THE UNIVERSITY *of* EDINBURGH

This thesis has been submitted in fulfilment of the requirements for a postgraduate degree (e.g. PhD, MPhil, DClinPsychol) at the University of Edinburgh. Please note the following terms and conditions of use:

- This work is protected by copyright and other intellectual property rights, which are retained by the thesis author, unless otherwise stated.
- A copy can be downloaded for personal non-commercial research or study, without prior permission or charge.
- This thesis cannot be reproduced or quoted extensively from without first obtaining permission in writing from the author.
- The content must not be changed in any way or sold commercially in any format or medium without the formal permission of the author.
- When referring to this work, full bibliographic details including the author, title, awarding institution and date of the thesis must be given.

New Methodologies and Scenarios for Evaluating Tidal Current Energy Potential

A. Sankaran Iyer

Thesis submitted for the degree of Doctor of Philosophy (PhD)
The University of Edinburgh
November 2011

Abstract

Transition towards a low carbon economy raises concerns of loss of security of supply with high penetrations of renewable generation displacing traditional fossil fuel based generation. While wind and wave resources are increasingly forecastable, they are stochastic in nature. The tidal current resource, although variable has the advantage of being deterministic and truly predictable. With the first Crown Estate leasing round complete for wave and tidal current energy, plans are in place to install 1000 MW of *tidal* capacity in the Pentland Firth and Orkney waters. The aim of the work presented in this thesis is to examine the role tidal current energy can realistically play in the future electricity mix.

To achieve this objective it was first necessary to develop new methodologies to capture the temporal and spatial variability of tidal current dynamics over long timescales and identify metrics relevant in a tidal energy context. These methodologies were developed for project scale resource characterisation, and provided a basis for development of a national scale dataset. The creation of project and national scale tidal datasets capture spatial and temporal variability at a level beyond previous insight, as demonstrated in case studies of three important early stage tidal current energy development sites. The provision of a robust national scale dataset enabled the development of realistic scenarios for the growth of the tidal current energy sector in UK waters. Assessing the various scenarios proposed indicates that first-generation technology solutions have the potential to generate up to 31 TWh/yr (over 8% of 2009 UK electricity demand). However, only 14 TWh/yr can be sensibly generated after incorporating realistic economic and environmental limitations proposed in this study.

The preceding development of methodologies, datasets and scenarios enabled statistical analysis of the matching characteristics of future tidal energy generation potential with the present UK electricity demand and trends of electricity usage. This analysis demonstrated that the UK tidal current energy resource is much more in phase than has

previously been understood, highlighting the flaws in previous studies suggesting that a combined portfolio of sites around the UK can deliver firm power. As there is negligible firm production, base-load contribution is insignificant. However, the time-series generated from this analysis identifies the role tidal current energy can play in meeting future energy demand and offer significant benefit for the operation of the electricity system as part of an integrated portfolio.

Acknowledgements

I would like to thank many people who have helped me along this mental odyssey. The following is a short list that I can think of, there are numerous others whom I have forgotten. To them, I am grateful and sorry I haven't listed you by name.

Supervisors Prof. Robin Wallace and Prof. Gareth Harrison, your guidance and at times doubts have only fuelled my need to find answers.

Many thanks to my colleagues at the Institute for Energy Systems and through out the School of Engineering for patiently listening to me and answering my GIS/Matlab/Fortran queries. I am also grateful for the period of employment I had at Flexitricity and particularly to Dr. Alastair Martin, the early morning were harsh but they taught me to be tough. To the ex-colleagues at Cineworld Edinburgh, your free films, tea and chat were constructive distraction. The Accommodation Manager and fellow Resident Assistants at Robbie Close, you made the job fun and I am most grateful for the subsidised accommodation.

I must thank my parents, for giving me this opportunity to do what I wanted, for their unconditional love and unwavering support even when I was being difficult. I could not have asked for more.

I am also grateful to Dr. Nicholas Johnson who offered to proofread this thesis without any bribe.

Finally, I cannot find the right words for the one person who I'd like to thank the most, my best friend and also my colleague Dr. Scott Couch who put up with me at home and at work. He had the unenviable task of being the critic as well as providing the shoulder for me to cry on. There is no doubt in my mind, without his kindness, generosity and hours of patience, I could not have completed this.

Financial support from EPSRC SuperGen FlexNet Consortium is gratefully acknowledged.

I also wish to acknowledge European Marine Energy Centre (EMEC) for the provision of Acoustic Doppler Current Profiler (ADCP) data; David Mummery at ScottishPower Renewables (SPR) for the ADCP data and the valuable interactions as well as Chris Zervas at National Oceanic Atmospheric Administration (NOAA) for providing the tidal analysis software.

The buoy records were supplied by the British Oceanographic Data Centre (BODC) as part of the Inter-Agency Committee on Marine Science and Technology funded, 'UK Moored Current Metre Data Set' DVD electronic publication. The data were collected by the Proudman Oceanographic Laboratory during the Mixing and sediment resuspension in shelf seas which was funded by the Natural Environment Research Council (NERC).

Software with the following trademarks were used within this study and are hereby acknowledged: Excel, Visio and Word of Microsoft, Inc.; ArcGIS (version 9.2) of Environmental Systems Research Institute, Inc.; MatLab (version 2008a) of Math Works, Inc.; and TotalTide (version 6.2) of the UK Hydrographic Office.

Declaration

I declare that this thesis has been written by myself. The research contained within is my own except where indicated otherwise. The work has not been submitted for any other degree or professional qualification.

.....

Abhinaya Sankaran Iyer

November 2011

Contents

Glossary

ACS	Average Cold Spell
AEP	Annual Energy Production
ADCP	Acoustic Doppler Current Profilers
ARC	Atlantis Resource Corporation
BERR	Department for Business, Enterprise and Regulatory Reform
BODC	British Oceanographic Data Centre
B&V	Black and Veatch
BP	British Petroleum
BWEA	British Wind Energy Association
CC	Cross Correlation
CFD	Computational Fluid Dynamics
CHP	Combine Heat and Power
CO_2	Carbon dioxide
CEC	Commission of the European Communities
CSM	Continental Shelf Model
CT	Carbon Trust
DoE	Department of Energy
DECC	Department of Energy and Climate Change
DTI	Department of Trade and Industry
DUKES	Digest of United Kingdom Energy Statistics
EIA	Environmental Impact Assessment
EMEC	European Marine Energy Centre
ENSG	Energy Network Strategy Group
EPRI	Electric Power Research Institute
ETI	Energy Technology Institute
EU	European Union
GB	Great Britain
GHG	Greenhouse Gas
GIS	Geographic Information System
GSP	Grid Supply Point
GW	Giga Watt
HRCS	High Resolution Continental Shelf
IDW	Inverse Distance Weighting
IEC - TC	International Electrotechnical Commission - Technical Committee
MaRS	Marine Resource System
MAE	Mean Absolute Error
MCT	Marine Current Turbine
MEC	Marine Energy Challenge
MRDP	Marine Renewable Development Fund
MRPF	Marine Renewable Proving Fund
NEA	North-East Atlantic

NG	National Grid
NGET	National Grid Electricity Transmission
NOAA	National Oceanic and Atmospheric Administration.
CO-OPS	Centre for Operational Oceanographic Products and Services
Ofgem	Office of the Gas and Electricity Markets
ORR	Operational Readiness Review
POL	Proudman Oceanographic Laboratories
RDI	RD Instruments
RES	Renewable Energy Strategy
RMAE	Relative Mean Absolute Error
RO	Renewables Obligation
ROC	Renewable Energy Certificates
SDC	Scottish Development Commission
SHETL	Scottish Hydro Electric Transmission Limited
SIF	Significant Impact Factor
SP	Scottish Power
SPT	Scottish Power Transmission
SPR	Scottish Power Renewables
SSE	Scottish and Southern energy
TAP	Technically Acceptable Power
TEC	Tidal Energy Converter
TECS	Tidal Energy Conversion System
TGL	Tidal Generation Limited
TRL	Technology Readiness Level
TS	Technical Specification
UK	United Kingdom
UKHO	United Kingdom Hydrographic Office

List of Symbols

Symbol	Description	Units
A	Area	m^2
a_o	Amplitude/ local tidal elevation	m
CC	Cross Correlation	-
c	Wave celerity	m/s
d	Distance	m
g	Acceleration due to gravity	m/s^2
g_n	Phase	°
H_n	Current velocity amplitude	m/s
H	Water depth	m
h	Bin size/ Water depth	m
hh	Hub Height	m
I	Eddy Intensity	%
N	Finite number	-
N_p	Number of pings per ensemble	-
n	Intrinsic noise	$/s^2$
$P_{cross\text{-}section}$	Power in a cross-section of water flow	W/m^2
p	peak weighting function	-
Q_{max}	Maximum flow discharge	m^3/s
T,t	Time	s
u, v	Velocity	m/s
u_k	Velocity at a known location	m/s
u_t	Velocity at time t	m/s
v'	Velocity anomaly	m/s
$\overline{v}$	velocity running average	m/s
w_k	Weighting	-
$\overline{x}$	mean value of x	-
x_i	i^{th} value of x	-
x, x_k	Value at a unknown/known point	-
X_n, Y_n	Two-dimensional velocity vectors	m/s
z	Elevation/ Reference height	m
z_r	Elevation of interest at r	m
Δz	Overall bin size	m
α	ADCP standard deviation	m/s
λ	Wavelength	m
θ	Tidal current direction	°
ρ	Density (water)	kg/m^3
σ	Standard Deviation (velocity)	m/s
$\sigma_n t$	Angular speed	℅hour

Units	Description	Value
kWh	kilo Watt-hour	1,000 Wh
MWh	Mega Watt-hour	1,000,000 Wh
GWh	Giga Watt-hour	1,000,000,000 Wh
TWh	Tera Watt-hour	1,000,000,000,000 Wh

Definitions

Array – A group of turbine in a farm.

Current –The horizontal flow of water is referred to as tidal current and is very sensitive to the size of the water area, bathymetry and the land mass surrounding the water.

Cut-in velocity – is the velocity at which the device starts to generate power. This is when there is enough kinetic energy to over come inertia and the rotor starts moving.

Diurnal –One high water and one low water daily.

Ebb – The movement of water level falling out of an estuary/channel into the open sea.

First Generation Technology – In order to set the context of the analysis presented in this thesis, 'First Generation Technology' is defined as iterations of existing prototype devices that are already undergoing pre-commercial demonstration. A *second generation* of technology is defined as being able to be deployed in deep water of greater than 50 metres. Examples of such generation technology solutions are under development, but are currently at the early stages of technology readiness, and hence unlikely to make a significant contribution to meeting 2020 electricity generation targets.

Flood– The movement of water level rising into an estuary/channel.

High water **–** is the maximum water level reached during a tidal cycle.

Low water **–** is the lowest water level in the tidal cycle.

Lunar day **–** is the time it take the moon to complete one full orbit around the Earth in 24 hours and 50 minutes.

Lunar month **–** is the time between two identical syzygies, 29.53 days.

Mean sea level **–** is the average hourly value of all the high water and low water experience at the site.

Neap tides **–** occur when the moon and the Sun are in quadrature where the Moon and the Sun counteract each other.

Power curve **–** shows the complete performance envelope of the device power output at specific velocity values. A power curve should indicate the exact cut in and rated velocity of the devices and the device operation between there two parameters.

Rated velocity – is when the device reaches maximum/ rated output for which it is designed for.

Semidiurnal – Variations with two high waters and two low waters daily. The UK experiences semidiurnal tides where high water and low water occur twice in a day.

Solar day – which is the time it take Earth to rotate on its own axis, 24 hours.

Spring tides are of increased amplitude and occur twice a month when the moon and the Sun reinforce each other

List of Figures

List of Tables

1. Introduction

The ever growing global population, along with the increasing need for electricity has put a lot of emphasis on the energy sector and the need to secure our energy sources. Global oil prices reached a record high in July 2008 and, although the current economic climate has stunted the rising prices, the age of cheap oil is coming to an end (UKERC, 2009). Moreover, continued extraction and combustion of fossil fuels has a negative impact on the environment. The main culprit being Greenhouse Gas (GHG) emissions. This has generated anthropogenic global warming, with 40% more carbon dioxide (CO_2) particles at present in the atmosphere, in over 130 countries, than prior to the Industrial Revolution (DECC, 2009).

The 2010 British Petroleum (BP) oil spill in the Gulf of Mexico (BBC, 2010) has raised public awareness of and increased the focus on finding alternative, sustainable sources of energy. One low carbon option is to opt for nuclear energy but the 2011 Tsunami in Japan has exacerbated public concern (BBC, 2011). For example, Germany is now planning to shut down all nuclear power plants by 2022 in response to this event (Guardian, 2011).

In the United Kingdom (UK), ambitious targets have been set by the government to reduce GHG emissions and to secure energy supply. An effective way of achieving this is the inclusion of renewable generation such as wind, wave and tidal energy in the energy mix. It is expected that there will be a transition from mostly carbon-based fossil-fuel generation to renewables. Hence, it is necessary to assess the generation potential of such energy sources and to address the issues that may arise when generation from these variable sources is connected to the electricity network.

The main aim of this work is to quantify the extractable proportion of tidal current energy available in the UK with specific regard to its spatial and temporal variability. The study will show how these datasets are assembled and define methodologies for combining a number of datasets to improve the overall temporal quality and spatial coverage of the study area. As an application, the new re-appraisal of the resource, presented in the form of time-

series for each site of interest, will be used to evaluate the variability of the aggregate resource. Of particular interest is characterising the matching of demand for electricity and generation. The impact of the time varying tidal resource at different levels of tidal energy penetration is also investigated.

1.1 Setting the Scene: Renewables and Electricity

A key driver for the UK government energy policy is to meet the European Union (EU) legally binding target of a 20% reduction in harmful GHG emissions (compared to the 1990's level) and a 20% share of energy generated for renewable sources by 2020. (CEC, 2008)

In the UK this translates into a demand for 30% of the electricity to be supplied from renewable sources in order to meet the target. Electricity faces a higher proportion of reduction as it is harder to reduce GHG emissions from other parts of the energy sector such as heat and transport.

This section introduces the various drivers and incentives that exist in the UK for decarbonising the electricity network.

1.1.1 Policies and funding support

One of the most important drivers towards renewables is the opportunity to increase secure energy supplies. Developing renewables will decrease the dependency on oil and gas imports. This would give more opportunities to allow the economy to develop with the emerging renewable sector. Economic growth can proceed with less adverse energy costs and environmental issues. It is reported that around 50% of EU's economically viable tidal current resource is available in the UK (B&V Phase II, 2005). Leading development of this sector could be of great advantage to the UK, with the potential to establish an industry to aid recovery from the recession.

The UK government has introduced numerous incentives to deliver these targets. The Renewable Energy Strategy (RES, 2009) was introduced in 2009 to help direct the sector towards meeting energy targets. RES has identified key areas as stimulants for renewable promotion. These financial incentives are:

1. In the form of Renewables Obligation (RO) where a mandatory requirement is placed on the electricity supplier to source part of their generation from renewable sources. This scheme is regulated by the Office of Gas and Electricity Markets (Ofgem). Renewable energy generators are awarded Renewable Energy Certificates (ROCs) for every megawatt hour (MWh) of electricity that is produced. With the introduction of the Energy Bill in 2008, ROC banding was introduced. This entitles emerging technologies to additional ROCs to give them bigger incentives. In Scotland, tidal technologies are allocated 3 ROCs/MWh as opposed to 2 ROCs/MWh in the rest of the UK.
2. Feed-in-tariffs are another form of financial incentive, where if a company generates its own renewable energy, they are then entitled to premium payment for the electricity and any excess exported to the electricity network.

Better planning for grid connection of large scale projects and improving grid coverage for faster provision of connections are also being considered.

Tidal current resources are abundant in the UK, placing it in a very favourable position to not only exploit this resource but to become one of the leading nations in the world for tidal energy. With the introduction of the Marine Renewable Proving Fund (MRPF), up to £6 million has been provided to successful applicants to help meet the capital cost and initiate prototype development. The Scottish Government also has funding programs offering additional grants to encourage device developers to come to Scotland. An additional funding avenue is the Saltire Prize, providing £10 million to the technology that can first demonstrate commercial viability in Scottish waters by generating an electrical output over 100GWh over a continuous two year period (The Scottish Government, 2011).

1.2 Project Objectives and Scope

The project objectives are as follows. To:

1. Determine how well correlated different sources of tidal current datasets for the UK are and see if they can be used together to assess the potential tidal current resource in UK,
2. Use site specific measurements; test and develop methodologies that can be used for project scale analysis,
3. Investigate the use of harmonic analysis to inform Annual Energy Production (AEP) assessment and assess the impact of data coverage and resolution on accuracy,
4. Use a Geographical Information System (GIS) to combine datasets. Develop constraints on parameters suitable for tidal current energy extraction,
5. Develop realistic scenarios of energy extraction for the sites identified and define a limit to the extraction based on an economic and environmental limit,
6. Explore the potential of continuous base-load generation potential from tidal current energy alone, and
7. Assess how well tidal generation matches demand for electricity.

1.3 Thesis Outline

This thesis is made up of eight chapters and two appendices. The scope, context, objective and aim of the research have been presented in chapter 1.

Chapter 2 presents all the development to date in the marine energy context with specific emphasis on tidal current energy. An overview of all the studies conducted so far and the present state of the industry is outlined.

The ideas developed in chapters 3, 4 and 5 assess individual sites of interest to evaluate the site specific characteristic presented at these different test sites. However, within

these chapters, different datasets are used that present how different each source of dataset is in terms of data quality and the level of site specific analysis that can be done using this data.

A novel way of combining datasets is presented in chapter 3 using publically available data sources, with the aim of evaluating how well each of the dataset represents a specific location. Site specific measurement is considered 'gold-standard' and therefore all the other datasets are compared to this benchmark. The analysis is presented as a case study for a site in Anglesey, Wales.

Chapters 4 and 5 demonstrate the use of site specific measurements. Using Acoustic Doppler Current Profiler (ADCP) data for the Sound of Islay and Fall of Warness, key metrics that are relevant in terms of energy extraction context and devices design are identified. The metrics presented are a combination of what has been identified in the existing studies as well as developing new methodologies where knowledge gaps are evident in support of the International Electrotechnical Commission (IEC) Technical Committee (TC) 114 Standards development activity.

Although the site specific characteristics are highly relevant at a project level, the level of information that feeds into a national scale study needs to be constricted so as to get an appropriate overview of the national resource. Chapter 6 presents a re-appraisal of the UK tidal current resource and develops realistic scenarios of 'first generation'[1] development that account for economic and environmental considerations. The scenario investigates if it is possible to generate a 'base load' like output using a combination of different sites that are thought to be out of phase.

Chapter 7 is an application of the datasets and methodologies generated in chapter 6. Analysis consists of evaluating how well demand and supply is matched, and methodologies to account for the variability.

Chapter 8 presents a summary of the thesis. It also identifies some of the limitations and areas of future work are also discussed.

[1] Exact description of first generation is provided in the Definition section.

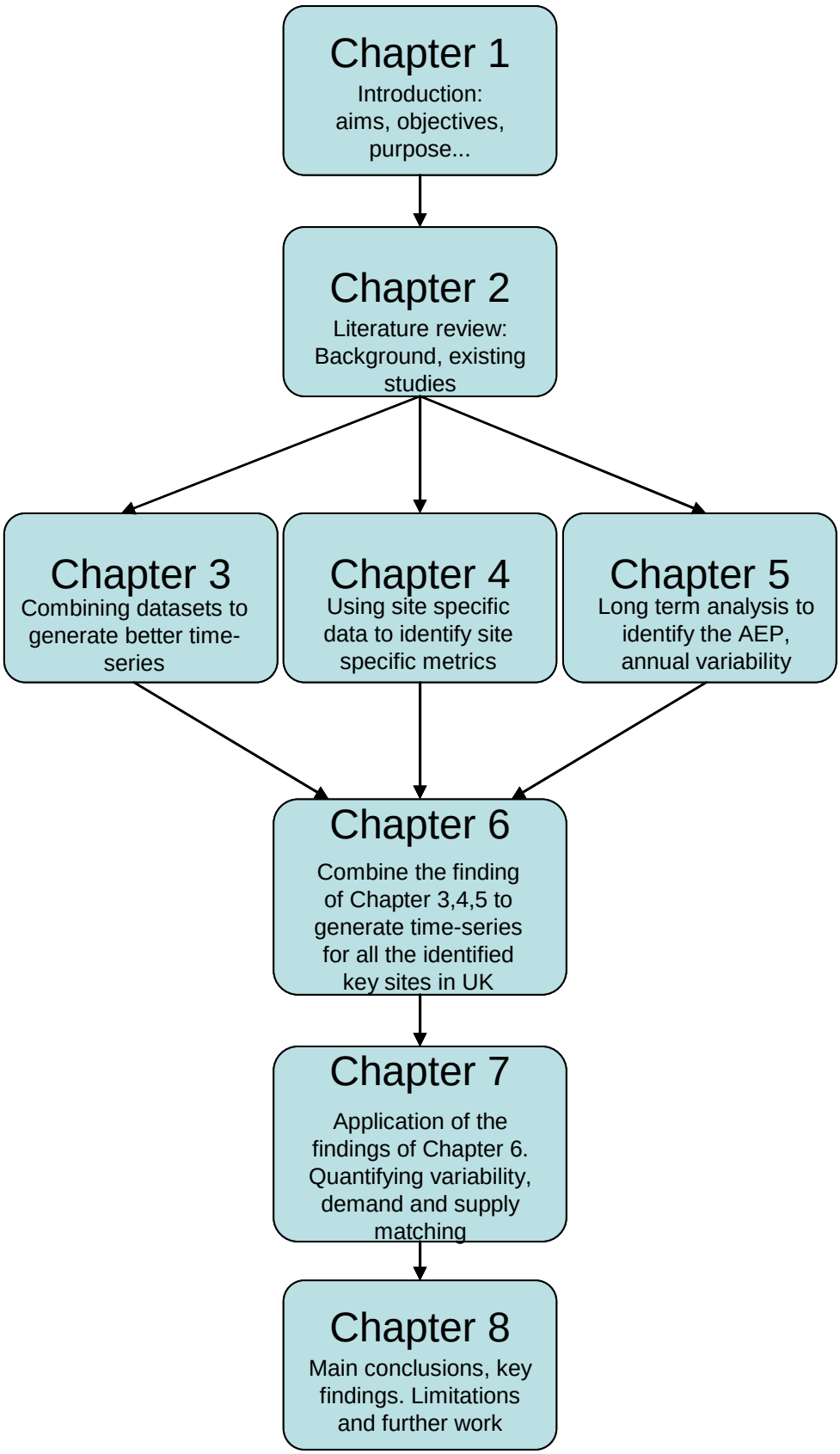

Figure 1.1 Outlining the objective and purpose of each chapter and how they are connected.

1.4 Contribution to Knowledge

The need for this research arises because, although numerous studies have been conducted to quantify the tidal current resource available in the UK waters, none of the estimates agree and it is important to have a robust assessment to provide policy advice. Some of the studies have simplified the assumptions behind the tidal physics and therefore reached incorrect conclusions, while others have simply used data that is of very low resolution and therefore not fit-for-purpose.

The research has established new datasets generated through the combination of a number of sources. The key addition is consideration of spatial *and* temporal variability, a significant improvement over existing studies. Using these datasets, a new estimate of the UK national resource based on enhanced data sources and understanding of the tidal physics and dynamics of energy extraction is presented.

The use of time-series data has enabled the evaluation of the phasing of all the sites included in the analysis. The analysis demonstrates that the UK tidal resource is much more in phase than previous findings suggest. This is predominantly because the study develops realistic and economic scenarios as would be the case over the next decade. The analysis demonstrates that there is negligible firm production and therefore base-load generation potential is insignificant compared to the installed capacity.

The marine renewable industry is still in its infancy compared to the wind industry. Over the years sets of standards and protocols in the wind industry have been developed that provide project developers with technical and practical guidelines through each major phase of project development. At the start of this PhD study (October, 2007), no full scale tidal current device had been tested and little knowledge existed of the best practice for site assessment and resource characterisation. One of the key contributions of this thesis is the demonstration and development of methodologies for appropriate site evaluations that are specific to the tidal current energy context and fit-for-purpose.

2. Tidal Current Energy

This chapter begins with a basic examination of how tides are formed, and introduces some of the terminologies used in this context. Definitions from Pugh (1996) and Boon (2004) have been assimilated to assist the reader in understanding the resource better. Specific discussion of tides with respect to tidal current energy extraction is also present by Polagye (2009). Key characteristics of an energetic site are presented and device characteristics are also discussed. Finally a literature review of the existing studies and methodologies are presented.

2.1 Tides

Regular water movements are a common feature on the shore of the ocean and seas. *Tides* are periodic movements which result from the gravitational force of the moon, and to a lesser extent, the sun, on the large bodies of water covering the Earth's surface. The vertical movement manifests itself as the rise and fall of water height. The horizontal movement is called *tidal current*. Tides formed this way are referred to as *Gravitational Tides* to distinguish them from change associated with *non-tidal components* which occur as a result of meteorological forces. The occurrence of Spring and Neap tides is determined by the position of the Sun and the Moon, see Figure 2.1 and Figure 2.2.

2.2 Harmonic Analysis

Tidal analysis can be conducted and used for prediction of tidal heights and tidal current time-series using harmonic analysis techniques. Tides are deterministic in nature, and are a sum of a finite number of harmonic constituents whose angular speed and phase is determined by the Moon and the Sun. A tidal constituent is a measure of one of these motions and has an amplitude and phase which varies from one location to another.

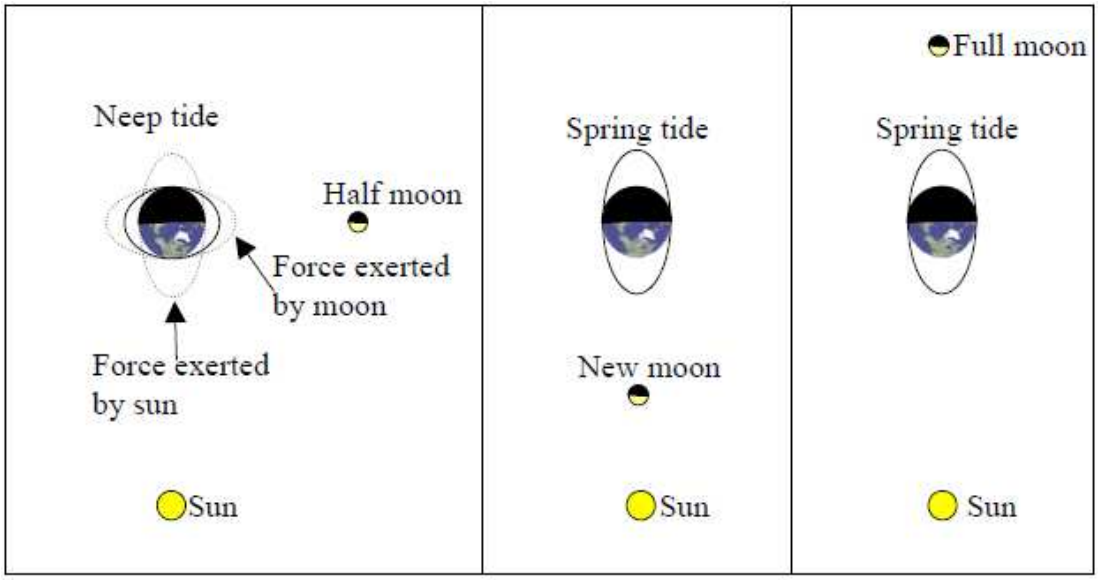

Figure 2.1 Spring and Neap tides based on the location of the Moon and the Sun. (Bryans, 2006)

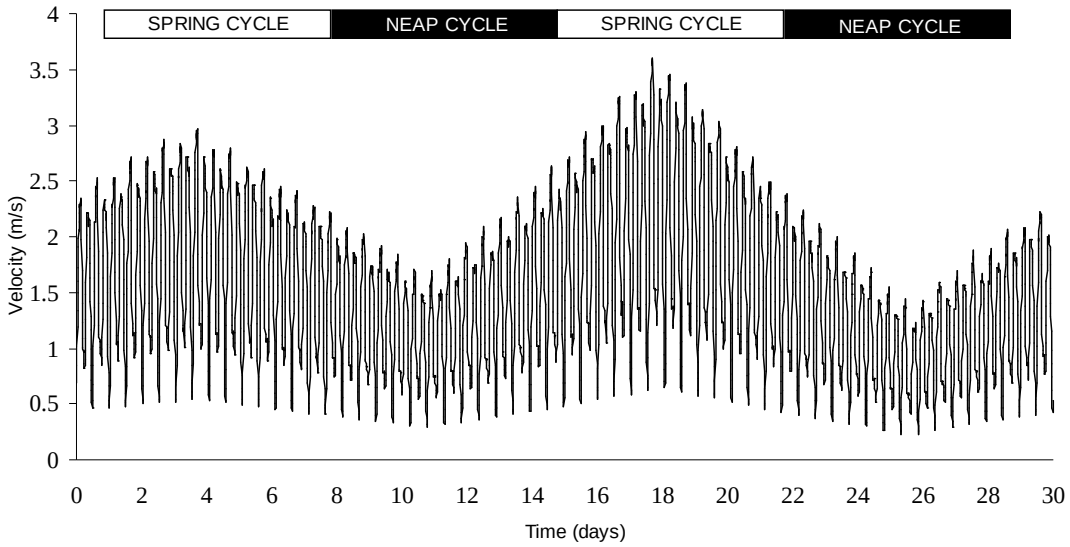

Figure 2.2 Complete tidal cycle over a month, with two spring and neap cycles.

Harmonic analysis can be represented by a finite number *N* of harmonic terms each of the form (Pugh, 1996):

$$H_n \cos(\sigma_n t - g_n) \tag{2.1}$$

where H_n is amplitude, $\sigma_n t$ is angular speed and g_n is phase lag of the Equilibrium tide, which is defined as:

> " A model under which it is assumed that the water covering the face of the Earth instantly responds to the tide-producing forces of the Moon and the Sun to form a surface of equilibrium under the action of these forces. The model disregards friction, inertia, and the irregular distribution of the land masses of the earth. The theoretical tide formed under these conditions is known as the equilibrium tide." (Boon, 2004)

The forces experienced by *Gravitational tides* consist of a number of discreet frequencies whose phase and amplitude is known. Local factors such as bathymetry can affect the flow and vary the amplitude and phase. However, the frequency remains the same. Least squares fitting is used to match the known frequency from the recorded time-series to the known frequency, which is used to identify the phase and amplitude. Table 2.1 shows the major astronomical tidal constituents with their respective periods, frequencies and angular velocities.

Constituent	Period (mean solar day)	Frequency (cycles per day)	Angular speed (°/hour)
M_2	0.518	1.932	28.984
S_2	0.500	2.000	30.000
N_2	0.527	1.896	28.440
K_1	0.997	1.003	15.041
M_4	0.259	3.865	57.968
O_1	1.076	0.930	13.943
M_6	0.173	5.797	86.952
MK_3	0.341	2.935	44.025
S_4	0.250	4.000	60.000
MN_4	0.261	3.828	57.424

Table 2.1 Major astronomical tidal constituents (Pugh, 1996).

Using this concept a number of tidal constituents can be extracted from measured data for a specific location. There are over 300 tidal constituents in total (Pugh, 1996), M_2 is generally the most dominant and has a period of 12.42 hours and represents the variations from the Moon's influence which has a daily diurnal pattern. S_2 is generally the second-most dominant constituent due to the Sun's influence with a period of 12 hours. The longest time period of variations is 18.6 years where the lunar cycle affects the inclination of the Moon's orbit relative to the Earth's plane. In order to get a true understanding of all the tidal

variations and be able to resolve all the 175 tidal constituents at a specific location, data for a minimum of 19 years is required. (Pugh, 1996)

Tidal current sites can experience semi-diurnal, mixed or mainly diurnal tidal regimes based on the Form Number, see Figure 2.3.

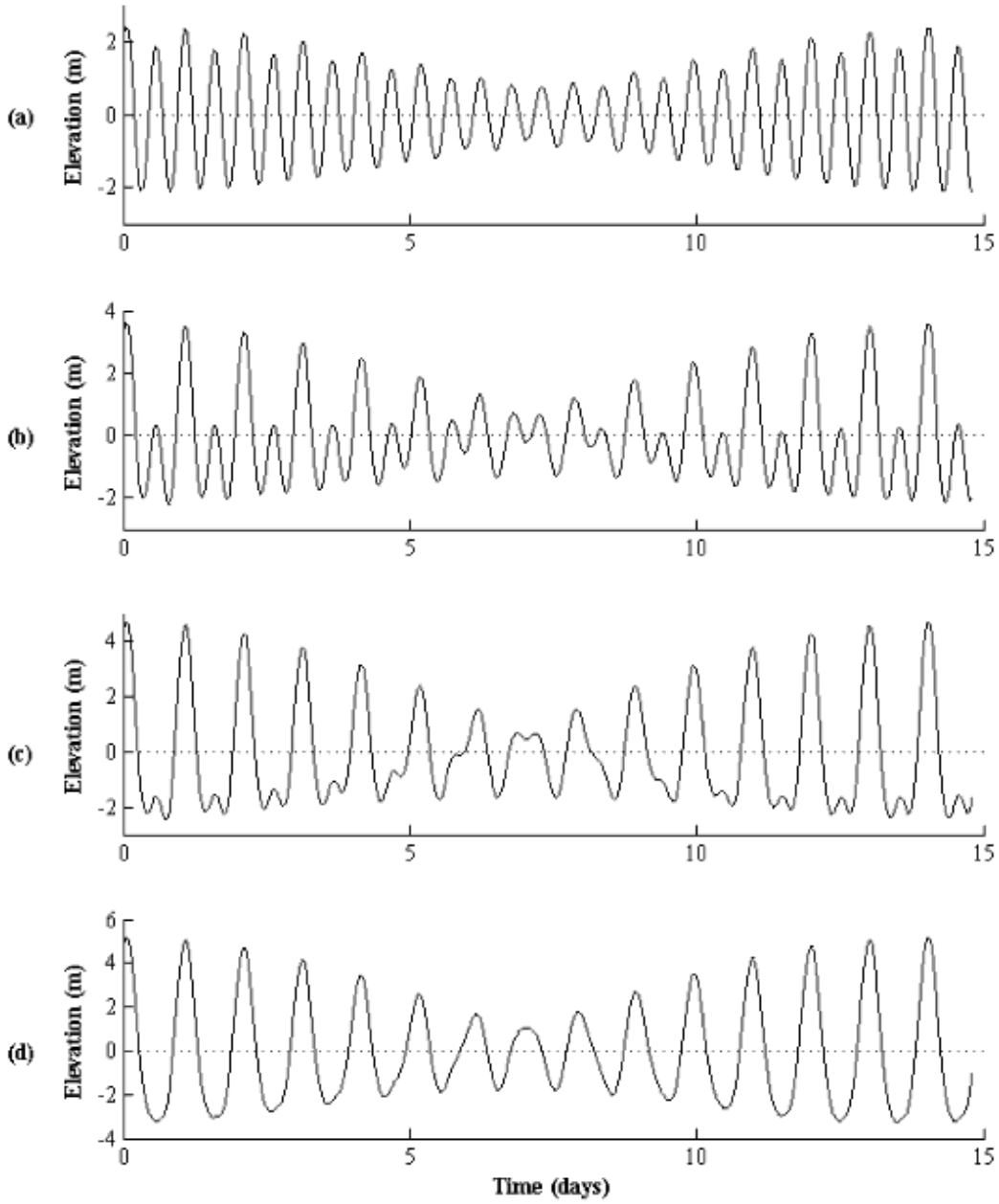

Figure 2.3 Tidal regimes, (a) semidiurnal (*F*=0.1), (b) mixed, mainly semidiurnal (*F*=0.9), (c) mixed, mainly diurnal (*F*=2.3) and (d) diurnal (*F* =4.7). (Polagye, 2009)

The Tidal Form number is an easy way to identify different types of tides experienced around the world. Tidal Form Number can be expressed as (Boon, 2004):

$$Form\ Number\ \ (F) = \frac{K_1 + O_1}{M_2 + S_2} \qquad (2.2)$$

If the Form Number is less than 0.25, the tides are semidiurnal, experiencing two high tides and two low tides each day. A tidal form number between 0.25 and 1.5 indicates mixed, predominantly semidiurnal tides. Between 1.5 and 3.0, the tides are mixed, predominantly diurnal and above 3.0 are fully diurnal with one high tide and one low tide each day. The UK coast is dominated by semidiurnal tides.

Collecting accurate data for a long period of time is expensive and time consuming. However, harmonic analysis can be used on datasets of 15 days or more of tidal current velocity measurements to create time-series of tidal heights and tidal currents for the location. Depending upon the signal-to-noise ratio and the *Rayleigh criterion*, 23 constituents can be consistently extracted from a 30 day record. In fact, the four major constituents M_2, S_2, K_1 and O_1 can between themselves account for more than 90% of the tidal variations in many locations. (Lu *et al.* 1999)

The selection of σ_n (equation 2.1) is based on the *Rayleigh Criterion* which requires each constituent to be separated by at least one complete period from their neighbouring constituent (Pugh, 1996). The Rayleigh Criterion is important as it helps determine which of the constituents can be evaluated in the harmonic analysis. This minimum period required to separate two constituents is called the *synodic period*. For example to resolve M_2 and N_2 required:

$$\frac{1}{(1.932 - 1.896)} \approx 28\ \ days$$

The frequency (cycles per days) for M_2 and N_2 can be obtained from Table 2.1. Table 2.2 shows the first 10 tidal constituents in the standard order, and the number of days needed to separate each of the constituents from the other. It is important to understand that a

minimum of *15 days* of data is required to do the basic harmonic analysis as it takes 14.77 days to separate the first two of the strongest tidal constituents.

Rayleigh criterion (in days)	M2	S2	N2	K1	M4	O1	M6	MK3	S4	MN4
M2		14.77	27.55	1.08	0.52	1.00	0.26	1.00	0.48	0.53
S2	14.77		9.61	1.00	0.54	0.93	0.26	1.07	0.50	0.55
N2	27.55	9.61		1.12	0.51	1.03	0.26	0.96	0.48	0.52
K1	1.08	1.00	1.12		0.35	13.66	0.21	0.52	0.33	0.35
M4	0.52	0.54	0.51	0.35		0.34	0.52	1.08	7.38	27.55
O1	1.00	0.93	1.03	13.66	0.34		0.21	0.50	0.33	0.34
M6	0.26	0.26	0.26	0.21	0.52	0.21		0.35	0.56	0.51
MK3	1.00	1.07	0.96	0.52	1.08	0.50	0.35		0.94	1.12
S4	0.48	0.50	0.48	0.33	7.38	0.33	0.56	0.94		5.82
MN4	0.53	0.55	0.52	0.35	27.55	0.34	0.51	1.12	5.82	

Table 2.2 Comparing different constituents and the number of day needed for each to resolve.

Sometimes the Rayleigh criterion can be very restrictive and it may not be possible to include additional constituents. However, by ignoring the signal-to-noise ratio it is possible to include extra constituents, although this can compromise the data quality. Aliasing is another major concern in terms of reproducing the data at a chosen sample period.

2.3 Tidal Wave Propagation

Tidal phasing stems from the fundamental concept of tidal wave propagation. The velocity of tidal wave propagation in shallow water is given by:

$$c = \sqrt{gh} \tag{2.3}$$

where c is the wave celerity (m/s), g is the gravitational acceleration (m/s^2), and h is the water depth.

For the purpose of illustration, a depth of 50 m is selected as being representative of UK coastal waters. From this, the wavelength λ of the tidal wave can be calculated as:

$$\lambda = cT \tag{2.4}$$

where T is taken as the time period 12.4 hours of the main tidal component M_2 (diurnal pattern of the Moon). In the vicinity of the UK the wavelength of the M_2 tidal component is approximately 988 km which is approximately the length of the UK landmass. This would suggest that that there are substantial differences in phase around the UK coastline. However the topology of the British Isles serves to complicate matters.

In the deep ocean, tides predominantly propagate as progressive waves. As they approach near-shore regions on the northern European continental shelf, their behaviour tends towards a standing wave characteristic where high and low water coincides with slack tide. Near-shore tidal velocities tend to peak when the gradient of the surface elevation is at a maximum. Figure 2.4 illustrates the current velocity and tidal heights for a randomly chosen location around the UK (Amlwch, near Holyhead - tidal diamond SN048J).

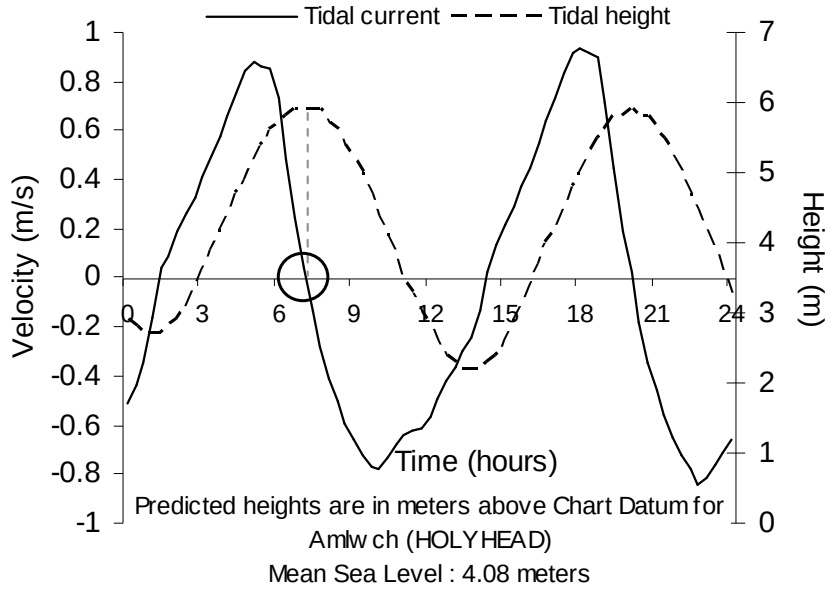

Figure 2.4 Tidal Current (solid line) and height data (dotted line) at Holyhead indicating relative phasing of current and surface elevation. Data obtained from TotalTide.

Slack tide occurs when the tidal current (solid line) changes direction. The change in flood to ebb direction is at the time of high water indicating standing wave characteristics. The Holyhead data is generically representative of large swathes of UK coastal waters, so Figure 2.4 represents broadly tidal wave characteristics throughout the UK waters. Although slight time lead/lag may be experienced at specific sites, the current will typically change direction coincident in time to the highest gradient of local surface elevation. This concept of tidal wave propagation and standing wave becomes particularly relevant in chapter 6 when tidal phasing is discussed.

2.4 Resource Characterisation

In the past, tidal data was primarily collected for navigational and oceanographic purposes. Therefore, regions of high tidal current velocity were generally considered unsafe and avoided and of minimal interest. Only in the last decade or so, since the concept of converting kinetic energy from tidal currents into electricity has been developed, have the areas of high current velocity become of greater interest. However, data for energetic locations is very scarce and of too poor resolution to be used for economic resource assessment and site characterisation.

2.4.1 Velocity and Power

Resource assessment and characterisation is a primary activity that plays a key role in identifying a site as suitable for tidal current energy extraction. Tidal current energy is spatially and temporally variable, typically concentrated in very small regions. The power available in a tidal current is proportional to the cube of the current velocity. To assess the potential energy that can be generated, it is essential to accurately evaluate the tidal current velocity observed at the site of interest. The kinetic tidal power is calculated as:

$$P_{cross-section} = \frac{1}{2} C_p \rho A u^3 \qquad (2.5)$$

where $P_{cross-section}$ is the theoretical power in Watts (W), C_p is power coefficient which can be considered as the water to wire efficiency of the device (for first generation devices, this in the order of 45%), ρ is the density of seawater (1025 kg/m^3), *A* is the cross section area or also referred to as device capture area and *u* is the instantaneous current velocity. It is often of interest to know the power in a metre square area, in which case power density per metre square (W/m^2) is calculated as:

$$P = \frac{1}{2}\rho u^3 \tag{2.6}$$

For a site to be considered economically viable, a power density of 1 kW/m^2 or above is considered acceptable, with exceptionally strong sites exceeding 5 kW/m^2 (Polagye, 2006). The tidal resource is geographically disperse and variable over time, although predictable. Appropriate devices need to be selected for each site to have optimised energy production. Therefore, adequate data needs to be collected to evaluate how strong a site is and assess the potential of economic tidal energy development.

2.4.2 Vertical Velocity Profile

Tidal current velocity varies through the water column. Close to the sea bed, the velocity is at its lowest due to friction. This is an important consideration in terms of energy extraction. Placing the hub of a tidal turbine in a low velocity region would mean the resource is underutilised. The Department of Energy (1990) guidelines for depth profile has also been used by The Department of Trade and Industry (DTI, 2004a, 2004b). The profile has a 1/7th power law for the bottom half of the water column followed by a constant velocity for the remaining top half of the water column. It is given by:

$$u_t(z) = \left(\frac{z}{0.32H}\right)^{1/7}\overline{u_t} \qquad \text{for} \qquad 0 \le z \le 0.5H \tag{2.7}$$

$$u_t(z) = 1.065\overline{u_t} \qquad \text{for} \qquad 0.5 \le z \le H \tag{2.8}$$

where $\overline{u_t}$ is depth averaged current at time *t*, and *H* is water depth. More commonly used are the 1/7th and the 1/10th power law profiles of the form:

$$\frac{v(z)}{v(z_r)} = \left(\frac{z}{z_r}\right)^{\frac{1}{x}} \tag{2.9}$$

where $v(z)$ is a known velocity at a known elevation z, and $v(z_r)$ is the unknown velocity at the elevation of interest, z_r. In the case of the 1/7th power law x = 7 or 10 in case of 1/10th power law. This method is often used to estimate the tidal velocity through the water column in cases where measurements are not available for the entire water column.

Figure 2.5 shows the three profiles applied to a region of 50 meters of water depth, with a known velocity of 1 m/s at the surface. In reality, the profile is very site specific and can often vary significantly over the tidal cycle and between ebb and flood cycles. Therefore, without in-situ data measured along the water column, is it not possible to determine which vertical profile is observed in the water column. Current direction can vary significantly down or across the water column.

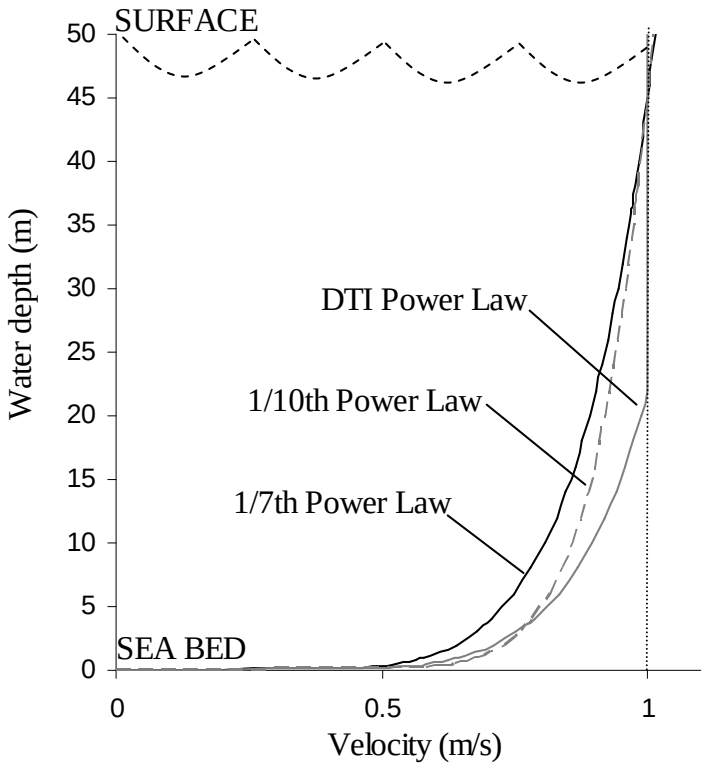

Figure 2.5 Vertical current velocity profile derived using different power laws.

2.4.3 Tidal Direction

Topography such as headlands and bathymetric variations in water depth impact on tidal flow direction in the coastal zone. In restricted regions such as narrow channels, tidal currents predominantly follow the local topography and the flow direction on the flood and ebb cycle are described as being rectilinear (180° apart). In less constrained flow domains, tidal current direction can constantly change as a result of the various forcing terms acting on the fluid (e.g. inertia, friction, Coriolis force). The contribution of the Coriolis forcing term often leads to elliptical or circular flow patterns as shown in Figure 2.6. Directionality is an important consideration when assessing tidal resource characteristics for tidal energy harvesting as the majority of existing devices are designed under the assumption of bi-directional flow. If a device is unable to yaw and located in a region where the flow in not rectilinear, a significant amount of the energy in the flow that could potentially be captured will be lost.

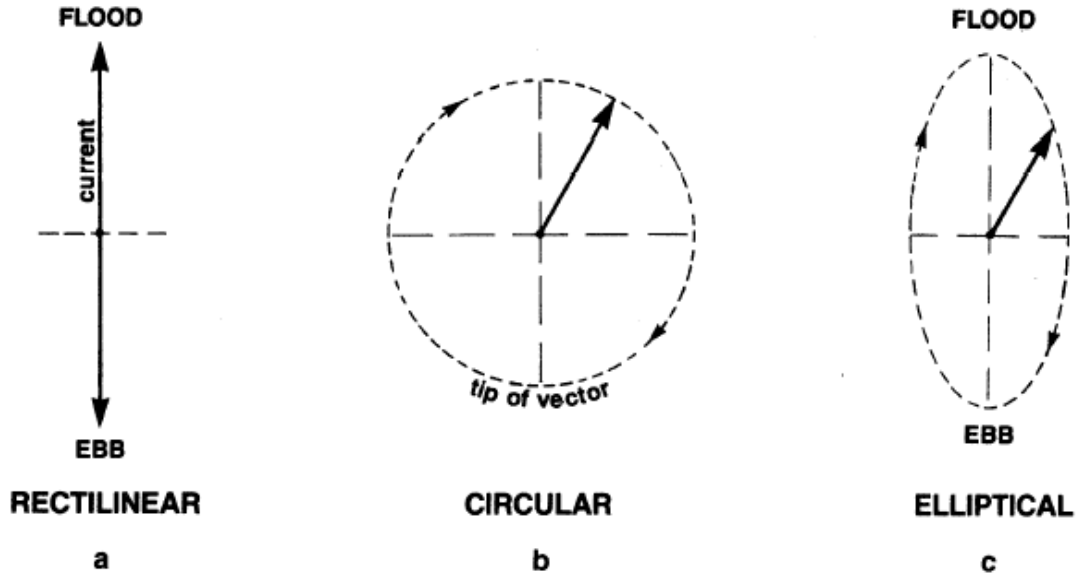

Figure 2.6 Tidal flow directionality, rectilinear, circular and elliptical (Cornett, 2008).

2.5 Existing Tidal Generation Technology

This section discusses the different methods of extracting energy. Some well known device designs are discussed. Section 2.5.1 explains the basic device concepts commonly used in the marine industry. This will give the reader an understanding of the current state of technology and an overview of the most established devices that have either undergone scale testing or had the opportunity to do a full scale testing.

2.5.1 Devices

To date a number of technology types have emerged that use different designs to harness power from tidal currents. The simplest and most commonly seen design uses a *horizontal axis turbine* where the current flow direction is perpendicular to the device rotor. Some device concepts include blades that *pitch* to optimise the angle of attack for the incoming tidal current velocity. Devices may also incorporate a *yawing* mechanism so that the rotor can orient to face the flow direction. This concept is predominantly designed for regions of depth 30 to 50 m to make optimum use of the velocity profile in the water column. The power generated by these devices is proportional to the device capture area and the current velocity cubed, as shown in equation 2.3.

In shallower waters a *vertical axis* turbine provides a possible alternative where a rectangular cross section defines the capture area. The power output is unaffected by device orientation and the turbine experiences even hydrodynamic loading. Another novel concept is the use of a hydroplane that moves vertically as the tidal current pass. Certain designs may choose to have a pitched hydroplane to change the angle of attack as the current moves through it. These basic device configurations are shown in Figure 2.7 and relate to real devices shown later.

A number of anchoring mechanisms have been developed to deploy and mount the devices. One concept is a *gravity base* foundation built with steel reinforced concrete which

holds the device and the device structure in place using its own weight. Many variations of the gravity based structure exist, where slabs of concrete are used to hold the device frame in place. Another common concept in use is the *monopile*, which is a single circular column of prefabricated metal plates. The structure is then either driven or drilled into the sea-bed. The friction between the pile and the material it is buried in then provides frictional resistance against loading on the device. Variations on this approach include the use of a tripod/ quadropod structure secured with rock bolts.

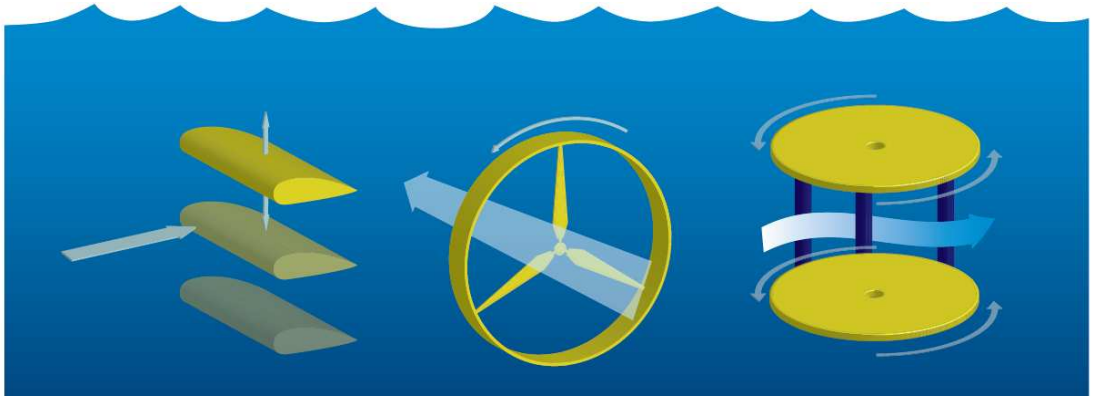

Figure 2.7 Different device configurations used to extract tidal current energy. (SDC, 2007f)

According to B&V Phase II (2005) approximately 50 % of the available resource is in deeper waters of depth above 40 metres, therefore the market for existing technologies will be limited by the available resource due to the depth restrictions. Further analysis demonstrated in chapter 6 presents scenarios and highlights the depth restrictions. Future generation of tidal devices are being designed to float so as to overcome depth limitations.

2.5.2 Technology Development

A number of devices have been designed and are undergoing large-scale open sea, pre-commercial testing. In order to identify how well each technology is progressing and to present an overview of what level of market readiness a specific device presents, a scale of Technology Readiness Level (TRL) is often applied to each technology as defined by the United States Department of Energy (US DoE, 2010) to assess how close each of the devices

is to full scale commercialisation. The concept of TRL's was first introduced by National Aeronautical Space Administration (NASA, 1995). A general definition of each TRL is presented in Table 2.3.

TRL 1	Basic principles observed and reported
TRL 2	Technology concept and/or application formulated
TRL 3	Analytical and experimental critical function and/ or characteristics proof-of-concept
TRL 4	Component/subsystem validated in laboratory environment
TRL 5	System/subsystem/component validation in relevant environment
TRL 6	System/subsystem model or prototyping demonstrating in a relevant end-to-end environment
TRL 7	System prototyping demonstration in an operational environment
TRL 8	Actual system completed and "mission qualified" through test and demonstration in an operational environment
TRL 9	Actual system "mission proven" through successful mission operations

Table 2.3 TRL's as defined by NASA (1995).

These TRL's can be applied to marine energy in general but the definitions used here have been adopted and modified to reflect tidal current energy specific development. A TRL of 4 or below indicates that the technology is undergoing laboratory testing but no large scale or commercial scale testing is underway. A TRL of 5 indicates that validation in a simulated environment is underway but full testing has not been done. TRL 6 indicates that the scaled prototype has been tested in a relevant operational environment that represents the actual environment the device will be deployed in. TRL 7 is actual full scale system demonstration and validation of the prototype meeting project requirements, includes supporting information. TRL 8 demonstrates that the technology is ready to be deployed commercially, and supporting documentation such as an Operational Readiness Review (ORR) will be carried out. Finally, TRL 9 indicates the technology is operational under all ranges of environment including demonstration of the actual system. Table 2.4 gives an overview of some of the top devices with proven technology and up-to-date development in terms of device testing and project development.

Technology Name/ Company	Technology type/ Configuration/ Capacity	Testing sites	Projects	TRL
 Marine Current Turbine/ Seagen *(MCT,2008)*	Two bladed, twin rotor, variable pitch, axial flow turbine. Full scale device tested with 16 meter rotor diameter.1.2 MW installed capacity. Mounted on a quadrapod structure. *(MCT, 2008)*	Full scale testing completed and grid connected at Strangford Narrows, N. Ireland, UK since 2008. Commercial scale array development is ongoing. *(MCT,2008)*	Kyle Rhea (UK), Anglesey (UK), Pentland Firth (UK), Bay of Fundy (Canada) *(MCT,2008, 2008c)*	**8**
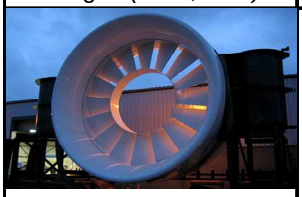 Open Hydro *(OpenHydro, 2007)*	Multiple bladed, duct shaped housing within a 6 meter rotor diameter. Open centre horizontal flow turbine. Scaled device tested with 250 kW installed capacity. Sea bed mounted. *(OpenHydro, 2010)*	1/3rd scaled, 250 kW testing is ongoing at EMEC since 2006. 1 MW device deployed in Bay of Fundy, Canada in 2009 – although not grid connected. *(OpenHydro, 2008, 2009)*	Race of Alderney (UK), Pentland Firth (UK), Paimpol-Brèhat (France), Bay of Fundy (Canada) (OpenHydro, 2008, 2008a, 2009)	**6**
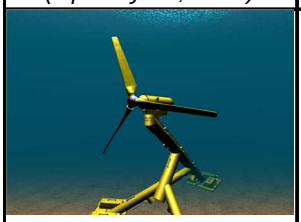 Hammerfest Strøm *(Hammerfest Strøm, 2010)*	Three bladed, fixed pitch, single rotor horizontal axis turbine. Gravity based, seabed mounted. Scaled 300 kW turbine tested, full scale testing for 1 MW underway.*(Hammerfest Strøm, 2010a)*	Scale testing at Kvalsund, Norway between 2003 to 2009. Full scale and array development underway and scheduled for testing at EMEC in 2011.*(Hammerfest Strøm, 2010a)*	Sound of Islay (UK) *(Hammerfest Strøm, 2010b)*	**6**
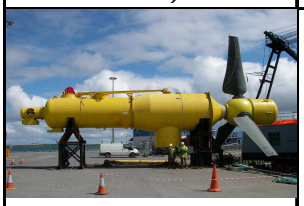 Tidal Generation Limited *(TGL,2010)*	Three bladed, upstream pitch controlled rotor. 500 kW installed capacity. Mounted on a light weight steel structure. 500 kW turbine successfully deployed and connected at EMEC in 2010. *(TGL, 2010)*	500 kW scale testing at EMEC since September 2010. 1 MW turbine currently being developed for testing in 2011/12. *(TGL, 2010)*	10 MW TGL contribution to the Inner Sound Pentland Firth, Maygen Project (UK) *(TGL,2010a)*	**5**
 Atlantis Resource Corporation (AR series) *(ARC, 2011)*	Twin rotor, fixed pitch, horizontal axis turbine. Full scale testing with 18 meter diameter and 1 MW installed capacity underway at EMEC blades were damaged during installation. Since re-installed. *(ARC, 2010, 2011a)*	AK series 1 MW testing underway at EMEC, however delays have been experienced due to technical problems and test is not grid connected. *(ARC, 2011a)*	Pentland Firth (UK), San Remo (Australia), Gulf of Kutch (India). *(ARC, 2011b)*	**5**

Table 2.4 Technology readiness levels of the devices at the forefront of full scale testing.

Each technology has evolved differently, which makes it difficult to compare them. For example IT Power's first device was tested in Loch Linnhe in 1994/5, well before any other technologies started testing. But the company then branched off and the technology moved to MCT (MCT, 1994). MCT has had more experience in developing their device and it is no surprise that MCT is therefore one of the leading device developers in UK. MCT's SeaGen is the third variation of the devices to be tested, now at full scale, grid connected (in UK) and ready for commercial deployment. The device is a twin rotor 16 metre diameter, axial-flow turbine rated to a 1.2 MW installed capacity, at a rated velocity of 2.4 m/s. The rotor blades can be pitched through 180°. The two rotor units are mounted on a horizontal beam on either side of the monopole. One of the most novel maintenance features of the device enables the horizontal beam to be raised above the sea level for inspection and maintenance. MCT are planning to deploy tidal arrays in Anglesey, off Wales and in Kyle Rhea in Scotland. However, MCT has suffered failures in its early days, a right of passage now being experienced by competing alternatives. While SeaGen was being commissioned in Strangford, two turbine blades were damaged, this is thought primarily to be due to control system fault and operator error (MCT, 2008a, 2008b).

OpenHydro is another leading tidal current turbine developer. The turbine has an open centre with a (relatively) slow-moving rotor. The blades are connected at the tip by an outer ring, so pitching is not possible. There is a duct on the outside to help align and potentially accelerate current flow (OpenHydro, 2010). OpenHydro was the first device to be tested at the EMEC site. An alternative OpenHydro offers in comparison with MCT is that the device is completely submerged underwater and therefore has no visual impact. OpenHydro have not publically disclosed device performance characteristics, however the device has had some technical problems. The recently recovered 1 MW full scale device in the Bay of Fundy, Canada (no grid connection) found all the turbine blades missing. The main cause for the lost blades has yet to be diagnosed (OpenHydro, 2010a).

Hammerfest Strøm is another device developer which has been testing their device since 2003 in Norway. The 300 kW device installed in Kvalsund was grid connected in 2004 becoming the world's first grid connected device. The turbine has been tested through a full cycle of operation, retrieval and maintenance. The test device has had two successful installations including re-deployment and a production track record of more than 16000 hours. The technology has been developed at a larger scale and a 1 MW device was expected to be installed at EMEC in summer 2011 (Hammerfest Strøm, 2010a). However, as of November 2011 installation had not taken place. A gravity or pinned foundation is used, the blades are variable speed and variable pitch up to 280°. The 1 MW device cut-in velocity is approximately 1 m/s with rated power at 2.25 m/s. The device can safely be deployed in depths of 40 to 100 meters. An array project development is due to be installed by Scottish Power Renewables in the Sound of Islay by 2013 (Hammerfest Strøm, 2010b).

Tidal Generation Limited (TGL, a subsidiary of Rolls Royce) is another developer that has been testing at the EMEC site since 2010. The turbine is an axial flow, variable pitch and speed, three bladed rotor. The turbine is buoyant so it can be towed to the site and attached to the foundation that is pinned to the seabed using a patented drilling technique. The nacelle is secured to the foundation through a mechanical clamp. The 1 MW device has a cut-in velocity of 1 m/s and rated power at 2.7 m/s with the device capable of operating at a maximum velocity of 3.4 m/s. The device rotor diameter is 18 meters and the rotor height above the sea bed is 19 meters. (TGL, 2010)

Atlantis Resource Corporation, originally from Australia has developed a series of devices based on different design strategies. The 'AN' series is a shallow water turbine that uses 'aquafoils' to capture kinetic energy from the tidal current. Tow testing of the AN-400 was carried out in 2008. The 'AS' series is a ducted horizontal axis turbine featuring a unique blade design. The turbines are rated for 2.6 m/s and are being developed in 100 kW, 500kW and 1 MW capacities. Although the devices have been developed for different markets, it appears that they are still in the learning stages. The AR-1000 (previously known

as AK-1000 which used a twin-rotor technology) turbine is a horizontal axis turbine featuring a rotor with fixed pitch blades, which is converging towards full scale commercialisation. The turbine is rated at 2.6 m/s and is designed for cost efficient nacelle retrieval. The AK series turbine which is installed and ready for testing at EMEC feature a twin rotor set with fixed pitch blades. Unfortunately the blades were damaged during installation, however the design has been modified into the AR-1000, such that it now has just one rotor and testing has commenced as of August, 2011. (ARC, 2010, 2011, 2011a).

2.5.3 State of the Industry

Over the last few years, a lot has changed. Full scale prototype devices were first tested in 2008 (MCT) and since then many other developers have reached a pre-commercial phase where the device performance and testing has won backing from major utilities (e.g. E.ON, Scottish Power, Scottish and Southern etc.) and investment from international companies (e.g. Alstom, Rolls Royce, Siemens etc.). The literature presented in this section identifies the 'state-of-play' in terms of where the current understanding is as seen by the UK Government.

The Renewable Energy Strategy (RES, 2009) has made more funding available to EMEC which is being used to construct further berths to accommodate the expected increase in the number of devices being tested with grid connection. (Renewable UK, 2010a)

The seabed surrounding the UK is owned by the Crown Estate, and the 2009/10 wave and tidal leasing round has been a major step forward in moving the industry towards commercialisation. The Crown Estate has developed a Maritime Spatial Planning tool, Marine Resource System (MaRS) for improved decision making between the different activities and managing their impact on the marine environment.

Sites in the Pentland Firth have been identified as likely to host the first generation of tidal current energy development. The first round of leasing by the Crown Estate has leased sites capable of accommodating 1.2 GW installed capacity of wave and tidal energy in

this region with an additional 400 MW of tidal development to take place in the Inner Sound region.

The Sound of Islay Tidal Energy Project has been fully consented by the Scottish Government. This is the first tidal array project in the world to be given consent and ScottishPower Renewables plan to build a 10 MW tidal farm ready for operation in 2013. (Islay Energy Trust, 2011)

2.6 Existing Studies

A large scale development of this sort needs a full scale understanding of the resource. A number of studies have tried to quantify the UK tidal current resource with estimates covering a range of values from 18TWh/yr (B&V phase II, 2005) to 96.4 TWh/yr (MacKay, 2008). The spread in the estimates is due to the differences in the technologies used to evaluate the resource as well as the differences in the interpretation of resource information between different studies. Sections 2.6.1 and 2.6.2 discuss some of the most recent national and project scale studies and the resource assessment methodologies employed by them.

2.6.1 National Scale Tidal Resource Assessment

In 2001, the Scottish Executive commissioned a study by Garrad Hassan & Partners to quantify the renewable resources available in Scotland (Garrad Hassan, 2001). The main task of the study was to estimate the resource size and development cost for the year 2010 and 2025 and to generate cost curves for different technologies in different network areas. The base case result for tidal current energy estimate for Scotland alone was 33.5 TWh/year with an installed capacity of 7.5 GW modelled at under 5-6 p/kWh in 2010 at an 8% discount rate. At the time this work was carried out, there was very little prior knowledge or understanding of tidal current resource and interaction with the devices. Ten years later, the input data used to carry out this analysis has been revised and updated. However, this is one of the first

studies that strived to quantify the renewable resource in the modern context. Since this study, many others have made an attempt to quantify the actual resource.

The Atlas of UK Marine Renewable Energy Resource (DTI, 2004a) was commissioned in 2003 by the then Department of Trade and Industry, DTI. The project was lead by ABPmer with the aim of producing a spatially representative map of the UK wave, tidal and offshore wind resources. The Atlas presents spatially averaged snapshots of mean spring and neap tides. The source for tidal data was obtained from the Proudman Oceanographic Laboratory (POL) Continental Shelf Model (POL CSM CS3), the High Resolution Continental Shelf model, (HRCS CS20) and the North-East Atlantic (NEA) model (POL, 2011). The resolution of each of the models are shown in Table 2.5.

	Latitude	Longitude	km	2D	3D
NEA	1/3°	1/2°	35	✓	-
CSM (CS3 & CS3-3D)	1/9°	1/6°	12	✓	✓
HRCS (CS20)	1/60°	1/40°	1.8	-	✓

Table 2.5 Resolution of each of the models used within the Marine Atlas

The main parameters included in the Atlas are tidal range, tidal flow and annual tidal power estimates. The tidal flows have been derived using the O_1, K_1, M_2 and S_2 harmonic constituents. CS3 is a depth averaged model where as the HRCS model uses 34 layers throughout the water column. The extractable power is a direct function of the cube of the tidal current velocity experienced at the site without considering the impact that development might have on the underlying tidal hydrodynamics.

The Marine Atlas shows the tidal resource as a map but also has been developed into a GIS based system which allows different layers to be interrogated by various users for their own purposes. The GIS layers can be manipulated with new constraints included within the map. For example, velocity data can be used to select specific locations that experience high tidal current velocity. In addition, water depth can be used as a constraint to specify which regions can be considered for development. However, the Atlas does not provide time-series,

it only provides long-term averages of parameters (such as mean spring peak, mean neap peak, average power/m^2) of use in the tidal energy context generated from the underlying model. Therefore, although the Atlas provides a wide spatial coverage, it lacks temporal variability. In 2007 the Marine Atlas was updated for the Department for Business, Enterprise and Regulatory Reform, (BERR, 2008). The updated Atlas has a higher vertical resolution and the vertical profiles are influenced in the model through the bottom friction transmitted through the water column by turbulent mixing. No additional tidal constituents were included as the purpose of the Atlas was to capture the average output (BERR, 2008). A map of the peak flow for mean spring tides is shown in Figure 2.8. The Atlas has a spatial resolution of 1.8 km^2.

In 2004, the Carbon Trust created an initiative known as the Marine Energy Challenge (MEC) (CT, 2004). The main aim of this project was to assess the potential to generate electricity from marine energy at a cost competitive manner compared to other renewable and conventional generation.

In an effort to achieve this aim Black & Veatch (B&V) was commissioned by the Carbon Trust to conduct a study to estimate the national tidal current resource available in the UK (B&V Phase I, 2004/B&V Phase II, 2005). In doing so they took account of newly identified environmental and theoretical constraints on power extraction in the scenario they developed. The result was the use of a 'Significant Impact Factor' (SIF) to determine the amount of energy that can be extracted from a site. The 'SIF-method' accounted for the energy that is extracted from the sites and indicates the fraction of energy that can be extracted beyond which further extraction can lead to environmental and economic impacts and affect the overall generation from the site. The key improvement offered by the SIF-method was that it progressed from the 'farm' approach to a 'flux' approach, thereby attempting to consider the impact that energy harvesting has on the underlying tidal hydrodynamics.

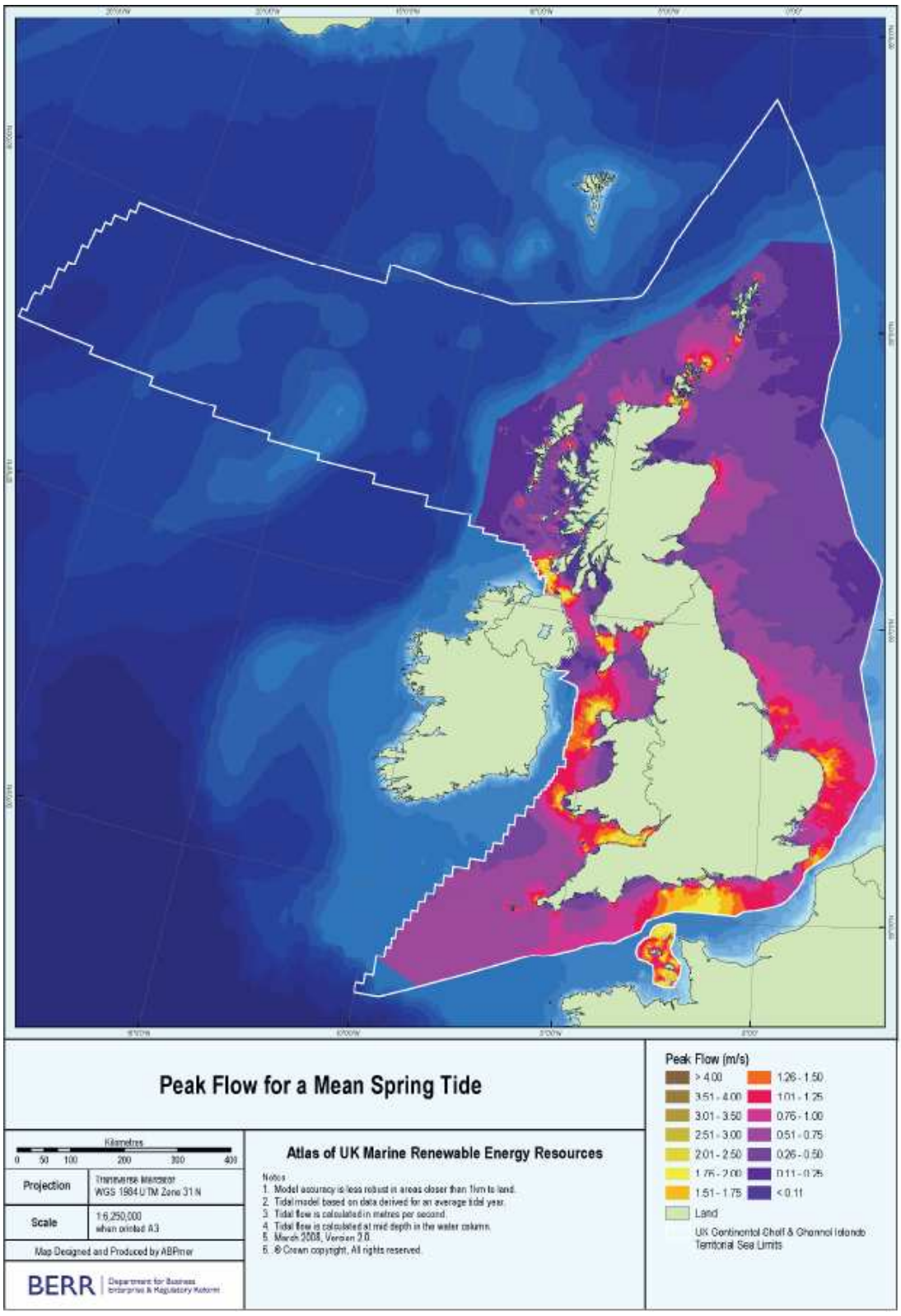

Figure 2.8 Peak Flow for mean Spring Tide (BERR, 2008).

The study was done in the early phase of tidal farm development and therefore had little understanding of the impact that different sites might experience. As a result the study assumed a SIF factor of 20%. According to this study (B&V Phase I, 2004), the total resource available in the UK was estimated to be 110 TWh/yr with a Technically Extractable Resource of 22 TWh/yr. Input data for this analysis was obtained from the Marine Energy Atlas (DTI, 2004a) and Admiralty Chart data. One of the key findings of this study suggested that the majority of the resource lies in the Pentland Firth. The report also identified the ten most energetic sites in the UK that contained 80% of the total UK resource, see Table 2.6.

Ranking	Site Name	Contribution	
		Individual (%)	Cumulative. (%)
1	Pentland Skerries	17.9%	17.9%
2	Stroma, P. Firth	12.7%	30.6%
3	Duncansby Head, P. Firth	9.3%	39.9%
4	Casquets, Channel Islands	7.6%	47.5%
5	S. Ronaldsay, P. Firth	7.0%	54.4%
6	Hoy, P. Firth	6.3%	60.8%
7	Race of Alderney, Ch. Is.	6.3%	67.0%
8	S. Ronaldsay, P.Skerries	5.3%	72.3%
9	Rathlin Island	4.0%	76.2%
10	Mull of Galloway	3.7%	79.9%

Table 2.6 Top 10 sites identified in Phase I with 80% of the total resource. (B&V, 2004).

The 2005 Black & Veatch Phase II study (2005) concentrated on refining the findings of the Phase I study. Specific aspects of the sites identified in the Phase I report were looked at. The Technically Extractable Resource was reduced due to double counting of flux across different sites and the SIF factor was 'fine-tuned' to be site specific. The SIF factors were updated for the top ten sites and reduced by 35% compared to the Phase I output estimate. The report concluded that 63% of the Extractable Resource is found in deep water of sites > 40 metres and about 20% is in 30-40 metres of water depth. The site needs to

experience spring velocity between 2.5 m/s to 4.5 m/s to be considered for economic development. Finally, the total extractable resource was reduced to 18 TWh/yr with a ±30% uncertainty. This was interpreted as being sufficient to meet 5% of existing UK electricity demand.

A further update to this study by B&V (2011) identifies different tidal hydrodynamics mechanisms that create high tidal current appropriate for tidal current energy generation. This study considers the physical environmental impacts of extracting energy from the system and presents a new way of assessing a 'theoretical' and 'technical' limit of power extraction based on acceptable environmental effects. These are particular to the physical environment and do not consider the benthic or marine environment.

In 2003, the Scottish Executive commissioned a study on Matching Renewable electricity generation and Demand in Scotland (Boehme, 2006a). The research was conducted by the Institute for Energy Systems at the University of Edinburgh. The purpose of the study was to determine if Scotland could meet 40% of its electricity demand from renewable resources by 2020. Contribution from on and offshore wind, wave and tidal energy generation were considered.

For tidal current resource assessment, data was primarily obtained from Admirality Chart tidal diamonds, and the TotalTide software package (a digitised version of the Admirality Charts). Data from the DTI Marine Atlas (DTI, 2004a) was also used. Different installed capacity scenarios for wind, wave and tide were considered. In the case of tidal, a 750 MW installed scenario (2.2 TWh/yr) was examined. The outcome of the overall study illustrated that on average 40% of Scottish electricity demand could be met by around 6 GW of installed renewable capacity. However, the study highlighted that the intended demand target is not met on a second-by-second basis in this scenario.

In his book, Mackay (2008a, 2008b) did a 'back of the envelope' calculation to evaluate the total potential tidal current energy in the UK waters. Mackay's methodologies differ substantially from the B&V 'flux method' discussed earlier. The analysis has very

controversial outcomes, the author bases his analysis on the maximum resource that can be extracted without considering economic, social or environmental impacts and suggested a rather large total of 96.4 TWh/yr can be extracted. Moreover, in his discussions Mackay assumes that extracting power will not affect the total resource or have an impact on the tidal hydrodynamics. Overall, the author tries to present a scenario where the total energy that can be extracted from all renewable sources is presented to evaluate if the UK can live on renewables alone.

Salter (2005) estimates the energy available in the Pentland Firth alone to be in the order of 876 TWh/yr. His calculations estimate the shear friction coefficient at 0.02 and suggest the fluid friction loss at the sea bed to be 100 GW. Furthermore, he proposes large vertical axis turbines (Salter, 2009) where 1200 close packed devices are laid out in lines with narrow gaps for navigational purposes, see Figure 2.9.

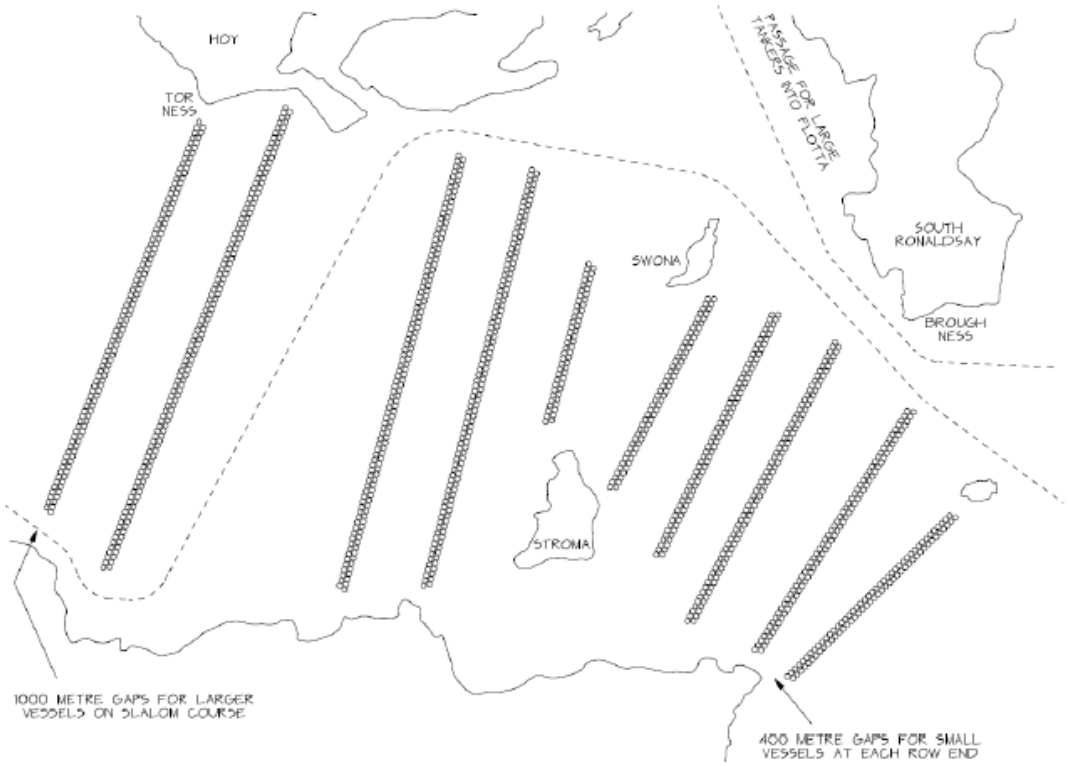

Figure 2.9 Possible layout of turbines as suggested by Salter (2009).

Salter also indicates that the installation will change the head difference at the entrance to the channel, which is thought to divert water around the north of the islands and improve the economics of the tidal farms situated further north. Mackay and Salter do not differentiate between theoretically ‘available’ energy and ‘extractable’ energy, nor do they acknowledge that there will be a reduction in the tidal current velocity and the underlying hydrodynamic effects as a result of extracting power.

The studies presented so far have mostly attempted to evaluate the national resource assessment. These studies evaluate the total extractable power in the UK continental shelf so present a wide spatial coverage but the data used in the analysis are average values of the Spring-Neap cycle and do not attempt to evaluate the temporal variability. In terms of project development, it is important to do a regional, site specific study to understand the local characteristics. The benefit of doing a site specific analysis is that the added local detail can be used to engineer the device and tune it to operate efficiently based on the local, site specific characteristics. Furthermore it becomes necessary to understand the impact local topography and bathymetry may have on the local flow structure and therefore to appropriately plan site and array layout including device orientation. The importance and use of project scale studies are presented in the following section.

2.6.2 Project Scale Tidal Resource Assessment

The data describing the majority of existing project-scale studies are commercially sensitive and are therefore not in the public domain. What is available is a set of standards, protocols and a small subset of research work that provides guidelines as to how such assessment could be conducted, best practice measurement techniques, analysis and reporting of tidal current energy device performance and operation.

In 2005, following the success of the prototype Marine Current Turbine (MCT) ‘Seaflow’, commissioned by DTI, “Development, Installation and Testing of Large Scale Tidal Current Turbine” (DTI, 2005) was written as the associated document reporting the

details. It also lists all the contender devices that were being tested at a smaller scale and moving towards achieving a full scale device. MCT's Seaflow at that time was one of the forerunners. The document outlines the different site selection and criteria needed for a successful tidal current energy project. Environmental Impact Assessment (EIA) is also discussed. Since 2008, the next generation of Seaflow, SeaGen has been successfully installed and tested in Strangford Narrows, Northern Ireland (MCT, 2008).

In 2007, the DTI commissioned a protocol to define procedures for assessing the tidal resource or comparing the performance of a device (DTI, 2007). The document outlines fit-for-purpose protocols that can be used in the initial stages of device performance characterisation. At the time of writing the document, no commercial scale deployment had taken place, therefore the document suggested guidelines on how it could be done using the existing understanding from theory and knowledge transfer from onshore wind approaches.

The Sustainable Development Commission (SDC) was the UK Government's independent advisor and watchdog until its demise in 2010 due to austerity measures. In 2006, the SDC invited various organisations and academics to produce a number of reports on tidal energy. Research Report 1 (SDC, 2007a) was a resource assessment exercise. All the existing studies were considered to obtain the best information about the tidal resource (including tidal barrage) in the UK. Grid connection constraints were assessed for each of the regions identified with tidal energy potential. The effect of tidal current extraction on coastal regions and sea level changes were also considered. Research Report 2 (SDC, 2007b) was an overview of various tidal technologies and investigated the economics of such development. Research Report 3 (SDC, 2007c) looked at various Severn Barrage proposals and Report 4 (SDC, 2007d) investigates non-Severn Barrage options and their environmental impacts, effect on sea level and impact on other marine industries. Report 4 specifically looked at social acceptance and compatibility with the grid. Research Report 5 (SDC, 2007e) is a UK case study that reviews a number of scenarios for tidal power development and presents case studies of developing tidal power in UK. The final report "Turning the Tide" (SDC, 2007f)

presented the possibility of tidal power around the UK with specific importance attached to the Severn Estuary. The focus throughout the SDC initiative however was tidal range resource and technology.

The Electric Power Research Institute Inc. (EPRI) is a US non-profit organisation that has carried out a range of assessments to provide methodologies to enable resource assessment of various sites experiencing high tidal current velocity and estimation of power production from various tidal devices. Their first document, (EPRI, 2006) produced in 2006 provides consistent methodologies to enable comparison between different sites and establish a 'baseline' performance for devices which can be used by the industry as it evolves. Subsequent work by the EPRI investigated the economic impact of tidal current generation on a large scale. A large part of the EPRI publications include site specific analysis of regions that are known to experience high tidal velocity. The assessment was carried out to determine if sites are suitable for tidal current energy extraction and if so, should they be considered for economic development.

The European Marine Energy Centre (EMEC) in Orkney offers developers the opportunity to test full scale devices with a grid connection to help assess the device performance. The tidal current test site at the Falls of Warness initially provided five berths (now expanded to seven) in depths ranging from 12 to 50 metres. The test sites are very energetic experiencing as much as 4 m/s velocity during the spring cycle (Norris *et al.*, 2007). EMEC is also involved in developing standards in an attempt to help develop the marine industry. A number of documents have been published covering a range of topics from resource assessment of tidal current energy to performance assessment of tidal conversion systems. Guidelines have also been provided to address health & safety, design considerations, grid connection and project development.

EMEC's 'Assessment of Tidal Energy Resource' (EMEC, 2009a) is a guide for conducting on-site measurements, analysing the findings and characterising the overall resource. Similarly 'The Assessment of Performance of Tidal Energy Conversion Systems'

(EMEC,2009b) and ‘Guideline for Project Development in the Marine Energy Industry’ (EMEC, 2009c) established a set of methodologies to measure the performance of tidal energy conversion systems (TECS) and outline project development methodologies key in the marine energy sector.

In 2007, the International Electrotechnical Commissions (IEC) established a Technical Committee (TC 114) to prepare standards for marine energy converters (Nadeau, 2010). The development of these standards is important as they provide a basis for ensuring reliability and safety and can be used as a set of benchmarks for comparisons between different resources and technologies locally and internationally as well as contribute to project ‘bankability’. The key areas addressed by the standard will include performance measurement, resource assessment, device design, survivability and electricity generated from wave and tidal energy converters. The IEC standard expects to generate guidelines and technical specifications that can cater to the world market.

Equimar is a European Union funded project that has developed a systematic suite of deliverables of assessment protocols for comparing marine energy devices. In 2010, it delivered a set of protocols that addressed various stages of project development, from tank testing to sea trials. The protocols highlight the need for consistency within the marine industry. The development of the protocols can be used as a template by device developers in various stages of project development. The project has also helped to identify existing knowledge gaps in the industry and involved a large number of stake-holders (EquiMar, 2011).

2.6.3 Tidal Resource and Power Generation Scenarios

The Carbon Trust published a further study (Sinden, 2005) that extracted power output time-series for tidal current from the POL CS20 tidal model alongside wave energy time series in order to explore their joint variability and potential match with demand. The analysis developed a scenario where all the available tidal energy identified in B&V Phase II (2005)

is developed, after accounting for SIF restrictions. The analysis does not differentiate between shallow and deeper sites where a different generation of technology will need to be deployed. First generation devices are considered to be the driver for tidal current energy development until at least 2025. Installation and operation in deeper water requires more radical 'second' and 'third' generation approaches that are as yet only in the very early stages of research and development. Therefore an analysis based on only first generation device specifications is required. The application of the SIF has since been superseded, therefore a revision of the 'Extractable Power' considered by Sinden (2005) and B&V Phase II (2005) is also necessary.

An interesting aspect that is yet to be fully understood is whether the aggregate output from different tidal sites can represent a form of 'firm' generation through combining various sites benefiting from diversified phasing of the incoming tidal waves. Clarke *et al.* (2006) demonstrates the potential for base load provision using tidal current by analysing three UK locations. The study does not demonstrate how the sites are selected. Therefore, no economic evaluation for the site selection is presented. A Nautical Almanac (2002) was used as input data. This data is primarily used by yachtsmen for navigation purposes and it has not previously or since been used for tidal current evaluation purposes. The analysis indicated that curtailing the maximum power output in the Spring cycle could be used to reduce variability over the Spring-Neap cycle, which is unlikely to be economical.

Similarly, Hardisty (2008) proposed that a careful selection of sites can generate a steady output. Back-testing this analysis has shown significant discrepancies. For instance, Hardisty purports to use data relating to tidal diamond SN040A (in Clyde, Scotland) and suggests that it has a spring peak velocity of 2.1 m/s. Interrogating the same tidal diamond using UK Hydrographic (UKHO) TotalTide software indicates that SN040A only reaches a spring peak of 0.57 m/s, a value inappropriate for tidal current energy development. Other discrepancies with reported tidal diamond data were also found while attempting to recreate

this analysis. The analysis concluded that a constant level of 45 MW can be generated from an installed capacity of 200 MW, a rather uneconomical scenario.

It is clear that much remains to be done with regard to the potential of tidal current energy meeting baseload ‘firm’ generation, Therefore one of the key aims of this work is to investigate the impact of tidal phasing on the tidal current energy resource potential around the UK and its match with historical electricity demand patterns.

2.7 New methodology

A lot can be learned from the studies done to-date. However, some of the methodologies and understand of the tidal hydrodynamics are outdated and could benefit from updating. A particular limitation of the majority of the resource assessment exercises is that they are done using long term average values and omit to assess the temporal variability. Therefore, a significant improvement would be the use of time-series datasets of tidal variability for specific locations of interest to evaluate specific local variability.

Traditionally, anchored buoys were used with current meters mounted on them to measure the tidal current velocity at specific locations. Ideally, tidal current velocities are measured using an ADCP where the velocity through the entire water column can be measured. The temporal resolution of the data varies depending upon the purpose of the data collection. ADCP measurements can be stationary, located in one place, (typically bottom mounted), or vessel mounted to provide spatial coverage of the area of interest.

Another way of understanding tidal flow is with the use of numerical or experimental tidal flow models. Scaled testing is often conducted in laboratories, these are physical models and often used for different purposes. Numerical models are often complex computer programs and have the added advantage of being used for a specific domain rather than a specific point and can be modelled for any duration of time, computational performance permitting. However, these numerical models need to be validated and verified with measured data to have a level of confidence in the model output. There are a number of

modelling options, a list of commercial and research modelling tools are provided in Table 2.7.

Models	Dimensions	Grid structure
ADCIRC	2D/3D	Unstructured
ADH	1D/2D/3D	Structured
CH2D/CH3D	2D/3D	Structured (curvilinear)
DELFT	2D/3D	Structured (curvilinear, rectilinear and spherical)
DIVAST	2D	Structured
ELCIRC	3D	Unstructured, flexible
ELCOM	3D	Structured (orthogonal)
GEMSS	1D/2D/3D	
GETM	3D	Structured (orthogonal curvilinear)
HRCS	2D/3D	
Mars	2D/3D	Structured
Mike Models (11, 21, 3)	1D/2D/3D	Structured
RICOM	2D/3D	Unstructured
RMA Models (2, 10, 11)	2D/3D	Unstructured
ROMS	2D/3D	Curvilinear structured
SELFE	3D	Unstructured
SUNTANS	2D/3D	Unstructured
TELEMAC	2D/3D	Structured
TFD	1D/2D/3D	Structured
TRIM	2D/3D	Structured
UnTRIM	2D/3D	Unstructured

Table 2.7 Commercial models used for tidal resource assessment (EMEC, 2009a).

The scope for the research in this document encompasses the entire UK continental shelf. Model data for this domain was not available and modelling such a region would require vast computational resource and man hours outwith the scope of this thesis. Therefore, it was decided that numerical models such as those presented in Table 2.7 would not be used in this study. Analysis presented by Cooper *et al.* (2006) suggests that *only 0.15% of the UK continental shelf has a peak flow of 3 m/s or greater and can be considered for economic development* of tidal current energy. Hence, to model the entire continental shelf is rather inefficient and redundant.

Instead the focus and approach adopted in this study was to use regional data in the form of tidal diamonds, and site specific measurements from buoy and ADCP data. An analytical approach is used to collate and combine existing datasets (mostly available in the

public domain) of different spatial and temporal resolutions. Data was obtained from Admirality Chart tidal diamonds using the TotalTide software package (a digitised version of the Admirality Charts) which provided temporal variations (see Figure 2.10) and from the DTI Marine Atlas (DTI, 2004a) which covers the entire continental shelf (see Figure 2.8) to provide vast spatial coverage. Combining these datasets itself will provide considerable improvement over the existing data availability.

SN028O
58°43.57'N 3°14.18'W Scotland

Time	Direction	Spring Rate	Neap Rate
-06h	355°	0.77 m/s	0.41 m/s
-05h	076°	0.87 m/s	0.46 m/s
-04h	097°	2.20 m/s	1.10 m/s
-03h	080°	2.30 m/s	1.10 m/s
-02h	089°	2.30 m/s	1.20 m/s
-01h	099°	1.30 m/s	0.67 m/s
HW	119°	0.46 m/s	0.26 m/s
+01h	258°	0.98 m/s	0.51 m/s
+02h	264°	2.00 m/s	1.00 m/s
+03h	264°	2.60 m/s	1.30 m/s
+04h	261°	2.80 m/s	1.40 m/s
+05h	311°	1.00 m/s	0.51 m/s
+06h	343°	0.98 m/s	0.51 m/s

Printed by Admiralty TotalTide

Figure 2.10 Example of a tidal diamond at Pentland Firth, Scotland.

High quality in-situ measured data is pivotal for assessing and quantifying the tidal energy resource. In terms of project development, site screening is one of the first key stages. Site characterisation is necessary in order to ensure certain conditions. In particular, the strength of the resource necessary for effective and economic utilisation needs to be understood, before further development and investment. The need for detailed analysis arises because the potential to generate power is proportional to the velocity cubed and first generation energy capture technologies are restricted to deployment in restrictive bathymetric conditions. Therefore, a site that experiences consistently high tidal current of high velocities will be much more economically advantageous than less energetic sites.

The predicament with highly energetic locations is that they are also often bodies of water that have not normally been considered of research interest, other than in identifying them to assist in safe navigation. Obtaining such data is expensive and difficult to collect over a large area, so little research or in-situ measurement data exists for such extreme locations. This lack of an existing historic database in highly energetic locations of interest for tidal current energy development and associated research has to some extent limited academic endeavour in support of industry development to date.

2.7.1 Approach

The first part of the research reported was predominantly focussed on developing methodologies to combine publically available datasets that did not coincide spatially or temporally. The analysis presented in chapter 3 identifies the existing publically available datasets and assesses how well the different datasets truly represent a specific site. This new method of combining datasets is a significant improvement over the use of each of the individual datasets and can be reproduced for other areas of interest.

Methodologies developed in chapters 4 and 5 use ADCP data to do further detailed site specific evaluation, as deemed necessary in the tidal energy context and vital to any project developer. Harmonic analysis is also used to extract the tidal constituents so as to enable long term AEP and the power output over the intended project lifetime. The methodologies are developed over different sites, to test the methodologies robustness and to understand how different topological and bathymetric features can impact the final findings.

Anglesey is the first case study region in the Irish Sea off the north Wales coast. The tidal flow accelerates around the headland presenting very interesting site specific flow characteristics. The potential suitability of this location for tidal energy development is the reason for selecting this site for analysis. The water depth is about 40 metres and potentially offers a highly energetic tidal current site, close to shore. These are conditions which suit first generation devices. Good landfall (beach, not cliffs) for bringing cables ashore,

appropriate local harbour facilities for installation, operation and management activities are also important project development constraints potentially addressed at this location. Additionally MCT and RWE Npower Renewables have collaborated and plans are in place to build a 10 MW tidal farm at this particular site (MCT, 2010a).

The Sound of Islay is the second case study site of interest presented in chapter 4. The case study region is a narrow channel between the islands of Islay and Jura where acceleration is caused by large volume of water being forced through a narrow channel (also known as hydraulic current). The chapter evaluates site specific metrics relevant in the tidal current energy context to determine the site suitability. As mentioned earlier, the Sound of Islay is the world's first full scale consented tidal array project. Therefore analysis specific to velocity, power, directionality were of interest. The development of these metrics also aided in bridging some of the knowledge gaps not covered by existing standards and protocols.

The Fall of Warness, tidal test site at EMEC is the final study area. The site is located in Orcadian waters and is of particular interest as multiple ADCP datasets were available at different sampling frequencies. This data enables analysis that can identify the effect of varying the ensemble period on harmonic analysis and then evaluate the effect on metrics like velocity and AEP.

The methodologies for combining datasets and time-series generated in chapters 3, 4 and 5 are used in chapter 6 to develop a national scale resource assessment. Site selection criteria particular to first generation technologies is presented as part of scenario development. The main aim of developing this national scenario is to evaluate, on a spatial and temporal level, how in or out-of-phase the different sites are and if there is any potential to generate base-load using tidal current generation alone. For sites where ADCP or buoy data is not available, the methodology introduced in chapter 3 is employed to combine nearby tidal diamond and Marine Atlas to generate times-series. A new and novel way of exploiting the resource is introduced so as to strike the right balance between environmental and economic considerations.

Chapter 7 is an application of the time-series generated in chapter 6 with the aim of developing methodologies to quantify the tidal variability on a national scale. The study does direct comparison between demand for electricity and hypothetical tidal power output to evaluate how much of demand can be matched by tidal current generation alone. Particular focus is to understand the timeliness and coincidence of peak demand with peak tidal generation.

3. Methodologies for Project Scale Assessment

The work presented in this chapter aims to develop a robust and repeatable method for generating resource time-series that reliably describe the available resource. The most recent analysis, Boehme (2006a) used TotalTide tidal diamonds as input. Before further analysis can be carried out, it is worth examining whether tidal diamonds at a specific site are a good representation of the resource. To do this they were compared to in-situ measurements from a current meter made available using buoy data from the UK moored current meter dataset from the British Oceanographic Data Centre (BODC).

Datasets were obtained for a specific geographic location where tidal current velocity is considered to offer potential for economic exploitation. Harmonic analysis enabled comparison of the datasets over a common time frame by time-shifting the data using the original data to generate harmonic constituent data which provided input to a harmonic prediction analysis. Interpolation techniques were used to combine point source data scattered around the site of interest to examine the spatial variability of the resource and test the interpolation techniques. Principal findings conclude that although the directionality of the dataset is well represented by the interpolation technique, velocity magnitudes, peak values and velocity exceedance histograms are not captured.

3.1 Approach

This chapter provides a preliminary analysis and comparison of time-series measurements from a case study region *Anglesey* in the Irish Sea near the Island of Anglesey off the north Wales coast. Figure 3.1 generated using the Marine Atlas data as layers in GIS highlighting Anglesey, the study area. The map is produced at a spatial resolution of 1.8 km^2.

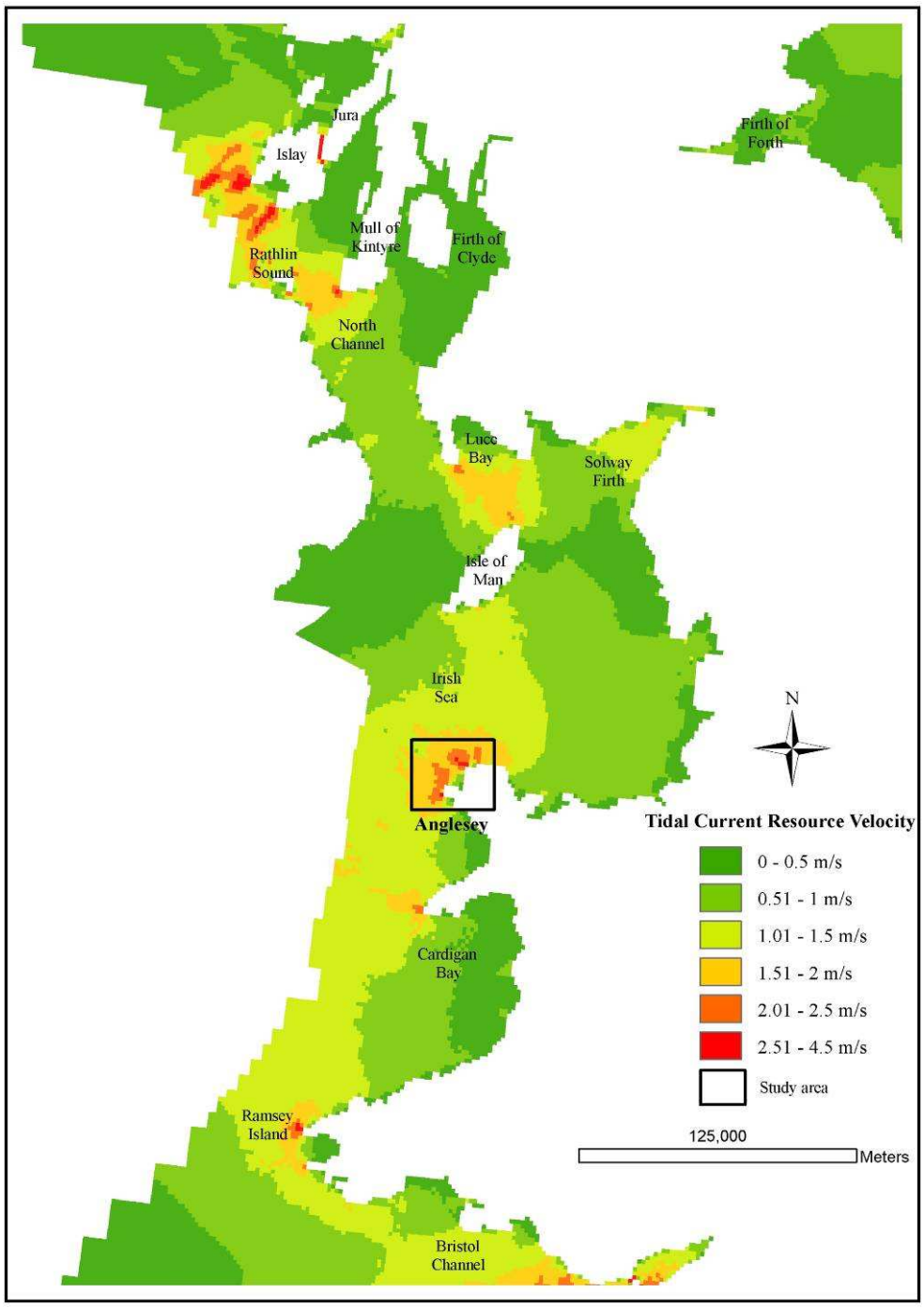

Figure 3.1 Figure showing mean spring peak current at the Anglesey study area. BERR © Crown Copyright. All rights reserved 2008.

3.1.1 Datasets

Different public domain datasets were used to assess the resource. These include the current meter dataset from the BODC, a national facility that archives marine data. One dataset,

available for academic purposes, provides time series measurements of ocean currents from temporarily moored instruments deployed in the shelf seas around the British Isles.

The first data sources are the tidal diamonds obtained from Admirality chart data and tidal stream atlases. Tidal diamond data is obtained by collecting hourly data using a current meter from an anchored boat at the specific location. Data is usually collected over a 13 hour period, approximately 5 metres below the water surface. These provide a series of descriptions of tidal current flows in terms of velocity magnitude and direction at hourly time intervals with respect to high water at a reference location. The data spans the period from 6 hours before high water through to 6 hours after high water for typical spring and neap tide conditions. This only captures the very basics of the tidal constituent picture equivalent to M2 and S2 (Bell *et al.,* 1998). The locations of these data are referred to as 'tidal diamonds', as their respective positions are indicated on Admiralty charts by diamond symbols. The Admirality chart tidal diamond data has been digitised and can be easily accessed using the 'TotalTide' software interface also provided by the UKHO.

The Marine Atlas (BERR) provides useful spatial information for offshore marine renewable technologies. The information provided in the atlas is managed and maintained in a structured Geographic Information System (GIS) database. The tidal current data presented in the Marine Atlas presents spatially averaged snapshots of mean spring and neap tides, water depth, tidal range and average power.

This case study site is considered as it is the only location where a number of datasets including measured buoy data spanning 29 days or more was identified within the existing BODC archive that coincides with a location of interest for tidal current energy development as identified in the existing literature (MCT, 2010a). This made it possible to carry out a detailed harmonic analysis to recreate the dataset. All comparisons were made for the period of August 2009, with the harmonic constituents derived from the original data records used to create a pseudo time-series at 10-minute intervals for this period for each buoy location. Tidal current data were also obtained for the relevant Admiralty tidal diamond

locations for the same time period using TotalTide. It should be noted that the location of the buoy data does not exactly coincide with the cells identified in the Marine Atlas or the tidal diamonds, but this exercise helps understand and test the integrity of the three datasets. Figure 3.2 shows the location of the buoy moorings and the tidal diamonds considered in this case study. The green and red squares in Figure 3.2 represent output from the Marine atlas where spring peak currents of greater than 2.5 m/s were predicted.

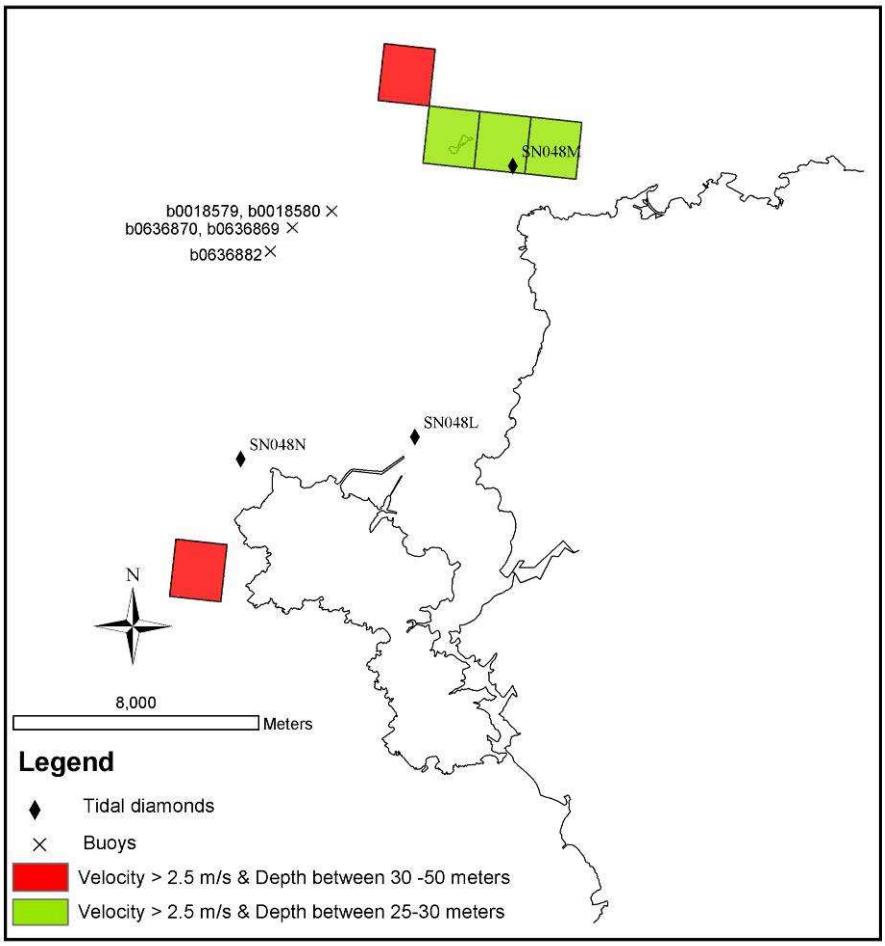

Figure 3.2 Location of the tidal diamonds, mooring buoys and the Marine Atlas identified cells of high energy. BERR © Crown Copyright. All rights reserved 2008.

The minimum data length for the selected mooring buoys was 29 days in order to enable a detailed harmonic analysis to be conducted. Other buoy records in the area were rejected as they were too short, for example buoy b0018579 and b0018580 are 6.1 km away from the nearest tidal diamond (SN048M) and spans the period between from 20/09/1970 to

04/10/1970, only 14 days long and therefore cannot be used adequately for reliable harmonic analysis.

The precise location of the buoys and tidal diamonds along with their position in the water column is indicated in Table 3.1. Buoy records buoy 1 (B1) and buoy 2 (B2) were gathered simultaneously, on the same mooring line. B1 was located 30 metres below the surface (i.e. near seabed) while B2 was positioned 3 metres below the surface. The water depth at this site is reported to be 40 metres (BODC, 2006).

	Name	Location (latitude, longitude)	Depth below mean sea level (metres)	Water depth (metres)
Buoy B1	b0636869	53.39°, -4.68°	30 m (near sea bed)	40 m
Buoy B2	b0636870	53.39°, -4.68°	3 m (near surface)	40 m
Buoy B3	b0636882	53.38°, -4.69°	3 m (near surface)	40 m
Diamond D1	SN0480	53.28°, -4.45°	5 m (near surface)	59 m
Diamond D2	SN048M	53.25°, -4.34°	5 m (near surface)	26 m
Diamond D3	SN048L	53.20°, -4.36°	5 m (near surface)	22 m
Diamond D4	SN048N	53.19°, -4.41°	5 m (near surface)	35 m
Diamond D5	SN048I	53.29°, -4.21°	5 m (near surface)	45 m
Diamond D6	SN048J	53.26°, -4.20°	5 m (near surface)	40 m
Diamond D7	SN048B	53.05°, -4.44°	5 m (near surface)	45 m
Diamond D8	SN062E	53.40°, -5.09°	5 m (near surface)	65 m

Table 3.1 List of buoys, tidal diamonds and location.

3.2 Assessment

The analysis takes the form of a series of comparisons:

1. Between individual moored buoy records;
2. Between individual Admiralty tidal diamond data (obtained from TotalTide);
3. Between buoy records and Admiralty tidal diamond data.

The data provided by BODC is presented in an excel file (.csv), where measurement data is presented as a velocity magnitude (cm/s) and direction (degrees) with a date and time stamp. Metadata also includes measurements for conductivity, sea pressure and salinity. For this

analysis, only velocity magnitude and direction along with the respective time stamp are used. The following steps were taken to prepare the dataset before conducting any analysis:

1. Comparing B1 to TotalTide tidal diamond, shows agreement in direction, however the directional angles for B2 and B3 are out by exactly 180°. For B1 and B2 the timestamps overlap, therefore on the assumption that the two buoys were deployed on the same mooring line. It is thought that the directional measurements for B2 are flawed. Further investigation shows that the current meter used to measure data for B2 was redeployed to measure B3 (same rig number). Therefore the error has been carried forward. In order to continue with the analysis, velocity directional values for B2 and B3 are assumed to be incorrect and needed to be manipulated in order to carry on with the analysis. A short program was written to correct the direction dataset for B2 and B3. This was done by adding 180° to the direction dataset and if the new angle obtained is greater than 360°, then 360° is subtracted for this new value to get the assumed correct direction.
2. The initial values from each of the datasets were omitted. They were mostly erroneous values and interpreted as being taken whilst the buoy was being deployed into the water column. The original start time used for all of the analysis for B1 is 28/05/2003 at 20:55, B2 is 29/05/2003 at 03:25 and B3 is 25/06/2003 at 13:15.
3. The time stamp was converted into Julian day, although later this information was discarded as the start time and ensemble period is defined in the parameter input file of the harmonic software. A short program was written to convert the data into a standard format as time, current velocity magnitude, current direction as a suitable input before any analysis was initiated.

In order to compare different buoy measurements, the data had to be recreated over a common time period. Least-squares harmonic analysis was conducted as explained in chapter 2, section 2.2 to obtain the tidal constituents for each of the buoy measurements. A number of programs written in FORTRAN have been used to perform specific tasks, in

particular data manipulation before harmonic analysis. 23 principal constituents were obtained following the methodology advocated by National Oceanic and Atmospheric Administration (NOAA) Centre for Operational Oceanographic Products and Services (CO-OPS) in their Tidal Current Analysis Procedures and Associated Computer Programs documentation (Zervas, 1999). The NOAA methodology uses different programs to carry out key tasks to obtain individual outputs. The method follows a sequential flow where the output from one program feeds into another program.

The program *prcmp.f* was used to determine the principal current direction of the tidal flow. The major axis is the component parallel to the principal current direction and the minor axis is offset by 90°. In a perfectly rectilinear flow the minor axis component will be non-existent. The principal current direction is used within the harmonic analysis procedure so that the tidal constituents can then be determined for components parallel and perpendicular to this direction (Zervas, 1999). *prcmp.f* is an interactive program where the user inputs the file name and the file format: 'date, speed, direction' or 'date, u component, v component'. The flood and ebb directions are verified using TotalTide tidal diamonds.

Next, the time-series is used to obtain the harmonic constituents. This can be done using either the *lsqha.f* or the *harm15.f* / *harm29.f* program. The *lsqha.f* program uses the least-squares method of obtaining the tidal constituents whereas *harm15.f* and *harm29.f* use Fourier analysis to obtain harmonic constituent details. *lsqha.f* and *harm29.f* require a minimum 29 day long dataset for analysis. *harm15.f* can be used on more than 15 days of data although it is restricted to only 16 tidal constituents. The input file for all programs is expected to be continually spaced and measured at equal time intervals.

Finally, *pred.f* can be used to create a new time-series using the harmonic constituents generated from the *lsqha.f* or *harm.f* programs. To test the credibility of the NOAA programs, the original input time-series are recreated to compare with the original measured data and the accuracy of the measurement and prediction is verified using various statistical tools (see Figure 3.4).

A control (parameter) file is used to provide user input information for each specific program. The input required is broken down into data specific to the dataset such as scalar/vector, simulated date and time for starting the analysis but certain parameters are left for the user to decide, e.g. which constituents to resolve and in what order. Metadata used in the different programs are listed in Table 3.2.

Program	Data specific INPUT	User specific INPUT	Program OUTPUT
prcmp.f	Data format in speed/direction or *u/v* format	-	Mean current velocity, Principal current direction, Major and minor axis variance
lsqha.f *harm15.f* *harm29.f*	Vector or scalar data - Tidal current velocity and direction. Principal current direction (obtained from *prcmp.f*). Start date, start time. Number of days in the dataset, total points to analyse, number of samples per hour. Longitude of the location where measurement was taken	Variance cutoff for the predictions, parameter for scaling, the number of constituents to resolve, specify the order of constituents to be resolved	Tidal constituents
pred.f	Tidal constituents (obtained from *lsqha.f/ harm15.f/ harm29.f*). Principal current direction (obtained form *prcmp.f*)	'*New*' prediction date and time, ensemble period. Type of prediction - scalar or vector. Specify which constituents to use.	Predicted speed and direction

Table 3.2 Tidal current analysis programs used. List of the inputs required by each of the program and the outputs obtained.

A number of changes to the original NOAA code provided by the author were implemented. The original program was written in FORTRAN 77 and over time various updates have been incorporated by different users. Some of the changes that had to be rectified or altered included:

1. Changing the path file directory so it did not point to the original author's C drive.

2. Changing the format of the *lsqha.f*/*harm15.f*/*harm29.f* output file *cons.out*, for all constituents such that enough significant digits were output to capture the high tidal amplitudes and sensitivities. For example, enabling constituent velocity to be recorded in m/s as opposed to cm/s.
3. Changing the format in *pred.f* to match the changes made to *cons.out*.
4. Changing the order in which the constituents are resolved in the *lsqha.f* program to be in the standard order.

3.2.1 Comparison of Buoys

The three individual moored buoy records are not coincident in time, although they were gathered during a coincident survey period. Direct quantitative comparisons between the buoy data to compare spatial variability over a common time frame is therefore not possible. Harmonic analysis and reconstruction was carried out to generate accurate tidal predictions that are coincident in time for all the three buoy datasets. To see what contribution each of the constituents make in the data set, Figure 3.3 illustrates the breakdown of the 23 constituents. For the three buoys the M_2 values have been scaled to 100 and the other constituents are scaled relative to this for each dataset. It can be seen that M_2, S_2, N_2 and M_4 are the most dominant constituents. The presence of these dominant constituents highlights that the site is predominantly semidiurnal. K_1, O_1 and M_6 play a small part but the contribution from the remaining constituents is insignificant. For some locations, it has been suggested that using M_2, S_2, K_1 and O_1, about 90% of tidal variation can be captured (Lu *et al.*, 1999). $_2SM_2$ and L_2 are shallow water constituents, and their presence is indicative of particular localised response to the tidal system.

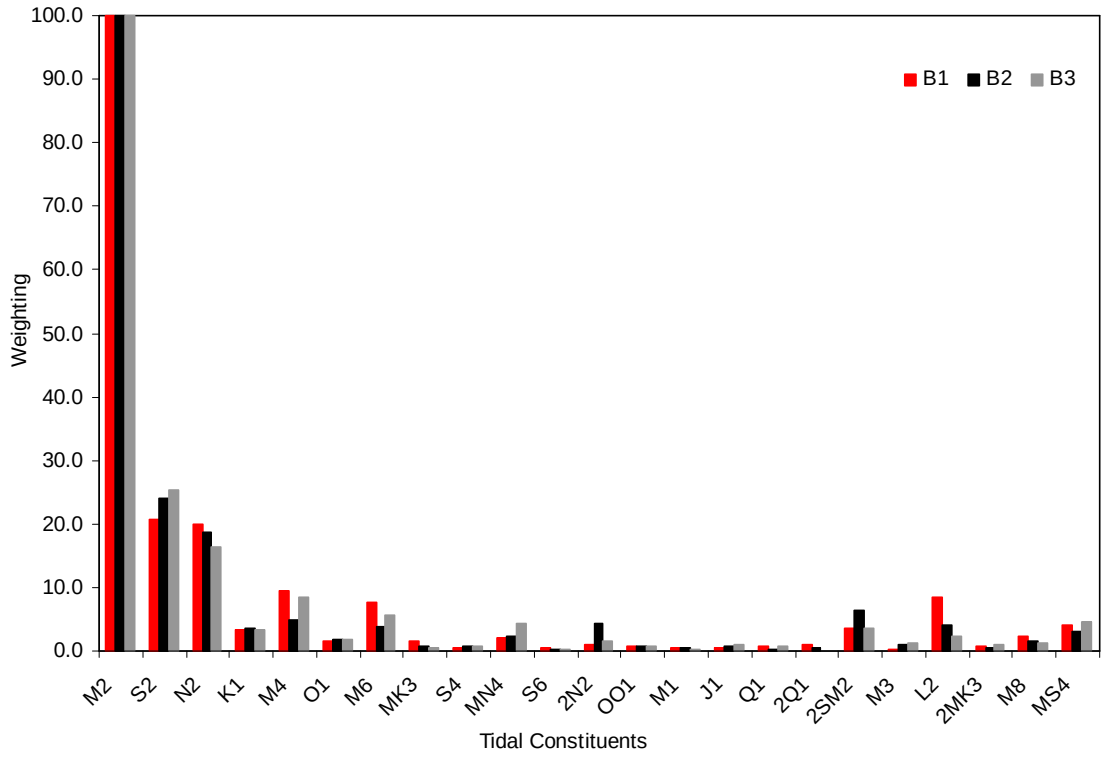

Figure 3.3 Breakdown of the constituents from the three buoys.

The harmonic analysis programs provided by NOAA have been validated, however it is necessary to verify how well the harmonic analysis captures the sites specific variability each time the program is used. The best way to do this is by re-creating the time-series using the 23 harmonic constituents to be coincident in time to the original time-series measured by the current meter data. Figure 3.4 shows a scatter plot of the original current data and the reconstructed data velocity magnitudes plotted on the X and Y axis respectively. It can be seen that while there is some scatter, the fit is good and exhibits good homogeneity. An R^2 value of 0.9014 is obtained. R^2 is a statistical indicator of how well one value represented the other. A R^2 value of 1 presents perfect prediction. Some of the variations are due to non-tidal events that cannot be captured by harmonics analysis, while others may be a result of the constituents that have not been resolved by harmonic analysis. The buoy data is a true in-situ record of sufficient length to allow confidence in its fidelity. Therefore, for this analysis, it is reasonable to treat reconstructed moored buoy data as the 'gold standard', where R^2 is greater than 0.9 and therefore with which other datasets it will be compared.

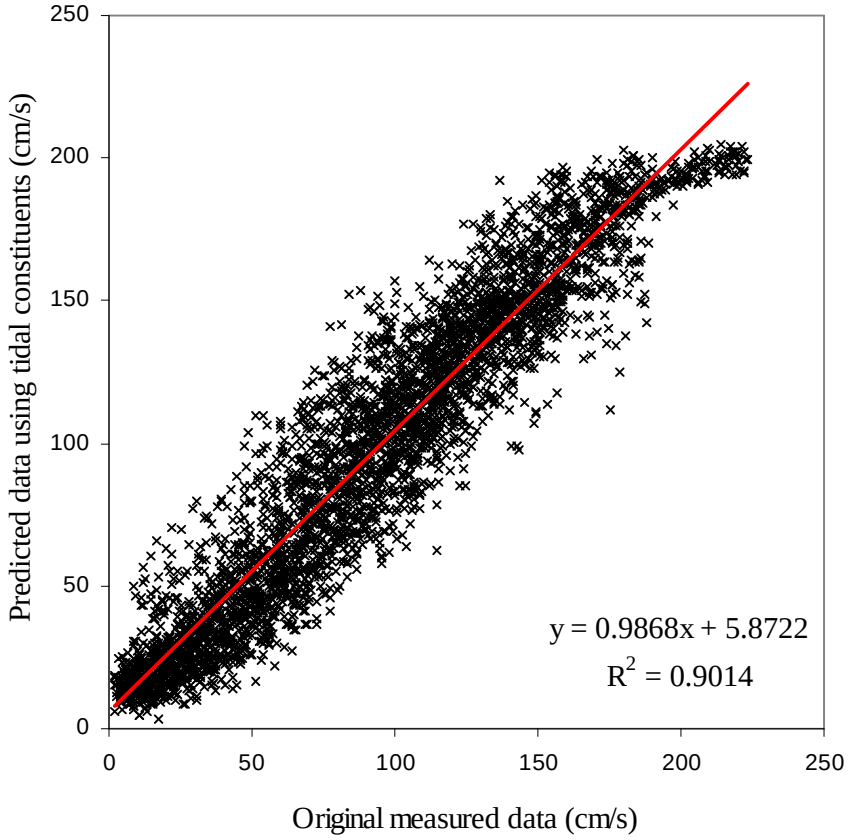

Figure 3.4 Scatter plot comparing between the original data record and the reconstructed data generated using 23 harmonic constituents for the period of 05/2003-06/2003.

The complete time-series of the measured and the predicted data for all the three buoys are shown in Figure 3.5 and Figure 3.6. Also presented are the residual errors which present the difference between the measured and the reconstructed data from harmonic analysis. The residual at the start of the records are particularly large as these are the erroneous measurements taken while the buoy was being deployed. For the harmonic analysis these valued were omitted as mentioned in section 3.2. The residuals are a combination of non-tidal events that cannot be captured by harmonic analysis and the fact that only 23 of the harmonic constituents are accounted for. An important observation to make is that the velocity observed at B1 is much smaller in magnitude compared to B2 and B3 (because it was measured near the sea bed). Figure 3.7 shows all the three datasets reproduced from harmonic analysis for the common time-period of August 2009. Further analysis using measured data and harmonic analysis is the focus of chapter 4 and 5.

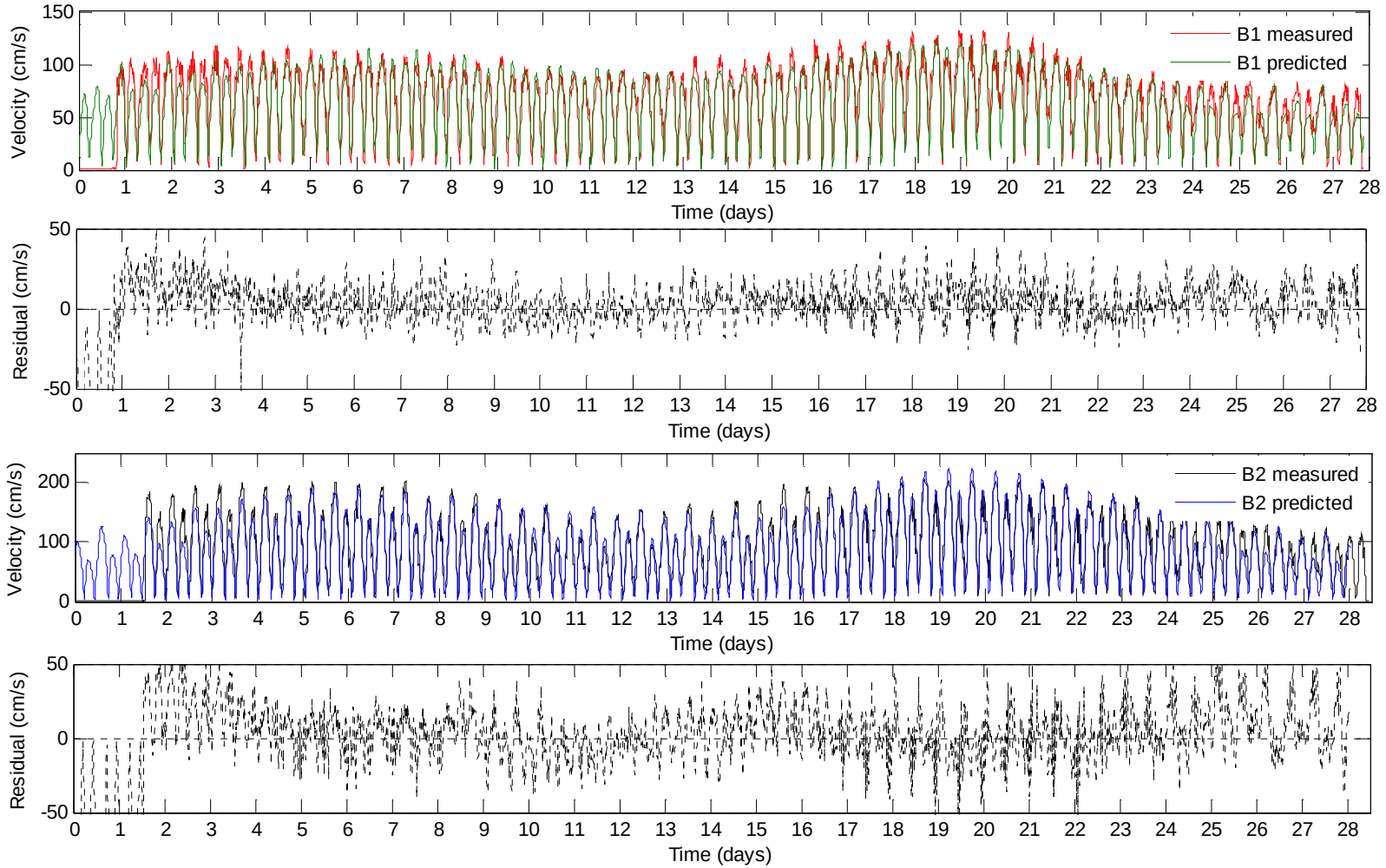

Figure 3.5 Measured and predicted time-series for buoy 1 (B1, top) and buoy 2 (B2, bottom). Residual values are also presented.

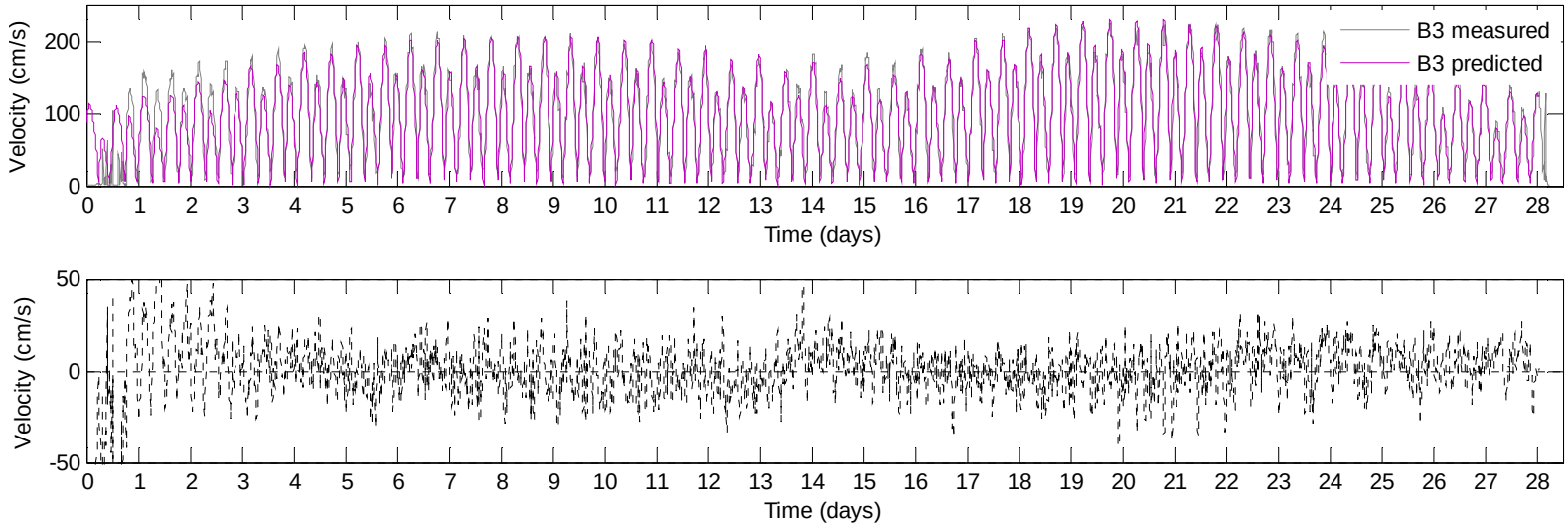

Figure 3.6 Measured and predicted time-series for buoy 3 (B3). Residual values are also presented.

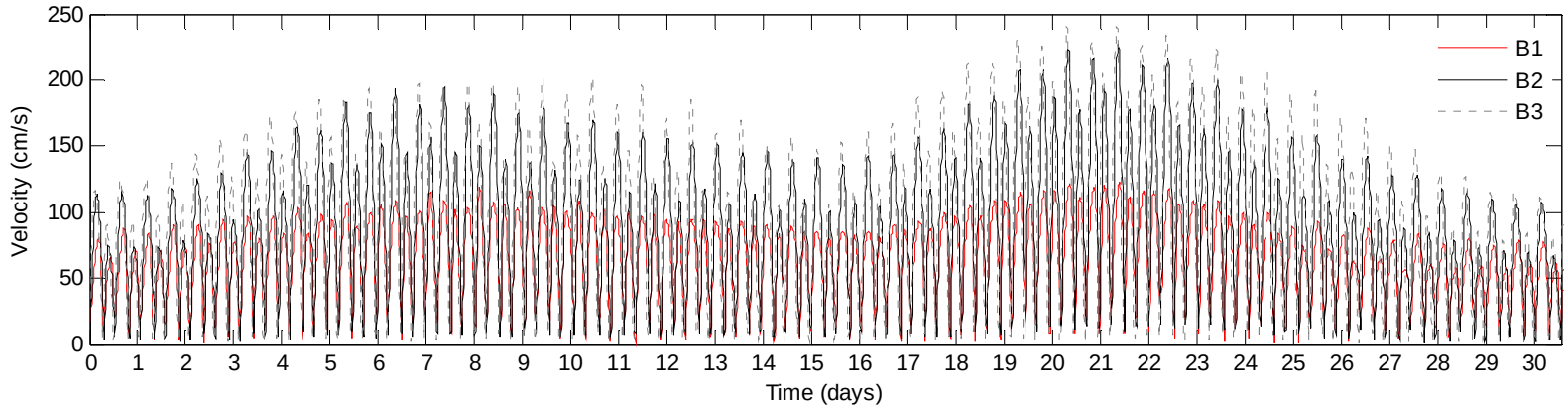

Figure 3.7 Buoy 1 (B1), buoy 2 (B2) and buoy 3 (B3) reproduced from harmonic constituents to a common time-period (August 2009).

3.2.2 Inter-comparison of Buoy Measurements

The first comparison presented is between the individual moored buoy records. Given the location of the buoys, within close physical proximity, the data could be expected to demonstrate some correlation. Figure 3.8 shows the velocity magnitude plot of all the three buoys on the day of the spring peak.

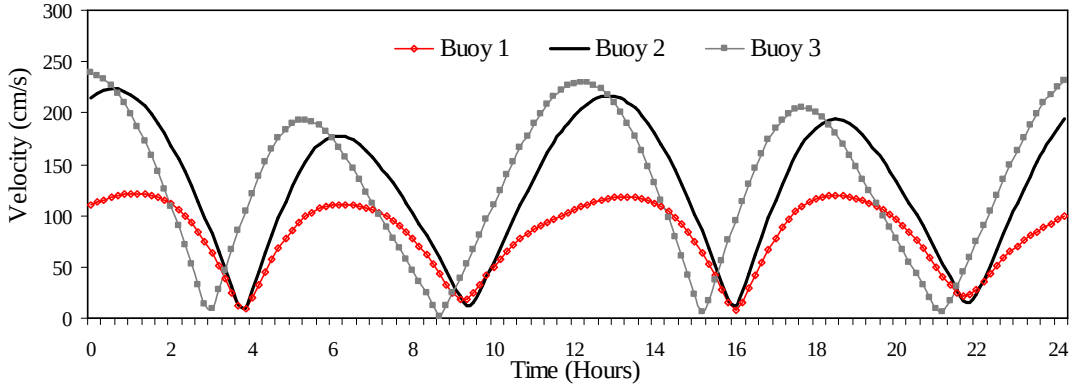

Figure 3.8 Current velocity observed by buoy 1, buoy 2 and buoy 3.

There is good phase agreement between the three records, B1 and B2 are located on the same mooring and therefore are almost exactly in phase. B2 and B3 are both located near the surface and 1.07 km apart, a slight phase lag is observed but the shape and size of the velocity magnitude plots compare well. The phase lag over such a small distance highlights the extent of the spatial variability.

To better represent the velocity variation, the velocity distributions of the three buoys are shown in Figure 3.9. B1 measurements are lower than both B2 and B3 because the original current meter measurements for B1 were taken near the seabed, whereas B2 and B3 were measured near surface. The velocity variations are indicative of the velocity profiling along the water column as discussed in chapter 2, section 2.3.2. A scaling factor would be required to account for the vertical velocity gradient between the sea-bed and the surface which skews the data in this case (e.g. $1/7^{th}$ power law).

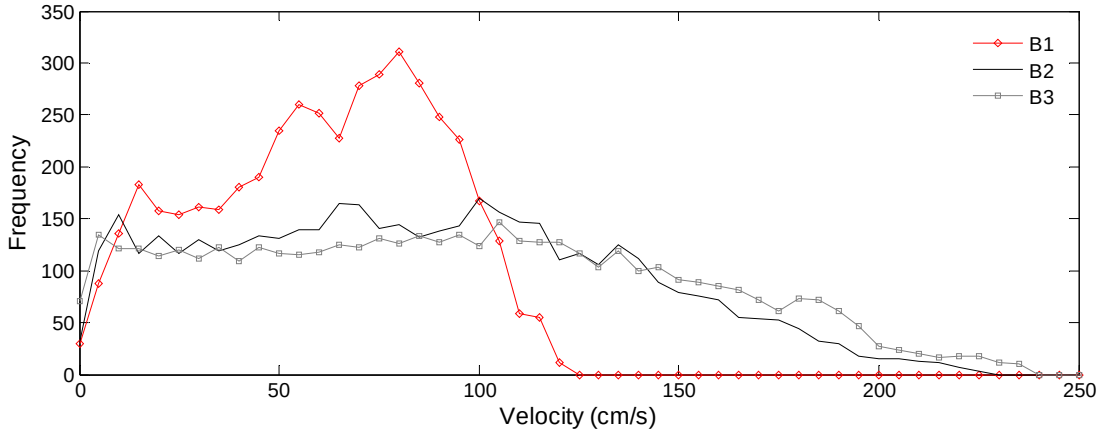

Figure 3.9 Current velocity histogram for buoy 1, buoy 2 and buoy 3.

To quantitatively compare these measurements, statistical methods were adopted, although it should be realised that none of the records themselves are 'accurate', as even the measured data could be distorted. However, this analysis presents a way to evaluate the spatial variability. The data to be compared is converted from velocity magnitude and direction into two-dimensional vectors X(X_{1n}, X_{2n}) and Y(Y_{1n}, Y_{2n}) where the indices 1 and 2 relate to the separate buoy datasets and *n* is the timestamp. The mean absolute error (MAE) is calculated as (Brière *et al*., 2006):

$$MAE = \frac{1}{N}\sum_{n-1}^{n}\sqrt{(Y_{1n} - X_{1n})^2 + (Y_{2n} - X_{2n})^2} \qquad (3.1)$$

where *N* is the number of data points. This statistically incorporates both errors in velocity magnitude and direction. The Relative Mean Absolute Error (RMAE) is a better means of comparison between the datasets as it incorporates the relative magnitude of the data considered to scale the error assessment (Brière *et al*., 2006):

$$RMAE = \frac{MAE}{\frac{1}{N}\sum_{n=1}^{N}\sqrt{(X_{1n} - X_{2n})^2}} \qquad (3.2)$$

An RMAE value of zero indicates a perfect match. As RMAE is a ratio of the mean absolute error over the mean values of the measured data, the further RMAE values deviate from 0 the higher the error ratio. This is a good indicator of how spatially variable tides in this

location are. Table 3.3 summarises MAE and RMAE values across the three records examined.

		B1	**B2**	**B3**
B1	MAE	-	31.16	51.86
	RMAE	-	0.49	0.82
B2	MAE	31.16	-	38.31
	RMAE	0.35	-	0.43
B3	MAE	51.86	38.31	-
	RMAE	0.54	0.40	-

Table 3.3 Comparing results from the buoys (cm/s).

As B1 and B2 are co-located, good quantitative agreement is expected and B1 has a much lower tidal velocity due to its relative depth accounting for the lower MAE and RMAE. B3 has better agreement with B2 than with B1. This is because B2 and B3 are both located close to the surface and except for a small phase lag have a very similar velocity magnitude.

3.2.3 Inter-comparison of Tidal Diamonds

The next set of experiments compared the tidal diamonds obtained from TotalTide. Tidal diamonds embody a set of numbers that depict the tidal current behaviour at a time relative to high water at a reference port. TotalTide can generate time-series over different sample periods. Therefore comparison between buoy data and tidal diamonds can be carried out.

A total of 8 tidal diamonds were used in this experiment, all within a 50 km radius of the central buoy location. The MAE and RMAE are calculated for the four closest tidal diamonds, SN0480 (D1), SN048M (D2), SN048L (D3) and SN048N (D4). The metrics are calculated for all the four diamonds and compared to quantify the spatial variability. Table 3.4 has a summary of MAE and RMAE. The error values are, in general, consistently bigger for the tidal diamonds compared with the buoy data. This is primarily because these data points are spatially more dispersed than the buoys. This gives a good indication of how

spatially variable tidal current velocity data can be, even within a relatively short distance, compared with the tidal wavelength.

		D1	D2	D3	D4
D1	MAE	-	68.49	88.51	91.6
	RMAE	-	0.83	1.07	1.11
D2	MAE	68.41	-	122.52	67.8
	RMAE	0.53	-	0.95	0.53
D3	MAE	88.38	122.44	-	92.78
	RMAE	3.14	4.35	-	3.29
D4	MAE	91.48	67.7	92.82	-
	RMAE	0.84	0.62	0.85	-

Table 3.4 Comparing results from the tidal diamonds.

The RMAE and MAE values for D3 are exceptionally poor compared to the rest of the tidal diamonds because this particular tidal diamond is sheltered by a headland. Further explanation as to the poor comparison is presented in the following section.

3.2.4 Comparison of Buoys and Tidal Diamonds

To better understand the quantitative agreement between the buoys and the tidal diamonds, Table 3.5 presents MAE and RMAE values for the buoys and tidal diamond. As expected, B2 and B3 present good agreement with the tidal diamond as they were measured near the surface. A model skill test was conducted (Warner *et al.*, 2005). The observed data considered are the measured buoys and the model data are the tidal diamonds. The skill is defined as:

$$Skill = \frac{\sum |X - Y|^2}{\sum \left(\left|X - \overline{Y}\right| + \left|X - \overline{X}\right| \right)^2} \tag{3.3}$$

where $\overline{X}$ is the mean model value (tidal diamond) and $\overline{Y}$ is the mean value of the measured data (buoy data). A value of one indicates perfect agreement and a value of zero indicates total disagreement. This value has been calculated separately in the Cartesian coordinate

system for *u*, the eastward velocity component and *v*, the northward velocity components to highlight the effect of directionality.

		D1	D2	D3	D4
B1	MAE	45.39	71.58	60.72	69.56
	RMAE	0.72	1.13	0.96	1.10
B2	MAE	48.73	51.60	87.30	61.27
	RMAE	0.55	0.58	0.99	0.69
B3	MAE	81.56	61.82	86.90	51.27
	RMAE	0.85	0.64	0.91	0.53

Table 3.5 Comparing results from the buoys and tidal diamonds (cm/s).

All three buoy records were compared against all eight tidal diamonds. The statistics are summarised in Table 3.6. Yet again, the model skill results for tidal diamond D3 which is 7.68 km away from B1 and B2 compares even worse than the distant D7 and D8 diamonds, particularly in the *v* direction. This relates to the earlier findings when the MAE and RMAE values were discussed. The effect is much more evident in the *v* direction.

		B1		B2		B3	
		u	***v***	***u***	***v***	***u***	***v***
Within 12 km	**D1**	0.91	0.88	0.94	0.90	0.81	0.77
	D2	0.87	0.82	0.92	0.96	0.91	0.94
	D3	0.71	0.29	0.64	0.28	0.79	0.27
	D4	0.78	0.84	0.79	0.93	0.90	0.97
Within 50 km	**D5**	0.90	0.10	0.94	0.14	0.86	0.15
	D6	0.90	0.05	0.94	0.11	0.85	0.09
	D7	0.16	0.91	0.29	0.93	0.31	0.82
	D8	0.87	0.94	0.80	0.86	0.69	0.78

Table 3.6 Comparing 'model skill' results from the buoys and tidal diamonds.

The standard deviation, σ of the datasets was calculated to provide a measure of the statistical spread of the data:

$$\sigma = \sqrt{\frac{1}{N}\sum_{i=1}^{N}(x_i - \bar{x})^2} \tag{3.4}$$

where *N* is the total number of observations, $\bar{x}$ is the mean velocity and x_i is the *i* th value. Standard deviation can also be used to calculate the cross correlation coefficient (*CC*) between two datasets, (in this case the buoy and the tidal diamond data):

$$CC = \sigma_x^{-1}\sigma_y^{-1}\frac{1}{N}\sum_{1}^{N}(x_i - \bar{x})(y_i - \bar{y}) \tag{3.5}$$

CC has been calculated between all the buoys and the four closest tidal diamonds (D1-D4). These values have been plotted and can be viewed in Figure 3.10. Perfect correlation is indicated by a value of 1, -1 indicates negative correlation. None of the *CC* show negative correlation.

Looking at the *CC* values it can be seen that all the buoys and tidal diamonds show values of 0.5 or above, however D3 consistently shows a poor correlation compared to all the tidal diamonds as well as the buoy data. The deviation becomes particularly evident for the *v*- velocity component (bottom graph).

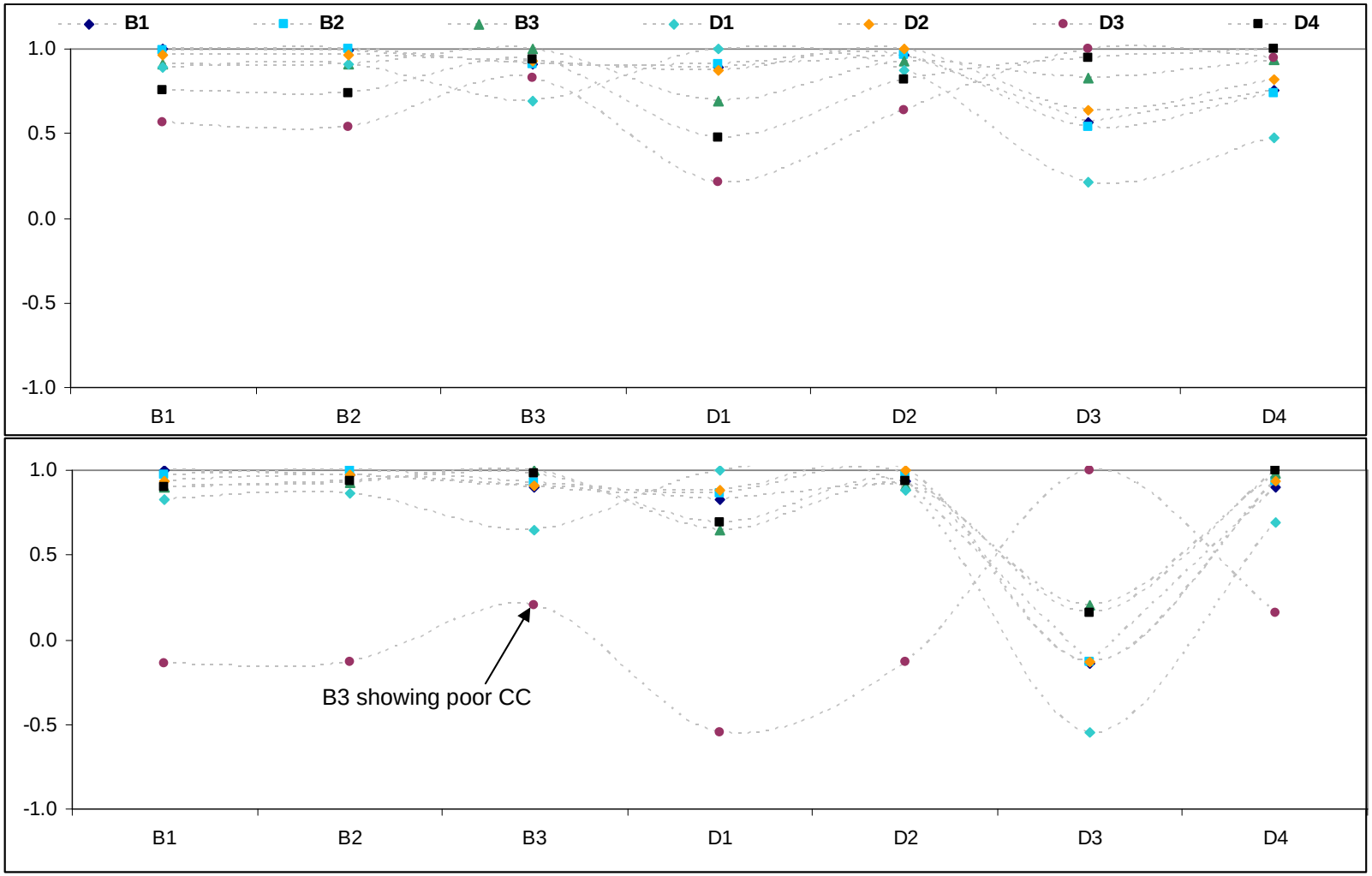

Figure 3.10 Comparing CC between buoys and tidal diamonds in directions (top) *u*-component, (bottom) *v*-component.

3.3 Effect of Interpolation

This section investigates the effect of interpolation on the tidal diamond datasets. The time-series are interpolated and compared to B2 as the tidal diamonds are interpolated to this point. B2 works best as it is a near surface measurement, similar to tidal diamonds and it represents the tidal flow conditions in this location well. The interpolation technique is advocated by Shepard (1968) for irregularly spaced data. The methodology is applied to the tidal diamond data, where the interpolated value u at a given point x is given by:

$$u(x) = \frac{\sum_{k=0}^{N} w_k(x) u_k}{\sum_{k=0}^{N} w_k(x)} \tag{3.6}$$

where u_k denotes the point the data is being interpolated from and w_k is the weighting, defined as:

$$w_k = \frac{1}{d(x, x_k)^p} \tag{3.7}$$

d is the distance between the two points x the unknown value and x_k the point the data is being interpolated from. $p = 2$ is adopted as recommended by Shepard (1968). Selection of the value of p enables the user to prescribe how sharp a peak the function exhibits by giving greater influence to nearby data points. A low value of p provides a smoother solution, with more 'smearing' of peaks (Shepard, 1968).

Inverse Distance Weighting (IDW) is used in this instance to create 'pseudo' diamonds from the tidal diamonds available in the location. To test the fidelity of these 'pseudo' diamonds, the interpolation locations are mapped onto existing buoy record locations. The further away a tidal diamond is from a specific location, the less weighting it will have in the calculation. Similarly, tidal diamonds located close to the buoy will have a higher weighting therefore having a more significant influence on the pseudo diamond. In order to preserve the directionality IDW was performed by converting all the speed and

direction datasets into the $u - v$ velocity Cartesian coordinate system. After IDW it was possible to convert the interpolated data back to speed and direction.

Three sets of IDW's were created. IDW1 indiscriminately included all the tidal diamonds within a 50 km radius of buoy 2. IDW2 only included the four tidal diamonds within 12 km of B2 and IDW3 was a 'selected' variation of IDW2 where tidal diamonds are selected based upon their statistical correlation. Table 3.7 summarises the distance between all the tidal diamonds and B2.

	Distance (km)
D 1	10.45
D 2	8.42
D 3	6.98
D 4	7.68
D 5	24.49
D 6	33.23
D 7	33.23
D 8	44.09

Table 3.7 Distance between each tidal diamond and buoy 2

For the purposes of comparison, IDW's are created for the same physical location of B2. Velocity magnitude plots of B2 along with IDW1, IDW2 and IDW3 are plotted in Figure 3.11.

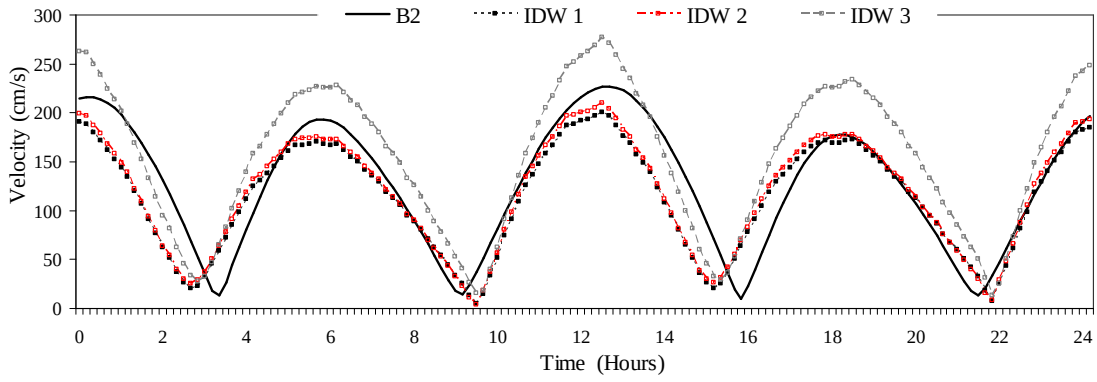

Figure 3.11 Velocity magnitude comparison of buoy with IDW 1, IDW 2 and IDW 3.

All the three IDW's present are in phase with B2 and there is good quantitative agreement between IDW1, which includes all the tidal diamond current data within the 50

km radius, and IDW2 which only includes the 4 closest buoys. The minimal difference between IDW1 and IDW2, which nearly overlap in Figure 3.11, is due to the inverse distance weighting ensuring that the distant tidal diamonds provide a limited impact, in this case where 4 tidal diamonds are relatively close and 4 are further away rather than an even dispersion.

Although the buoy data encapsulates 23 constituents and the Totaltide diamond data generally only captures 2 of the major constituents, M2 and S2 (Bell *et al.*, 1998), there is a good qualitative agreement and correlation. Velocity magnitude peaks and phasing in Figure 3.11 indicate reasonable qualitative agreement between the different records. The shape and the general envelope of the Spring-Neap cycle are also well captured as shown in Figure 3.12 (only for IDW2 and B2). However, the envelope highlights that the tidal diamonds fail to meet the peak velocity values. They either overestimate in the *u* direction or underestimate in the *v* direction depending upon which combination of tidal diamonds is being considered. Therefore, estimated tidal currents based on the IDW1 and IDW2 values from tidal diamonds will always underestimate whereas IDW3 will tend to overestimate the resource.

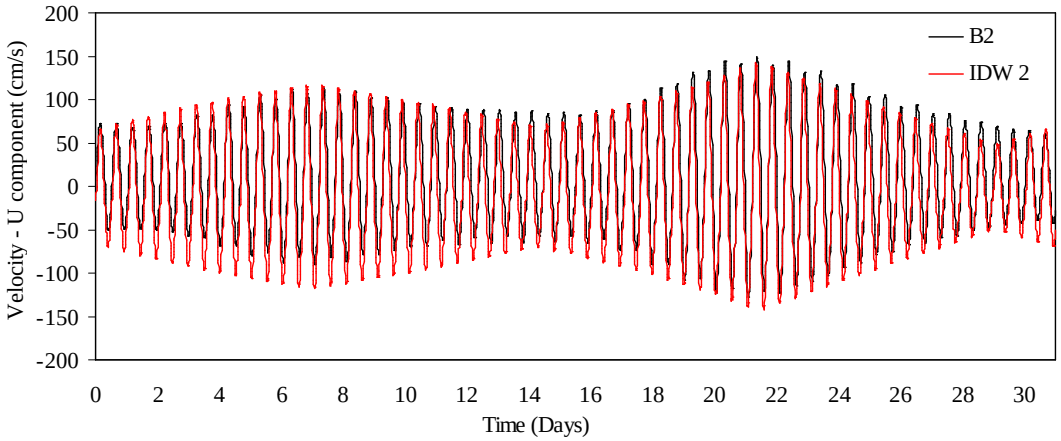

Figure 3.12 Velocity magnitude comparison of B2 with IDW 2. Data showing the Spring-Neap envelope.

To better understand how skewed the velocity distribution between the three IDW's were, Figure 3.13 shows a velocity histogram of all the IDW's and B2. In the context of energy extraction, the extreme velocities are of significant importance in determining the

AEP. IDW1 and IDW2 over estimate the velocity distribution compared to B2 up to 100 cm/s. Beyond this value, the IDW's under estimated and missed the peak values. For IDW3, the distribution underestimated the values below 100 cm/s, but towards the tail end of the spectrum IDW3 overestimated the peak values. For Comparison, B2 is also plotting along with all tidal diamonds D1, D2, D3 and D4 in Figure 3.14.

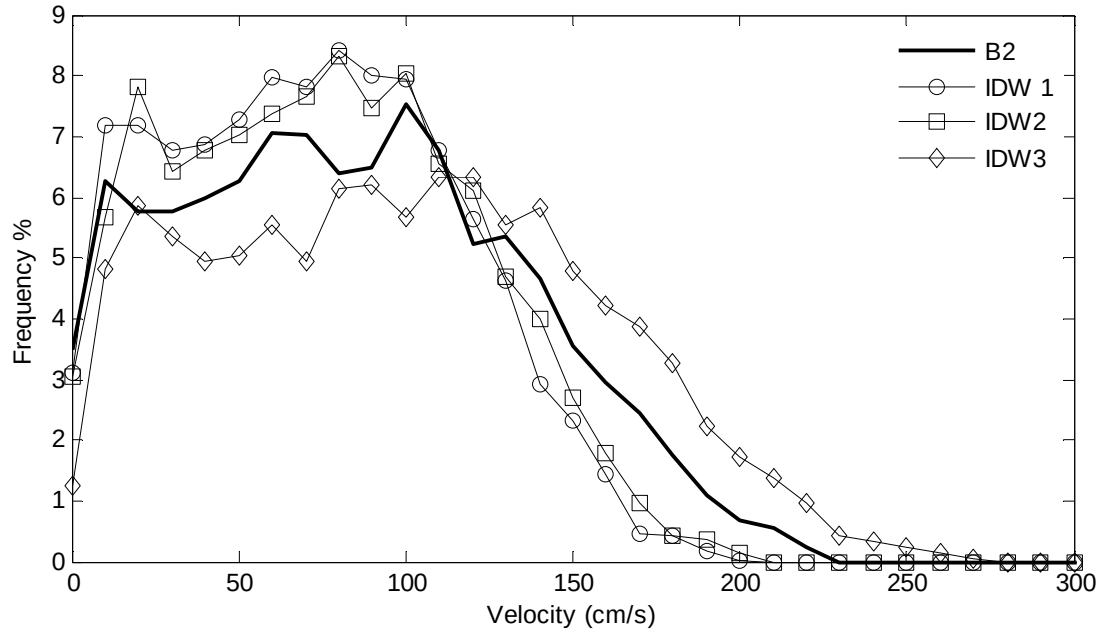

Figure 3.13 Velocity magnitude comparison of buoy with IDW 1, IDW 2 and IDW 3.

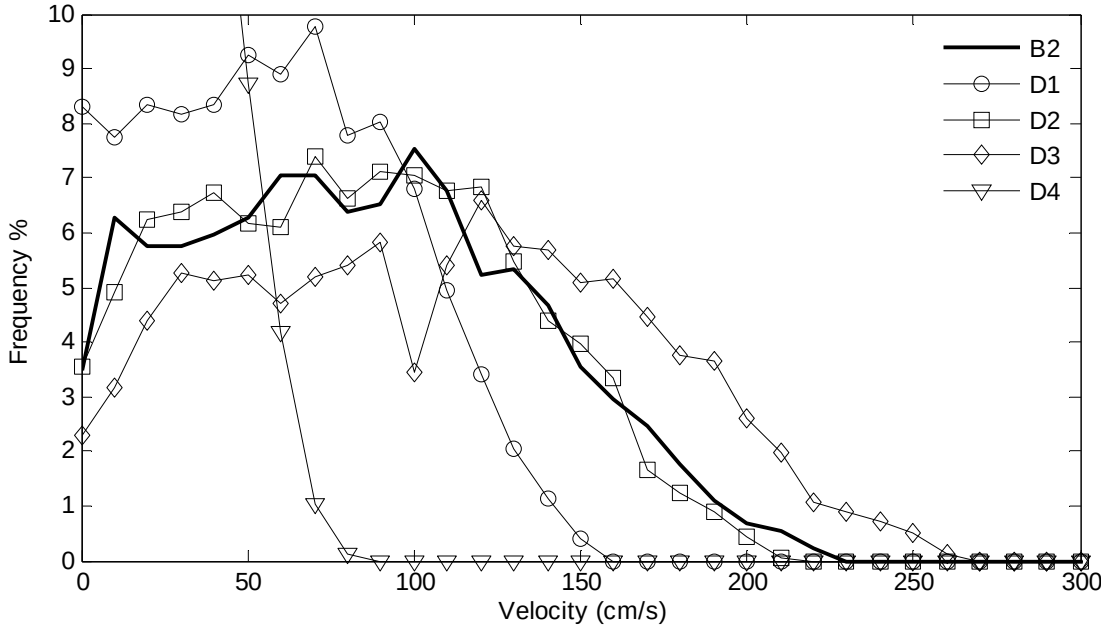

Figure 3.14 Velocity magnitude comparison of buoy with D1, D2, D3, D4.

For all the distributions, velocity data was placed in bins of width 10 cm/s. Interestingly, D2 presents a better match to B2 than any of the IDW's. D3, which is the nearest tidal diamond, under-predicts at lower velocities and over-predicts at higher velocities (similar to IDW 3). The poor performance from D4 is evident where no velocity above 100 cm/s is recorded by this tidal diamond, despite being the second closest tidal diamond. D1 presents characteristics similar to IDW1 & IDW2. The fact that D2 alone represents B2 so well is coincidence and is unlikely to occur at any other site of interest. Without having measurements taken at the specific location, it would not have been possible to know scientifically which dataset would provide the best match.

This exercise had helped in understanding that an interpolation technique cannot fully capture the complex tidal hydrodynamics occurring at the site. But, without performing the analysis it would not have been possible to understand how well the interpolation technique worked. Even though D2 presents good velocity magnitude match, it will also be of interest to observe if D2 can present similar directionality when compared to B2. This analysis is presented in the following section compares directionality.

3.3.1 Comparison of Tidal Ellipses Hodographs

Tidal ellipse comparisons have been plotted in Figure 3.12, where the local individual tidal diamond ellipses (left) are compared with all the IDW ellipses (right). The IDW ellipses were created by resolving the $u - v$ velocity component back into speed and direction. D3 presents the worst spread in directionality. Each individual tidal diamond presents poor directional comparison to B2. The IDW ellipses show a much better qualitative agreement suggesting that this methodology improves the representation of some of the tidal characteristics. The bi-directionality of the tides suggests that this location is very desirable for tidal current energy deployment which is captured well by the IDW's.

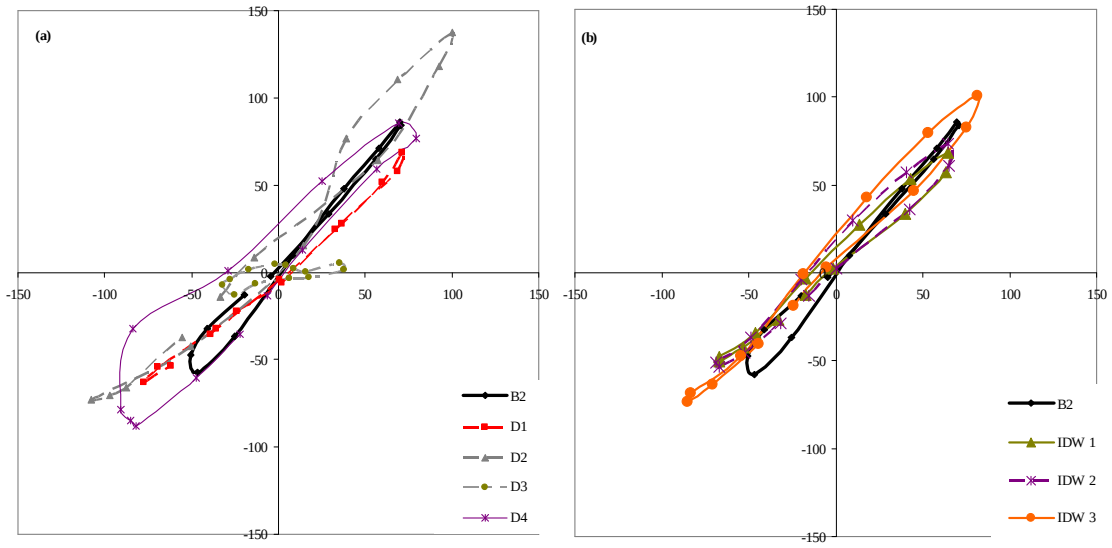

Figure 3.15 Tidal ellipse hodographs (a) comparing buoy data with tidal diamond data and (b) comparing buoy data with IDW data constructed from tidal diamond records.

3.3.2 Comparison with the Marine Atlas

It is estimated that only 0.15% (1269 km^2 Area) of the UK continental shelf has a peak flow of 3 m/s or greater (Cooper *et al.*, 2006). These are the very high energy sites that make tidal energy extraction economically viable. Before devices are deployed into the water, it is important to precisely identify these locations and study the individual site characteristics.

Depth averaged data is often used during calculations but in this analysis buoy data is available from near the surface, at 37 meters from the seabed, and near the seabed at 10 metres. The TotalTide data is measured approximately 5 meters below the surface. Current velocity estimates can be extrapolated from measurements at a specific depth by using a scaling value. A 1/7th power law is often considered appropriate in fluid flows (Falconer *et al.*, 1997). The POL (POL, 2011) model used to construct the Marine Atlas uses a vertical velocity profile. Alternatively, Black & Veatch (B&V Phase II, 2005) uses a variable power law similar to equation 2.9, presented in chapter 2. This formula can be used to estimate the tidal velocity at a specific height in the water column. This enables the calculation of velocity at the device hub-height for the intended device.

Figure 3.16 shows spring peak measurements for B2 which is located at 37 meters (near surface), scaled to 10 meters using the scaling factor as suggested by the DoE (1990). Also plotted is the measured data obtained at 10 metres in the same location. The Marine Atlas scaling factor is 0.9. Figure 3.16 indicates that the current velocity is nearly half, when compared to the 10 metres depth data, a scaling factor of approximately 0.5 would be more appropriate in this case. The Marine Atlas uses layers obtained from the POL HRCS model and this scaling factor to obtain their depth averaged current velocity and power. However, it is observed that for this particular site the $1/7^{th}$ and DTI scaling factors overestimate the current velocity significantly. If this is manipulated to produce an estimate of the energy that can be harvested at this location, the overestimation would then be compounded.

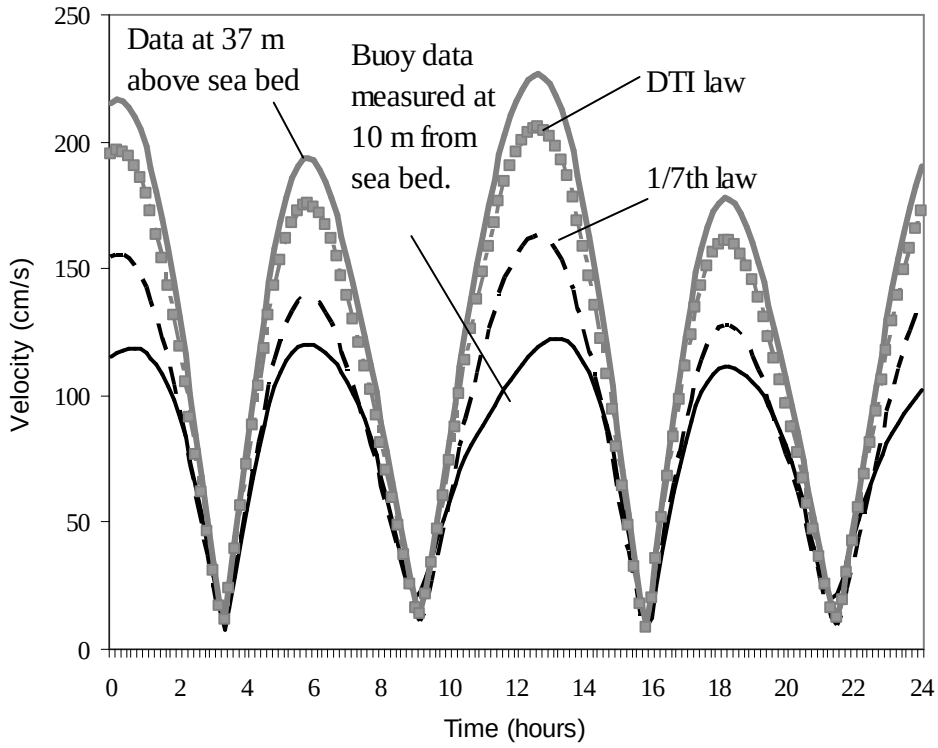

Figure 3.16 B2 scaled down using the $1/7^{th}$ and DTI scaling factors.

Figure 3.17 shows current vertical velocity profiles along the water column, in a water depth of 40 meters. The figure compares the various commonly applied power law plots with two data points obtained from the buoys.

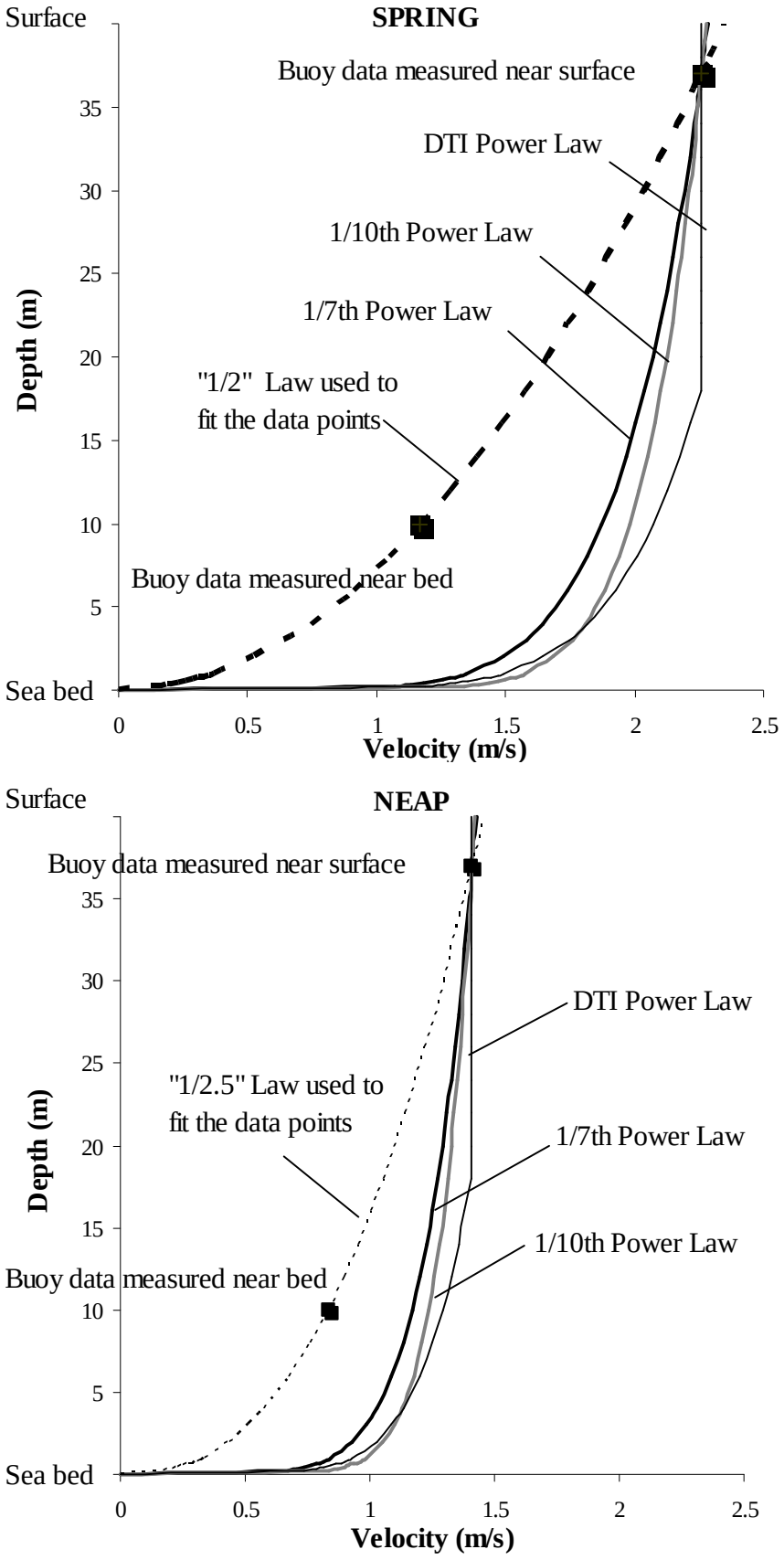

Figure 3.17 Tidal current velocity profiles, during spring and neap tide.

The power law curves have been derived from the near surface buoy data. To best represent the profile characteristics, the tidal current characteristics are broken down into Spring and Neap. As suggested earlier, the flow in the Spring cycle best fits a scaling factor of 0.5. Neap tide data were best fitted using a similar scaling factor.

It remains unclear whether overestimation of the resource in this case by the $1/7^{th}$, $1/10^{th}$ and DTI power law would be replicated at other locations. Analysis presented in chapters 4 and 5 present vertical velocity profiles at other sites and attempt to evaluate different ways of quantifying the velocity profile variation. However, it is notable that the extreme tidal velocities of interest for tidal energy development are potentially not well represented by traditional vertical velocity variation assumptions and require updating.

3.3.3 Comparing Power Outputs

Power output for all the three IDW's and B2 have been calculated for the month considered. Power was calculated using equation 2.6. Similarly, the power output from the Marine Atlas for this region is obtained by extracting the mean annual power (kW/m^2) from the atlas and multiplying by the number of hours in a year (8760 hours) to obtain the annual energy output. Table 3.8 summarises the output resource assuming that the simulated month is representative of the entire year. B2 is used as the base value here for comparison and the annual energy yield is compared with the three IDW outputs and the average value obtained from the Marine Atlas (BERR, 2008).

	Annual energy resource available per square metre (kWh/ m^2)
B2	6395
IDW 1	4038
IDW 2	4538
IDW 3	9875
BERR Atlas	10319

Table 3.8 Power output for B2, IDW1, IDW2 & IDW3.

From the preceding analysis, the error margin between the velocity magnitudes were substantially reduced between the IDW representations of the tidal diamond data over consideration of the individual tidal diamond data when compared with the moored buoy derived data record. However, when these datasets are used to conduct a long-term monthly or AEP assessment, even the IDW representation of the tidal diamond data show poor agreement as demonstrated by the varied values presented in Table 3.8, as prediction of long-term energy yield is at the heart of any sensible economic appraisal. The application of the IDW methodology for use in tidal energy resource assessment presented through this example demonstrated error that can be introduced as a result of this methodology. This is a combination of the error introduced as a result of interpolation as well as the extent of the variability of the datasets. Therefore, other locations may present higher or lower velocity and power discrepancies depending upon the site specific variability.

None the less, it is important to mention that these error margins make a significant impact on site selection and lifetime production costs. If this was to be considered over 25 years, the typical intended lifecycle of tidal energy development projects, these error margins would have a significant impact on the project economics.

3.4 Conclusion

The spatial variability of tides is governed by complex non-linear physics, topography, the bathymetry and the fluid interaction at the site. For this reason, interpolating spatially diffuse tidal data records is always going to lead to inaccuracies. These complex phenomena cannot be well represented by simple interpolation. This is particularly true when the current velocity derived will inevitably be used to conduct tidal energy generation calculations and scenarios analysis. Even though statistical analysis shows the MAE and RMAE of velocity records to be relatively small, the error is magnified when the power output is estimated for a site. This is mainly because the power output is proportional to the velocity cubed. Therefore an error of 2% can cause a 6.12% error in the power output. The significant variations in the

available energy in the water column derived using the improved IDW representations demonstrates that site selection and evaluation should not be done simply based on this methodology, instead, this can be the first screening process following which full site survey and high resolution data collection can take place.

The most important issue to highlight is that it is essential for developers, before committing to a site for development, to conduct an appropriate survey of the available resource as the next stage of project development. Gathering multiple ADCP records across the intended site at a minimum temporal resolution of 29 days is recommended to enable an appropriate spatial and temporal representation of the tidal currents to be determined. A suitable site specific analysis using ADCP data is presented in chapter 4. An immediate observation is the improved resolution and quality of the data gathered using ADCP. The analysis will make assessments of the future energy yield through appropriate harmonic predictions that can feed into power production calculations and economic assessment models. Ultimately, this type of data will enable project developers to better estimate future revenue generation or, conversely be able to pre-determine that a site is in fact uneconomic for development.

The purpose of the analysis presented in this chapter was to quantify how well different sources of datasets represent the tidal flow conditions in a specific location. It was understood that, where available, in-situ measured data is most appropriate for site assessment. For the majority of the sites, tidal diamonds are the only source of data available to the author from the public domain. As tidal diamond data is generated from measurements taken over a 13 hour period, it does not capture the detailed variability that is obtained from a longer period of measurement. However, tidal diamond datasets are available for most of the UK coastal region and therefore are easily accessible. On the other hand, the Marine Atlas data is an output from a number of complex nested models (POL) that provide long term average snapshots over a spatial resolution of 1.8 km^2. Therefore, a way to *improve* the time-series generated is by combining the interpolated dataset obtained using tidal diamonds

and scaling it to the long term average values from the Marine Atlas for each of the specific sites. This way it is possible to generate a time-series that combines the temporal variability obtained from tidal diamond measurements but also benefits from the model runs used to produce the Marine Atlas.

Although tides are highly spatially variable, as highlighted in this chapter, the IDW methodology presented in section 3.3 presents a *consistent, repeatable and scientific* means of combining datasets without the need to perform a full-scale site assessment and modelling, necessitating an extensive and expensive in-situ survey data and numerical modelling campaign beyond the scope of this analysis and although highly desirable is, as yet, unavailable on a UK wide scale. Therefore, using this methodology it is possible to generate time-series for any site of interest in the UK that is captured by the Marine Atlas and tidal diamonds.

The final outcome of this work is to use a combination of datasets, tidal diamonds, Marine Atlas and buoy/ADCP measurements to carry out a *national scale resource assessment*. This final analysis is presented in chapter 6.

4. Site Characterisation using ADCP

The analysis presented in chapter 3 used buoy data, which uses a current meter to measure the velocity. One of the limitations of using buoy data measurements is that it only captures the velocity at a specific depth. An updated and more accurate way to measure tidal currents is using ADCP which uses the theory of Doppler shift to determine the current velocity. This method of measurement can be highly accurate and depending upon the ADCP setup be used to measure the velocity vertically along the water column. An overview of ADCP setup and workings is presented in section 4.1.2.

This chapter presents analysis carried out using ADCP datasets to demonstrate the detailed information and site characterisation that is necessary for project scale development. A number of publications exist that highlight various methodologies for assessing the energy characteristics of the tidal resource and associated turbine generation performance in combination with a resource definition (DTI, 2007; EMEC, 2009a; EPRI, 2006). These documents primarily provide guidance on how to carry out a resource assessment study to estimate the AEP from the deployment of a device or an array of devices in a farm. However, important knowledge gaps have been identified in the publications, the analysis presented in this chapter strives to fill some of these gaps.

The analysis presented is a set of the methodologies developed using previous documentation and knowledge to build on the understanding of site specific characterisation. This work is in support of the International Electrotechnical Commission (IEC) Technical Committee (TC) 114 (62600-1-3) Resource Characterisation and Assessment Standards development activity. TC114 was established in 2007 to develop standards for wave and tidal energy converters with the current focus being development of Technical Specification (TS) documents embodying existing best practice for the development of tidal current energy technologies and projects. The TS documents under development address design requirements for marine energy converters, resource characterisation, performance and

quality assessment of electricity generated from wave and tidal energy converters (Nadeau, 2010).

The development of these international standards is important as they provide a basis for ensuring reliability and safety and can be used as a set of benchmarks for comparisons between different technologies locally and internationally. Development of these documents is hindered by the lack of experience in the community in defining good examples of best practice. Addressing this issue, the research presented here is focussed on embodying evidence, advice and examples of suggested best practice in support of the development of the IEC TC 114 documentation and methodologies.

4.1 Site Selection

Initial site screening should take the form of regional studies using existing datasets like tidal diamonds and the Marine Atlas to identify an appropriate site perimeter of interest. If the site shows any potential, the specific region should be considered for a pre-feasibility study to identify relevant characteristics. This should be followed by surveys in the form of vessel mounted transects and bottom mounted ADCP data in order to do a detailed analysis. Bathymetry information is also highly relevant. The data collected will be primarily used for site assessment but can also be used to tune the device to the specific site in order to optimise generation.

Although ADCP data interpretation has a long track record, application in a tidal energy context is under developed. It is the intention of this chapter to highlight the use of ADCP data for site specific analysis. The case study demonstrates the use of data in identifying key metrics relevant for project planning and development.

4.1.1 Sound of Islay

The site, the Sound of Islay - is a narrow channel between the islands of Jura and Islay, in the Inner Hebrides, Scotland. This site is a fairly sheltered location and the water depth in the

channel ranges from approximately 12 to 60 meters. Tidal velocity acceleration is due to hydrodynamic mechanisms where large volumes of water are forced through narrow channels. The adjoining water bodies can be out of phase, resulting in a pressure gradient that drives the current. Figure 4.1 is a detailed map of the site and the location of the two ADCP deployments.

As of March 2011, the Sound of Islay is the world's first fully consented tidal array project, with lease, grid connection and planning consent. Construction is due to commence in 2013. The project is being developed by SPR as part of their phased approach to Marine Energy. The candidate device (HS1000 by Hammerfest Strøm) will initially be tested at EMEC's test site to establish technology performance and operation, followed by the 10 MW demonstration array project at Sound of Islay and finally the 95 MW project at Duncansby in the Pentland Firth.

4.1.2 ADCP Overview

An Acoustic Current Doppler Profile (ADCP) can be used to record water current velocity. ADCPs can record current velocity along the entire vertical water column. The device in its most common configuration comprises of a number of diverging acoustic beams that measure the water velocity at regular intervals (usually referred to as bins). The ADCP data used in this analysis was obtained from bottom mounted instruments with the beams facing upward. Four beams are used in the ADCP to obtain velocity in three dimensions, with an error velocity calculation to evaluate data quality.

The measurements are taken assuming horizontal homogeneity of the water body. The devices operate at a frequency of 300, 600 and 1200 kHz. ADCPs used at higher frequencies have a better vertical resolution whereas lower frequency ADCPs can accept a much larger range of returning frequencies. Therefore, there is a trade-off between range and resolution.

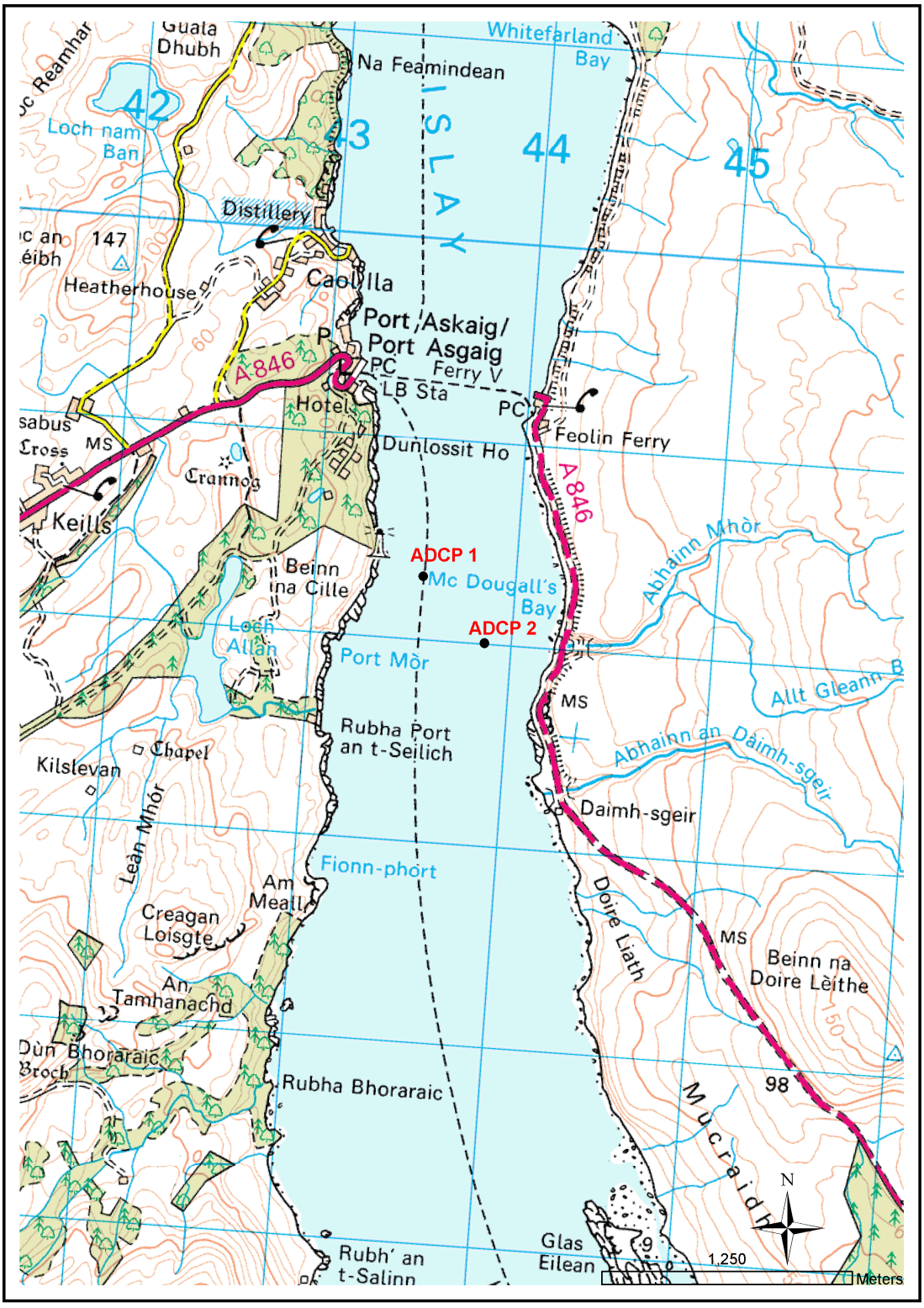

Figure 4.1 Sound of Islay map showing location of the ADCP deployment. Contains Ordnance Survey data © Crown copyright and database right (2010).

Figure 4.2 shows the most commonly used RD Instruments Workhorse Sentinel 4 beam ADCP in the 'Janus' configuration, named after the Roman god who looks both forward and back.

Figure 4.2 Standard RDI ADCP in 'Janus' configuration.

It is important to optimise the ADCP setup to get the best use out of it. There is a trade-off between the range the ADCP needs to work over, the resolution (depth) it needs to work at and random noise. Increasing the depth resolution linearly increases the noise and power consumption. Planning software such as PlanADCP is used to determine the amount of battery pack, memory and spatial/temporal resolution that are needed for the intended period of deployment.

The ADCP 'pings' at a fixed frequency and listens to echoes of returning sound waves from small particles suspended in the water. Depending upon the motion of the tidal currents, the returning scatter is Doppler shifted to a lower or higher frequency which is used to deduce the velocity and direction of the tidal current. However, often the echo near the sea surface is much stronger than anywhere else from the rest of the water column due to cavitations and side lobe suppression. Consequently, a certain amount of data near the surface needs to be rejected. This is particularly important where wide beam angles are used. Figure 4.3 shows the transducer beams at 20° where only 6% of the data can be contaminated but when the angle is increased to 30°, the contaminated area increases to 15%.

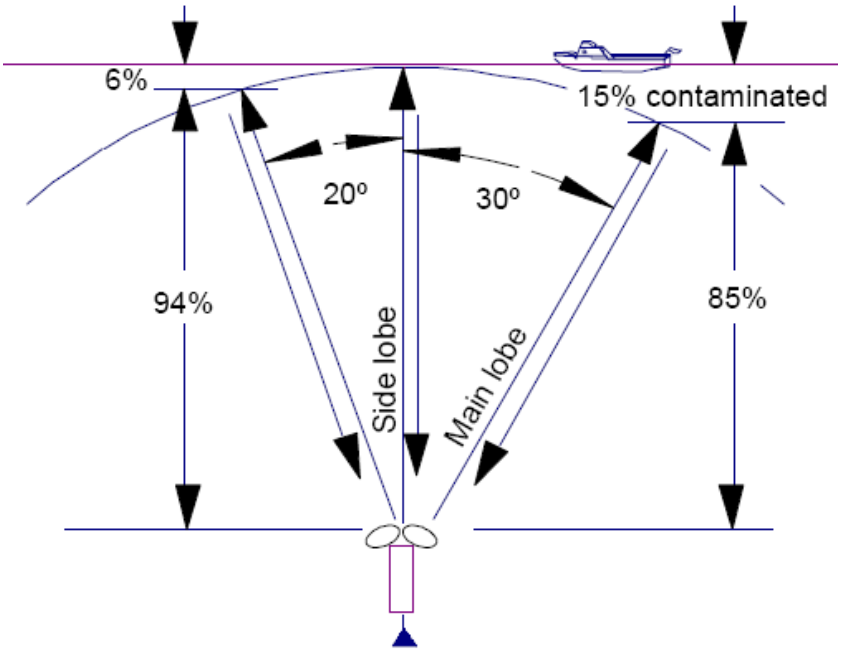

Figure 4.3 Side view of the ADCP showing the transducer, showing the 4 beams (RDI, 1996).

To maintain horizontal homogeneity in the measurements, velocity measurements are averaged over the same depth for measurements taken across different cells. This becomes particularly relevant at high pitch and roll angles, see Figure 4.4.

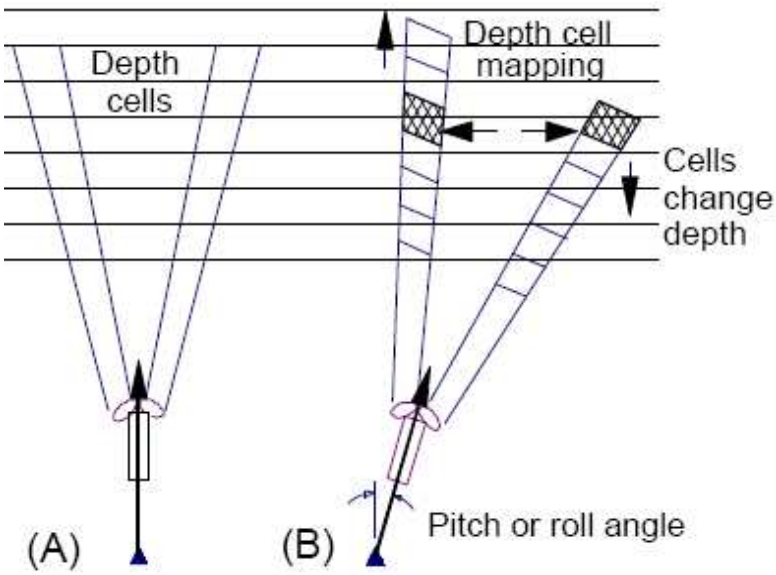

Figure 4.4 ADCP tilt and velocity averaging over different cells (RDI, 1996).

A number of quality control measures are in place to check that the data measured is 'good' and meets the necessary criteria. These quality control measures take the form of (RDI, 1996):

1. Testing the *Echo Intensity* where the decibel measure of the return echo is compared to the original ping.
2. *Correlation* between the different beams to measure data quality.
3. *Percent-good* is a threshold that identifies the proportion of data that passes a variety of conditions such as correlation, error velocity and fish detection.

4.2 Dataset Analysis

This analysis aims to define and use a standardised set of metrics so that direct comparisons can be made between the data presented here and other sites. The methodology is applied to two ADCP datasets from the site 500 metres apart to allow the degree of spatial and temporal variability in the tidal currents at this location to be quantified. The degree of variability is of significant interest in considering how representative a particular set of in-situ measurement data may be in the wider surrounding area of interest for large scale project developments.

For the ADCP measurements used in this study, any that had *Percent-good* data less than 80% is considered unacceptable and therefore tagged as 'bad'. The ADCP records collected have 7% of the datasets labelled 'bad', mostly from the surface bins, which is the area of highest error due to surface reflection.

The original data was presented in an Excel file where the measurements are tabulated as speed and direction for each bin along the water column. The first 9 values of the dataset were omitted for ADCP 1, so the data used in the analysis starts at 15/06/2009 at 16:02 and finishes at 17/07/2009 06:01. For ADCP 2, the start time is 15/06/2009 15:08 and finishes at 17/07/2009 16:44. Both the datasets have an ensemble period of 1 minute. Therefore, the majority of the deployment overlaps and is coincident in time.

The missing data was in small clusters and occurs all over the time-series. The measured data spanned over 32 days and the current velocities are measured every minute. Therefore, it was possible to conduct harmonic analysis using the Least Square Harmonic Analysis and Prediction programs provided by NOAA (Zervas, 1999). Before conducting any analysis, the missing data gaps had to be bridged. Data from different depths could not be used to fill the missing gaps as clusters of missing data spanned over time and across various depths. Additionally, at this point in the analysis the velocity variation along the vertical profile was unknown.

Linear and cubic interpolation was used to fill in the missing data. Interpolation works well as the period of the constituents in the time series varies slower than the sampling interval. Figure 4.5 illustrates an example where missing data is interpolated using the two mentioned techniques at the 44th bin.

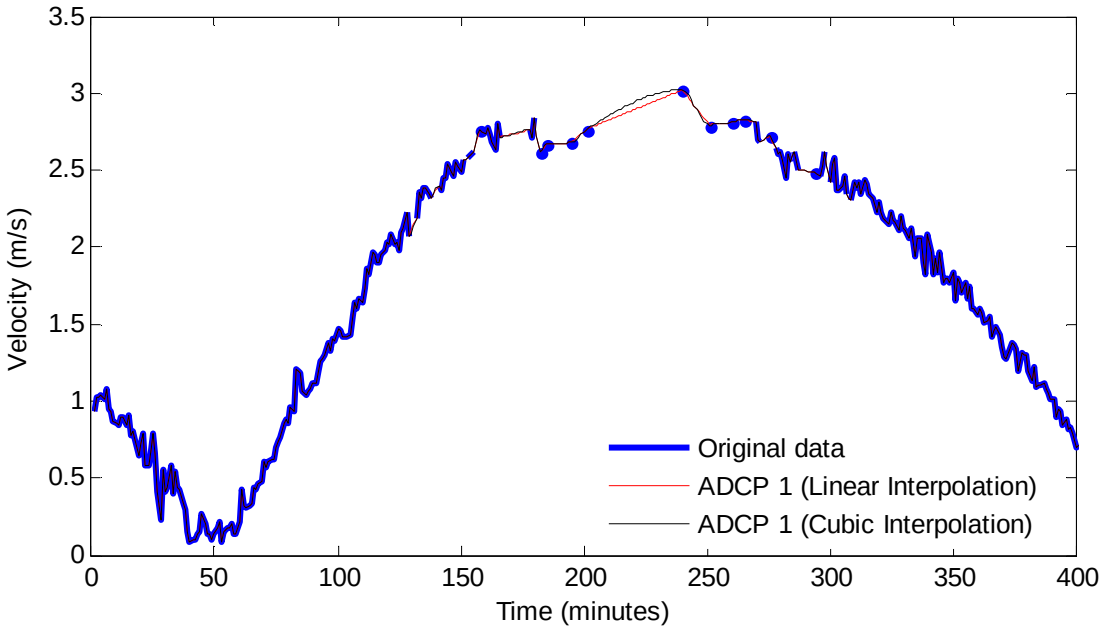

Figure 4.5 Example of Linear and Cubic Interpolation used to fill 'bad' data.

The data presented in this graph is one of the worst cases where no data was collected for nearly an hour. The interpolation was necessary in order to facilitate the calculation of depth averaged velocity values and enable harmonic analysis to be conducted. The high temporal resolution of the dataset meant that both the interpolation techniques

worked well, as although 7% of data is reported as ‘bad’, it is spread throughout the record and not all clusters of missing data occur at high velocities. The final analysis was conducted using cubic interpolation as it better maintained the sinusoidal envelope of the tidal time series. Moreover, the absolute error from the recreated time series (for the original time period) using harmonic analysis (discussion in section 4.3) when compared to the original measurements has a marginally smaller error value for the cubic technique than the linear interpolation technique.

For the purpose of calculating the available power a device hub height of 20 m above the sea bed is assumed, as depth averaged values could produce lower velocity and power values, giving an underestimation for the site. No further assumptions were made about device characteristics. All the calculations are prepared using bin 17 from the ADCP dataset which corresponds to a region between 19.7 m and 20.7 m in the water column, so that no assumptions need to be made about the device swept area. This is done assuming that measurements are made at the ‘centre’ of the bin rather than the ‘edge’ of the bin and include the 3.2 m bin range from the bottom. Therefore, the water depth is calculated using:

$$3.2 – 0.5 \text{ (to the edge of the bin)} + 17 = 19.7 \text{ m.}$$

The total depth of the water column is 55 metres as recorded by the ADCP sensor. The depth averaged velocity as presented here is obtained by averaging only the first 45 bins from the bottom. The top 5 bins are removed from the record as including the rise and fall of the tides would cause variations in the water height. With most of the data missing in the top bins due to contamination from strong surface echo scatter, this also reduces averaging across the interpolated data. Moreover, no device will operate in this region due to restrictions such as device diameter and the device blades possibly inducing cavitation leading to premature failure. Therefore, the top 5 meters are not included.

It should be noted that the first bin measurements are at 3.2 m above the sea bed (due to blanking range where measurements cannot be taken. The transducer does not operate well in this region because the signal is contaminated.), and hence the expected

lowest velocity occurrence measurements are unavailable. In this context it is also acceptable to ignore the top 5 bins as both the top and bottom boundary layers are missed out. Although referred to as depth averaged velocity, when presented, the data is averaged between 3.2 m and 48.2 m. (Note: most of the metrics are calculated at hub height, depth average data is only used to present the data graphically.)

For all the analysis carried out for site characterisation, the metrics are separated into ebb, slack and flood tide where all velocities below 0.5 m/s are considered slack and discarded. In terms of energy generation, velocities of 0.5 m/s or less are not significant, as they do not provide enough torque to rotate the turbine and generate power or at least not in the first generation technologies considered at present. Ebb and flood regimes are determined using the principal axis decomposition, based on the direction of the current flow. The two regions are treated separately as each has specific characteristics and when combined together, this detail is missed out by amalgamation. The entire record is also analysed for all metrics, as this can be used to understand how biased the data is in any one direction.

Results from all the analysis on the two ADCP datasets are tabulated in Table 4.1. Discussions of how the metrics were calculated and their purpose is presented in the following section. Where relevant and available, they are compared with results from other sites and locations. The next section identifies eight parameters that characterise tidal flow and site assessment qualities using the Sound of Islay as a case study. The metrics presented are in the form of velocity, direction, power and vertical velocity profile.

4.2.1 Velocity

Figure 4.6 shows the complete tidal cycle for 32 days (depth-averaged data), with two spring and two neap cycles for each of the ADCPs. Nominally, for a tidal site to be considered economically viable and suitable for energy extraction mean Spring peak velocity should be above 2.5 m/s (B&V Phase II, 2005).

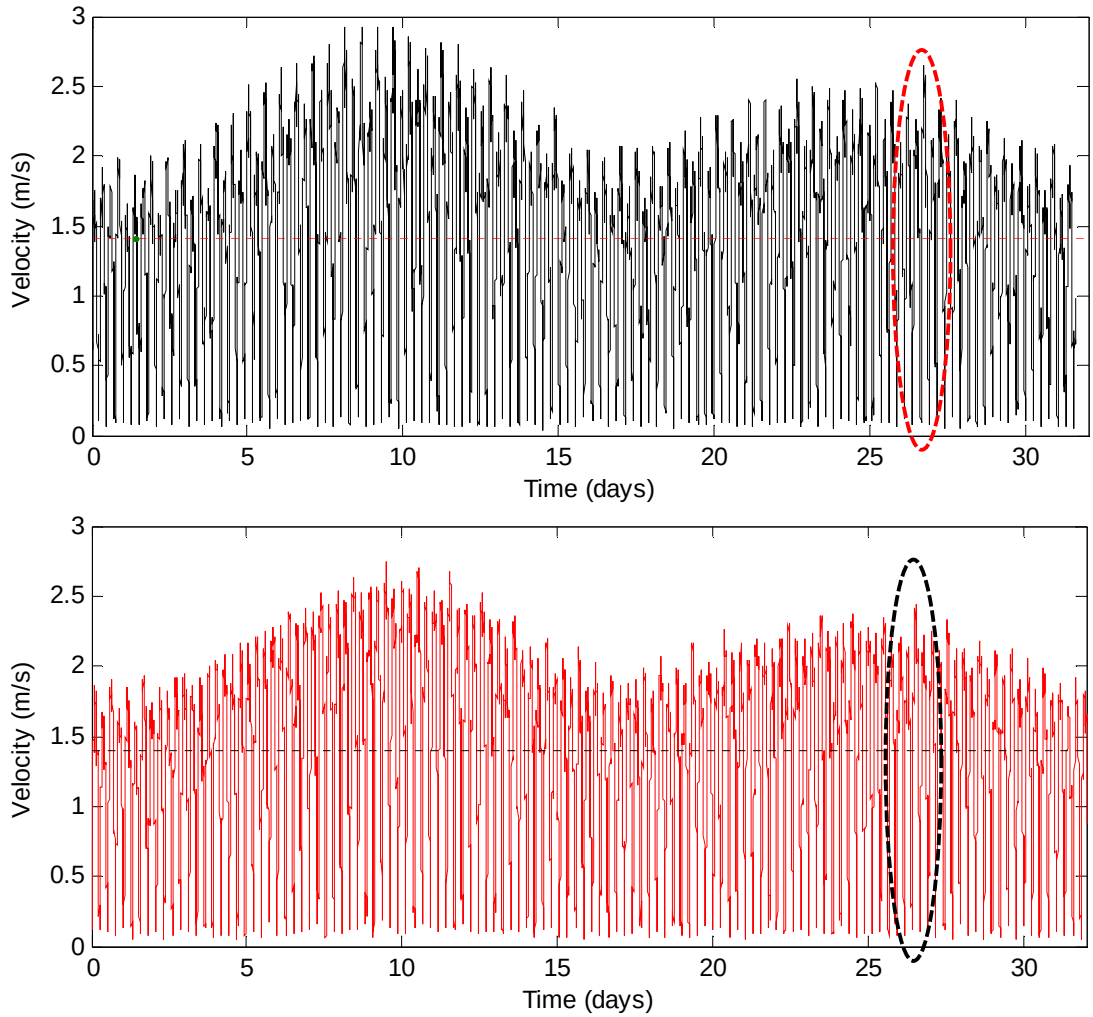

Figure 4.6 Depth averaged one month time series from ADCP 1 (top) and ADCP 2 (bottom). Circled region indicates outliers.

The mean depth averaged velocities for both the ADCP records are approximately 1.4 m/s, shown with a horizontal line in Figure 4.6. When compared to the Puget Sound sites in Washington as discussed in Gooch *et al.*, (2009), the Sound of Islay has a higher mean velocity. However, Culina *et al.*, (2011) report 6 observations at the Bay of Fundy, out of which 3 values are higher than the values presented here. Already, this initial presentation confirms that the Sound of Islay is a strong site and presents a good opportunity for tidal current energy extraction.

The ratio of average spring and average neap velocities (Spring-Neap ratio) is 0.7, higher than usual observations of 0.5 where the spring cycle is double the neap cycle. This is of particular interest as a higher ratio indicates that the site has a high overall capacity factor.

The value of using these metrics becomes useful when comparing spatial variability at other sites or in the process of identifying the most economic site.

On the 27th day of the measured time series a maximum wind gust speed of 35 knots was observed at a nearby port, Port Ellen. Although the wind speed is not very high, the direction coincides with the flow direction of the tidal current of approximately 140°, relative to 0° north (see section 4.2.2). Hourly values measured at this port along with the wind direction are shown in Figure 4.7. The meteorological effect reinforces the current velocity and can be identified as the outlier in both tidal envelopes, circled in Figure 4.6. This is an example of *non-tidal component* as introduced in section 2.1. The wind direction coincides with the principal current direction of ADCP 1 and therefore the reinforcement is much more evident for this particular set of measurements.

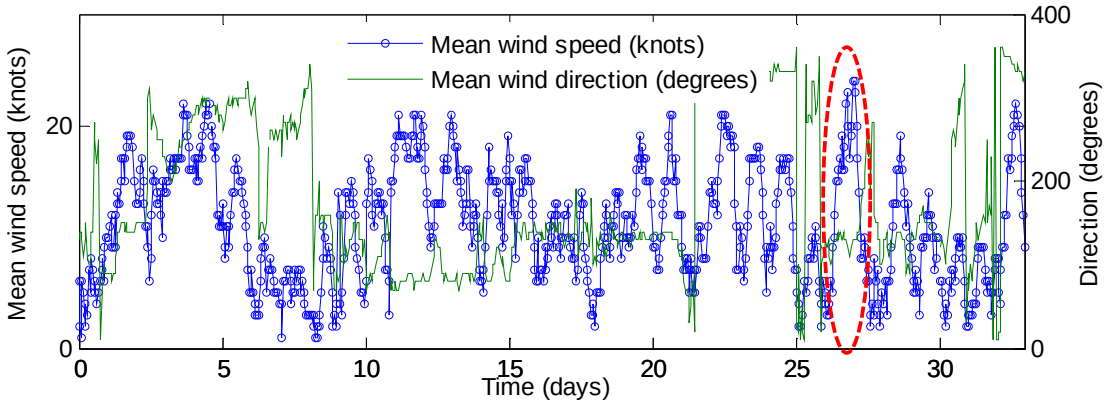

Figure 4.7 Mean wind speed and direction at Port Ellen.

4.2.2 Direction Plots

The flow direction provides vital information for device orientation, as most first generation tidal devices employ a fixed orientation axial flow turbine, primarily to keep the mechanics underwater simple. Tidal flow in a channel can be perfectly bi-directional but variations and skews can occur due to bathymetry or the surrounding land mass. If a rotary current is observed, then the device should be designed to yaw for maximum power capture. The sites presented by Gooch *et al.*, (2009) show asymmetrical ebb and flood conditions which may best suit devices that can yaw.

Directionality can also play a key role in designing the support structure and assessing the impact the device and the supporting structure must withstand (streamlining for wake effects, etc). Therefore it is important to have the optimum orientation for effective energy extraction. Figure 4.8 is an x-y scatter plot showing the bi-directional nature of this site. The lines indicate the principal current direction for ebb and flood along with the standard deviation for each case. In both cases, the standard deviation on the flood tide is slightly higher than that of ebb. Both the ADCPs present broadly rectilinear flow conditions that are ideal for a device not designed for yawing.

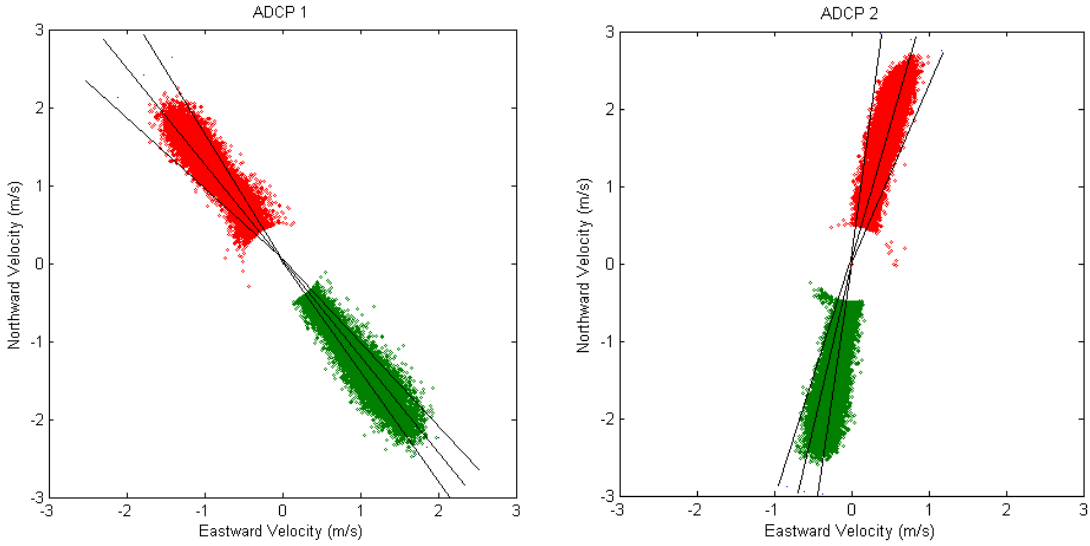

	ADCP 1	ADCP 2
Ebb (green)	142 ± 4°	192 ± 5°
Flood (red)	324 ± 8°	15 ± 8°

Figure 4.8 X-Y scatter plot, mean axes and standard deviation of ebb (green) and flood (red) tides at hub height for ADCP 1 and ADCP 2.

Note that the two ADCP measurements have significantly different principal current directions. ADCP 2 was deployed 500 metres south-west of ADCP 1 (see Figure 4.1). Although both the ADCP's are deployed in similar depths, the bathymetry and the channel appears to steer the flow. Also, it has been observed that the channel has a 'V' shape vertical profile, the Sound is narrower at the bottom and opens up towards the top. This could

potentially cause blockage in the bottom-most layers and offer an explanation for the significant directional change between ADCP 1 and ADCP 2.

4.2.3 Power Plots

Figure 4.9 shows the velocity histogram at the assumed hub height. The tidal velocity is binned into 0.10 m/s bins (0 m/s to 0.10 m/s = 0.05m/s). Both the ADCP datasets present similar velocities and power values. Comparing this output to the American sites in Gooch *et al.*, (2009) suggest that this is a more productive site, the 'peak' occurrence between 1.5 and 2 m/s creates a higher power density. The distinct peak between 1.5 and 2 m/s is best explained due to the site's high spring to neap velocity ratio. A spring to neap ratio of 0.5 would have an even velocity distribution, but a higher value than this will result in a hump towards the higher end of the velocity distribution. Similarly a value below 0.5 would result in a peak towards the lower end of the distribution. A rated velocity of 2 m/s would be appropriate for this site, for two reasons:

1. It has a high percentage of occurrences and,
2. It follows the rule of thumb where rated velocity is 70% of the maximum spring peak velocity (B&V Phase II, 2005).

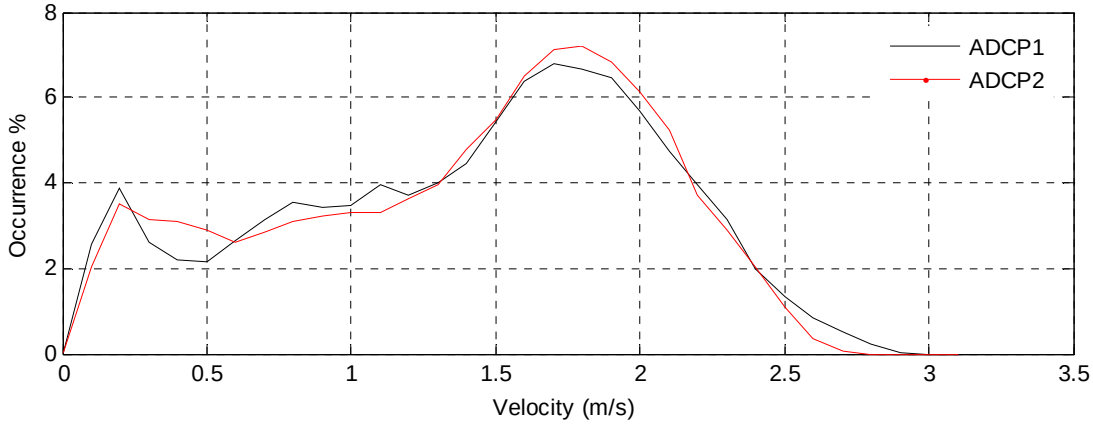

Figure 4.9 Velocity histogram as a percentage of total occurrences for ADCP 1 and ADCP 2.

The guidelines by EMEC (2009a) and DTI (2007) suggest that this histogram should be multiplied by the device power curve to obtain power output. If the velocity histogram

covers a relevant period of time (1 month), then it is accepted that the data captures the majority of the velocity distribution and is suitable for project feasibility evaluation. For tidal currents, seasonal variations are negligible compared to wind or wave resource. This velocity distribution can potentially be used to calculate power output for the project lifetime without the need for further analysis. This is a very important assumption and analysis presented in chapter 5 uses various methods to quantify and compare between different durations of datasets to assess how this affects power output.

A better way to present this data is shown in Figure 4.10, where an exceedance curve is used to show the velocity distribution between the two datasets. From these curves it can be identified that for 80% of the time, the velocity exceeds 0.7 m/s. The majority of the first generation devices do not cut-in until the velocity is above this value. Therefore from this graph, it is evident that for 20% of the time an installed device will generate no power.

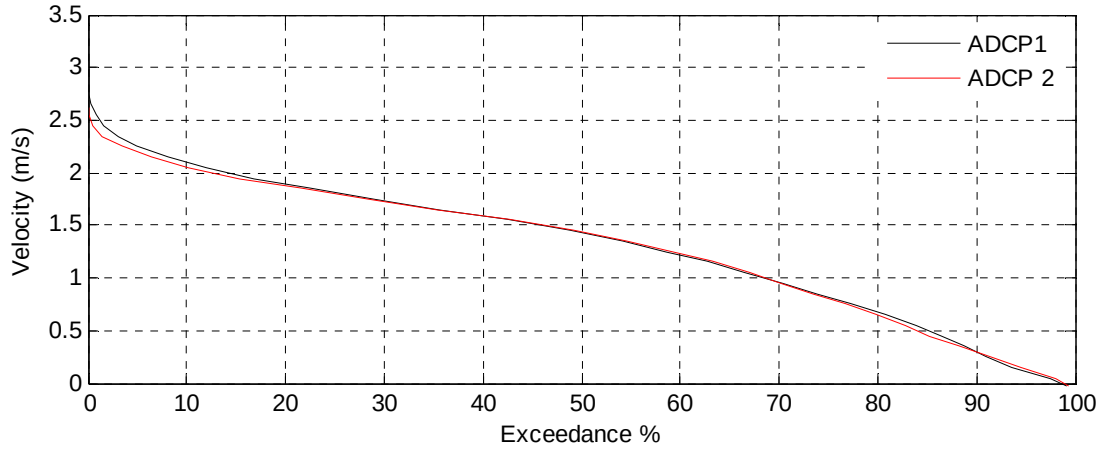

Figure 4.10 Tidal current velocity exceedance histogram for ADCP 1 and ADCP 2.

The exceedance curve presents the percentage of time velocity exceed a certain value. It should be possible to determine the rated velocity by understanding the amount of time the generic device needs to operate at rated power to obtain an economically acceptable capacity factor (of 30% adopted from the wind industry). The exceedance plots of other energetic sites are presented in chapter 6, where a different method of determining the device rating is identified. The findings of chapter 6 suggest that in order to have an economically

viable device and capacity factor, a rated velocity based on the 10% velocity exceedance is considered sensible. This method delivers a consistent capacity factor across a number of sites compared to the B&V Phase II method of device rating, see Figure 6.9.

Another aspect to consider is that the maximum velocity measured at this site does not exceed 3 m/s. This is an important consideration when building a device, as they must be able to withstand the maximum load imposed by the tidal currents. The kinetic power density of the two ADCPs is shown in Figure 4.11 (in 1 kW/m^2 bins) as calculated using equation 2.6 (chapter 2).

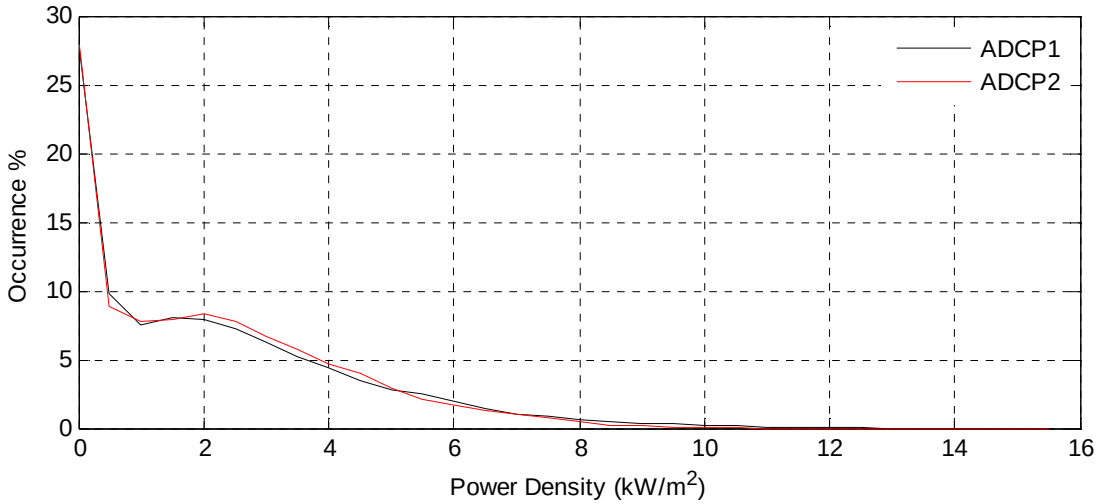

Figure 4.11 Power histogram probability density function.

Device characteristics such as cut-in, rated velocity and efficiency are not considered, just the raw energy available in the resource. The small 'hump' present between 1 and 3 kW/m^2 is related to the peak in velocity occurrence observed in Figure 4.9 between 1.5 and 2 m/s. Power exceedance curve is presented in Figure 4.12.

4.2.4 Maximum Sustained Velocity

Maximum sustained velocity is a measure of the highest velocity sustained for a period of 5 minutes. This is calculated by considering velocities over 5 minute windows, until the highest moving persistence level is obtained. A similar metric has been proposed by the EMEC standards (2009a), suggesting a 10 minute window. In reality the window period is

dependent on the ensemble period of the measured data. Both the ADCPs have 5 minute periods where the velocity is sustained at above 2.6 m/s. The absolute highest velocity occurs elsewhere in the dataset. For example, the maximum velocity measured by ADCP 1 was 2.93 m/s, but this velocity is not sustained for more than a minute and is of less importance in characterising the site. This metric has more merit when making assumptions about the forces experienced by the device for a sustained short term period and the rated velocity in the pre-design and evaluation phase.

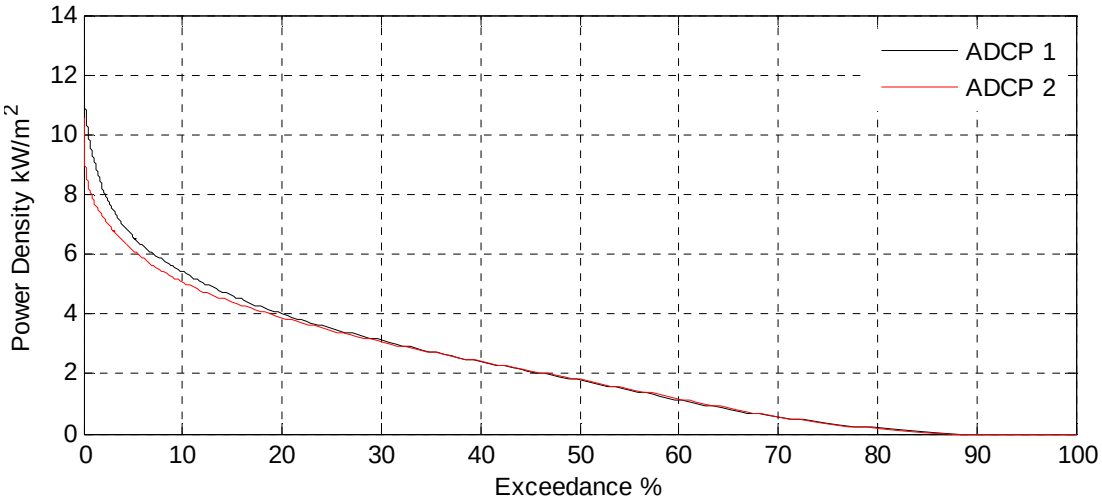

Figure 4.12 Power density histogram for ADCP 1 and ADCP 2.

4.2.5 Eddy Intensity

Eddy intensity (or turbulence intensity) is the ratio of the velocity fluctuation in the horizontal plane over a much larger area with respect to the background velocity. These fluctuations are characterised as turbulent structures caused by flow conditions and the local bathymetry. Turbulence metrics are important in terms of device design. A thorough analysis using high frequency ADCP data is presented by Osalusi (2011). However, for the Sound of Islay, limited by the temporal resolution, eddy intensity is calculated as suggested by Gooch *et al.*, (2009):

$$I = \left\langle \frac{v'}{\bar{v}} \right\rangle - \left\langle \frac{n}{\bar{v}} \right\rangle \tag{4.1}$$

where I is the eddy intensity, $\bar{v}$ is a 15 minute centred running velocity average, v' is the velocity anomaly where $v' = v - \bar{v}$ represents the velocity with its temporal mean removed. The angle brackets imply a mean over the entire dataset. This value is only computed for bin 17, at the 20 m hub height, shown in Table 4.1.

The value of n is the intrinsic noise in the ADCP measurements, which depends on the ADCP set up (frequency, bin size and pings per ensemble). In the analysis presented here n is calculated as:

$$n = \frac{1}{\sqrt{N}_p \times h} \times \alpha \tag{4.2}$$

where Np is the number of ping per ensemble, h is the bin size of the ADCP and α is the single ping standard deviation (obtained from the Workhorse Sentinel ADCP data sheet[2]). For ADCP 1 and ADCP 2, *n* is calculated as 0.0141. When comparing these values to the sites presented in Gooch *et al*., (2009) the eddy intensity values for all the sites are within the same range. However, the overall eddy intensity for ADCP 1 is 5.27%, a little higher than the ADCP 2 value of 3.88%. The higher values are also consistent for the ADCP 1 ebb/flood region compared to the ADCP 2 values. This shows that, even though the two ADCP measurements are nearby, ADCP 1 experiences much higher turbulence than ADCP 2, highlighting the need for multiple ADCP deployments to get a full site survey.

4.2.6 Flood/Ebb Asymmetry

Symmetrical flow implies that the device rotor, blades and machinery will experience the same loading and wear during both the flood and ebb flow. Large asymmetry can cause difficulty as device performance may be affected and generation may be biased. Asymmetry can cause premature failures due to uneven wearing and can be computed as the difference between the ebb and flood angles:

[2] RDI Workhorse Sentinel datasheet can be obtained from http://www.rdinstruments.com/datasheets/wh_sentinel.pdf

$$Asymmetry = | \theta_{ebb} - \theta_{flood} - 180 | \quad (4.3)$$

A perfectly bi-directional site would have an asymmetry of zero degrees. ADCP 1 and ADCP 2 have small asymmetry, about 1°, indicating a small percent of uneven loading on the device. Larger asymmetries can cause premature loading, which can amount to large maintenance and operation cost, highlighting the importance of this metric.

4.2.7 Vertical Shear

The force exerted by strong tidal currents can be very large especially when considering specific design aspects of the device. The turbine needs to withstand a number of forces created by the velocity variations. Vertical shear can be defined as the change in velocity with height. In terms of device specification, the change in velocity along the blades is highly relevant. The shear is calculated using the bins below and above the assumed hub height. Ebb and flood regimes are considered separately but are based on ebb and flood flow values of the hub height bin. The average shear is expressed as a scalar magnitude as in Lu *et al.*, (1999) and in Gooch *et al.*, (2009) as:

$$\frac{d\,|v|}{dz} = \frac{|v_{hh-1} - v_{hh+1}|}{\Delta z} \quad (4.4)$$

Subscript *hh* is for the bin closest to hub height. Δz is the overall bin range, in this case 2 m as each bin is 1 m in size. Even though only the velocity magnitudes are considered, it is assumed that the flow direction above and below hub height are similar. This assumption worked well in this case as the bins are only 1 metre apart. Figure 4.13 shows that the direction does not change above and below the hub height, because the channel is rather narrow, the flow direction is restricted. However, in wider channels and out in the open sea, the flow direction may not be the same throughout the water column.

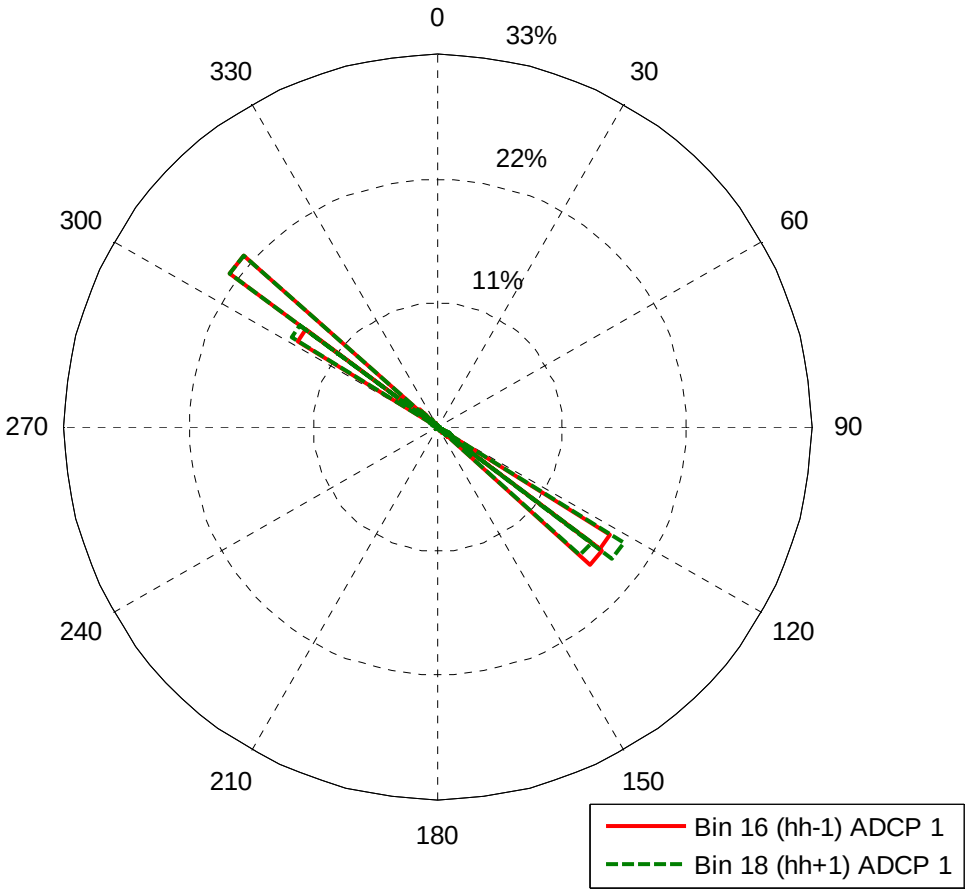

Figure 4.13 Tidal rose showing the flow direction above and below hub height.

Average shear velocity for ebb and flood are tabulated in Table 4.1. The values are similar for ebb and flood showing consistency and indicating no persistent uneven loading in any one specific direction. The average values are in the range of 0.015 - 0.02 m/s per m. The maximum shear for each record is as high as 0.2 m/s per m, however this force does not accumulate across the rotor diameter. Vertical shear calculated across the rotor diameter, assuming a 16 metre diameter is 0.01 m/s per m with maximum values of the order of 0.05 - 0.06 m/s per m; these values are much smaller as it is an average value cross the rotor diameter. The maximum shear occurs nearest to the sea bed. For specific design calculations, data of much higher temporal resolution is desirable for detailed analysis.

4.2.8 Vertical Velocity Profile

It was necessary to understand the vertical velocity profile so that an appropriate hub height could be determined for the device or to assess the impact of pre-selecting a specific hub height. The power law profile is best estimated using equation 2.9 (chapter 2). This formula can be used to estimate the tidal velocity at a specific height in the water column. These values are typically applied in fluid mechanics and have been carried over from the wind industry. Although wind and tidal energy have similar characteristics, particularly as power is proportional to velocity cubed and tidal turbines are often referred to as 'under-water wind turbines'. However, there are some fundamental differences, for example wind resource only considers the average profile but tidal has recurring patterns of ebb and flood.

The metrics presented so far have identified differences between ebb and flood flow conditions and these variations become significant in locations that are not rectilinear, where ebb and flood are not 180° apart. Upstream conditions can also alter the strength of the flow, which may be in the form of a slope or other bathymetric conditions. These can affect the strength of the flow in one particular direction. Additionally, no power is generated during slack tide as velocity is below cut-in, the profiling should be specific and split into ebb and flood cycles to identify how these variations may affect device performance.

Figure 4.14 shows the profile for measurements from ADCP 1 averaged over time. The profile is broken down into flood and ebb periods based on the velocity and direction at bin 17 to assess how the flow profile varies under different conditions. (Note, only velocity magnitudes are shown in the figures.) A fit for the profiles was obtained by using the MATLAB Curve Fitting Toolbox. The exponential power value is left unknown and computed using a nonlinear least square fitting methodology. For ADCP 1 the fit was uncomplicated and ranges from a $1/7.1^{th}$ profile in the ebb region to a $1/8.4^{th}$ profile in the flood region. Overall, the region can be presented using a $1/7.5^{th}$ fit profile. In this case the generic $1/7^{th}$ profile represents this measurement well, with the tendency to slightly over

estimate velocity near the bottom and top of the water column, but with a good match in the vicinity of the hub height (20 m).

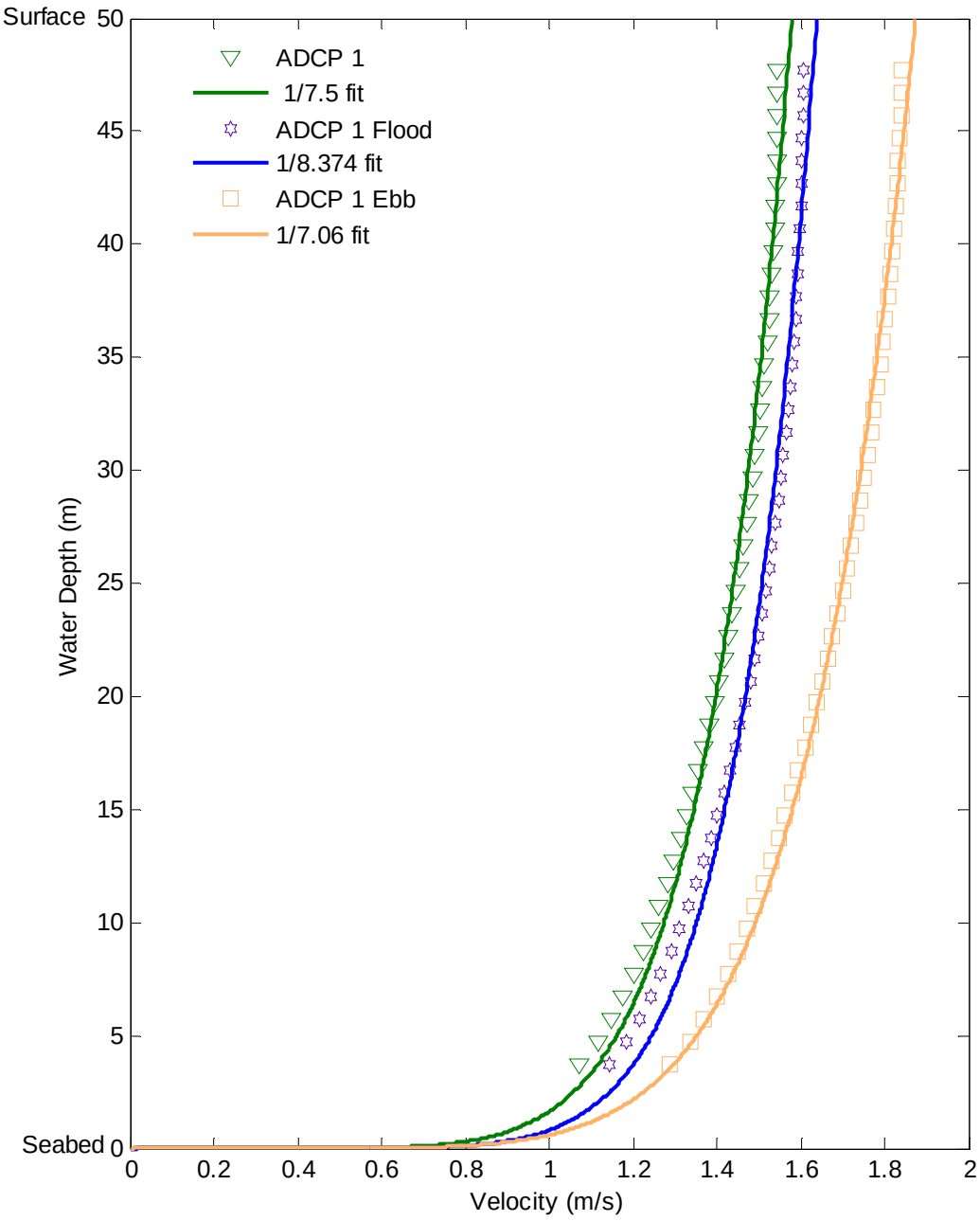

Figure 4.14 Average vertical velocity profile for ADCP 1.

The profile measurements from ADCP 2 are complicated by the seabed bathymetry, as shown in Figure 4.15. This effect is highlighted in the ADCP 2 flood regime, where two different power profiles have been used to fit the measured values. The profile suits well at different depths, the bottom half is a 1/6.9th profile up to 20 metres and the above 20 metres a

1/19th profile is identified as a suitable fit. The top half is similar to a linear profile for the rest of the water column where average velocity is 1.6~ 1.8 m/s (see Figure 4.16). This profile is similar to the scaling factor used in the DTI Marine Atlas (DTI, 2004b) and also shown in equation 2.7 and 2.8.

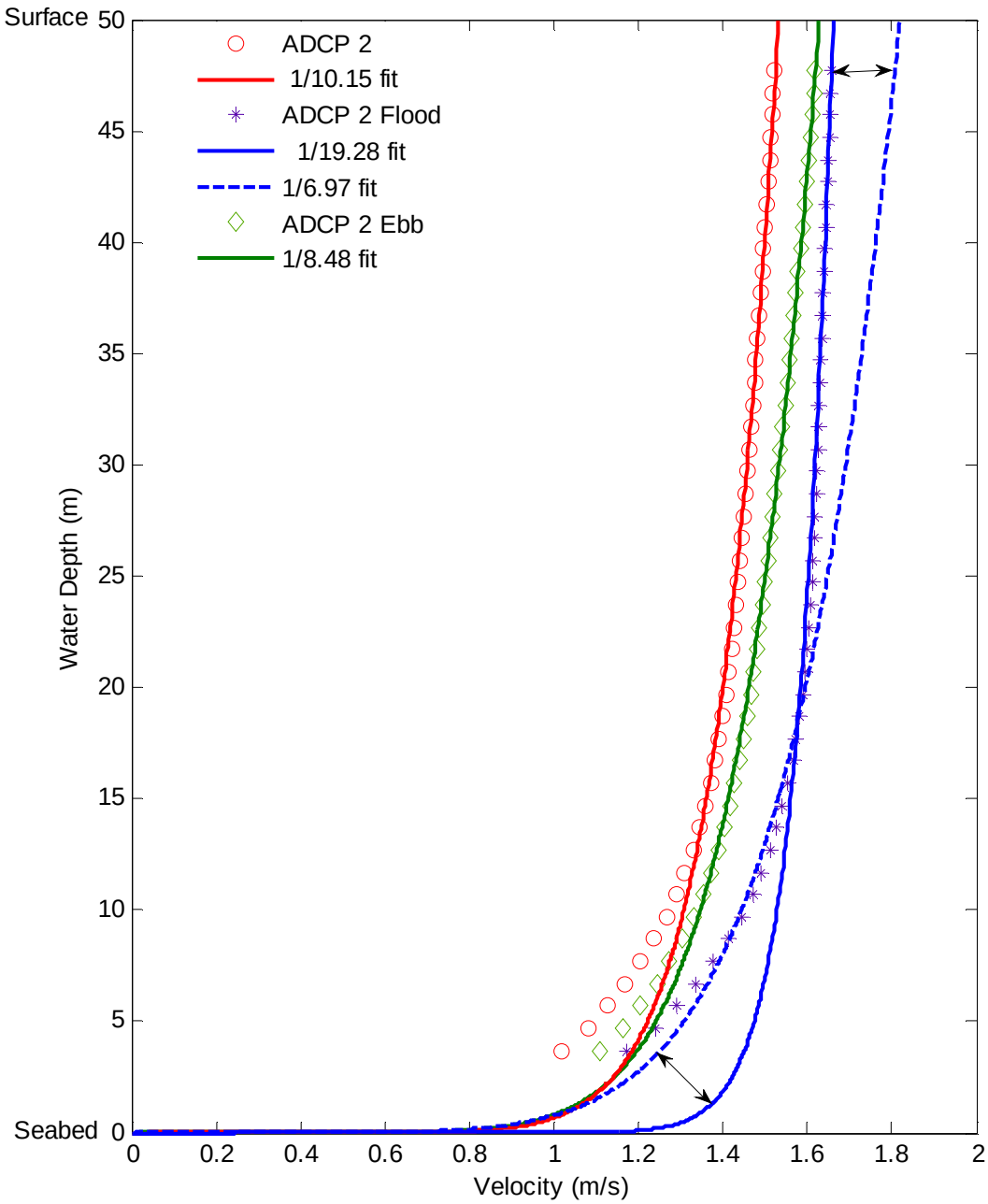

Figure 4.15 Average vertical velocity profile for ADCP 2.

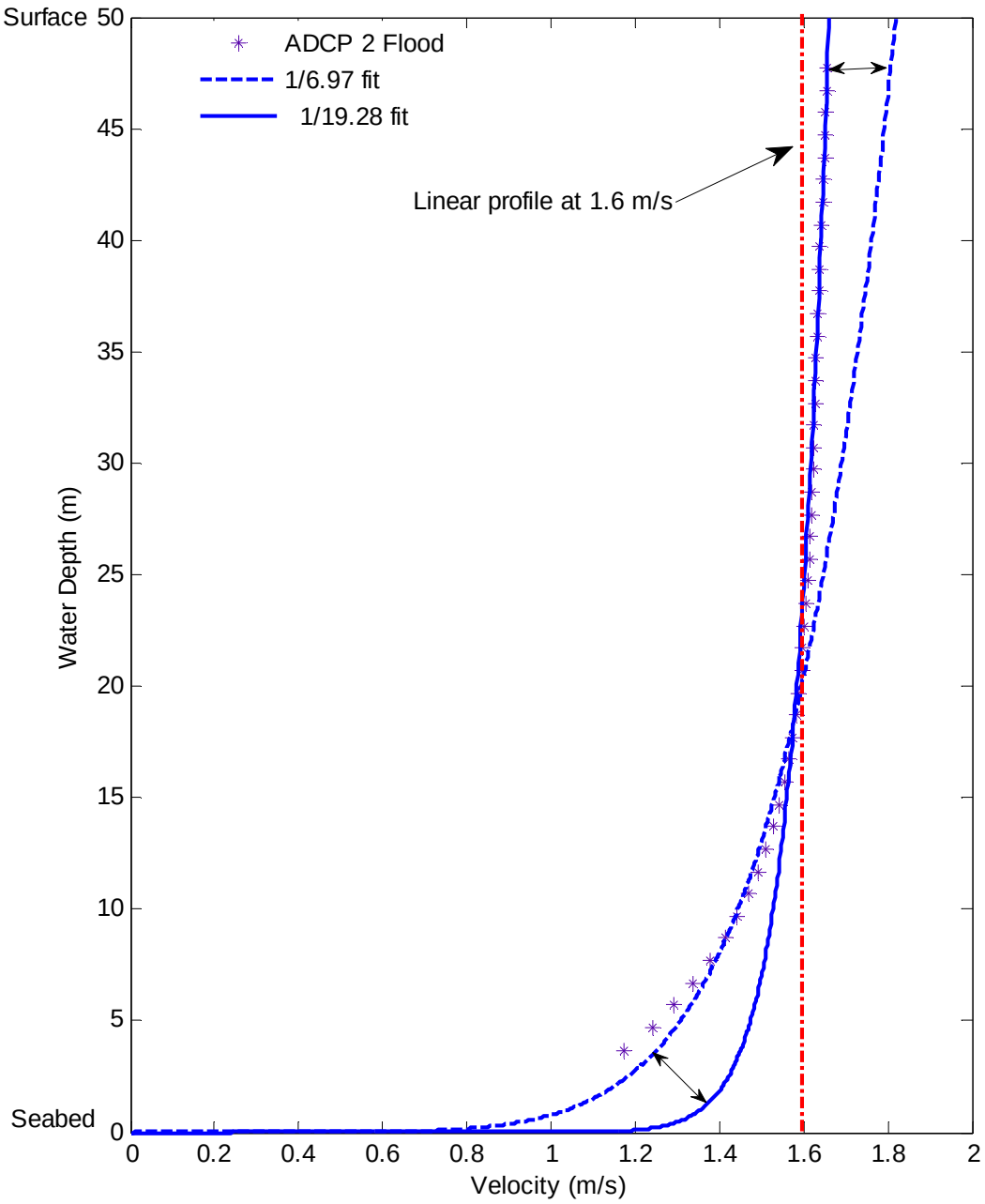

Figure 4.16 Linear profile for the top half of the water column in the ADCP 2 flood region.

The findings of Iyer *et al.*, (2009a), present vertical velocity profiles split for the Spring and Neap tidal conditions. It is thought that splitting the profile based on ebb and flood conditions is a better way of characterising the flow conditions as it omits slack tide when no power is generated. Analysis from both sites (Anglesey and the Sound of Islay) suggests that most sites do not fit any of the common profiles. All the sites discussed by

Gooch *et al*., (2009) present a number of vertical profile variations ranging from 1/5th profile to 1/10th profile.

The velocity profile also enables to understand the flow variation along the diameter of the device rotor and this can be used to evaluate how strong the rotor will need to be to withstand this thrust. As thrust is proportional to velocity squared, assuming a 16 metre device diameter, variation of 1.3 m/s to 1.7 m/s from top to bottom of the blade amount to a 23.5% variation in velocity and a 41.5% variation in the thrust force.

The most significant understanding that emerges from this is that depending upon the ebb and flood angle alignment and the strength of the flow in each direction, the device power curve and efficiency will vary between the cycles. Instead of developing a generic power curve for the device in the design phase, it is suggested that, based on the vertical velocity profiles, the strength of the flow in the ebb and flood direction and the angle alignment *two* power curves should be developed which will reduce inaccuracies when calculating AEP. To demonstrate this idea, Figure 4.17 shows the power curve for MCT's SeaGen, a full scale prototype device tested at Strangford Narrows. The power curve indicates that ebb flow is marginally stronger than flood. Calculating AEP based on these two curves will give a more accurate estimate of AEP than using a generic power curve.

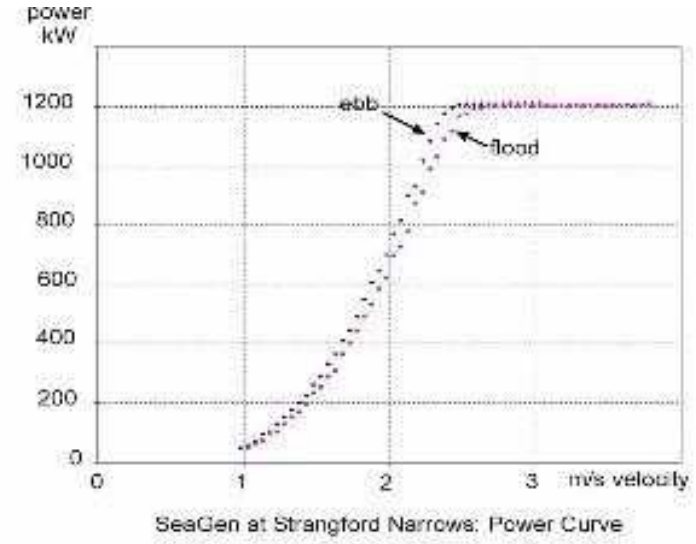

Figure 4.17 MCT SeaGen's power curve. (MCT, 2010b)

			ADCP1	ADCP2
	SITE			
		ADCP Measurement duration (days)	32	32
		ADCP Vertical resolution (m)	1	1
		ADCP Sampling interval (min)	1	1
		Mean depth (m)	52	50
		Assumed hub height (m)	20	20
	VELOCITY			
		Mean velocity magnitude (m/s)	1.39	1.41
		Neap Spring Ratio	0.68	0.74
		Max sustained velocity (m/s)	2.72	2.67
		Eddy intensity %	5.27	3.88
		Flood/ Ebb asymmetry	1.12	0.92
		Average Vertical shear (m/s per m)	0.018	0.015
		Maximum Vertical shear (m/s per m)	0.210	0.180
	DIRECTION			
		Principal axis direction (deg)	142.82	12.52
		Standard deviation (deg)	18.27	18.27
		Flood/ Ebb asymmetry (deg)	10.30	7.06
	POWER			
		Mean power density (kW/m^2)	2.23	2.28
		Ebb/flood asymmetry	1.45	0.79
	VERTICAL PROFILE			
		Power law exponent 1/(α)	7.5	10.2
		R -squared (α)	0.98	0.99
EBB	**VELOCITY**			
		Mean velocity magnitude (m/s)	1.64	1.51
		Max sustained velocity (m/s)	2.72	2.44
		Eddy intensity %	3.69	2.42
		Avg Vertical shear (m/s per m)	0.019	0.015
		Max Vertical shear (m/s per m)	0.185	0.162
	DIRECTION			
		Principal axis direction (deg)	141.83	191.74
		Standard deviation	3.89	4.53
	VERTICAL PROFILE			
		Power law exponent 1/(α)	7.1	8.4
		R -squared (α)	0.99	0.99
	POWER			
		Mean power density (kW/m^2)	2.97	2.30
FLOOD	**VELOCITY**			
		Mean velocity magnitude (m/s)	1.47	1.64
		Max sustained velocity (m/s)	2.47	2.67
		Eddy intensity %	3.97	2.24
		Avg Vertical shear (m/s per m)	0.018	0.015
		Max Vertical shear (m/s per m)	0.206	0.180
	DIRECTION			
		Principal axis direction (deg)	323.50	15.01
		Standard deviation	8.33	8.01
	VERTICAL PROFILE			
		Power law exponent 1/(α)	8.4	7.0
		R -squared (α)	0.99	0.97
	POWER			
		Mean power density (kW/m^2)	2.06	2.95

Table 4.1 Key metrics for site characterisation from ADCP 1 & 2.

4.3 Harmonic Analysis

As the ADCP data was collected over a month long period, harmonic analysis can be used to predict tidal time series using Least square or Fourier analysis. This process, if reproduced accurately can significantly reduce the amount of time and money spent collecting data as it provides a credible means of 'extending' the time-series. It is becoming critically important to get good current measurement data for sites of potential economic interest, as such analysis will essentially estimate the life time production of the site and provide good revenue estimates.

The least square harmonic analysis conducted on the ADCP data presented here follows the same methodology as discussed in chapter 3, section 3.2.

4.3.1 Least Square Harmonic Analysis using ADCP data

Table 4.2 shows a brief explanation of the resolved constituents for ADCP 1. The 23 constituents resolved by the *lasha.f* program for a representative 'mean year' as well as the amplitude and phase for the specific year the data comes from. M_2 is the most dominant constituent, with a magnitude H of 2.14. This alone accounts for 89% of the site's variation. 99% of the tidal variations were resolved for this dataset using the harmonic analysis program. The remaining 1% was missed due to non-tidal components and unresolved harmonic constituents. Short term variability in the record has limited impact on harmonic analysis using the least squared analysis technique.

To verify the harmonic constituents generated and asses how well they represent the site, the constituents are used by the prediction program *pred.f* to recreate the time-series spanning the original measured period. Figure 4.18 shows a scatter plot of the original current data and the reconstructed data for ADCP1. The regression line shows as linear fit with a high R^2 value indicating good agreement.

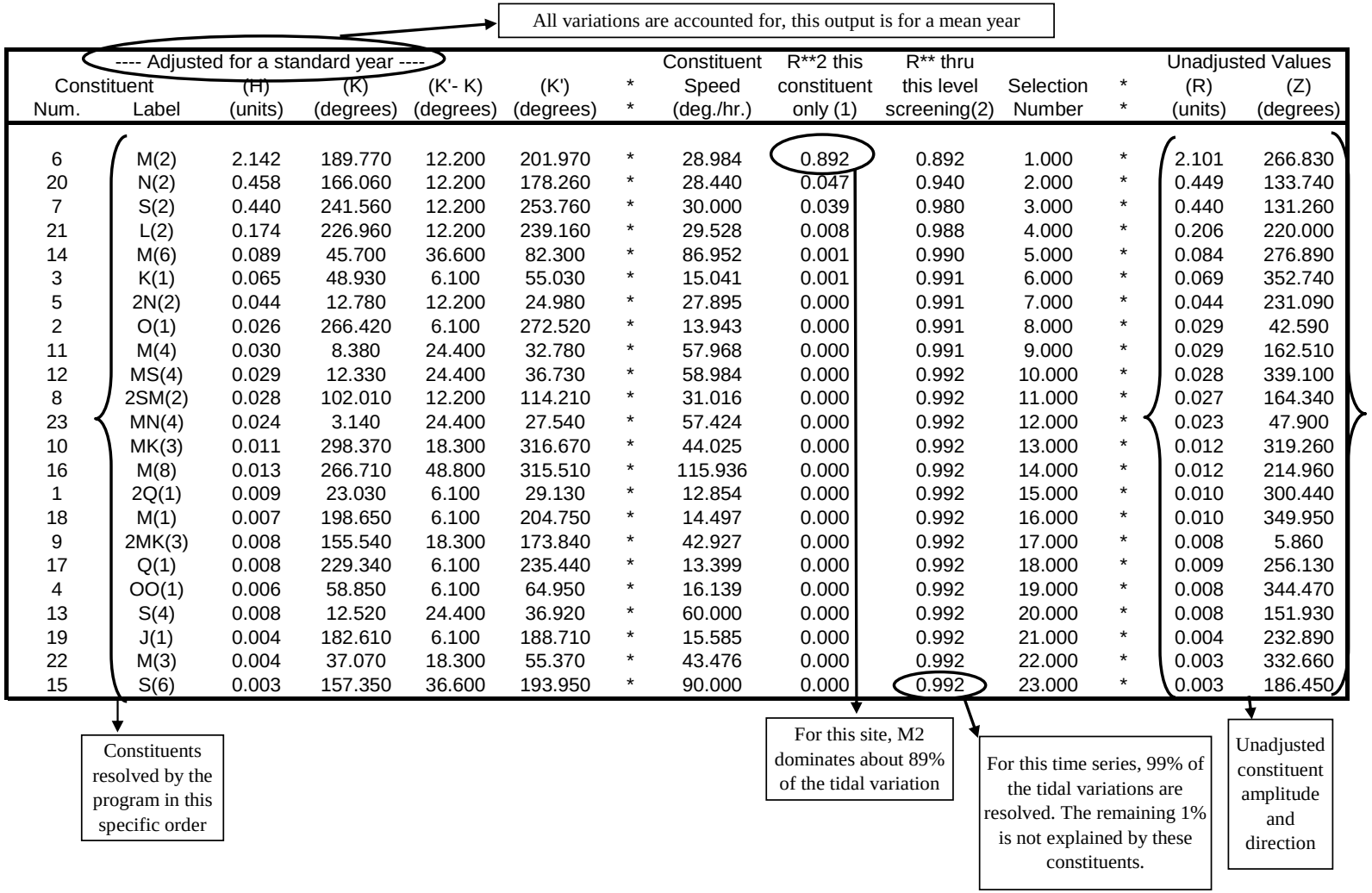

Table 4.2 Output from the NOAA Least Square program explained.

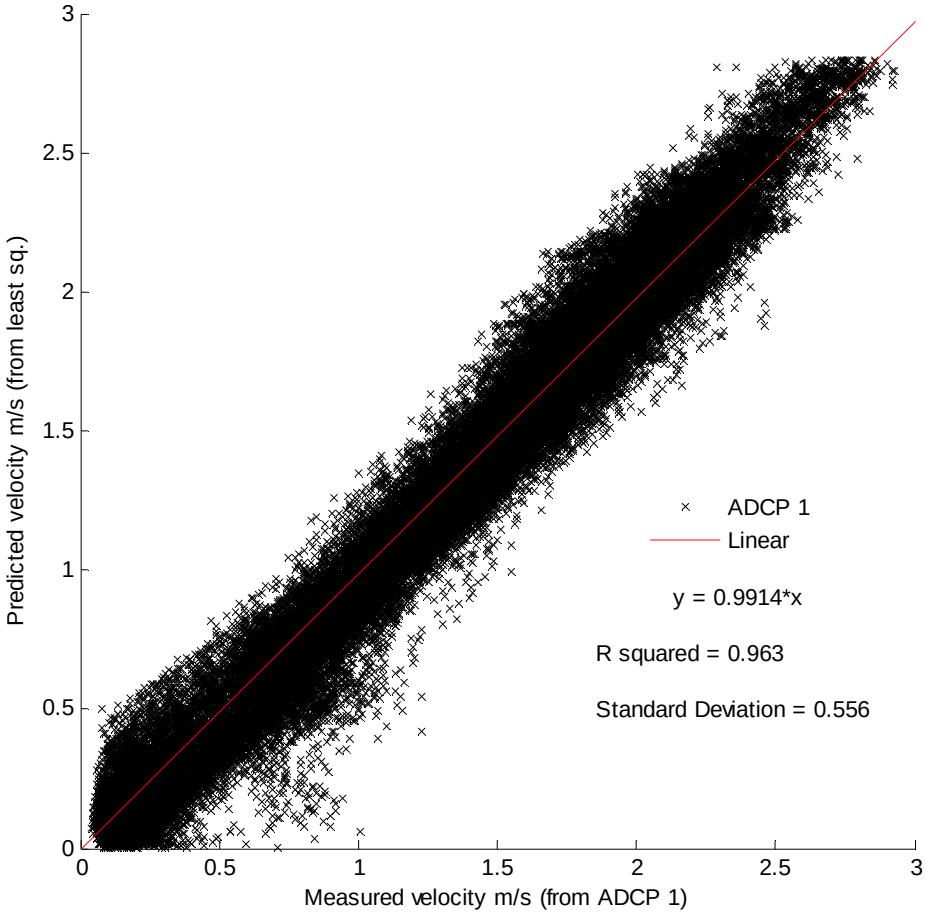

Figure 4.18 Plot comparing between the original and reconstructed data using 23 harmonic constituents.

Figure 4.19 shows the output from the prediction program compared with the measured values from ADCP 1, as well as the residual error. It can be seen that, while there is some scatter, the fit is good and exhibits good homogeneity. The data recreated using the prediction program shows good correlation and follows the tidal envelope well. The outlier on the 27th day as shown in section 4.2.1 can be seen. The residual between measured and predicted value is the largest here, as harmonic analysis does not account for any local meteorological variations.

Looking at the residual velocity, it was identified that a lot of the peak velocity values around the spring peaks were missed. This is a limitation of using 23 constituents and highlights the errors introduced by using harmonic analysis. Over a short period, these errors

do not accumulate but, if harmonic analysis were to under predict peak values for the entire lifetime of a project, it could have significant impact on the AEP and adversely impact the site economics. Harmonic analysis provides an easy and reliable way of predicting tidal current over long periods of time and depending upon the quality of the input data, can provide very valuable insight into the site. Further analysis presented in chapter 5, evaluates the errors introduced using harmonic analysis.

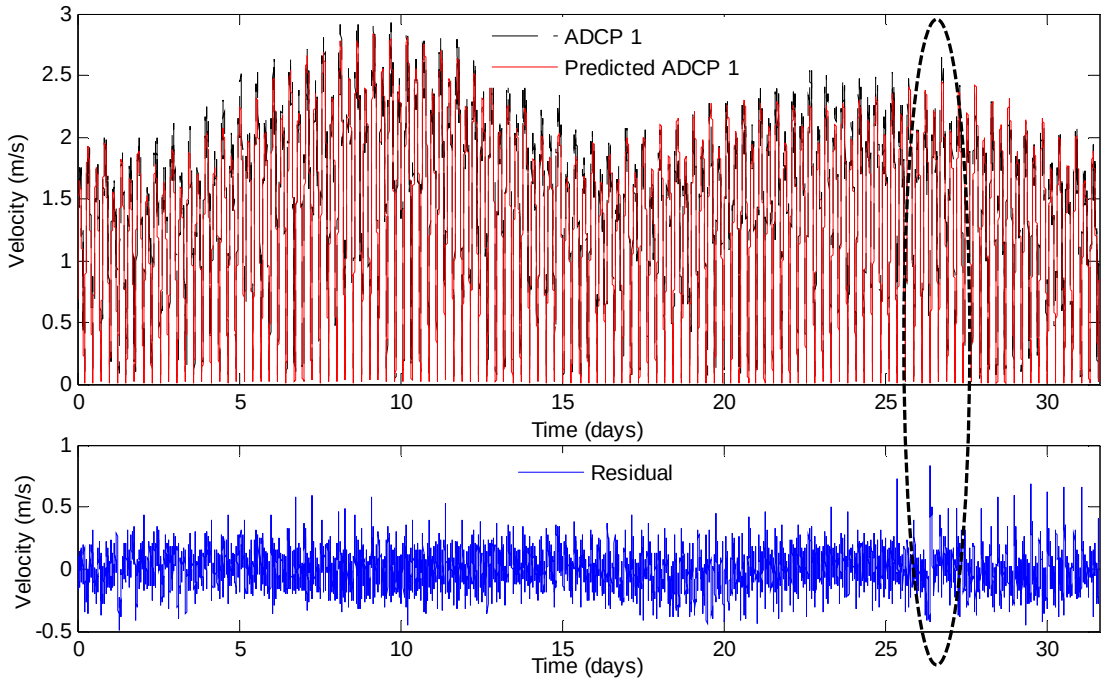

Figure 4.19 Plot comparing ADCP 1 measured and predicted. Residual variation shown as well.

In order to compare the constituents obtained from the different ADCPs, Figure 4.20 shows the weighting of all the constituents obtained from the *lsqha.f* program. For both the ADCP data, M_2 values have been scaled to 100 and all the other constituents are scaled relative to it for each dataset. Small differences can be observed between the two set of constituents. Note that the magnitude of the constituents significantly diminishes after the first ten constituents. Resolving any additional constituents will have negligible impact on the overall output. Only the amplitude of the constituents are presented here, the phase angle also plays a key role.

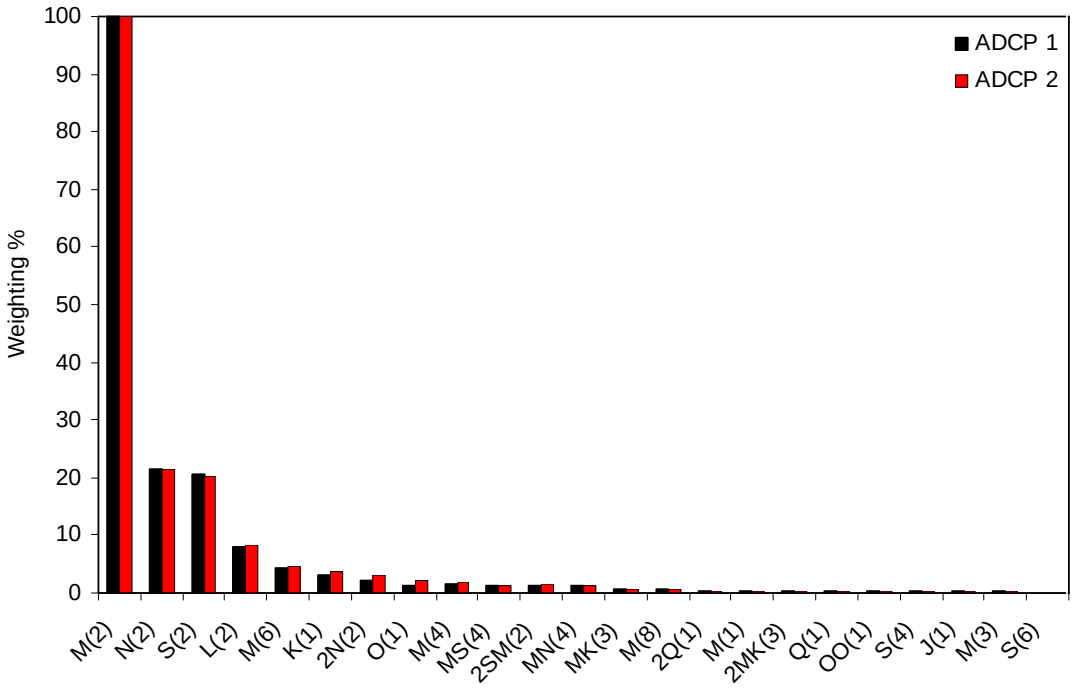

Figure 4.20 Constituent weightings form different ADCP measurements.

4.3.2 Statistical Analysis using ADCP Data

To qualitatively compare between the measured data and the recreated data, statistical methods have been adopted. The MAE, RMAE, Model skills and Cross Correlation coefficient as defined in chapter 3 are presented here. Table 4.3 presents values for ADCP 1 and ADCP 2 measured values compared to the predicted values using the harmonic analysis. The RMAE varies less than 10%, indicating a good match. (Note, values presented in chapter 3 are not expressed as percentages.) A model skills value of 0.9 suggests that this harmonic analysis represents the data well as 1 indicates perfect agreement. Similarly, the cross correlation coefficients for both the datasets agree well too.

Performance Metrics	Units	ADCP 1	ADCP 2
Mean Absolute Error (MAE)	(m/s)	0.132	0.127
Relative Mean Absolute Error (RMAE)	(%)	9.336	9.063
Model Skills (u)	(m/s)	0.997	0.986
Model Skills (v)	(m/s)	0.989	0.991
Cross Correlation (u)	(m/s)	0.994	0.973
Cross Correlation (v)	(m/s)	0.994	0.995

Table 4.3 Performance measure of measured vs. predicted values for ADCP 1 and ADCP 2.

4.4 Effect of Time Varying Ensemble Periods

The next analysis investigates the effect of varying ensemble periods for the data measured. This is akin to altering the set-up of the ADCP to have different levels of resolution. An additional point of interest is to understand the accuracy of the NOAA harmonic analysis program utilising data with different sampling period. Similar analysis has been presented by Stiven, (2010) for datasets obtained from EMEC.

Data for ADCP 1 measured in 1 minute intervals was used to create an average over 5 minutes, 10 minutes, 15 minutes, 30 minutes and 1 hour periods to generate data with different sampling intervals. This is a similar effect to setting the ADCP device to have equivalent ensemble averaging periods but it maintains the resolution of the number of 'pings' in the record.

Table 4.4 shows the set up to test the outcome of different sampling periods with the NOAA software. Case (a) examines the impact of varying the data sample input from 5 minutes to 1 hour and simulates output resolution of 1 minute data. Case (b) examines the impact of down sampling the original 1 minute dataset to a lower value to compare the performance of the harmonic analysis. Case (c) is a combination of the previous two cases, where the input and output samples are of the same temporal resolution.

The first line in bold is the predicted data for ADCP 1 using harmonic analysis. This first output is considered the 'gold standard', and all the outputs are compared to this value. Results from case (a) highlight that, as the ensemble period is increased, peak measured velocity values are missed (through amalgamation over a longer ensemble period), and averaged values are similarly reduced (generally only slightly). This would lead to an underestimation of predicted power available. However, the percentage difference in the calculation is generally very small, less than 1% in all the cases except for the hourly data.

	Data resolution		Velocity m/s Output		Average Energy kWh/m^2		Average Energy Difference	%
	Input	Output	Mean	Peak	Input	Output		Difference
Case (a)	1 min	1 min	**1.388**	2.835	2.2483	**2.2540**	base case	
	5 min	1 min	1.388	2.835	2.2388	2.2541	0.0001	0.003
	10 min	1 min	1.387	2.835	2.2349	2.2513	-0.0027	-0.122
	15 min	1 min	1.387	2.833	2.2314	2.2479	-0.0061	-0.269
	30 min	1 min	1.384	2.827	2.2160	2.2352	-0.0188	-0.834
	1 hr	1min	1.369	2.801	2.1641	2.1690	-0.0850	**-3.772**
Case (b)	1 min	5 min	1.388	2.834	2.2540	2.2539	-0.0001	-0.005
	1 min	10 min	1.388	2.833	2.2540	2.2538	-0.0002	-0.009
	1 min	15 min	1.388	2.831	2.2540	2.2538	-0.0002	-0.009
	1 min	30 min	1.387	2.819	2.2540	2.2531	-0.0009	-0.039
	1 min	1 hr	1.389	2.795	2.2540	2.2539	-0.0001	-0.003
Case (c)	5 min	5 min	1.388	2.835	2.2388	2.2540	-0.0001	-0.002
	10 min	10 min	1.387	2.833	2.2349	2.2510	-0.0030	-0.132
	15 min	15 min	1.387	2.829	2.2314	2.2478	-0.0063	-0.277
	30 min	30 min	1.384	2.813	2.2160	2.2350	-0.0190	-0.841
	1 hr	1 hr	1.370	2.763	2.1641	2.1688	-0.0852	**-3.779**

Table 4.4 Test setup to show the velocity and power output using different ensemble periods.

Case (b) uses 1 minute data as input and compares the effect of increasing the sampling resolution on the output dataset. It is observed that the percentage difference between all the datasets is negligible, even the 1 hour dataset. Therefore, as long as the original input data is of a high temporal resolution, down sampling at a later stage does not significantly impact on the velocity and power accuracy. It also highlights that the harmonic analysis programs ability and performance is dependent on data resolution used to obtain the harmonic constituents.

Case (c) is a combination of the previous two cases and confirms what is understood from (a) and (b). In order to test this, the time-series was fed into the program at different resolutions and the results are output at the same resolution as the input. In this case the effect of varying ensemble period along with the software's capability to cope with the changes is tested. The percentage difference is essentially a composite of case (a) and case (b).

The analysis so far has averaged the existing data when reducing the data to lower resolution. This is equivalent to maintaining the number of pings in the full record, but reducing the ensemble period. This would be of benefit to reduce data storage requirements on the ADCP unit, but would still have a similar drain on the battery. The alternative, where the number of pings is reduced and spread more widely across a lower resolution ensemble period, would likely introduce more error into the harmonic analysis and hence reduce the accuracy of the power calculations presented in Table 4.4.

To clarify this, in order to generate the equivalent 5 minute input ensemble record used in Table 4.4, the 5 surrounding 1 minute data records (82 pings per ensemble) have been averaged together – equivalent to capturing 410 pings within the 5 minute period. If the intention was to save battery usage[3], a reduced number of pings could be used within the 1 minute records, or a similar density of pings across a longer time period could be selected. If a longer time period was utilised (say 5 minutes), with the same ping density (82 pings in the ensemble), then both battery and memory storage usage would be reduced, hence enabling a longer deployment.

4.5 Conclusions

Reducing uncertainties and errors are key to successful project development. The analysis presented in this chapter identifies a fit-for-purpose set of metrics that can be used for site specific analysis which can help reduce errors and uncertainties. The use of existing documents (DTI, 2007; EMEC, 2009a) has provided a good starting point, however implementing the methodologies suggested by these documents has identified distinct knowledge gaps. Applying the methodology to a real site and a set of measured data has enabled 'learning-by-doing', for example none of the documents specified a way of filling in for missing data. The chapter presents the metrics for the overall data as well as splits it into

[3] Battery use reduces because the number of pings emitted is less, therefore reducing the energy required to emit pings. One of most limiting factor in terms of ADCP usage is memory and battery life, particularly for longer deployments. Therefore, increasing battery life in this way can often be a huge benefit.

ebb and flood. This is predominantly to understand if the flow is skewed in any one direction and how this may affect the overall power output.

The metrics can be used as an indicator to evaluate how economic the site is and provide a way of comparing different sites and help target appropriate device and technology type suitable for the site. Understanding the variation in the vertical velocity profile and the difference in the profile variation between the flood and the ebb cycle has also provided valuable insight. These findings will make a significant contribution to the IEC Standards currently under development.

The time-series generated from the harmonic analysis is still subjected to spatial variability. In order to get a complete understanding of the spatial variability at a specific site, numerical models need to be coupled with harmonic analysis for validation. The variability of the resource is likely to increase in locations that are more open and exposed to weather related such as strong wave action, wind action and storm surge. This would undoubtedly reduce the accuracy of any predictions made using harmonic analysis techniques. Although harmonic analysis is a powerful tool for removing small scale background ‘noise’ in a data record, it is unclear how it would be impacted by a record subject to many storm related events. More importantly, prediction from a harmonic analysis constituent set would not capture any weather related effects and hence would not be as accurate in predicting a record (or any time period) subject to such conditions. An obvious extension would be to include weather models and implement operational oceanography and forecasting to further reduce errors.

The exercise of varying the ensemble period indicates that increasing the measurement intervals up to 30 minutes does not significantly affect the velocity and power output estimates obtained from the measurements taken at this specific site. An ensemble period of greater than half an hour will under predict the overall AEP and will have an impact on the project economics and development. For example, a specific installed capacity may be chosen based on an under predicted AEP, which will be below optimum and

adversely affect the project economics when a larger installed capacity (based on a higher AEP with smaller error bars) could have been viable.

Finally, it was identified that two sets of ADCP measurements should be taken. The first set of measurements with the purpose of resource assessment and site characterisation can be taken at a lower ensemble period, up to 30 minutes, but be deployed for a long duration of time, 29 days or more. The second set of measurements should be taken at a much higher resolution to calculate metrics specific for device design, but can be deployed for a shorter duration of time.

5. Project Feasibility Study

With the intention of further reducing uncertainty and error, the analysis presented in this chapter is a follow on from chapter 4. Site specific metrics are calculated for the Fall of Warness, a tidal test site in Orkney. The data used in this analysis has been collected by the European Marine Energy Centre (EMEC) over the period from 2005 to 2007. Only specific records were considered for full analysis based on the total length of each of the records. The aim of this chapter was to better understand the spatial variability of tidal currents by assessing multiple data points. The Fall of Warness is a more open channel than the Sound of Islay and exhibits higher spatial variability. Errors introduced by harmonic analysis and long term variability over the intended project life time are also presented.

5.1 EMEC Dataset

Table 5.1 shows the EMEC Surveys available for the Fall of Warness. Figure 5.1 maps the location of all the deployments. In the analysis presented here, site specific metrics identified in chapter 4 have been calculated for Surveys 6a, 6b 7, 10, 11 and 13.

Survey / Action	Latitude deg minutes N	Longitude deg minutes W	Depth (m)	*Number of Days*	*Ensemble period (s)*	*Packets*	File Size
Survey 3	59°08.581'	002°48.449'	35.7	*13.9*	*1200*	*yes*	62.8MB
Survey 6a	59°08.040'	002°48.440'	41.8	*16.0*	*1200*	*yes*	80.5MB
Survey 6b	59°08.040'	002°48.440'	41.8	*16.4*	*20*	*no*	91.2MB
Survey 7	59°08.443'	002°48.757'	49.3	*33.2*	*600*	*no*	5.51MB
Survey 8	59°07.909'	002°47.996'	36.0	*14.0*	*1200*	*yes*	62.5MB
Survey 9a	59°09.292'	002°49.572'	30.5	*8.0*	*1200*	*yes*	36.2MB
Survey 9b	59°09.292'	002°49.572'	30.5	*20.9*	*1200*	*yes*	94.0MB
Survey 10	59°09.323'	002°49.515'	26.4	*40.7*	*1200*	*yes*	183MB
Survey 11	59°09.430 '	002°49.540'	15.1	*25.0*	*1200*	*yes*	157MB
Survey 12	59°08.208'	002°48.469'	44.6	*6.9*	*1*	*no*	600MB
Survey 13	59°08.147'	002°48.391'	36.2	*32.0*	*30*	*yes*	175MB
Survey 14	59°09.046'	002°48.935'	35.2	*31.4*	*0.5*	*no*	1.91GB

Table 5.1 EMEC Survey data available for this analysis (EMEC)

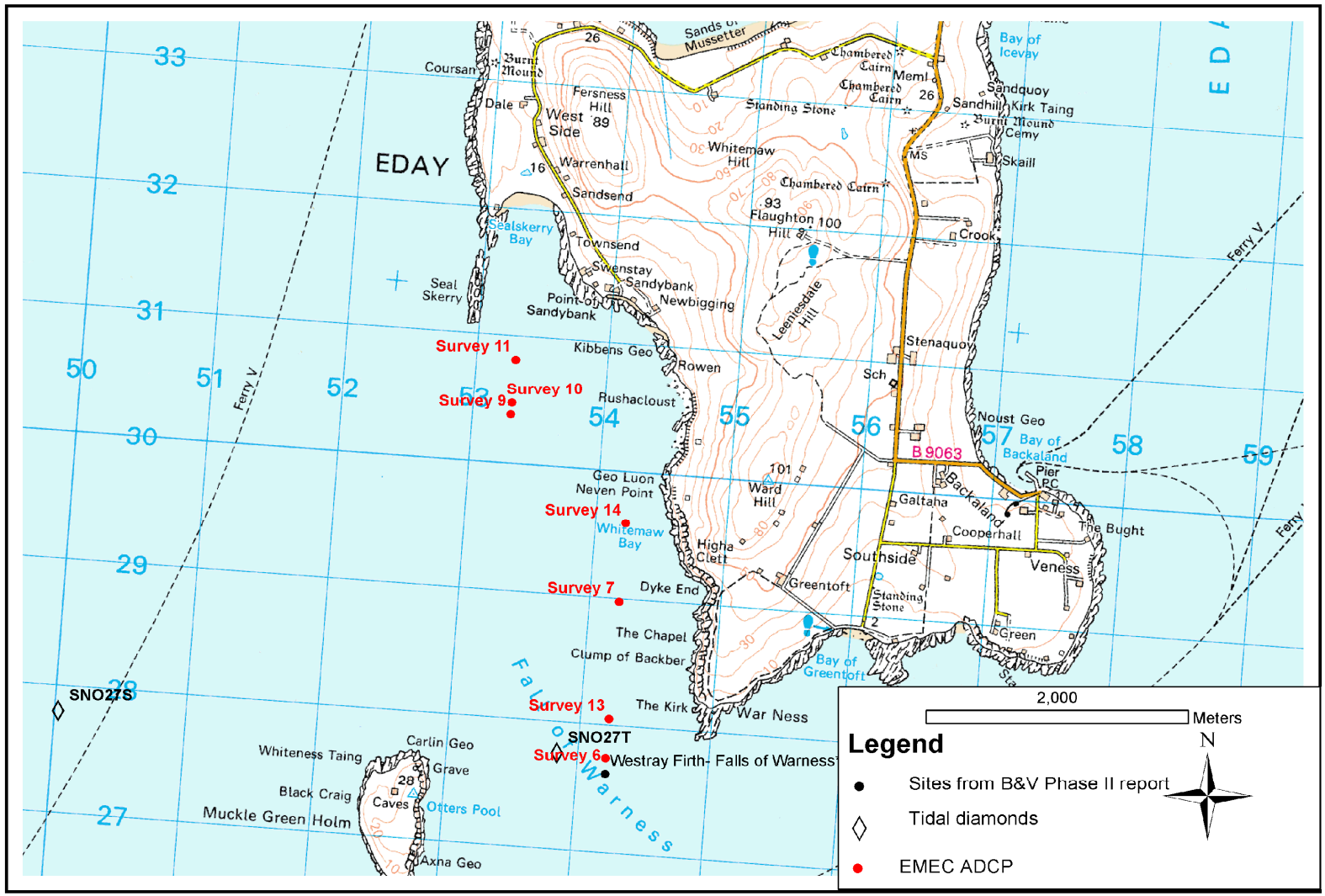

Figure 5.1 EMEC Survey location of deployment. Contains Ordnance Survey data © Crown copyright and database right (2010).

Surveys that span less than 15 days have not been included in the analysis. Survey 9b had to be excluded as there were too many missing data points. The dataset was not robust enough and it was thought that the remaining data was biasing the depth average values. For similar reasons Survey 14 was excluded.

EMEC have carried out in-house quality control to ensure the quality of the data. The standard quality control threshold has been doubled to make allowance for the highly turbulent flow experienced at this site. The data in its original format was presented in a text file where the velocity measurements were taken in a Cartesian coordinate system. Some of the initial data preparation was conducted by Tim Stiven, as part of his MSc dissertation (Stiven, 2010). The data preparation step identified below and developed by Stiven (2010) has been adopted for the analysis presented here:

1. The data was primarily separated into three arrays, East, North and Error velocity in mm/s. Where necessary the first few measurements were omitted. This is usually when the ADCP was set up and can have random values which may bias the overall average results.
2. The top 5 meters of data near the surface was removed from the record as including the rise and fall of the tide would bias the results as velocities in the upper water column tend to be higher. Near the seabed, the lower 25% of the total depth was removed unless the depth was less than 25 metres. This is to avoid under-estimating the depth averaged data, as velocity near the seabed is usually lower that the rest of the water column.
3. The remaining bins were averaged across the depths to give a single column of East and North velocity vectors. For certain scalar analyses the data was converted into speed and direction before depth averaging.

Section 5.1.1 presents the metrics identified in chapter 4 necessary for site characterisation. In section 5.2 harmonic analysis is used to recreate Survey 7, 10 and 13 at the same ensemble period as that of the measured data (Survey 7: 10 minutes, Survey 10: 20

minutes, Survey 13: 0.5 minutes) and spanning over the original time-period that each of the data was measured for. Analysis was presented to see how harmonic analysis performs over different ensemble periods. Section 5.3 presents analysis where all the data is recreated to a coincident time period, at a 10 minute ensemble period so that a direct comparison can be carried out between the three locations to assess the spatial variability. Section 5.4 investigates the long term variations that can affect tidal current velocity over years and presents analysis that investigates how these variations may affect to power production over a project life time.

5.1.1 Stationary, Bottom Mounted ADCP Analysis

Following the same methodology as presented in chapter 4 allows direct comparisons to be made between the data presented here and data considered from other sites in future. The degree of spatial and temporal variability is of significant interest in considering how representative a particular set of in-situ measurement data may be of the wider surrounding area of interest for large scale project developments.

As detailed in chapter 4, the metrics are separated into ebb, flood and slack tide, where tidal velocity below 0.5 m/s is considered slack. Ebb and flood is separated based on the principal axis decomposition. The entire record is also analysed for all the metrics. Results from all the analysis on the three ADCP datasets are tabulated in Table 5.2 and Table 5.3. For the purpose of power calculation, device hub height (from the sea bed) is assumed to be mid depth, as depth averaged values could produce lower velocity and power values, giving an underestimation for the site considered. No further assumptions are made about device characteristics.

		Survey 6a	Survey 6b	Survey 7	Survey 10	Survey 11	Survey 13
OVERALL	**SITE**						
	Measurement duration (days)	16.0	16.4	32. 9	40.7	25.0	31.9
	Vertical resolution (m)	1	1	1	0.75	0.50	1
	Sampling interval (min)	20	0.3333	10	20	20	0.5
	Mean depth (m)	35	35	48	26	10	36
	Assumed hub height(m)	Mid depth	Mid depth	Mid depth	Mid depth	Mid depth	Mid depth
	VELOCITY						
	Mean velocity magnitude (m/s)	1.63	1.63	1.58	1.66	1.55	1.69
	Neap Spring Ratio	0.37	0.42	0.34	0.38	0.53	0.41
	Max sustained velocity (m/s)	3.34*	3.46**	3.57 *	3.38 *	3.18*	4.22 **
	Eddy intensity %	***	7.67	***	***	***	9.63
	Flood/ Ebb asymmetry	0.15	0.16	-0.24	0.19	0.30	-0.26
	AvgVertical shear (m/s per m)	0.015	0.039	0.014	0.017	0.056	0.024
	Max Vertical shear (m/s per m)	0.065	0.356	0.075	0.131	0.283	0.326
	DIRECTION						
	Principal axis direction (deg)	168	149	158	145	148	146
	Standard deviation (deg)	50.99	28.32	34.71	31.58	40.74	36.01
	Flood/ Ebb asymmetry (deg)	-9.86	-4.49	-3.65	-19.75	-40.79	-5.84
	POWER						
	Mean power density (kW/m sq)	4.11	4.31	3.74	4.04	3.18	4.70
	Flood/ Ebb asymmetry	0.79	0.83	0.63	1.30	0.56	0.69
	VERTICAL PROFILE						
	Power law exponent 1/(α)	7.146	6.34	5.4	10.5	4.7	11.4
	R -squared (α)	0.997	0.993	0.999	0.991	0.962	0.944

* For survey 6a, 7,10 &11 max sustained velocity in an hour. ** For survey 6b, 13 max sustained velocity in 5 minutes.

*** Sampling interval too high

Table 5.2 Key metrics for site characterisation for the overall dataset.

		Survey 6a	Survey 6b	Survey 7	Survey 10	Survey 11	Survey 13
EBB	**VELOCITY**						
	Mean velocity magnitude (m/s)	1.86	1.87	1.85	1.72	1.65	1.96
	Max sustained velocity (m/s)	3.34*	3.46**	3.49 *	3.30 *	3.18*	4.22**
	Eddy intensity %	***	7.61	***	***	***	7.14
	Avg Vertical shear (m/s per m)	0.018	0.075	0.013	0.014	0.036	0.029
	Max Vertical shear (m/s per m)	0.065	1.652	0.062	0.099	0.172	0.326
	DIRECTION						
	Principal axis direction (deg)	338.55	322.79	341.19	311.05	301.12	317.78
	Standard deviation	12.41	11.71	6.87	20.28	24.53	10.38
	VERTICAL PROFILE						
	Power law exponent 1/(α)	6.59	5.32	6.2	14.7	7.1	10.2
	R -squared (α)	0.984	0.984	0.998	0.991	0.840	0.893
	POWER						
	Mean power density (kW/m sq)	5.16	5.27	5.08	3.96	4.38	6.16
FLOOD	**VELOCITY**						
	Mean velocity magnitude (m/s)	1.71	1.71	1.61	1.91	1.42	1.70
	Max sustained velocity (m/s)	3.04*	3.27**	2.95 *	3.38 *	2.62*	4.05**
	Eddy intensity %	***	7.70	***	***	***	7.18
	Avg Vertical shear (m/s per m)	0.012	0.0375	0.016	0.021	0.081	0.022
	Max Vertical shear (m/s per m)	0.049	0.326	0.075	0.131	0.283	0.161
	DIRECTION						
	Principal axis direction (deg)	168.41	147.29	155.56	150.80	161.99	143.62
	Standard deviation	12.67	15.19	7.34	11.71	16.67	14.79
	VERTICAL PROFILE						
	Power law exponent 1/(α)	8.06	7.83	4.6	8.0	2.9	11.7
	R -squared (α)	0.999	0.999	0.999	0.994	0.993	0.940
	POWER						
	Mean power density (kW/m sq)	4.08	4.4	3.22	5.14	2.44	4.27

* For survey 6a, 7,10 &11 max sustained velocity in an hour. ** For survey 6b, 13 max sustained velocity in 5 minutes.

*** Sampling interval too high

Table 5.3 Key metrics for the Ebb/Flood site characterisation.

5.2 Comparing Measured and Reconstructed Data

Missing data in this dataset has not been interpolated, instead the *NaNmean* function in MATLAB has been used to depth average the data where the missing values are simply omitted. This method is deemed appropriate as only small clusters of data are missing at any given point.

Figure 5.2 shows the scatter plot of the original measured data from Survey 7 vs. the predicted data generated using harmonic analysis as presented in chapter 4, spanning the original measurement period.

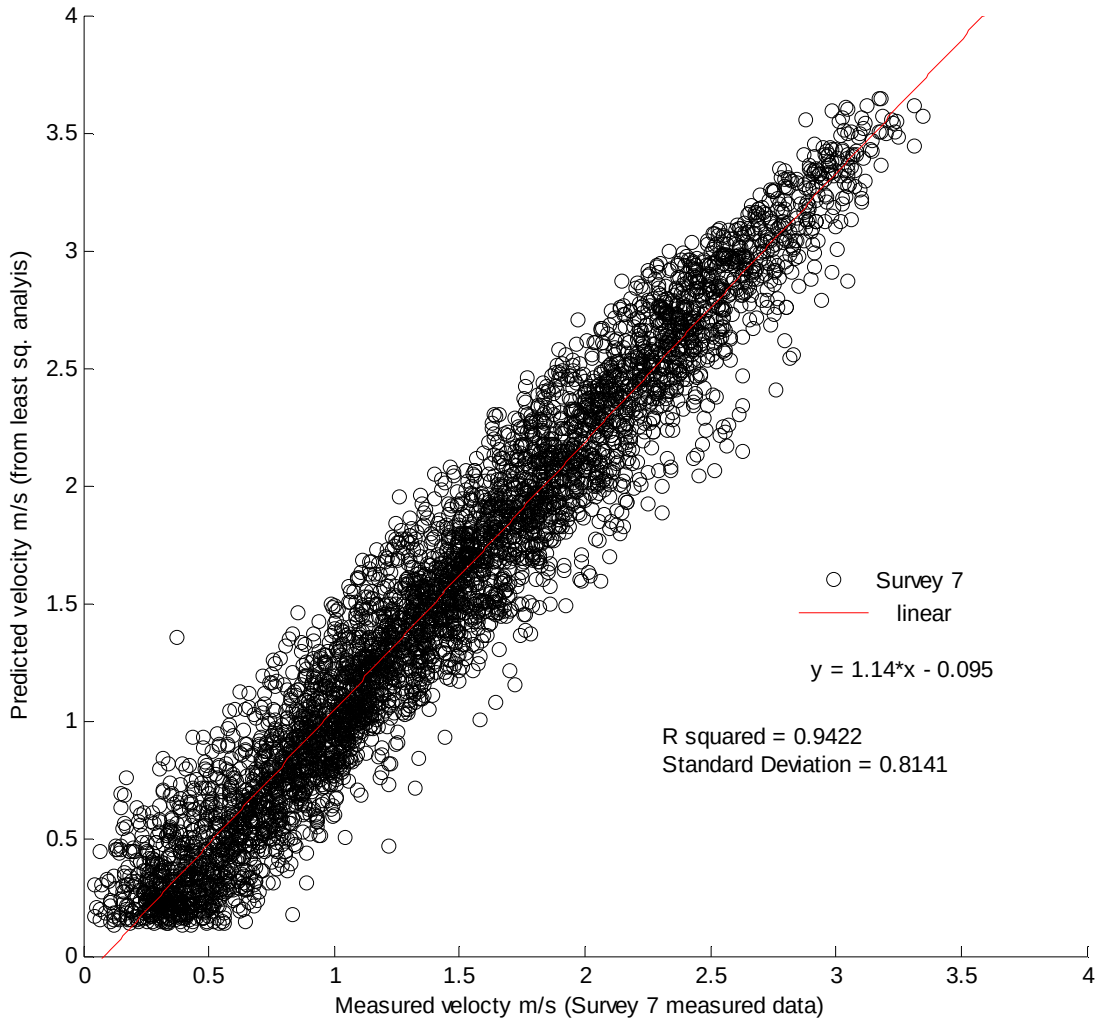

Figure 5.2 Scatter plot of Survey 7, measured vs. predicted data.

The scatter plot shows velocity measured compared to velocity predicted spanning the same time period and at the same sample frequency of 10 minutes for Survey 7. This is the ensemble period at which the original data is measured. Figure 5.3 shows the scatter plot for Survey 10 sampled at 20 minutes.

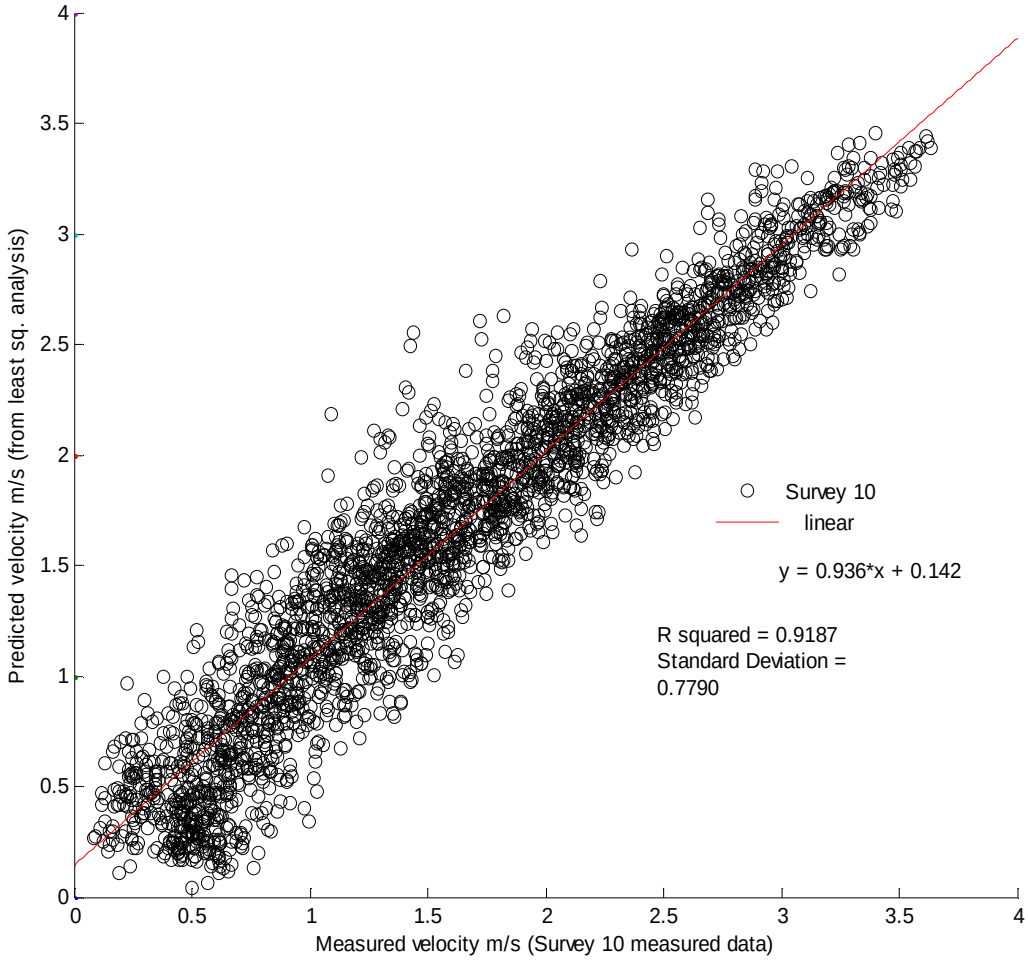

Figure 5.3 Scatter plot of Survey 10, measured vs. predicted data.

The scatter shows that the fit is good and, therefore, the constituents generated from this harmonic analysis can be used to recreate the time-series. The high R^2 value and the regression line demonstrates that the model presents a near 1:1 ratio. Small bias is present and is shown by the value of the linear regression intercept on the axis. This bias is a representation of all the variations that are not accounted for and the addition of meteorological variations observed on site that is not represented by harmonic analysis.

Survey 13 was sampled at a much higher resolution of 30 seconds. The higher resolution allows the measured data to capture more of the variation and some of this is random background noise, therefore a bigger spread is observed between the measured and the predicted data. In future, the use of a digital filter has been suggested to remove low frequency noise. Table 5.4 presents statistics from all the three scatter plot.

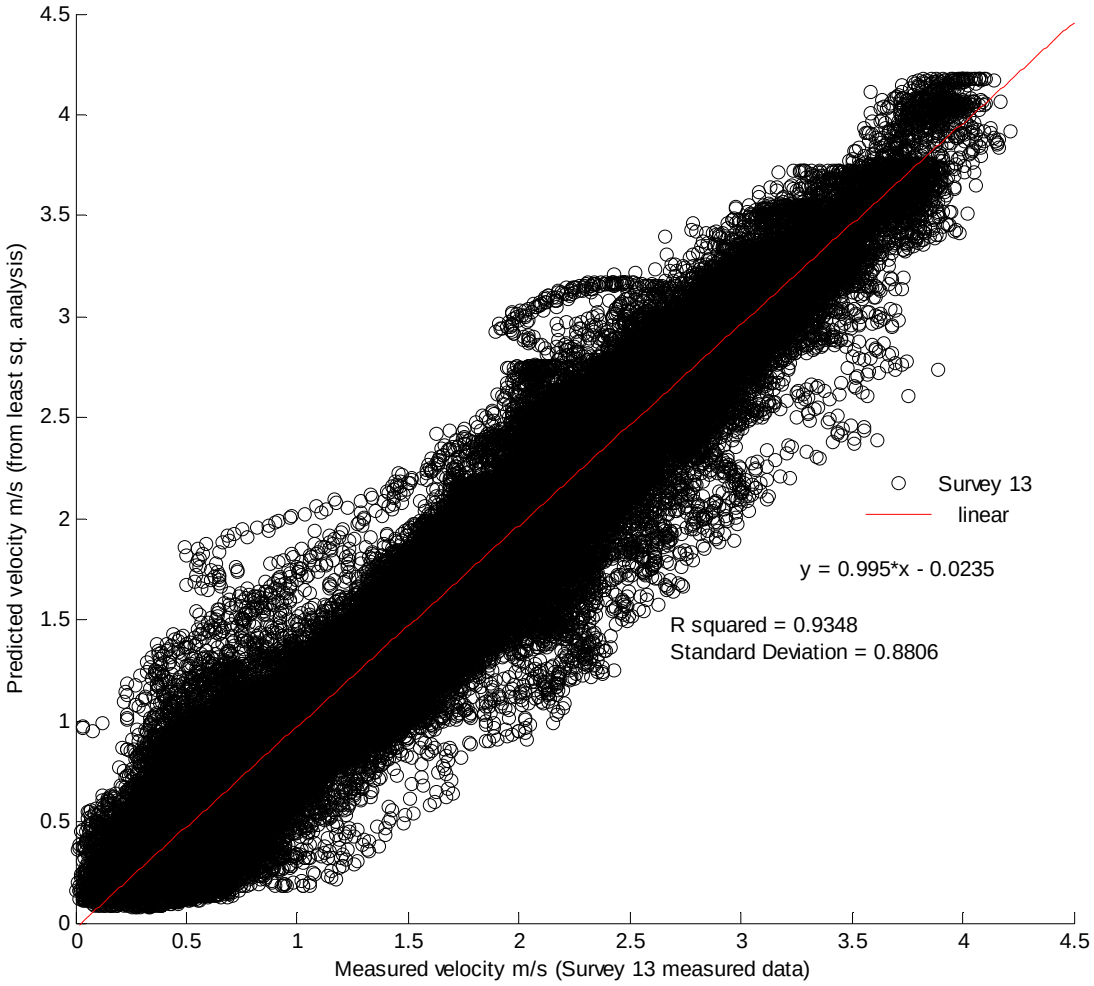

Figure 5.4 Scatter plot of Survey 13, measured vs. predicted data.

	Equation	R^2	Standard Deviation
SURVEY 7	y = 1.14*x -0.095	0.942	0.814
SURVEY 10	y = 0.936*x +0.142	0.919	0.779
SURVEY 13	y = 0.995*x -0.0235	0.935	0.881

Table 5.4 Table presenting statistics from the scatter plot.

Figure 5.5 shows the weighting of the different constituents that have been obtained using the NOAA's *lsqha.f* program. For all the three surveys, M2 values have been scaled to 100 and all the other constituents are scaled relative to it for each dataset. It is interesting to note that even though the three surveys are nearby, weighting for some of the constituents are significantly different. This highlights the spatial variation expected at high energy sites. It is important to note that only the amplitudes are presented here, the phase angle also makes a significant contribution.

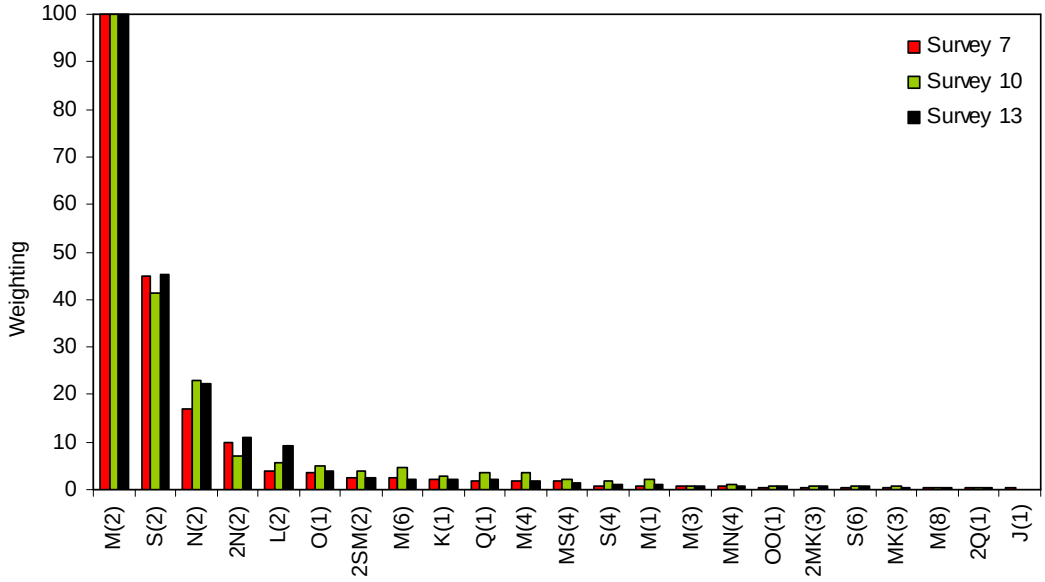

Figure 5.5 Constituent weightings from different Surveys.

5.2.1 Velocity Variations

The velocity distribution between the measured and reconstructed data is shown in Figure 5.6. For Survey 7 and 13, the velocities are slightly over predicted, up to 0.5 m/s, small over prediction occurs throughout the remaining velocity distribution. For Survey 10, the model slightly under predicts at velocities ranging from 0.5 m/s to 1.5 m/s, followed by small over-predictions at higher velocities. However, for all the Surveys, the mean values are similar.

5.2.2 Directionality

So far, comparisons show a good velocity match but do not show what the directionality looks like. A way of incorporating this is to superimpose X-Y scatter plots of the original measured data with the reconstructed data (over the original common measured time-period). This demonstrates good matching between speed and direction. Scatter plots for Survey 7, Survey 10 and Survey 13 are shown in Figures 5.7; prediction from the harmonic analysis is shown in black.

The general envelope of the scatter plot matched the measured data well. The degree of scatter is much higher in the measured data when compared to the recreated data, particularly for Survey 10. One of the limitations of the NOAA program is that it only works with one principal current direction (ebb or flood). The other direction is assumed to be 180 degrees off the direction that is fed into the control file if the current is rectilinear. Survey 10 is located such that the current is forced into a narrow flow along the south-east (flood direction) because of the land mass structure. However, the flow varies and has a large scatter in the north-west (ebb direction) because of the way the island steers the flow. Additionally, the Seal Skerry lies a few hundred metres ahead, which influences the flow further (see Figure 5.1).

Another reason for the scatter is most likely meteorological effects caused by wind/wave interactions superimposed on tidal variations. Non-tidal variations are not captured in this harmonic analysis. A suitable way of verifying these meteorological effects would be to obtain wind/wave data from a nearby met station as presented in chapter 4 for the Sound of Islay.

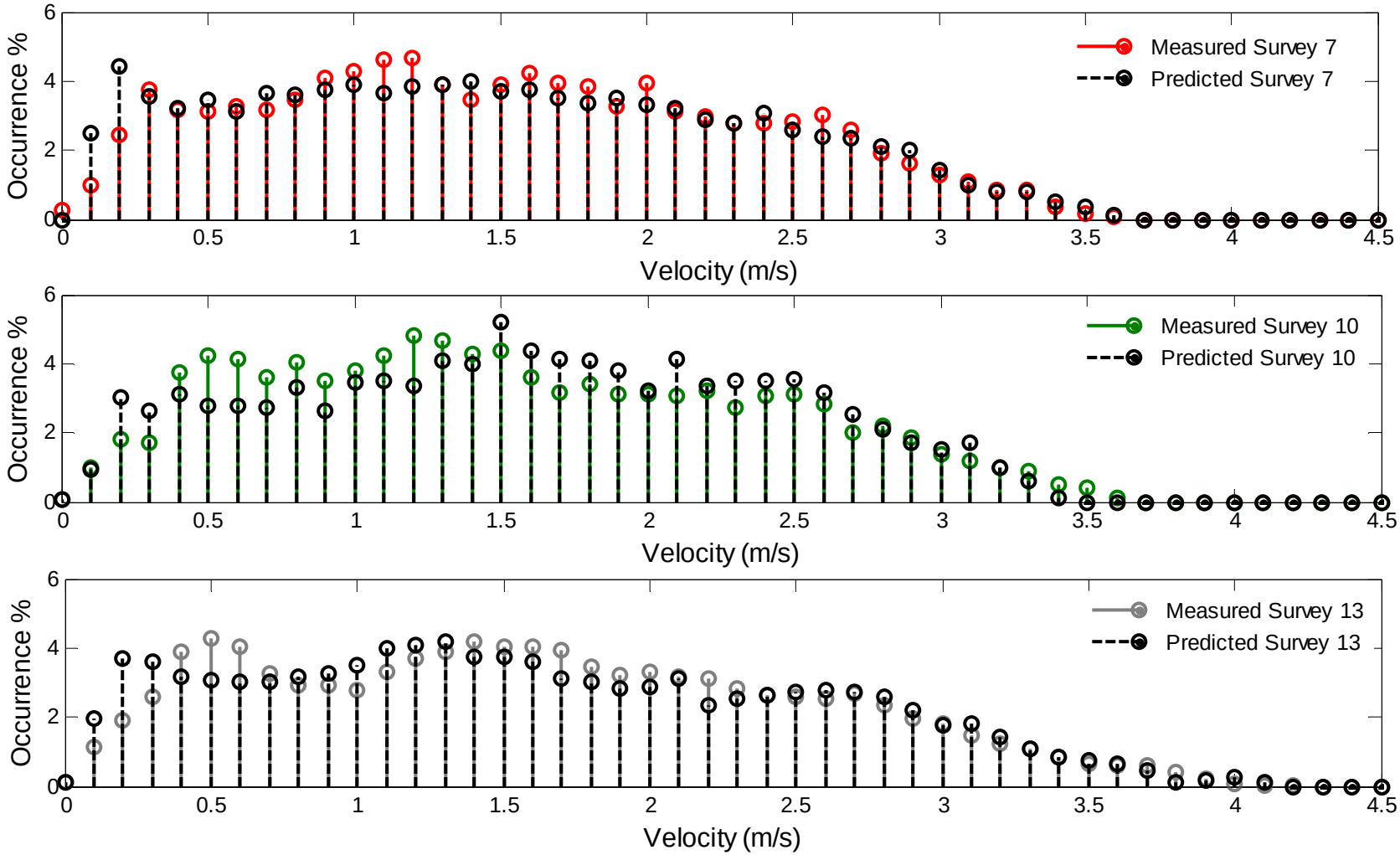

Figure 5.6 Velocity histogram comparing measured and predicted data spanning over the original measurement period. Survey 7 (top), Survey 10 (middle) and Survey 13 (bottom).

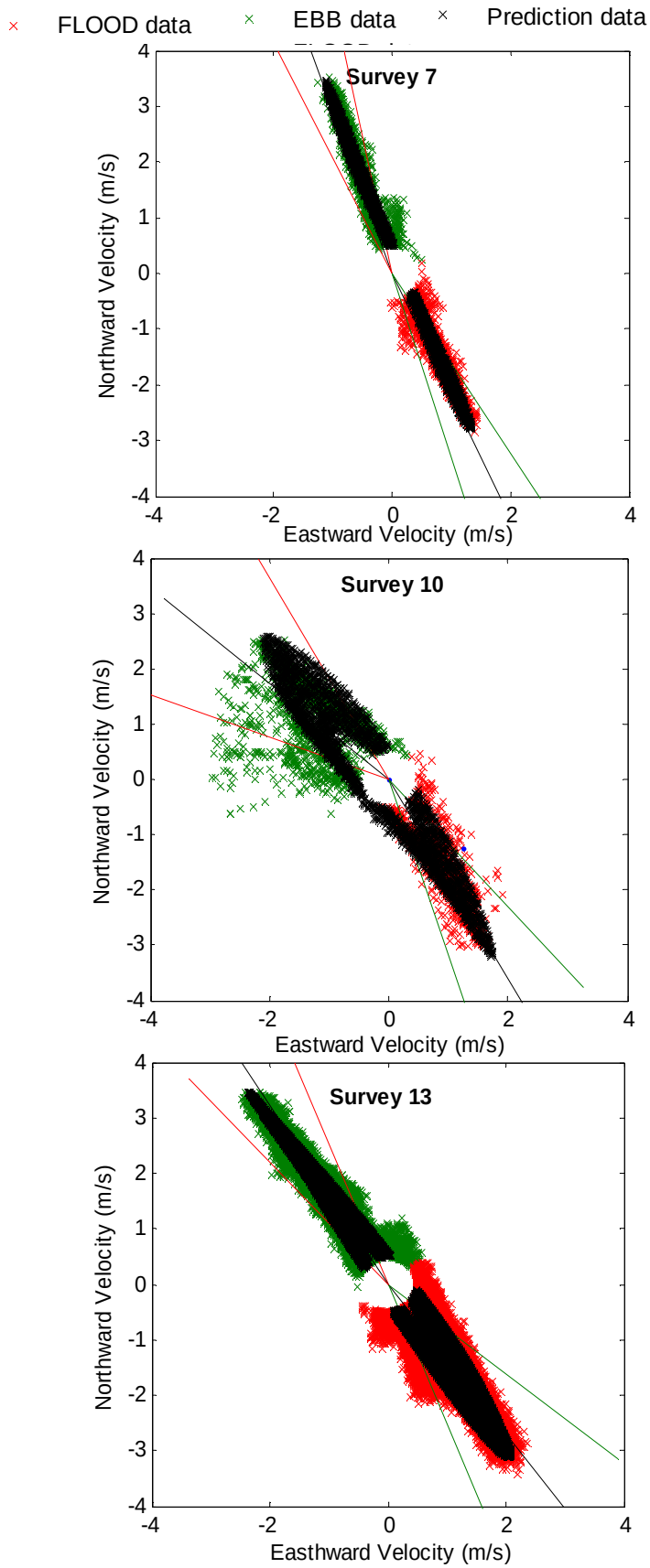

Figure 5.7 X-Y scatter plot for Survey 7, 10 and 13. Comparison between measured and predicted data.

5.2.3 Power Variation

The analysis presented so far shows how well velocity measured and predicted data from harmonic analysis perform. However, power is the key metric and small errors in velocity can scale up as power is proportional to velocity cubed. It is of interest to know how much the energy output varies between the original measured data and the data generated from harmonic analysis and is another way of assessing the accuracy of harmonic analysis. Table 5.5 presents the values of the power output for each of the surveys. A standard rated velocity is assumed between the measured and predicted scenarios to simulate the characteristics of 'one generic device' in both the measured and the predicted cases. For Survey 7 and 10, a rated velocity of 2.6 m/s is chosen, whereas for Survey 13, a much higher rated velocity of 2.8 m/s is used. The rated velocity is choosen using the velocity exceedance curve, using the 10^{th} percentile as suggested in section 6.3.3. The predicted power output and consequently capacity factor in all the cases is lower than the measured value. This is primarily because harmonic analysis smoothes out the small scale variations as it does not account for non-tidal variations and instrumental errors as identified in Figure 4.19. As more constituents are resolved, the difference becomes smaller.

Survey		Energy (MWh/yr)	Capacity Factor	% Reduction
	Measured	3557.20	35.84	
7	Predicted	3476.07	35.02	-2.28
	Measured	3790.06	38.19	
10	Predicted	3566.37	35.93	-5.90
	Measured	4393.89	35.44	
13	Predicted	4352.31	35.11	-0.95

Table 5.5 Comparing power output between measured and predicted velocity.

Survey 13 has the smallest percentage reduction and Survey 10 has the largest. The fact that these measurements are not coincident in time could mean that a meteorological event such as extreme wave/wind interaction could have occurred when Survey 10

measurements were taken while Survey 13 measurements occurred over a calm period. These historical events can play a significant part in establishing and identifying the reason behind the reduction/inaccuracies. Another explanation could be the significant spatial variation, it is already understood that Survey 10 has a large directional scatter due to variation in the local bathymetry, which also affects velocity. Local bathymetric changes are not fully captured by harmonic analysis. The temporal resolution of the data could also be a factor.

5.3 Spatial Variability

Having established that the constituents capture the majority of the tidal variability, it would be valuable to further understand the spatial variability inherent at this location. A direct comparison between the different datasets needs to be carried out, where the three datasets span a common time-period. In order to achieve this, the harmonic constituents obtained earlier are used to recreate the time-series using *pred.f* over a common time-period. This enables a comparison between the three surveys that are coincident in time and are not affected by meteorological events.

5.3.1 Velocity and Power

Although the data measured at each of the sites is of a different ensemble period, the recreated data is predicted at a 10 minute ensemble period. Figure 5.8 shows the dataset for Survey 7, 10 and 13 over a common time period of two weeks, showing the transition from Spring to Neap. In terms of velocity magnitude, Survey 13 is the strongest. There appears to be negligible time lag between the three measurements and all three datasets maintain the tidal envelope. However, upon closer inspection, as shown in Figure 5.9, it can be seen that Survey 10 presents a slight time lag and the highest velocity magnitudes vary between Survey 7 and 10.

Survey 7 is located between Survey 10 and Survey 13 (see Figure 5.1). The distance between Survey 7 and 13, and 7 and 10 are 1 km and 1.7 km respectively. The phase lag between the three Surveys is of significant interest as it highlights the extent of spatial variability. This provides some insight into how out of phase the power output will be if devices were to be deployed in these specific locations.

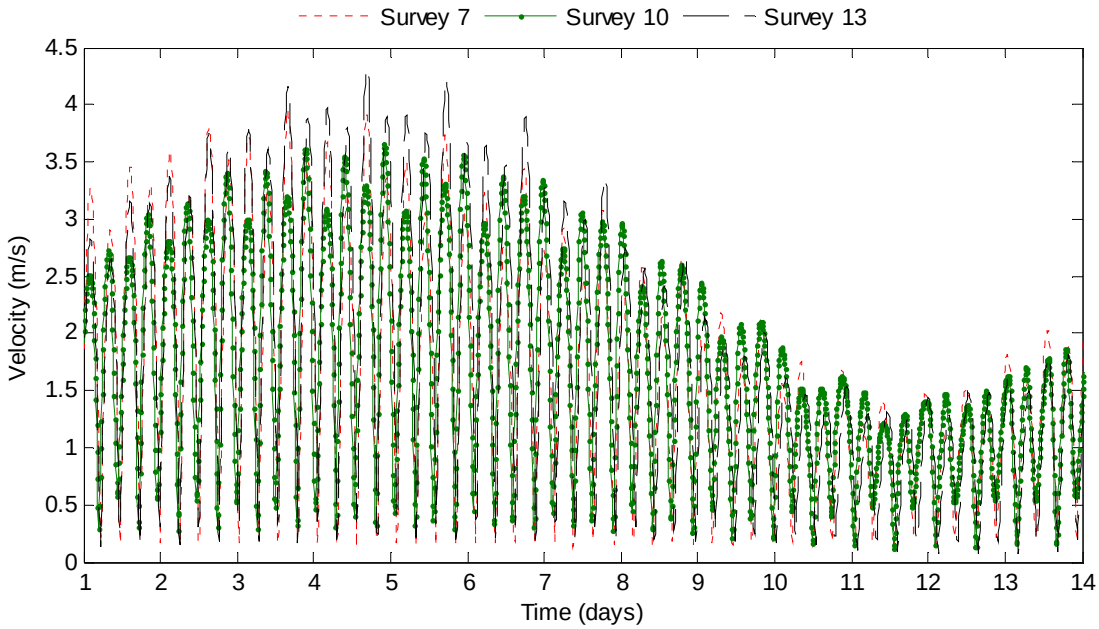

Figure 5.8 Velocity variation over a week for Survey 7, 10 and 13.

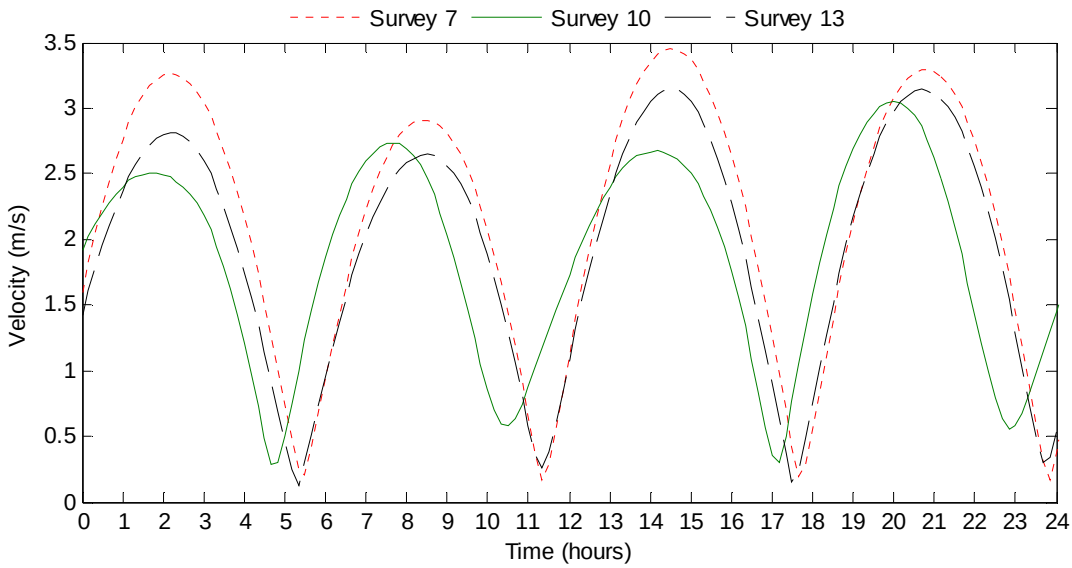

Figure 5.9 Velocity variation over a day for Survey 7, 10 and 13.

Figure 5.10 shows the variation over the entire year. From the figures, it can be seen that Survey 13 experiences the highest velocity. This variability can also be understood by

looking at the position of the different survey locations. Because Survey 13 is the closest to the tip of the headland, it is expected that the water would accelerate most around this region.

The velocity histogram (see Figure 5.11) shows that Survey 7 has a higher occurrence of velocities at lower magnitude than the other two surveys. This is of particular relevance as velocity below 0.7 m/s is below the device 'cut-in' velocity and therefore no power is produced during this time. The exceedance curve identifies that for approximately 80% of the time, the flow velocity is above 0.7 m/s. Therefore, for 20% of the time, there is not enough kinetic energy in the tidal current to generate power. Based on these measurements, the rated velocity for the device should be chosen at the 70^{th} percentile as suggested by B&V Phase II (2005), around 2.2 m/s. In terms of project economics, it is understood that the longer a device operates at or close to rated capacity, the higher the capacity factor will be. Therefore, choosing a rated velocity is a design and economic consideration. A very high capacity factor indicates that the device is underrated for the specific site; a low capacity factor may imply that the site is uneconomical or the device is over-rated. Figure 5.12 shows the kinetic power density of the three measurements in 1 kW/m^2 bins. Also plotted are the power exceedance plots.

5.3. Direction Plots

Predictions for Survey 7, 10 and 13 for the year of 2009 show good bi-directionality, see Figure 5.13. The largest variation is observed in the ebb flow which is predominantly thought to be because of the land topology. Asymmetry of 4° is observed for Survey 7 as calculated using the principal current direction, compared with 6° for Survey 13. A perfectly bi-directional site will have an asymmetry of 0°. Measurements from Survey 10 show a larger scatter, particularly in the ebb flow. The huge scatter is due to the variation in the bathymetric contours and the location of the site measurement with respect to the landmass. As the water flow moves towards the headland, the flow becomes more rectilinear.

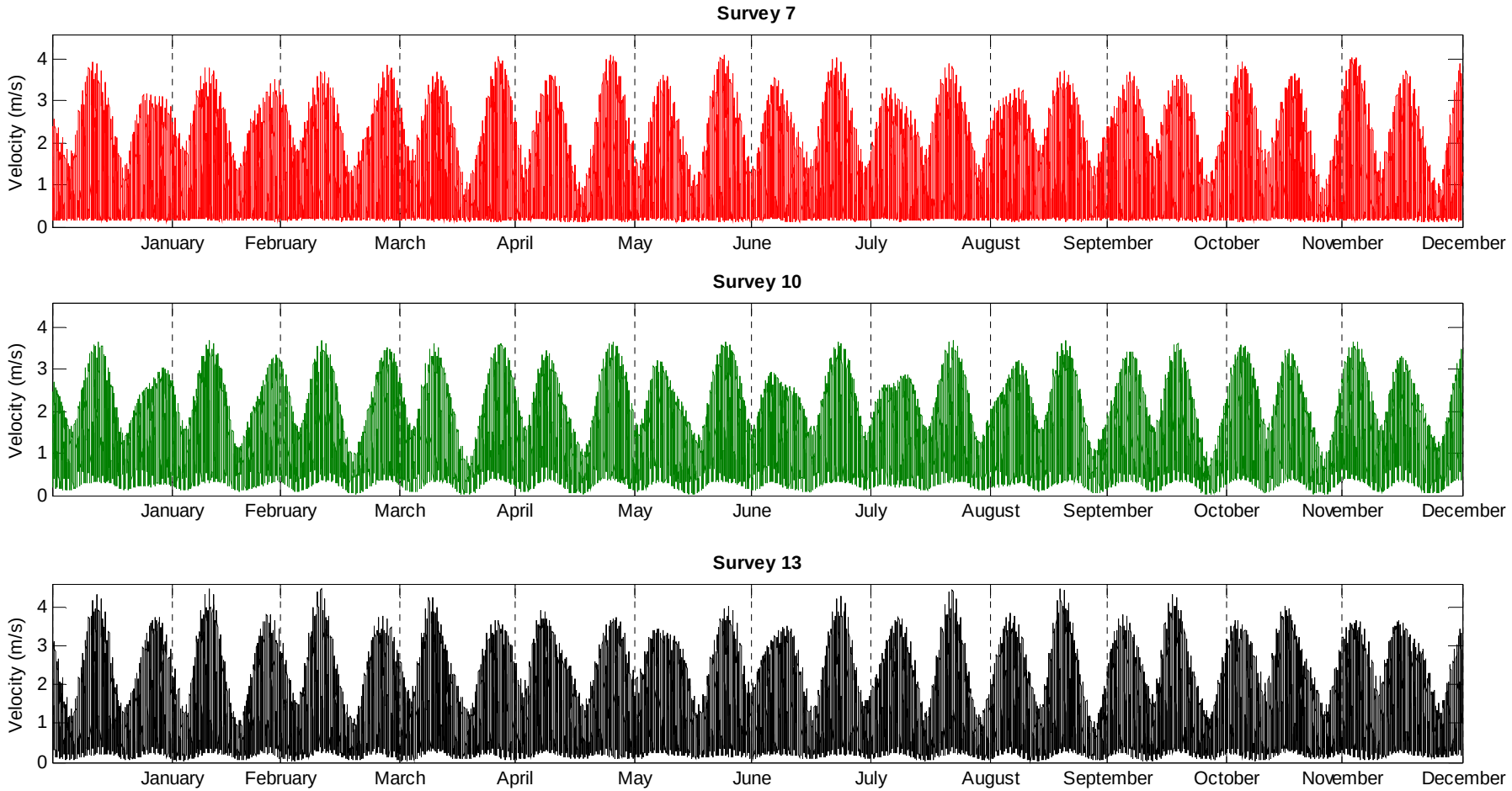

Figure 5.10 Tidal velocity profile for Survey 7, Survey 10 and Survey 13.

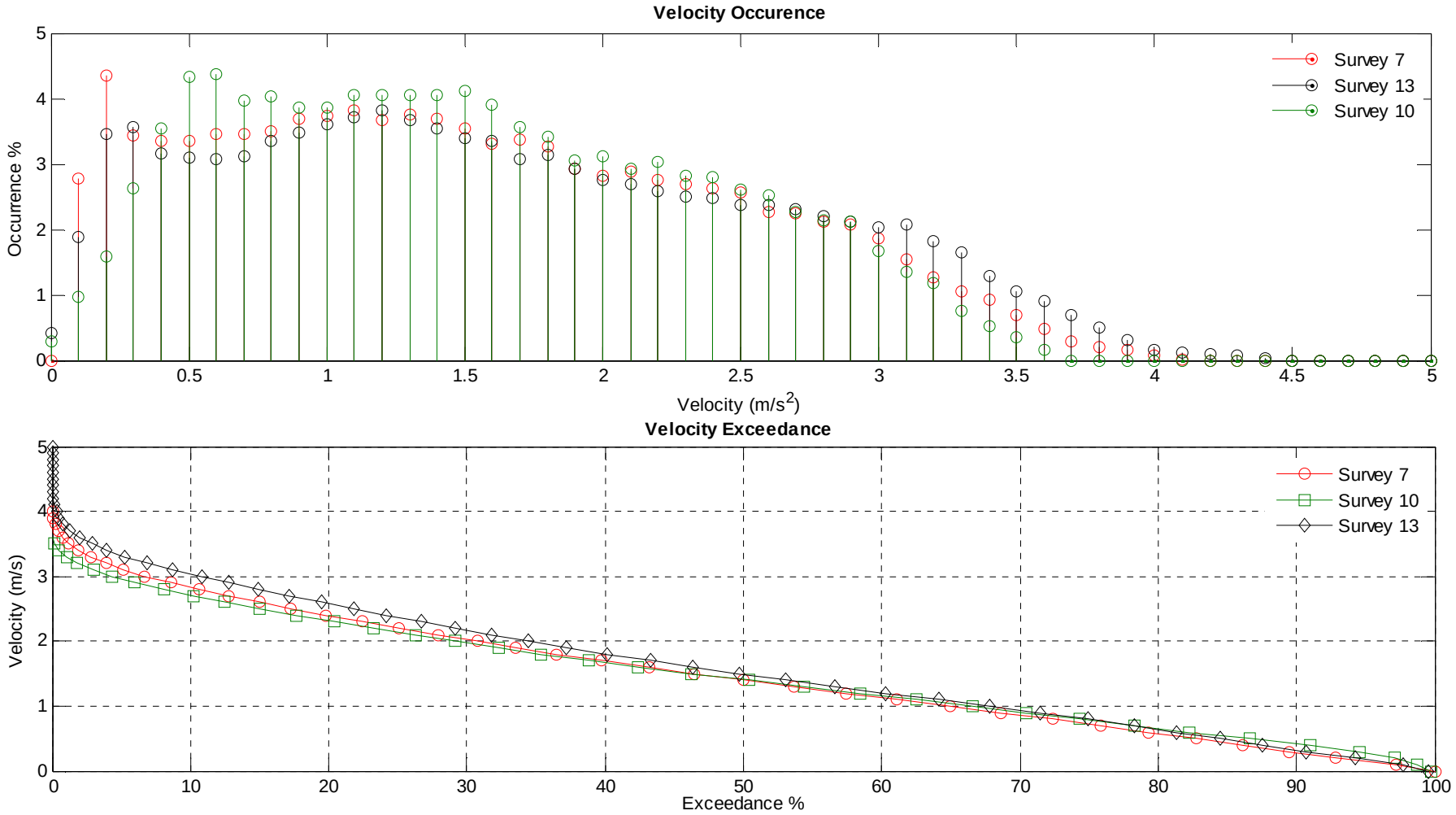

Figure 5.11 Velocity occurrence and velocity histogram for Survey 7, Survey 10 and Survey 13. Analysis for the year 2009.

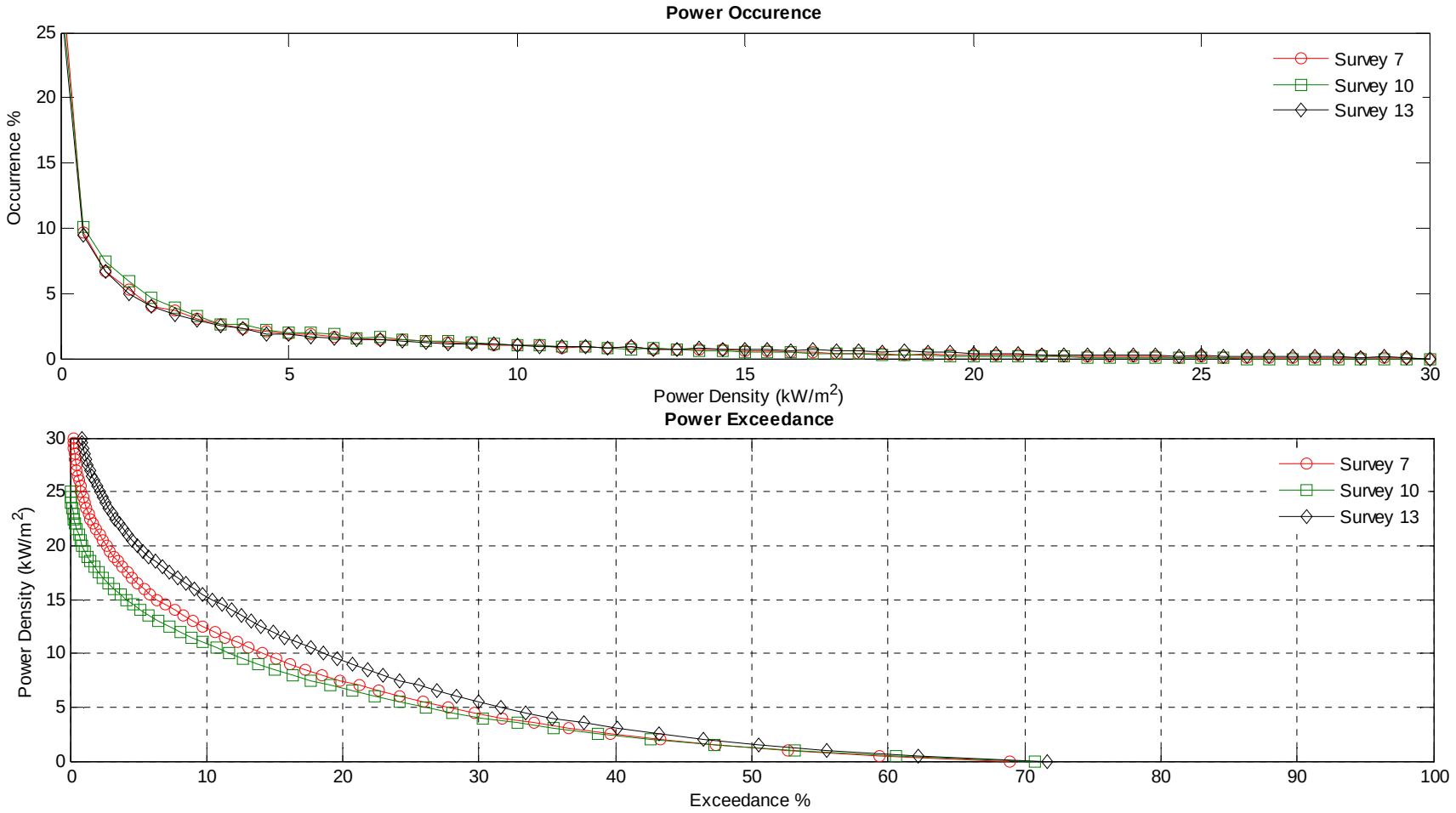

Figure 5.12 Power occurrence and power histogram for Survey 7, Survey 10 and Survey 13. Analysis for the year 2009.

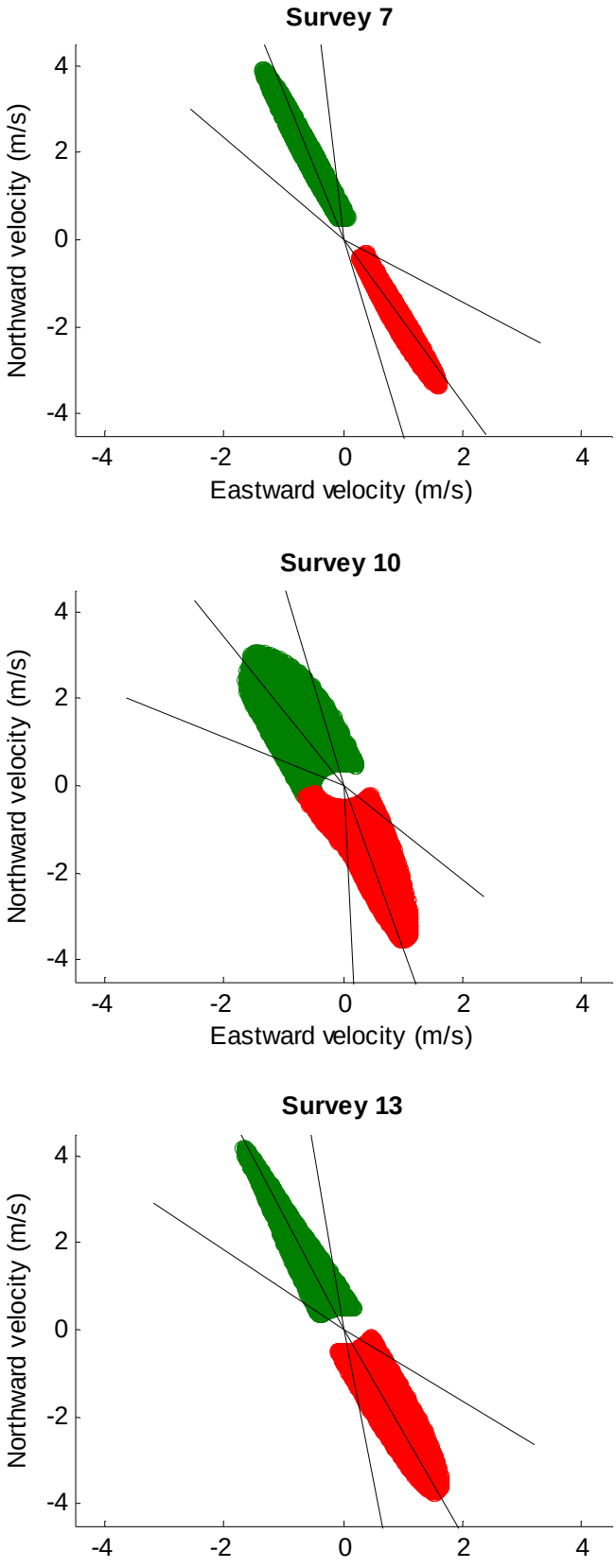

Figure 5.13 X-Y scatter plot showing the directionality of each of the Surveys.

Survey 10 measurements were taken in a location where changes in the water depths were observed, the changing water depth does affect uniform flow and can cause large scale turbulence. The scatter also gives rise to large asymmetry, of the order of 20°. Directionality and symmetry are an important aspect of site assessment and can highlight major differences between sites. The principal current directions along with the standard deviation are tabulated in Table 5.2 and 5.3.

Amongst the scatter plots presented here, Survey 7 stands out as the most rectilinear site and best suited for placing a device that would not require any yawing. The variation between the different surveys also highlights the need for high resolution modelling that can identify what the flow is doing between these measurement data points for optimal device placement and orientation.

Comparing the scatter between Figure 5.7, which presents scatter plots of the measured data (one month), and Figure 5.13 shows that the variations in one year's predicted data is well represented by one months measured data. However these predictions do not capture any meteorological and non-tidal events and therefore extreme variations caused by these events will not be represented by the predicted data.

5.3.3 Power Output

As previously mentioned, power is the most important metric. As part of assessing the spatial variability, it is valuable to know the power output distribution variation across the three surveys. In order to get a true understanding of the power distribution, a single generic hypothetical device is assumed, with a cut in velocity of 0.7 m/s and a rated velocity of 2.8 m/s. The rated velocity may not be the most ideal velocity for the three surveys but it is chosen to be a constant so a true comparison can be done to see what the power output from each of the surveys is if the same device is deployed in each location. Table 5.6 presents the values of the power output for each of the surveys in the year 2009.

2009 analysis	SURVEY 7	SURVEY 10	SURVEY 13
Energy (MWh/yr)	3951.57	3795.49	4424.46
Capacity Factor %	31.88	30.62	35.69

Table 5.6 Comparing power output for the year 2009.

Survey 13 has the highest energy output and capacity factor followed by Survey 7 and then Survey 10. The energy output presented here is evaluated based on the current velocity; directionality is not accounted for. In reality, because of the large scatter experienced at Survey 10, even with a device that can yaw, less energy is likely to be extracted.

5.3.4 Vertical Velocity Profile

Figure 5.14 shows the profile for measurements from Survey 7 averaged over time. The profile is broken down into flood and ebb to assess how the flow profile varies under different conditions. As presented in chapter 4, the MATLAB Curve Fitting Toolbox was used to fit the profile. No data was available for the bottom 3 metres because of the blanking distance (section 4.2). For Survey 7 the fit ranges from a $1/6.2^{th}$ profile in the ebb region to a $1/4.6^{th}$ profile in the flood region, with an overall fit of $1/5.4^{th}$ for the entire dataset.

Note that the data generated using NOAA is depth averaged, therefore the values obtained from the prediction cannot be used for comparing the vertical profile. The only way harmonic analysis could be used here, is if the velocity time-series for each of the depths is used to generate a different set of constituents and each of these sets of constituents is then used to recreate the time-series for each depth bin.

Figure 5.15 shows the profile for Survey 10. Interestingly a distinct reduction in velocity is noticed near the surface where the profile appears to curve inwards. Often strong echoes from the sea surface can cause error measurements. It is thought that the velocity reduction observed here is in fact what is observed in the water column due to surface roughness created by wind. For Survey 10 an overall fit of $1/10.5^{th}$ is best, in the ebb region a

fit of 1/14.7th and a 1/8th fit for the flood region. Although the fit does not match well near the surface, the most important region where a good fit is necessary is mid-depth where the rotors are likely to be placed.

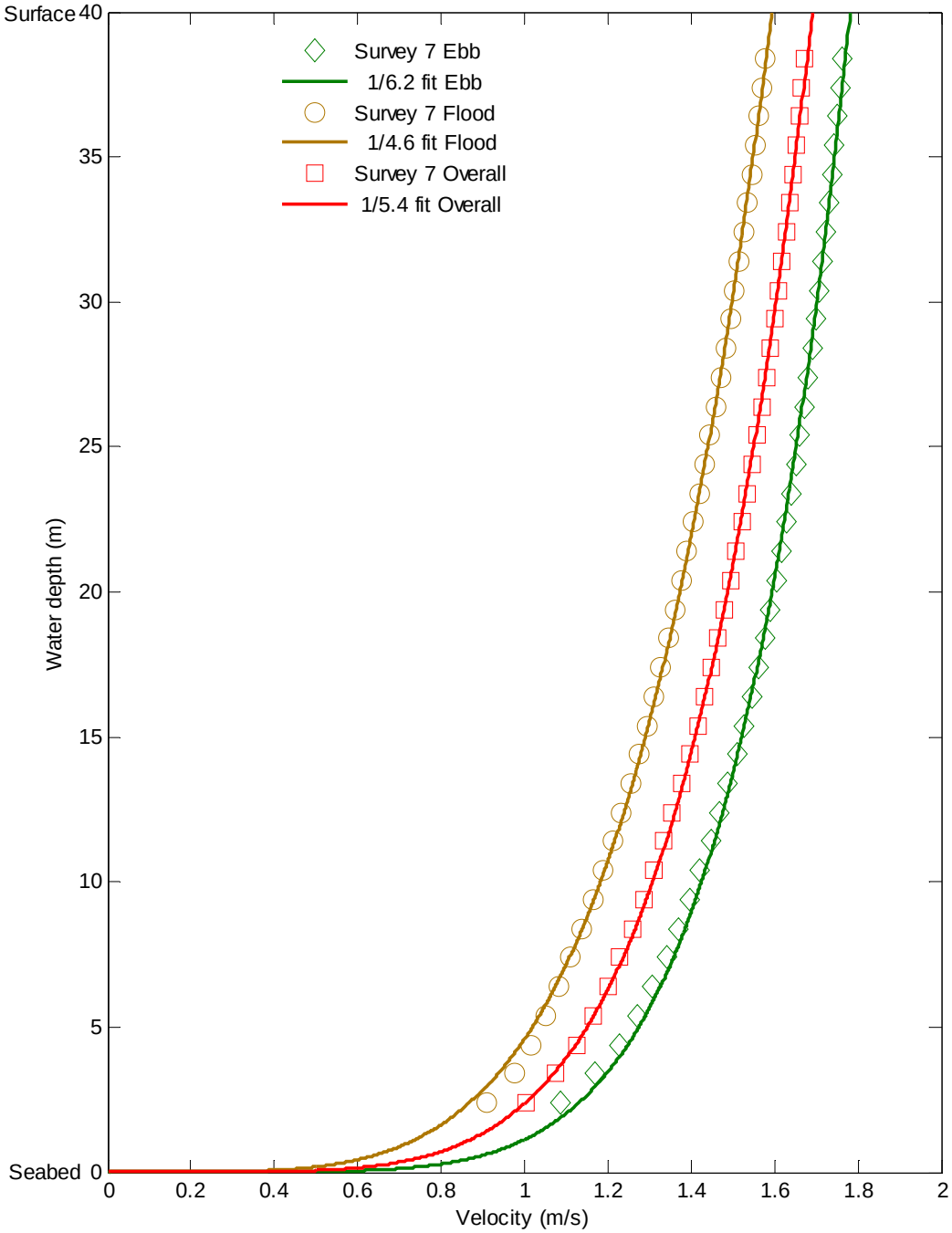

Figure 5.14 Average vertical velocity profile for Survey 7.

There also appears to be a 'twist' in the profile for survey 10 in the predicted profile very close to the sea bed. As no recorded measurements exist for this depth, it is difficult to

say if the twist in the profile is merely an attempt of the toolbox to fit the data or if this is an actual physical occurrence.

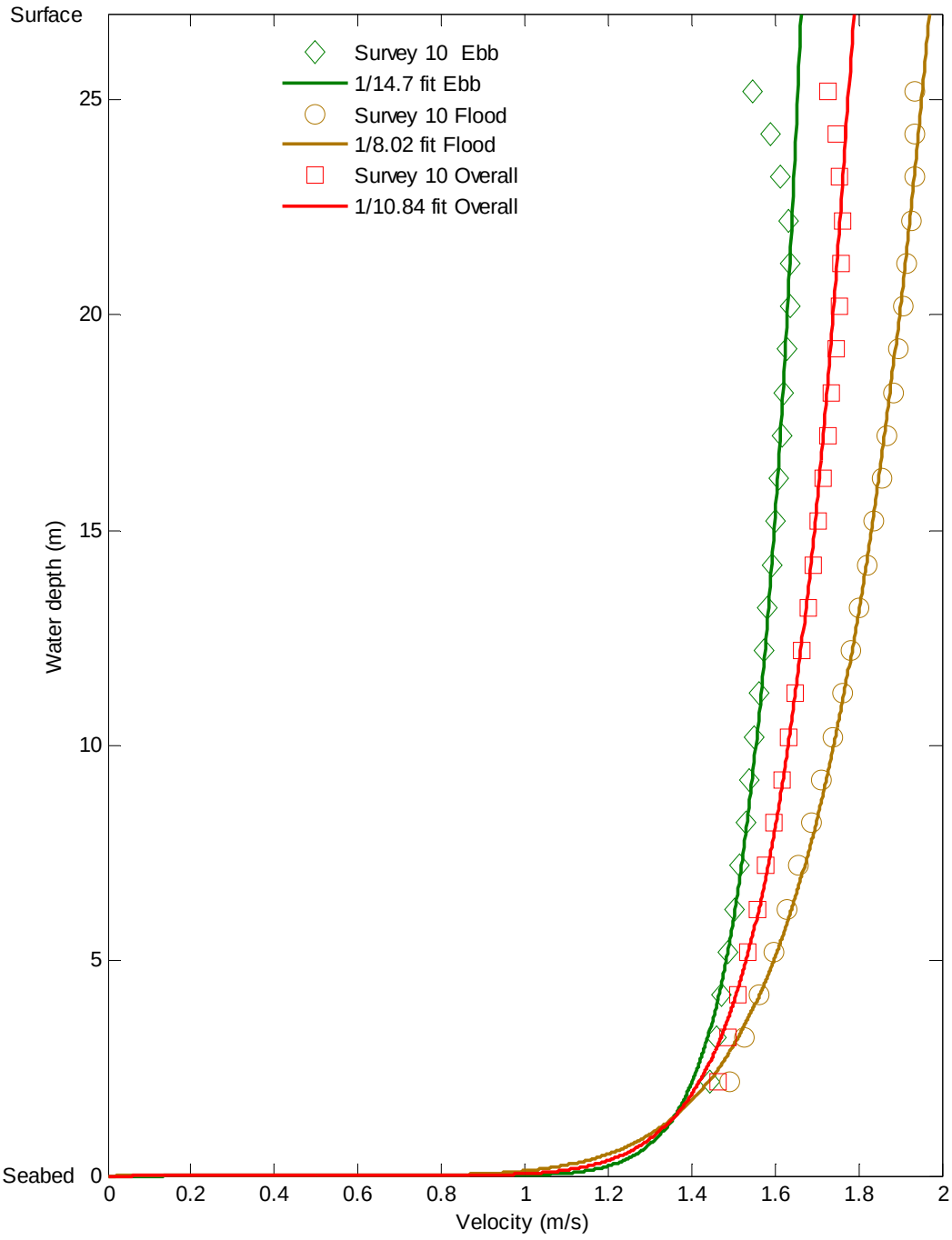

Figure 5.15 Average vertical velocity profile for Survey 10.

Figure 5.16 shows the vertical velocity profile for Survey 13. Like Survey 10, reduction in the flow velocity near the surface is observed. Some sporadic values are also

observed here. The overall profile fits a 1/11.3th profile, a 1/10.5th profile fits well in the ebb flow and 1/11.8th profile for the flood flow.

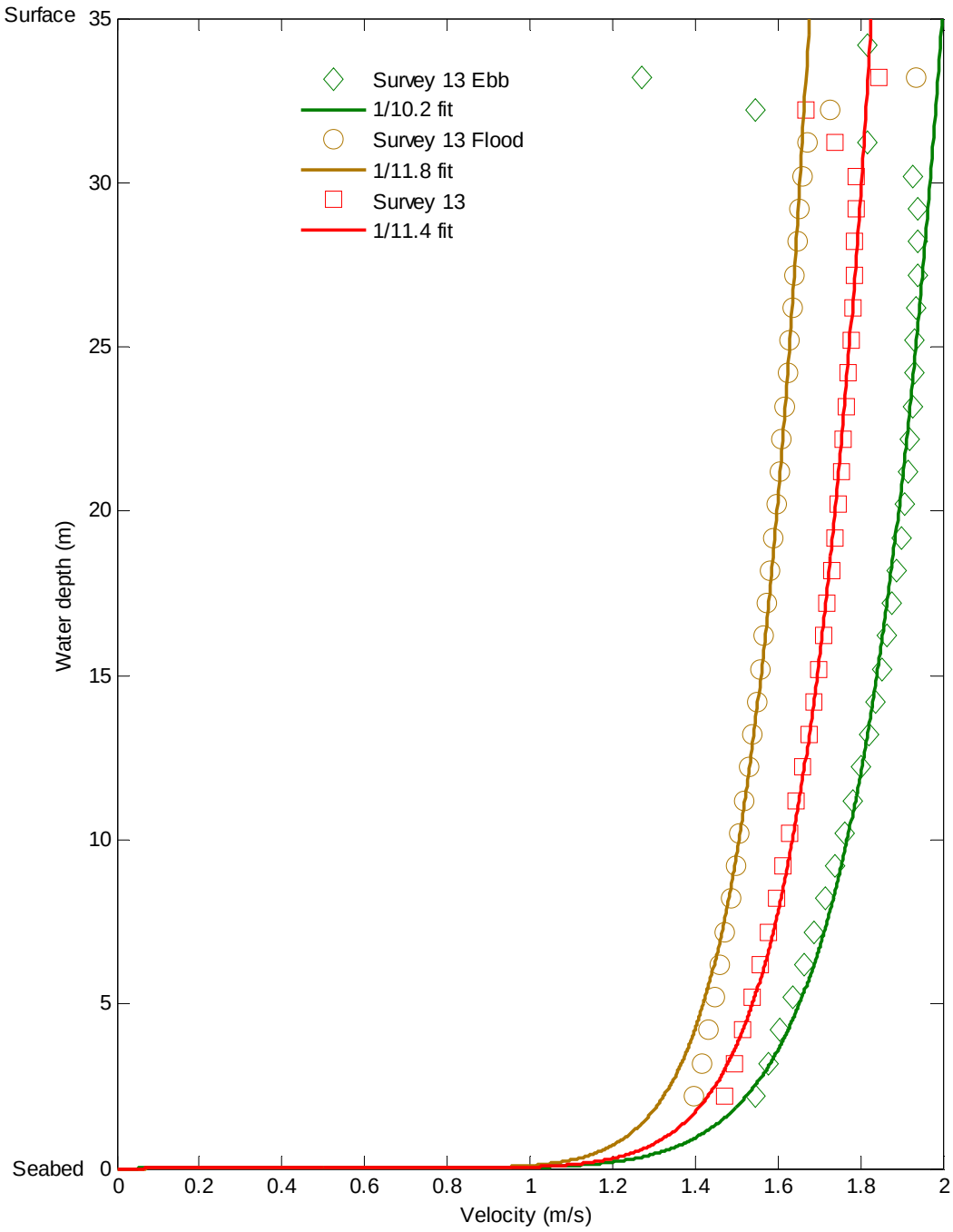

Figure 5.16 Average vertical velocity profile for Survey 13.

The range of profile fits shown here emphasises that the generically used 1/7th and 1/10th profile do not truly represent the velocity variation along the water column. This

emphasises the understandings developed in chapter 4 and further highlights the need for developing two power curves, tuning the device to operate in ebb and flood flow conditions and the variations in thrust acting on the turbine rotor.

5.4 Temporal Variations

The analysis presented in this section aims to investigate the temporal behaviour from short term variations that takes place over a day to the long term variations that can be experienced in the tidal cycle. Factors such as the Earth's tilt, elliptical orbit and the range of the lunar declination can cause variations, some of these variations can be seen over small duration of time, roughly monthly, while other can be gradual over a few years with the largest one being 18.6 years long. These are of particular importance, as these variations can influence power output on a daily basis and over a Spring/Neap cycle.

5.4.1 Daily Variability

The UK experiences semidiurnal tides, therefore each site will experience two high and two low tides a day. The tidal pattern shifts by 50 minutes each day as a result of the Moon's lunar cycle of 24 hours and 50 minutes. Therefore, it is of interest to see if any patterns emerge on a daily basis, particularly over long term.

Figure 5.17 shows a daily profile of tidal current velocity obtained from survey 13 (original measured data) in a 3-D plot over a two week period. The plot shows the tidal variation on a daily basis for each hour of the day. It can be observed that, as expected, the tidal pattern shifts each day by 50 minutes. This verifies the semidiurnal pattern (two ebbs and two floods in a day) and highlights the daily variability. Although not shown in Figure 5.17, the Neap cycle following the Spring cycle have peaks that do not coincide with the Spring peak. However, the consecutive Spring cycle that will occur will have peaks coinciding with all the Spring peaks identified in Figure 5.17

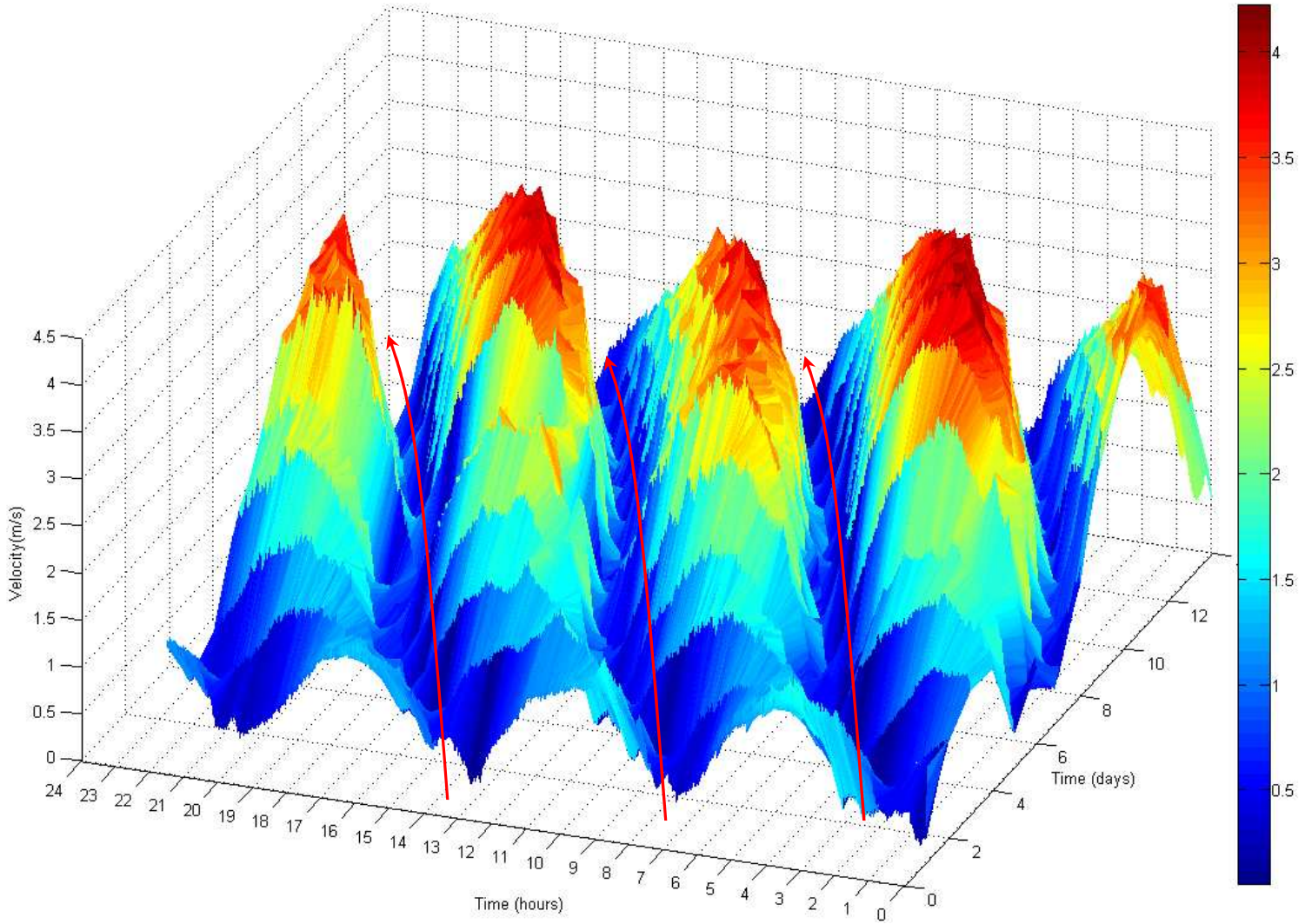

Figure 5.17 3-D plot showing daily tidal variation profile over a two week period. Note how tidal pattern shifts each day by 50 minutes.

To verify this semidiurnal behaviour recurring, data from a nearby tidal diamond was extracted for the year 2009 (Figure 5.18). The location of the tidal diamond is closest to Survey 13 and can be seen in Figure 5.1. Tidal diamonds only capture two constituents (Bell *et al.,* 1998). However, over a longer period, it is observed that the time of the Spring and Neap peaks coincide over a (solar) day. Figure 5.19 shows the output for Survey 13 genrated using NOAA, also for the year of 2009. The daily 50 minute shift is hard to see in Figure 5.18 and 5.19 because of the longer time-period. However, a trend can be seen where the timing of the Spring and Neap peak cycles re-occur at the same time across each Spring-Neap variation.

In order to further investigate the variations, data for 25 years is generated using harmonic analysis. The prediction period ranges from year 2000 to 2024 for Survey 7, 10 and 13. Variations over a 25 year period for Survey 13 are shown in Figure 5.20. Over this 25 year period, despite the daily 50 minute shift in the tidal patterns the long term Spring-Neap peaks do not shift in time. The trend over this period can be used to represent the project life time of a first generation tidal farm. The figure highlights that the time of peak generation in each day broadly remains the same. It can be assumed that daily peak power generation will occur at 3 am, 8 am, 3 pm and 8 pm at this location.

2-D plots of all the three surveys are shown in Figure 5.21. The daily profile is averaged across each year and averaged again over the 25 year period. A similar semidiurnal pattern was present by Bryans (2006) observed due to the Sun's influence on tides. For tidal heights, Shaw *et al.,* (2003) and Radtke *et al.,* (2011) also show a similar pattern for two different time-periods in the Severn Estuary.

This important finding prompted further investigation of how the velocity and power output from different locations around the UK could be phased. A UK-wide analysis to assess the phasing of potential high energy sites and matching of the power output to electricity demand is the focus of chapters 6 and 7.

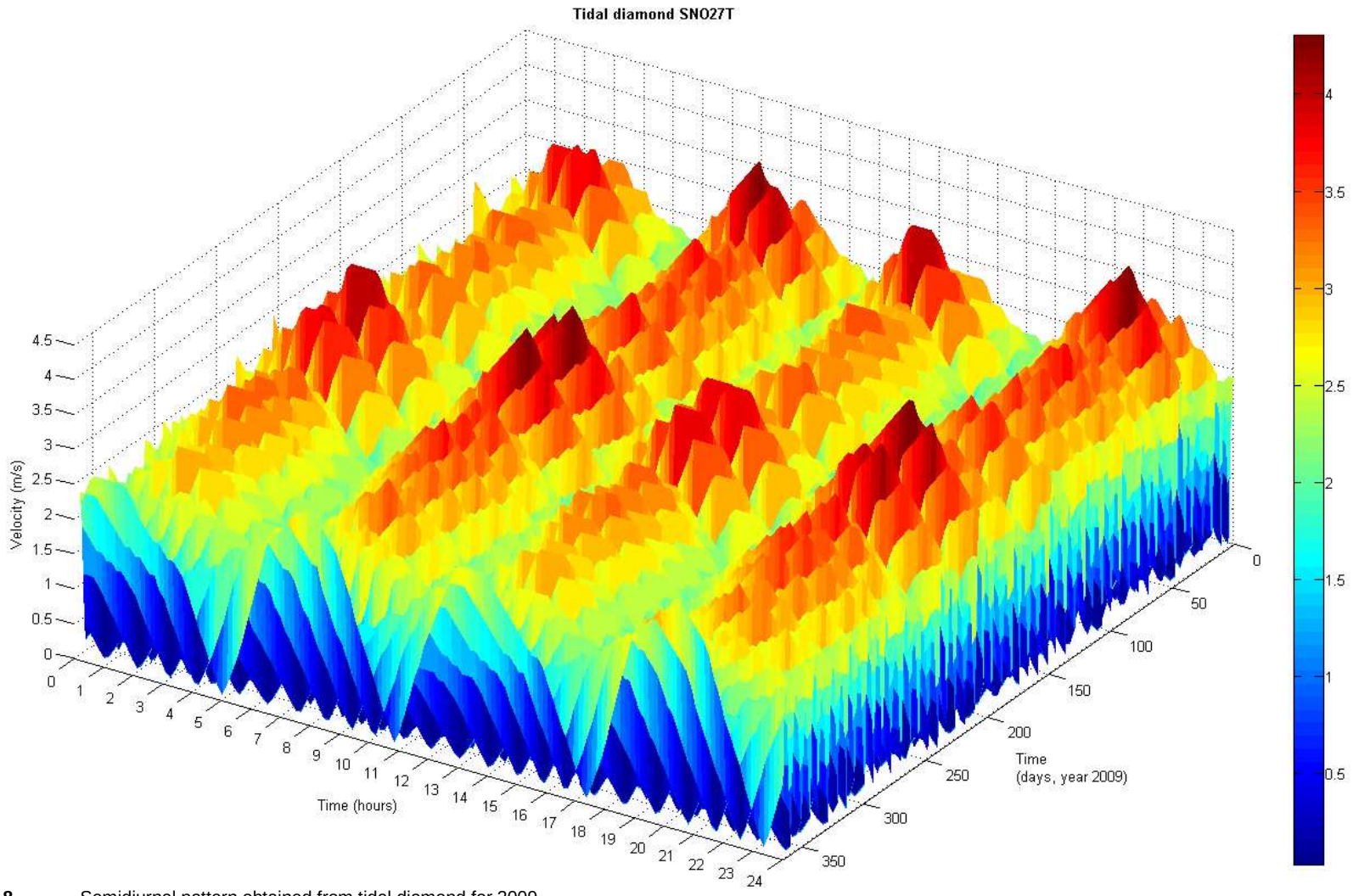

Figure 5.18 Semidiurnal pattern obtained from tidal diamond for 2009.

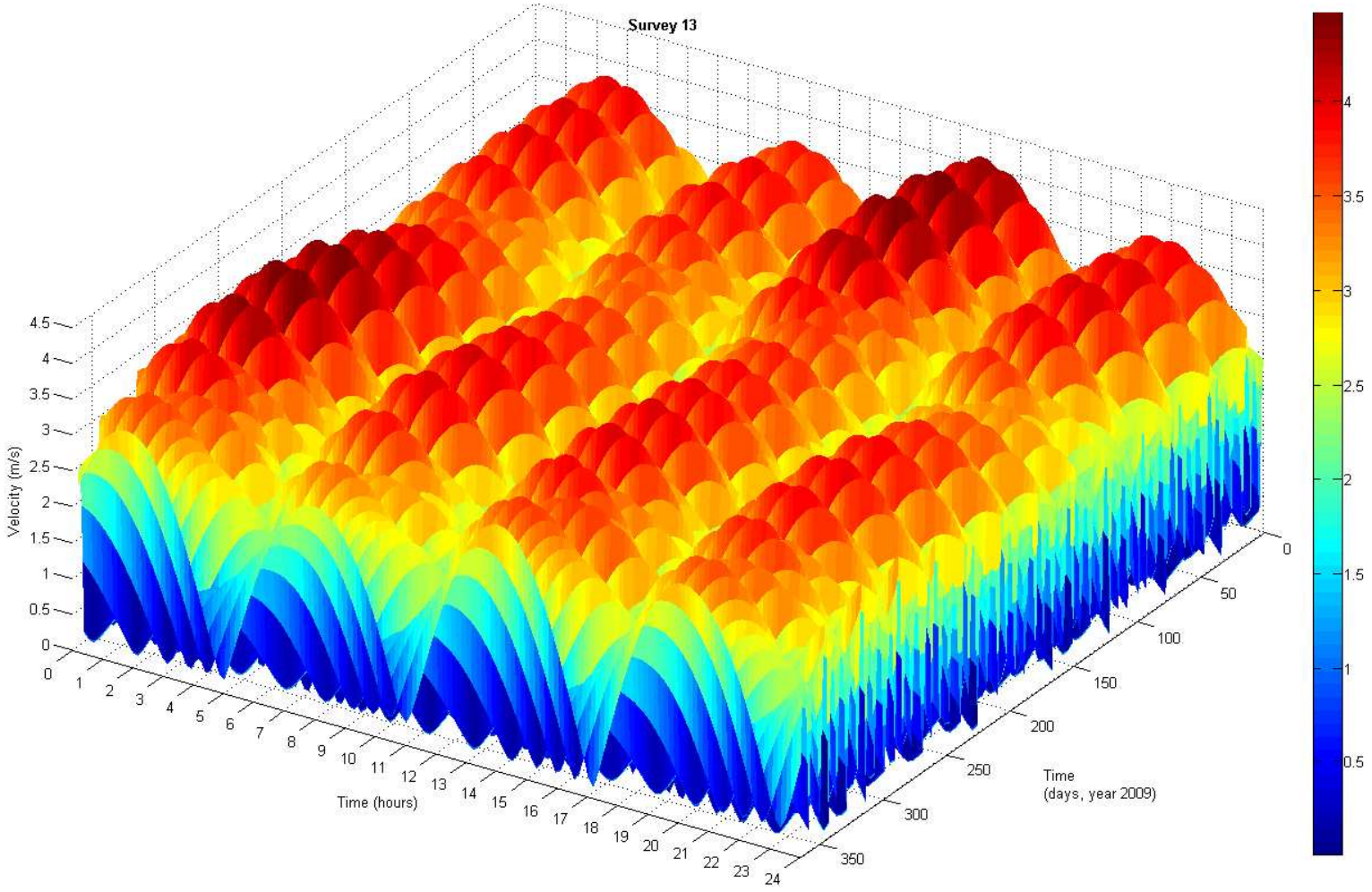

Figure 5.19 Semidiurnal pattern obtained from Survey 13 for 2009.

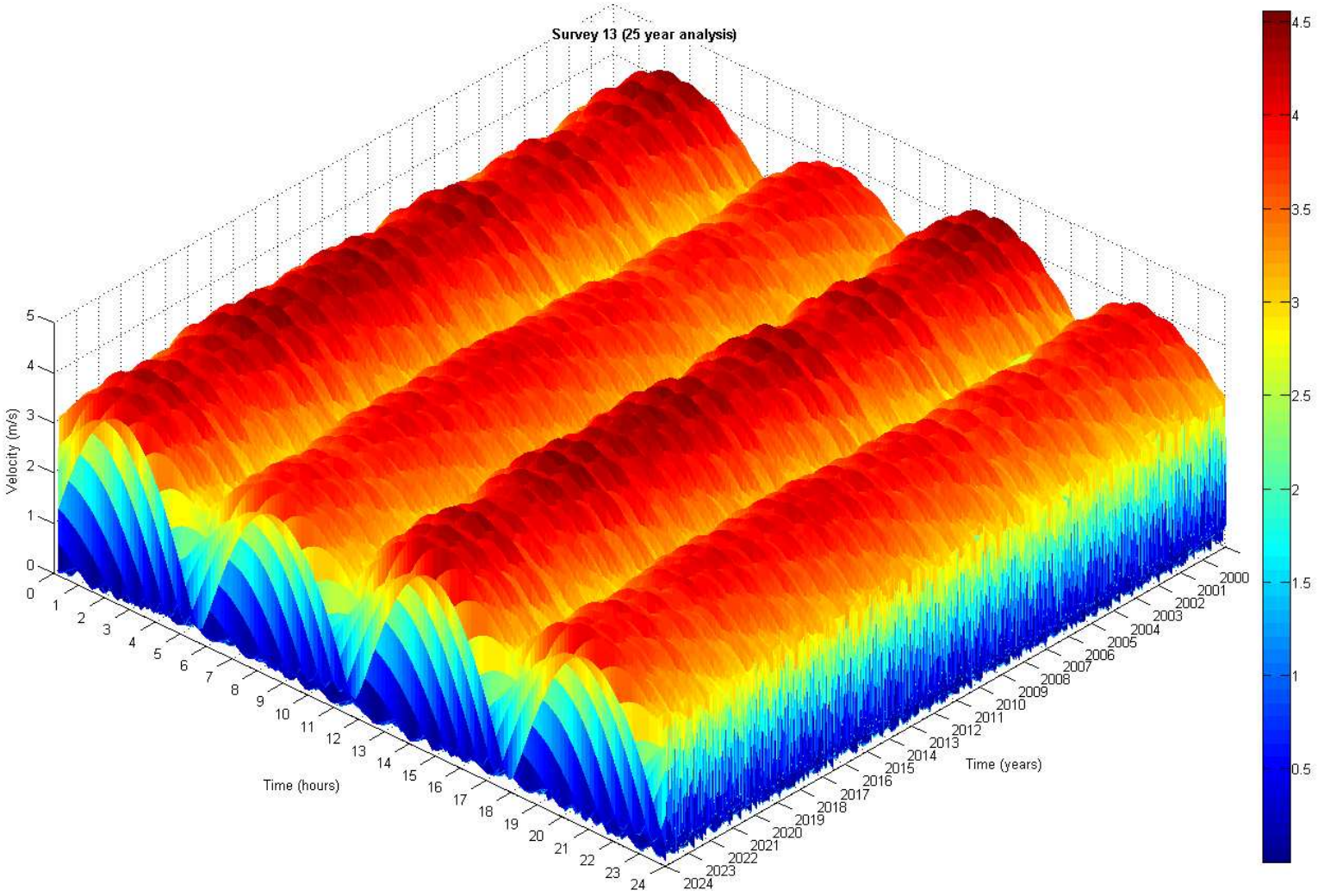

Figure 5.20 Semidiurnal pattern obtained from Survey 13 for 25 years, from 2000 to 2024

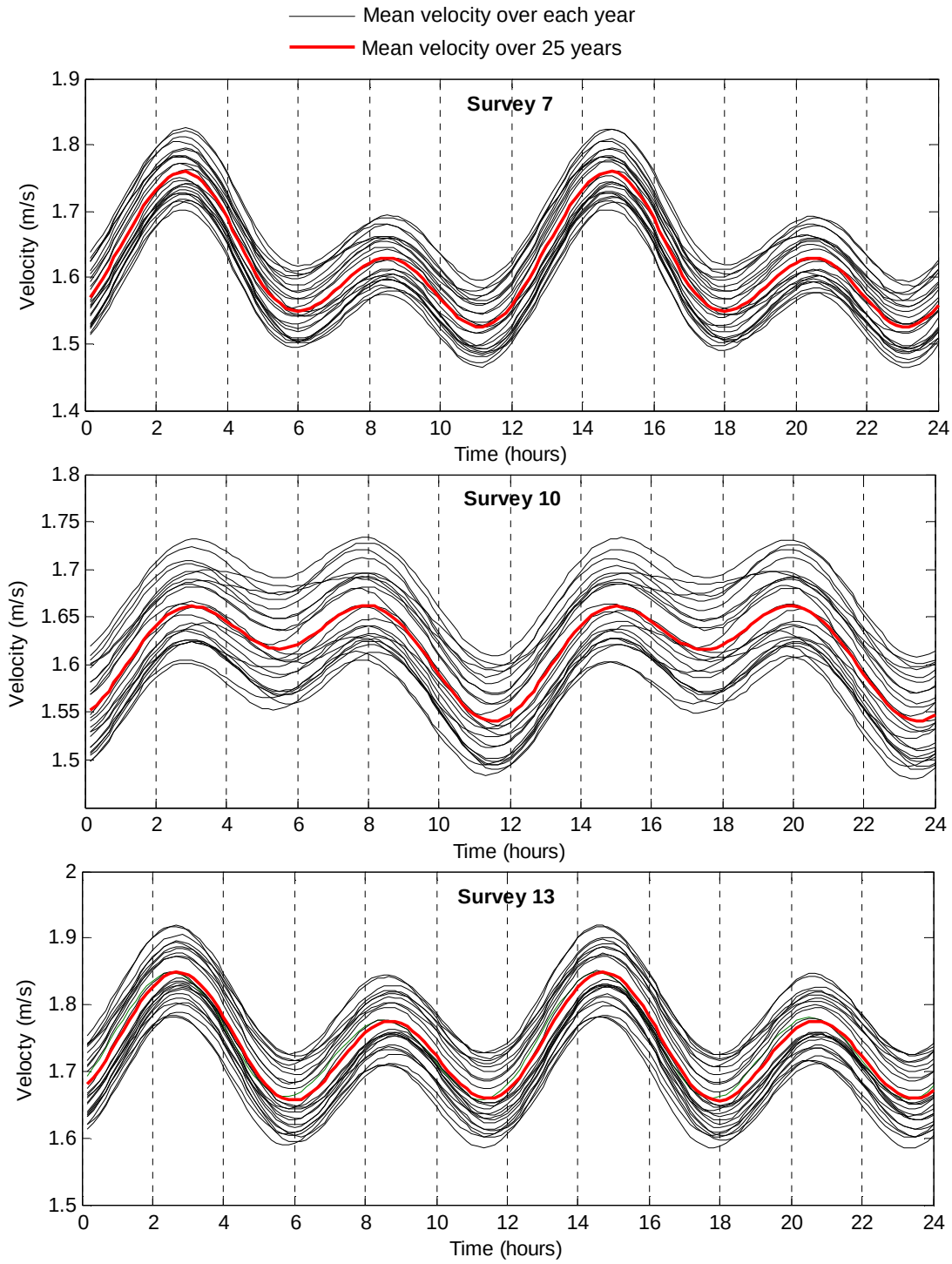

Figure 5.21 Mean velocity in a day. Data obtained by averaging yearly data from 2000 to 2024.

5.4.2 Monthly Variability

The data predicted for the year 2009 is split into different months. The purpose is to evaluate if seasonal variations affect tidal current velocity. It is understood that unlike wind and wave

seasonal variations have little effect on tidal currents, although often meteorological factors can influence the tidal currents to a small extent. The different harmonic constituents can also have an impact on the seasonal variations. Figure 5.22 shows the monthly mean values experienced at Surveys 7, 10 and 13 for the 2009 year recreated record. The largest swing is observed for Survey 13; between the month of June and August the velocity reduced by 5%. The swing between the three surveys is a change of 11%. The graph shows opposite variation between Survey 7 and 13 with Survey 10 showing least variations. Before further analysis is presented it is important to highlight that although 25 years of data is predicted, the data only presents variations observed in the 23 constituents because the original measured data which was used to extract the harmonic constituents only spanned a month. Therefore, fortnightly, monthly, semi-annual and annual constituents (MF, MSF, MM, SSA and SA) are not presented as several years of data are required to accurately determine these constituents (Zervas, 1999).

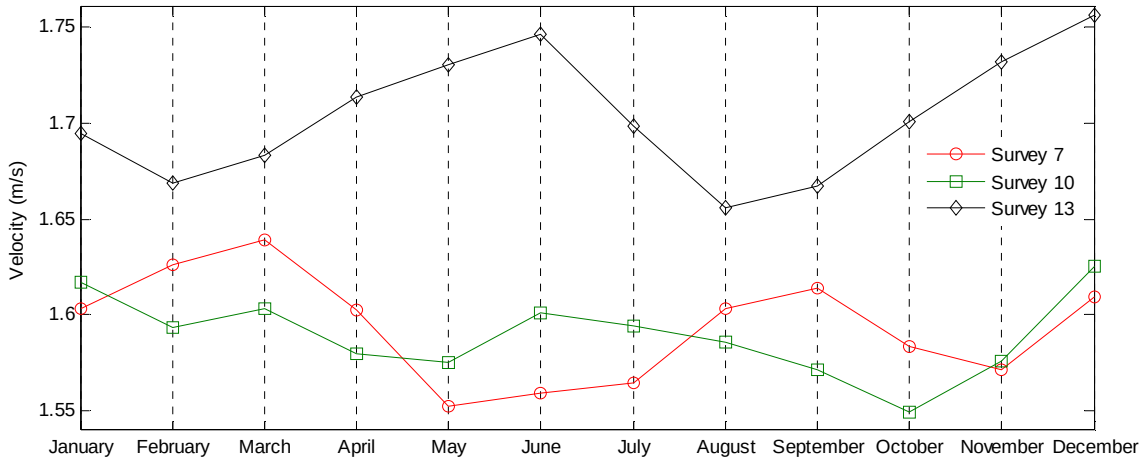

Figure 5.22 Monthly mean velocity variation as seen at Survey 7, 10 and 13 for the year 2009.

The mean value observed in each month for a 25 year period, obtained from harmonic analysis, can be seen in Figure 5.23. Only the maximum/minimum and mean values are plotted to show the general trend and the extreme values experienced.

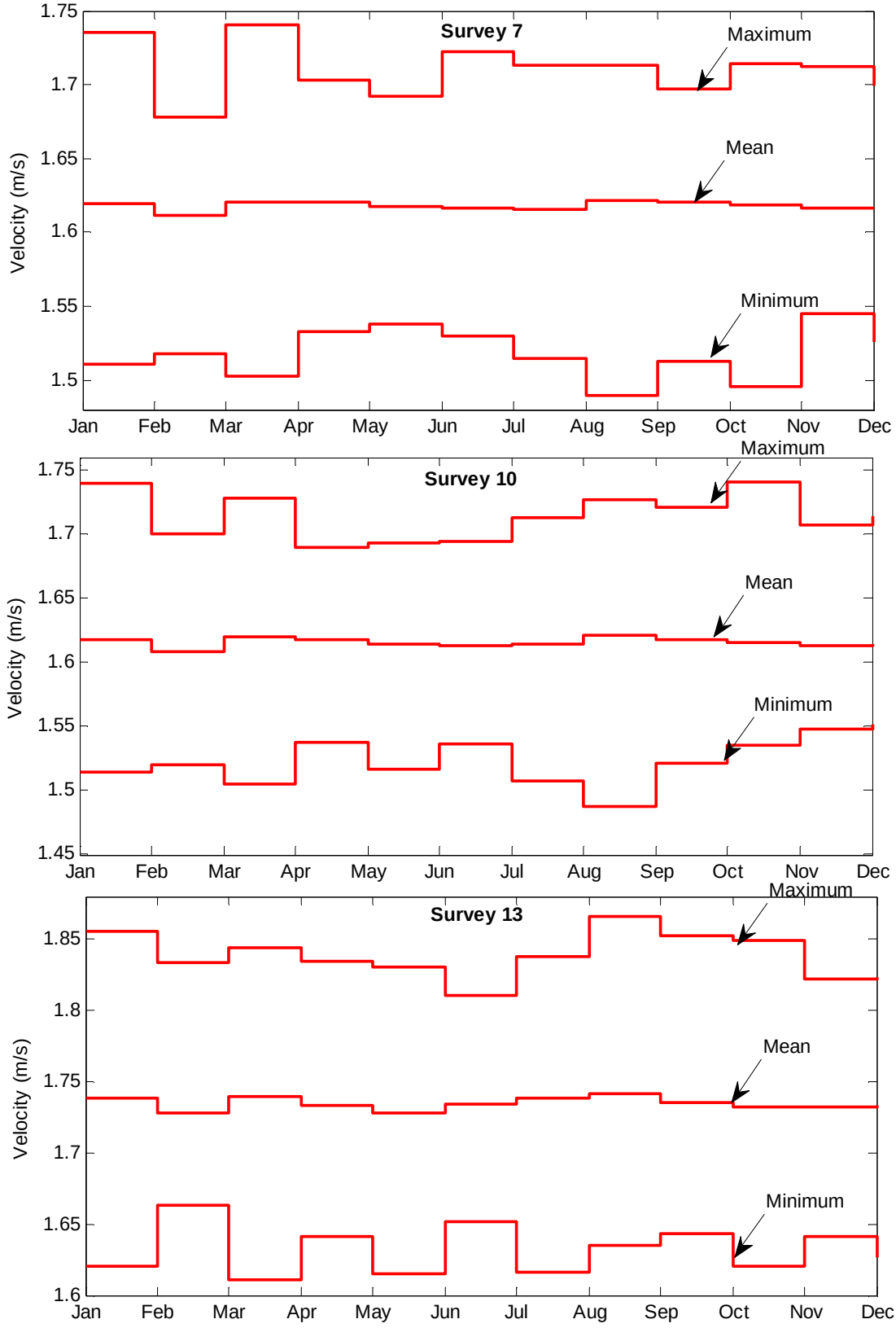

Figure 5.23 Seasonal variation over 25 years of data. Lines show mean/minimum/maximum values.

Although no obvious seasonal trend can be seen here, each month varies from the other because the 23 constituents used in the harmonic analysis have different frequencies and amplitude. Therefore, splitting them into different months implies that the constituents have not completed their cycle leading to small variations. February, for example, always appears to have a lower mean simply because there are fewer days in this month compared to the other months.

Without the inclusion of the fortnightly, monthly, semi-annual and annual constituents, it is difficult to observe any specific trend. Further analysis assumed no monthly variability although it is important to be aware that monthly and seasonal variabilities do exist, they just cannot be accounted for in this analysis.

5.4.2 Yearly Variability

The most significant variations over yearly values are caused by the 18.6 years nodal factor. The extent of these variations becomes obvious when looking at Figure 5.24. In the 18.6 year nodal cycle 2001, 2011 and 2020 are the years that are either one quarter or three quarter way through the cycle. This nodal factor related to the obliquity of the moon's orbit. These years are determined by nodal factors closest to 1 and essentially represent 'a mean year' (Zervas, 1999).

Variations of ±4% swings can be observed between a mean year, such as 2001, 2011 and 2020, to either extreme. Similar variations have also been reported by Jeuken (2003). Maximum swings of 7.5% can be observed between the minimum and maximum values. Since power is proportional to velocity cubed. Even small variations can have significant changes, about 12% in the energy output.

To evaluate the variation in power output, power is calculated for each year. A velocity exceedance curve is plotted for the entire 25 year period (not shown) and the rated velocity for each of the surveys is picked as the velocity exceeding the 10^{th} percentile. This methodology is presented in detail in chapter 6, section 6.3.2. A rated velocity of 2.8 m/s for

Survey 7, Survey 10 is rated at 2.7 m/s and Survey 13 at 3 m/s is evaluated. Figure 5.25 show the potential energy output for the 25 year period.

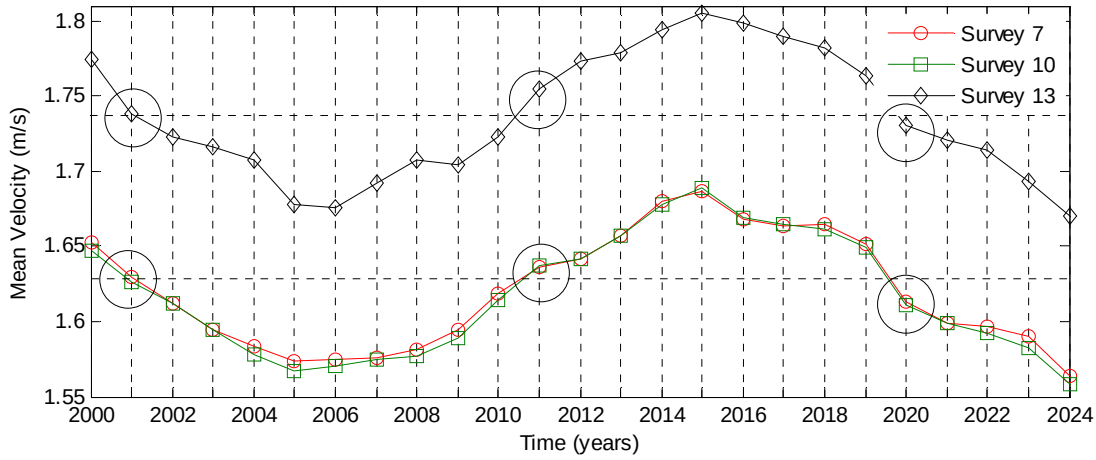

Figure 5.24 Mean velocity variation over 25 year's highlights to 18.6 year nodal cycle.

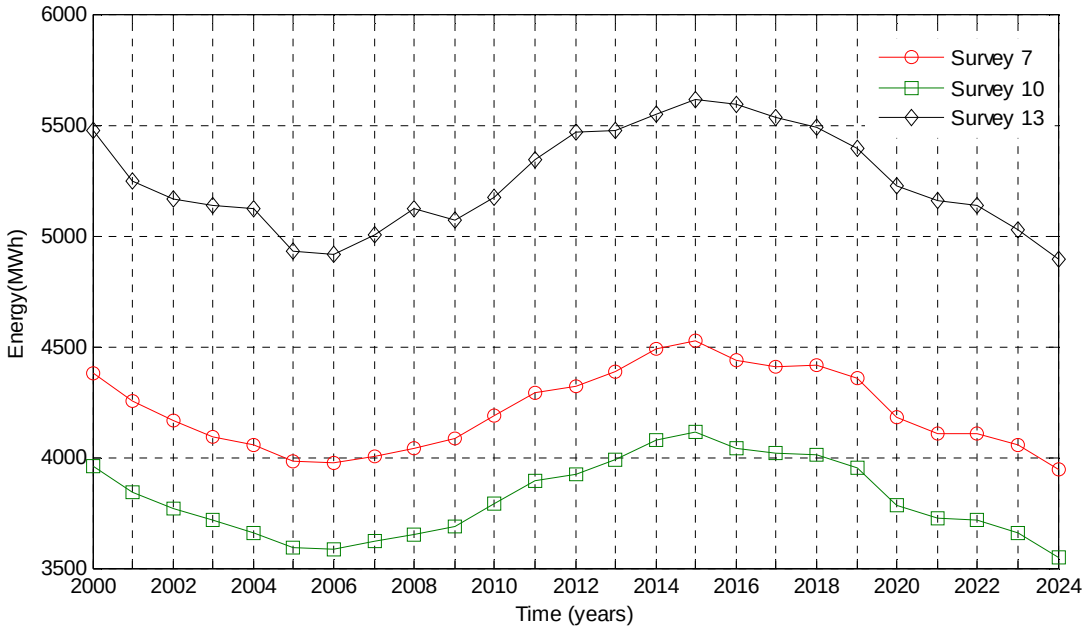

Figure 5.25 Total energy variation over 25 years.

Energy output variations for all three surveys are in the order of ±6% and maximum variation of 12 to 13% can be seen. An assessment of what the energy output for the project life time will be (assuming a 25 year tidal farm project) based on a 'mean' year where the nodal factor is closest to 1 will be very different to say a 'maximum/ minimum' year. Often only one month long deployment measurements are used to evaluate the AEP.

Table 5.7 shows the energy output calculated over different mean, maximum and minimum years compared to the power output calculated over the entire 25 year period. Also presented is energy output based on the original one month ADCP data recorded at the specific locations. It should be emphasised that no down time is assumed in this case and external meteorological factors have not been accounted for either.

		25 years	1 mean year	1 max year	1 min year	1 month measured	1 month predicted
	Energy (GWh)	105.24	104.71	113.14	98.62	99.84	98.72
SURVEY 7	Avg CF (%)	31.57	31.41	33.94	29.58	29.95	29.61
	% difference	-	-0.50	7.51	-6.29	-5.13	-6.20
	Energy (GWh)	95.32	94.72	102.88	88.70	100.24	94.76
SURVEY 10	Avg CF (%)	32.88	32.67	35.48	30.59	34.57	34.57
	% difference	-	-0.63	7.93	-6.95	5.16	-0.58
	Energy (GWh)	131.26	131.23	140.28	122.39	123.22	122.38
SURVEY 13	Avg CF (%)	32.23	32.22	34.44	30.05	30.25	30.05
	% difference	-	-0.02	6.88	-6.75	-6.13	-6.77

Table 5.7 Difference in power output based on mean/minimum/maximum yearly output compared to the 25 year analysis.

In all the cases, the mean year presents the least difference of less than 1%. However, AEP based on the minimum or maximum year show variation in the order of 6 to 7%. Calculations based on one month of data also present variations of 6% and more. By coincidence, the one month predicted data for Survey 10 has the least percentage difference when compared to any of the other values within the analysis. Yet again, this highlights the variability that can be seen at high tidal current energy sites. To put these variations into context, if the energy is sold at £40/MWh (not accounting any discounts, ROC's etc.), a difference of 6% in generation will result in a difference of £265,000, which could significantly affect the project economics.

The evidence of 5-7% variation is specific to this location. Similar analysis should be performed for other sites to fully understand the extent of the variation. What does become obvious is that multiple long term deployments need to be carried out and detailed site survey are necessary to better understand the local flow conditions.

Additionally, analysis is carried out to assess how constant the 18.6 year distribution is. For example, within the 25 year period, will any set of 18.6 year periods have the same power output? In theory, 18.6 years of data should capture all the variations, therefore every set of 18.6 years of data should be identical and for a specific survey, produce the same velocity/power output, apart from weather and other non- harmonic influences. Table 5.8 presents two scenarios where power output from 18.6 years is presented as spanning from year 2000 to 2018 (the top of the 18.6 year cycle) and from year 2006 to 2024 (the bottom of the 18.6 year cycle). The difference between the two values is negligible, and shows how well NOAA's harmonic analysis performs. Moreover, this supports the theory that any 18.6 year period should be alike.

	Energy output (GWh)		
18.6 year period	SURVEY 7	SURVEY 10	SURVEY 13
2000 to 2018	78.720	71.336	98.223
2006 to 2024	78.728	71.349	98.212
% difference	-0.010	-0.017	0.012

Table 5.8 Comparing power output over different 18.6 year cycles.

5.5 Conclusion

The analysis presented in this chapter investigates the spatial and temporal variability of ADCP data collected over different time-periods and at different resolutions. The analysis follows a systematic approach of first calculating all the site specific metrics so that if, for example, a developer was interested, direct comparison could be done between the Fall of Warness and the Sound of Islay.

The main focus of this chapter, however has been to investigate the spatial and temporal variability that is inherent of high energy tidal current sites. Section 5.2 presents a comparison between the measured data and the reconstructed data. Since none of the measurements are coincident in time, a like-for-like comparison is not possible. Therefore the time-series were re-created to a coincident period of time to evaluate how they performed. It is observed that the difference between the measured data and the predicted

data varies from 1% to 5%. The error between the two datasets could be due to various factors including local meteorological events, bathymetry affecting the flow in ways that cannot be recreated by harmonic analysis and possibly the ensemble period used to measure the data.

It was identified that Survey 13 experienced the highest velocity. All three surveys present good bi-directionality, although Survey 7 is the most rectilinear and therefore best suited for a device that does not require a yawing mechanism. Survey 10 has a large scatter caused by the landmass steering the flow and, because the harmonic analysis is unable to recreate the same scatter, a large difference between the measured and the predicted data is observed.

The vertical velocity showed a range of profiles. Survey 7 profiles ranged from $1/4^{th}$ to $1/6^{th}$ profile, whereas Survey 10 suits a range of $1/10^{th}$ to $1/15^{th}$ profile. Survey 13 has a range of $1/10^{th}$ to $1/12^{th}$. For Survey 10 and 13, velocity reduction is observed near the surface. It is thought that these reductions are caused due to surface roughness created by strong winds.

Section 5.4 recreated the data for all the three surveys spanning a 25 year period from 2000 to 2024. It covers the same period as a first generation tidal energy project life time and it covers the 18.6 year tidal variations. Semidiurnal patterns have been observed and it has been identified that the peaks in the Neap and Spring cycle occur at the same time. Further analysis for other regions will be useful in assessing weather or not the times of peak generation are the same.

It has been difficult to establish specific monthly/seasonal patterns as the 23 constituents do not capture these variations. It is suggested that years of data are needed before the monthly, annual, semi-annual and yearly constituents can be identified with any accuracy. However, it has been possible to mimic the 18.6 year variations caused by the obliquity of the moon’s orbit. It is observed that 4% variations are observed in the velocity values compared to a mean year and swings of 6% can be seen for power output. Analysis

was also performed to confirm that any 18.6 year cycle is alike and for project planning and AEP any two 18.6 year cycles can be treated equally.

Multiple and high frequency ADCP deployments have enabled such a detailed analysis. Unfortunately, ADCP data is expensive to collect and is not available for other sites of interest around the UK. However, the methodology and ideas presented in chapters 4 and 5 need to be adapted and re-calculated for each site considered for economic tidal energy development. Chapter 6 presents a national scale analysis. However, the depth of the analysis is not as detailed as presented in chapters 4 and 5. The obvious reason is lack of in-situ data. The purpose of and aim of chapter 6 is to evaluate the overall tidal resource and assess their phasing. The data and methodologies generated from chapters 3, 4 and 5 are applied in chapter 6.

6. National Scale Tidal Resource Assessment

This chapter presents an assessment of the total potential tidal current energy that can be extracted within the UK waters and examines the impact of a portfolio of tidal sites, their phasing and characteristics on an aggregated fleet of tidal turbines. There is step change in the level of detailed site specific measurement presented in this study. This chapter bring together all the learning and understanding developed previously in chapters 3, 4 and 5. The depth of evaluation in some sites is limited by the input data but, more importantly, the wider spatial coverage needs to be at a consistent level so that a like-to-like comparison can be done on a national scale.

Under the Marine Energy Challenge, Black & Veatch, (B&V Phase II, 2005) estimated the extractable resource to be 18 TWh/yr (±30% uncertainty). This is the most widely referenced assessment at a national scale. The analysis presented by B&V utilises input data from a combination of sources, the UK Marine Renewable Energy Resource Atlas (2008) by the (then) Department of Trade and Industry (DTI), Admiralty chart data from the UK Hydrographic Office, and local port data where available. A 'Significant Impact Factor' (SIF) was proposed to limit the energy that can be exploited without adversely affecting the environment and the overall resource itself. A constant value of 20% of the total available kinetic energy flux was applied by B&V (2005).

First generation devices are considered to be the driver for tidal current energy development until at least 2025. Installation and operation in deeper water requires more radical 'second' and 'third' generation approaches that are, as yet, only in the very early stages of research and development. Therefore, an analysis based on just first generation device specification is required. The application of the SIF has since been superseded, for this reason a revision of the 'Extractable Power' considered by B&V Phase II (2005) and Sinden (2005) is also necessary.

Findings of Clarke *et al.*, (2006) and Hardisty (2008) with regard to tidal phasing are flawed and would also benefit from a re-evaluation. Given the identified deficiencies of existing efforts to assess the potential for aggregate tidal current energy generation at a national level that also considers the temporal variability, this chapter is concerned with understanding the scope for portfolios of credible first generation tidal current locations to provide firm power. This involves a re-assessment of the UK tidal current resource by identifying appropriate development locations incorporating the latest thinking on power extraction limits and examines aspects of generation yield, variability and temporal phasing.

The majority of the data used are publically available. Two different datasets were used to provide spatial and temporal accuracy as identified using IDW in chapter 3. With additional processing, the datasets were combined to achieve considerable improvement in analysing the resource. The data obtained from the Marine Atlas was available through a web interface (BERR, 2008). The Geographic Information System (GIS) data layers downloadable from the web interface were interrogated using ArcGIS and manipulated. Admiralty chart data was accessed utilising Admiralty TotalTide, to provide time-series at identified locations. The site specific data applied in chapters 3, 4 and 5 was also used. ADCP data was made available to the author on request for Orkney by the European Marine Energy Centre (EMEC) and for Sound of Islay by Scottish Power Renewables (SPR). Additionally, measured buoy data was obtained from British Oceanographic Data Centre (BODC) for Anglesey. Time-series for all these sites needed to be coincident in time, therefore the buoy and ADCP data had to be recreated using harmonic decomposition and predicted using the methodology advocated by the US National Oceanic Atmospheric Administration, NOAA (Zervas, 1999), as demonstrated in previous chapters.

6.1 Tidal Resource Phasing

Figure 6.1 shows the co-tidal lines around the UK that represent the time of high water at each location.

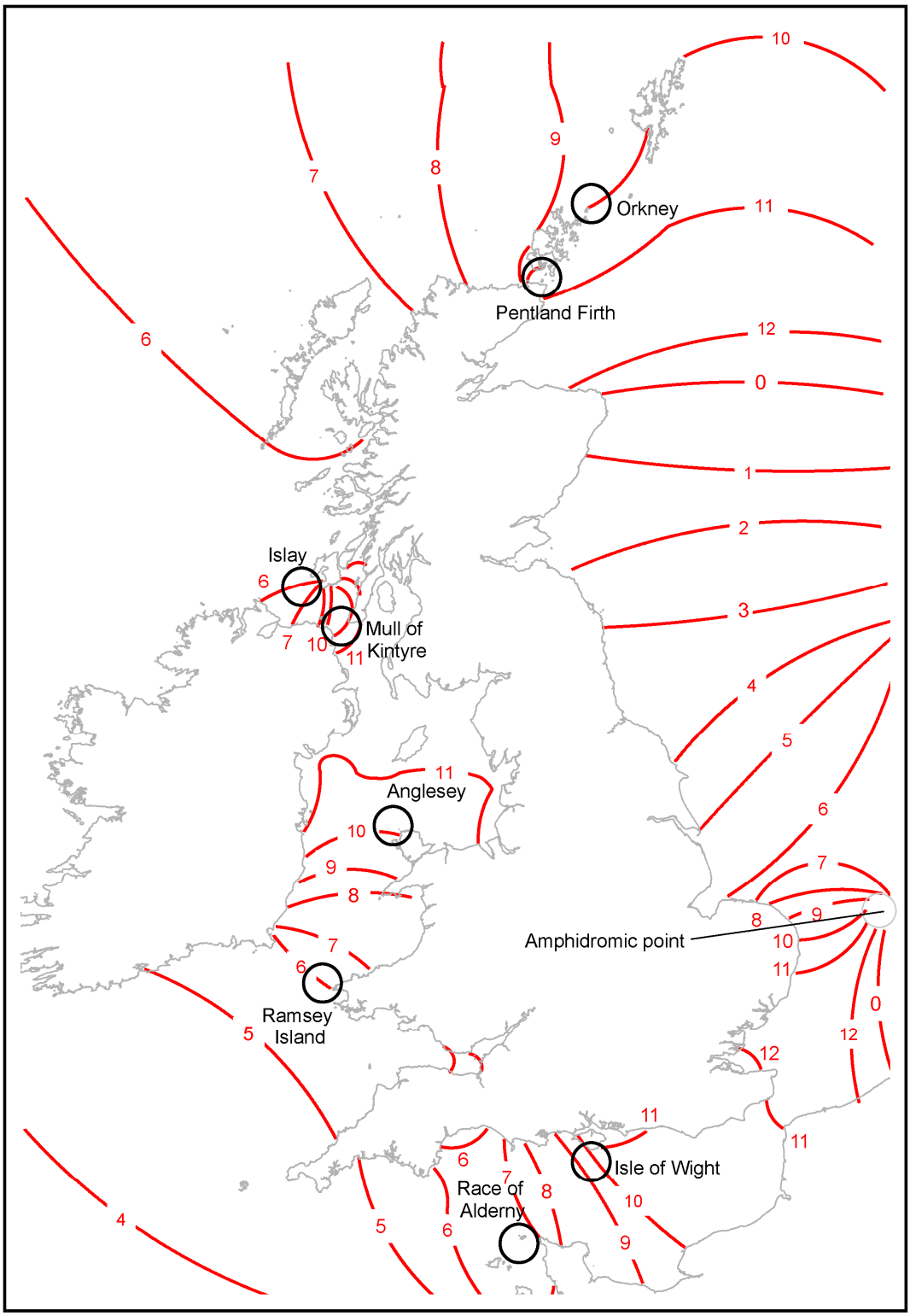

Figure 6.1 Co-tidal lines for the coast of UK. Areas indicated by the circles are regions identified to be of interest for tidal current energy development.

This broadly illustrates the phasing of tidal currents. Although coincidence in the time of high water does not necessarily mean that the tidal currents in each location are also in-phase, as this is highly dependent upon the local variation of surface elevation. Tidal interaction with local bathymetry and the coastal topography also play an important role in the local phasing of tidal currents. However, for UK waters, near-shore tidal wave propagation behaves like standing waves, as suggested in section 2.3. In addition, the characteristics of tidal current generators, particularly the shape of the power extraction curve will also play a significant role in the phasing of power production. (This is in reference to the ramp rate of the device, see Figure 6.12. The power generation is asymmetrical.)

The locations circled in Figure 6.1 have been identified by B&V Phase II (2005) as being sites of interest for tidal current energy extraction. Ideally a phase difference of 90° or 270° (three or nine hours) between two locations is optimal for tidal sites to provide best potential for generating firm power. However, the locations highlighted here experience high water at broadly similar times. This suggests that there is also a good likelihood that these locations will also exhibit tidal current patterns that are also to be in-phase (as introduced in section 2.3). If this coincidence of tidal velocity phasing can be verified for instance in the case of the Pentland Firth and Channel Islands, the phasing will have significant negative impact on the potential for tidal current energy to generate a large proportion of its output as firm power, as these two locations alone have been identified as embodying about 70% of the technically extractable UK tidal current energy resource (B&V, 2004).

Sites in the Pentland Firth have already been identified as the first significant tidal current energy developments, as established by the recent round of site leasing by the Crown Estate, with 1.2 GW installed capacity of wave and tidal energy proposed for this region (Crown Estate, 2010a). An additional 400 MW of tidal energy developments have since been leased in the Inner Sound region of the Pentland Firth (Crown Estate, 2010b). As a result of these geographically clustered developments, there will likely be very small phase difference

between these initial tidal sites. The ‘in-phase’ character of the tidal sites is entirely coincidental and specific to the UK. Such coincidence of phasing of so many key locations in one country may not be replicated in other territories, when the tidal current energy resource is accurately assessed. This is simply because of the uniqueness of the land topology and bathymetry which is unlikely to be reproduced elsewhere!

6.2 Methodology

The methodology aims to make best use of publicly available data to identify locations suitable for deployment of first generation tidal current devices and to generate credible time-series of energy production from generic tidal current technologies at these locations. It also allows the latest methods on power extraction limits to be incorporated. The three main stages of the method as outlined in Figure 6.2 are:

1. Identification of locations suitable for large scale first generation tidal current device developments;
2. Estimation and validation of the tidal current time-series at these locations;
3. Estimation of generic tidal generator size, rating and hence time-series of energy generation at each identified location.

The time-series generated provide a suitable format to enable comparison between aggregate assessment of the energy generation potential of specific regions as well as for the UK as a whole. The output is primarily a re-appraisal of the UK tidal resource, but the generated time-series will also assess how much can tidal contribute to the UK’s demand for electricity. Therefore, the time period for this analysis had to be recent, so as to make comparison to recent demand trends. With this thought, the analysis was conducted for the year of 2009. The choice of the year is such that demand data is easily available and the nodal factor is as close to unity as possible for the 18.6 years nodal cycle. For the present period, this happens to be in the year 2011 as demonstrated in chapter 5, section 5.4.2. To

allow comparison between the resource and present demand, 2009 has been used as the base year.

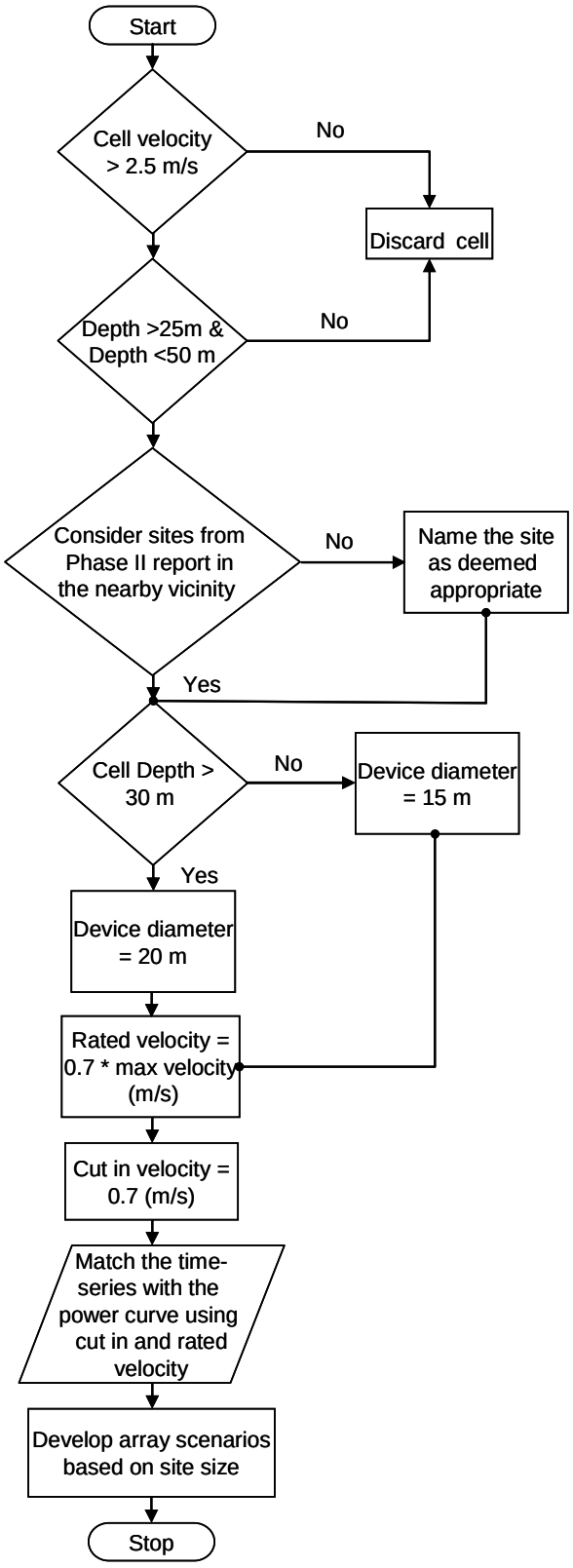

Figure 6.2 Flowchart showing the steps embodying the methodology.

6.2.1 Locations for First Generation Tidal Devices

The first stage of the process outlined in Figure 6.2 aims to identify sites that are viable for the deployment of first generation tidal current devices. Data accessed from downloadable GIS layers of the Atlas of UK Marine Renewable Energy Resources (BERR, 2008) were used here. This was a similar approach to that adopted by B&V Phase II (2005). The GIS data itself is derived from the POL CS20 Model (POL), which was also utilised in the analysis conducted by Sinden (2005). The Atlas provides mean spring and neap tide velocity magnitude and water depth data within the UK territorial waters at a spatial resolution of approximately 1.8km^2. Figure 6.3 shows the mean spring peak current for the UK and several regions of particular interest for first generation tidal deployment included in this scenario.

Using ArcGIS, the Marine Atlas data was interrogated to select specific cells meeting certain criteria. For a site to be considered economically viable for first generation tidal farms, the mean spring peak current velocity must exceed 2.5 m/s. The second criterion needs the water depth to be within the range of 25 to 50 metres which is the expected operational depth for first generation devices, as suggested by B&V Phase II (2005).

The specific cell selected through interrogating the Marine Atlas for Westray firth, Orkney are shown in Figure 6.4. This site is in the same channel as Fall of Warness, EMEC's test site (and the subject of analysis in chapter 5). The 1.8 km^2 cells are too large to accurately assess the resource in the narrow channels. Although the cells identified by the Marine Atlas are not spatially coincident to the ADCP data, the analysis conducted in chapter 5 demonstrates the strength of the resource in this region. Therefore, for this particular analysis, data from EMEC's Survey 7 is being used, where a current velocity of 3.5 m/s has been recorded. In-situ measurements are considered 'gold-standard' and the surveys carried out by EMEC provides enough confidence in considering this region as a highly energetic site.

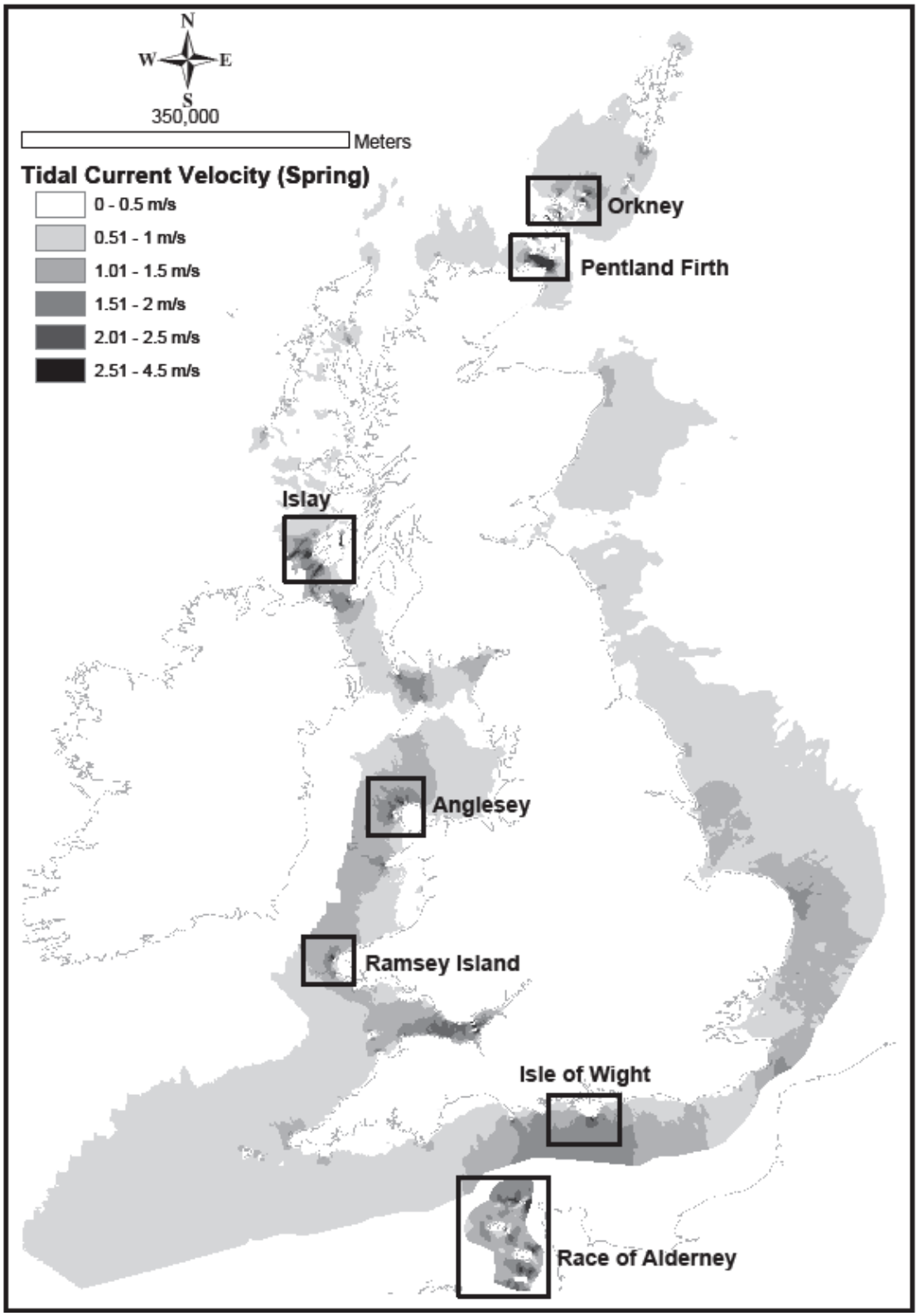

Figure 6.3 Figure showing mean spring peak current and specific regions of interest. BERR Marine Atlas. © Crown Copyright. All rights reserved 2008.

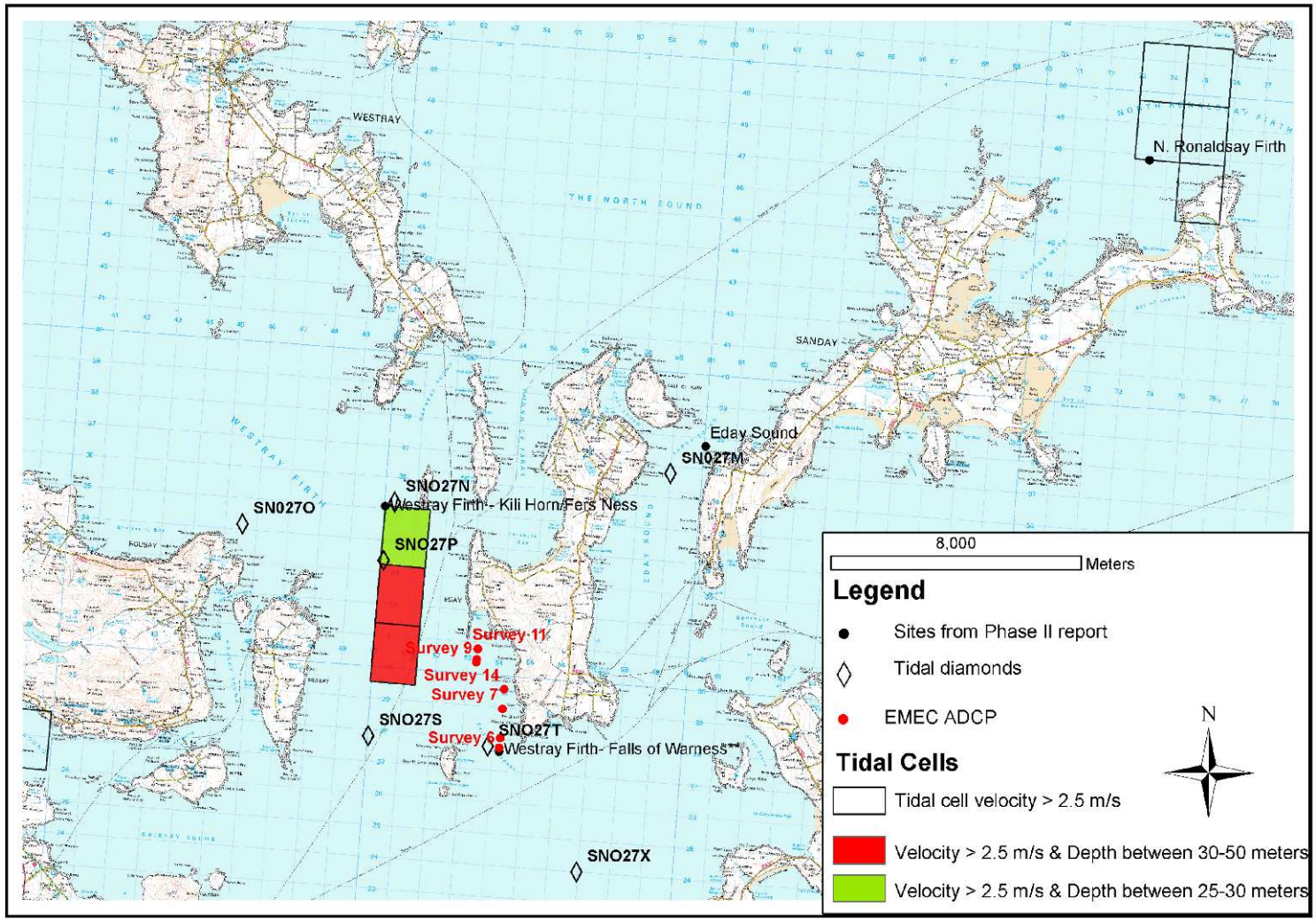

Figure 6.4 Cell selection at Orkney using the Marine Atlas. © Crown Copyright/database right 2011. An Ordnance Survey/EDINA supplied service.

As previously indicated in chapter 5, the ADCP data is a 1 month long measurement taken in 2005. To re-create the dataset in this national resource assessment for the common time period of 2009, harmonic constituents generated using NOAA's *lsqha.f* program were used in *pred.f* to generate the necessary time-series. All the datasets generated for this national scale resource assessment were obtained at a temporal resolution of 10 minutes.

In the Pentland Firth region, identified in Figure 6.5, there are 89 cells in total that experience current velocity of 2.5 m/s or higher, but the majority of these cells are too deep to be considered for first generation development. All the sites considered by the Black & Veatch Phase II (2005) are located in regions where the cell depth is too deep for deployment. Only 17 cells have been identified to be of 30 to 50 metres of water depth, with 2 cells in water depths of 25-30 metres. The time-series for this region is generated using tidal diamonds, as no measured datasets was made available to the author. There were a limited number of tidal diamonds to extract data from. Therefore, to differentiate between different sites the-time series are scaled up for each cell using specific average spring peak velocity obtained from the Marine Atlas:

$$Atlas\ \ scaled\ \ data = IDW\ \ genrated\ \ data * \frac{Marine\ \ Atlas\ \ mean\ \ spring\ \ peak\ \ value}{Spring\ \ peak\ \ value\ \ in\ \ the\ \ IDW\ \ data} \quad (6.1)$$

This maintains the local phasing and Spring-Neap variability as prescribed by the tidal diamond data, while also utilising the improved resolution of the numerical model output to identify local peak current velocities.

Table 6.1 lists all the sites considered in this study using the selection criterion outlined in Figure 6.2. The sites identified in Figure 6.4 and 6.5 were included in the B&V Phase II (2005) study as well.

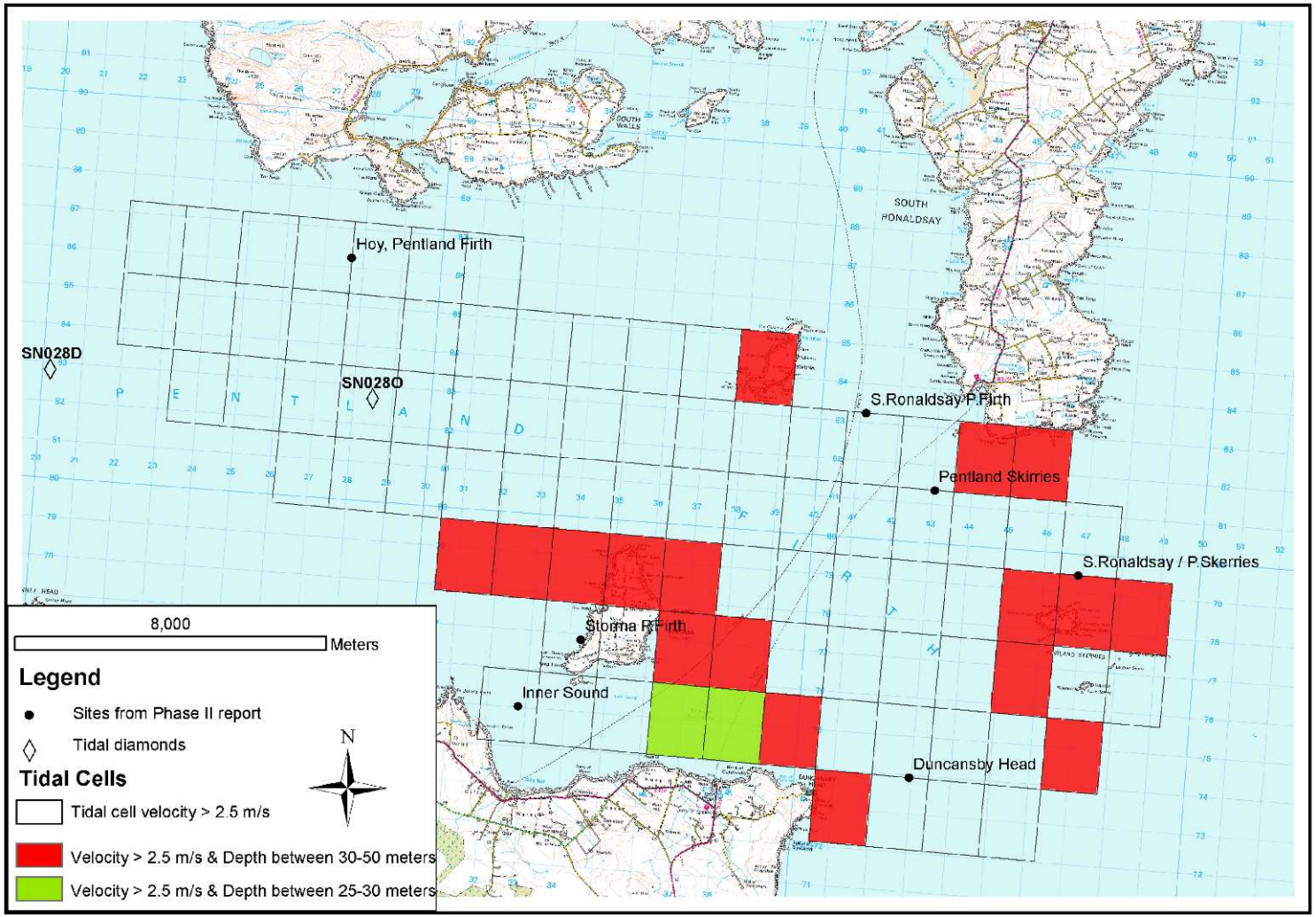

Figure 6.5 Cell selection at Pentland Firth using the Marine Atlas. © Crown Copyright/database right 2011. An Ordnance Survey/EDINA supplied service

	Site name	Grid reference		No. of cells	Region	Average Depth (m)	Average Velocity Spring Peak (m/s)
Pentland Firth	Pentland Skerries	58.72 N	-2.95 W	2	Scotland	35.50	3.60
	S. Ronaldsay P.Firth	58.74 N	-3.06 W	1	Scotland	39.00	3.19
	S. Ronaldsay/ P.Skerries	58.69 N	-2.92 W	5	Scotland	43.20	2.93
	Duncansby Head	58.64 N	-3.01 W	1	Scotland	36.00	3.25
	Inner Sound	58.66 N	-3.06 W	3	Scotland	28.67	3.27
	Stroma P.Firth	58.68 N	-3.12 W	7	Scotland	39.29	3.44
Orkney	Westray Firth	59.17 N	-2.86 W	2	Scotland	29.00	3.81
	N. Ronaldsay Firth	59.39 N	-2.34 W	1	Scotland	34.00	2.57
Islay	Islay North	55.67 N	-6.84 W	7	Scotland	29.00	2.75
	Islay Centre	55.67 N	-6.63 W	12	Scotland	27.75	2.76
	Islay South	55.54 N	-6.39 W	8	Scotland	38.88	2.63
	Sound of Islay	55.86 N	-6.09 W	2	Scotland	50.00	2.95
Anglesey	Anglesey North	53.42 N	-4.61 W	4	Wales	30.00	2.59
	Anglesey South	53.29 N	-4.71 W	1	Wales	31.00	2.60
	Ramsey Island	51.41 N	-5.41 W	3	Wales	35.00	2.66
	Race of Alderney	49.69 N	-2.11 W	19	England	31.68	3.38
	Isle of Wight	50.56 N	-1.23 W	2	England	27.50	2.76

Table 6.1 List of all the sites considered in this study.

Clusters of cells have been identified just off the Island of Islay where high tidal velocity is experienced. The Marine Atlas performs well in more open seas, but for the Sound of Islay (which is a narrow channel), the model is not resolved sufficiently to identify that this area meets the necessary criteria. The Marine Atlas identifies the Sound of Islay as a region of high velocity but considers it too shallow to meet the depth criteria. This example is indicative of some of the limitations of the Marine Atlas as a data source. It has wide area coverage, but this is only achievable because the resolution is lower than necessary for the purpose of identifying suitable tidal current energy development sites. Scottish Power Renewables (SPR, 2010) indicated that the Sound of Islay reaches 48 metres deep and is appropriate for first generation development. The ADCP measurement for this site has also been analysed in chapter 4 and supports SPR's findings.

6.2.2 Estimation and Validation of Tidal Current Time-Series

The next stage of the analysis is to generate credible tidal current time-series data for each of the sites identified in Table 6.1. In order to do this, it is necessary to identify which sources of datasets are available for each of the sites identified. Table 6.2 lists the different datasets available. For majority of the sites, the Marine Atlas and tidal diamonds are the only source of data. For these sites, multiple calibrations between different tidal diamonds were employed to find IDW's that best represented the sites as presented in chapter 3 and scaling factors using the Marine Atlas as suggested in equation 6.1 were applied.

For Westray Firth, Sound of Islay and Anglesey, local measured data was used as it provides improved accuracy and encapsulates the tidal variability better than the tidal diamonds.

	Site name	Marine Atlas	Tidal diamond	ADCP	Buoy
Pentland Firth	Pentland Skerries	✓	✓		
	S. Ronaldsay P.Firth	✓	✓		
	S. Ronaldsay/ P.Skerries	✓	✓		
	Duncansby Head	✓	✓		
	Inner Sound	✓	✓		
	Stroma P.Firth	✓	✓		
Orkney	Westray Firth	✓	✓	✓	
	N. Ronaldsay Firth	✓	✓		
Islay	Islay North	✓	✓		
	Islay Centre	✓	✓		
	Islay South	✓	✓		
	Sound of Islay			✓	
Anglesey	Anglesey North	✓	✓		✓
	Anglesey South	✓	✓		✓
	Ramsey Island	✓	✓		
	Race of Alderney	✓	✓		
	Isle of Wight	✓	✓		

Table 6.2 Datasets available for each site

6.2.3 Tidal Generator Size and Rating

The third stage uses a simple generic model of a 3-bladed horizontal axis tidal current device to estimate time-series of power generation at each site from local current velocity time-series. For the purpose of assessing energy extraction, it is assumed that each device is sited such that the flow direction is aligned axially with the device axis of rotation. Two device models are used to reflect the differences required for operating in different water depths. In cells with minimum water depths of 25 to 30 metres a device rotor diameter of 15 metres provides appropriate surface and seabed clearance, avoiding conflict with vessel navigation in the region. In depths greater than 30 metres, a device diameter of 20 metres is specified.

An appropriate rated current velocity for each cell is determined by taking 70% of the Spring peak velocity of the specific cell. This follows similar practice to B&V Phase II

(2005), utilising understanding of the optimal economic balance between capturing maximum available energy and the cost of the energy capture device. If, for instance, the device was rated to coincide with maximum Spring peak velocity, then the drivetrain would have to be rated to operate for condition that occurs only for a short instant each month, and the structural support element of the device would similarly have to be designed to withstand the thrust acting on the turbine for only a minute fraction of the operational period.

The device power curve is based on the published power curve for MCT's SeaGen device currently being tested in Strangford Narrows. Figure 6.6 illustrates the device's operating power curve. The hypothetical device power curve used in this scenario is developed based on the device characteristics of MCT's SeaGen full scale prototype (MCT, 2010b).

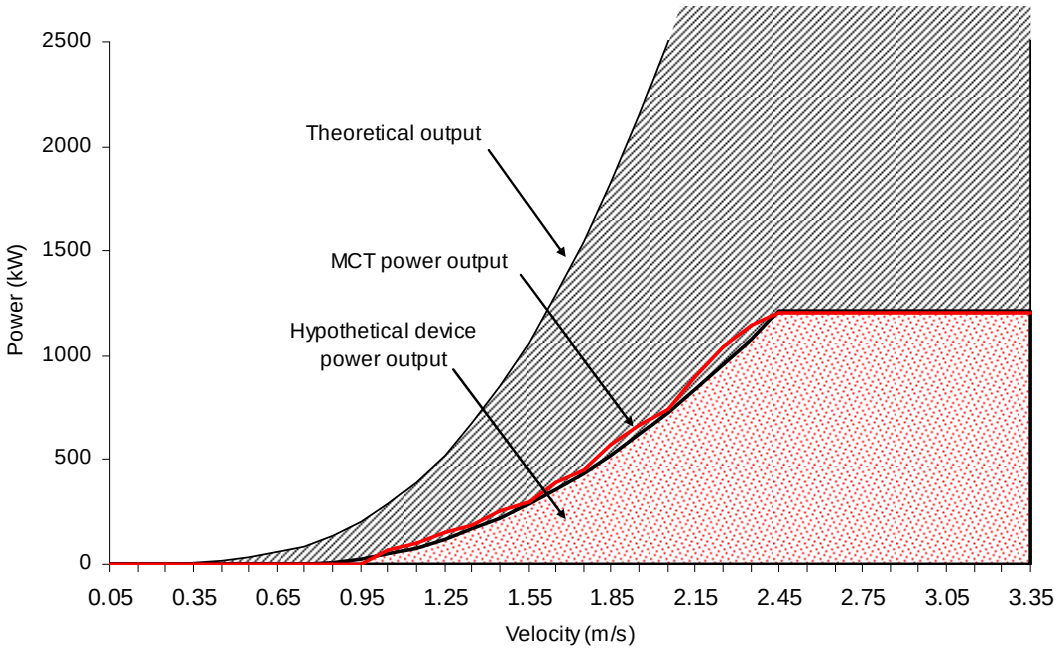

Figure 6.6 Hypothetical device curve based on MCT's Seagen. Curve built based on the actual device power output.

Figure 6.7 shows the power curve for a generic 0.5 MW rated turbine and demonstrates the difference in rated velocity necessary to generate 0.5 MW with a 15 and a 20 metre rotor diameter. A cut in velocity of 0.7 m/s is assumed in each case for both the hypothesised generic turbines and a constant efficiency of 42% is considered in both the

cases as suggested by DTI (2005) and identified by the power curve shown in Figure 6.6. A 25% reduction in the capture area from 20 metres to 15 metres results in a 17.5% increase in rated velocity from 1.98 m/s for the 20 metre diameter device to 2.4 m/s for the 15 metre diameter for the same rated power (0.5 MW).

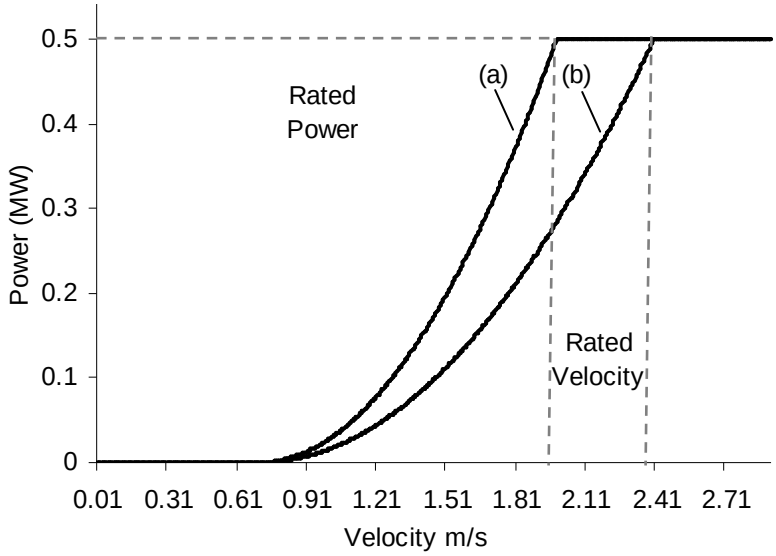

Figure 6.7 Hypothetical power curve for a generic 0.5 MW tidal current device: (a) rated velocity of 1.98 m/s with 20 m diameter rotor; (b) rated velocity of 2.39 m/s for a 15 m rotor.

Multiple tidal devices populate each of the 1.8km^2 cells. The device rating for each cell is a function of the velocity distribution experienced at the site. Two techniques of rating the device are presented in section 6.3. EMEC Standards (EMEC, 2009a) suggest devices are spaced two and a half diameters between the rotor axis perpendicular to the current and ten diameters apart parallel to the current. The assumed device array spacing in this study is more conservative with three diameters apart laterally and ten diameters spacing upstream/downstream of each device. This means that 480, 15 metres diameter devices or 270, 20 metre diameter devices can populate each 1.8km^2 cell. It is acknowledged that actual array layout is unlikely to be as regimented, employing staggering of devices, and would have to adapt to the real world variability of appropriate bathymetric conditions (e.g. bed slope).

6.3 Analysis

This section reports the results obtained from application of the methodology described in section 6.2.1 when applied to the sites identified in Table 6.1 as being suitable for first generation tidal current sites (also see Figure 6.3). The power potential of each site, the phasing of the sites and the impact of the environmental extraction limits at each location are considered in this section.

6.3.1 First Generation Tidal Current Resource

The installed capacity of each cell was calculated from the relevant cell rated velocity and peak power output. These are aggregated for each site as shown in Table 6.3 along with a breakdown of the number of each turbine size. Overall, first generation sites would support an installed capacity of 13.4 GW of tidal current devices. The installed capacity is a simple assessment of the number of devices that can be placed in each of the identified cells without considering any impact this may have on the current flow velocity or the environment. There is a substantial range of installed capacity with the largest single site capacity identified as 3855 MW in the Race of Alderney and the smallest being the 105 MW Anglesey South site. The largest regional group is the Pentland Firth at 4352 MW installed capacity. For the purposes of the analysis presented here, the interaction of devices with wakes generated by upstream devices and device downtime due to planned or unplanned maintenance have been ignored, as these aspects are likely to be highly site and project specific. However, it should be acknowledged that these assumptions do need to be considered at a detailed level when doing a site specific study.

	Site name	No. of cells	No. of device (20 m)	No. of device (15 m)	Installed Capacity MW	Yield TWh/yr	Capacity Factor %
Pentland Firth	Pentland Skerries	2	540		708	1.8	28.8
	S. Ronaldsay P.Firth	1	270		194	0.4	26.2
	S. Ronaldsay/ P.Skerries	5	1350		759	1.7	25.2
	Duncansby Head	1	270		205	0.6	32.6
	Inner Sound	3	270	960	813	1.4	23.3
	Stroma P.Firth	7	1890		1673	3.9	24.7
	Regional Total				**4352**	**9.7**	
Orkney	Westray Firth	2	540		620	2.6	32.4
	N. Ronaldsay Firth	1		480	180	0.2	23.8
	Regional Total				**800**	**2.9**	
Islay	Islay North	7	810	1920	875	2.5	32.5
	Islay Centre	12	2160	1920	1526	4.5	33.2
	Islay South	8	1620	960	879	2.6	33.3
	Sound of Islay	2	40		23	0.1	43.6
	Regional Total				**3302**	**9.6**	
Anglesey	Anglesey North	4	270	1440	418	1.0	26.2
	Anglesey South	1	270		105	0.3	32.4
	Regional Total				**523**	**1.3**	
	Ramsey Island	3	540	480	**340**	**0.7**	24.8
	Race of Alderney	19	3658	1178	**3855**	**10.4**	30.0
	Isle of Wight	2		960	**255**	**0.7**	29.6
	TOTAL				**13427**	**35.2**	

Table 6.3 Sites with installed capacity, annual energy yield and capacity factor. Based on rated velocity obtained by using 70% of Spring peak as suggested by B&V (2005)

The gross annual energy yield from each of the cell is calculated from the tidal current time series at each cell matched with the device power curve identified as appropriate for that cell. As reported in Table 6.3, the results from each cell within a site are summated and suggest that over 35 TWh/ year could be produced across each of the sites which equates to approximately 10% of UK electricity demand based on 2009 demand levels. The productivity of each site broadly reflects the installed capacity, although the match between current flow conditions and generator characteristics means that the production from each site varies. For example, the Race of Alderney has the highest energy yield despite not possessing the largest installed capacity. This is reflected in the site capacity factors, (the ratio of production from a given generator to the production if the same generator operated at rated output with 100% availability over a given period of time). The overall average capacity factor across all the sites is 29.9% but the values for individual sites vary between 23.3 and 43.6%, respectively for the Inner South (Pentland Firth) and the Sound of Islay.

6.3.2 Alternate Rated Velocity

Capacity Factor can be used as a simplified indicator of how 'economic' a site is by indicating how well the capital investment in generation capacity is being utilised. In the wind industry a capacity factor of 30% (BWEA, 2005) or greater is regarded as a high performing site. A low capacity factor may indicate a lower economic performance on a per kW basis but the overall investment may perform very well. The variation in capacity factors is also a consequence of the simple generic turbine sizing which under-rated the device characteristics at some of the higher capacity factor sites, while being too large for low capacity factor sites. The important point in decision-making however, is the balance between revenue from energy sales and the cost of the installation. With the cost of the devices and importantly the grid connection not part of the selection criteria, it would be anticipated that sites further from land represent a more challenging investment, particularly at prices of £52,000/MWkm for subsea 132-275 kV HVAC cable (Boehme, 2006a). It is

important to highlight that such additional externalities will impact on potential site selection, differentiating projects as installation costs rise.

The selection of rated velocity at 70% of spring peak velocity has been reported in B&V Phase II (2005) as demonstrating an appropriate balance between maximising energy yield at minimum unit cost of energy and optimum for locations that experience tidal current velocities of 2.5 m/s or greater. It is thought that the capacity factors indicated in Table 6.3 for some of the sites that are known to be highly energetic were lower than expected. For example, majority of the sites in Pentland Firth have a capacity factor below 30%. Discussion with Black & Veatch highlighted that using 70% of the peak value does not fully consider the site economics and they have moved on to an 'in-house' cost optimisation model that chooses a device rating accordingly. Unfortunately this model is not available in the public domain. Therefore, in order to instigate the balance between maximum power generation and economic capacity factor an alternative simplified method of assigning the rated velocity has been identified.

Figure 6.8 is a velocity exceedance curve for all the cells of interest identified in Table 6.3. All the sites experience spring peak velocity above 2.5 m/s, but examining the exceedance curves it becomes clear that for some sites this occurrence is very low. To choose a rated velocity based solely on the spring peak characteristics for a site could mean that the device would spend only a small proportion of its time operating at rated power and hence have a low capacity factor.

The interpretation of capacity factor statistics is complicated by the fact that increasing the rated power of a turbine increases the energy harvested but decreases the overall capacity factor. A compromise needs to be made between maximising generation at the expense of engineering the device to withstand the forces at higher rated velocity. It is considered uneconomic to engineer a device that will only be operating at its rated value for a small percentage of the time.

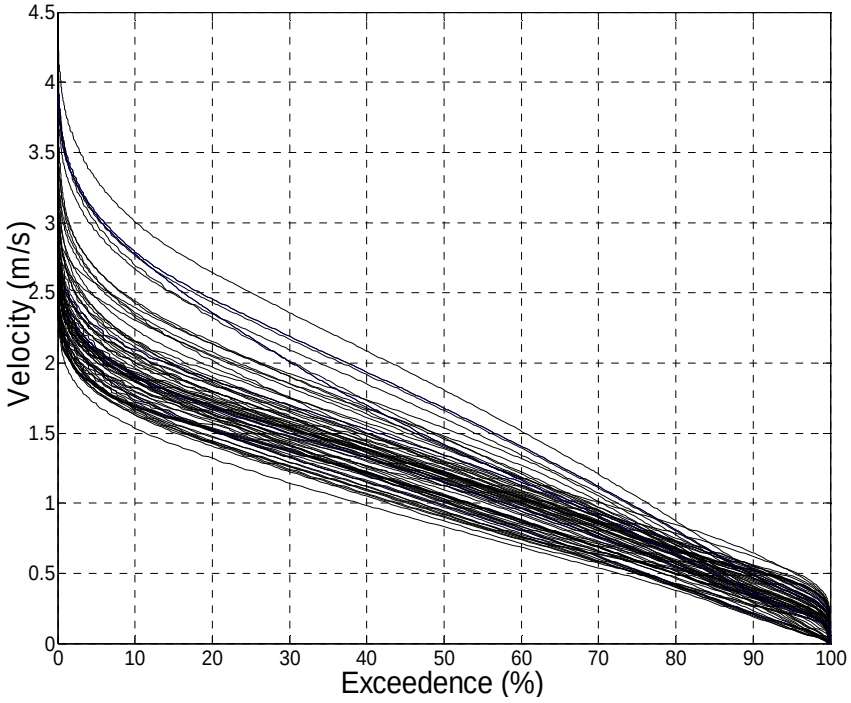

Figure 6.8 Velocity exceedance curve from all the selected cells.

The problem behind B&V's rule, assuming a rated velocity based in 70% of the mean Spring peak value is that it does not account for the velocity distribution or consider what percentage of time the velocity exceeds a specific value. In order to reach an effective balance, the approach adopted herein specified the rated velocity as the velocity value associated with 10% velocity exceedance. The idea behind choosing the rated velocity this way is that using the 10^{th} percentile value forces the device specified in each cell to operate at rated power for 10% of the operational time (assuming no downtime). Examining the exceedance curve in Figure 6.8 indicates that for roughly 20% of the time, the majority of sites experience velocity below 0.7 m/s. This equates to the cut-in velocity expected of first-generation tidal current technologies. For the remaining 70% of the time the device will be generating but will be operating somewhere between cut-in and rated velocity.

This method of using the exceedance plot therefore provides a sensible way of understanding the power generation distribution over tidal cycles and assists in identifying a rated velocity appropriate for each cell location that will lead to a capacity factor of around

30%, although an arbitrary value but similar in experience with the wind industry. Further detailed work on the economics of project at different scales would be necessary to verify this 10% exceedance value.

Figure 6.9 shows the capacity factor for each of the cells already identified in the analysis using the two different approaches for selecting the rated power. From the graph, it can be seen that the updated method of assessing the rated velocity maintains better consistency of capacity factor (around 30% as desired).

6.3.3 Technically Acceptable Power Extraction

So far the analysis has not taken any account of the fact that there is a limit to the amount of energy that can be extracted from the tidal system. The analysis to date has been using the 'Farm' approach to developing projects in the proceeding scenarios. Therefore the preceding scenario will from now on be referred to as the Farm Technically Acceptable Power (TAP). The SIF of 20% extractable kinetic energy used in many tidal assessments to restrict project development on environmental and economic grounds has been substantially revised by B&V (2011) to reflect improved understanding of the hydrodynamic mechanisms that underlie the tidal current resource. The numerical modelling carried out by Couch *et al.*, (2006) assesses representations of various relevant hydrodynamic mechanisms as presented here:

1. Tidal streaming: To maintain continuity, when a body of water is forced through a constraint such as a narrow channel, the flow accelerates.
2. Hydraulic currents: When two adjoining bodies of water are out of phase, a hydraulic current is created in response to the pressure variation induced as a result of the varying water levels in the different water bodies.
3. Resonance: Occurs as a result of standing wave when the incoming tidal wave and the reflecting wave interfere constructively. This can create large tidal amplitudes and associated currents.

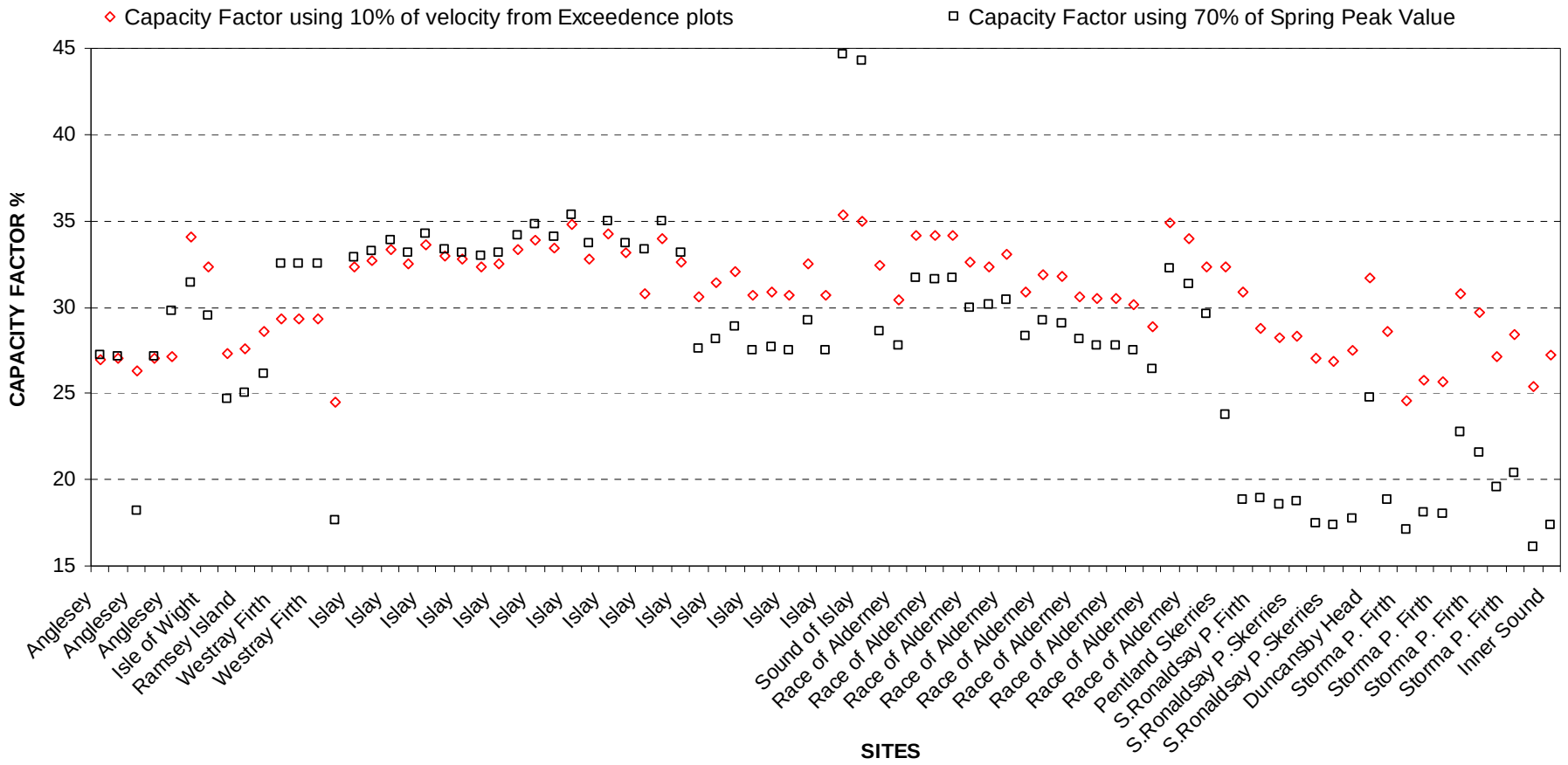

Figure 6.9 Capacity Factor evaluation for all the cells of interest appropriate for first-generation device deployment.

These are the flow phenomena that create the tidal current conditions necessary for economic project deployment. The same analysis also demonstrated that when too much energy is extracted from the system, it impacts on the underlying dynamics of the tidal system. These are the flow phenomena that create the tidal current conditions necessary for economic project deployment. The same analysis also demonstrated that excess energy extraction from the system can impact on the underlying dynamics of the tidal system. The evidence suggest that, beyond what is referred to as the theoretical harvesting limit, attempts to extract more energy by installing additional devices would in fact result in a reduction of the overall energy harvested as each device in the farm would experience a reduction in kinetic energy flux. This has previously been demonstrated analytically for hydraulic current tidal flow regimes by Sutherland *et al.* (2007) and Polagye *et al.* (2009). A further limit has also been defined in B&V (2011) by imposing constraints to limit far field environmental[4] impacts beyond which energy harvesting is likely to be restricted by environmental regulations and/or economic impact on the project due to reduction in available energy. Applying a similar approach in this analysis will generate a Flux Technically Acceptable Power (TAP) scenario.

Figure 6.10 illustrates the response of various non-dimensional parameters across a range of energy extraction scenarios. The parameters have been expressed as a fraction of the maximum value and the parameters evaluated over complete ebb and flood cycle. Q is the flow discharge, U represents the velocity and P is power. Reading the graph from right to left, when there is no power extraction (Q/Q_{max} = 1, ratio of flow over maximum flow) velocity and flow are unchanged. Moving along the axis when (U/U_{max} = 0.8), 80% of the power can be extracted with a 20% reduction in the velocity and a 40% reduction in head loss. In the case when P/P_{max} peaks, U/U_{max} is approximately half (56%), and Q/Q_{max} reduces by nearly 70%. Looking past peak power extraction, the overall power that can be extracted

[4] Although referred to as environmental, this is specific to the physical environment and does not account for the marine environment.

reduced due to a significant reduction in U and Q, the ratio of the flow over maximum flow continues to decrease and consequenty the velocity continues to reduce. (B&V, 2011)

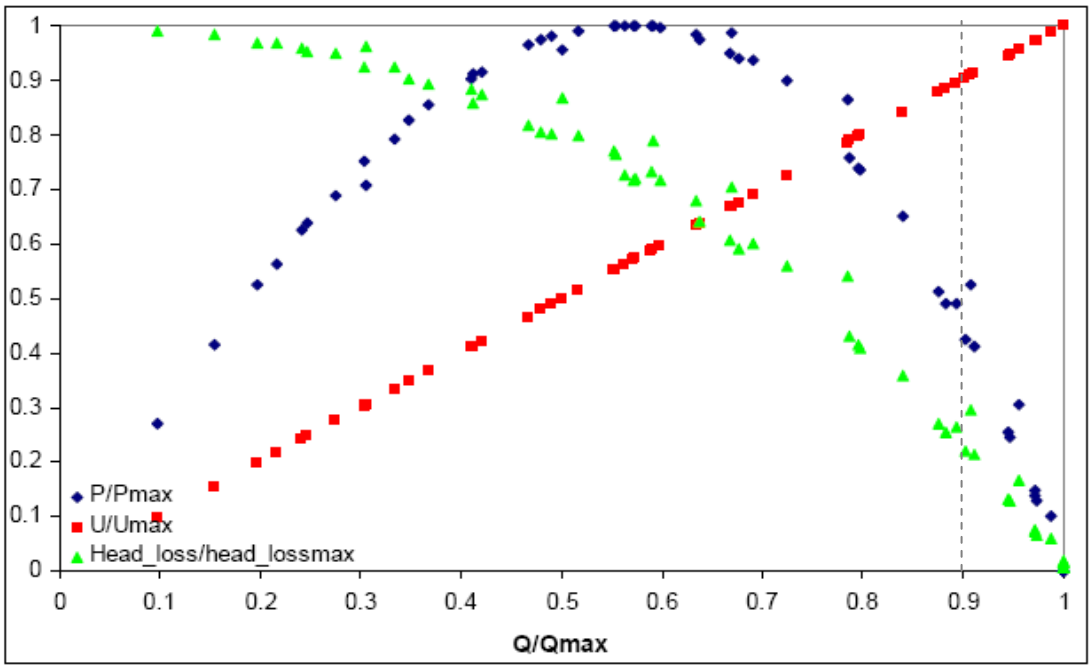

Figure 6.10 Key non-dimensional parameters for hydraulic current (B&V, 2011).

The parameters needed for this calculation are shown in Table 6.4 where Q_{max} is the maximum flow discharge and a_o the amplitude of the sinusoidal sea level difference between the two ends of the channel in the case a hydraulic current. For tidal streaming and resonance a_o is the local tidal elevation amplitude.

Tidal Mechanisms	Theoretical limit of tidal current energy harvesting.	'Technically acceptable' limit of tidal current energy harvesting.	Hydrodynamic response limiting energy harvesting.
Hydraulic current	$P_{Theoretical} = 0.2\rho g Q_{\max} a_o$	$P_{acceptable} = 0.086\rho g Q_{\max} a_o$	Velocity reduction
Resonant basin	$P_{Theoretical} = 0.2\rho g Q_{\max} a_o$	$P_{acceptable} = 0.033\rho g Q_{\max} a_o$	Downstream tidal range
Tidal streaming	$P_{Theoretical} = 0.16\rho g Q_{\max} a_o$	$P_{acceptable} = 0.020\rho g Q_{\max} a_o$	Downstream tidal range

Table 6.4 Summary of technically acceptable power (TAP) extraction limits for the three identified tidal flow driving mechanisms (B&V, 2011).

To evaluate the level of power that can be harvested from each of the sites, their respective hydrodynamic mechanism is identified and a TAP value defined. Regions with multiple sites are treated in one of two ways: the sites at Orkney, Islay and Anglesey are considered to be sufficiently geographically and hydraulically dispersed to be evaluated separately while for the Pentland Firth, sites are considered interdependent and are handled jointly by a single set of limits. For many sites, the high flow velocities experienced areas are a result of a combination of mechanisms.

Table 6.5 uses the 70% rule identified in B&V Phase II as the rated velocity. It lists all the sites and attempts to identify the dominant hydrodynamic mechanism experienced. Using the dominant system, the annual 'Environmentally acceptable' energy that can be extracted from each of the sites is assessed (Flux TAP) also reported in Table 6.5. This limit is identified using the different mechanisms as suggested by Table 6.4. Note however, these values are only calculated for a randomly chosen month (August) in the year 2009 and scaled up to present values for the entire year. These results have also been presented in Iyer *et al.,* (2011b). As identified in chapter 5, seasonal variations cannot be represented in the datasets used in this study.

Table 6.6 presents a different scenario, the rated velocity is obtained using the 10% exceedance value for all the sites identified in Table 6.6. Additionally, analysis presented in this scenario uses values for the entire year of 2009. Although a much more economic capacity factor is obtained for all the sites, the overall extractable energy is reduced. Extracting 9.76 TWh/yr from Race of Alderney as developed for the Farm TAP case would reduce the free stream velocity by 25% and alter tidal height variation by more than 35%. Therefore, the Farm TAP scenario would in reality never be considered.

The Flux TAP yield values listed in Table 6.5 place limits on the development at each site. The capacity factor for each cell was used to define the 'least economic' cell and these cells are prioritised for removal from the analysis to reduce output to meet TAP constraints. This was achieved either by removing the cell entirely or by reducing the

	Site name	Tidal Site System	ANNUAL YIELD TWh/yr				CAPACITY MW		
			Farm TAP	Flux TAP	Actual	% Reduced	Farm TAP	Flux TAP	% Reduced
Pentland Firth	Pentland Skerries	HC	1.8	Calculated as one system	1.8		708	708	
	S. Ronaldsay P.Firth	HC	0.4		0.4		194	194	
	S. Ronaldsay/ P.Skerries	HC	1.7		1.7		759	759	
	Duncansby Head	HC	0.6		0.6		205	205	
	Inner Sound	HC	1.4		1.4		813	813	
	Stroma P.Firth	HC	3.9		3.4		1673	*1526*	
	Regional Total		**9.7**	**9.2**	**9.2**	-5%	**4352**	**4205**	-3%
Orkney	Westray Firth	HC	2.6	0.7	0.7		620	*259*	
	N. Ronaldsay Firth	TS	0.2	0.2	0.2		180	180	
	Regional Total		**2.9**	**1.0**	**1.0**	-67%	**800**	**439**	-45 %
Islay	Islay North	TS	2.5	0.5	0.5		875	*167*	
	Islay Centre	TS	4.5	0.6	0.6		1526	*192*	
	Islay South	TS	2.6	1.2	1.2		879	*393*	
	Sound of Islay	HC	0.1	0.7	0.1		23	23	
	Regional Total		**9.6**	**2.9**	**2.3**	-76%	**3303**	**775**	-77 %
Anglesey	Anglesey North	TS	1.0	0.8	0.8		418	*363*	
	Anglesey South	TS	0.3	0.4	0.3		105	105	
	Regional Total		**1.3**	**1.2**	**1.1**	-10%	**523**	**468**	-11 %
	Ramsey Island	TS	**0.7**	**0.6**	**0.6**	-16%	**340**	**285**	-16 %
	Race of Alderney	TS	**10.4**	**2.1**	**2.1**	-80%	**3855**	**747**	-81 %
	Isle of Wight	HC	**0.7**	**1.2**	**0.7**	-	**255**	**255**	-
	TOTAL		**35.2**	**18.2**	**17.0**	-52%	**13428**	**7174**	-42 %

HC = Hydraulic current TS = Tidal streaming

Table 6.5 Technically Acceptable Power that can be extracted from each of the sites and the final annual energy yield including TAP. Values obtained using device rated velocity by taking 70% of the spring peak value as suggested by B&V phase II (2005). Values in red indicate that the Flux TAP value is higher than the Farm TAP scenario.

	Site name	Tidal Site System	ANNUAL YIELD TWh/yr				CAPACITY MW		
			Farm TAP	Flux TAP	Actual	% Reduced	Farm TAP	Flux TAP	% Reduced
Pentland Firth	Pentland Skerries	HC	1.2	Calculated as one system	1.2		422	422	
	S. Ronaldsay P.Firth	HC	0.3		0.3		114	114	
	S. Ronaldsay/ P.Skerries	HC	1.1		1.1		447	447	
	Duncansby Head	HC	0.4		0.4		148	148	
	Inner Sound	HC	0.9		0.9		368	368	
	Stroma P.Firth	HC	2.7		2.7		1058	1058	
	Regional Total		**6.5**	**9.2**	**6.5**	0%	**2556**	**2556**	0%
Orkney	Westray Firth	HC	2.9	0.7	0.7		1122	*291*	
	N. Ronaldsay Firth	TS	0.1	0.2	0.1		67	67	
	Regional Total		**3.0**	**0.9**	**0.9**	-70%	**1189**	**358**	-70%
Islay	Islay North	TS	2.6	0.5	0.5		894	*167*	
	Islay Centre	TS	4.6	0.6	0.6		1582	*194*	
	Islay South	TS	2.1	1.2	1.2		766	*421*	
	Sound of Islay	HC	0.1	0.7	0.1		34	34	
	Regional Total		**9.4**	**3.0**	**2.3**	-76%	**3276**	**816**	-75%
Anglesey	Anglesey North	TS	0.9	0.8	0.8		370	*353*	
	Anglesey South	TS	0.3	0.4	0.3		121	121	
	Regional Total		**1.2**	**1.2**	**1.1**	-8%	**492**	**474**	-4%
	Ramsey Island	TS	**0.7**	**0.6**	**0.6**	-14%	**297**	**255**	-14%
	Race of Alderney	TS	**9.8**	**2.1**	**2.1**	-79%	**3405**	**710**	-79%
	Isle of Wight	HC	**0.7**	**1.2**	**0.7**	0%	**227**	**227**	0%
	TOTAL		**31.2**	**18.2**	**14.3**	-54%	**11443**	**5397**	-53%

HC = Hydraulic current TS = Tidal streaming

Table 6.6 Technically Acceptable Power that can be extracted from each of the sites and the final annual energy yield including TAP. Values obtained using device rated velocity by taking 10% of the exceedance curve as presented in section 6.3.2. Values in red indicate that the Flux TAP value is higher than the Farm TAP scenario.

number of devices deployed in the cell. The energy yield reductions imposed by Flux TAP constraints range from 14% reduction for Ramsey Island to 79% for the Race of Alderney. Aggregate reduction for all the sites combined was in the order of 54%.

The analysis indicates that for most of the identified sites, the limit to the energy extracted is determined by the TAP constraint limiting energy harvesting due to excessive impact on the energy flux. In the Flux TAP scenario presented here (for both methods of rated velocity), most of the sites already meet or exceed the TAP limitations imposed. For example using the 10% exceedance values, only the Pentland Firth (consisting of Pentland Skerries, S. Ronaldsay P. Firth, S.Ronaldsay/P.Skerries, Duncansby Head, Inner Sound and Stroma P. Firth), N. Ronaldsay Firth, Sound of Islay, Anglesey South and Isle of Wight can undergo further development, provided suitable depth conditions exist suitable for second/third generation tidal energy devices (when they become available). However, at locations where the TAP constraint has already been reached, further development with newer generations of technology will be constrained by the existing first generation deployments assuming the TAP limitations are shown to be credible.

Figure 6.11 shows the combined power output from all the sites for the Farm TAP and the Flux TAP scenario (using the 10% exceedance values). Only the peak value far each 12 hour period is plotted so an envelope of the generation can be seen representative of the variation of the spring-neap cycle.

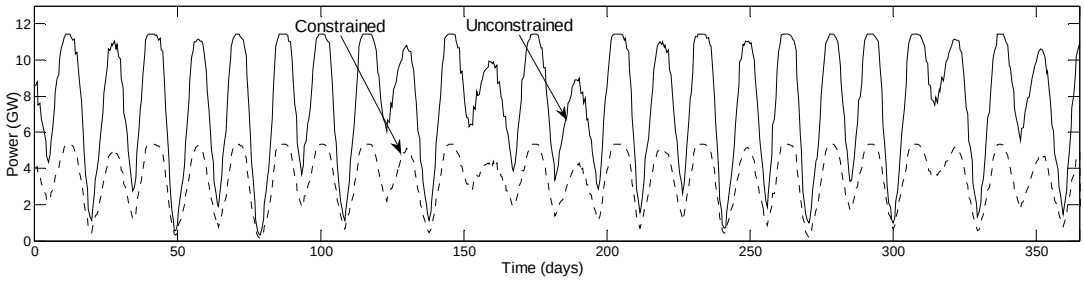

Figure 6.11 Time series of all sites showing aggregate production at spring peak with environmental constraints ignored using the 10% exceedance values.

6.3.4 Site Phasing

The generation time series were now used to examine the relative phasing of the production from each site. Figure 6.12 is a stacked time-series plot for a typical spring peak day highlighting the Farm TAP (top) and Flux TAP (bottom) scenario, using the B&V Phase II (2005) methodology of rating the device. It can be seen that the majority of generation contributions are from the Pentland Firth, Islay region and the Race of Alderney. The periods of generation at rated output can be clearly seen in many of the traces particularly for the Pentland Firth. Also observe the asymmetric nature of the power production cycle with aggregated output ramping up slower than it reduces highlights the differences between the ramp rates.

The location of individual sites determines their phasing and, in terms of tidal wave propagation, Islay and Pentland Firth are in-phase due to the coincidence of the local tidal phasing at these locations. The Race of Alderney is out-of-phase (behind) by approximately one hour. The aggregate effect of this can be seen in the total power output generated. Continuous output can be achieved for a number of days around Spring peak. However, the output is sustained as a very small fraction of the generation potential. This causes the base of the total output to be a very ‘lumpy’ production cycle. It should be noted that the base of aggregate generation is much wider than any of the individual outputs, caused by slight phase differences. This shows that there is a small portfolio aggregate effect exploiting the phase variations between sites. For example, Pentland Firth generates power for 3.5 hours; with all the other sites included the duration can be increased for 4 hours. However, this effect is not sufficient to generate significant firm output as none of the large sites are completely out-of-phase. Even the smaller contributions from the Orkney, Anglesey, Isle of Wight and Ramsey Island sites are more or less in-phase with each other, and with the Pentland Firth and Islay.

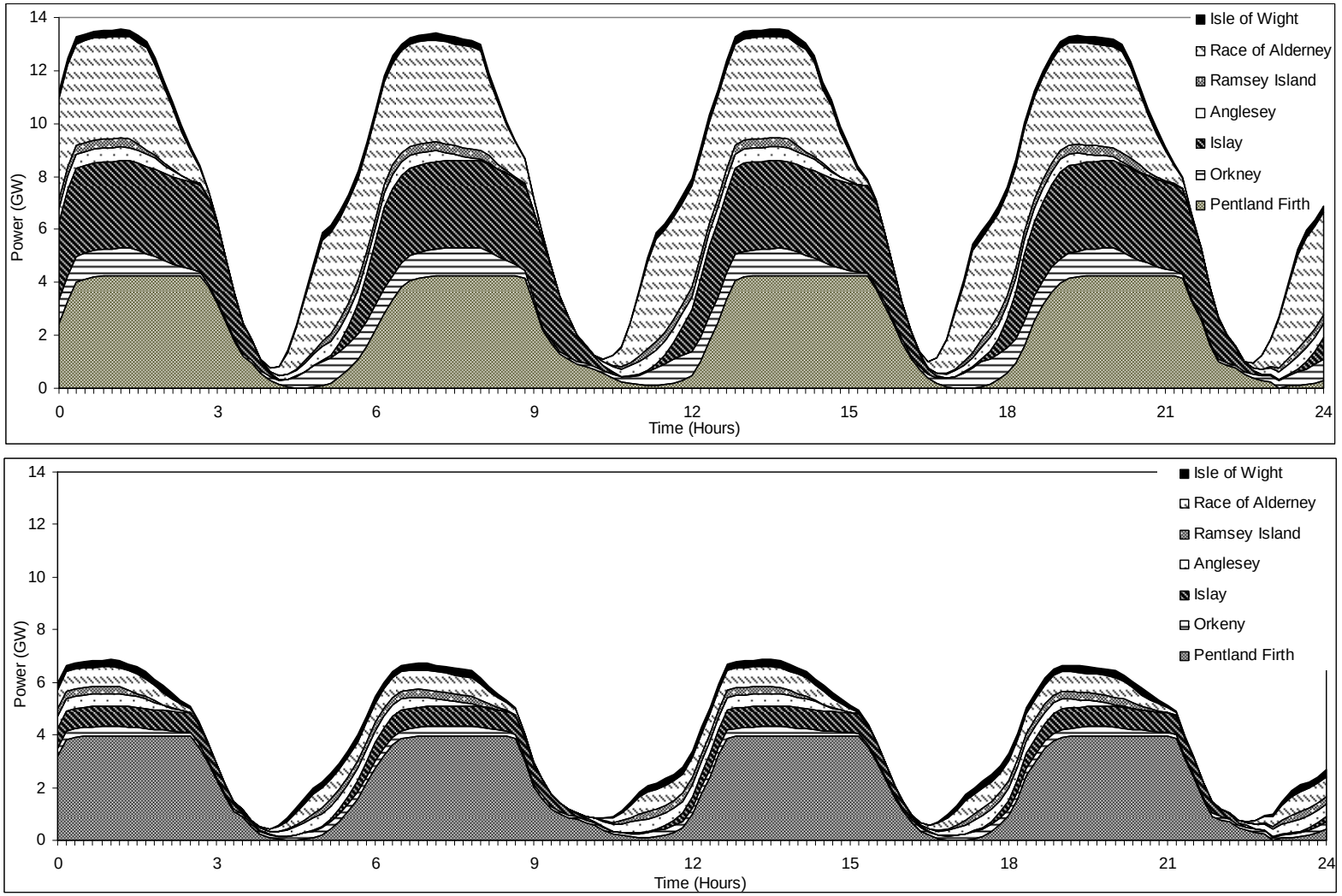

Figure 6.12 Stacked time series of all sites showing aggregate production at spring peak. Farm TAP (bottom) and Flux TAP (top).

6.4 Discussion

The analysis presented here suggests that with an installed capacity of 11.4 GW around 31.2 TWh/year of tidal current energy could be extracted using only first generation tidal current devices installed at suitable UK sites (Farm TAP scenario). However, when accounting for environmental acceptability limitations and reduction of the in-situ resource a lower overall Technically Acceptable Power output of 14.3 TWh/yr is suggested based on the restricted site selection and assumptions detailed (Flux TAP scenario). Approximately 5.4 GW of installed capacity is necessary to meet this scenario of generation. With several smaller but energetic sites excluded by the analysis, the energy yield estimates compare favourably with the 29 TWh/year suggested by B&V in their base case, P50 (B&V, 2011).

While the analysis presented here lacks the very high temporal and spatial resolution data necessary to inform individual project development detailed design, it offers a credible and broad resource analysis suitable for understanding the nature of the UK tidal resource and its phasing. A true understanding, with a high level of accuracy of the resource will only be gained by extensive site measurements combined with new generations of hydrodynamic tidal current models incorporating the complex interaction of device operation alongside the evolving hydrodynamics.

In terms of answering the question as to whether first generation tidal current devices can offer a sufficient degree of firm power supply in the UK, the results suggest that it is not possible except for a number of days around Spring peak. This can be confirmed by aggregating the time series output of all the sites and presenting them as a power exceedance curve over a period of a year, Figure 6.13 shows curves for aggregate tidal current generation in the Farm TAP and Flux TAP scenario. In both cases, aggregate output at 100% exceedance is zero, indicating that there is no true capability for firm power generation with first generation tidal current devices.

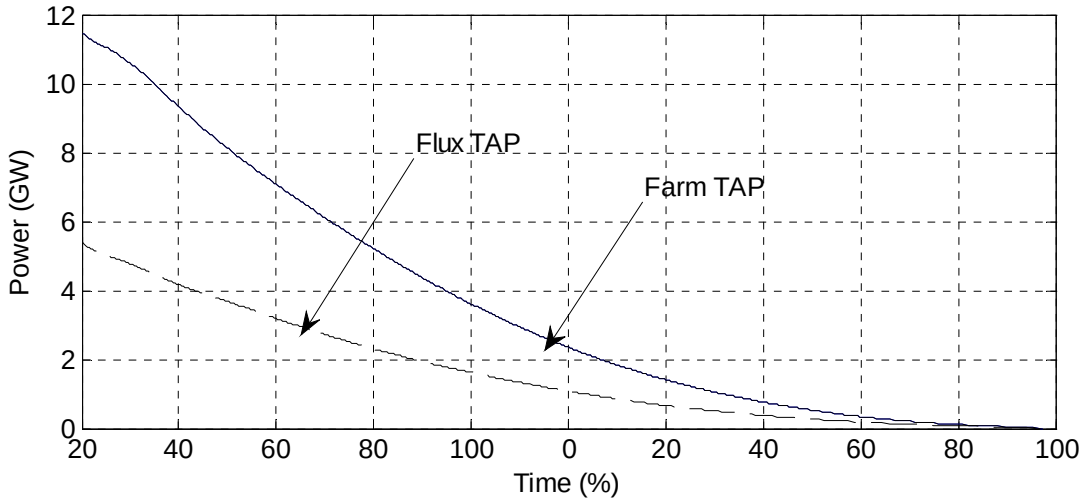

Figure 6.13 Power Exceedance curve from instantaneous tidal generation for Farm TAP and Flux TAP over a year.

To further investigate the phasing aspect, the correlation between power output at individual sites is presented in Table 6.7. All combinations are shown, and correlations in excess of 0.5 are shown in bold. This analysis obviously does not take any consideration of the relative magnitudes of each site, only the relative phasing. The majority of the locations in the study show either a degree of or strong positive correlation. Maximum correlation is observed between Pentland Firth, Orkney and Islay and between Anglesey, Race of Alderney, Ramsey Island and Isle of Wight.

	Pentland Firth	**Orkney**	**Islay**	**Anglesey**	**Race of Alderney**	**Ramsey Island**	**Isle of Wight**
Pentland Firth	1.00	0.63	**0.96**	0.21	0.29	0.42	0.64
Orkney	0.63	1.00	0.64	0.63	**0.80**	**0.85**	**0.89**
Islay	**0.96**	0.64	1.00	0.26	0.32	0.44	0.69
Anglesey	0.21	0.63	0.26	1.00	**0.71**	**0.76**	**0.70**
Race of Alderney	0.29	**0.80**	0.32	**0.71**	1.00	**0.93**	**0.85**
Ramsey Island	0.42	**0.85**	0.44	**0.76**	**0.93**	1.00	**0.91**
Isle of Wight	0.64	**0.89**	0.69	**0.70**	**0.85**	**0.91**	1.00

Table 6.7 Correlation coefficient for production between each site

It is also interesting to observe the high correlation between Orkney and Race of Alderney, Ramsey Island and Isle of Wight, particularly as they are geographically distant. It would be preferable from the point of view of generating continuous base load profile if the sites indicated a wide spread of both positive and negative correlations. It is anticipated that the use of second generation tidal current devices will open up more areas to exploitation, potentially improve the spread of phasing and raise the opportunity for firm aggregate production from tidal current sources.

Although lying within the British Isles, the Race of Alderney is a significant distance from the UK mainland and the resource may be more readily exploited by connection to the French electricity grid. This will mean that any benefit of the phasing provided by this site will be hidden by the bulk transfers across the UK-France interconnector but arguably it transfers the issue of integration to the French system.

Despite the apparent lack of a firm production capability, tidal current energy can be predicted accurately over long periods. This may make its integration with the electricity network more straightforward than other renewables. Chapter 7 presents a detailed analysis comparing the temporal variability of tidal currents power output generated in this scenario with demand for electricity in the UK.

6.5 Conclusions

This work presents an improved method of assessing the total UK tidal current resource by combining multiple datasets including Marine Atlas, TotalTide tidal diamonds and measured tidal current information where available. First generation device installation is considered in regions where spring peak velocity exceeds 2.5 m/s in water depths of 25 to 50 metres.

Based on the approach suggested by B&V Phase II (2005) a total installed capacity of 13.4 GW is suggested that can generate 35 TWh/year (Farm TAP scenario) using only first generation tidal current devices installed at suitable UK sites. However, when accounting for environmental acceptability limitations and the consequent reduction of the

in-situ resource, a lower overall output of 17 TWh/yr (Flux TAP scenario) is suggested based on the restricted site selection and assumptions detailed. Approximately 7.8 GW of installed capacity is necessary to meet this scenario of generation.

A new approach to identifying the device rated velocity is introduced to help achieve an overall economic capacity factor and aid development of realistic scenarios. This new approach is based on understanding the velocity distribution and bases the rated velocity as the value that exceeded at the site for 10% of the time and allows it to attain a capacity factor of around 30%. Based on an economic assessment of the capacity factors for each of the sites considered, it is concluded that 31 TWh/yr (updated Farm TAP) can be extracted with an installed capacity of 11.4 GW, meeting 8.24% of UK demand (based on 2009 demand data). When including TAP constraints 14.25 TWh/yr (updated Flux TAP) can be extracted with an installed capacity of 5.4 GW without significantly impacting the underlying resource at the identified sites.

In both the scenarios presented, the analysis shows that the high energy sites in the UK considered are largely in phase and that tidal current *cannot* be seen as offering significant base load generation in the UK. Numerous small sites exist that may provide a small percentage of generation out of phase but this will amount to a small proportion of the total installed capacity. Generation from the constrained scenario (using the 10% exceedance value) presented here can meet 4% of present UK demand based on 2009 demand levels. Two of the largest sites, the Pentland Firth and Race of Alderney together contribute 60% of this total generation.

7. Demand for Electricity and Supply

Following the analysis and discussion of tidal current energy extraction scenarios, this chapter aims to evaluate how well tidal current generation can be matched with demand for electricity. The following section introduces the inherent variability that exists within the electricity system and how variable demand can be over short and long term time scales. Demand patterns and trends play a key role in understanding local, regional and national energy needs. Analyses to quantify the variation of demand for electricity are discussed to see how much and how often can demand be met by tidal current energy. Part of the discussion looks at the various sources of fuel that have been used for energy generation and how the trend is expected to change.

7.1 The Electricity Supply System

Electricity in the UK is predominantly generated by fossil fuels. Gas and coal play a key role in meeting energy needs. Figure 7.1 shows pie charts of the different supply sources used to generate electricity in 1999 and 2009 with gas playing a much more dominant role than any other fuel.

In 2009, 7% of the generation was contributed by renewables (DUKES, 2010). If the UK is to stay on target for the 2020 reductions of 20% in GHG emissions as part of the EU obligations, nearly 30% of electricity generation is expected to be sourced from renewables by then (RES, 2009). Inclusion of renewables in the system in such a large scale will have significant impact on the way the system operates, as it will introduce huge amounts of variable generation into the electricity system. The section that follows discusses some of the network aspects that need to be considered when integrating renewables in the system.

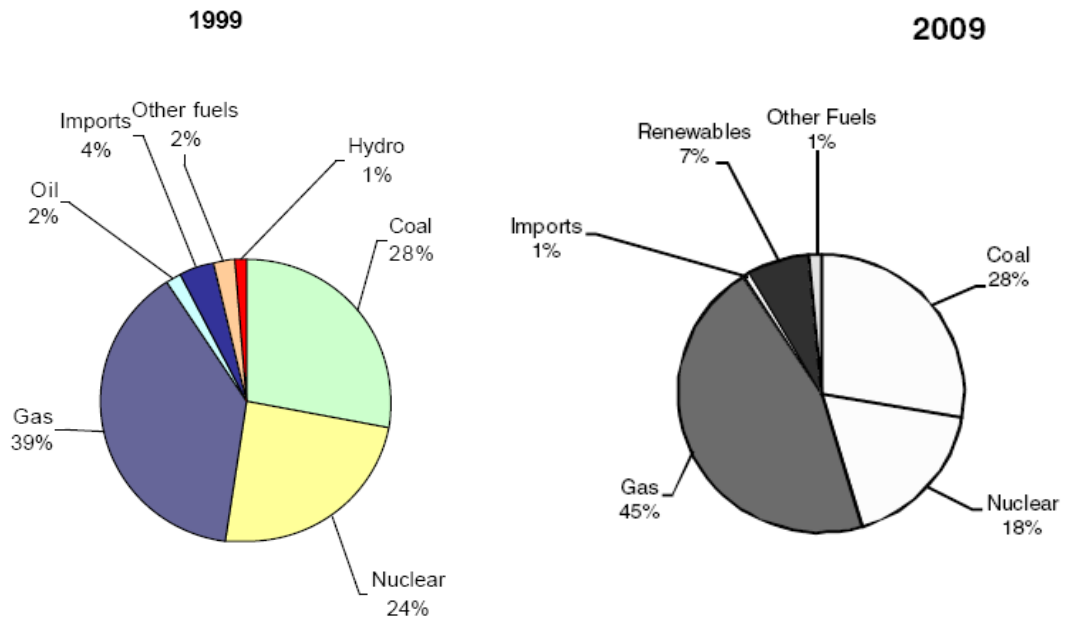

Figure 7.1 Net electricity supplied fuel input (DUKES 2005, DUKES 2010).

7.1.1 Existing Network

In the UK, National Grid (NG) own the transmission network in England and Wales and operate the Great Britain (GB) Grid. In Scotland the network is owned by Scottish and Southern Energy (SSE) and Scottish Power (SP). The existing network operates on a largely centralised basis where large power plants generate power that flows through the transmission and distribution networks from many central locations to various domestic and industrial consumers at progressively decreasing voltages in progressively more distant areas.

With the introduction of renewables, numerous variable generation sources that are dependant on resource availability as opposed to hydrocarbon fuel in store will be used to generate electricity. This potentially creates concern over the network's ability to cope with this form of operation. Ofgem have estimated the cost of integration in order to meet the 2020 renewables target to be in the order of £30 billion, largely in the form of transmission and distribution network upgrades (Ofgem, 2011). Figure 7.2 shows the electricity supply network in GB.

Figure 7.2 The electricity supply system in Great Britain in 2009 (Dukes,2010).

The structure of the network is usually weakest at locations that are best for the exploitation of tidal current energy, especially in the north and west coast of Scotland. Moreover, these regions are sparsely populated where local demand for electricity is low with much of the power generated expected to be exported south. As identified in chapter 6, the best region for tidal current energy extraction is the Pentland Firth. Table 7.1 and Figure 7.3 highlight some of the network constraints on accepting tidal energy in the Pentland Firth region. Due to network constraints that could strand assets or sterilise new development, additional connection to many of the rural feeders and substations are mutually exclusive (Xero Energy, 2009). Similarly, constraints in the north of England also limit potential to add any more capacity without a sustained programme of grid upgrade.

Connection point geographic location	Voltage	Capacity [MW]	Approx costs [£k]	Grid issues & Consents
Duncansby Head	11kV	0.15	160	Voltage limit
Gills Bay	11kV	0.24	160	Voltage limit
Scarfskerry NOP east	11kV	0.16	160	Voltage limit
Scarfskerry NOP west	11kV	0.27	160	Voltage limit
West Brough	11kV	0.35	160	Voltage limit
Dunnet Head Lighthouse	11kV	0.24	160	Voltage limit
Mains of Murkle	11kV	1.42	160	Voltage limit
Orkney cable pothead	33kV	0	260	Thermal limit due to Orkney gen'
Mount Pleasant Primary Substation	11kV	15.6	402	Thermal limit of 33kV line
	33kV	15.6	260	Thermal limit of 33kV line
Thurso GSP	33kV	26.5	533	Firm thermal capacity of 132/33kV transformers

Table 7.1 Possible connection points to the mainland distribution network from the Pentland Firth (Xero Energy, 2009).

7.1.2 Network Planning

In the nationalised industry before privatisation, generation and transmission was centrally planned. Today National Grid must plan the network on the basis of where private generators might choose to connect. However, without a contract underwriting the connection, National

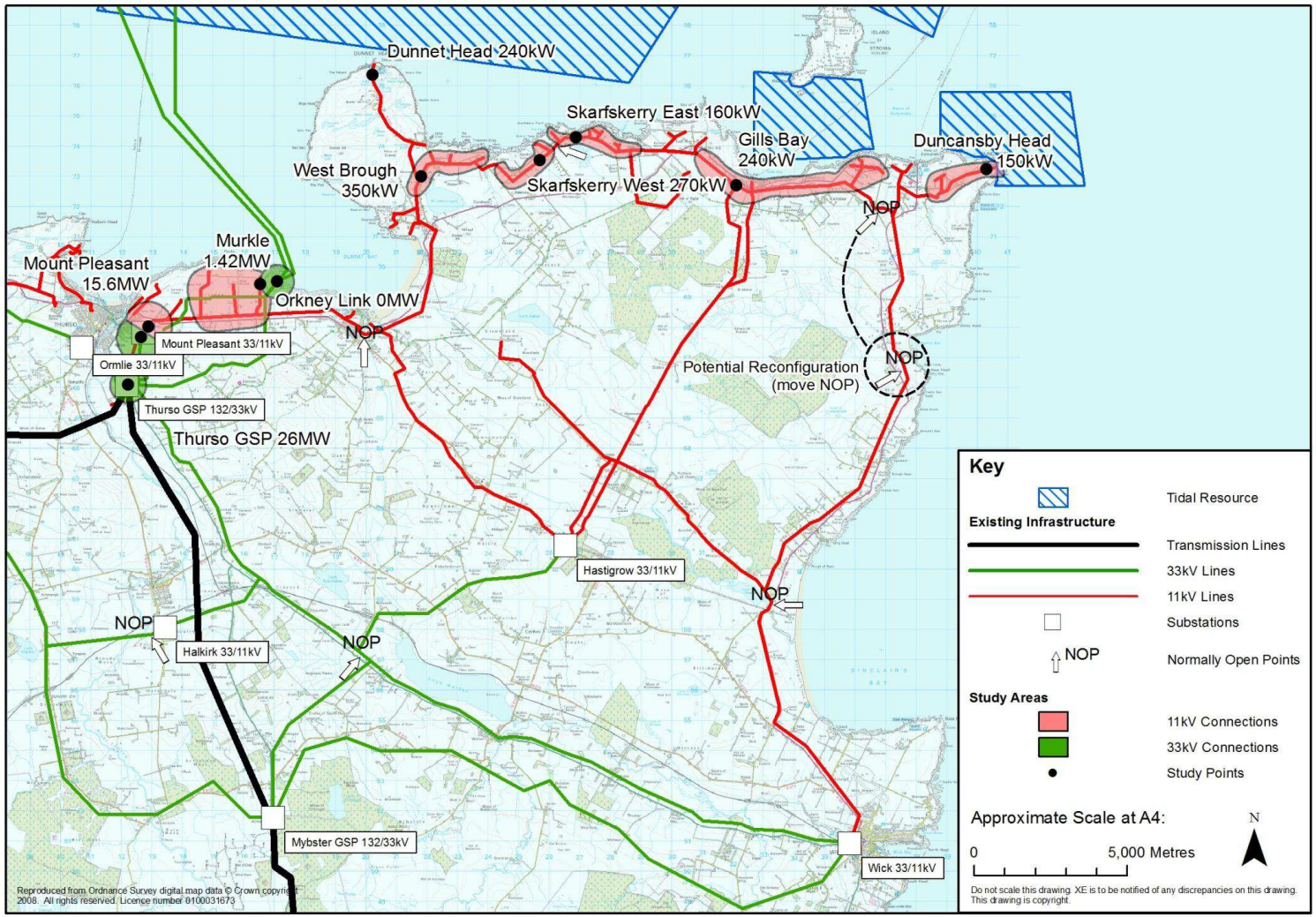

Figure 7.3 Possible connections to the existing mainland distribution system. (Xero Energy, 2009)

Grid were unable to build transmission capacity. Pre-privatisation connection was on a 'fit-and-forget' basis but post privatisation the 'invest and connect' approach was used where all upgrades to the network had to be implemented before generator connection could take place. However, this system did not work well for the connection of large capacitiess of renewable generation, as projects that needed a network connection were being offered connection dates eight to ten years in future. (Tocardo BV Tidal Energy, 2008).

The queuing system implemented saw projects that required little work given consent but this system did not work well as other projects in the pipeline caused delays which took even longer to get consent (SDC, 2007a). This prompted the need for transmission access reform to accelerate connections.

One of the most debated upgrades is the Beauly-Denny line, stretching 137 miles across the Scottish highlands. In 2005 Scottish Hydro Electric Transmission Limited (SHETL) and Scottish Power Transmission Limited (SPT) proposed a project to upgrade an existing 132 kV transmission line to 400 kV, which could increase the transmission entry capacity up to 6 GW (SDC, 2007f). This proposal was referred to a public enquiry and finally consented in January 2010. As of November 2011 construction is yet to begin and disagreements continue. This highlights the bottlenecks that occur in the transmission planning system and the topicality of connecting tidal energy – the need to truly understand its potential as an electricity source.

7.1.3 Electricity Demand and Variability

The need for electricity varies over time and this variability can be defined over short timescales of seconds to longer durations of weeks and seasons. For most North European countries, the UK included, the winter season is dominated by periods of long cold spells and short daylight periods. Electricity demand is therefore concentrated during this time when additional need for heat and lighting becomes necessary, along with the usual daily domestic and industrial load on the system. Figure 7.4 highlights the daily demand profile for typical

and extreme summer and winter demand in 2009. The demand data presented here corresponds to the year 2009 to allow comparison with the tidal current energy analysis.

Traditionally, operation and long term planning looks at a very small number of extreme cases in projecting how much generation will be required and the network capacity necessary to deliver it. These are system peak demand and system minimum demand.

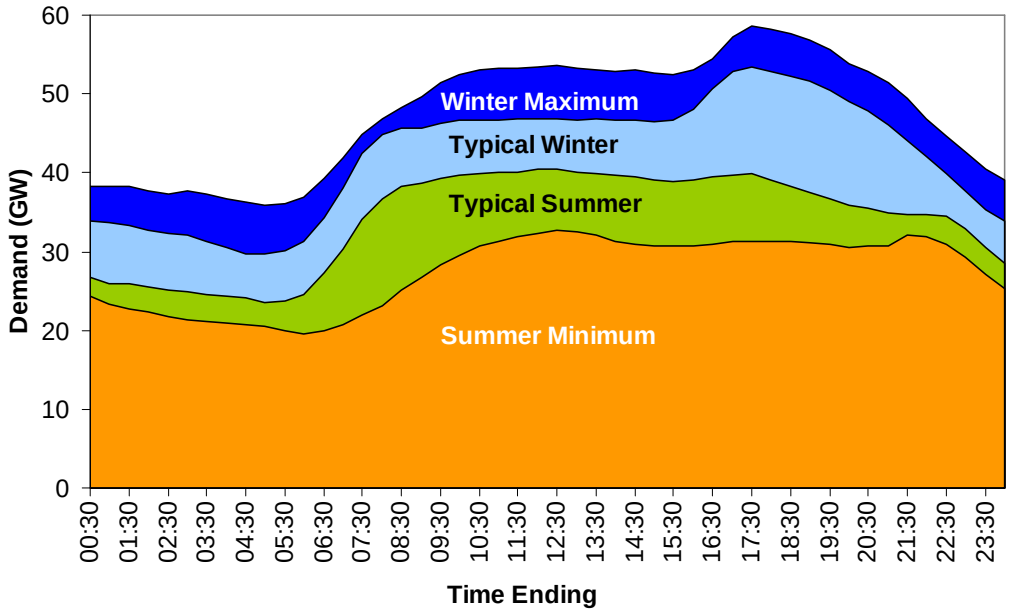

Figure 7.4 GB summer and winter daily profile in 2009 (NG,2010).

The need to understand and identify demand patterns is crucial to allow the system operator to schedule generation. Most of the analyses conducted in this study is based around system peak demand as this is the maximum load the system is expected to deliver. Therefore, all the parameters are associated around system peak and what the maximum expected demand for electricity will be. National Grid expectes to plan and schedule generation for electricity demand at a growth rate of 1.2% per year (NG, 2010).

In 2009 the UK electricity system had an average demand of 36.4 GW, with a standard deviation of 7.7 GW and electricity demand peaked at 59.1 GW on the 6th January at 17:30. Figure 7.5 shows the two week period when peak demand occurred in January and

a trace shows where demand is at its lowest on the 2nd of August at 06:00. Load patterns are very distinct with, for example, demand for working days (Monday to Friday) easily distinguished from non-working days (Saturday and Sunday). The seasonal variation can also be identified here. On average winter demand exceeds summer demand by about 7 GW.

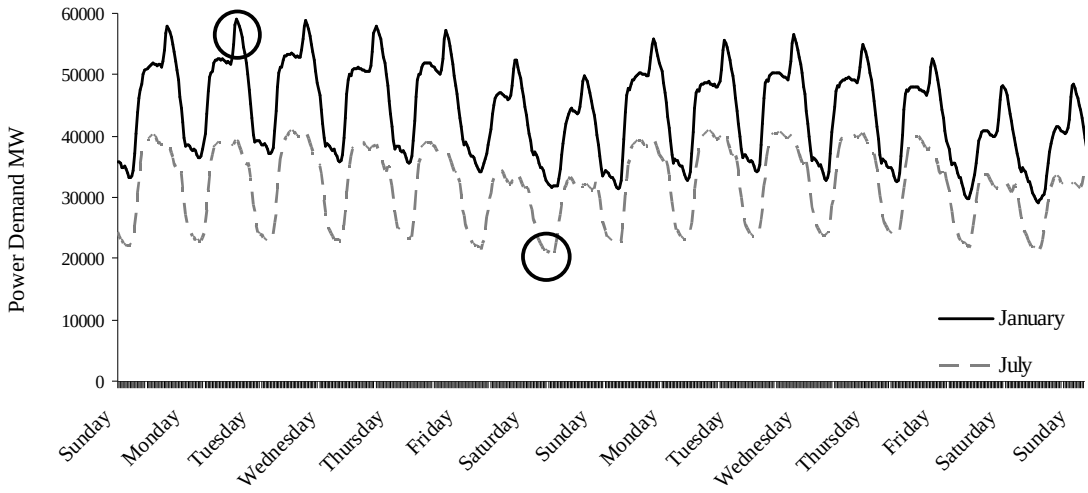

Figure 7.5 Demand in UK over two 14 day periods in 2009. Data for the month of January from 15th to 18th and for July 27th to 9th August. The circles show periods of peak demand (6th January, 1730) as well as period of lowest demand (2nd August, 0600).

Figure 7.6 shows the mean demand for each half hour period in a standard day determined from the complete 2009 data record. Although the average demand for the entire year is 36.4 GW, it can fall as low as 20.15 GW (2nd August), 34% of the peak value. However, demand for electricity never drops to zero, therefore base load capacity of 20~22 GW is always necessary to meet even the lowest of the demands with some reserve margin.

The analysis and discussion so far show that demand is not constant and there is an inherent variability in the need for electricity. Therefore, before adding any inherently variable generation into the system it is prudent to assess just how variable demand for electricity is. Figure 7.7 shows an inter half-hourly analysis of demand fluctuation obtained by measuring the difference in demand between each half hour period for 2009. It is interesting to note that the tail end of the negative load change is longer than the positive end highlighting that demand ramps up faster than it drops down.

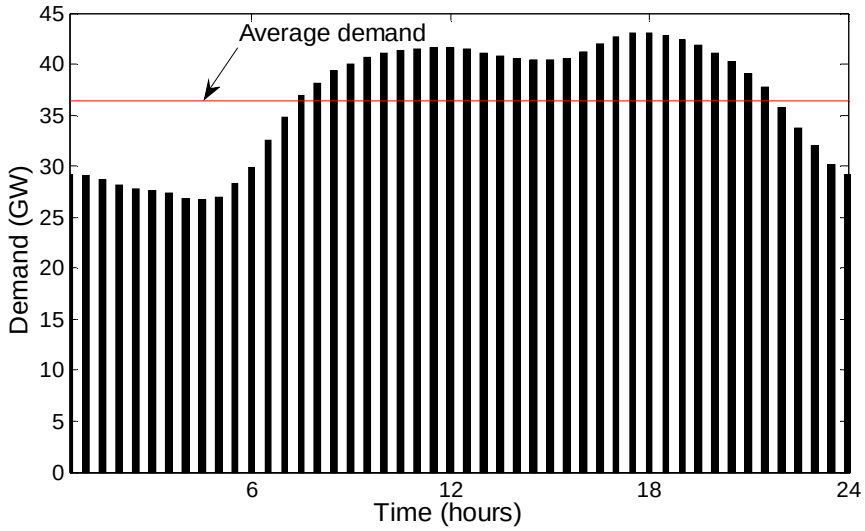

Figure 7.6 Mean demand for each half hour period in the day for 2009.

The inter half hourly load change (Figure 7.7) shows that the system is already capable of coping with substantial variability in terms of variable demand operations and scheduled/unscheduled plant shutdowns. Therefore, the inclusion of tidal current energy or any other variable generation into the system must be considered as adding to the overall variability as well as increasing the complexity of planning and operating the system.

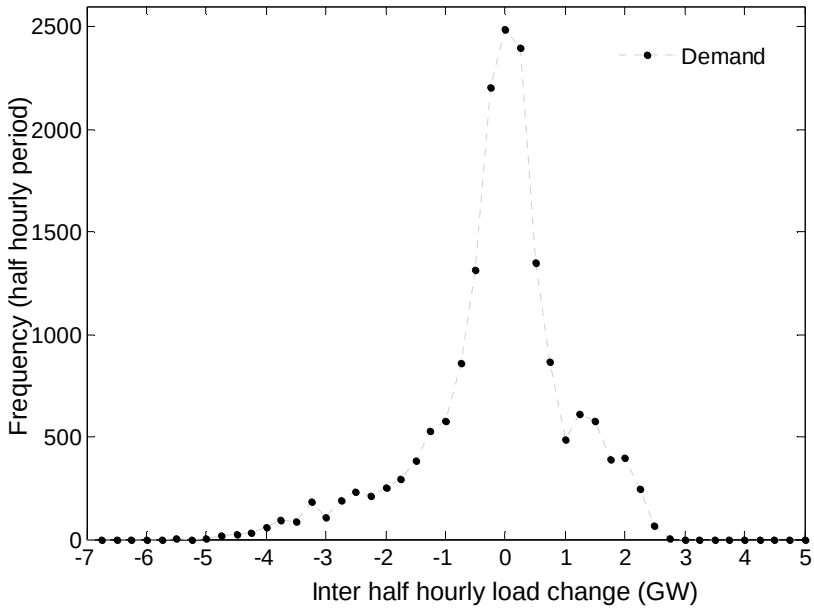

Figure 7.7 Inter half hourly demand changes in GB for 2009.

7.1.4 Future Demand Trends

Demand trends are vital for forecasting future demand patterns. This can in turn be used to understand the scope, to 'match' with variable resources. Timing is a key factor as demand for electricity is currently high at very specific times of the day and supply response needs to be instantaneous for the system to be stable.

Looking at the demand trend over the past few years shows that the year 2009 has had the lowest demand. A number of factors contributed to this including weather, low economic activity, high energy prices, increased energy efficiency and demand side management (NG, 2010). There is substantial uncertainty in future demand and these variables add to the uncertainties. National Grid Electricity Transmission (NGET) forecasts for GB demand are shown in Figure 7.8 and future demand scenarios are presented. The NGET high and low scenarios are considered with a number of assumptions including the strong growth in the renewable sector, take up of combined heat and power (CHP) etc. Of course these assumptions can be very varied depending upon the market conditions.

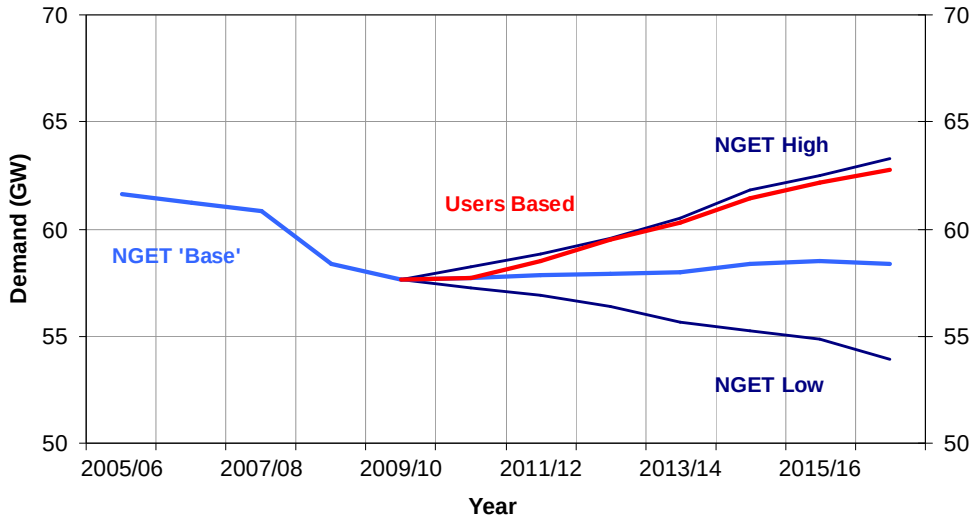

Figure 7.8 Comparison of NGET's future projections (NG,2010)

A report published by the Energy Networks Strategy Group (ENSG, 2009) has extended these scenarios up to 2030. Based on these model scenarios, it is projected that demand would increase up to 2020 and plateau from then on for the remaining period as

presented in Figure 7.9. This forecast takes into account the overall demand growth but as transmission losses reduce with the inclusion of embedded generation, the overall effect is for these to cancel each other out. The average cold spell (ACS) winter peaks can be seen to decline from 2015 as other sources of heat are used for domestic and central heating.

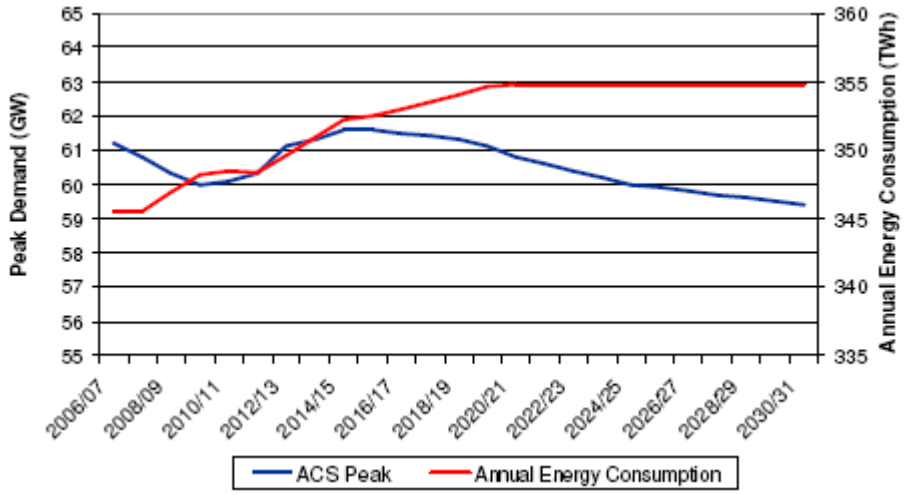

Figure 7.9 Comparison of Annual Energy consumption and change in Average cold spell (ACS) peak demand from 2006-2030. (ENSG, 2009)

7.1.5 Demand at Grid Supply Point

The analysis presented in the following sections presents matching between demand for electricity and generation from tidal current energy. The changes introduced in the network are at the Grid Supply Point (GSP), which is the connecting point for the distribution network, GB transmission network and other power plants. All the analysis presented, including the change in demand, will be observed by the system operator at the GSP and shall be referred to as *residual demand*. This does not refer to consumer demand.

7.1.6 Definition of Penetration Level

The scenarios presented in this chapter consider different levels of penetration. The level of penetration can be defined as the ratio of the installed capacity to peak system demand:

$$Penetration\ \ Level = \frac{Installed\ \ Capacity}{Peak\ \ Demand} \tag{7.1}$$

7.2 Tidal Energy Matching Case Study - Anglesey

Presented here, are methodologies of assessing and evaluating the impact of tidal current energy from a specific site on the electricity network, with the aim of developing the scenario to a UK wide set of sites as identified in chapter 6 and assessing the aggregate impact on the network. The analysis presented here is the first step in this process, developing the methodological approach and demonstrating application through a case study scenario developed using Milborrow (2010).

Figure 7.10 shows the power output along with the variation in current velocity for Anglesey, one of the case study sites presented in chapter 3. Note that, although the change in current velocity is relatively minor on this particular day, the power output during the flood tide is twice as much as during the ebb tide. Similarly, Figure 7.11 shows the power available for the same site over a period of a week. It is important to highlight the Spring-Neap variability, During the Spring cycle the peak power output ranges from 2-6 kW/m^2 but during the Neap cycle peak output only ranges from 0.5-1 kW/m^2. This generation needs to be integrated with all other sources of power and connected to the end user. Therefore, connecting such a predictable but variable source of generation is going to be challenging. This case study was presented in Iyer *et al.,* (2009b).

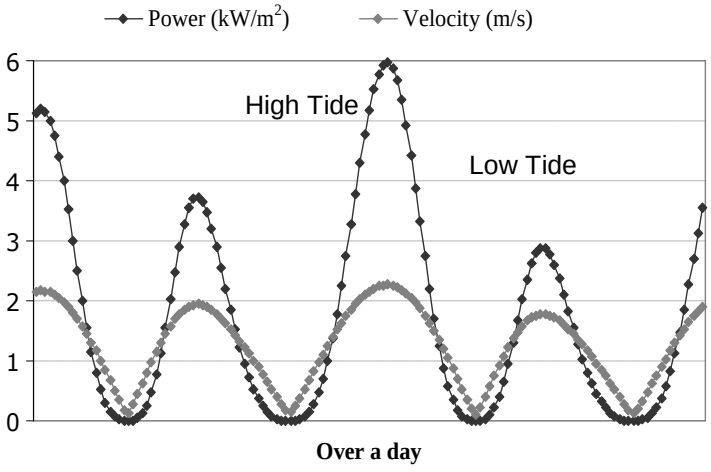

Figure 7.10 Power available (per m^2 cross-sectional area) and current velocity for Anglesey. Note the change in velocity relative to the change in power output.

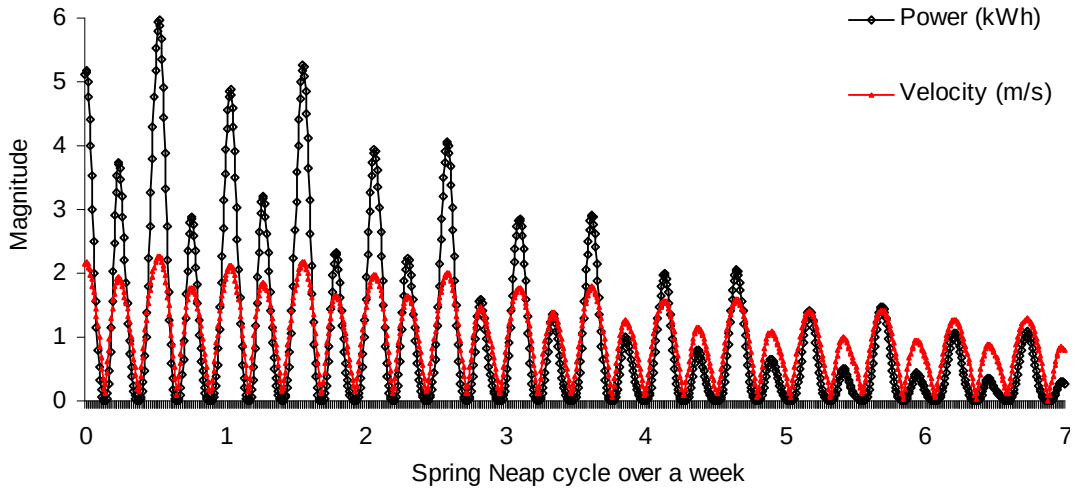

Figure 7.11 Power availability (per m^2 cross-sectional area) and current velocity over a week at Anglesey.

7.2.1 Anglesey Demand and Supply Scenario

As this scenario only considers power generation from one area of Anglesey waters, it is necessary to use an appropriate level of demand for a regional distribution network. From the size of the Anglesey site, 20 MW and 40 MW installed capacity scenarios are developed. However, disaggregate demand for Anglesey was not available but it was possible to obtain seasonal daily load profiles for the distribution system in Merseryside, Cheshire and North Wales, see Figure 7.12.

The regional distribution network presents similar characteristics to the national demand presented in Figure 7.4. Given the lack of disaggregated demand for the Anglesey region, national demand for the UK has been scaled down from 59.1 GW peak demand to 200 MW[5], so that demand and supply for tidal generation are a similar magnitude to each other, while maintaining likely demand variability patterns. The scenarios developed are intended to evaluate the effect of 10% and 20% penetration into the system. The power generation scenario presented here was also published as Iyer *et al.*, (2010).

[5] It is acknowledged that this value for the local distribution network is an arbitrary selection. However the aim of this exercise is the see the effect of a 10% and 20% penetration level, which is primarily the reason for choosing this value.

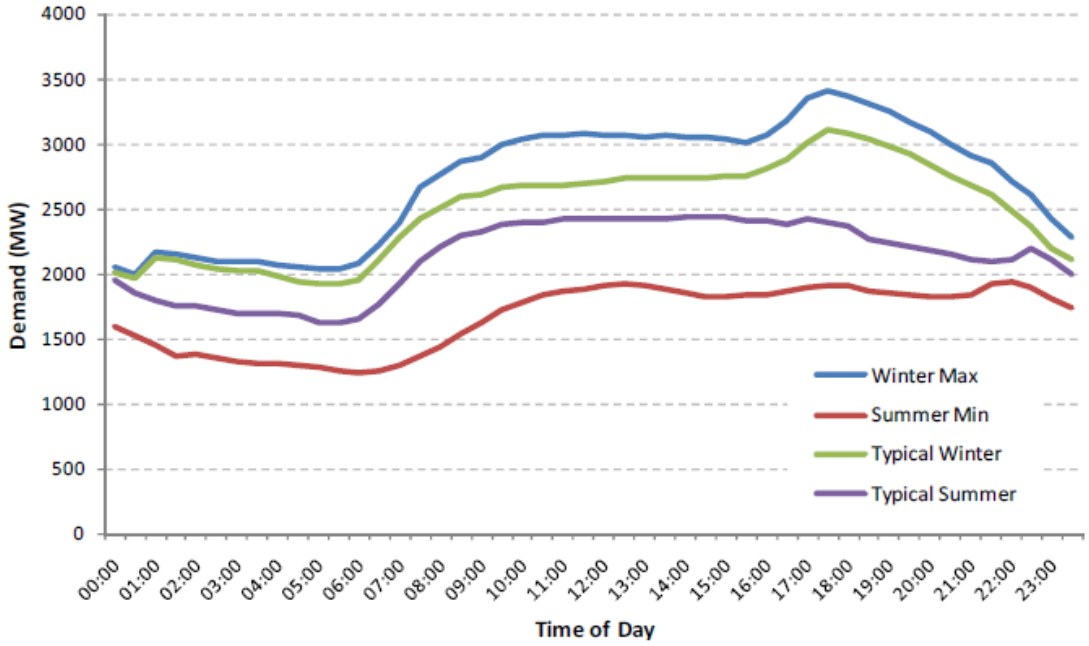

Figure 7.12 Seasonal demand profile for Merseyside, Cheshire and north Wales.(SP, 2010)

7.2.2 Power Generation

The supply scenarios considered here are the output obtained for the chosen site with two tidal turbine hypothetical farms. The first scenario consists of 40 devices, each with a rated power of 0.5 MW (a total installed capacity of 20MW). The second scenario consists of 80 devices with a total generation potential of 40 MW. For both scenarios it has been assumed that the tidal current energy resource itself is not impacted by the operation of extraction devices. As the scale of energy extraction increases, the energy available in the system for extraction will be reduced to some extent (as shown in chapter 6, section 6.3.3). Here this is ignored but for a larger development it will become important to take appropriate consideration of the reduction in resource harvest. Figure 7.13 shows the power curve of the hypothetical generic tidal turbine appropriate for this site, akin to the MCT power curve presented in chapter 6. The diameter is assumed to be 16 metres, with a cut in velocity of 0.7 m/s and the rated velocity of the device is 2.25 m/s.

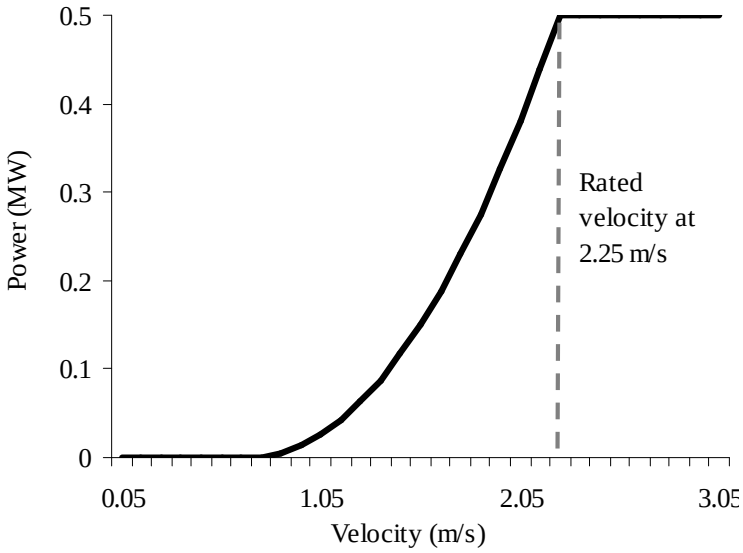

Figure 7.13 Power curve of a hypothetical tidal device. Power rated at 0.5 MW.

For this device, power efficiency (taken as a measure of the overall water to wire efficiency), *Cp* has been assumed to be about 42% on the basis of DTI (2005). The annual energy production for each device at this site is the sum of all the energy produced within the operational range of the turbine. In this case, the actual production is 1327 MWh/year, which represents a capacity factor of 30.3%. Figure 7.14 illustrates the percentage of time the device generates a specific amount of power. The device characteristics are such that it operates at rated power for 10% of the time and is idle for 27% of the time. The device rating is based on the velocity exceedance curve identified for Anglesey in chapter 6. Using the 10% exceedance value forces the device to operate at rated power for a minimum of 10% of time, therefore obtaining desirable capacity factor of about 30%.

The variability of power output is one of the key challenges for successful matching. Figure 7.14 illustrates the inter-half hourly variability of generation by one 0.5 MW tidal turbine. It shows a broadly symmetrical pattern of upward and downward shift in production. It is dominated by the periods when there are no inter-half hour changes. No generation occurs during slack and neap cycles when the velocity is too low for generation. Also, when the device is operating at rated power, the change observed is very small. Outputs from Figure 7.15 are substantially different to the wind generation patterns observed by

Milborrow (2010) as the nature of the resource is different. Importantly Milborrow looks at the aggregated output from a number of sites. Combination of a number of sites adds to the diversity and presents a wider spread. The asymmetry of the graph can be attributed to a combination of device power curve and site specific characteristics.

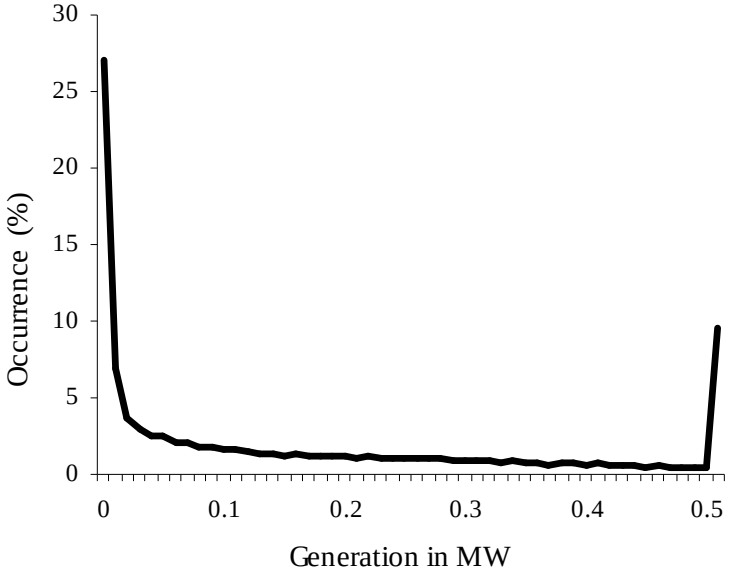

Figure 7.14 Tidal power generation and its occurrence using the hypothetical generic tidal device.

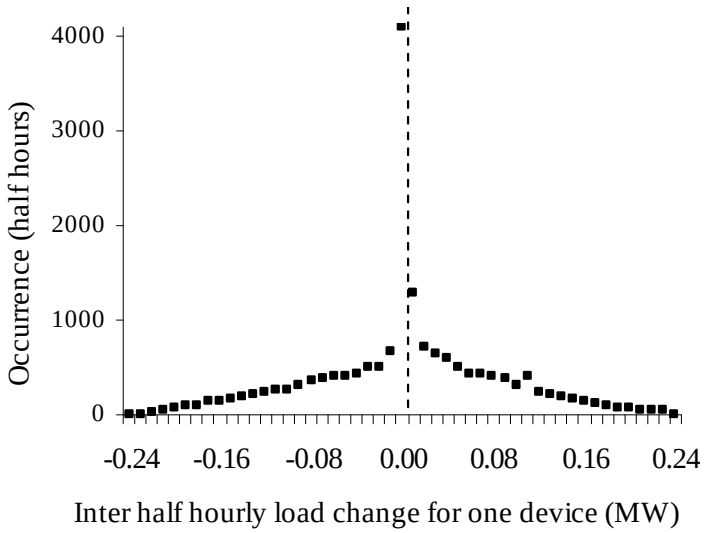

Figure 7.15 Tidal power fluctuation for one device over a year.

7.2.3 Contribution at 10% and 20% Penetration

Figure 7.16 shows demand fluctuations on the day of peak and as well as minimum demand in 2009. Plotted on the same graph are the simulated 20MW and 40MW generation scenarios. On the day of peak demand, the tidal resource is generating limited power with peaks of around half the installed capacity in both the scenarios. Because the tides are in their neap cycle, generation potential was low. Also interesting to note was that generation starting at 15:00 hours does not help service peak demand. As demand is increasing, tidal generation is reducing – therefore this reduction in generation suggests a larger swing for the system to cope with. However, this is just one instance – a longer period of data is needed to further understand the coincidence of peak demand with tidal generation. As tidal generation shifts by 50 minutes each day, there will be periods when spring peak generation will coincide with peak demand.

Alternatively, looking at the day when demand is lowest, generation from tidal production can at instances meet more than 50% of the demand. On the regional level this represents a significant contribution, but may equally create local problems of network overloading, perhaps leading to curtailment of tidal generation or other generators. It is important to point out that this combination of high and low tidal output and demand occurrence is for the year 2009, but that other combinations at peak and minimum demand would occur in other years.

To further investigate matching phenomenon at peak demand level, demand and generation patterns over the two weeks around peak demand are presented in Figure 7.17. The spring peak generation occurs the week after peak demand so, although in this particular scenario where there is negligible contribution to peak demand itself, there is contribution around the days of peak demand as a whole.

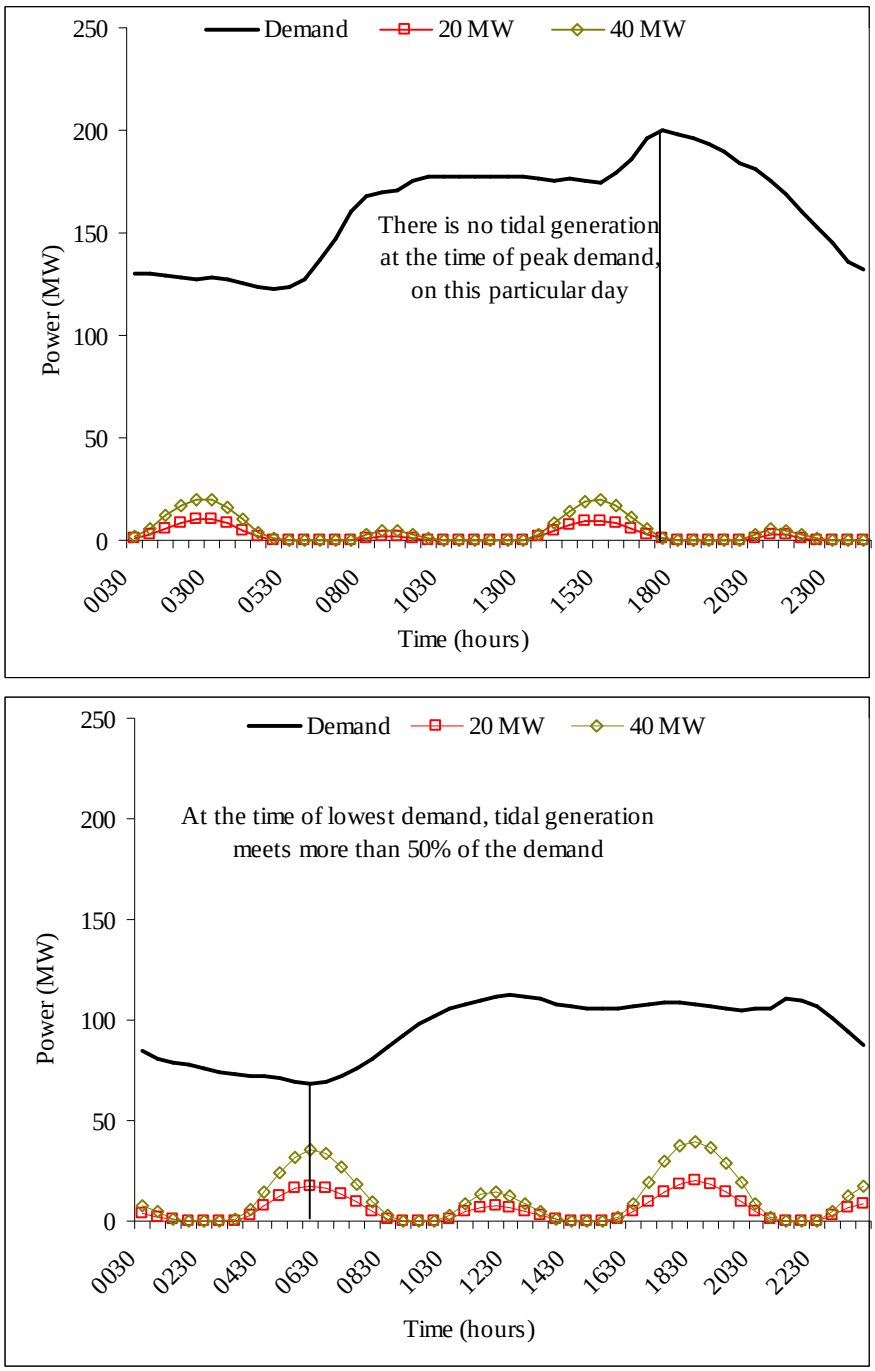

Figure 7.16 Tidal current generation contribution towards peak demand (top) and minimum demand (bottom) in the 10% and 20% penetration scenario.

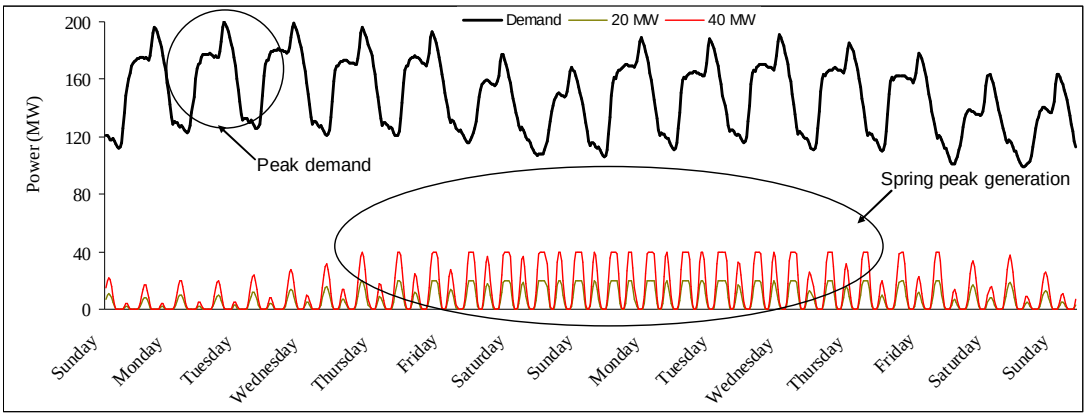

Figure 7.17 Tidal current generation contribution over a two week period following peak demand.

Figure 7.18 shows the extent to which the introduction of tidal energy is visible to the distribution system operator. It shows the scaled demand without any tidal in the system compared to the introduction of the 20 MW and 40 MW case. The residual demand curve shows demand minus tidal generation. The extreme cases at the tail of the graph are of interest. For emphasis, negative changes above 17MW are considered: in the scaled demand scenario, number of decreases below 17MW occurs once, but with tidal included the frequency of occurrence increases. Similarly, changes below 9MW are also considered, and the summary is presented in Table 7.2. The general trend observed here shows that large changes in demand are to become more frequent while periods of negligible change fall drastically.

The negative load change, although useful in terms of understanding the system, are less important compared to the positive load change as negative load change implies that there is a reduction in the demand for electricity. Therefore, if generation is in excess of demand, it can be exported or, depending upon network constraints, be curtailed.

Comparing this to the work done by Milborrow (2010) shows that there are more excursions at both of the tails of the distribution curve. This is mainly because only the output from one generation location is being considered here and does not benefit from aggregation of locations to smooth the ‘peaky’ operational characteristics of tidal current

generation. The aggregate effects of a number of tidal current energy locations would be expected to produce an excursion characteristic more in line with those produced for wind. Additional sites will be geographically diverse and bring individual site characteristics to the mix.

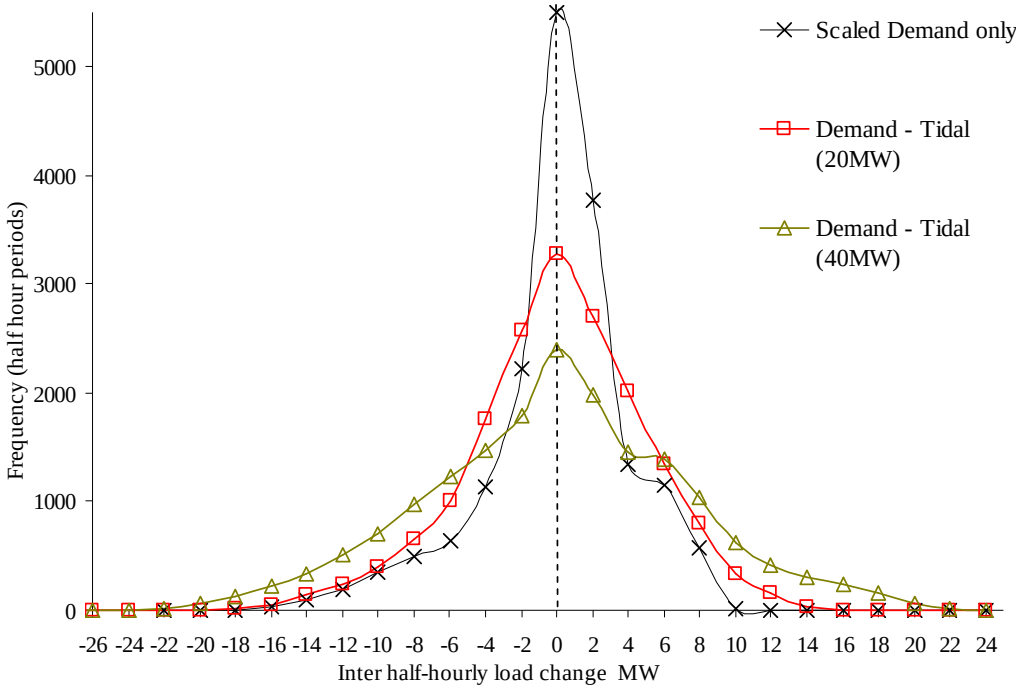

Figure 7.18 Inter half-hourly demand changes in UK for 2009 along with what the system operator would see if there was 20 MW and 40MW (Demand – Tidal) tidal generation.

Tidal Penentration %			
	None	10%	20%
Maximum inter period decrease: MW	18.5	20.8	26.0
Number of decreases of 17 MW and above	1	17	211
Maximum inter period increase: MW	9.4	15.8	23.9
Number of increases of 9 MW and above	12	538	1811
Zero load change %	31.4	18.7	13.6

Table 7.2 Key data for half hour power excursion in scaled demand.

7.3 Aggregate Tidal Energy Generation Matching

The methodology identified in section 7.2 will now be applied to all the UK sites identified in chapter 6 as part of the first generation development scenario. Since the physical environment impacts of full resource exploitation are likely to be unacceptable, only the Flux TAP scenario developed in chapter 6 of 5.4 GW installed capacity is taken into account here.

7.3.1 Variability

Chapter 6 assesses the total UK tidal current resource by combining multiple datasets including Marine Atlas, TotalTide tidal diamonds and measured tidal current information. A new approach to identify device rating has been developed during this study to help suggest an overall economic capacity factor and aid development of realistic scenarios. It has concluded that 14.25 TWh/yr can be extracted with a total installed capacity of 5.4 GW, without significantly impacting the underlying resource at the identified sites.

Figure 7.19 shows the fluctuation of tidal generation potential simulated every half hour for each of the individual sites: Pentland Firth, Orkney, Islay, Anglesey, Ramsey Island, Race of Alderney and Isle of Wight used in the Flux TAP scenario development. Extreme fluctuations above 0.5 GW can only been seen at the Pentland Firth as it has the largest installed capacity (2.5 GW). The asymmetry in the power swings are significant at Orkney, Islay and Pentland Firth exacerbated particularly for the negative change. The analysis and scenario developed in chapter 6 identified that all these sites are predominantly in-phase.

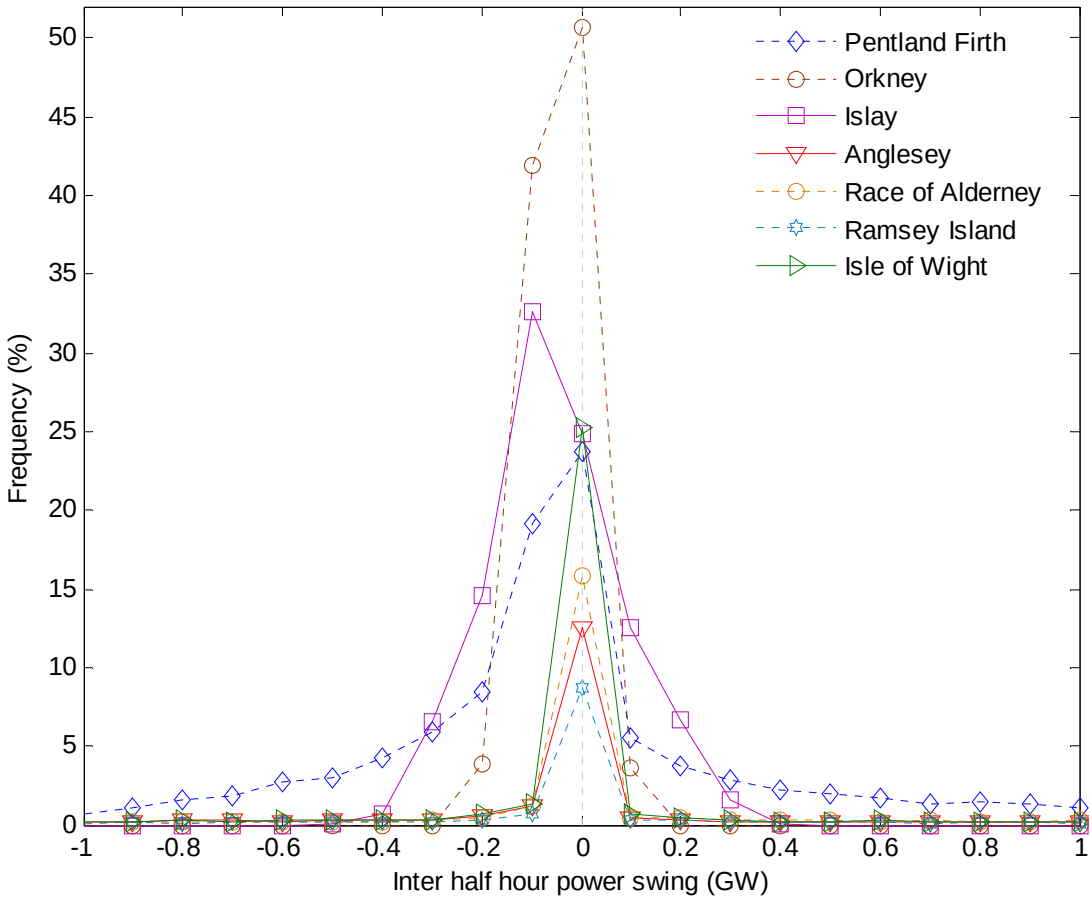

Figure 7.19 Frequency of load change at each individual site.

Inter half-hourly aggregated output obtained from the Farm TAP and Flux TAP tidal scenarios are presented in Figure 7.20. Extreme fluctuations of ±4 GW are observed for the Farm TAP and ±2 GW for the Flux TAP scenario. Considering the total installed tidal capacity of 5.4 GW in this scenario, the maximum indicated half-hourly swing is a significant proportion of installed capacity. However smaller swings are generally the norm. The asymmetry observed from each individual site is smoothed over when aggregated. However, the negative and positive swings still are not symmetrical. In particular for the constrained scenario, a second peak can be observed at 1.5 GW load change.

The modular approach to tidal current generation installation ensures that sudden ‘switch-off’ is avoided. A key distinction to be made here is that failure or shutdown of a unit or a number of units will reduce output but near–zero output from an entire fleet of

conventional generation units does not occur, while for tidal generation the output is constantly variable dependent upon the resource. Diversification and multiple device farms reduce the risk of a complete shutdown.

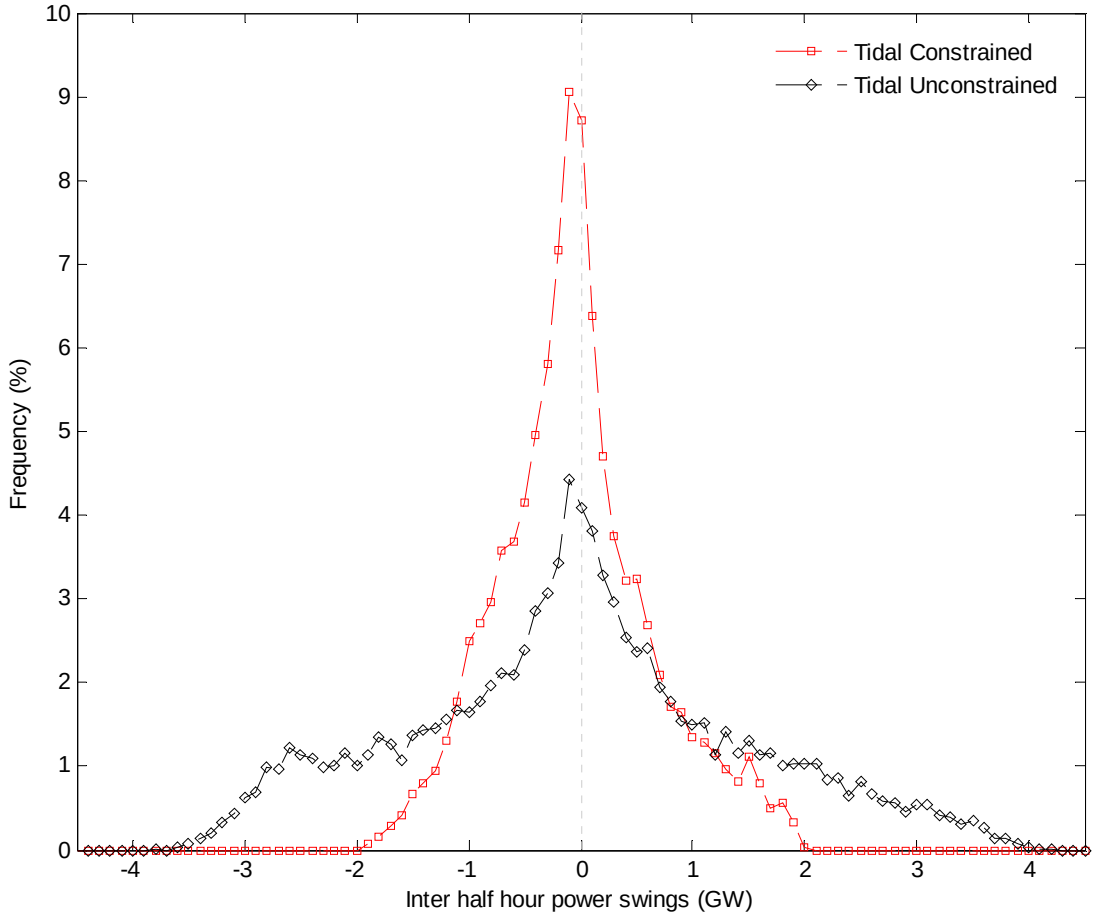

Figure 7.20 Inter half hourly power output fluctuations from Farm TAP and Flux TAP scenario.

An advantage tidal generation has over wind and wave power is the absence of extremities of operation. For example, a standard wind turbine may be rated at 12 m/s and cut out at 25 m/s. This is necessary as gust speeds of 50 m/s are common across the UK (Met Office UK). A cut-out velocity or survival strategy is therefore necessary for these technologies as sites can experience extreme gust speeds (wind) or wave heights (wave) that are far beyond the operating region of the wind or wave generators. For tidal current this is not a major issue, as the operating conditions are not that far removed from the extreme conditions (as shown in Figure 6.8). Most tidal devices are therefore not designed to cut out

and can operate at rated power during extremes by pitching the blades to alter the angle of attack and shed load.

Figure 7.21 shows two curves. The first is the UK demand over the week when peak demand occurred, from the 5th to 11th of January 2009 with peak demand occurring on the 6th of January. The second curve shows residual demand (demand – tidal) for 5.4 GW installed capacity (the Flux TAP scenario). This scenario presents a 9.4% (approximately 10%, similar to the Anglesey case study) penetration level. The contribution of tidal current energy to the system would only reduce the annual system peak on the 6th by 0.5 GW. Two days later, on the 8th, maximum demand for the day was 57.3 GW, 12th highest for the year, is reduced by 3 GW with tidal current included in the system. The biggest reduction that can be obtained with the inclusion of tidal in the system will be in the order of 5 GW, which occurs around midnight on the 11th; in this instance, peak generation does not coincide with a significant demand peak.

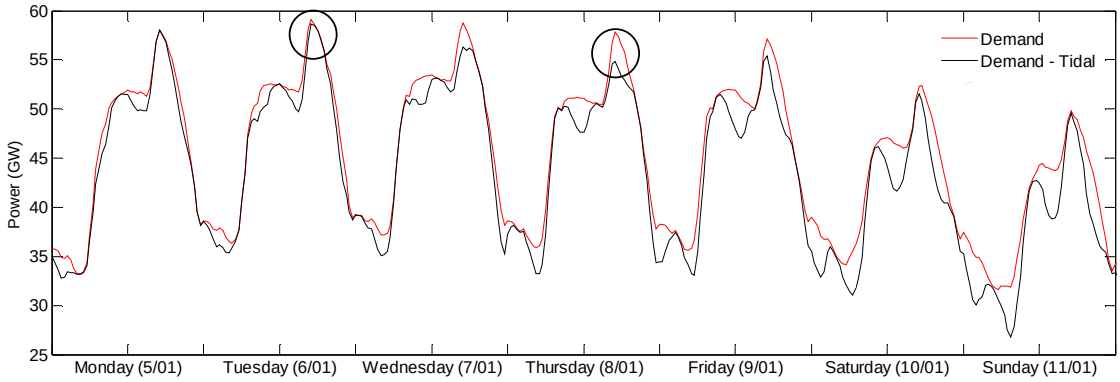

Figure 7.21 Change in demand with tidal in the system being considered as negative demand. Circle on Tuesday indicates day of peak demand. Circle on Thursday indicates largest tidal contribution to demand.

As part of the Spring-Neap cycle, even if in this instance tidal does not make a significant contribution to peak demand, there are occasions in the winter period (usually considered from November to February) when tidal does make a significant contribution to reducing net peak demand. This can be seen in Figure 7.22 where 10% of the peak demand hours are binned and the average reduction with tidal in the system are shown. The bars

indicate minimum and maximum value for each percentile. It can be seen that, although tidal does not contribute towards all of the half-hourly periods, there is reduction. Particularly in the 94th percentile where a reduction of 10% can be seen. This equates to the total tidal installed capacity.

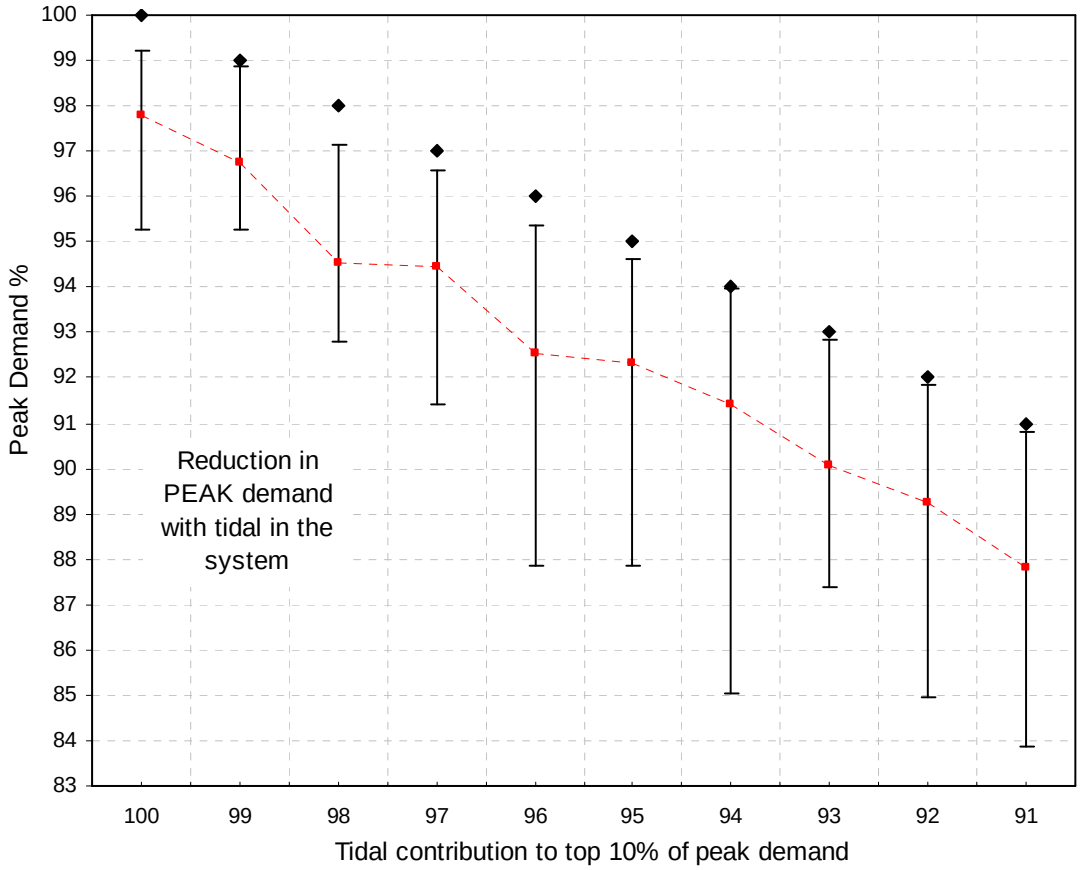

Figure 7.22 Average reduction in the top 10% of demand half hours with tidal in the system. Bars indicate minimum and maximum values of reduction.

Because of the inherent characteristic of the resources, the majority of the sites experience velocity below 0.7 m/s (the cut-in velocity) for about 30% of the time. Therefore, it is implicit that, for approximately 30% of the time, tidal will make no contribution towards generation. Figure 7.23 shows a reduction in demand for the whole year obtained by considering what percentage the demand is reduced by and for what percent of time. As expected for nearly 37% of the time there is less than 1% reduction in demand but for nearly

60% (obtained by adding all the other bins) of the time there is some reduction in net demand.

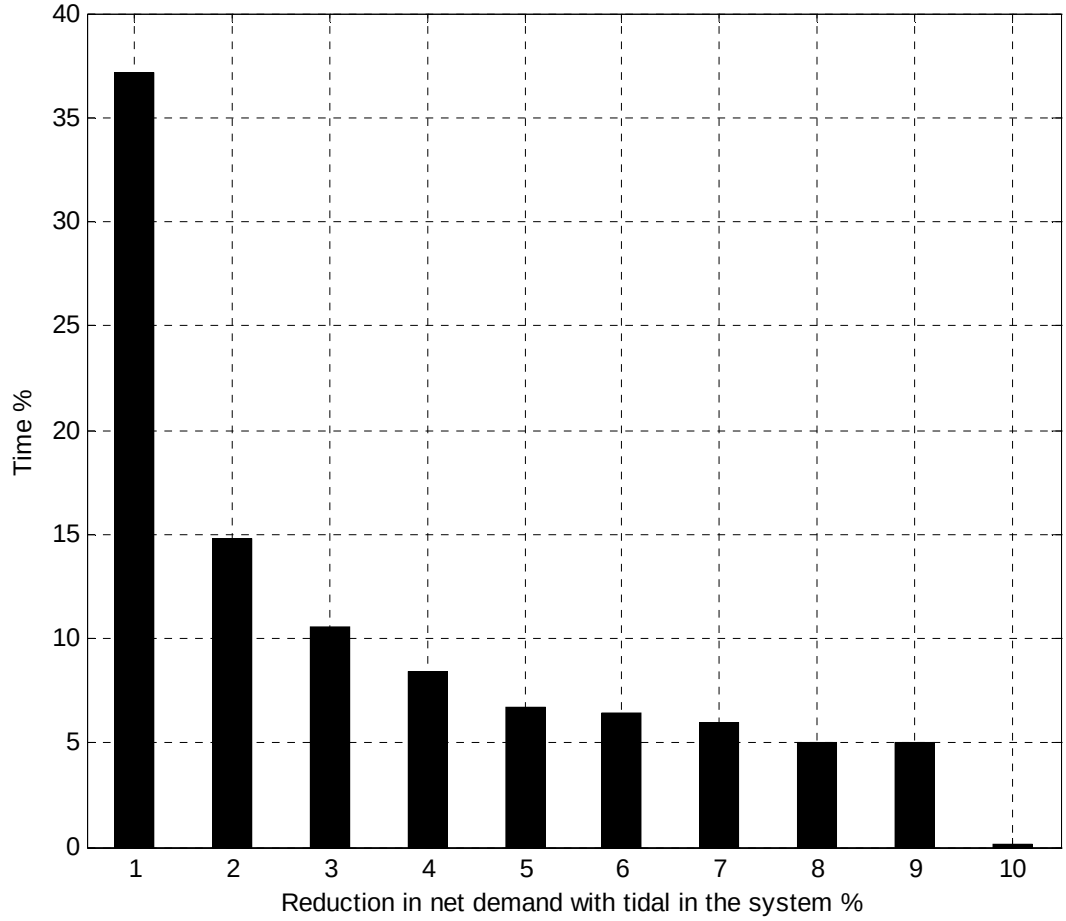

Figure 7.23 Reduction in net demand for the entire year with tidal in the system.

7.3.2 Contribution to Demand from Tidal

A method of assessing the variability for the whole year is presented in the Load Duration Curve in Figure 7.24. The two curves show demand with and without the inclusion of tidal in the system using the 14.25 TWh/yr, Flux TAP generation potential. The reduction in the load duration curve with tidal in the system is an even spread indicating a potential correlation. However, due to the lack of any causal relationship tidal is independent of demand.

Although the reduction appears to be small and only meets about 4% of the demand, this is a significant contribution. For comparison in 2009, only 9 TWh/yr was generated by wind and 26 TWh/yr from all of renewables aggregated (DUKES, 2010). In terms of

meeting 2020 targets, tidal can contribute as much as 12.6% using only first generation sites and technologies. Expansion to second and third generation will have the potential to increase the impact, with potential to double this contribution.

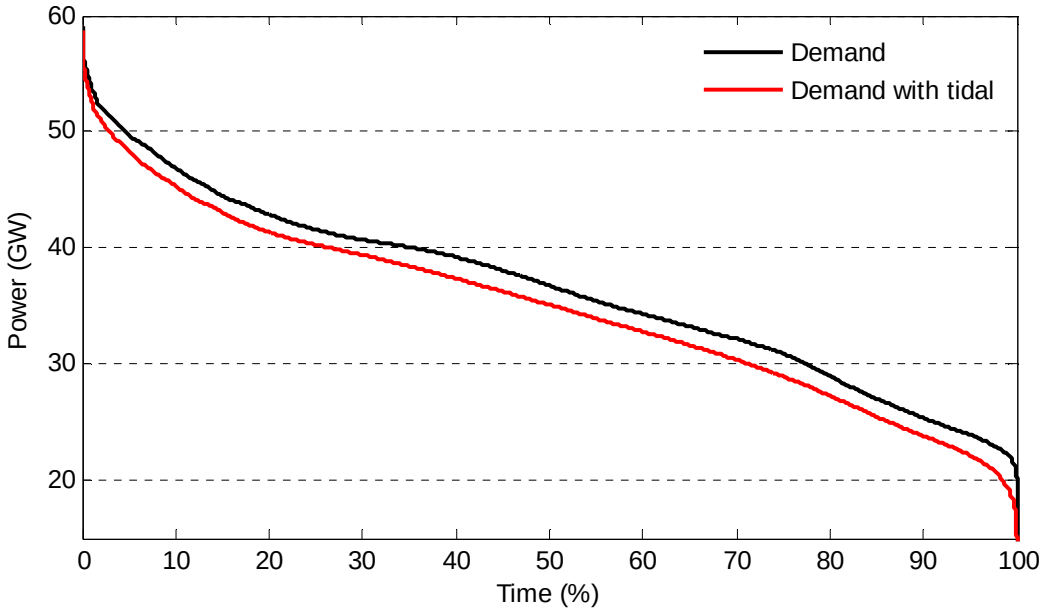

Figure 7.24 Half hourly demands and tidal generation presented as Load Duration curve.

Despite its usefulness, the load duration curve does not show how demand and tidal generation scenario interact in time. Therefore, the coincidence of occurrence of demand and supply is shown in Figure 7.25. Demand is normalised with respect to peak demand and tidal generation is presented as a percentage of the total installed capacity, 5.4 GW from the Flux TAP scenario. Each column in the bivariate histogram shows the amount of time (in %) for which a particular combination of generation and demand *coincide*.

As demand never falls below 20 GW, there are no coincidences for the first 30% of peak demand. Appendix A presents a histogram where only the distribution above 20GW is considered. The worst-case, as defined by Boehme (2006a), is identified as the period when demand is ≥90% and tidal generation is ≤10%, the right-most column in the histogram. This corner is significant as it defines the time when generation is low and demand is high and therefore a very critical period for the system. The histogram highlights that the largest

match occurs when generation is ≤10% and demand is ≥70%. With the inclusion of second and third generation tidal into the energy, this histogram should present a better mix.

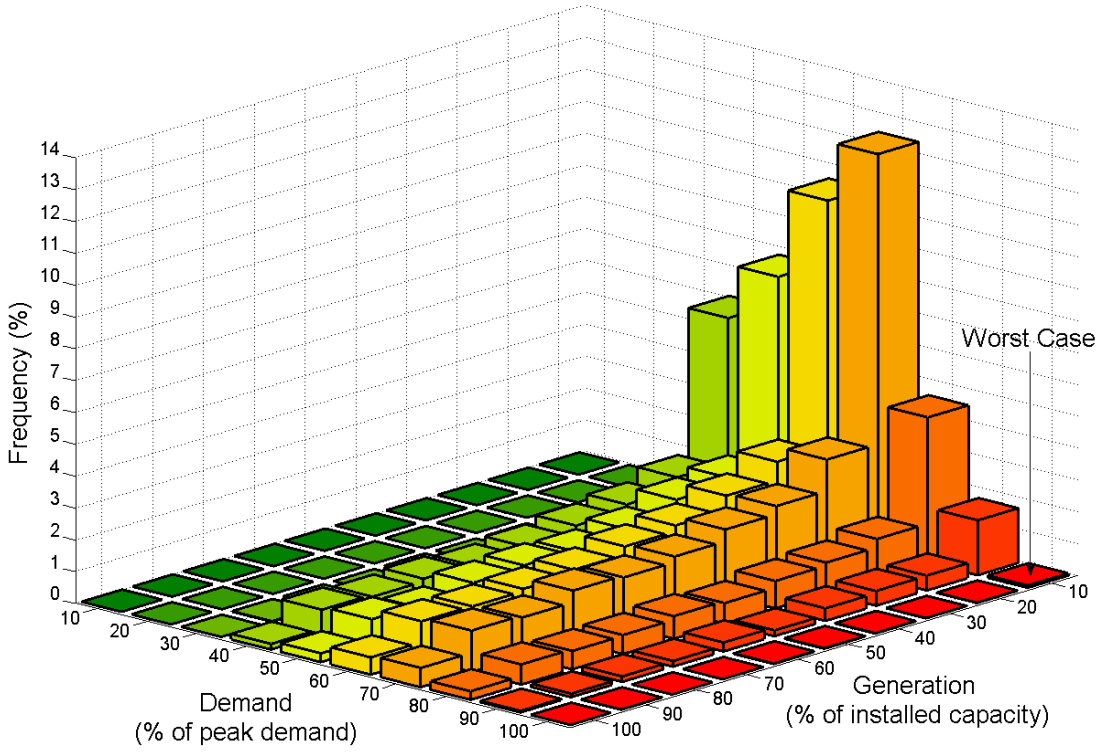

Figure 7.25 Bivariate histogram showing the frequency of coincidence between demand and supply.

7.3.3 System Adequacy

One of the key concerns with higher levels of penetration of renewables in the electricity system is system adequacy. As mentioned, periods of, and around, peak demand are the most important in terms of planning generation capacity and account for scheduled and un-scheduled outages. A concern with large levels of wind penetration are the high-pressure weather systems that bring calm winds but periods of cold weather, leading to high demand for electricity with little generation from wind, as suggested by Kean *et. al.*, (2011) and explained by Cradden *et al.*, (2011). However, tidal should not suffer from this problem. Table 7.3 and Figure 7.26 explore the tidal current generation time-series relative to time-series of demand and identify distribution of power output level with respect to demand levels. Similar analysis for wind is also presented in the National Grid Winter Outlook (NG,

2008). The analysis was conducted by presenting demand as a percentage of peak demand and grouping the percentage tidal (Flux TAP scenario) generation as capacity factor within each of these bins. Table 7.3 presents the number of hours power is generated for a specific percentage of peak demand at a specific capacity factor. For example, 41 hours in a year tidal current generation will operate between 0 and 10% of installed capacity while demand is between 90 and 100% of peak demand.

% Peak Demand	Tidal Current Capacity Factor										Total hours	Average CF %
	0 to 10	10 to 20	20 to 30	30 to 40	40 to 50	50 to 60	60 to 70	70 to 80	80 to 90	90 to 100		
30 to 40	138	57	33	23	25	15	17	23	19	23	370	31
40 to 50	518	234	158	115	114	87	89	87	76	44	1519	30
50 to 60	750	305	203	163	143	114	116	110	92	92	2085	30
60 to 70	926	342	263	223	172	158	143	125	107	84	2540	29
70 to 80	516	192	151	112	94	87	76	73	82	71	1452	31
80 to 90	225	99	71	65	40	42	40	40	29	31	680	31
90 to 100	41	19	14	13	8	8	6	4	3	1	116	26
Total	3113	1246	891	711	595	508.5	484	461	406.5	344	8760	30

Table 7.3 Hours spent at mean capacity factors as a percentage of peak demand.

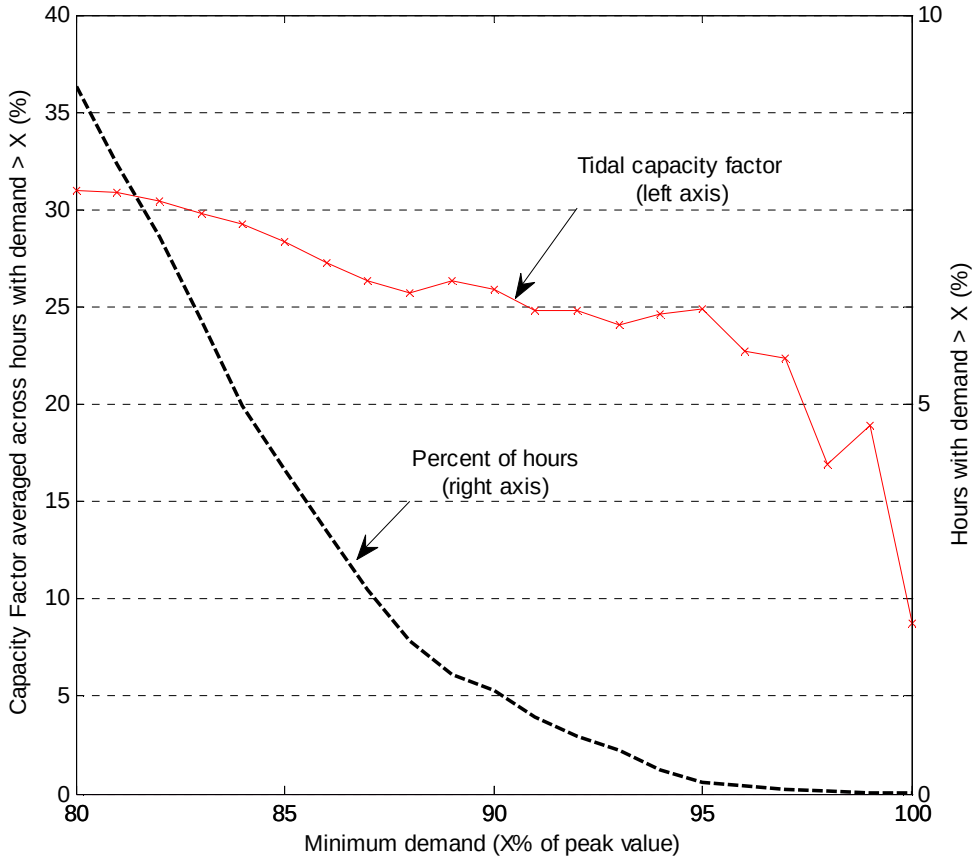

Figure 7.26 Average capacity factor for high demand levels.

Note that the average capacity factor drops as demand increases, illustrated in Figure 7.26. Kean *et al.*, (2010) and Hawkins *et al.*, (2011) find similar results for wind and Cradden *et al.*, (2011) presents a combined wind/wave scenario. However, the drop in the capacity factor of wind is lower than that of tidal as considered in this scenario.

7.3.4 Load change

The effect of the aggregate tidal variability on the system can be examined by considering the residual that generation sources other than tidal must provide. Figure 7.27 shows the frequency of inter-half hourly demand changes, before and after tidal is introduced as per Figure 7.17 for Anglesey only. The shape of the graph with and without tidal is similar. This highlights that extent of variability already inherent in the demand for electricity.

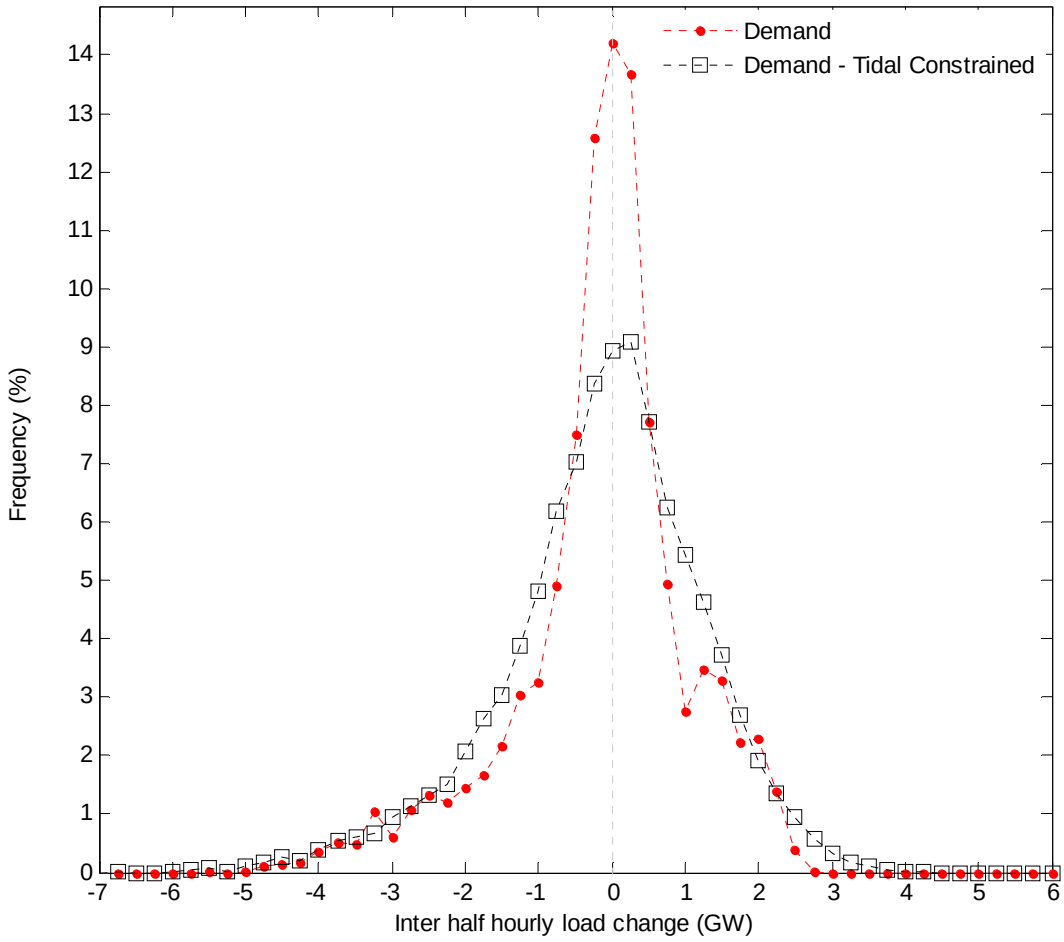

Figure 7.27 Inter half hourly demand change with and without tidal current in the system.

The impact of including tidal to the overall system significantly reduces the number of small changes at the GSP. Table 7.4 summarises the key changes and highlights that the largest swings are increased and become more frequent with the addition of tidal to the system. Maximum negative swings of the order of 6.7 GW and positive swing above 4.4 GW have increased. The increased swings indicate that additional fast reacting reserve will need to be included in the generation mix to account for these changes.

This outcome relates back to the initial findings (in chapter 6) of the relative phasing of UK tidal current energy resources. If the resource was more out of phase, the variability felt by the system would be reduced as power generation would generally be smoother, with potential for continuous generation. Because of the phasing of all the sites considered in this scenario, the aggregated output is, in effect, one big site; therefore the analysis presents output similar to the Anglesey case study. As expected, the number of small load changes in the system fall from 14.2% to 9.1%. A log scale on the Y-axis plot of Figure 7.27 is presented in Appendix A to highlight the excursions occurring at the tail end.

Tidal Penentration %		
	None	Constrained
Maximum inter period decrease: GW	5.5	6.7
Number of decreases of 5.25 GW and above	1	21
Maximum inter period increase: GW	2.8	4.4
Number of increases of 2.5 GW and above	2	220
Zero load change %	14.2	9.1

Table 7.4 Key data for half hourly power excursions with the inclusion of tidal in the system.

7.3.5 Semidiurnal Pattern

In chapter 5 (section 5.4.1), it was identified that the tidal current time-series presented a semidiurnal pattern when averaged over a long term. It is of interest to evaluate if all the individual sites will present a semidiurnal pattern and consider how they vary. The mean power output from each of the sites is presented in Figure 7.28.

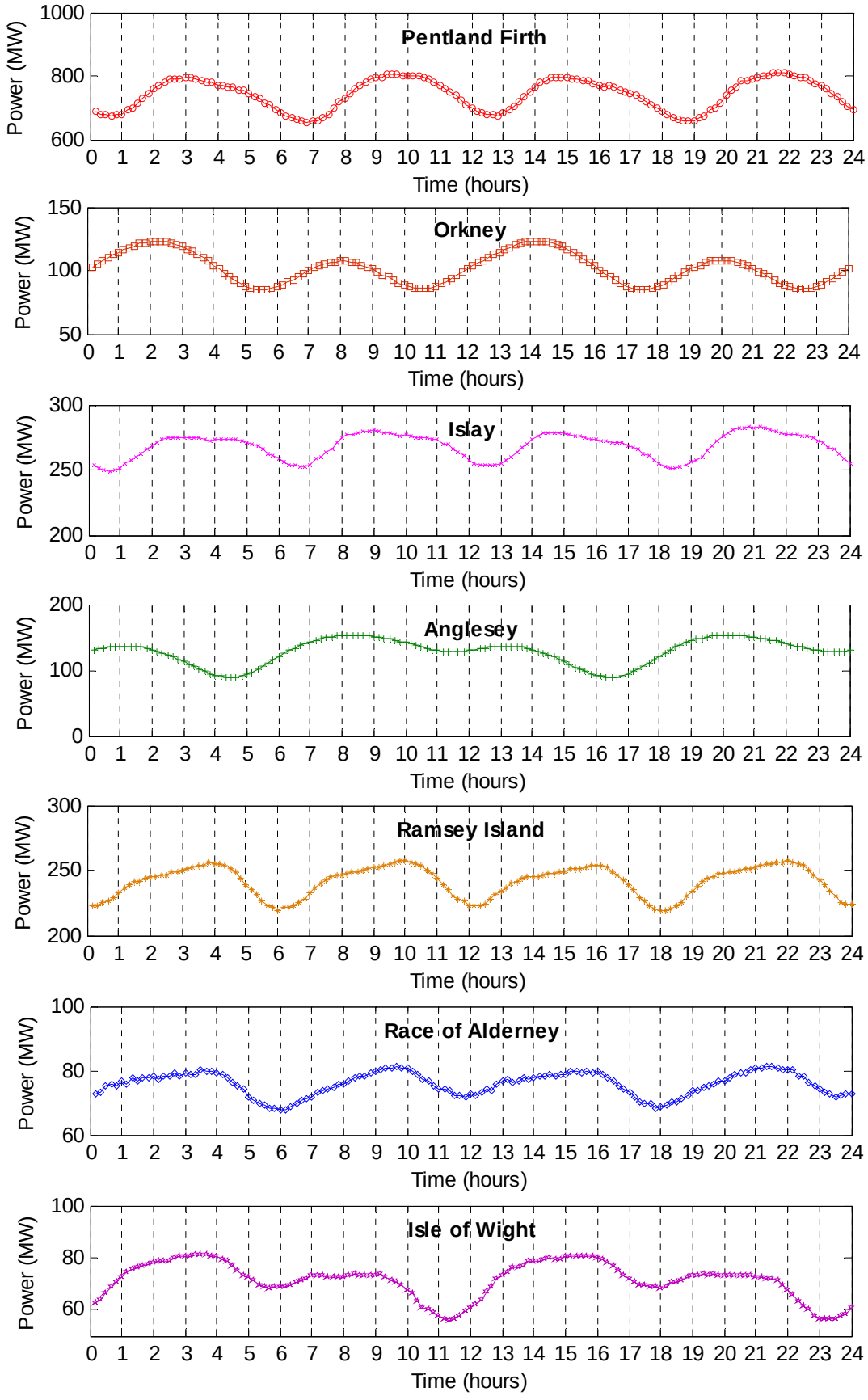

Figure 7.28 Semidiurnal pattern experienced at each of the sites in the year 2009.

The daily pattern was obtained by averaging, for each ensemble period, in a standard day. All the sites show a semidiurnal pattern, although the timings of the peaks and troughs do not coincide for most of the sites. The observation of a semidiurnal pattern is of particular interest as the coincidence of peak generation coupled at the time of peak demand will benefit the system. Due to the size of the installed capacity, the aggregate effect of combining the power output from all the sites is dominated by the Pentland Firth. Therefore, the timings of the total power output looks similar to the Flux TAP scenario output from the Pentland Firth alone, as shown in Figure 7.29.

Diurnal patterns analysis have been presented over a 25 year period for EMEC datasets (Survey 13) in chapter 5, suggested that the timing of the Spring and Neap peaks and troughs in the diurnal patterns coincide. Therefore, unless additional sites are included as part of second/third generation development that are much larger than Pentland Firth (which is highly unlikely) and present different timings, the aggregate power output will continue to look similar to Figure 7.29.

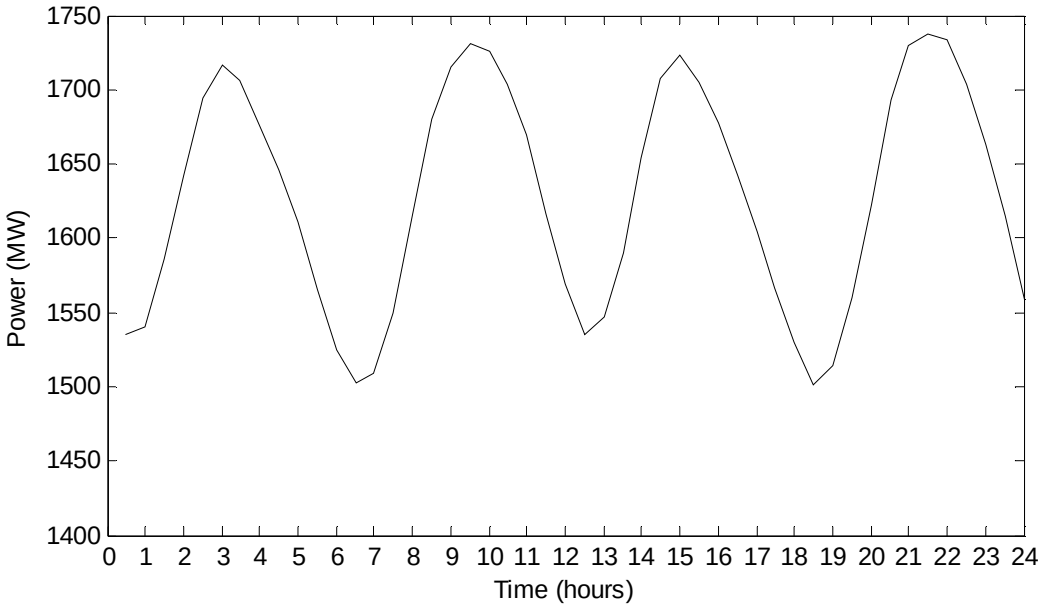

Figure 7.29 Diurnal pattern of the aggregated total output.

This analysis can also be used to develop a statistical model of tidal current generation to evaluate what percent of conventional generation can be displaced by tidal

current generation. A basic analysis presented in Iyer *et. al.,* (2011a) follows the methodologies identified by Dent *et. al.,* (2010) suggests an Effective Load Carrying Capability (ELCC) of 0.82 GW or 15.19% for the Flux TAP scenario. The author intends to do a detailed study in future.

The capacity values presented for tidal current is similar to the wind capacity credit presented by Aguirre *et al.,* (2009), Hawkins *et al.,* (2011) and the capacity value evaluate for tidal barrages presented by Radtke *et al.,* (2011). It is also understood that as the overall installed capacity increases, the capacity credit decreases. Therefore with higher penetration, the need to maintain the same level of risk index would incur a higher cost of balancing.

7.4 Trading Tidal

Having identified the power output characteristics (production and time-series) of each of the tidal sites and explored the aggregated output, it is useful to consider how such a predictable but variable power output could be traded in the electricity market. At present the trading arrangements for renewable generators depends on the installed capacity. Plants that are larger than 10 MW need to be licensed and are required to comply with the Balancing and Settlement Code.

7.4.1 Spot Price

Wind is traded over a short-term period. This can be in the form of day-ahead or hours ahead before gate closure, but wind does not lend itself for long term trading as, over time, the errors associated with the wind forecastability increases. Tidal does not suffer from this problem of inaccurate forcastability and can be predicted over long time-periods with high levels of accuracy. So, given the high level of accuracy with which tidal currents can be predicted, this study explores whether tidal current energy are potentially better suited to trade in the spot market or, perhaps, a medium to long term fixed price contract. Figure 7.30

shows the system spot market price for the year 2009, obtained from Elexon[6]. The average price for the whole year is £36.9/MWh.

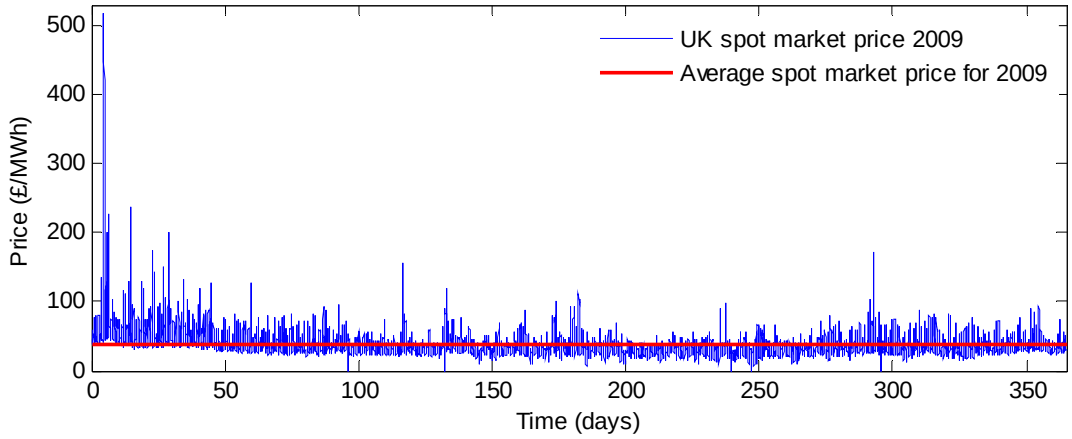

Figure 7.30 UK electricity spot market price for 2009.

Figure 7.31 shows the ten day period when the spot price reaches its maximum value of £517.46/MWh (on the 5th of January) and the tidal aggregated output developed under the Flux TAP scenario.

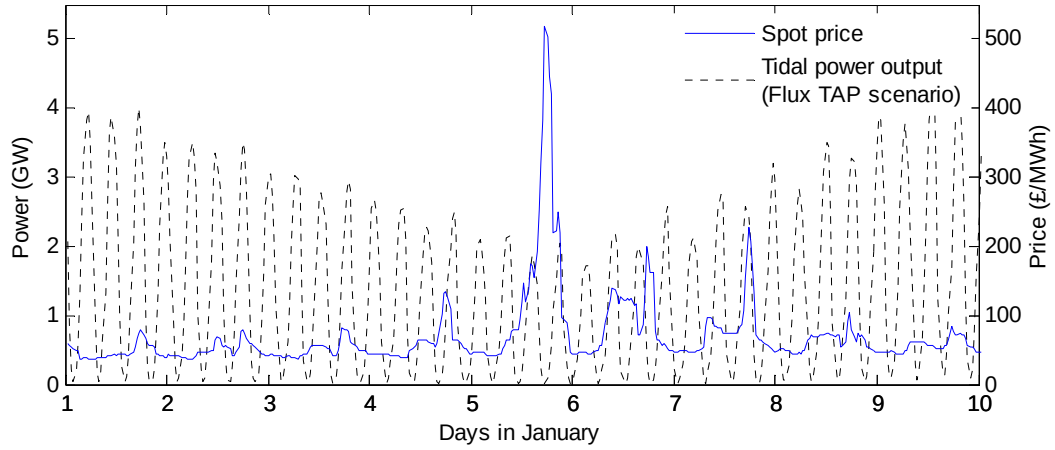

Figure 7.31 Tidal generation on the day of maximum spot price.

Unfortunately, on this occasion there is no tidal generation and therefore it would not have benefitted from the high spot price. However, there are other occasions when a higher spot price coincides with tidal generation, indicating that there is some opportunity to trade in the spot market. An exceedance curve of the system spot price from 2005 to 2010 is

[6] http://www.elexon.co.uk/Pages/home.aspx

shown in Figure 7.32 which highlights that the spot price variability and characteristics are predominantly the same from one year to another. The occurrence of very high price exceeding £220/MWh diminishes very quickly.

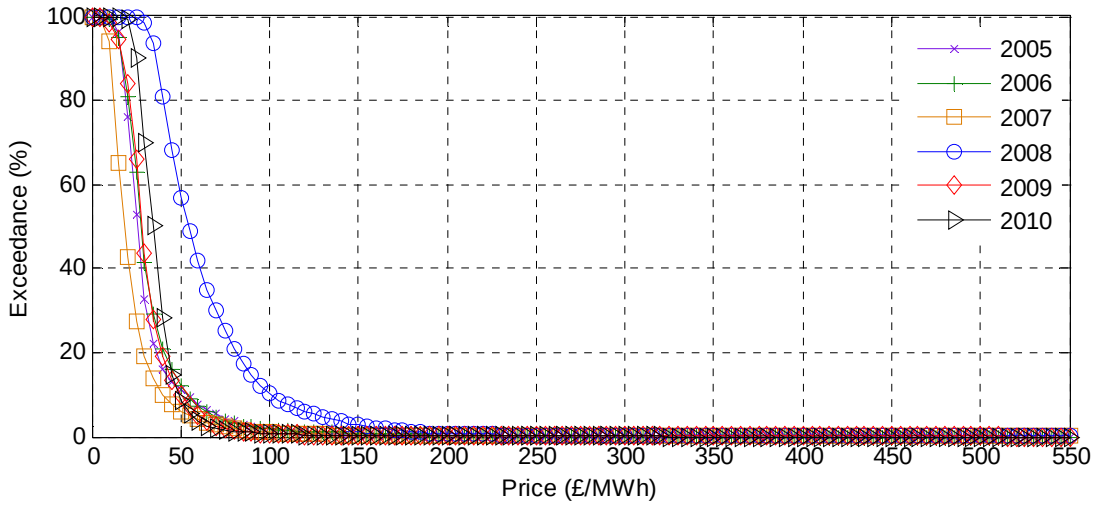

Figure 7.32 Spot price exceedance curve from 2005 to 2010.

To further investigate, Figure 7.33 shows a bivariate histogram of the coincidence of high spot price and tidal generation. For the year of 2009, it appears that the majority of generation occurs around £50/MWh. The top histogram shows data binned in £50/MWh. In this case, generation exceeding £200/MWh occurs 13 times (0.074%). The bottom histogram bins the data in £10/MWh and it can be seen that majority of the coincidence occurs around £30 to £50/MWh. Understanding, based on this analysis, suggests that at least for the year 2009, coincidence of high spot price and tidal generation was small. A few years of data will be necessary to completely understand the coincidence between price and generation but, even then, although tidal is predictable, it is still a variable resource and the coincidence of (maximum) generation occurring at a time that benefits from high spot market price remains uncertain until a few hours before real time.

Additionally, Martin (2011) informed that operating just before gate closure will mean that tidal will operate in a market that is short of liquidity. Tidal will just have to accept the spot price without any influence on the price. National Grid initiates all within-

gate trades and not very much can be done with an instruction to turn up the tides at a time when there is no/minimum generation.

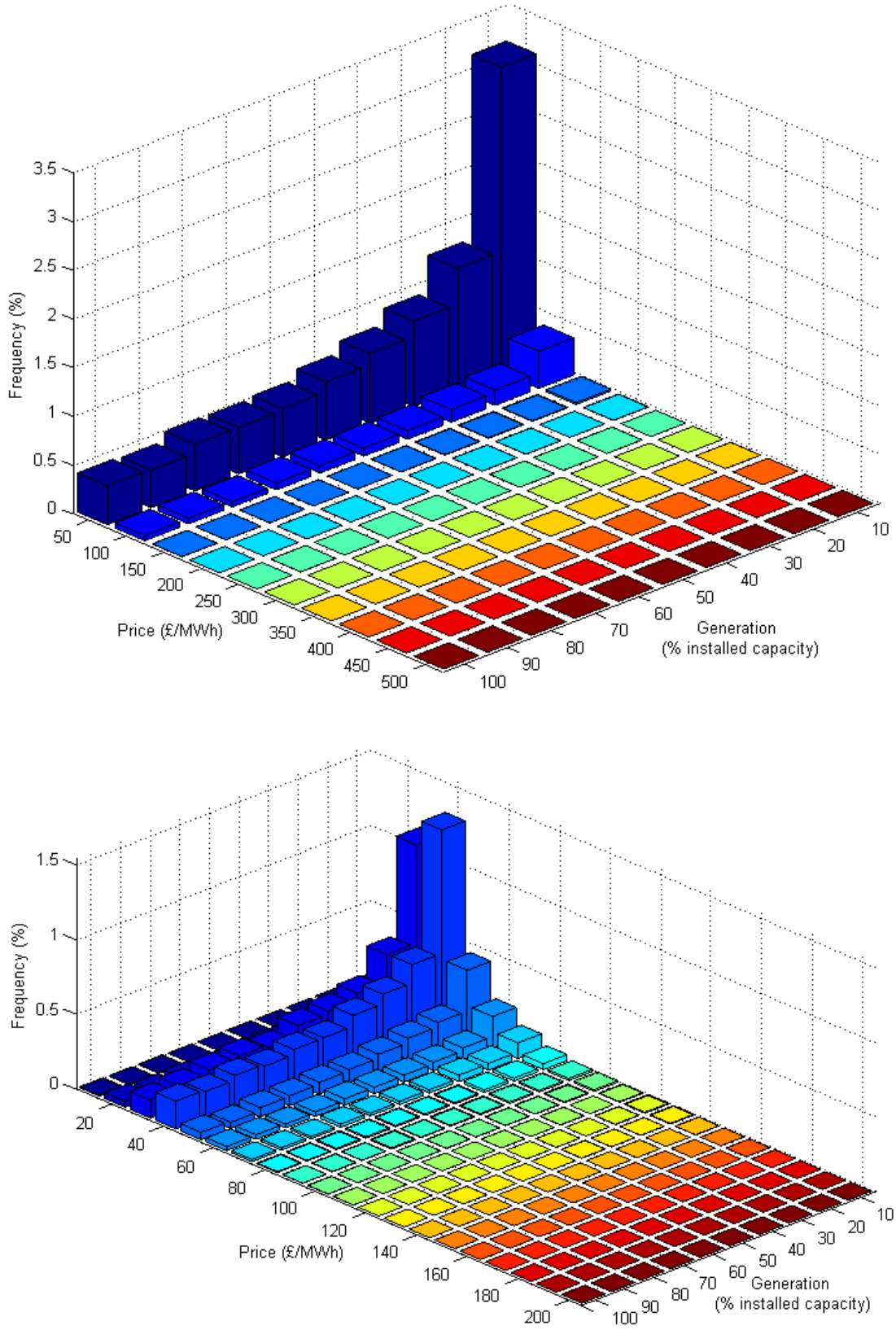

Figure 7.33 Bivariate histogram showing the coincident of high spot price and tidal generation.

7.4.2 Additional Incentives

At present, Renewables Obligation Certificates (ROCs) are the main form of subsidies in the UK (for generators above 5 MW). Initially ROCs were technology neutral but changes have been incorporated to reflect the difficulties certain technologies may face. Therefore, high level of support is provided to technologies that are much more expensive.

Under the current scheme tidal generators receive 2 ROCs/MWh (BERR, 2009). However, the Scottish government has provided additional incentive and offers 3 ROCs in Scotland (Scottish Government, 2008). Figure 7.33 shows the value of ROCs obtained in e-ROC auction achieved since 2002(e-ROC, 2011).

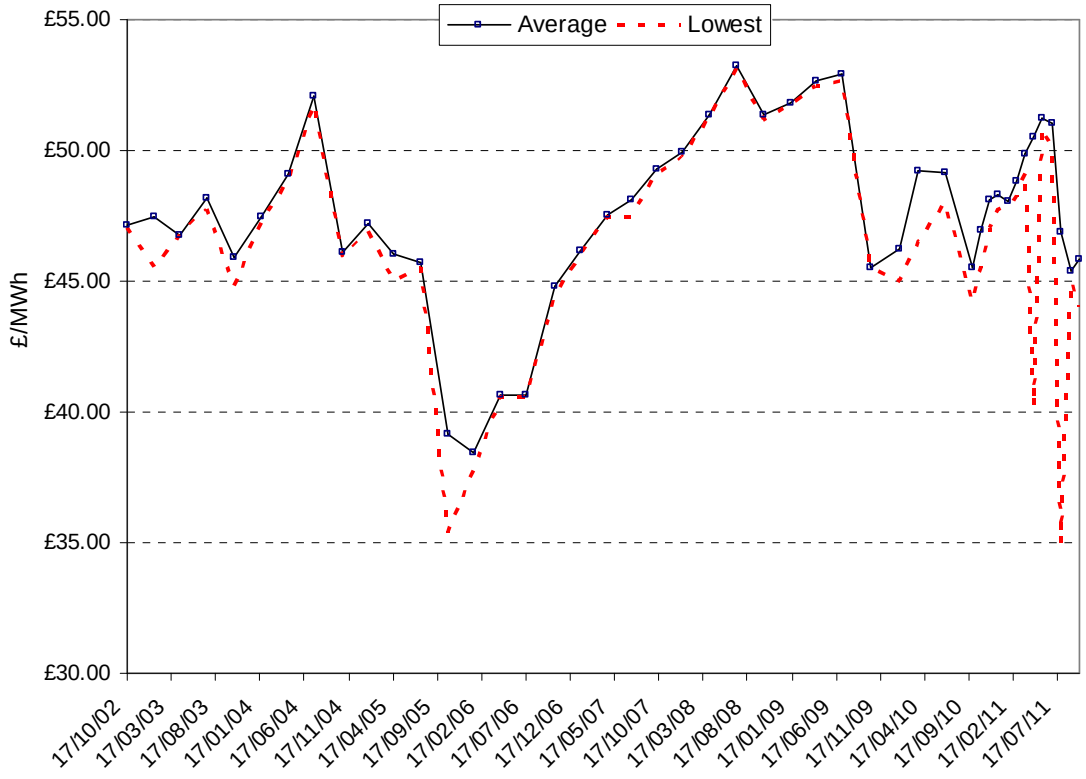

Figure 7.34 ROC auction price (e-ROC, 2011).

It can be seen that even the lowest price does not drop below £35/MWh and maintains an average value of £47/MWh. Therefore, the ROCs themselves substantially increase the revenue for the generator and play a much more significant role than the actual trading price of electricity. For example, the average spot price for the whole year in 2009 is

£36.9 /MWh, but ROCs will be in the order of £94.2/MWh for 2 ROCs and £141.3/MWh for 3 ROCs. Similarly, the EU Emissions Trading System (EU ETS, 2008) implements a cap on the CO_2 emissions by businesses and as a result has created a market for carbon trading where shares can be auctioned. This is another avenue to subsidise renewable generations.

For the future, incentives like a supplement to the EU ETS have been indicated by the recent White Paper by DECC (2011a). The UK government in addition to EU ETS aims to introduce a Carbon Price Floor (CPF) to 'top up' the carbon price. For 2013, the CPF begins at £15.70/tCO_2 and is expected to rise as high as £70/tCO_2 by 2030. Additionally, the UK government understands the need for long-term investments and therefore has identified long-term contracts such as Feed-in-Tariffs (FiT) with Contracts for Difference (CfDs), which will replace ROCs to helps obtain a steady level of revenue as agreed at the start of the contract for the duration of the contract. A 'two-way' scheme operates where, if the monthly electricity price is below the agreed contract strike price, the generator will be given additional payment such that it meets the strike price. On the other hand, if the monthly electricity price is above the strike price, the generator is to pay back the difference.

7.4.3 Long Term Power Purchase Agreements

In reality, tidal generation schemes without impoundment do not have a choice of delaying generation and therefore cannot choose when they can trade. The purpose of AEP and accurate predictions is that the project developer can build a case and use it to borrow as the project guarantees income over the project lifetime. To guarantee debt finance the lender will need to have confidence in the prediction and be guaranteed the value (£/MWh) of the energy to be produced. Therefore, to minimise project risk, the project developer is much more likely to enter into a (flexible) power purchase agreement (PPA) for selling electricity simply because it guarantees a certain payment.

The added advantage that tidal is predictable up to a high level of accuracy significantly reduces the risk and can attract higher payment (Robertson, 2011). In reality

tidal power output will rarely be traded by itself and, if this is the case, then it will be small scale. Most tidal farms will form a part of a portfolio and the power output will be aggregated. If hydro (with pump storage) or open cycle gas turbine (OCGT) form part of this portfolio, they could compliment tidal generation such that the aggregate power output presents a base-load like characteristic. This aggregate power can then be traded under a PPA. It can also be argued that tidal, with some form of storage or complement generation, will have 100% capacity credit as suggested by Barbour *et al.*, (2011)

To make the most of the incentives (ROCs, EU ETS) tidal power output should not be curtailed (unless it is a network constraint), particularly since it is predictable with negligible operational costs. Instead, other forms of variable generations (including other renewables) should be used to complement tidal generation so as to reduce the overall variability of the aggregate output and reduce the overall change observed by the system at the GSP.

7.5 Conclusion

This chapter presents an overview of the existing electricity supply system in the context of the challenges that are presented, while considering integrating tidal current generation as part of the electricity network. There are a number of technical, policy, environmental and planning issues that need to be addressed in time, so as not to pose a physical constraint in terms of development. But the main focus of this chapter is to evaluate how the variable power output obtained from tidal current generation may be related to demand variability.

New methodologies are presented that analyse and compare the hypothetical power output generated from tidal current and how well it matched with demand for electricity. It is shown that tidal can make a meaningful contribution towards meeting energy needs. With a 5.4 GW installed capacity, 14.25 TWh/yr can be generated from the scenario presented. Although this only meets 4% of our current energy demand, it can make a 12.6% contribution towards the renewables target set by the UK government.

Demand is inherently variable and the inclusion of tidal in the system increases the number of extreme short-term changes in net demand but they do not appear to be severe and seem manageable as suggested by National Grid (2010). In order to fully comprehend the additional variability, a portfolio analysis needs to be done, not necessarily on a national scale but on a more regional level accounting for network constraints. It is suggested that in a portfolio scenario, when power is aggregated from tidal current and a number of other generators, the variability of the output can be smoothed by operating the other generators to compliment tidal power output.

System risk and adequacy with higher levels of penetration can cause concern over security of supply. Ultimately the aim is to 'keep the lights on', even at times of peak demand. Analysis suggests that, for the year of 2009, because of the timing of peak demand and the variation of tidal cycle, only 0.5 GW was contributed towards peak demand. However, within the winter season, when peak demand is likely to occur, tidal does make contribution to hours up to peak demand, see Figure 7.22.

Further statistical analysis of the semidiurnal pattern is required to fully understand the role this will play in contributing to demand. However, tidal is truly predictable and deterministic, which is a significant advantage over wind and wave as they are stochastic in nature. Due to this predictability, tidal is better suited to trade under a long term PPA or potentially venture into the spot market when combined with some form of storage.

8. Conclusions

In a recent consultation document by DECC (2011b) on reassessing the Renewables Obligation Banding Review, the following was said about support for tidal:

> "It should also be noted that there are potential beneficial balancing cost implications to consumers from a significant contribution from marine energy within a high renewables generation mix. This is particularly true for tidal stream because tidal is predictable, and with phasing of generation around the coast it can contribute towards baseload generation. Wave although intermittent is predictable over much longer timescales than wind." (DECC, 2011b)

The UK government is making incorrect assumptions about tidal current energy in the UK and its potential to generate base load. Although the technology itself could be used to provide base load generation, the resource potential in the UK waters indicates that majority of the sites are in phase and generating a significant continuous output from a combination of sites is unlikely. The government continues to make incorrect policy decisions based on inappropriate understanding of the tidal resource and the marine sector to a larger extent. There is a great concern that these false expectations could taint public perception of tidal energy and renewable energy in general. This particular misunderstanding highlights the pressing need for understanding the extent of contribution tidal can realistically make and portray it in way that will manage public expectations.

It was the aim of the work presented in this thesis to provide a better understanding of tidal current energy and the role it can play in meeting future energy needs.

8.1 Thesis Summary

The main research questions at the start of this PhD were:

1. What is the spatial and temporal variability for the UK tidal resource?
2. Can aggregate output from a number of sites around the UK waters provide base-load?
3. How does tidal variability compare with demand for electricity?

The focus of this thesis has been developing methodologies for tidal current resource assessment; firstly on a site specific level and then expanding this understanding to a national scale. The thesis begins with a re-appraisal of the UK tidal resource using a combination of datasets, the majority of which are publically available. It is thought that this new re-appraisal is an improvement over the existing methodologies and provides a better spatial and temporal coverage. This final chapter summarises the key findings and their implications. The limits of the study are also discussed and potential plans for further work are presented.

8.1.1 Analysis of Datasets

New methodologies were presented to combine different datasets that has enabled a better analysis and comparison of the local resource, spatially and temporally. The BERR Marine Atlas and its spatial snapshots of the tidal current velocity for the UK continental shelf was used to assess the spatial variability of the tidal resource. This dataset, however, lacked temporal resolution. Therefore, time-series of tidal current velocity variability were obtained by using TotalTide tidal diamonds, buoy data or high resolution ADCP data where available. With additional processing, these datasets were combined to gain considerable improvement in assessing the UK tidal energy resource over existing analyses that have generally neglected the temporal variability.

Inverse distance weighted interpolation was applied to tidal diamonds to create time-series for specific locations of interest. Statistical analysis shows that, although the data captures the tidal phasing, the interpolation technique tends to miss the peak velocity magnitudes. However, the average values obtained from the Marine Atlas can be used to scale the velocity magnitudes to better represent the tidal variations. Given the lack of in-situ measurements, this method of generating datasets has been beneficial, as the method can be reproduced for any location that has nearby tidal diamonds and is covered by the Marine

Atlas. The combination of the two datasets generates a better set of data that has improved temporal variability and also provides a wider spatial coverage.

8.1.2 Velocity Profile

It is understood that tidal current vertical velocity profiles generally follow a power law through the water column. It is necessary to understand this profile so that an appropriate hub height can be determined and to assess the impact of velocity shear. Previously, generic 1/7th or 1/10th power law profiles have been pre-supposed to define the water column. Analysis presented using buoy data for Anglesey and ADCP data obtained at the Sound of Islay and EMEC's Fall of Warness site demonstrates that the velocity profile through the water column can vary significantly from one location to another. In fact, at sites where multiple ADCP deployments were available, it was identified that even within close proximity the profiles varied significantly.

Analysis also indicates that the characteristic power law profile fit varies between the ebb and flood cycle and, therefore, would benefit from device power curves tuned to operate in the individual flow conditions. Based on the strength and directional alignment of the flow conditions, one of the cycles may be stronger than the other producing asymmetrical power output. Another use of the vertical velocity profile data was to identify the variation in the flow velocity across the device rotor.

Often measurements are only obtained near the surface or near the seabed and a generic power law profile is assumed for the hub height. This analysis highlights that such assumptions could significantly over-or under-estimate the power output and the necessary design considerations for the device to withstand such velocity shear.

8.1.3 Site Specific Analysis

For project scale analysis, site specific characterisation is required. In-situ data is necessary to support the detailed design of tidal current energy development, including the array layout

and device specification. ADCP data is the key source of resource data appropriate for such assessment. Although ADCP data interpretation is well establish, application in a tidal energy context has not, until now, been fully developed. An assessment was conducted of existing techniques for quantifying tidal resource characteristics such as principal current direction, mean velocity and vertical velocity profile. Additional metrics relevant in a tidal energy context were further developed, such as power output, eddy intensity, annual energy production, flood/ebb asymmetry and vertical shear.

Where necessary, new methodologies were developed to fill knowledge gaps. Specifically, data processing before calculating the metrics. A standard methodology for obtaining all these metrics has been developed and presented so that similar analysis can be conducted for other sites of interest and a like-to-like comparison can be conducted to assess which site is, for example, more energetic or better suited to a particular device.

8.1.4 Harmonic Analysis

Harmonic analysis was applied to hindcast and predict datasets over a period spanning the intended lifetime of the tidal energy project, so that long and short term variations of velocity and power generation can be observed and assessed. The temporal resolution and sampling rate of the datasets from the Sound of Islay were also varied to assess the impact on power output and project economics (section 4.4). In addition, the effect of the 18.6 year nodal variability can be seen in the AEP as demonstrated by using the EMEC ADCP dataset to conduct a 25 year long analysis (section 5.4.2).

Additionally, sensitivity and statistical analysis is carried out to evaluate the amount by which the velocity, and therefore the power output, varies with the resolution of the original measured data capturing the tidal current velocities. Another interesting outcome is an apparent diurnal variability that emerges over long term averaging.

All the site specific assessments have helped inform and contribute to the progress and development of the IEC TC 114 Standards which will pave the way for tidal industries around the world.

8.1.5 Scenario Development

GIS techniques were used to interrogate the Marine Atlas data to identify locations that exhibit appropriate depth and velocity characteristics for economically harvesting tidal energy. After suitable locations were identified, scenarios were developed to explore the distribution and yield from potential large scale tidal farm developments. To populate these scenarios, a new way of evaluating the rated velocity is introduced that considers capacity factor as an economic indicator as well as sensible device design considerations. This new rated velocity is assessed by evaluating the velocity exceedance curve for each of the time-series considered, where the 10% velocity exceedance value is assigned as the rated velocity. This is found to ensure the matching of resource and device characteristics produces a credible target capacity factor of around 30% (which is comparable to present wind capacity factors). The methodology presented can also be used to select a higher capacity factor by targeting a different exceedance value, presenting a streamlined process of selecting the rated velocity.

It is also understood that increasing energy extraction can have unacceptable effects on the physical local environment and underlying tidal resource characteristics. This feeds back into reducing the overall energy available for extraction and hence the economic viability of that particular scenario, see section 6.3.3. Therefore, a ‘Technically Acceptable’ power limitation is imposed to balance development scale against environmental and economic disincentives.

A key outcome of this analysis has been to counter previous studies that have suggested a combined portfolio of sites around the UK can deliver firm power. The scenarios developed within the thesis demonstrate that the nature of tidal wave propagation around the

UK coast indicates that the high energy sites considered are largely in-phase and that tidal current cannot be seen as offering significant base load generation potential in the UK. However, the research has identified that the first generation scenario for tidal current energy can play a significant role in meeting future energy needs and contribute to meeting 4% of present UK demand. More importantly, it can contribute 12.6% towards meeting the UK Governments 2020 renewable energy targets.

8.2 Contribution

In terms of contribution to knowledge, the study develops a methodology that uses publically available datasets that ultimately provides better spatial coverage and improved temporal resolution. One of the most significant findings has been the statistical analysis of future tidal energy generation potential. This analysis demonstrated that the UK tidal current energy resource is much more in phase than has previously been understood. As there is negligible firm production and base-load contribution compared to the total installed capacity.

Analysis from the data for 2009 indicates that at peak electricity demand levels, a reduction in the capacity factor is observed (see Figure 7.26), and, in this scenario, it is identified that tidal energy does not provide a significant contribution to peak demand (see Figure 7.21). However, the predictability of the resources is a huge advantage, in terms of scheduling alternate generation to accommodate tidal production as part of a future energy portfolio mix.

8.2.1 Immediate Impact

Part of the PhD process requires actively disseminating the findings of the research in the form of posters, publication and presentations. A reprint of all the publications is provided in Appendix B. As a result, the study has benefitted from a number of collaborations and has also had an immediate impact on other industry studies, analysis and Standards documentation that overlapped or developed in parallel with the PhD as summarised:

1. Following the initial interaction with SPR to obtain the ADCP data for the Sound of Islay, a report was produced identifying the key site characteristics and provided relevant advice for their in-house technical team. (The contents of this report forms part of chapter 4). Further interactions involving the development of the project which is the world's first fully consented tidal array project, included providing ad-hoc advice on various occasions. This has led to discussions of another project where SPR is interested in conducting a study specific to Islay to evaluate the combined power output of the 10 MW tidal farm aggregated with the onshore wind farm at Beinn an Turic with an overall installed capacity of 30 MW and the 2 MW Inver Hydro project on the local distribution network. The project will aim to investigate the potential combinations and scenarios of firm generation from the aggregated power output.
2. The resource assessment requirements under the IEC TC 114 62600-1-3 Resource Characterisation and Assessment Standards are at the time of writing still a working document. The site characterisation assessment presented as part of this PhD is an example of 'learning-by-doing' which has scoped all the existing literature that outline the best practice in this field. The analysis has also identified and tailored practices that are suitable for site specific assessment and attempted to fill some of the existing knowledge gaps. This has provided the Standards committee a better understanding, particularly about the ADCP data resolution, the effect of harmonic analysis on the dataset, variations in the vertical velocity profile and provided some understanding of the long-term variations that can be expected over the intended project lifetime. These findings have informed the evolving standards documentation.
3. The EMEC site characterisation, datasets and analysis for Fall of Warness has been used by Marina Platform (2011a) as part of their Work Package 2 to identify suitable site for deploying combined wind and tidal devices, entitled 'Site Assessment –

Review of existing test sites' (Marina Platform, 2011b). The contribution has mainly been in the form of providing hypothetical power outputs of potential tidal devices, highlighting site specific characteristics relevant for the study and identifying the semidiurnal pattern of the tidal power output that will be relevant when combining with wind power output.

8.3 Future Work and Improvements

This section discusses some of the unavoidable real-world and operational limitations of the research presented in this thesis and presents suggestions for future work. The majority of the limitations presented highlight the need for improved input data, but also presented are restrictions of the methodology used. Enhancing the work presented in this thesis, by further application of some or all of these suggested measures would make an extremely valuable contribution in understanding the role and benefit tidal current energy generation will make in the UK marine energy industry and electricity mix.

8.3.1 Data Resolution and Updated Input Data

The majority of the analysis presented in this thesis relies on the BERR Marine Atlas and TotalTide tidal diamonds. Although the Marine Atlas covers a wide area and the GIS friendly layers provide valuable information in terms of enabling interrogation of the data and applying depth and velocity constraints, the low resolution of the Atlas has been a limitation as narrow channels and smaller sites like Strangford Lough could not be included as part of the study.

Tidal diamonds are extrapolations of measurements taken over a thirteen hour period and capture approximately two of the tidal harmonic constituents. The measurements are also taken mostly for navigation purposes and are near the surface. Therefore these measurements are not taken at the most energetic locations, nor do they provide further information about the characteristics of the vertical velocity profile.

An updated version of the BERR Marine Atlas has been made available since June 2011 that includes smaller sites like Kyle Rhea. A re-analysis of the resource to include some of the smaller sites that were omitted at lower resolution would be highly beneficial. In terms of site specific analysis, each of the sites considered in this study would benefit from detailed data that provides improved spatial and temporal coverage. If possible, ADCP data should be collected for one month at each of the sites for better sites characterisation and to enable harmonic analysis. With better understanding of second and third generation devices, the methodology should also be extended to other sites to be considered as future scenario developments or to expand the first generation sites.

8.3.2 Lack of Model Data and Site Specific Measurements

Time-series data from an appropriate numerical tidal hydrodynamic model was not available for the purpose of this study (although average snap shots were made available from the Marine Atlas that is derived from the POL numerical model). The possibility of developing a model for such a large spatial coverage was beyond the scope of the study. The need for a high resolution model on a national scale for this purpose has been identified and is currently being addressed by an Energy Technology Institute (ETI) project that aims to bridge this gap and make model datasets available for such analysis. Further details about the proposed model development can be found at ETI (2011).

Where possible site specific measurements were obtained and used to improve the quality of the input data. ADCP data was purchased from EMEC for the Fall of Warness and Scottish Power Renewables kindly provided ADCP data for their demonstration site at the Sound of Islay. Buoy data was obtained for Anglesey from BODC datasets. Extensive analysis of the existing BODC datasets identifies a lack of historic oceanographic data in locations of interest for the development of tidal energy projects. The methods used for the majority of sites use a combination of tidal diamonds and Marine Atlas, which is an

improvement over the existing datasets but the analysis would significantly benefit from better site specific ADCP data to truly capture the spatial and temporal variability.

8.3.3 Resource Reduction Feedback

Although a technically acceptable limitation is imposed as to how much power can be extracted from each of the sites considered, the limitation assumes a 10% reduction in velocity. This is the extent to which reduction in velocity and therefore power is considered acceptable before the energy extraction can significantly impact the physical environment. Therefore, the power outputs should be recalculated accounting for the velocity reduction as expected from the scenario development throughout the intended time-period to truly account for the reduction in velocity as the devices are deployed. Not all the sites will experience a 10% reduction, therefore to fully understand the feedback effect each sites will have to be modelled individually.

8.3.4 Longer Time-period

The analysis and scenario development was initially done for a month long duration. However, after developing the methodologies, it became evident that the analysis would benefit from expanding to a longer time-period. Harmonic analysis was applied to measured data and the recreated without much difficulty. However, TotalTide tidal diamonds were rather limiting. Because of the commercial nature of the software, only one week could be extracted at a specific moment. Therefore, extracting data for the whole year from all the tidal diamonds of interest was monotonous and time consuming. Better methods of interrogating the software would be invaluable.

In terms of scenario development, the period of the analysis does not significantly affect the study. However, for demand and generation matching, the study could benefit from expanding over at least a few years of differing demand regimes so that the analysis

can capture demand trends varying over years as influenced by seasonal changes and the economy.

8.3.5 Operational Oceanography and Forecasting

Operational oceanography uses atmospheric measurements and wind/wave measured data to run numerical models that can provide accurate nowcasts and forecasts. In addition to harmonic analysis that can predict tidal variability, operational oceanography can be used to account for the non-tidal meteorological events that will affect the tidal variability. These analysis techniques will be particularly useful when tidal current energy reaches a commercial scale and can be used by system operators to accurately determine how much tidal will be able to contribute to the system as well as give the project developers accurately AEP assessment, that could influence the project economics. Simultaneously, such forecasting will also be relevant for monitoring offshore deployment and maintenance weather windows. However, as the tidal energy industry is as yet immature and future large-scale development prospects remain uncertain, application of operational oceanography and forecasting is beyond the current needs of the sector.

8.3.6 Additional Constraints

Although an economic constraint is included by selection of specific depths and Spring peak velocity exceeding 2.5 m/s, this is predominantly a characteristic of site selection. However, the analysis could benefit from additional financial constraints and cost models that help better differentiate and reflect the true cost of developing each site. These constraints can take the form of costs associated with water depth and factors that are dependant on how far a specific site is from shore or the nearest appropriate grid connection point. Other constraints can take the form of marine spatial planning and include aspects of other competitive marine users over a common site of interest.

8.3.7 Use of Network Model

The time-series generated from the scenario development could be used in an electrical network model to evaluate how the network power flows will be affected. The majority of the sites are small enough to connect to the local distribution network, therefore a site-by-site analysis will be necessary and will be very relevant. A water-to-wire model that investigates interactions between the devices in an array, power-take-off, generation and control would also be highly desirable.

8.4 Concluding Remark

The work presented here identifies that tidal current energy can make a meaningful contribution to meeting the UK Governments renewable energy targets. However, integration of this new energy generation technology will require detailed planning and a thorough understanding of the resource and its variability, as the identified sites and power generation scenarios indicate no potential for base load generation.

Reference

Atlantis Resource Corporation, (2010) Atlantis Unveils the World's Largest Tidal Turbine, The AK1000 (Accessed on 01/09/11) http://www.atlantisresourcescorporation.com/media/press-release/23-press/105-atlantis-unveils-the-worlds-largest-tidal-turbine-the-ak1000.html

Atlantis Resource Corporation, (2011) Atlantis Technology (Accessed on 01/09/11) http://www.atlantisresourcescorporation.com/marine-power/atlantis-technologies/ar-series.html

Atlantis Resource Corporation, (2011a). Update on Atlantis Resource Corporation's AK1000 test turbine. (Accessed on 01/09/11) http://www.atlantisresourcescorporation.com/media/press-release/23-press/129-update-on-atlantis-resources-corporations-ak1000-test-turbine-march-10th-2011.html

Atlantis Resource Corporation, (2011b). Projects. (Accessed on 01/09/11) http://www.atlantisresourcescorporation.com/projects.html

ARC…see Atlantis Resource Corporation.

Barbour, E & Bryden, I. G. (2011) Energy storage in association with tidal currenr generation systems. *Proceedings of the Institution of Mechanical Engineers, Part A: Journal of Power and Energ, 225, 443-455.*

BBC News 2010, Gulf of Mexico Oil leaks 'worst US environmental disaster'. (Accessed on 01/09/11) http://www.bbc.co.uk/news/10194335

BBC News 2011, Japan 'unprepared' for Fukushima nuclear disaster. (Accessed on 01/09/11) http://www.bbc.co.uk/news/world-asia-pacific-13678627

Bell, C. & Carlin, L. (1998) Generation of UK Tidal Stream Atlases from Regularly Gridded Hydrodynamic Modelled Data. *The Journal of Navigation,* 51**,** 73-78.

BERR … see Department for Business Enterprise and Regulatory Reform.

Black & Veatch (2004) Phase I. UK Tidal Stream Energy Resource Assessment. The Carbon Trust, London.

Black & Veatch (2005) Phase II. UK Tidal Stream Energy Resource Assessment. The Carbon Trust, London.

Black & Veatch (2011), UK Tidal Current Resource and Economics, The Carbon Trust, London.

B&V... see Black & Veatch

British Oceanographic Data Centre UK Moored Current Meter Data Set. (2006). DVD Electronic Publication. http://www.bodc.ac.uk/

BODC … see British Oceanographic Data Centre

Boon, J. D. (2004) *Secrets of the Tide*. Tide and Tidal Current Analysis and Applications, Storm Surges and Sea Level Trends.

Boehme, T., Taylor, J., Wallace, A. R. & Bialek, J. (2006) Matching Renewable Electricity Generation with Demand. The Scottish Executive.

Boehme, T. (2006a) Matching Renewable Electricity Generation with Demand in Scotland (PhD Thesis). *Institute for Energy Systems.* Edinburgh, University of Edinburgh.

Brière,C., Abadie, S., Bretel, P., and Lang, P., (2006) Assessment of TELEMAC system performance, a hydrodynamic case study of Anglet, France.

British Wind Energy Association, (2005) Blowing Away the Myths. A critique of the Renewable Energy Foundation's report: *Reduction in carbon dioxide emissions: estimating the potential contributions from wind power.*

Bryans, G. A., (2006) Impacts of Tidal Stream Devices on Electrical Power Systems. (PhD Thesis). *School of Electronics, Electrical Engineering and Computer Science.* The Queen's University Belfast.

BWEA...see British Wind Energy Association

Carbon Trust, (2004) Annual report (Accessed on 27/09/11) http://www.carbontrust.co.uk/SiteCollectionDocuments/PDF/CTC508.pdf

CEC… see Commission of the European Communities

Clarke, J. A., Connor, G., Grant, A. D. & Johnstone, C. M. (2006) Regulating the output characteristics of tidal current power stations to facilitate better base load matching over the lunar cycle. *Renewable Energy*, 31**,** 173-180.

Commission of the European Communities (CEC) (2008) 20 20 by 2020. Europe's Climate Change Opportunity. Communication from the Commission to the European Parliament, The Council, The European Economic and Social Committee and the Committee of the regions.

Cooper, W. S., Hinton, C. L., Ashton, N., Saulter, A., Morgan, C., Proctor, R., Bell, C. & Huggett, Q. (2006) An introduction to the UK marine renewable atlas. *Proceedings of the ICE - Maritime Engineering, Volume 159, Issue 1, pages 1 –7.*

Cornett, A., (2008) Guidance for Assessing Tidal Current Energy Resources, Report by NRC-CHC for the OES IA Annex II Task 1.2 Generic and site related tidal data.

Couch, S. J., and Bryden, I. G., (2006) Tidal current resource assessment. *Proceedings of the IMechE, Part A: Journal of Power and Energy*, 221, pp.125-135.

Cradden, L., Mouslim, H., Duperray, O. & Ingram, D., (2011) Joint Exploitation of Wave and Offshore Wind Power. Proceedings Ninth European Wave and Tidal Energy Conference *(EWTEC).* Southampton, UK.

Crown Estate (2010a), Press Release: World's First Wave and Tidal Energy Leasing Round to Power up to Three Quarters of a Million Homes. (Accessed on 16/05/10) http://www.thecrownestate.co.uk/newscontent/92-pentland-firth-developers.htm

Crown Estate (2010b), Press release: Inner Sound Tidal Project Awarded, Crown Estate, London. (Accessed on 27/10/10) http://www.thecrownestate.co.uk/newscontent/92-inner-sound-tidal-project-awarded.htm

CT... see Carbon Trust

Culina, J., Karsten, R., & Walter, R. (2011) Comparison of Different Resolution Models and Observed Current Profiles in the Bay of Fundy, Canada using Turbine-Relevant Metrics. Proceedings Nineth European Wave and Tidal Energy Conference *(EWTEC).* Southampton, UK.

Dent, C.J., Keane, A., and Bialek, J.W., (2010) Simplified Methods for Renewable Generation Capacity Credit Calculation: A Critical Review, IEEE PES GM.

Department for Business, Enterpriser and Regulatory Reform. (2008). Atlas of UK Marine Renewable Energy Resource. http://www.renewables-atlas.info/

Department for Business, Enterpriser and Regulatory Reform. (2008). Reform of the Renewables Obligation. Statutory Consultation on the Renewables Obligation Order 2009. http://webarchive.nationalarchives.gov.uk/+/http://www.berr.gov.uk/files/file46838.pdf

Department of Energy (1990), Offshore Installations: Guidance on Design and Construction, 4th edition, HMSO London

Department of Energy and Climate Change, (2009) The UK Low Carbon Transitions Plan: National strategy for climate and energy. http://centralcontent.fco.gov.uk/central-content/campaigns/act-on-copenhagen/resources/en/pdf/DECC-Low-Carbon-Transition-Plan

Department of Energy and Climate Change, (2011a) Planning our electricity future: a White Paper for secure, affordable and low-carbon electricity. (Accessed on 16/10/11) http://www.decc.gov.uk/en/content/cms/legislation/white_papers/emr_wp_2011/emr_wp_2011.aspx

Department of Energy and Climate Change, (2011b) Consultation on proposals for the levels of banded support under the Renewables Obligation for the period 2013-17 and the Renewables Obligation Order 2012. http://www.decc.gov.uk/assets/decc/11/consultation/ro-banding/3235-consultation-ro-banding.pdf

Digest of United Kingdom Energy Statistics, 2005. Department of Energy and Climate Change (2005).

Digest of United Kingdom Energy Statistics, 2010. Department of Energy and Climate Change (2010).

Department of Trade and Industry, (2004a) Atlas of UK Marine Renewable Energy Resource: Atlas. ABP Marine Environmental Research Ltd., Southampton

Department of Trade and Industry, (2004b) Atlas of UK Marine Renewable Energy Resource. Technical Report. A Strategic Environmental Assessment Report. ABP Marine Environmental Research Ltd., Southampton

Department of Trade and Industry, (2005) Thake, J. Development Installation and Testing of a Large Scale Tidal Current Turbine.

Department of Trade and Industry, (2007). Couch, S. J. & Jeffrey, H. Preliminary Tidal Current Energy Device Performance Protocol

DECC… see Department of Energy and Climate Change

DTI… see Department of Trade and Industry

DUKES… see Digest of United Kingdom Energy Statistics

Electrical Network Strategy Group, (2009) 'Our Electricity Transmission Network: A vision for 2020'

Electric Power Research Institute Inc., (2006) HAGERMAN, G., POLAGYE, B.: Methodology for Estimating Tidal Current Energy Resource and Power Production by Tidal In-Stream Energy Conversion (TISEC) Devices.

EMEC, The European Marine Energy Centre Ltd. http://www.emec.org.uk/index.asp.

EMEC (2009a) LEGRAND, C. Assessment of Tidal Energy Resource. Marine Renewable Energy Guides.

EMEC (2009b) SWIFT, R. Assessment of Performance of Tidal Energy Conversion Systems

EMEC (2009c) CROLL, P. & ANDINA-PENDAS, I. Guidelines for Project Development in the Marine Energy Industry.

Energy Technology Institute (2011) UK's Tidal Energy Resource To Be Modelled by the ETI (Accessed on 22/11/11) http://www.energytechnologies.co.uk/Home/news/11-10-18/UK%E2%80%99s_Tidal_Energy_Resources_To_Be_Modelled_by_the_ETI.aspx

ENSG…see Electrical Network Strategy Group

EPRI... see Electric Power Research Institute

Equimar (2011) Ingram, D.M., Smith, G. H., Ferriera, C. B. & Smith, H. Protocols for the Equitable Assessment of Marine Energy Converters.

ETI...see Energy Technology Institute

EU Emissions Trading Scheme. Cutting Carbon in Europe: The 2020 plans and the future of the EUETS. 2008 (Accessed on 16/10/11) http://www.carbontrust.co.uk/Publications/pages/PublicationDetail.aspx?id=CTC734

EU ETS... see EU Emissions Trading Scheme

Falconer, R.A. & Ismail, A.I.B.M. (1997) Numerical modelling of tracer transport in a contact tank. Environment International, 23, 763-773.

Garrad Hassan (2001), Scotland's Renewable Resource 2001:Volume I – The Analysis.

Guardian News 2011, Germany to shut all nuclear reactors. (Accessed on 15/10/11) http://www.guardian.co.uk/world/2011/may/30/germany-to-shut-nuclear-reactors

Gooch, S., Thomson, J., Polagye, B. & Meggitt, D. (2009) Site characterization for tidal power. *OCEANS 2009, MTS/IEEE Biloxi - Marine Technology for Our Future: Global and Local Challenges.*

Hammerfest Strøm (2010), Images (Accessed on 27/05/11) http://www.scottish-enterprise.presscentre.com/Media-library/Hammerfest-Strom-1eb.aspx

Hammerfest Strøm (2010a), Research and development (Accessed on 01/09/11) http://www.hammerfeststrom.com/research-and-development/

Hammerfest Strøm (2010b), Sound of Islay Tidal Power Project (Accessed on 01/09/11) http://www.hammerfeststrom.com/products/tidal-turbines/sound-of-islay-tidal-power-project/

Hardisty, J. (2008) Power intermittency, redundancy and tidal phasing around the United Kingdom. *Geographical Journal*, 174**,** 76-84.

Hawkins, S., Eager, D. & Harrison, G.P. (2011) Characterising the Reliability of Production from Future British Offshore Wind Fleets. Proceedings First IET Renewable Power Generation Conference *(RPG).* Edinburgh, UK

Islay Energy Trust, (2011) Consent Given for Sound of Islay Tidal Energy Project. http://islayenergytrust.wordpress.com/2011/03/17/consent-given-for-sound-of-islay-tidal-energy-project/

Iyer, A.S., Couch, S.J., Harrison, G.P. & Wallace, A.R. (2009a) Analysis and comparison of Tidal Datasets. Proceedings Eighth European Wave and Tidal Energy Conference (*EWTEC*). Uppsala, Sweden.

Iyer, A.S., Couch, S.J., Harrison, G.P. & Wallace, A.R. (2009b). Analysis and comparison of Tidal Datasets for Resource Assessment and Network Modelling. Forty Fourth International Universities' Power Energy Conference (*UPEC*). Glasgow, Scotland.

Iyer, A.S., Couch, S.J., Harrison, G.P. & Wallace, A.R. (2010). Developing Methodologies for Quantifying the Impact of Tidal Current energy Variability. Third International Conference on Ocean Energy (ICOE). Bilbao, Spain.

Iyer, A.S., Couch, S.J., Harrison, G.P. & Wallace, A.R. (2011a) Phasing of tidal current energy around the UK and potential contribution to electricity generation. Proceedings Ninth European Wave and Tidal Energy Conference *(EWTEC)*. Southampton, UK.

Iyer, A.S., Couch, S.J., Harrison, G.P. & Wallace, A.R. (2011b). Variability and phasing of tidal current energy around United Kingdom. *Renewable Energy* (In Review)

Jeuken, M.C.J.L., Wang, Z.B., Keiller, D., Townend, I. & Like, G.A., (2003) Morphological response of estuaries to nodal tide variation. *International Conference on Estuaries and Coasts*. November, 11-19. China

Kean, A., Milligan, M., Dent, C.J., Hasche, B., Annunzio, C.D', Dragoon, K., Holttinen, H., Samaan, N., Soder, L., O'Malley, M., (2011) Capacity value of wind power, IEEE Transactions on Power Systems, vol. 26, May. 2011.

Lu, Y. & Lueck, R. G. (1999) Using a Broadband ADCP in a Tidal Channel. Part II: Turbulence. *Journal of Atmospheric and Oceanic Technology*, 16**,** 1568-1579.

Mackay. D.J.C (2008a) Sustainable Energy – Without the Hot Air. UTI Cambridge, ISBN 978-0-9544529-3-3. Available online from www.withouthotair.com.

Mackay. D.J.C (2008b) Under-estimation of the UK Tidal Resource. Cavendish Laboratory, University of Cambridge

Marina Platform (2011a), (Accessed on 16/10/11) http://www.marina-platform.info/index.aspx

Marina Platform. Cradden, L., Duperray, O., Mouslim, H. & Iyer, A.I. (2011b), Site Assessment – review of existing test sites. http://www.marina-platform.info/documentation.aspx

Marine Current Turbine Ltd. (1994), Loch Linnhe (Accessed on 18/08/2011) http://www.marineturbines.com/6/background/15/loch_linnhe/

Marine Current Turbine Ltd. (2008), Images (Accessed on 27/05/11) http://www.marineturbines.com/

Marine Current Turbine Ltd. (2008a), Strangford Narrows, N. Ireland. SeaGen Enter Final Stage of commissioning. (Accessed on 18/08/11) http://www.marineturbines.com/3/news/article/14/seagen_enters_final_stage_of_commissioning/

Marine Current Turbine Ltd. (2008b), Delay in commissioning one of SeaGen's rotor. (Accessed on 18/08/2011) http://www.marineturbines.com/3/news/article/11/delay_in_commissioning_one_of_seagen_s_rotors/

Marine Current Turbine Ltd. (2008c), Projects, The Skerries (Accessed on 18/08/2011) http://www.marineturbines.com/18/projects/20/the_skerries/

Marine Current Turbine Ltd. (2010a), Anglesey Tidal Energy Plan Moves Forward. (Accessed on 18/08/2011) http://www.marineturbines.com/3/news/article/37/anglesey_tidal_energy_plan_moves_forward_/

Marine Current Turbine Ltd. (2010b), DNV confirms SeaGen's Powerful Performance. http://www.marineturbines.com/3/news/article/38/dnv_confirms_seagen_s_powerful_performance_/

Martin, A. (2011), Flexitricity Ltd. Personal Communication

MCT… see Marine Current Turbine

MEC… see Marine Energy Challenge

Milborrow, D. (2010) Quantifying the Impacts of Wind Variability. *Proceedings of the Institute of Civil Engineers. Energy 162 Issue EN3.*

Met Office UK. Met office Gust speed record by district. http://www.metoffice.gov.uk/climate/uk/extremes/gust_district.html

Nadeau, M. (2010) Developing International Standards for Marine Energy Converter. *Proceedings of the 3rd International Conference on Ocean Energy (ICOE).* Bilbao.

NASA... see National Aeronautical and Space Administration

National Aeronautical and Space Administration, Mankins, J.C., (1995). Technology Readiness Levels. A white Paper

National Grid Electricity Transmission Plc, (2010) National Electricity Transmission System (NETS) Seven Year Statement, London, http://www.nationalgrid.com/uk/Electricity/SYS/

National Grid Winter Outlook Report, (2008) http://www.nationalgrid.com/NR/rdonlyres/0CA133C5-4BC3-4442-883D-8D298335ACB4/35402/Winter_Outlook_2008_final.pdf

Nautical Almanac, The Macmillan Reeds, (2002). B. D'Oliveira, B. Goulder and E. Lee-Elliott, [ISBN 0 333 781821]

NG … see National Grid

Norris, J. V., Droniou, E., (2007) Update on EMEC activities, resource description, and characterisation of wave-induced velocities in tidal flow. Proceedings Seventh European Wave and Tidal Energy Conference *(EWTEC).* Porto, Portugal.

Office of Gas and Electricity Markets, Press Release: Promoting choice and value for all gas and electricity customers. Press Release, Sustainable Energy Networks: RIIO Demand Innovation and Efficiency.

Ofgem…see Office of Gas and Electricity Markets

OpenHydro (2007), Images (Accessed on 27/05/11)
http://www.openhydro.com/images.html

OpenHydro (2008), OpenHydro Becomes First Tidal Energy Company to Generate Electricity onto the UK National Grid (Accessed on 01/09/11)
http://www.openhydro.com/news/OpenHydroPR-270508.pdf

OpenHydro (2008a), OpenHydro secures substantial shareholding in Alderney Renewable Energy Ltd (Accessed on 01/09/11)
http://www.openhydro.com/news/OpenHydroPR-201108.pdf

OpenHydro (2009), OpenHydro successfully deploys 1MW commercial tidal turbine in the Bay of Fundy (Accessed on 01/09/11)
http://www.openhydro.com/news/OpenHydroPR-171109.pdf

OpenHydro (2010), Open centre turbine technology overview (Accessed on 01//09/11)
http://www.openhydro.com/technology.html

OpenHydro (2010a), OpenHydro tidal turbine recovered – blades missing.
http://www.renewableenergyfocus.com/view/14766/openhydro-tidal-turbine-recovered-blades-missing/

Osalusi, E., (2011) Analysis of Wave and Current Data in a Tidal Energy Test Site (PhD Thesis). *Institute of Petroleum Engineering*. Heriot-Watt University.

Polagye, B., (2009) Hydrodynamic Effects of Kinetic Power Extraction by In-Stream Tidal Turbine (PhD Thesis). *Department of Mechanical engineering.* Washington, University of Washington.

Polagye, B., Kawase, M., Malte, P., (2009) In-stream tidal energy potential of Puget Sound, Washington. Proceedings of the Institution of Mechanical Engineers Part A: Journal of Power and Energy, 223, pp. 571-587

POL … see Proudman Oceanographic Laboratories

Proudman Oceanographic Laboratories. (2011) POL Model Details. Information Sheet;
http://www.pol.ac.uk/appl/downloads/POL_Model_Details-all.pdf

Pugh, D. T. (1996) *Tides, Surges and Mean Sea Level*, John Wiley & Sons.

Radtke, J., Dent, C.J., Couch, S.J., (2011) Capacity Value of Large Tidal Barrages. Power Systems, IEEE Transactions on , vol.26, no.3, pp.1697-1704.

RDI … see R D Instruments

R D Instruments (1996), Acoustic Doppler Current Profiler. Principles of Operation. *A Practical Primer.*

Renewable UK, (2010) Marine Renewable Energy –State of Industry Report.
http://www.bwea.com/pdf/publications/RenewableUK_Wave_tidal_report_%202010.pdf.

RES… see The UK Renewable Energy Strategy

Robertson, I. (2011), Smartestenergy. Personal Communication

Salter, S. (2005) Possible Under-Estimation of the UK Tidal Resource. *DTI Energy Review*

Salter, S. (2009) Correcting the Under-estimate of the Tidal-Stream Resource of the Pentland Firth. *Proceedings Eights European Wave and Tidal Energy Conference.(EWTEC).* Uppsala, Sweden.

Scottish Government, 2008. Renewables Obligation (Scotland) Introduction of Banding Statutory Consultation. http://www.scotland.gov.uk/Resource/Doc/917/0065773.pdf

ScottishPower, SP Manweb (2010) Distribution Long Term Development Statement www.scottishpower.com/uploads/SPM2010LTDS.pdf

ScottishPower Renewables, SPR. (2010) Sound of Islay Demonstration Tidal Array Environmental Statement. Non Technical Summary.

SDC … see Sustainable Development and Commission.

Shaw, T.L., & Watson, M.J. (2003) Flexible power generation from the tides. Proceedings of the IEC – Engineering Sustainability, Volume 156, Issue 2, pages 119- 123.

Shepard, D. (1968) A two-dimensional interpolation function for irregularly-spaced data. *In Proc. ACM National Conference.*

Sinden, G. (2005) Variability of UK Marine Resource. The Carbon Trust.

SP...see Scottish Power

SPR...see Scottish Power Renewables

Sutherland, G., Foreman, M., Garrett, C.,(2007) Tidal current energy assessment for Johnstone Strait, Vancouver Island. Proc. IMechE Part A: Journal of Power and Energy, 221, pp. 147-157.

Sustainable Development Commission (2007a) Tidal Power in the UK. Research Report 1 - UK tidal resource assessment.

Sustainable Development Commission (2007b) Tidal Power in the UK. Research Report 2 – Tidal technologies overview.

Sustainable Development Commission (2007c) Tidal Power in the UK. Research Report 3 – Severn Barrage Proposals.

Sustainable Development Commission (2007d) Tidal Power in the UK. Research Report 4 – Severn Non-Barrage Options.

Sustainable Development Commission (2007e) Tidal Power in the UK. Research Repoert 5 - UK Case Studies.

Sustainable Development Commission (2007f) Turning the Tide, Tidal Power in the UK.

Stiven, T. (2010) Assessing the impact of resolution and sampling rate on tidal energy project economics. (MSc Theise). *Institute for Energy Systems.*University of Edinburgh.

Stiven, T., Couch, S.J. & Iyer, A.S. (2011) Assessing the Impact of ADCP resolution and sampling rate of tidal current energy projects economics. IEEE-OS Oceans'11 Conference. Santander, Spain

TGL… see Tidal Generation Limited

The Scottish Government (2011) Saltire Prize
http://www.scotland.gov.uk/Topics/Business-Industry/Energy/Action/leading/saltire

The UK Renewable Energy Strategy (2009) HM Government, Department of Energy and Climate Change.
http://www.decc.gov.uk/assets/decc/what%20we%20do/uk%20energy%20supply/energy%20mix/renewable%20energy/renewable%20energy%20strategy/1_20090717120647_e_@@_theukrenewableenergystrategy2009.pdf

Tidal Generation Limited (2010), DeepGen Tidal Stream Turbine Brochure (Accessed on 30/08/11)
http://www.tidalgeneration.co.uk/wpcontent/uploads/2010/12/TGL_Brochure.pdf

Tidal Generation Limited (2010a), Tidal Development In Pentland Firth, Set For MeyGen (Accessed on 01/090/11)
http://www.tidalgeneration.co.uk/content/news/

Tocardo BV Tidal Energy (2008), Tidal Energy in the Pentland Firth – Pre-Feasibility Report. (Accessed on 30/08/11)
http://www.tocardo.com/cms/files/PDF-downloads/pre-feasibilityreport.pdf

UKERC... see UK Energy Research Centre

UK Energy Research Centre, (2009). Global Oil Depletion. An assessment of the evidence for a near-term peak in global oil production.

UK Hydrographic Office, Admiralty Charts, UKHO, Taunton, UK,
http://catalogue.ukho.gov.uk/home.asp.

US Department of Energy, (2010) Financial Assistance Funding Opportunity announcement. Marine and Hydrokinetic Technology Readiness Advancement Initiative. Funding Opportunity Announcement Number: DE-FOA-0000293.
http://www.stoel.com/files/FY10_Water_MHK_FOA.pdf

US DoE… see US Department of Energy

Warner, J. C., Geyer, W. R. & Lerczak, J.A. (2005) Numerical modelling of an estuary: A comprehensive skill assessment. *Journal of Geophysical Research,* Vol. 110.

Xero Energy (2009) Scott, N.C., Smeed M.R., M^{C}Laren A.C., Pentland Firth Tidal Energy Project Grid Options Study.

Zervas, C. (1999) NOAA Technical Memorandum NOS CO-OPS 0021. Tidal Current Analysis Procedures and Associated Computer Programs.

Appendix

A.1 Bivariate Histogram

The bivariate histogram presented in Figure A.1 here shows demand from 20.15 MW, 34.1% of the peak demand. The 10 bins are split into 7.32% each to present the detailed variation that is otherwise missed out in Figure 7.24.

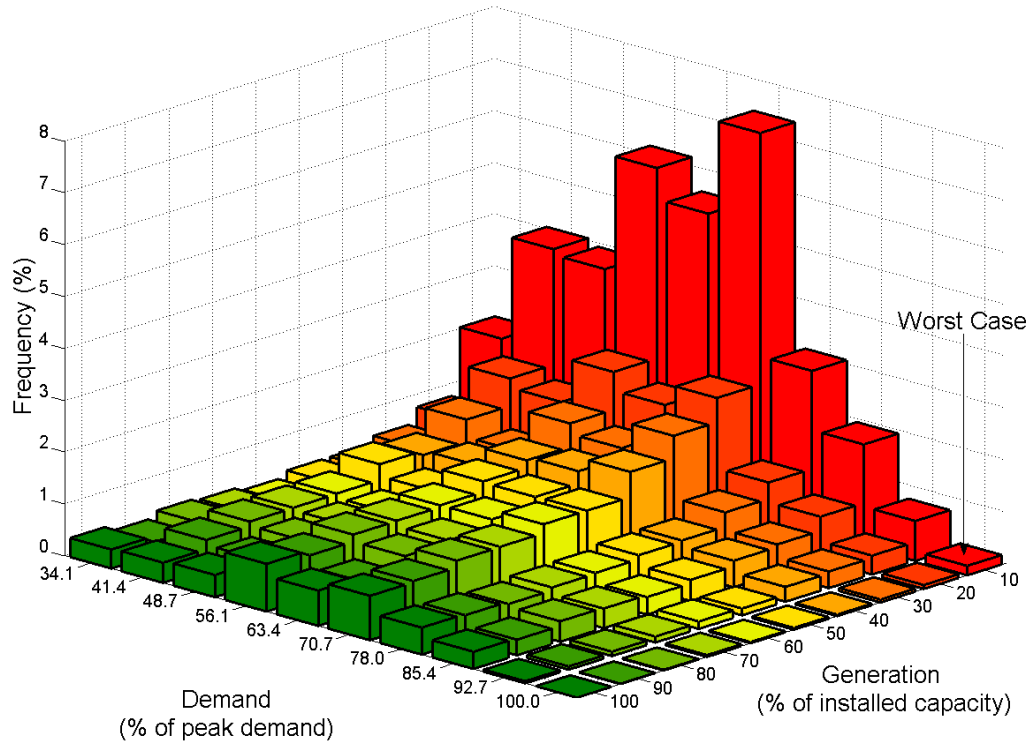

Figure A.0.1 Bivariate histogram presenting demand from 34.1%.

2.08	4.08	3.97	6.19	5.59	7.42	3.11	1.97	0.77	0.18	10
0.8	1.84	1.67	2.52	2.16	2.57	1.22	0.84	0.37	0.07	20
0.5	1.31	0.98	1.79	1.59	2.11	0.91	0.57	0.32	0.06	30
0.36	0.89	0.98	1.34	1.41	1.67	0.63	0.51	0.29	0.03	40
0.36	0.98	0.75	1.2	1.18	1.19	0.61	0.41	0.13	0.03	50
0.25	0.67	0.59	1	1	1.19	0.53	0.34	0.14	0.02	60
0.33	0.66	0.62	0.96	0.86	1.02	0.51	0.38	0.11	0.03	70
0.37	0.66	0.58	0.96	0.82	1.01	0.45	0.39	0.09	0.01	80
0.25	0.57	0.47	0.82	0.59	0.88	0.5	0.3	0.06	0.01	90
0.37	0.39	0.43	0.92	0.68	0.86	0.52	0.33	0.04	0	100
34.1	41.4	48.7	56.1	63.4	70.7	78	85.4	92.7	100	

Generation (% of installed capacity)

Demand (% of peak demand)

Table A.1 Bivariate histogram table.

A.2 Inter-half hourly load change

The inter-half hourly load change presented in Figure A.2 is the same as Figure 7.26. to highlight the excursions occurring at the tail ends, the Y-axis is presented on a log scale.

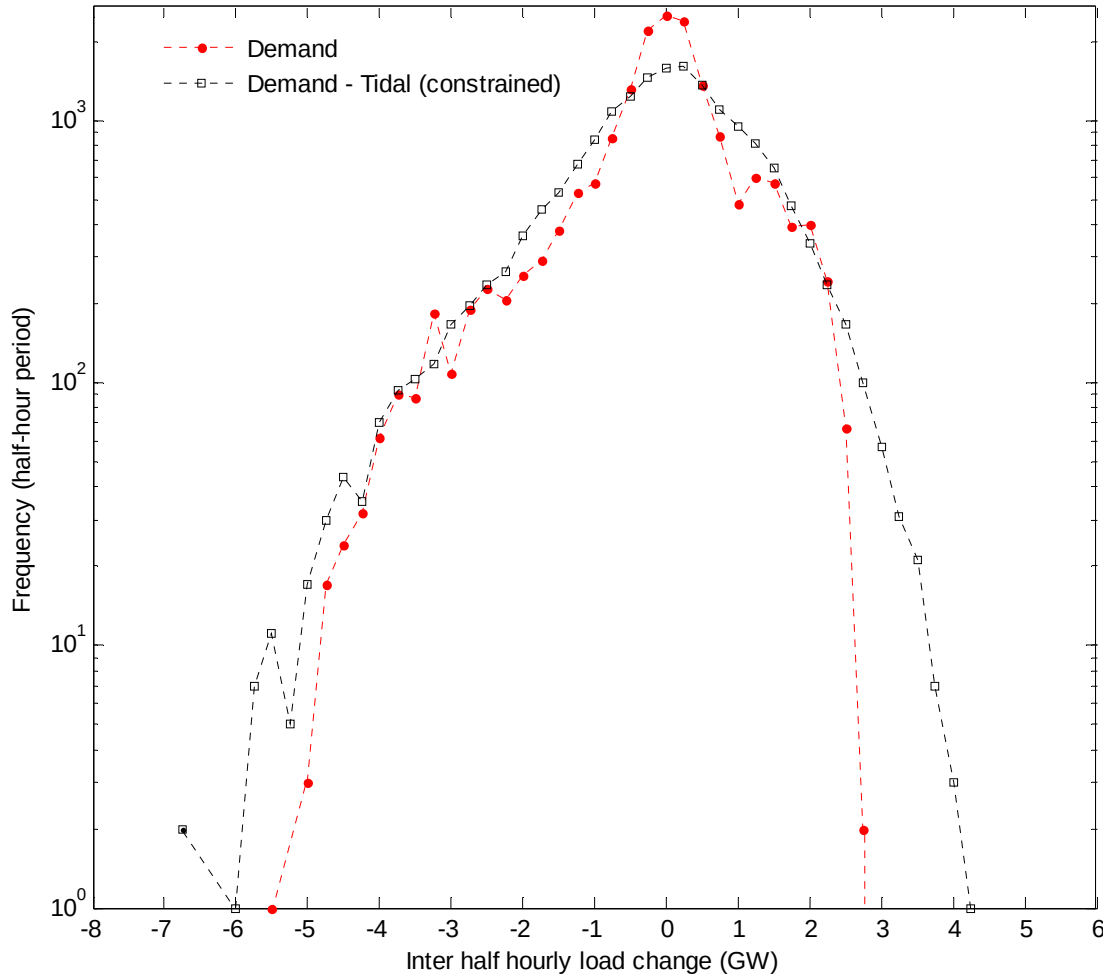

Figure A.0.2 Inter half hourly demand change with and without tidal current in the system. Y-axis is log scale to highlight excursions occurring at the tail end.

B.1 Publications

The following papers are bound into the back of this thesis:

Iyer et al. (2009a): Iyer, A.S., Couch, S.J., Harrison, G.P. & Wallace, A.R. (2009a) Analysis and comparison of Tidal Datasets. Proceedings Eighth European Wave and Tidal Energy Conference (*EWTEC*). Uppsala, Sweden.

Iyer et al. (2009b): Iyer, A.S., Couch, S.J., Harrison, G.P. & Wallace, A.R. (2009b). Analysis and comparison of Tidal Datasets for Resource Assessment and Network Modelling. Forty Fourth International Universities' Power Energy Conference (*UPEC*). Glasgow, Scotland.

Iyer et al. (2010): Iyer, A.S., Couch, S.J., Harrison, G.P. & Wallace, A.R. (2010). Developing Methodologies for Quantifying the Impact of Tidal Current energy Variability. Third International Conference on Ocean Energy (ICOE). Bilbao, Spain.

Stiven et al. (2011): Stiven, T., Couch, S.J. & Iyer, A.S. (2011) Assessing the Impact of ADCP resolution and sampling rate of tidal current energy projects economics. IEEE-OS Oceans'11 Conference. Santander, Spain

Iyer et al. (2011a): Iyer, A.S., Couch, S.J., Harrison, G.P. & Wallace, A.R. (2011a) Phasing of tidal current energy around the UK and potential contribution to electricity generation. Proceedings Ninth European Wave and Tidal Energy Conference *(EWTEC).* Southampton, UK.

Iyer et al. (2011b): Iyer, A.S., Couch, S.J., Harrison, G.P. & Wallace, A.R. (2011b). Variability and phasing of tidal current energy around United Kingdom. *Renewable Energy* (In Review)

Analysis and Comparison of Tidal Datasets

A. Sankaran Iyer, S. J. Couch, G. P. Harrison and A. R. Wallace

University of Edinburgh
Institute for Energy Systems
Kings Buildings
Mayfield Road
Edinburgh EH9 3JL
United Kingdom

E-mails: A.Sankaran-Iyer@ed.ac.uk, Scott.Couch@ed.ac.uk, Gareth.Harrison@ed.ac.uk, Robin.Wallace@ed.ac.uk

Abstract

Tidal resources are highly variable, spatially and temporally. For tidal current energy to be economically exploited, certain conditions need to be fulfilled. Principally the strength of the resource needs to be quantified before it can be effectively utilised. This paper will build on and expand the simplified tidal analysis methods adopted in [1] and other simplified regional and national scale resource assessments. High quality data collection for interesting sites is highly desirable but expensive, difficult to extrapolate over a larger area, and hence unsuitable for national scale resource analysis. Existing publicly available datasets have so far typically been used to examine the resource. A methodology to combine all of the available datasets to produce an improved resource assessment methodology is desirable.

Combining datasets will only be suitable if there is good correlation and consistency between them. The suitability of combining three UK wide datasets will be examined in this analysis. The data sources considered are:

- UK Moored Current Meter Data,
- UK Hydrographic Office publications, and the
- DTI Atlas of UK Marine Renewable Energy Resource.

The datasets do not generally coincide spatially or temporally. Analysis to enable direct comparison of these datasets for a case study region will be presented. This will inform whether the methodology of analysis and combining of datasets has potential for application at larger scales. If with additional processing, datasets can be combined, considerable improvement will potentially be realised in analysing the UK tidal energy resource. Future work is intended to combine outputs from this research with similar datasets for other intermittent renewable resources in order to examine their combined output and their potential integration into the existing electrical network infrastructure.

Keywords: Resource assessment, Tidal analysis, Harmonic tidal analysis, model skill.

Nomenclature

X	= two dimension vector
Y	= two dimension vector
$\overline{X}$	= mean of X
$\overline{Y}$	= mean of Y
Skill	= Model Skill
CC	= Cross Correlation Coefficient
x, y	= Cartesian co-ordinate system
σ	= Standard Deviation
N	= Total number of observations
$v(z)$	= The velocity at some elevation in question z
$v(z_r)$	= The velocity at a unknown elevation z_r
P	= Power
ρ	= Density of sea water (1025 kg/m^3)
v	= Velocity

1 Introduction

The UK has an excellent tidal current energy resource around its coastline. The development of these resources can potentially contribute to meeting future renewable energy requirements. Many studies have tried to quantify this resource with estimates including 18 TWh/yr [2], 13.3 TWh/yr [3], and 96.4 TWh/yr [4] to around 25 TWh/yr for Scotland alone [5]. The spread in the estimates is due to difficulties in evaluating the resource as a result of complex local tidal interaction as well as differences in use of resource information between the various studies. Simplified and often inaccurate assumptions can have a significant impact on the estimate arrived at within each study. With a range of tidal current devices in development, eventual deployment will be enhanced by reliable evidence about the resource, its characteristics, environmental impacts and costs.

© Proceedings of the 8th European Wave and Tidal Energy Conference, Uppsala, Sweden, 2009

The work described here is part of an effort to accurately model the UK tidal resource, both spatially and temporally. This will form part of a larger renewable resource model being developed by the Engineering and Physical Sciences Research Council's Supergen FlexNet consortium [6]. The aim is to develop a robust and repeatable method for generating resource related time series that reliably describes the available resource across the UK.

This paper provides a preliminary analysis and comparison of time series measurements from a case study region in the Irish Sea near the Island of Anglesey off the north Wales coast. The potential suitability of this location for tidal energy development is the reason for selecting this site for analysis. The water depth is about 40 metres and potentially offers a high tidal energy site, close to shore, conditions which suits first generation devices. Good landfall (beach, not cliffs) for bringing cables ashore, appropriate local harbour facilities for installation, operation and management activities are also important project development constraints potentially addressed at this location.

The datasets include current measurements from several buoys that were moored temporarily over relatively short periods but covering several spring-neap cycle tidal variations. The study is also re-evaluating the methodology used by Boehme *et al*. [1] to estimate the potential of the tidal resource in Scotland; the study used point source data from tidal diamonds obtained from Admiralty charts, to generate spatially consistent resource maps by means of Inverse Distance Weighting interpolation (IDW) [7]. The fidelity of this methodology will be considered.

The paper is structured as follows. Section 2 looks at the datasets available in the study area and explains the approach used. Details of the methodology used and the numerical experiments conducted are presented in section 3, discussion of the results obtained from the statistical analysis are also discussed here. Details of the comparison between the buoys, tidal diamonds and the effect of interpolation are also looked at followed by a summary and discussion in section 4.

2 Approach

Ongoing work at the University of Edinburgh is examining different datasets available for tidal resource assessment in UK. These include the UK moored current meter dataset made available through the British Oceanographic Data Centre (BODC), a national facility that archives marine data. One of the datasets available for academic purposes provides time series measurements of ocean currents from temporarily moored instruments deployed in the shelf seas around the British Isles [8, 9].

The second data source examined here is analysis of Admiralty chart data and tidal stream atlases. These provide a series of descriptions of tidal current flows in terms of velocity magnitude and direction at hourly time intervals with respect to high water at a reference location. The data spans from 6 hours before high water through to 6 hours after high water for typical spring and neap tide conditions. The locations of these data are referred to as 'tidal diamonds', as their respective positions are indicated on Admiralty charts by diamond symbols. The UK Hydrographic Office (UKHO) TotalTide software package [10] contains fundamentally the same information as the Admiralty charts but provides a means of interrogating the tidal current data through time at the tidal diamond locations. The tidal current data in TotalTide would appear to only encapsulate variability of the available data prescribed by the two generally dominant tidal harmonic constituents, M_2 and S_2 [11].

The DTI Atlas of UK Marine Renewable Energy Resources also provides useful spatial information for offshore marine renewable technologies [12]. The information provided in the atlas is managed and maintained in a structured Geographic Information System (GIS) database and is available online [13].

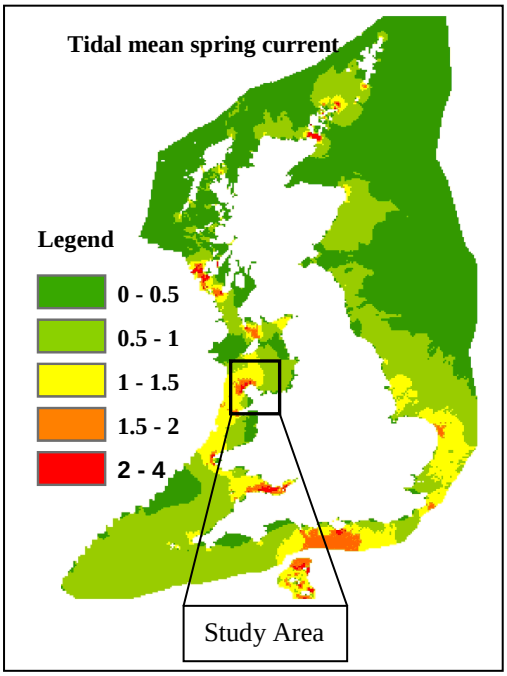

Figure 1: Figure showing mean spring peak current.
© Crown Copyright. All rights reserved 2008.

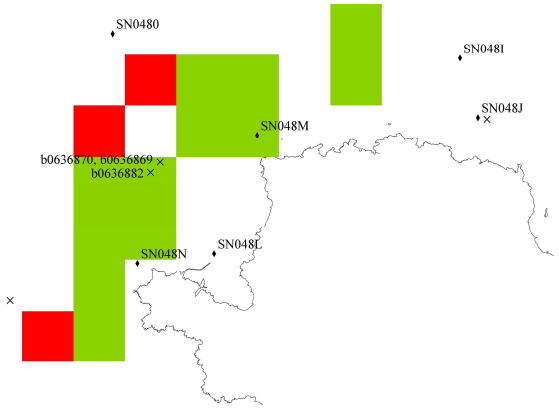

Figure 2. Location of tidal diamonds, mooring buoys and DTI Atlas identified tidal energy potential locations.

Figure 1 is an extract from the DTI Atlas showing the site of interest. The tidal current data presented in the DTI Atlas presents spatially averaged snapshots of mean spring and neap tides. It is based on data from continental shelf models developed by the Proudman Oceanographic Laboratory (POL). Times series data from the POL modelling effort have not been available for use in this analysis, only the output presented in the DTI Atlas is considered.

Figure 2 shows the location of the three buoy moorings and the eight tidal diamonds considered in this case study. The green (depth <40 metres) and red squares (depth > 40 metres) in figure 2 represent output from the DTI atlas where spring peak currents of greater than 2.0 m/s were predicted The minimum data length for the selected mooring buoys was 29 days in order to enable a detailed harmonic analysis to be conducted. Other buoy records in the area were rejected as they were of length less than 29 days. The tidal diamonds are all within a 50 km radius of the buoy locations. The location of the buoys and tidal diamonds along with their position in the water column is indicated in Table 1. Buoy records B1 and B2 were gathered simultaneously, on the same mooring. B1 was located 10 metres above the sea bed while B2 was positioned 37 meters above the sea bed (near surface). The water depth at this site is reported to be 40 metres [8].

	Name	Location	Depth below mean sea level (metres)
B1	b0636869	53.39°, -4.68°	30 m (near sea bed)
B2	b0636870	53.39°, -4.68°	3 m (near surface)
B3	b0636882	53.38°, -4.69°	3 m (near surface)
D1	SN0480	53.28°, -4.45°	5 m (near surface)
D2	SN048M	53.25°, -4.34°	5 m (near surface)
D3	SN048L	53.20°, -4.36°	5 m (near surface)
D4	SN048N	53.19°, -4.41°	5 m (near surface)
D5	SN048I	53.29°, -4.21°	5 m (near surface)
D6	SN048J	53.26°, -4.20°	5 m (near surface)
D7	SN048B	53.05°, -4.44°	5 m (near surface)
D8	SN062E	53.40°, -5.09°	5 m (near surface)

Table 1: List of buoys (B), tidal diamonds (D) and location.

3 Assessment

The analysis takes the form of a series of comparisons between:

1. the individual moored buoy records themselves,
2. the individual Admiralty tidal diamond data obtained from TotalTide
3. the individual moored buoy records and Admiralty tidal diamond data obtained from TotalTide.

Comparison of Buoys

The three individual moored buoy records do not coincide in time, although they were gathered during a coincident survey period. Direct comparison between the buoy data is therefore not possible. However, harmonic analysis and reconstruction can be used to generate accurate tidal predictions that are coincident.

The harmonic constituents of the tides contained within each of the three current meter datasets was determined using least-squared analysis. 23 principal constituents were obtained following the methodology advocated by National Oceanic and Atmospheric Administration (NOAA) Centre for Operational Oceanographic Products and Services (CO-OPS) in their Tidal Current Analysis Procedures and Associated Computer Programs documentation [14].

To verify how representative a prediction was generated through this analysis, the 23 constituent records were used to recreate the original time series and compared with the original current meter data. Fig 3 shows a scatter plot of the original current data and the data created using the 23 tidal constituents. It can be seen that while there is some scatter, the fit is good to excellent, and exhibits good homogeneity. The buoy data is a true in-situ record of sufficient length to allow confidence in its fidelity, therefore for this analysis it is reasonable to treat reconstructed moored buoy data as the 'gold standard' with which other datasets will be compared.

All comparisons are made for the common period of August 2009, with the harmonic constituents derived from the original data records used to create a pseudo-time series at 10-minute intervals for this period for each buoy location. Tidal current data are also obtained for the relevant Admiralty tidal diamond locations for the same time period using TotalTide.

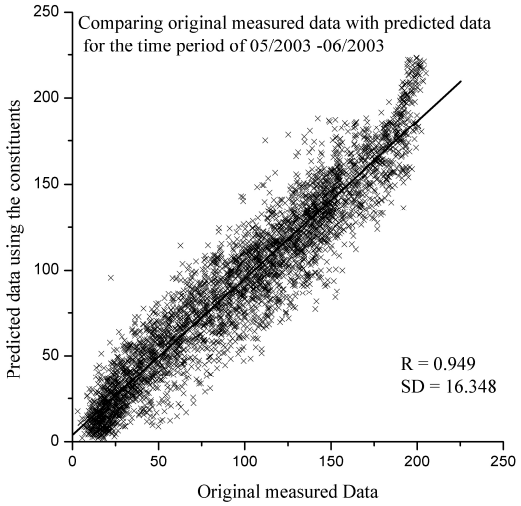

Figure 3: Scatter plot comparing between the original data record and the reconstructed data generated using 23 harmonic constituents.

The first comparison presented is between the individual moored buoy records. Given the location of the buoys (close physical proximity) the data would be expected to demonstrate good correlation. Figure 4 shows the velocity magnitude plot of all the three buoys for a randomly selected day in August 2009.

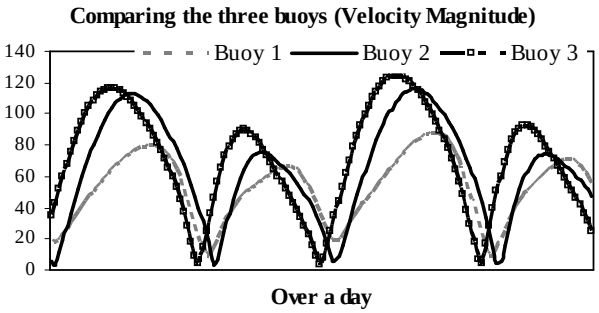

Figure 4: Figure showing currents at buoys B1, B2 and B3.

Buoy 1 and Buoy 2 are located on the same mooring, there is good phase agreement between the three records. Buoy 2 and buoy 3 are both located near surface and only 1.07 km apart, a slight phase lag is observed but the shape and size of the velocity magnitude plots compare well. To quantitatively compare these measurements statistical methods are adopted. First the mean absolute error (MAE) and relative mean absolute error (RMAE) are calculated. The data is converted from velocity magnitude and direction into two-dimensional vectors X(X_{1n},X_{2n}) and Y($Y_{1n,}Y_{2n}$). The MAE is calculated as [15]:

$$MAE = \frac{1}{N}\sum_{n=1}^{N}\sqrt{(Y_{1n}-X_{1n})^2+(Y_{2n}-X_{2n})^2}$$

This statistically incorporates both errors in velocity magnitude and direction. The relative mean absolute error is a better means of comparing between experiments as it incorporates the relative magnitude of the data considered.

$$RMAE = \frac{MAE}{\frac{1}{N}\sum_{n=1}^{N}\sqrt{(X_{1n}-X_{2n})^2}}$$

An RMAE value of zero indicates a perfect match. This will be a good indicator of how spatially variable tides in this site are. Table 2 has a summary of MAE and RMAE between the three records examined.

		B1	B2	B3
B1	MAE	-	31.16	51.86
	RMAE	-	0.49	0.82
B2	MAE	31.16	-	38.31
	RMAE	0.35	-	0.43
B3	MAE	51.86	38.31	-
	RMAE	0.54	0.40	-

Table 2: Comparing results from the buoys

Because B1 and B2 are co-located, good qualitative agreement is expected but with B2 having a much lower tidal velocity (due to its relative depth). A scaling factor would be required to account for the vertical velocity gradient between the sea-bed and the surface which skews the data in this case (e.g. 1/7th power law).

B3 has better agreement with B2 than with B1 because B2 and B3 are both located close to the surface and except for a small phase lag have a very similar velocity magnitude.

Comparison of Tidal Diamonds

The next set of experiments compared all the tidal diamonds obtained from TotalTide. Tidal diamonds are a set of numbers that depict the tidal current behaviour at certain time relative to high water at a reference port [16].

A total of 8 tidal diamonds were used in this experiment - all those within 50 km radius of the buoys (see Figure 2). The MAE and RMAE are calculated for the four closest tidal diamonds, SN0480, SN048M, SN048L and SN048N. Table 3 has a summary of MAE and RMAE between the tidal diamonds. The error values are in general consistently bigger for the tidal diamonds compared with the buoy data. This is primarily because these data points are spatially more dispersed than the buoys. This gives us a good indication of how spatially variable tidal current velocity data can be even within a (relatively) short distance.

		D1	D2	D3	D4
D1	MAE	-	68.49	88.51	91.6
	RMAE	-	0.83	1.07	1.11
D2	MAE	68.41	-	122.52	67.8
	RMAE	0.53	-	0.95	0.53
D3	MAE	88.38	122.44	-	92.78
	RMAE	3.14	4.35	-	3.29
D4	MAE	91.48	67.7	92.82	-
	RMAE	0.84	0.62	0.85	-

Table 3: Comparing results from the tidal diamonds.

The RMAE and MAE values for D3 are exceptionally bad compared to the rest of the tidal diamonds because this particular tidal diamond is located just over the edge of the head land, therefore none of the strong tidal currents are observed at this location as it is shielded by the land mass.

Comparison of Buoys and Tidal Diamonds

To better understand the quantitative agreement between the buoys and the tidal diamonds, a model skills test [17] is conducted. The observed data considered are the measured buoys and the model data are the tidal diamonds. The skill is defined as:

$$Skill = \frac{\sum|X-Y|^2}{\sum\left(\left|X-\overline{Y}\right|+\left|X-\overline{Y}\right|\right)^2}$$

Where $\overline{Y}$ is the mean value of the observed data. A value of one indicates perfect agreement and a value of zero indicates total disagreement. All the three buoy records were compared against all eight tidal diamonds. The statistics are summarised in table 4. The values of least agreement within a 12 km radius and within the 50 km radii are shown in bold. Yet again, the model skill results for tidal diamond D3 which is 7.68 km away from buoy 1 and 2 compares even worse than the distant D7 and D8 diamonds, especially in the V direction. This has been explained

earlier when the MAE and RMAE values were discussed. The effect is much more evident in the V direction as this is the stronger principal current direction.

		B1		B2		B3	
		U	**V**	**U**	**V**	**U**	**V**
Within 12 km	**D1**	0.91	0.88	0.94	0.90	0.81	0.77
	D2	0.87	0.82	0.92	0.96	0.91	0.94
	D3	**0.71**	**0.29**	**0.64**	**0.28**	**0.79**	**0.27**
	D4	0.78	0.84	0.79	0.93	0.90	0.97
Within 50 km	**D5**	0.90	0.10	0.94	0.14	0.86	0.15
	D6	0.90	**0.05**	0.94	**0.11**	0.85	**0.09**
	D7	**0.16**	0.91	**0.29**	0.93	**0.31**	0.82
	D8	0.87	0.94	0.80	0.86	0.69	0.78

Table 4: Comparing 'model skill' results from the buoys and tidal diamonds.

Standard deviation σ was also calculated to get a measure of the statistical spread of the values.

$$\sigma = \sqrt{\frac{1}{N}\sum_{i=1}^{N}(x_i - \bar{x})^2}$$

Where N is the total number of observations and x_i is the ith value. Standard deviation can also be used to calculate the cross correlation coefficient (CC) between the buoy and the tidal diamond data:

$$CC = \sigma_x^{-1}\sigma_y^{-1}\frac{1}{N}\sum_{1}^{N}(x_i - \bar{x})(y_i - \bar{y})$$

CC has been calculated for all the buoys and the four closest tidal diamonds (D1-D4). These values have been plotted and can be seen in Figure 5. Perfect correlation is indicated by a value of 1 and -1 indicates negative correlation.

Effect of Interpolation

The inverse distance weighting (IDW) interpolation methodology advocated by Shepard [7] was applied to the tidal diamond records.

$$u(x) = \frac{\sum_{k=0}^{N} w_k(x)u_k}{\sum_{k=0}^{N} w_k(x)}$$

Where:

$$w_k = \frac{1}{d(x, x_k)^p}$$

Here $p = 2$ is adopted as recommended by Shepard. Selection of the value of p enables the user to prescribe how sharp a peak the function exhibits by giving greater influence to nearby data points. A low value of p provides a smoother solution, with more 'smearing' of peaks. IDW is used in this instance to create 'pseudo' diamonds from the tidal diamonds available in the location. To test the fidelity of these 'pseudo' diamonds, the interpolation locations are mapped onto existing buoy record locations. The further away a tidal diamond is from a specific location, the less weighting it will have in the calculation. Similarly, tidal diamonds located close to the buoy will have a higher weighting therefore having a more significant influence on the pseudo diamond.

Three sets of IDW's are created. IDW 1 indiscriminately includes all the tidal diamonds within 50 km radii of B2. IDW 2 only includes the four tidal diamonds within 12 km of B2 and IDW 3 is a 'selected' variation of IDW 2 where tidal diamonds are selected based upon their statistical correlation.

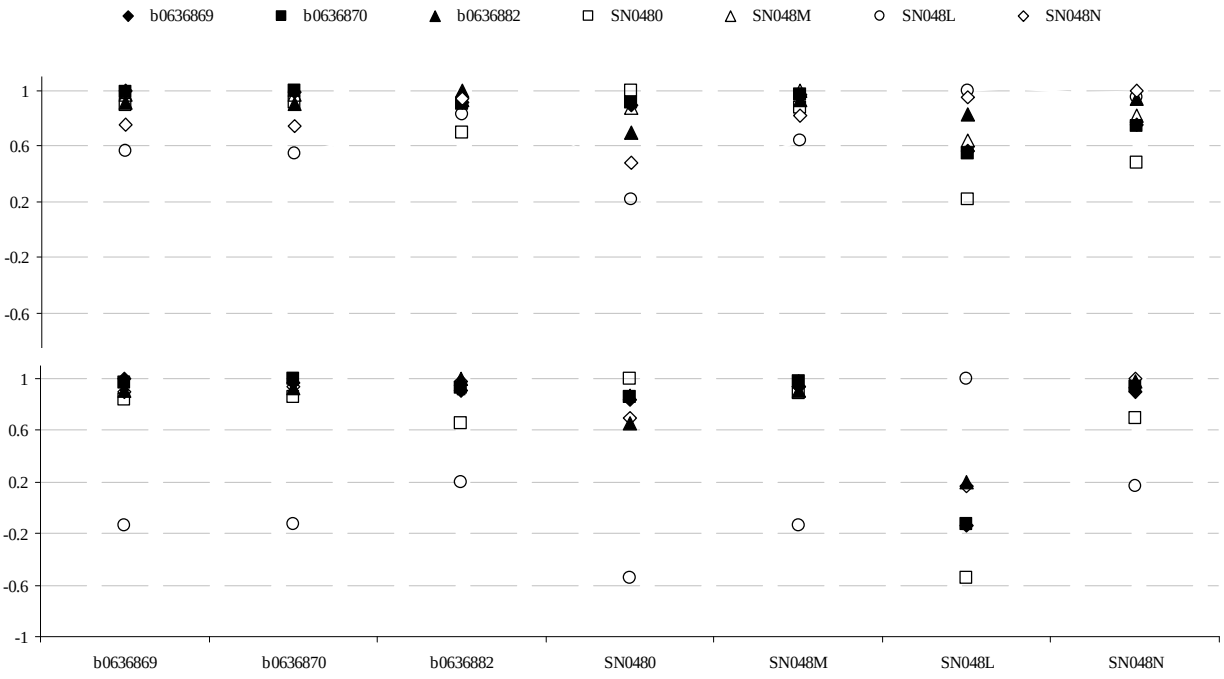

Figure 5: Comparing CC between buoys and tidal diamonds n directions (top) West-East, (bottom) South-North.

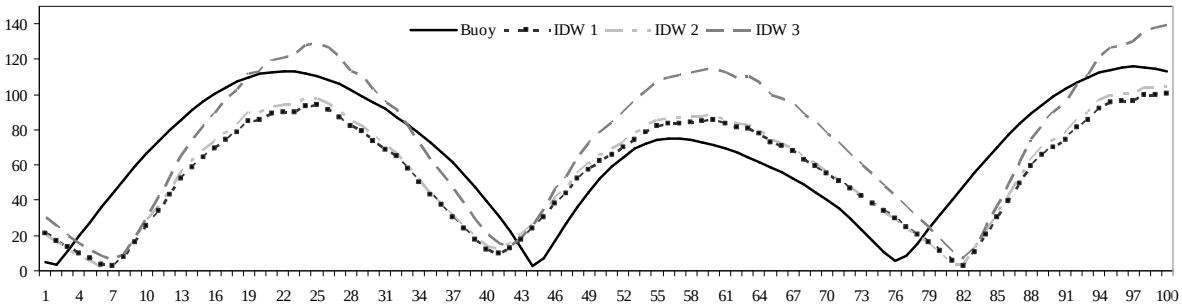

Figure 6: Velocity magnitude comparison of buoy with IDW 1, IDW 2 and IDW 3.

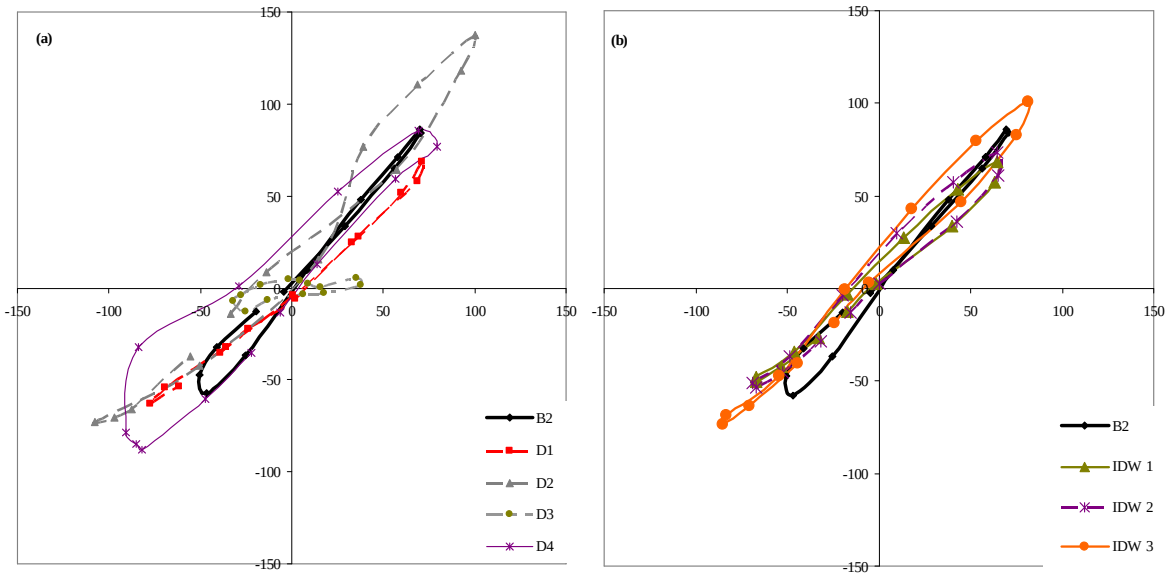

Figure 7: Tidal ellipse hodographs (a) comparing buoy data with tidal diamond data and (b) comparing buoy data with IDW data constructed from tidal diamond records.

Table 5 summarises the distance between all the tidal diamonds and B.

	Distance (km)
D 1	10.45
D 2	8.42
D 3	6.98
D 4	7.68
D 5	24.49
D 6	33.23
D 7	33.23
D 8	44.09

Table 5: Distance between each tidal diamond and B2

Statistical analysis has been carried out to better understand the correlation between IDW 1, IDW 2 and IDW 3 and see how theses representations compare with the individual buoy record.

Vector magnitude plots of B2 along with IDW 1, IDW 2 and IDW 3 are plotted in Figure 6. There is good quantitative agreement between IDW 1, which includes all the tidal diamond current data within the 50 km radii, and IDW 2 which only includes the 4 closest buoys. The minimal difference between IDW1 and IDW 2 (they nearly overlap in figure 6) is due to the inverse distance weighting ensuring that the distant buoys provide a limited impact in this particular case (see table 5).

As the buoy data encapsulates 23 constituents where as the Total Tide diamond data generally has only 2 constituents, [11] there is a surprisingly good qualitative agreement and correlation. The shape and the general envelope of the spring-neap cycle are also well captured (not shown).

Velocity magnitude peaks and phasing in figure 6 indicate reasonable qualitative agreement between the different records, certainly offering improvement over the comparison with individual TotalTide sourced tidal diamond records are presented in the preceding section.

Comparing tidal ellipses hodographs

Tidal ellipse comparisons have been plotted in figure 7, where the local individual tidal diamond ellipses (left) are compared with all the IDW ellipses (right). The IDW ellipses show a good qualitative agreement and the IDW presents substantially graphically reduced errors, suggesting that this methodology does in fact improve the representation of some of the tidal characteristics. The bi-directionality of the tides makes this location very desirable and this is shown well by the IDW's.

Comparison with the DTI Atlas data

It is estimated that only 0.15% (1269 km^2 Area) in the UK continental shelf has a peak flow of 3 m/s or greater [18]. These are the very high energy sites that can make tidal energy extraction economically viable. Before devices are deployed into the water, it is important to precisely identify these locations and study the individual site characteristics.

Depth-averaged data is often used during calculations; in this study we have buoy data near surface, at 37 metres and near bed at 10 metres. TotalTide data is near surface, approximately 35 metres. Current velocity data can be obtained at specific depth by using a scaling value. A 1/7th power law is often considered appropriate in fluid flows [19].

The POL (CS3) model used to construct the DTI Atlas [11] uses a depth-variation profile. Alternatively, [2] uses a variable power law:

$$\frac{v(z)}{v(z_r)} = \left(\frac{z}{z_r}\right)^{\frac{1}{x}}$$

Where $v(z)$ is a known velocity at a known elevation z, and $v(z_r)$ is the unknown velocity at the elevation of interest, z_r, and x = 7 in case of 1/7th power law or 10 in case of 1/10th power law (these values are typically applied in the fluids community, and carry over into the wind industry).This formula can be used to estimate the tidal velocity at a specific height in the water column. This would enable the calculation of velocity at the height intended for installation of a selected tidal turbine from data records elsewhere in the water column.

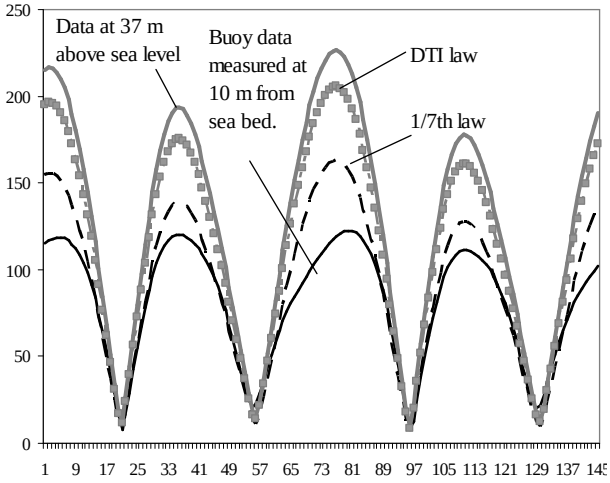

Figure 8: B2 scaled down using the 1/7^{tn} and DTI scaling factors.

Figure 8 shows spring peak measurements for B2 which is located at 37 metres (near surface), scaled to 10 metres using the scaling factor as suggested by the DTI (Dept. of Energy). Also plotted is the actual measured data obtained at 30 metre in the same location.

The scaling factor used by DTI is about 0.9. However figure 8 indicates that the current velocity is nearly half at 10 metres depth, suggesting that a scaling factor of approximately 0.5 would be more appropriate in this particular case. The DTI Marine Atlas uses layers obtained from the HRCS model and this scaling factor to obtain their depth averaged current velocity and power. For this particular site this scaling factor overestimates the current velocity significantly. When then manipulate to produce an estimate of the energy that can be harvested at this location, this overestimation would then be compounded.

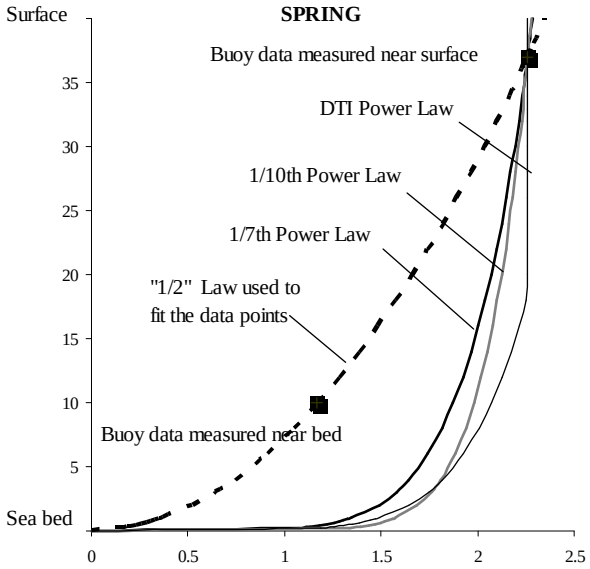

Figure 9: Tidal current velocity profile.

Figure 9 shows current vertical velocity profiles in a water depth of 40 metres. The figure compares various commonly applied power law plots with two data points obtained from the buoys. The power law cures have been derived from the near surface buoy data. As suggested earlier, a scaling factor of 0.5 is appropriate for fitting a power curve to the data. Similarly calculations for neap tide data were best fitted using a similar scaling factor. It remains unclear weather overestimation of the resource in this case by the 1/7th, 1/10th and DTI power law would be replicated at other locations without further evidence. However it is of significant interest that the extreme tidal velocities of interest for tidal energy development are potentially not well represented by traditional vertical velocity variation assumptions.

Comparing Power outputs for B2 buoy and IDW's

Power output for all the three IDW's and B2 have been calculated for the month considered for case study analysis. Power was calculated using:

$$P = \frac{1}{2}\rho A v^3$$

Where

$\rho = 1025$ kg/m^3 and A is taken as 1m^2

Similarly, the power output from the DTI Atlas for this region is also obtained, the mean annual kw/m^2 was extracted from the atlas and multiplied by the number of hours in a year (8760 hours) to obtain the annual energy output. Table 6 summarises the output

resource assuming that the simulated month is representative of the entire year. B2 is used as the base value here for comparison and the annual energy yield is compared with the three IDW outputs and the DTI Atlas.

	Annual energy resource available per square metre (kWh)
B2	6395
IDW 1	4038
IDW 2	4538
IDW 3	9875
DTI Atlas	10319

Table 6: Power output for B2, IDW1, IDW2 & IDW3

From the preceding analysis, the error margin between the velocity magnitudes were substantially reduced between the IDW representations of the tidal diamond data over consideration of the individual tidal diamond data when compared with the moored buoy derived data record. However, when these datasets are used to conduct a long-term monthly, or annual energy yield assessment, even the IDW representation of the tidal diamond data show poor agreement. As prediction of long-term energy yield is at the heart of any sensible economic appraisal of a particular development project, the application of the IDW methodology for use in tidal energy resource assessment must be questioned.

These error margins make a significant impact on site selection and lifetime production costs. If this was to be considered over 25 years, the typical intended lifecycle of tidal energy development projects, these error margins would be unacceptable.

4 Conclusion

The spatial variability of tides is governed by complex non-linear physics, topography, the bathymetry and the fluid interaction at the site. For this reason, interpolating spatially diffuse tidal data records is always going to lead to inaccuracies. These complex phenomena cannot be well represented by simple interpolation. This is particularly true when the current velocity derived will inevitably be manipulated to conduct tidal energy generation calculations and scenarios analysis. Even though statistical analysis shows the MAE and RMAE of velocity records to be relatively small, the error is magnified when the power output is estimated for a site. The significant variations in the available energy in the water column derived using even the improved IDW representations demonstrates that this methodology is not robust for serious resource or development project economic assessment.

The most important issue the authors wish to highlight is that it is essential for developers before committing to a site for development to conduct an appropriate survey of the available resource. Gathering multiple Acoustic Doppler Current Profiler (ADCP) records across the intended site at a minimum temporal resolution of 29 days is recommended to enable an appropriate spatial and temporal representation of the tidal currents to be determined. This will also assist in making assessments of the future energy yield through appropriate harmonic predictions that can feed into power production calculations and economic assessment models. Ultimately this type of data will enable project developers to better estimate future revenue generation, or conversely be able to pre-determine that a site is in fact uneconomic for development.

Additional case studies are necessary to support the various conclusions reached here. Further analysis is ongoing to support and expand upon the current work.

Acknowledgements

The moored buoy records were supplied by the British Oceanographic Data Centre as part of the, Inter-Agency Committee on Marine Science and Technology funded, 'UK Moored Current Meter Data Set' DVD electronic publication. The data were collected by the Proudman Oceanographic Laboratory during the Mixing and sediment resuspension in shelf seas which was funded by the Natural Environment Research Council (NERC)

The authors also wish to acknowledge the contributions from the scientists of Assessment of the National Ocean Service's Tidal Current Program which was provided by NOAA.

This work is funded by the EPSRC Supergen FlexNet Consortium.

References

[1] Thomas Boehme, Jamie Taylor, Dr. Robin Wallace and Prof. Janusz Bialek. Matching Renewable Electricity Generation With Demand. 2006.

[2] Black & Veatch, Tidal stream Energy Report. 2004

[3] Carbon Trust, Variability of UK marine resources. 2005

[4] David JC MacKay. Sustainable Energy –without the hot air. UTI Cambridge, 2008.ISBN 978-0-9544529-3-3. Available free online from www.withouthotair.com.

[5] Garrad Hassan and Partners. Scotland's Renewable Resource 2001 –Volume I : The Analysis.

[6] Supergen FlexNet consortium, www.supergen-networks.org

[7] Donald Shepard. A two-dimensional interpolation function for irregularly-spaced data. *In Proc. 1968 ACM National Conference.*

[8] UK Moored Current Meter Data Set. DVD Electronic Publication. 2006

[9] http://www.bodc.ac.uk/about/what_is_bodc/ BODC website

[10] United Kingdom Hydrographic Office (2005) Admiralty TotaTide

[11] Colin Bell and Lisa Carlin. Generation of UK Tidal Stream Atlases from Regularly Gridded Hydrodynamic Modelled Data. The Journal of Navigation , Volume 51, Issue 01, January 1998, pp 73-78

[12] DTI Atlas of UK Marine Renewable Energy Resource. A Strategic Environmental Assessment Report. 2004

[13] DTI Marine Atlas http://www.renewables-atlas.info/

[14] NOAA Technical Memorandum NOS CO-OPS 0021. Tidal Current Analysis Procedures and Associated Computer Programs, 1991.

[15] C. Brière, S. Abadie, P. Bretel and P. Lang. Assessment of TELEMAC system performance, a hydrodynamic case study of Anglet, France. 2006.

[16] Colin Bell and Lisa Carling. The Generation of UK tidal stream atlases from regularly gridded hydrodynamic modelled data.

[17] John C. Warner, W. Rockwell Geyer and James A Lerczak. Numerical modelling of an estuary: A comprehensive skill assessment.

[18] W.S Cooper, C.L. Hinton, N. Ashton, A. Saulter, C. Morgan, R. Proctor, C. Bell and Q. Huggett. An introduction to the UK marine renewable atlas.

[19] Roger A. Falconer and A. I. B. M. Ismail. Numerical modelling of tracer transport in a contact tank.

Analysis and Comparison of Tidal Datasets for Resource Assessment and Network Modelling

A. Sankaran. Iyer:
Institute for Energy Systems,
University of Edinburgh
A.Sankaran-Iyer@ed.ac.uk

Prof. A Robin Wallace:
Institute for Energy Systems,
University of Edinburgh
Robin.Wallace@ed.ac.uk

Dr Gareth P Harrison:
Institute for Energy Systems,
University of Edinburgh
Gareth.Harrison@ed.ac.uk

Dr Scott J Couch:
Institute for Energy Systems,
University of Edinburgh
Scott.Couch@ed.ac.uk

***Abstract*—This paper presents research being undertaken as part of the EPSRC Supergen FlexNet consortium to analyse the spatial and temporal behaviour of the UK wave, tidal, on- and off- shore wind resources. The UK has extensive renewable resources that can potentially be developed to reduce harmful greenhouse gas emissions from electricity generation. The study explores the availability of tidal current energy in terms of its timing, location and extent. The tidal resource is highly spatially and temporally variable. For tidal current energy to be economically exploited, certain conditions need to be fulfilled. Principally the strength of the resource needs to be quantified before it can be effectively utilised. This paper looks at the energy output from a case study site and considers matters that need to be addressed with intermittent but predictable energy such as tidal currents. Tidal current velocity distributions for this site are obtained and used to evaluate the energy that can be exploited by a typical device. Future work is intended to combine outputs from this research with similar datasets for other renewable resources in order to examine their combined impact and integration into the existing electrical network infrastructure.**

***Index Terms*—Network integration, Renewable resource assessment, Tidal current energy**

I. INTRODUCTION

Developments in tidal power show that this renewable resource can achieve impressive results and contribute to meeting future energy requirements [1]. However, device performance is based upon the energy available at a particular site; therefore it is important to evaluate exactly what resource is available. Different studies have in the past tried to quantify the resource available [2]-[5]. There appears to be a spread in the estimates made and this is put down to the difficulties arising from the complex tidal interactions and the different methodologies used. A better understanding of the tidal energy resource is key to enabling more deployment of tidal technology, therefore meeting UK renewable energy targets and reducing emissions [6]. However large scale deployment of this emerging technology may be ultimately limited by network constraints.

The current work looks at expanding the analysis in [7] and investigates some of the techniques used. This methodology can then be used to more accurately model the UK tidal resource, both spatially and temporally. The work forms part of a larger renewable energy resource model being developed by the Engineering and Physical Sciences Research Council's Supergen FlexNet consortium [8]. The aim is to find a robust and repeatable method for predicting tidal energy generation scenarios for the UK. This initial analysis will then be used in conjunction with a UK network model to investigate what new procedures are required for effective and efficient network management.

Tidal energy, not to be confused with wave or hydro energy is a result of the gravitational pull of the Moon and Sun on the large water bodies covering the earth. All the sites around UK experience semi-diurnal tides, exhibiting two periods of high tides and two low tides a day [9]. Tidal currents tend to be more bi-directional in narrow channels and estuaries, and are often accelerated in these regions due to concentration of tidal energy.

As the rise and fall of the tide depends upon the rotation of the Moon and Sun, it makes them highly predictable, with small additional local variations due to other factors such as meteorological conditions. The predictability of tidal energy is a major advantage over other intermittent renewable energy resources for integration into the network. Even with numerical weather prediction models wind and wave predictions are not nearly as accurate or precise as tidal analyses based upon appropriate data sources and application of harmonic analysis. However, a challenge with tidal energy is that the peak power that can be extracted occurs 50 minutes later each day as it is governed by the Moon's orbital period of 24 hours and 50 minutes. This may or may not coincide with the peak demand potentially causing some complications. None the less, the predictability of tides should help with the planning of day to day network integration hence avoiding any serious issues.

For a tidal device to work efficiently, it is essential to select a bi-directional site with peak spring current velocity of 2 m/s or more. The preferred water depth would be 20-50 metres for first generation devices. Further advances in technology could make it possible to deploy in deeper water. Access to network for grid connection and integration is another important consideration; even with a high energy site grid connection is the biggest constraint that will limit the power supplied to the network. If the network is required to be reinforced then potentially significant additional costs will be incurred. The timing of peak tidal velocities varies around the UK dependant upon the propagation of tidal energy around the UK continental shelf. There is therefore potential that when a number of sites are connected to the network a consistent level of continuous background output

would be produced with a level of additional variation on top.

The current work is trying to assess the tidal resource available for harvesting around the UK with a high spatial and temporal resolution so that a good estimate of the resource is obtained. This will enhance understanding of how intermittent, but predictable, tidal energy impacts the network on a site by site basis as well as the cumulative impact of the technology in the future energy mix.

II. Tidal Energy: Case Study

High quality data collection for interesting sites is highly desirable but expensive, difficult to extrapolate over a larger area, and hence unsuitable for national scale resource analysis. Existing publically available datasets have so far typically been used to examine the resource. A methodology to combine all of the available datasets to produce an improved resource assessment methodology is desirable. This work is validating the techniques used in [7].

The suitability of combining three UK wide datasets is considered. The datasets do not coincide spatially or temporally. If with additional processing, datasets can be combined, considerable improvement will be achieved in analysing the UK resource by improving the spatial coverage of data available. The data sources considered are:

1.British Oceanographic Data Centre (BODC) UK Moored Current Meter Data, [10];

2.TotalTide software, a UK Hydrographic Office publication [11];

3.DTI Atlas of UK Marine Renewable Energy [12, 13].

Fig 1 is an extract from the DTI Atlas showing the site of interest. Three BODC buoys records are being used for this study. Two of the buoys are located on the same mooring, one located at 3 metres depth (near surface) and the other one located at 30 metres depth (near bed), in a total water depth of approximately 40 metres. The third buoy is located 1.07 km away at 3 metres depth also in approximately 40 metres of water depth. As the buoy records did not coincide in time, direct comparison between the data is not possible. Therefore, harmonic decomposition and analysis were used to construct datasets based on the buoy data that are coincident in time. This was achieved through least square analysis using National Oceanic and Atmospheric Administration (NOAA) Centre for Operational Oceanographic Products and Services (CO-OPS) Tidal Current Analysis Procedures and Associated Computer Programs [14].

The buoy data is a true record of sufficient length to allow confidence in its fidelity, therefore for this analysis it is reasonable to treat reconstructed buoy data as the ‘gold standard’. Inverse distance weighting (IDW) [15] interpolation was applied to the TotalTide tidal diamond data as in [7] in order to derive ‘pseudo’ diamonds for comparison with the BODC buoy datasets. Details of all the analysis conducted can be obtained from [16]

The comparisons in [16] demonstrate that there is good qualitative agreement between the current velocity measured from the buoys and the dataset created using IDW on the TotalTide data. However, it is important to emphasise that [16] demonstrates that it is not always appropriate to simply interpolate tidal data, as the physical processes being approximated are highly complex and non linear. Interpolation, even by well regarded numerical methods is inappropriate. Complex phenomena, non-linear physics, the sea bed bathymetry, and the land topology affect tides in various ways that are not well represented using interpolation. Although the data shows good homogeneity, and the current velocity show small errors, power calculations using interpolated output can produce significant errors as demonstrated in [16] due to cubing of velocity to produce power.

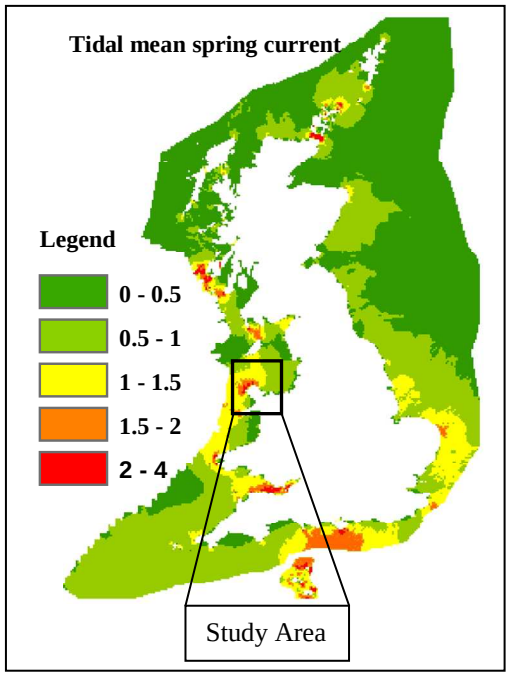

Fig. 1 Figure showing mean spring peak current. © Crown Copyright. All rights reserved 2008.

III. Tidal Energy Integration

The power output from a tidal device depends upon the local current velocity, device efficiency and matching of device characteristics to the local resource [17, 18]. Fig 2 shows the power output of one of the case study sites along with the variation in current velocity. This demonstrates the spatial variability that tidal currents exhibit, as it is well known that tidal currents in the Skerries region around Anglsey can peak at much higher velocities than captured in these data records. Note that although the change in current velocity is relatively minor, on this particular day, the power output during the flood tide is nearly double that occurring at ebb (because of the cubing of velocity during derivation of the kinetic energy that would be acting on the device).

Similarly, fig 3 shows the power available for the same site over a period of a week. It is important to highlight the spring-neap variability; during the spring cycle the peak power output ranges from 2-6 kW/m^2, but during the neap cycle, peak output only ranges from 0.5-1 kW/m^2

This electricity needs to be integrated with all other sources of power and connected to the end user. One of the biggest challenges is to feed the output from such a site to the network. Timing is important as tidal cycles are on a 24.8 hour period 'Lunar day' where as an 'Earth day' is 24 hours. Every day the peak generation will occur around 50 minutes later and hence may not coincide with peak demand.

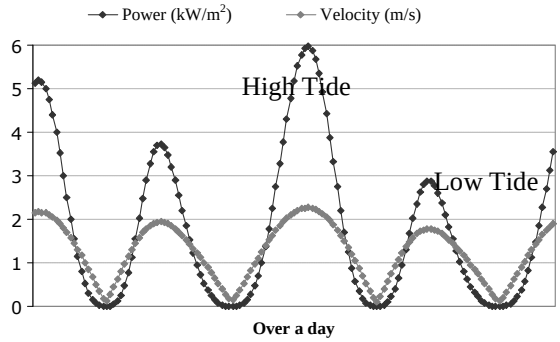

Fig. 2 Power available (per m^2 cross-sectional area) and current velocity for a location. Note the change in velocity to the change in power output.

The power curve of a tidal current energy device relates electrical generation from the unit to the incident tidal velocity. The power curve is influenced by the rotor swept area, power take-off properties of the device and characteristics of the site. Cut-in velocity is the minimum current velocity required for the device to start operating and the rated velocity describes when the power output from the device is at maximum.

Unlike wind, tidal current velocities will never reach such extremes beyond the typical operating condition that the device will need to be switched off (cut-out). Fig. 4 shows the power curve of a typical tidal device appropriate for deployment at this site.

The device is assumed to have a diameter of 14 metres giving a rated power of 500 kW at rated velocity. The cut in velocity in this case is assumed to be 0.75 m/s and the rated velocity is 1.85 m/s in an attempt to match the characteristics of the site under investigation. Above this velocity, the device will continue to generate its rated output and remain at this output level even as the velocity increases.

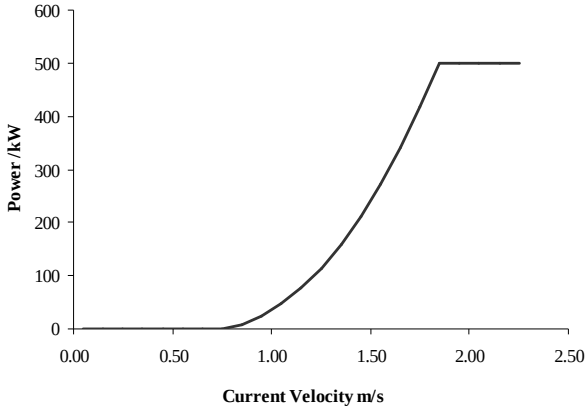

Fig. 4 Power curve of a typical tidal device with rated power of 500 kW.

A good way to assess the resource at a particular location is by using a frequency distribution of the current velocity at the site. In fig. 5 (a), the histogram shows the number of times the current velocity falls within a 0.11 m/s 'class' or 'bin' (0.01 to 0.10 = 0.05 m/s) over a 31-day month with data resolution of 10 minute intervals. The power generated at a site with these characteristics for a device as specified in figure 4 is presented in fig 5 (b), where the accumulated energy production for specific velocity bands are plotted.

The total power output through the device for this site is the sum of all the energy produced within the operational range of the turbine, in this case 61 MWh. As the device will not cut in till about 0.7 m/s, there will be power production for about 53% of the time and operation at rated power for 4% of the time when this hypothetical 500kW rated device is matched with this local resource.

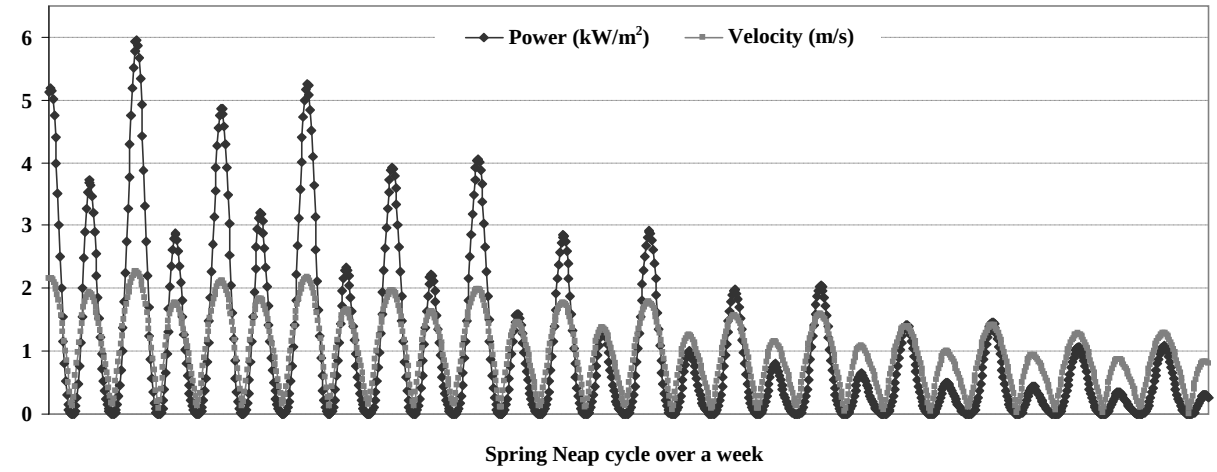

Fig. 3 Power availability (per m^2 cross-sectional area) and current velocity over a week

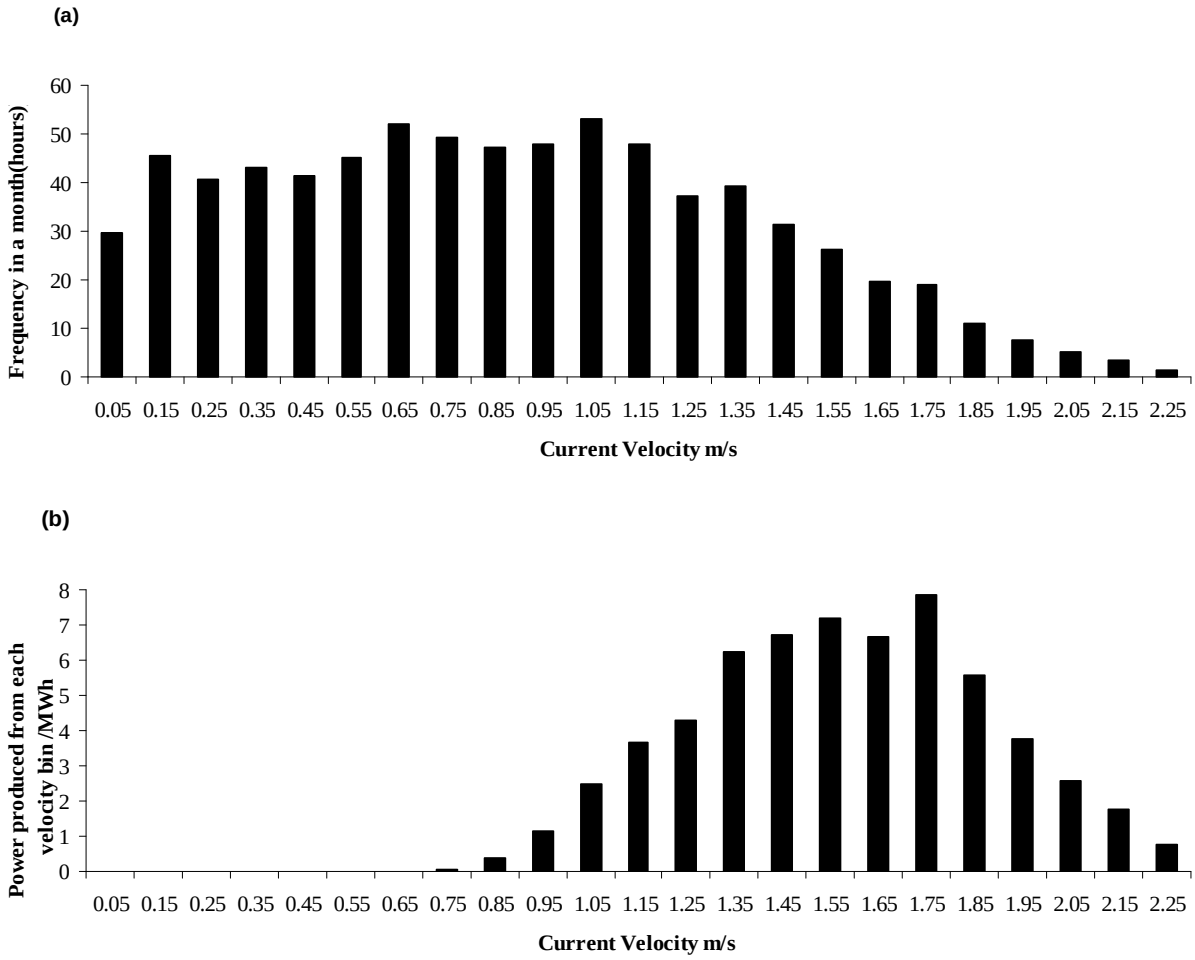

Fig. 5 (a) Frequency distribution of tidal current velocity in a month. (b) Tidal energy distribution for the site, power output calculated using power curve shown in Fig 4.

The load factor achieved in this scenario is about 17%. This is substantially lower than typical load factors achieved by conventional power plant. In this instance the load factor is also lower than other intermittent renewable plant such as onshore wind would typically achieve (approx. 25-30%). This indicates that this *exact* location is not optimal for tidal current energy development; as a site with a stronger resource is typically capable of producing load factors competitive with onshore wind.

IV. Network Integration

The case study presented here considers the simple situation of output from one device at a specific site. Small energy generation plants (renewable or conventional) are normally connected to the local distribution network. Hence early stage tidal energy developments of single devices or a small number of devices in an array are likely to be connected to the local distribution network. This is typical of the resurgence of distributed generation even in well integrated modern energy networks where embedded generation has been the standard approach for the last 30 years or so. This is the best way to enable incorporation of small renewable energy developments into the wider energy supply system in order to begin to address greenhouse gas emission concerns. Increasing amounts of tidal energy and larger arrays of devices will inevitably require integration into the transmission network, as is currently occurring for onshore wind as it matures and begins to make a substantial contribution to the energy mix. In both the distribution and transmission network, increasingly sophisticated active management methods are required to be developed in order to assist in integrating all the potential intermittent renewable energy produced from sources such as wind, wave, tidal current energy, tidal barrage schemes and solar energy. The inherent predictability of the intermittence of tidal current (and barrage) energy offers assistance in developing appropriate management systems. However, it is obvious that in the near future significant decisions will be necessary regarding development and management of the existing electricity infrastructure to ensure that modern renewable energy generation methodologies do not adversely impact on the security of supply.

V. Conclusion

The work described here is intended to raise issues and provoke thinking towards future solutions. A process is being developed to understand the nature of the intermittent tidal energy resource. From this scenarios are being developed to examine the

matching of supply and demand using tidal current energy, and how this will integrate with the existing electricity infrastructure and working practices.. Two major issues are being addressed; one is the intermittent nature of tidal currents that takes place over small periods of time and its coincidence with the demand for electricity. Second is effectively predicting and managing the collective output from a large number of sites, each with its own unique characteristics and integrating this new energy generation methodology into the network infrastructure.

ACKNOWLEDGEMENTS

The buoy records were supplied by the British Oceanographic Data Centre as part of the, Inter-Agency Committee on Marine Science and Technology funded, 'UK Moored Current Meter Data Set' DVD electronic publication. The data were collected by the Proudman Oceanographic Laboratory during the Mixing and sediment resuspension in shelf seas which was funded by the Natural Environment Research Council (NERC).

The authors also wish to acknowledge the contributions from the scientists of Assessment of the National Ocean Service's Tidal Current Program which was provided by NOAA.

This piece of work is funded by the EPSRC Supergen FlexNet Consortium.

REFERENCES

[1] MCT, Marine current Turbine wins prestigious new energy award. http://www.marineturbines.com/3/news/article/19/marine_current_turbines_wins_prestigious_new_energy_award/
[2] Black & Veatch, Tidal stream Energy Report. 2004
[3] Carbon Trust, Variability of UK marine resources. 2005
[4] David JC MacKay. Sustainable Energy–without the hot air. UTI Cambridge, 2008.ISBN 978-0-9544529-3-3. Available free online from www.withouthotair.com.
[5] Garrad Hassan and Partners. Scotland's Renewable Resource 2001 –Volume I: The Analysis. Scottish Executive, 2001.
[6] Meeting our energy challenge, A white Paper on Energy, DTI, May 2007.
[7] Thomas Boehme, Jamie Taylor, Robin Wallace and Janusz Bialek. Matching Renewable Electricity Generation with Demand. Scottish Executive, 2006.
[8] Supergen FlexNet consortium, www.supergen-networks.org
[9] Pidwirny, M. "Ocean Tides". Fundamentals of Physical Geography, 2nd Edition. 2006
[10] http://www.bodc.ac.uk/about/what_is_bodc/ BODC website
[11] http://www.neptune-navigation.com/totaltide.htm UKHO TotalTides
[12] DTI Atlas of UK Marine Renewable Energy Resource. A Strategic Environmental Assessment Report. DTI. 2004
[13] DTI Marine Atlas http://www.renewables-atlas.info/
[14] NOAA Technical Memorandum NOS CO-OPS 0021. Tidal Current Analysis Procedures and Associated Computer Programs, 1991.
[15] Donald Shepard. A two-dimensional interpolation function for irregularly-spaced data. *In Proc. 1968 ACM National Conference.*
[16] A. Sankaran Iyer, S. J. Couch, G. P. Harrison and A. R. Wallace Analysis and Comparison of Tidal Datasets. Proceedings of the 8th European Wave and Tidal Energy Conference, Uppsala, Sweden, 2009
[17] I Bryden and G T Melville. Choosing and evaluating sites for tidal current development. Centre for Research into Energy and the Environment. The Robert Gordon University, Aberdeen, UK. 2004
[18] G. Hagerman and B Polagye. Methodology for Estimating Tidal current Energy resources and Power Production by Tidal In-Stream Energy Conversion (TISEC) devices EPRI-TP-001 NA Rev 3 http://oceanenergy.epri.com/attachments/streamenergy/reports/TP-001_REV_3_BP_091306.pdf

Developing Methodologies for Quantifying the Impact of Tidal Current Energy Variability

Abhinaya Sankaran Iyer[1],
Scott J. Couch[1], Gareth Harrison[1] & Robin Wallace [1]

[1] University of Edinburgh
Institute for Energy Systems
Kings Buildings
Mayfield Road
Edinburgh
EH9 3JL,

Abstract

This paper presents research being undertaken as part of the EPSRC Supergen FlexNet consortium to analyse the spatial and temporal behaviour of tidal current resources. The study explores the availability of tidal current energy at a particular location and examines its timing with respect to electricity demand. Actual performance data from a tidal device is not available; therefore a representative hypothetical device is used to simulate electrical generation output from the available tidal resource. The variability of the power generated is compared with realistic demand data and the level of perturbation is calculated. As the study only considers generation output at one location, the importance of aggregation is highlighted. Two scenarios are presented; 10% and 20% penetration of tidal current energy generation in a small network with variability characteristics similar to the UK system demand. Increasing penetration leads to larger power excursions in the system due to the addition of variable generation.

Keywords: Demand and supply fluctuations, Electricity network integration, Resource assessment, Tidal analysis.

1. Introduction

The United Kingdom has excellent tidal current energy resource potential, and the development of this resource could make a meaningful contribution to meeting our future energy requirements. With a range of tidal current devices being developed and prototype full scale devices being tested, deployment will be enhanced by reliable evidence about the resource, its characteristics, potential environmental impacts and economic cost.

It is important to assess the generation potential at each location where tidal current energy resources are to be deployed, and understand what might be the consequence of absorbing the energy generated into the existing network system. No electricity system can be 100% reliable, since even with conventional generation there is a small chance of major power failure. Addition of variable generation will introduce additional uncertainty, which needs to be quantified.

Each tidal site has very specific characteristics so no two sites are exactly the same, but it is possible to compare some of the generic responses of energetic tidal current sites and assess how much these locations can contribute to the future energy mix if appropriately developed. The aim of this paper is to explore issues associated with the operation of the electricity network with the addition of tidal current energy.

This paper looks at the output from one particular location and assesses its potential impact on the network with the future intention of expanding this analysis to all the key tidal current locations in the UK. The aggregate effect of wind is studied in a similar manner in [1]. The work in [1] draws upon actual wind data from the western Denmark electricity system to illustrate the variability of wind and makes comparisons with demand fluctuations. The outcome from [1] highlights that the system is inherently capable of coping with intermittency and shows that there already exists room for perturbations. Importantly, there are large power excursions that need to be managed by the system when significant amount of wind generation is included, but the number of extreme excursions and their occurrences are manageable.

Current work would involve using a similar methodology to evaluate the impact of tidal current energy from a specific site in the network with the aim of developing a number of test sites to assess the aggregate impact on the network. The analysis presented here is the first step in this process, developing the methodological approach and

demonstrating application through a case study scenario.

Conventional generation can lose output as a result of mechanical or electrical faults and the entire plant can shut down. For a farm of (tidal) devices, it is much more likely that one or two devices will shut down due to failure but the shutdown of the entire farm is unlikely. Renewable resources are often termed 'intermittent'. For example wind and wave can stop generation instantaneously at the point of cut-out in extreme conditions for example. For tidal generation 'variable' is a much better description. It has periods of no generation but there will be a constant transition from rated to no generation over a period of time. This makes the output variable, but instantaneous shutdowns are unlikely.

2. Tidal Resource

As the rise and fall of the tide depends upon the rotation of the Earth-Moon-Sun system, tidal variability is highly predictable, with small additional variations due to other factors such as local meteorological conditions. The predictability of tidal energy is a major advantage over other intermittent renewable energy resources for integration into the network. Even with numerical weather prediction models wind and wave predictions are not nearly as accurate or precise as tidal analyses based upon appropriate data sources and application of harmonic analysis. The accuracy of numerical weather predictions diminish over time, whereas tidal perditions can be conducted accurately for many years.

However, a challenge with tidal energy is that the peak power that can be extracted occurs 50 minutes later each day as it is governed by the Moon's orbital period of 24 hours and 50 minutes. This may or may not coincide with the peak demand potentially causing complications. None the less, the predictability of tides should help with the planning of day to day network integration of electricity generated from this resource.

2.1 Case Study

Only about 0.15% (1269 km^2) of the UK continental shelf has a peak flow of 3 m/s or greater [2]. This represents the main region of interest in terms of economic energy extraction due to the characteristics of the technologies proposed for harnessing the available energy. Therefore obtaining data across all of UK continental shelf area is not necessary. Instead what would be most beneficial would be a detailed survey of sites that have high peak flow velocities. This would capture all the information needed to carry out the analysis and assess the sites feasibility, but high quality tidal data tends not to exist for the areas of interest. Prior to the rise of interest in tidal current energy, these regions were not previously deemed of much interest, and therefore not much data exists. A methodology to combine publically available datasets to produce an improved resource assessment methodology is discussed in [3].

The sources of data being considered here as in [3] are:

1. British Oceanographic Data Centre (BODC) UK Moored Current Meter Data, [4];
2. DTI Atlas of UK Marine Renewable Energy [5-6].

Figure 1 shows an extract from the DTI Atlas indicating the case study region in the Irish Sea near the Island of Anglesey off the north Wales coast. The potential suitability of this location for tidal energy development as identified by a leading early stage tidal current energy technology developer [7] is one reason for selecting this site for analysis. The other key driver to select this region is the existence of three historic BODC buoy records available in this region. Two of the records are located on the same mooring, one located at 3 metres depth (near surface) and the other one located at 30 metres depth (near bed), in a total water depth of approximately 40 metres. The third buoy is located 1.07 km away at 3 metres depth also in approximately 40 metres of water dept

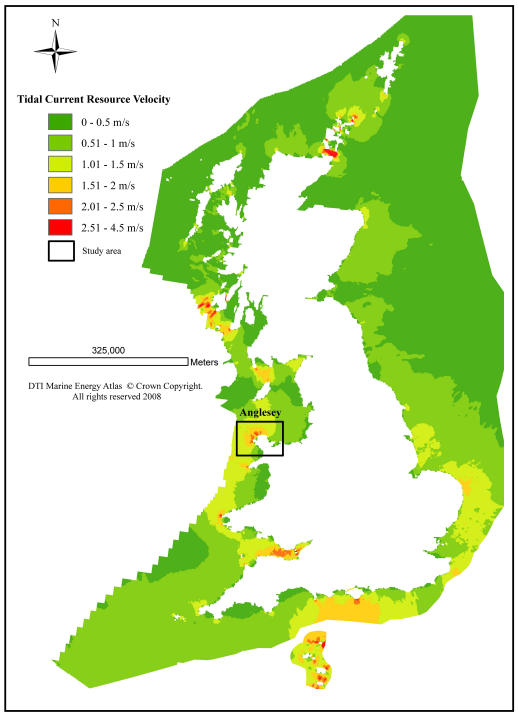

Figure 1: Mean spring peak current.

The buoy records do not coincide in time, so direct comparison between the data is not possible. Therefore, harmonic decomposition and analysis of the original buoy data is used to construct datasets that are coincident in time. This was achieved through least square analysis using National Oceanic and Atmospheric Administration (NOAA) Centre for Operational Oceanographic Products and Services (CO-OPS) Tidal Current Analysis Procedures and Associated Computer Programs [8].

The data is reconstructed from the derived harmonic constituents to generate a time series for the complete year of 2009. The choice of the year is such that it has a nodal factor as close to unity as possible

for the nodal cycle (18.6 years). For the present period this happens to be in the year 2011, but demand data is only available from April 2001 to April 2010 [10].

The buoy data is a true in-situ record of sufficient length to allow confidence in its fidelity, therefore for this analysis it is reasonable to treat reconstructed moored buoy data as the 'gold standard'. The only concern is that this data is not for the exact location of interest, the original buoy data was recorded about 7.5 km from the area of interest. The average peak values identified in [5-6] are used to scale up the resource. Using this approach helps retain the correct phase of the tidal signal as well as provide the most accurate tidal current velocity for the location. Although tides are spatially very varied, this is the best way to combine the data sets without carrying out a full scale site assessment which would require extensive and expensive in-situ survey and numerical modelling activity.

3. Demand

Half hourly demand data is published online and available from National Grid, the Transmission System Operator in Great Britain. The IO14_DEM values are used; this is the sum of all the generation. It takes into account station load but not pump storage pumping [10].

Figure 2 shows the mean daily profile demand for the year 2009. Also illustrated are the days when peak and lowest demand occurred in 2009. This graph shows the extent of diurnal variation in electricity demand and how they vary reflects seasonal effects. It is worth noting that the mean day has very distinct characteristics. There is an increase in the profile between the hours of 1600 and 1800. This two hour slot is usually when demand reaches its peak over the winter period, used by National Grid to determine the charge it levies on the electricity supplier know as Triad demand.

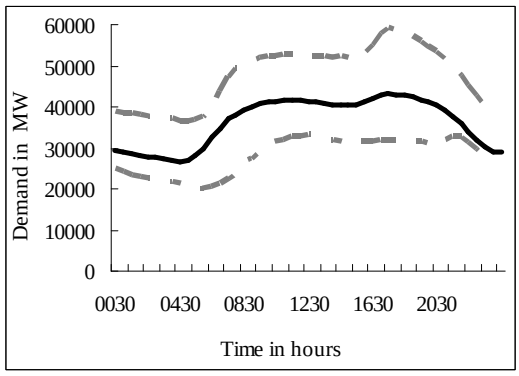

Figure 2: Mean demand daily profile for the year 2009.

3.1 Fluctuation in Demand

The UK electricity system has an average demand of 36449 MW, with a Standard Deviation of 7774 MW. Demand for electricity peaked at 59140 MW in 2009. The lowest demand is 34% of this peak value and the average demand is about 62% of this peak. This peak is estimated to be around 62.8 GW by 2016/17, assuming a growth rate of 1.2% per year [11]. Figure 3 shows the load profile covering two 14 day periods in January (winter) and July (summer). The January period includes the occurrence of peak demand, on the 6th of January between the hours of 1700 and 1730. The July trend shows where demand is at its lowest on the 2nd of August at 0600.

Load patterns are very distinct in this graph, for example demand for working days (Monday –Friday) can easily be distinguished from non-working days (Saturday and Sunday). The seasonal variation can also be identified here. On average about 7GW are consumed more during the winter period than during the summer period. This demand pattern is distinct to the UK and most northern European countries where the winter season is dominated by short daylight time and the need for heating along with the normal

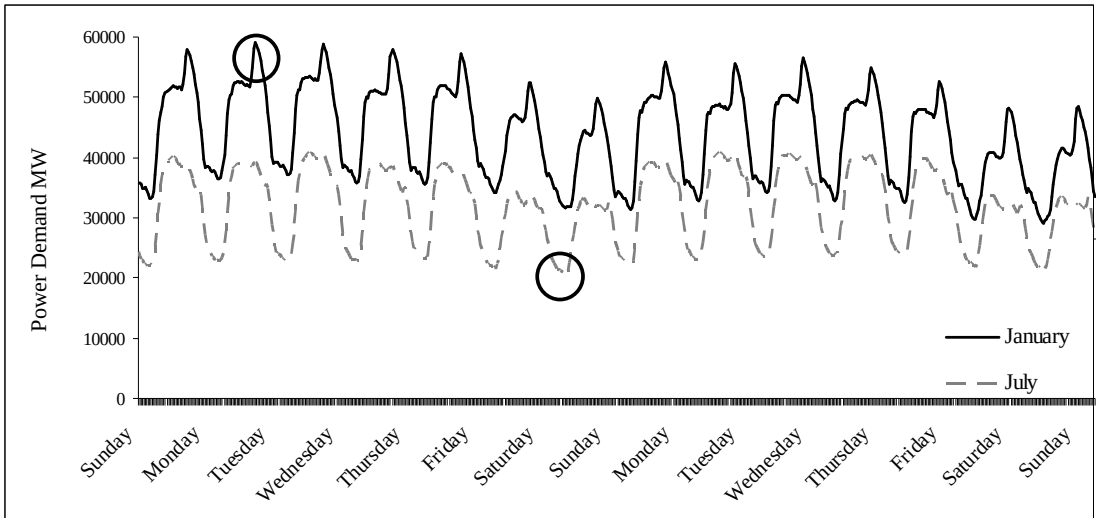

Demand in UK over a 14 day period in 2009. Data for the month of January from 5th to 18th and for 27th July to 9th of August. The graphs caputre periods of peak demand (6th January, 1730) as well as periods when the demand is at its lowest (2nd August, 0600).

Figure 3: Demand in UK over a 14 day period in 2009

working load gives it its 'peaky-ness'. The daily and seasonal demand pattern can significantly vary in countries that experience different weather conditions or work practices.

Generators require periodic maintenance and occasionally there will be unplanned outages. Therefore power systems are designed to deal with demand fluctuations and periods when several power stations are unavailable due to planned shutdown or unexpected failure. A range of plants are used to meet the daily demand, from some that mainly provide a base load output and can be slow in reaction to change in demand to flexible plant that meet rapid swings in demand [12].

Understanding demand trends will help forecast future demand patterns. This can in turn be used to 'match' with variable resources. Timing is a very crucial and a key factor as demand for electricity is high at very specific times of the day and supply response needs to be instantaneous for the system to be stable. Figure 4 shows inter half-hourly analysis of demand fluctuation in 2009, obtained by measuring the difference in demand between each half hour period.

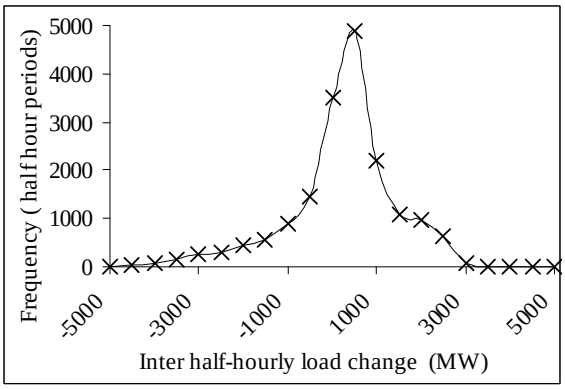

Figure 4: Inter half-hourly demand change in UK during 2009.

3.2 Scaled Demand

As this paper is only investigating the impact of one generation facility on the network, it is necessary to scale the demand down to simulate the response of a regional distribution network. It is assumed that the scaled demand will have similar demand timing characteristics to a local distribution network which would likely be the connection point of a small array of first generation tidal turbine devices.

Demand for electricity has been scaled down from 59.1 GW peak demand to 200 MW, so that demand and supply for tidal generation are comparable to each other while maintaining likely demand variability patterns.

4. Supply

The supply considered here is the output obtained for the chosen site with two hypothetical farms. The first scenario consists of 40 devices that has a rated power of 0.5 MW, making total rated power generation to be 20MW. The second scenario consists of 80 devices with a total generation potential of 40 MW.

For both scenarios, it has been assumed that the tidal current energy resource is not impacted by the operation of extraction devices. As the scale of energy extraction increases, the energy available in the system for extraction will be reduced to some extent [13]. For a larger development project, it will become more important to take appropriate considerations of the potential reduction of resource available for harvesting.

Figure 5 shows the power curve of the hypothetical generic device appropriate for this site. The diameter is assumed to be 16 meters, cut in velocity of 0.7 m/s and the rated velocity of the device is 2.25 m/s. This velocity was obtained by considering the 3rd quartile of the highest velocity recorded in the time series [14].

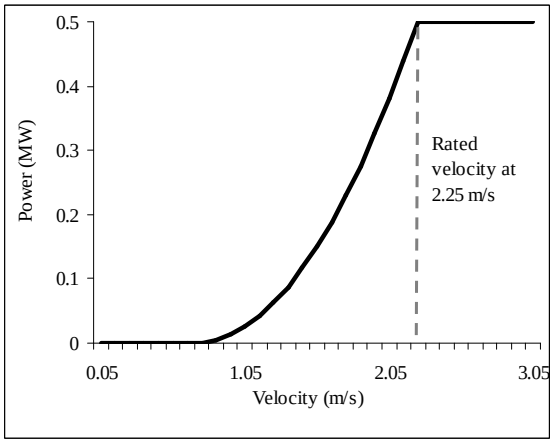

Figure 5: Power curve of a typical tidal device. Power rated at 0.5 MW

For this device the efficiency has been assumed to be about 42% on the basis of [15].The annual energy production for each device at this site is the sum of all the energy produced within the operational range of the turbine. In this case, the actual production is 1327.3 MWh which represents a capacity factor of 30.3%. This is substantially lower than what conventional power plants achieve but comparable with other variable renewable technology approaches such as wind.

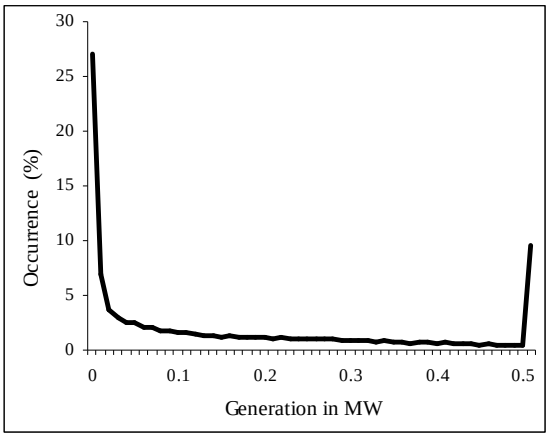

Figure 6: Tidal power generation and its occurrence by the postulated hypothetical generic tidal device.

Figure 6 illustrates the percentage of time the device generates a specific amount of power. Device characteristics are such that, it operates at rated power for 9% of the time and is idle for 27% of the time.

4.1 Supply variation

Intermittency is part of the electricity system; it needs to cope with plant shutdown and variability in demand as it follows different daily and seasonal trends (as already discussed). How much difficulty will the addition of variable generation from tidal energy harvesting pose the network operator with increasing levels of penetration?

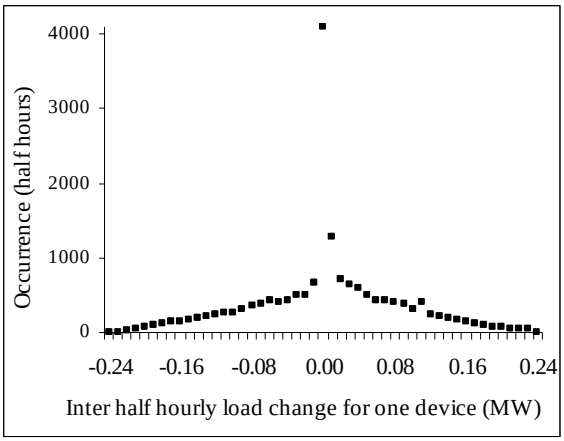

Figure 7: Tidal power fluctuation for one device.

Figure 7 illustrates the fluctuations generated by one 0.5 MW tidal power device. The frequency of occurrence (change over a half-hour period) is very high at 0 MW as there are periods of no generation during slack and neap cycles when the velocity is too low for generation. When the device is operating at rated power, the change observed is also zero hence adding to the accumulative 0 MW change. Outputs from figure 7 are different to the wind generation pattern shown in [1] as the nature of the resource is different and importantly [1] looks at the aggregated output from a number of sites. The asymmetry of the graph is an indication of site specific resource characteristics.

5. Demand and Supply fluctuations

Figure 8 shows demand fluctuations on the day of peak and lowest demand. Also plotted on the same graph are the simulated 20MW and 40MW generation scenarios. At the exact moment of peak demand, the tidal resource is generating no power. The tides are in their neap cycle, so generation potential is low even if the demand and supply peak were coincident. The generation at 1500 hours does not help service peak demand. As demand is increasing, tidal generation is reducing – therefore it is an even bigger swing for the network to cope with in this case. This may potentially imply that this site has a low capacity credit, depending upon the variation of the tidal cycle and how it progresses with respect to demand. This would require further analysis that is currently under development.

On the other hand, looking at the day when demand is lowest – generation from tidal production can meet more than 50% of the demand. This could be cause for concern as combined with base load generation supply may exceed demand. If this is the case, the system operator may choose to export excess power or curtail the output of the tidal power plant depending upon the network capacity. This will in turn affect the operational cost as the site may be underutilised.

The penetration level at which supply exceeds demand is not a limit for the resource. After this initial level of generation the market value and cost of generation will change to accommodate the need for curtailments or exporting energy elsewhere [1].

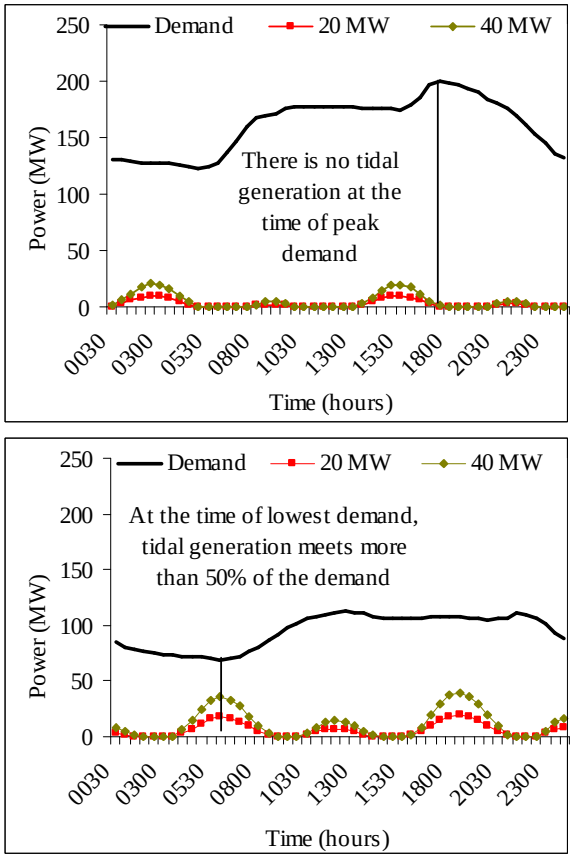

Figure 8: Demand and tidal production in the two scenarios.

5.1 Perturbation at 10% and 20%

Figure 9 shows a more systematic way of investigating the extent to which the introduction of tidal energy affects the perturbation observed by the system operator. Comparing this to the work done in [1] shows that there is more excursion at both the tails of the distribution curve. This is mainly because only the output from one generation location is being considered here and does not benefit from aggregation of locations to dampen the 'peaky' operational characteristics of tidal current energy generation. The aggregate effects of a number of tidal current energy locations would be expected to produce an excursion characteristic more in line with those produced for wind. Additional sites will be geographically diverse and bring individual site characteristics to the

equation along with phasing aspects associated with tidal energy. The extreme case for negative changes above 17MW and below 9MW are summarised in table 1.

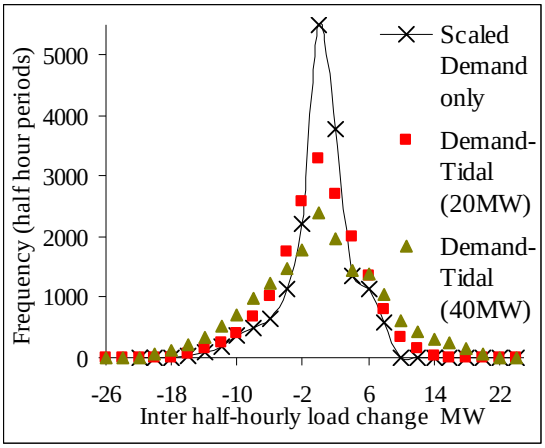

Figure 9: Inter half-hourly demand changes in UK for 2009 along with what the system operator would see if there was 20 MW and 40MW (Demand –Tidal) tidal generation.

Tidal Penentration %			
	None	10%	20%
Maximum decrease: MW	18.51	20.83	26.03
Number of decreases of 17 MW and above	1	17	211
Maximum increase: MW	9.38	15.82	23.91
Number of increases of 9 MW and above	12	538	1811

Table 1: Key data for half hour power excursion in scaled demand.

6. Conclusions

This work presents outcomes from examining one generation facility. This analysis shows that more and larger power excursions are created that need to be handled by the system operator. Another aspect to consider is the aggregate impact of a number of sites on the network. Further work will look UK wide and assess the potential cumulative impact on the network.

The electricity network will potentially require extra reserves to deal with higher power excursions. These extra reserves add to the cost of increasing variable generation on the network. The idea is not very different from adding conventional generation, except in this case the plant may have a low capacity credit. At higher levels of penetration this situation may change.

The consensus presented for wind demonstrates that there are no barriers to the implementation of wind in the network and the cost associated with the uncertainty can be as little as £2/MWh with 10% penetration [1]. Further work needs to be done in the tidal current energy case before a similar conclusion can be reached. The work presented is being further expanded to work towards this final goal.

Acknowledgements

The buoy records were supplied by the British Oceanographic Data Centre as part of the, Inter-Agency Committee on Marine Science and Technology funded, 'UK Moored Current Meter Data Set' DVD electronic publication. The data were collected by the Proudman Oceanographic Laboratory during the Mixing and sediment resuspension in shelf seas which was funded by the Natural Environment Research Council (NERC).

The authors also wish to acknowledge the provision of tidal analysis software by Chris Zervas at NOAA.

This research work is funded by the EPSRC Supergen FlexNet and SuperGen Marine Consortia.

References

[1] D. Milborrow (2009): Quantifying the Impact of wind variability. Proceedings of the Institution of Civil Engineers. Energy 162 Issue EN3.

[2] W.S Cooper, C.L. Hinton, N. Ashton, A. Saulter, C. Morgan, R. Proctor, C. Bell and Q. Huggett. An introduction to the UK marine renewable atlas.

[3] A. Sankaran Iyer, S. J. Couch, G. P. Harrison and A. R. Wallace (2009): Analysis and Comparison of Tidal Datasets. Proc. of the 8th European Wave and Tidal Energy Conference (EWTEC), Uppsala, Sweden.

[4] http://www.bodc.ac.uk/about/what_is_bodc/ BODC website (accessed on 31/05/10)

[5] DTI (2004): Atlas of UK Marine Renewable Energy Resource. Technical Report.

[6] http://www.renewables-atlas.info/ DTI (BERR) Marine Atlas.

[7] Marine Current Turbine (Accessed on 31/05/10) http://www.marineturbines.com/18/projects/20/the_skerries/

[8] C. Zervas (1999): NOAA Technical Memorandum NOS CO-OPS 0021. Tidal Current Analysis Procedures and Associated Computer Programs.

[9] J. D. Boon (2004): Secrets of the Tide. Tide and Tidal Current Analysis and Applications, Storm Surges and Sea Level Trends.

[10] National Grid (2009): Demand Data (Accessed on 31/05/10) http://www.nationalgrid.com/uk/Electricity/Data/Demand+Data/

[11] 2010 National Electricity Transmission System Seven Year Statement.

[12] R. Gross, P. Heptonstall, D. Anderson, T. Green, M. Leach, J. Skea (2006): The Cost and Impact of Intermittency. An assessment of the evidence on the cost and impact of intermittent generation on the British electricity network.

[13] G.Sutherland, M. Foreman and C Garrett (2007) Tidal current energy Assessment for Johnstone Strait, Vancouver Island. Proc. IMechE Vol. 221

[14] Phase II.UK Tidal Stream Energy Resource Assessment. BLACK & VEATCH 2005.

[15] J. Thake (2005): DTI Development, Installation and Testing of a large scale tidal current turbine.

Assessing the impact of ADCP resolution and sampling rate on tidal current energy project economics

Tim Stiven[*], Scott J. Couch[**] & A. Sankaran Iyer
Institute for Energy Systems, School of Engineering, University of Edinburgh, EH9 3JL, Scotland, UK
[*] Now with Ocean Power Technologies Ltd, Warwick Innovation Centre, Gallows Hill, Warwick CV34 6UW, UK
[**] Corresponding and presenting author

***Abstract* - This research examines the impact of accuracy in tidal current energy resource assessment on the likely economics of a tidal array project, ultimately estimating the impact of resource uncertainty on overall lifetime project economics. The analysis utilises field data gathered at 3 key locations at the European Marine Energy Centre (EMEC) tidal test-site in the Fall of Warness, Orkney. Data analysis techniques appropriate for application to tidal current energy projects are presented and the results obtained interpreted. The widely adopted Matlab code *t_tide* is then used to conduct harmonic analysis of the tidal current velocity data records. The adjacent ADCP records enable analysis of the spatial variability of the tidal resource at the EMEC site. Electricity generation potential and project revenue estimates are generated using simple and clear assumptions regarding typical tidal turbine topology and array layout. The impact of resource uncertainty on the prediction of Annual Energy Production (AEP) of the idealised array is calculated by varying the temporal and spatial resolution of the ADCP data utilised as input to the analysis, and similarly by using various lengths of the measured tidal records. These scenario based predictions are analysed in a simple financial model to examine the effect resource estimate uncertainty has on the projected returns on investment. Overall, the results suggest one clear conclusion: the range of impacts on project economics of uncertainties introduced by the resource estimation process warrant greater investment of time and money by project and technology developers at an early stage of development.**

***Index Terms* — Renewable Energy, Marine Technology, Tides.**

I. Introduction

In the wind energy industry there are established tools, techniques and procedures for resource assessment enabling project developers and their lenders to agree on the 'certainty' of their project return estimates. Characterising the resource is a critical part of estimating project revenues and is a key risk for project finance. No equivalent tools or techniques have been established for the nascent tidal energy industry. This will hinder deployment of commercial scale arrays and hence industry development.

Though appropriate technologies exist to measure the tidal resource, much less is understood about how to make cost-effective use of the technology to produce 'bankable' estimates. This research draws on the historic database of tidal resource measurements from the European Marine Energy Centre (EMEC) in Orkney to make recommendations on how to optimise tidal resource assessments.

A. Background

Across Europe, challenging targets have been set for the reduction of overall Greenhouse Gas (GHG) emissions. A key foundation of achieving these targets is the rapid de-carbonisation of the energy industry. In many European states, electricity generation is primarily derived from centralised coal and gas burning power stations. For example, the major electricity supply providers by resource type in the UK for 2010 can be broken down as 47.4% gas, 28.4% coal, nuclear 15.6%, and 6.9% renewable [1]. Hence, displacing carbon intensive fossil-fuel electricity generation plants with renewable energy generation solutions has become a cornerstone of 21st Century energy policy. Development and application of renewable energy approaches and technologies has rapidly become established as a major industrial activity (e.g. total renewable electricity capacity increased by 12% in the UK between 2009 and 2010 [1]).

Tidal current energy resources around the UK coastline are among the most energetic in Europe, created by tidal propagation through straits, resonant systems and around headlands linking the Atlantic and North Sea [2]. These energy resources are variable but largely predictable as the underlying tide generating forces are the product of gravitational attraction between the combined Earth-Sun-Moon system. Hence, tidal energy has the potential to offer complementary availability in a future energy mix with other variable renewable energy sources such as on- and off-shore wind, wave and solar energy. Tidal current energy research, development and demonstration have been gathering momentum in the UK over the last decade, in no small part due to financial support from UK government organisations [3]. Development of pioneering tidal current energy converter (TEC) technologies has now reached pre-commercialisation

T.S. acknowledges support for his MSc studies from the Panasonic Trust and the Royal Academy of Engineering who administer the scheme on behalf of the Panasonic Trustees. S.J.C. acknowledges the support of the EPSRC Supergen Marine research consortium (Grant number [EP/E040136/1]). A.S.I. acknowledges the support of the EPSRC Supergen Flexnet research consortium (Grant number [EP/E04011X/1]).

demonstration of full-scale devices in the open sea. Nonetheless, there is still much to learn about technology optimisation, the tidal energy resource, its conversion and economic delivery, and the operating environment for TEC technologies on the way to development of a mature industry.

B. Learning from the experience of the wind industry

There are high-level similarities between the emerging tidal industry and the more mature wind industry. Hence, given the immaturity of TEC technology development and the lack of experience of utility scale generation of electricity from TEC devices, the emerging tidal sector often looks to the more established wind industry for knowledge transfer. This can be seen at a technology development level, in terms of the necessary infrastructure at a project and industry scale, and in terms of policy support mechanisms. The focus of the research being reported herein is in understanding the impact of tidal resource uncertainty on utility scale project economics. This is an area where it is possible for tidal industry development to benefit from the experiences of the wind industry by assessing the potential for adoption and adaptation of existing methodologies underpinning wind energy resource characterisation tools and procedures.

II. An Investor's Perspective on Tidal Energy Economics

Aside from the obvious technological, and operational developments that are required to deliver commercial scale marine energy projects (e.g. scaling up the technology, demonstrating reliability, development of the installation and maintenance supply chain), it is critical that the finance community considers marine energy projects a sound investment offering returns at least as good as those available elsewhere in the energy market. The role of 'project finance' has been instrumental in the commercial deployment of wind power, both on and off- shore; it is likely to be similarly vital in the marine energy sector.

Potential investors in energy projects (tidal or otherwise) will consider a wide range of risk factors; typical considerations are listed in table I. Many of the risks in a project can be appropriately managed through time. For instance failing contracts can be terminated (and new suppliers found) or renegotiated, and Government agencies seldom apply new legislation in retrospect. Where then do resource estimates sit in the consideration of project risk? The role of resource estimation is informing decisions to ensure correct sizing of the plant and enable accurate forecasting of the revenues from generation.

An important metric of the economic effectiveness of any energy project is the capacity factor – the ratio of the potential output of the plant over a period, to the maximum theoretical 'nameplate' output delivered over the same period (which itself is a function of the reliability of the plant, its power curve characteristic and the distribution of the resource (wind/ tide speed) over the period of interest). The higher the capacity factor, the more quickly the plant will recover the capital invested. More importantly, if the cost curve for installed capacity (in terms of £/MW installed capacity versus rated plant output) is known for an array of devices, then the optimum array size (and hence investment) for the given resource can be derived. For these considerations to work effectively, the resource availability at the site of interest must be accurately forecast. Hence, accurate resource estimates have a significant part to play in successful financing of tidal energy projects. It is clear then that resource prediction is potentially a substantial risk for the economics of tidal energy projects. Looking instead at the opportunity, it should follow that accurate resource estimates hold the promise of reducing the risk of tidal energy projects: increasing the likelihood that they will attract investment and reducing the cost of the project. Even in the more established wind industry, there is evidence that better wind forecasting is reducing the cost of finance for projects. The Economist magazine recently reported [4]:

> "[project] developers use a statistical model to obtain a 'P90' wind value - the average wind speed in which they can be 90% confident. The closer the P90 reading is to the measured average speed, the more attractive the site becomes to investors. If the P90 wind-speed is within 12-15% of the average, banks are usually happy to stump up. But a difference of 20% or higher renders a wind farm "un-financeable". …Conversely, reducing the error margin to 7-10% can reduce a project's cost of funds by 0.5-0.75 percentage points, resulting in higher investor returns."

In case this seems insignificant, a basic hypothetical example will illustrate the potential impact on overall project economics: Suppose an offshore marine energy plant project with a lifetime of 20 years is proposed with an installed capacity of 100MW at a capital cost of £1.5M per MW of installed capacity. The project capital requirement is £150M. If the split between debt and equity is 66/33, the bank loan required is approximately £100M. Assuming the cost of the debt is 7.75% in the 'high' case (where the resource

TABLE I: Typical risk considerations in energy projects

Category	Risk Consideration
Regulatory	How is the electricity market structured and regulated? Can cost increases be passed on to consumers through price increases?
Regulatory	How stable and long-lived are revenue support mechanisms for renewable electricity (e.g. ROCs in the UK)
Merchant/ Market	What are the anticipated price variations for electricity? What proportion of the project's output should/ can be sold forward in a Power Purchase Agreement?
Project execution	What are the supply Chain risks? What is the ability of sub-contractors to deliver against the requirements of their contracts? How competitive is the market for supply if alternatives are required?
Revenue	What is the confidence in the plant's reliability?
Revenue	What is the confidence in the estimate of the available resource for electricity generation? Has the plant been sized correctly given the available resource?

estimate error is in the range 12-15%) and 7% in the 'low' case (with a more accurate resource estimate), then, applying an approach outlined in [5], the capital cost of the project is reduced by more than £11M in current cash terms (or if a discount rate of 15% is applied, capital cost is reduced by more than £4M when considering Net Present Value).

III. Energy Resource Measurement and Prediction

There are broad analogies, for resource estimation, between the wind and tidal energy markets. Principles for resource assessment and prediction in the wind industry are well established with many engineering consultancies offering appropriate services to project developers and operators. Similarly, device performance assessment is documented in appropriate international standard documentation [6]. The existence of this institutional experience and know-how gives lenders and potential investors confidence. Development of similar technology performance assessment approaches have been proposed for tidal energy application [7, 8], and separate 'Technical Specification' documents are now under development for tidal energy resource characterisation and TEC device performance assessment under the stewardship of the IEC. However it must be recognised that at heart, the wind and tide are different natural process: the variation of wind is stochastic, but tidal variation is deterministic. As such the tide lends itself to harmonic analysis, based on a least squares decomposition of a measured record of tidal velocity [9]. The industry standard for measuring tidal velocities is an Acoustic Doppler Current Profiler (ADCP). When a tidal prediction is subsequently generated from harmonic analysis, the estimation of Annual Energy Prediction (AEP) from the velocity probability distribution is theoretically straightforward.

A. Wind Energy Approach

The IEC International Standard document [6] lays out agreed procedures for measuring and predicting the wind resource at a given site and for forecasting the AEP for a given design of turbine. The Standard requires that actual wind velocity measurements are taken at the site of interest for a period of sufficient length to generate a representative sample of the long-term average wind velocity and its distribution around the mean. Measurements are typically made using a mast mounted cup anemometer and wind vane (the measurement of wind speed and direction is conducted at, at least 1Hz or higher and reported as averaged over 10 minutes). Equipment set-up and measurement procedures are closely prescribed by the Standard, as are methods for quantifying measurement uncertainty. When the wind speed distribution at a given site has been established a 'method of bins' is used to segment the data to give a probability of occurrence of a wind speed within a defined range over a representative year. If the variation of turbine power output with wind speed is also characterised by measurement, then the Annual Energy Production can be estimated from summing the power output across each 'bin' multiplied by the total number of hours for which that wind speed occurs in a given year.

Accurate characterisation of the mean wind speed at a given site requires many years of continuous measurement; other important characteristics (e.g. wind shear and turbulence intensity) require 6-12 months of data. To shorten project timescales, the wind industry typically applies a 'Measure – Correlate – Predict' technique, where shorter-term measurements (e.g. over 6 months) at the project site are correlated with a known long-term data series from a nearby location (e.g. data from a nearby airfield). Long-term predictions for the project site are then derived assuming that the distribution of wind speeds around the mean are the same as at the reference site. For detailed site design ('micro-siting', in the industry jargon), numerical models are validated against local site measurements to determine the wake effects of terrain and other turbines in the array. A wide range of proprietary software tools supports this market (e.g. WAsP, GH WindFarmer). Additionally, processes for application of detailed bespoke CFD numerical simulations exist for application to particularly complex projects (e.g. complex terrain) where the extra investment in ensuring accurate understanding of wind resource variability is deemed beneficial.

B. Tidal Energy Approach

The principles of tidal and wind resource assessment are common, in so far as, actual measurement of the resource variation with time combined with an accurate description of the energy extraction device performance characteristics can deliver long term estimates of energy production over the life of the project. However, the long-term variation of wind speed is a stochastic process, whereas tidal variability is deterministic. Hence the detailed analysis of the variation of tidal velocity over time has some critical differences. In particular the use of the measured record is different. Typically, a wind resource assessment uses the measured record to determine the mean wind speed and a Weibull or Rayleigh distribution is assumed to describe the parametric variation of wind speed around the mean for future prediction [10]. In contrast, for tidal energy, the analysis of the measured record requires a different approach. Harmonic analysis is used to determine tidal constituents representative of that exact location that can then be used for future prediction, again using harmonic analysis techniques. Harmonic analysis uses a least squares approximation to 'fit' the measured tidal record to the known forcing frequencies and seeks to determine the phase and amplitude of those dynamic constituents at the site of interest. In both the wind and tidal cases, the predictions extrapolated from real world measurements can be used to validate numerical models representing the detailed characteristics of the project site, which in turn enable informed decisions to be made regarding the optimal installed capacity and siting, which, finally, allows economic calculations based on Annual Energy Production from the whole site and return on capital to be projected.

C. *Difficulties associated with the tidal energy approach*

Typically harmonic analysis has been the preserve of oceanographers studying the long-term variation of the seas. Engineering interest has generally been reserved for shoreline interactions and navigational safety – the purpose of utilising harmonic analysis for tidal energy prediction is distinct.

If a tidal measurement record is visualised in the frequency domain (a plot of spectral density against frequency), then the tidal energy elements will appear as peaks around the discrete forcing frequencies of the harmonic constituents. Non-tidal energy will be evident as broadband noise (or long period seasonal effects may appear at discrete frequencies). By their nature, these non-tidal phenomena are longer-term processes with lower temporal variability. A tidal current measurement for energy extraction is concerned primarily with the tidal element of the measured signal and hence will require a relatively short sample period. One of the purposes of this research effort is to examine the sensitivity of resource estimates to measured resource data characteristics (e.g. sample periods). Another potentially significant part of the measured record will be instrument error and noise and shorter-term wave and wind effects, which will have an influence in coastal regions at limited depth. It is important to be able to separate and analyse both tidal and non-tidal elements of the record to understand their impact on TEC device performance.

Potentially the most significant determinant for the quality of the measured record and the subsequent resource prediction is the total length of the record and the sample interval. The length of the measurement record directly impacts the number of tidal constituents that can be derived from the harmonic analysis. The longer the record length, the easier it becomes to resolve between constituents of similar frequency. To develop confidence in the resource estimate derived from harmonic analysis, it is important to understand what the key determinants of the quality of the measured record are.

IV. Methodological Approach

A tidal energy resource assessment should most appropriately be based on a harmonic analysis prediction for the location of interest assuming a suitable ADCP record is available. The most complete understanding of the impact on project economics is made possible by taking account of the characteristics of typical tidal turbines. It is then possible to derive simplified predictions of AEP following [7] (which itself broadly follows [6]). This approach has the advantage of super-imposing the limitations of the selected TEC turbines in extracting energy from the flow. The first step of the analysis is to generate a velocity probability distribution based on the tidal resource characteristics generated from the harmonic prediction (in this case the bin width is set at 100mm/s). When the velocity distribution is known the AEP is calculated from equation (1):

$$AEP = 8760.A_v.\sum_{i=1}^{i=N_B} P_i.f_i \qquad (1)$$

Where 8760 is the number of hours in the year, and A_V is the mechanical availability of the machine as a percentage (assumed to be 100% in this study - though this is far from realistic, as long as the value is maintained as a constant throughout the comparisons, the absolute value is not important). P_i is the power output of the machine in the i^{th} velocity bin, and f_i is the probability that the velocity (the average of the velocity bin range) of the i^{th} bin will occur. Finally, N_B is the total number of velocity bins. The power output of the turbine in any given bin, i, is then:

$$P_t = 0.5.\rho.A.C_p.U_i^3 \qquad (2)$$

Assuming a typical horizontal axis TEC configuration of turbine diameter 16 metres (to assess the swept area, A), in water of uniform density (ρ) 1025 kg/m^3, we only have to estimate the machine's C_p and rated speed to generate a 'typical' power curve to give P_i and then an AEP prediction. If the machine operates on the principle of variable speed/ controllable pitch, it is a reasonable approximation to assume that it achieves a relatively constant C_p up to its rated speed. Assuming a C_p of 0.42 and a rated speed of 2.4 m/s gives a power curve as shown in fig. 1 (rated power of 600kW). All of the assumed turbine characteristics have basis in proven existing operating device performance. The results of the AEP analysis can then be used to understand the performance of an idealised turbine. For this analysis, the assumption of uniform inflow conditions across the rotor swept area with flow consistently perpendicular to the plane of the rotor disc has been applied. Clearly this is a substantial simplification over

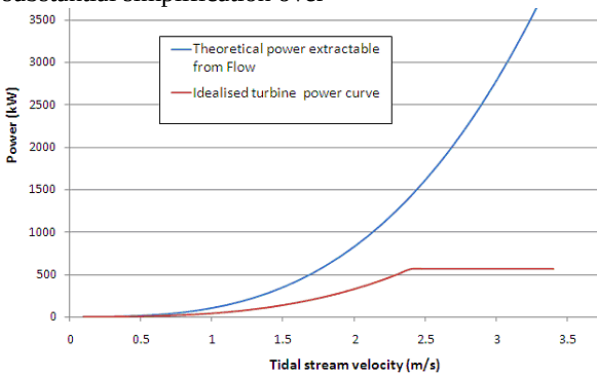

Figure 1: Idealised TEC device power curve used in the analysis.

the real world scenario where the velocity shear across the turbine swept area should be modelled, but is adequate for consistent comparisons of AEP based on different approaches to measuring and predicting the tidal currents in an area of interest. An estimate of annual revenue generated by a hypothetical project is possible after making some further assumptions. An array of approximately 50MW is taken to represent a typical early stage commercial project (at 0.6MW rated output per machine this gives a total of 83 turbines). The wholesale electricity price is assumed to be £30/ MWh and the Renewable Obligation Certificates received by the project owner for each MWh generated are assumed to have a buy-out price of £30 each (a conservative approximation of the value

set by Ofgem of £36.99/ MWh for 2010-2011 [11]). Under the assumption of a project based in Scottish waters, the venture would benefit from government support of 3 ROC payments for early stage tidal energy projects. This basic scenario will in later sections provide a means of comparing the revenue generation of various simulated development scenarios.

The principles of operation of an ADCP device are straight forward, but it is important to understand the errors and uncertainty that they introduce to any resource prediction. Hence, a brief description of key ADCP operational and quality control measures follows. Interested readers can address a more comprehensive treatment by one of the available device manufacturers (upon which this description is based), in [12].

The operator sets the ADCP device 'ensemble period' and returns from each 'ping' are averaged across the ensemble. As random measurement errors are normally distributed about the mean, increasing the number of pings per ensemble reduces the standard deviation of the error (in proportion to the square of the number of pings). This is useful to the point where the random error is less than the bias of the machine, which cannot be corrected ([12] reports bias of the order of 10mm/s velocity as typical). In general, the ADCP unit does both depth and ensemble averaging before transmitting results to the data collection system (this can be over-ridden by the user, however, it has the advantage of reducing the data volume needing transmission, and the ADCP automatically corrects velocity vectors to earth co-ordinates and corrects for beam pointing angle errors). However, external errors (from turbulence in the water column, for example) tend to dominate ADCP error. These can be estimated by computing the standard deviation of the reported velocity errors. In addition the ADCP reports 3 other quality control measures to enable judgement of measurement quality (summarised in table II). Neither sound speed variation with depth or thermoclines substantially effect data quality. However strong echoes from the sea surface (for bottom mounted units) must be removed from the data record.

TABLE II: Quality control measures for ADCP operation (source [12]).

Quality Control Measure	Detail
Echo intensity	Data output in units proportional to decibels (dB) and are a measure of the proportion of the energy in the return echo to the energy sent out by the ping. The stronger the echo intensity, the more reliable the data.
Correla-tion	A measure of data quality (ping/ echo signal correlation for detecting small phase changes - well correlated ping/ echo signals look similar). Output is scaled in units such that the expected correlation (given high signal/noise ratio) is 128.
Percent-good	Data tell you what fraction of data passed a variety of criteria. Rejection criteria include low correlation, large error velocity and fish detection (false target threshold).

V. Source Data

The data set informing this research utilises a range of surveys conducted by the European Marine Energy Centre (EMEC) in the period 2005 -2007 at the tidal test-site located in the Fall of Warness, Orkney. A number of criteria were applied to identify those surveys most suitable for this analysis from the suite of surveys made available by EMEC – these were:

- Record length – a record of greater than 30 days duration is desirable, for better constituent resolution and to allow the effect of record length on resource prediction to be analysed.
- Temporal resolution – short ensemble periods are desirable to allow post measurement 'down-sampling' of the record to examine the effect of temporal resolution on resource predictions.
- Spatial resolution – surveys that are well separated around the location are desirable to develop an understanding of the impact of channel bathymetry on the optimal spatial resolution of samples.

For these reasons, surveys 7, 10 and 13 were selected as a baseline for further investigation and comparison. The approximate locations of these survey measurements are shown in Fig. 2 (page 10). Alongside the data sets, EMEC issue separate quality control reports on each of the surveys against the criteria outlined in table II and limits defined by the ADCP Original Equipment Manufacturer (OEM). They conclude that, all three surveys represent good quality data.

The ADCP data provided comprise text files that represent north, east, vertical and error velocities (units mm/s) against ensemble number and time across the full range of depth bins. Having removed the ancillary data from the record, the following procedures were applied:

- Where necessary, remove the start and end of the time series when the instrument is deployed but no measurements are made.
- Replace identified 'bad' data in the record with NaN entries (which are then ignored by Matlab during analysis).
- Remove the top and bottom of the water column record from the dataset. At the water surface the top 5m of the record is removed to take account of:
  - Surface reflection/ side-lobe suppression (see [12]);
  - The variability of water depth through the tidal cycle;
  - The envisaged practical limit of the top of a TEC device's swept area for navigational safety clearance and to avoid excessive cavitation;
- At the bottom of the water column, the record from the lower 25% of the total depth is removed, because in a realistic turbine deployment project:
  - The resource close to the seabed tends to be of limited economic value for harvesting - strongest flow characteristics are experienced in the upper half of the water column.
  - Additionally, this minimises shear loading on the turbine due to the strength of the boundary layer near the sea-bed;

- Depth-average the East and North velocities across the remaining depth bins for every ensemble sample in the record, giving a single column velocity vector for both components.
- Where the temporal resolution of the record is to be investigated, sample the depth averaged velocity vector at the user specified resolution according to one of two approaches: discrete sampling or period averaging. At the same time the time series vector is 'down-sampled' so that the ensemble number corresponds with the new temporal resolution of the velocity record.

The data presented for harmonic analysis is therefore representative of an idealised water column with no velocity variation with depth. The harmonic analysis is conducted using *t_tide*; a suite of programmes implemented in Matlab code [13]. In order to validate the *t_tide* results the authors conducted some basic comparisons with model output against the model described in [14] (not shown). The two models were in excellent agreement in terms of harmonic analysis outputs, often in agreement to the level of insignificant decimal places. Output from subsequent harmonic predictions were also in generally excellent agreement, although the more refined selection of harmonic constituents for inclusion in the analysis provided by *t_tide* did in certain cases lead to some divergence in the predictions generated.

Before conducting harmonic analysis, the properties of the raw survey datasets were analysed. Table III summarises the key characteristics following adoption and adaptation of a methodology presented in [15]. Following a common approach to data presentation allows comparisons to be made between the data presented here and data from other location in the future. To aid understanding and interpretation in a tidal energy context, the metrics are presented representing the entire dataset, and additionally separated into flood and ebb, with tidal velocities below 0.5 m/s considered as slack. In terms of energy generation, velocities of 0.5 m/s or less are of limited significance, as a typical TEC device will not operate under such conditions. This is because a TEC turbine requires significant input thrust to provide enough rotational torque to overcome friction in the turbine system. Ebb and flood regimes are determined using principal axis decomposition. Presenting the flood and ebb tides separately highlights that the two regions have specific characteristics. The mean power density figures presented have been assessed for an assumed device hub height at mid depth. No further assumptions are necessary. There are important similarities and differences between the three surveys. The reader must keep in mind that the data presented in table III relates to 3 different time-periods. The main variations are in flow direction and vertical profile. The significant variation in vertical profile is potentially of major significance from a tidal current energy perspective (and general interest relating to properties of extreme tidal regimes), but is beyond the scope of this paper – it is mentioned in passing to highlight an area requiring further research effort.

TABLE III: Characteristics of the 3 survey records

		Survey 7	Survey 10	Survey 13
	SITE			
	1 Measurement duration (days)	32. 93	40.74	32
	2 Vertical resolution (m)	1	0.75	1
	3 Sampling interval (min)	10	20	0.5
	4 Mean depth (m)	48	26	36
	5 Assumed hub height(m)	Mid depth	Mid depth	Mid depth
	VELOCITY			
	6 Mean velocity magnitude (m/s)	1.58	1.66	1.69
	7 Neap Spring Ratio	0.34	0.38	0.41
	8 Max sustained velocity (m/s)	3.57 *	3.38 *	4.05 **
	9 Flood/ Ebb asymmetry	-0.24	0.19	-0.26
	10 AvgVertical shear (m/s per m)	0.014	0.017	0.024
	11 Max Vertical shear (m/s per m)	0.075	0.131	0.326
	DIRECTION			
	12 Principal axis direction (deg)	158	145	146
	13 Standard deviation (deg)	34.71	31.58	36.01
	14 Flood/ Ebb assymetry (deg)	-3.65	-19.75	-5.84
	POWER			
	15 Mean power density (kW/m sq)	3.74	4.04	4.70
	16 Flood/ Ebb asymmetry	0.63	1.30	0.69
	VERTICAL PROFILE			
	17 Power law exponent 1/(α)	5.4	10.5	11.3
	18 R -squared (α)	0.999	0.991	0.992
EBB	**VELOCITY**			
	19 Mean velocity magnitude (m/s)	1.85	1.72	1.96
	20 Max sustained velocity (m/s)	3.49 *	3.30 *	4.05**
	21 Avg Vertical shear (m/s per m)	0.013	0.014	0.029
	22 Max Vertical shear (m/s per m)	0.062	0.099	0.326
	DIRECTION			
	23 Principal axis direction (deg)	341.19	311.05	317.78
	24 Standard deviation	6.87	20.28	10.38
	VERTICAL PROFILE			
	25 Power law exponent 1/(α)	6.2	14.7	10.5
	26 R -squared (α)	0.998	0.991	0.963
	POWER			
	27 Mean power density (kW/m sq)	5.08	3.96	6.16
FLOOD	**VELOCITY**			
	28 Mean velocity magnitude (m/s)	1.61	1.91	1.70
	29 Max sustained velocity (m/s)	2.95 *	3.38 *	3.65**
	30 Avg Vertical shear (m/s per m)	0.016	0.021	0.022
	31 Max Vertical shear (m/s per m)	0.075	0.131	0.161
	DIRECTION			
	32 Principal axis direction (deg)	155.56	150.80	143.62
	33 Standard deviation	7.34	11.71	14.79
	VERTICAL PROFILE			
	34 Power law exponent 1/(α)	4.6	8.0	11.8
	35 R -squared (α)	0.999	0.994	0.994
	POWER			
	36 Mean power density (kW/m sq)	3.22	5.14	4.27

* For survey 7 & 10, max sustained velocity in an hour.
** For survey 13, max sustained velocity in 5 minutes.

VI. Impact of Data Variability on Resource Estimates

This section describes the results of the tidal analyses using *t_tide*, examining the effect on resource estimates of varying:

- The temporal resolution of samples at survey site 13;
- The overall record length at survey site 13;
- Spatial resolution across survey sites 7, 10 and 13;
- Signal to Noise Ratio (SNR) at survey site 7.

As a basic measure of the quality of the prediction, *t_tide*, reports the variance of the predicted tidal velocities as a proportion of the variance of the measured velocities. Clearly the higher the ratio, the better the prediction is considered to be. In all of the following results, the proportion "variance predicted to variance measured" was greater than 90%.

A. The impact of temporal resolution

Survey 13 was selected to examine the effect of temporal resolution of resource estimation because it spanned more than 30 days and had a basic ensemble period of 30 seconds, allowing 'down-sampling' to simulate the effect of a range of sample intervals. Initially both discrete sampling at different time

periods and period averaging were investigated. But the results for period averaging only are presented because it is considered more closely representative of the actual measurement process of an ADCP deployed with longer ensemble periods. As described in section IV, the standard ADCP process averages returns from all pings within a given ensemble to reduce measurement error; in effect period averaging a record with a short temporal resolution best simulates the effect of a longer ensemble period. Initially the record was analysed at the recorded ensemble period of 30 seconds. Then the measured record was period averaged to simulate a record measured at ensemble periods of 5, 20 and 60 minutes. *T_tide* was then used to generate predictions over the full length of the original time series from constituents based on a harmonic analysis of each of these records (including only those constituents with a calculated SNR greater than 2 as recommended by [13]). Brief inspection shows that there is effectively no variation in the predicted constituents for sample periods 30 seconds and 5 minutes. At a simulated sample interval of 60 minutes, 2MN6 is not significant, but the harmonic analysis picks up the long period (around 28 days) constituent MM at a frequency of 0.0015 cph; at a magnitude which is unlikely to materially affect the predicted currents. Plotting overlapping scatter diagrams using the measured and predicted velocity based harmonic analyses conducted at temporal resolutions of 30 seconds and 60 minutes clearly indicates that the temporal resolution of the sample has limited impact on the predicted velocity pattern (not shown).

To examine the impact, not just on the statistical distribution of the predicted tidal currents but on project economics, a simple analysis of likely AEP was conducted. The results of this analysis are presented in table IV. Again it is clear that there is very little difference in the predictions based on sample intervals in the range 30 seconds to 20 minutes. Only at an interval of 60 minutes are substantial differences in the predicted velocity distribution evident. Probably the most significant indicator here is the predicted Capacity Factor (a measure of the cost effectiveness of the investment in turbines as a function of the revenue generated from the available tidal current). With details of the potential impact on AEP in hand, the impact of the difference in tidal velocity predictions in terms of project economics (on the basis of the simple assumptions set out in section IV) can now be considered. If we assume that the most accurate forecast of the total revenue available from the project should be based on the prediction from the highest resolution tidal record at 30s sample interval (the original measurement record), then the total annual project revenue would be £22, 230, 170 and the maximum 'delta' caused by lengthening the sample interval to as much as 60 minutes would represent as much as 1.56% of the overall projected annual revenue.

TABLE IV: Survey 13 – Impact of temporal resolution on AEP predictions.

Sample interval	AEP (kWh)	AEP (MWh)	Capacity factor
30 seconds	2231945	2231.94	42.46%
5 minutes	2231652	2231.65	42.46%
20 minutes	2228365	2228.36	42.40%
60 minutes	2197145	2197.15	41.80%

B. The impact of record length

The survey 13 measurement record was also chosen to examine the impact of record length on the accuracy of prediction and the uncertainty of the resulting AEP estimate. The original record length of the full survey is 31.92 days. To examine the impact of shortening the record length on the harmonic analysis and subsequent prediction, the original data was split into 2 half records, each 15.96 days long. Importantly, each half record is still longer than the Spring/Neap cycle, suggesting that it should be possible to resolve the major constituents. Table V details the predicted significant major axis constituents for each case, and the data is alternatively presented in fig. 3 (page 10). Only 4 constituents are common to all 3 analyses: the principle semi-diurnal lunar and solar constituents M2 and S2; and then M6 (a higher shallow water overtide of the principal lunar constituent M2) and 2MS6 of period around 4 hours. Surprisingly, the harmonic analysis of the second half of the record returns two constituents that are not significant in the full record analysis: the approximately fortnightly Luni-solar synodic, MSF and the3MK7 constituent of period 3.53 hours. It should be noted that both these constituents are resolved in the full record, but they are not deemed 'significant' for use in the prediction because their SNR is below the user-defined threshold of 2. This emphasises the importance of improving the understanding of the error estimation technique employed by *t_tide* for tidal current energy application. In both cases, the shorter records significantly under predict the peak tidal velocities. Detailed analysis highlights that the largest reduction of peak velocity between the full and half records is 309 and 405 mm/s (East and North components respectively). This represents the introduction of what is considered significant potential error into the analysis dependent upon the selection of ADCP measurement record length for tidal current energy projects. The impact on projected AEP is detailed in table VI as for the preceding case. The impact on project economics represents a variation of as much as 14.92% of annual project revenue in the worst-case scenario (the difference in capacity factor can be seen as a simple indication of the potential economic impact). This is now indicative of resource uncertainty having a significant potential impact on project economics, even on the basis of 'judgement' rather than more detailed analysis.

TABLE V: Impact of data record length on harmonic analysis outputs.

Constituent	Frequency (cph)	Major axis constituent amplitude (mm/s)		
		1st half	2nd half	Full record
MSF	0.00282		61.855	
Q1	0.03722			49.208
O1	0.03873		85.663	100.882
K1	0.04178		61.593	66.544
EPS2	0.07618			127.911
MU2	0.07769			278.712
N2	0.079			520.203
M2	0.08051	2667.682	2326.934	2485.788
L2	0.08202			221.001
S2	0.08333	1007.398	1250.212	1141.182
MO3	0.11924			14.732
M3	0.12077	52.013		28.341
MK3	0.12229			13.689
SK3	0.12511	21.926		
M4	0.16102		59.704	61.785
MS4	0.16384		66.995	43.396
2MK5	0.2028			11.589
M6	0.24153	82.623	36.94	61.318
2MS6	0.24436	94.176	95.526	92.48
2SM6	0.24718		45.403	32.599
3MK7	0.28331		7.351	
# significant constituents:		***6***	***11***	***18***

TABLE VI: Survey 13 - Predicted AEP using various record lengths

Record length	AEP (kWh)	AEP (MWh)	Capacity factor
First half	2300413	2300.41	43.77%
Second half	1967361	1967.36	37.43%
Full record	2231945	2231.94	42.46%

C. The impact of spatial resolution

Surveys 7, 10 and 13 were selected to examine the impact of spatial resolution of resource estimates because: they all have record lengths in excess of 30 days; they are well separated with some differences in the local bathymetry; and the range of ensemble sample intervals (at 30 seconds to 20 minutes) had already been demonstrated to have limited potential impact on subsequent predictions. Fig. 2 (page 10) indicates the actual locations of each survey and table VII reports the latitudes and longitudes of each site and their physical separation in terms of distance and bearing.

TABLE VII: Position and spatial separation of surveys 7, 10 and13.

	Position		***Spatial separation***		
	Latitude	Longitude		Distance	Bearing
7	59° 08' 27"	02° 48' 59"	7 - 10	1,684 m	342°
10	59° 09' 09"	02° 49' 31"	7 - 13	797 m	134°
13	59° 08' 09"	02° 48' 23"	10 - 13	2,416 m	153°

The measured record data for surveys 7 and 13 were 'down-sampled', using the approach to 'period averaging' described earlier, such that all 3 records had effective measurement period ensemble intervals of 20 minutes. Harmonic analyses of each record (at the common ensemble interval) were conducted at a common threshold SNR of 2 against their original time base (start times range from March 2005 to March 2007). To assess the impact of spatial resolution, harmonic predictions were then generated from each set of constituents for a common start time and period length (19 Mar 2005 10:47:37, for 33.15 days, the start and duration of survey). As a result, the predictions based on surveys from all 3 sites can be compared directly. Figure 4 displays a scatter plot of the predicted velocity vector tips based on harmonic analyses of the measured records at survey sites 7, 10 and 13, with predictions to a common time base. Substantial variations are evident. All of the plots correspond well with the orientation of the bathymetry local to the survey locations. The most northerly dataset, survey 10, displays rotary aspects, although the plot is still substantially bi-directional. Site 10 also shows lower peak velocities than are predicted from the harmonic analyses of the records at sites 7 and 13. The prediction based on the record at site 7 shows an almost perfectly bi-directional tidal pattern with the highest peak velocities – which is consistent with its mid channel position at the point of greatest 'constriction'. If the flood tide is considered to be flow from NW to SE, then the prediction at 7 shows modestly greater velocities on the ebb. The prediction at site 13 is a little less linearly bi-directional, a minor East – West rotary element is indicated.

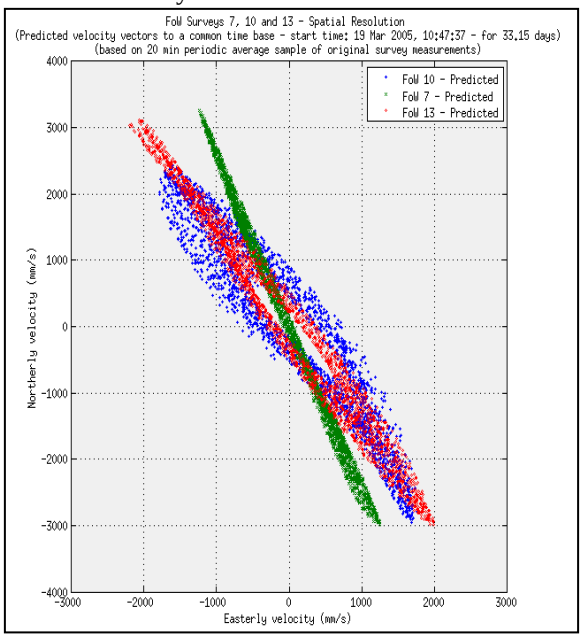

Figure 4: Comparison of spatial velocity variability between three adjacent ADCP records (maximum linear separation less than 2.5km – see table VII).

Continuing with the previous assumptions regarding typical turbine topology and the numbers required for a tidal array with installed capacity 50MW (16 metre diameter; and 83 turbines respectively) and further assuming that each machine is separated by 15 diameters downstream and 2.5 diameters perpendicular to the flow, the area of seabed required to accommodate the array can be assessed. At a 'per turbine' footprint of approximately 240m (length) by 40m (width), a 50MW array is likely to occupy an area of around 2000 metres by 400 metres if bathymetry variability enables a uniform distribution of devices in an array. Comparing this estimate with the linear separation of the survey sites listed in table VII, it is evident that the variation of predicted velocities presented here is a reasonable representation of what might be experienced across an array.

Fig. 5 (page 10) presents the significant constituents (at SNR threshold of 2, major axis amplitude only) generated by harmonic analyses for each of the survey records. It is evident that there is reasonable

agreement in both frequency and amplitude for surveys 7 and 13, located relatively closely in mid-channel. The prediction for site 10 shows significant variation, mainly in that different constituents at shorter periods are evident. Constituents clustered around the semi-diurnal frequencies dominate all the harmonic analyses. The resulting velocity probability distributions are plotted in fig. 6 (page 10). The lower probability of peak velocities for survey 10 is evident, and lower prediction of AEP for this location is therefore expected (table VIII), despite a higher probability of lower velocities in the approximate range 250 – 1000 mm/s (which are of limited use for energy generation as a typical turbine will not 'cut-in' until around 0.7 m/s).

TABLE VIII: AEP predictions based on different spatial representations

Input data	AEP (kWh)	AEP (MWh)	Capacity factor
Survey 7	2038619	2038.62	38.79%
Survey 10	1917435	1917.44	36.48%
Survey 13	2133190	2133.19	40.59%

Based on these predictions, the maximum total revenue from an array (assuming the flow conditions across the array are uniform and best described by the prediction at site 13) for a given year is £21,246,575. The largest simulated variation (based on an assumption that flow conditions are uniformly as at site 10) is 10.1% of this revenue – which is obviously a significant impact on project economics. A point of relevance should be considered here. In the development of a larger scale tidal array, it is very likely that tidal hydrodynamic numerical models will be developed to optimise the array design and take full account of the local bathymetry. An important question arises: how many ADCP surveys are required and in what locations to validate the numerical modelling? A high-level assessment of these results suggests that – where the channel geometry is reasonably constant, i.e. in the region of survey sites 7 and 13, then reasonable agreement is obtained for surveys separated by nearly 800m (at least for absolute velocity, if not for direction of flow). However, in regions characterised by varying local topography, like survey site 10, a greater density of surveys may be required to ensure the model in question is representing the local flow conditions effectively.

D. The impact of spatial signal to noise ratio

Given the significance in the *t_tide* code of the method of estimating errors and the subsequent calculation of the Signal to Noise Ratio, a brief study was conducted on the sensitivity of resource estimates to the SNR limit. In the notes accompanying *t_tide*, it is suggested that the range techniques applied to error estimation give reasonable results in the range SNR 10 to SNR 1 (see [13], for a more detailed discussion). Fig. 7 (page 10) shows the significant constituents calculated from the harmonic analysis with varying SNR thresholds from 1 to 10. To interpret this figure: look first for the highest SNR limit 10 (in cyan), these are the only constituents included in a prediction based on this limit. As the SNR threshold is reduced, so the other colours show which constituents are included in the prediction (so for an SNR threshold of 4, both the constituents coloured cyan and red are included). At all threshold levels, the principal lunar and solar semi-diurnal constituents that dominate the tidal response at this site are included in the prediction.

Table IX summarises the simulated AEP in each case, and the impact on project economics of the variation between the resource estimates. Taking the case where the SNR threshold is set to 1, the maximum possible annual revenue that the project could deliver is £20,643,293. The largest possible delta from setting another SNR threshold represents 3.36% of this total. This relatively small variation is mainly due to the predominance in this location of the main lunar and solar semi-diurnal constituents. In other locations where shallow water over-tides are particularly important or where non-tidal process dominate the observed record, the choice of SNR may be far more significant in the energy yield assessment.

TABLE IX: Survey 7 - annual energy production at various SNR.

Signal to Noise Ration	AEP (kWh)	AEP (MWh)	Capacity factor
SNR1	2072620	2072.62	39.43%
SNR2	2058107	2058.11	39.16%
SNR4	2003053	2003.05	38.11%

VII. CONCLUSION

The results demonstrate that the following variables (listed in order of decreasing significance) impact accuracy of energy resource assessments: total record length; spatial resolution (in relation to the total area covered by a projected array); the user selected signal to noise ratio (which is particular to *t_tide* and determines the number of constituents which are carried forward from the harmonic analysis to the subsequent prediction); and, finally, the temporal resolution (or sample interval) of the recorded survey. The relatively low significance of the temporal resolution of the survey is an unexpected result. If this trend can be confirmed by analysis of data from other tidal sites suitable for energy extraction, it would suggest a clear recommendation could then be made that tidal surveys should be conducted with a sample interval less than or equal to 20 minutes (results indicate that the change in the resource estimate below this level is insignificant for the purpose of AEP assessment). This has advantages for project and technology developers who are currently utilising much higher resolution sampling - it would allow a better trade-off, within the constraints of ADCP battery life and data storage capacity, between the total survey length (shown to be of key importance), the sample interval and the number of pings per ensemble (which reduces the instrument measurement error). On the other hand, significant increases in temporal resolution are required to inform certain key TEC device design (e.g. turbulence characteristics of a particular site). Given the conflicting requirements of high resolution, short recording periods to suit device design, and (relatively) low resolution and long recording periods for energy yield assessment, the authors recommend that data gathering for the two purposes is conducted separately.

The results assessing the impact of spatial resolution suggest that project developers will need to give careful consideration to the number and geographical distribution of in-situ measurements utilised to characterise a tidal energy development, particularly as the industry moves towards deployments of arrays of multiple devices. As projects increase in scale, it is likely that there will be a tendency to rely on 3D hydrodynamic numerical models as the basis for detailed large-scale resource assessment. Validation of the model results from in-situ tidal survey data will remain key to ensuring confidence in the resulting resource estimates. The number and length of surveys required for these purpose will remain a matter of judgment for some time, but it should be possible to develop effective best practice guidance once data from a larger sample of locations become available in the public domain.

The motivation for conducting this analysis has been to raise awareness of the potential detrimental longer-term economic impact on project returns of failing to appropriately invest in assessing the specific tidal current energy site characteristics. This is currently an area where tidal energy project developers are minimising cost expenditure. Evidence of the potential impact on project returns have been highlighted. The research presented has also been conducted with the intention of informing the recently initiated moves to develop International Standard documentation for the tidal current energy industry under the auspices of the IEC TC114.

ACKNOWLEDGMENT

ADCP data provision by the European Marine Energy Centre is gratefully acknowledged, without which this analysis would not have been possible. The authors also wish to acknowledge the provision of tidal analysis software associated with [14] by Chris Zervas.

REFERENCES

[1] Department of Energy and Climate Change, "Energy Trends, March 2011", *Department of Energy and Climate Change URN 110/794*, ISSN 2040-6029, 92 pp. (March 2011).

[2] S.J. Couch and I.G. Bryden, "Tidal current energy extraction: Hydrodynamic resource characteristics", *Proc. ImechE Part M: J. Engineering for the Maritime Environment*, **220**, pp.185-194. DOI: 10.1243/14750902JEME50. (2006).

[3] RenewableUK "Wave and Tidal Energy in the UK – State of the industry report", RenewableUK, www.bwea.com/pdf/publications/WandT_SoI_Report.pdf. (March 2011).

[4] The Economist, "And now, the electricity forecast". *The Economist magazine. (*June 2010).

[5] H, Khatib**, "**Economic Evaluation of Projects in the Electricity Supply Industry: IEE Power and Energy Series", *The Institution of Engineering and Technology*, ISBN: 978-086341-3049, 232 pp. (2003).

[6] International Electrotechnical Commission, "Wind turbines – Part 12-1: Power producing measurements of electricity producing wind turbines", *IEC 61400-12-1:2005(E)*, ISBN 2-8318-8333-4, 90 pp. {2005).

[7] S. J. Couch and H.F. Jeffrey, "Preliminary Tidal Current Energy Device Performance Protocol", *DTI/DBERR URN 07/838*, www.berr.gov.uk/files/file38991.pdf, (2007).

[8] R. Swift**,** "Assessment of Performance of Tidal Energy Conversion Systems", EMEC, via the British Standards Instititue, ISBN 978-0-580-65031-4. (2009).

[9] J.D. Boon, "Secrets of the Tide: Tide and Tidal Current Analysis", *Horwood*, ISBN: 978-1-904275-17-6 (2004).

[10] A.N. Celik, "A statistical analysis of wind power density based on the Weibull and Rayleigh models at the southern region of Turkey". *Renewable Energy*, **29**(4), pp. 593-604. (2004).

[11] Ofgem, "The Renewables Obligation buy-out price and mutualisation regime, 2010 – 2011". (2011).

[12] Teledyne RDI**.** "Acoustic Doppler Current Profiler - Principles of Operation - A Practical Primer", *Teledyne RDI.* http://www.rdinstruments.com/mm_papers.aspx. (1996).

[13] R. Pawlowicz, R. Beardsley and S. Lentz, "Classical tidal harmonic analysis including error estimates in Matlab using t_tide", *Computer and Geosciences*, **28,** pp. 929–937. s.l. : Pergamon, 2002, Vol. Computers & Geosciences. (2002).

[14] C. Zervas, "Tidal Current Analysis Procedures and Associated Computer Programs". NOAA Technical Memorandum NOS CO-OPS 0021, (1999).

[15] S. Gooch, J. Thomson, B. Polagye, and D. Meggitt "Site characterization for tidal power". *Oceans 2009*, Biloxi, MI, October 26-29. (2009).

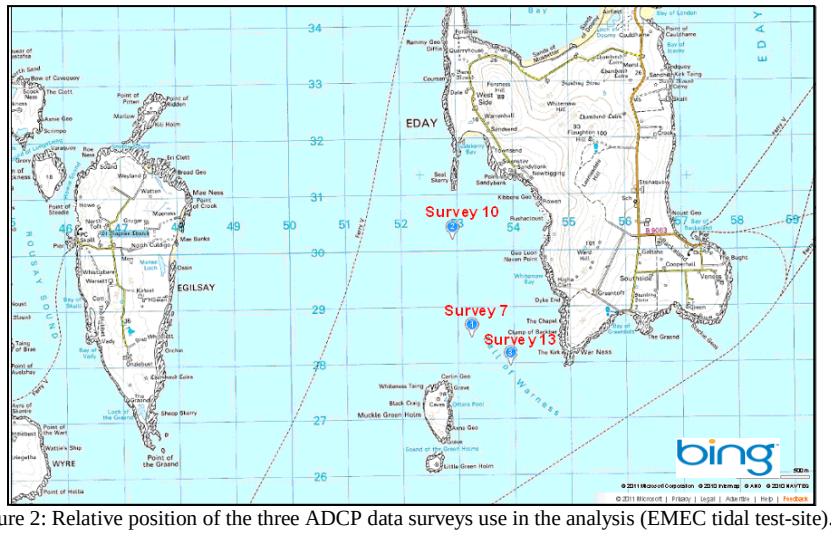

Figure 2: Relative position of the three ADCP data surveys use in the analysis (EMEC tidal test-site).

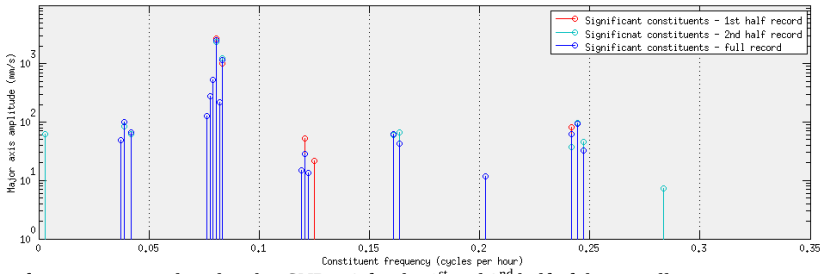

Figure 3: Comparison of constituents predicted with a SNR > 2 for the 1st and 2nd half of the overall measurement record and from the full record.

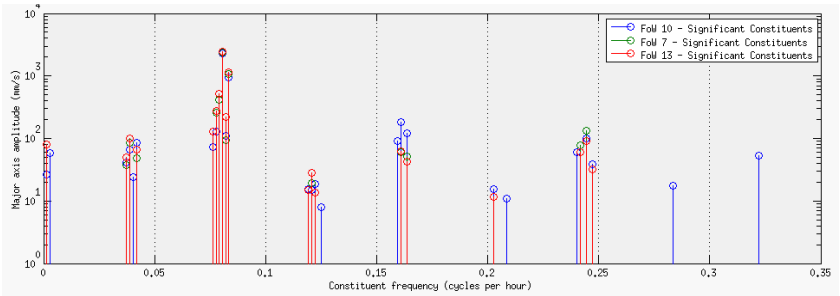

Figure 5: Comparison of constituents wih a SNR > 2 for predictions at a common time basis for surveys 7, 10 and 13.

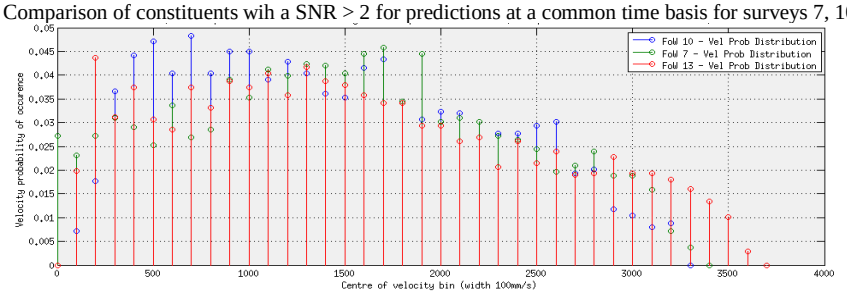

Figure 6: Comparison of velocity distributions based on predictions at a common time basis for surveys 7, 10 and 13.

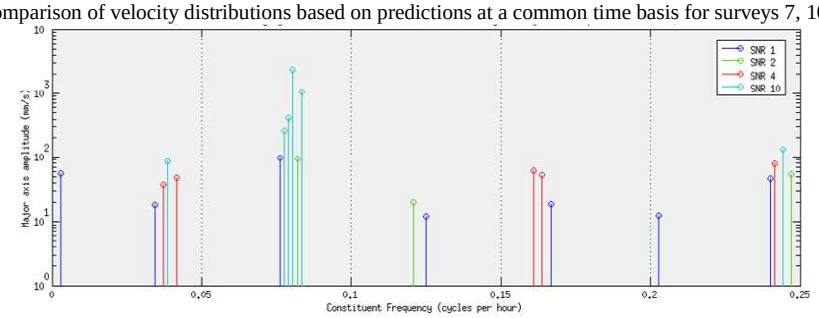

Figure 7: Survey 7 - major axis amplitude constituents obtained from harmonic analysis utilising various signal to noise ration for a single measured record.

Phasing of tidal current energy around the UK and potential contribution to electricity generation

A. Sankaran Iyer, S. J. Couch, G. P. Harrison & A.R. Wallace

Institute for Energy Systems, University of Edinburgh

Kings Building, Mayfield Road, Edinburgh, EH9 3JL

A.Sankaran-Iyer@ed.ac.uk

Scott.Couch@ed.ac.uk

Gareth.Harrison@ed.ac.uk

Robin.Wallace@ed.ac.uk

***Abstract*— Tidal current energy has the potential to play a key role in meeting UK renewable energy targets. Although tides are periodic and predictable, there are times when the current velocity even at high energy sites is too low for power generation. However, it has been proposed that a portfolio of diverse sites located around the UK will deliver firm aggregate output due to the relative phasing of the tidal signal around the coast. This paper analyses whether firm tidal power is feasible with 'first generation' tidal current generators suitable for relatively shallow water, high velocity sites. This is achieved through development of realistic scenarios. Time-series data for sites identified as high energy are obtained using a combination of sources for the year 2009. Scenarios incorporate constraints relating to assessment of the economically harvestable resource, tidal technology potential and practical limits to energy extraction dictated by environmental response. Spatial availability of appropriate bathymetric conditions are assessed which provides an additional limit on the energy harvesting potential. Finally, the variability of power generation from tidal current energy is compared with the existing variability of UK electricity demand using National Grid data.**

***Keywords* – Tidal Current Energy, Marine renewables, Resource assessment, Network integration, Supply and demand matching**

I. INTRODUCTION

The European Union (EU) has ambitious targets to meet future energy demand while reducing carbon emissions. These targets include achieving a 20% reduction in harmful greenhouse gas (GHG) emissions on 1990 levels by 2020, and increasing final energy consumption from renewable sources to 20% on the same timescale [1]. In the UK, more than 30% of electricity generation needs to be supplied through new, clean and carbon free sources in order to meet the EU mandated target, as other parts of the energy sector have less ability to reduce GHG emissions [2]. In order to achieve this, substantial investment in new energy sources such as on- and offshore wind, wave and tidal energy is necessary. Tidal current energy has the potential to play a key role in meeting these targets as around 50% of the economically viable tidal resource in the EU lies in UK coastal waters [3]. Various assessments have equated this tidal current energy resource potential to around 5% of UK electricity demand (e.g. [3]). Ongoing analysis by the authors suggests that assessment may be conservative. Further potential to harvest energy from the tidal resource using barrage and lagoon technologies is also possible [4]. The assessment presented herein is specifically focussed on the potential of tidal current energy solutions.

The marine energy industry is moving towards large scale deployment with regions identified as high energy sites in the Pentland Firth being leased by the Crown Estate for commercial development [5]. However, the introduction of variable sources of energy where supply dependency is related to resource availability as opposed to mechanical availability is a potential cause for concern from an electricity network operator's perspective. Tidal energy resources are driven by the gravitational interaction of the Earth–Sun-Moon system. Therefore, although variable with time, tidal energy production patterns can be reliably predicted on both short and long timescales. However, a challenge with tidal energy is that the peak power at a particular site occurs approximately 50 minutes later each day as the tidal signal around the UK is dominated by the M2 tidal constituent associated with the periodicity of a lunar day (24 hours and 50 minutes). This discontinuity between the solar and lunar day ensures that peak generation and demand are rarely coincident.

Accurate assessment of the output and variability of individual tidal current sites and the impact of aggregation of output from various sites would be highly desirable to facilitate network planning and operation. Such information would also be instructive for scoping the future potential of tidal current energy, and hence planning development and investment in the emerging technology and project development industry.

The research presented in this paper uses methodologies that initially quantifies the total available resource in the UK that can be extracted using 'first-generation' technology options as outlines in [6,7]. The resource assessment utilises a combination of available datasets. The analysis is based on tidal current characteristics for the calendar

year 2009. For the purpose of developing power generation scenarios, representative generic first-generation device characteristics are considered. The overall analysis involves examining aspects of generation, yield, variability, phasing and ultimately the fit with existing UK electricity demand. The potential impacts of introducing tidal generation into the existing electricity mix are thus considered. The work presented uses various methodologies to quantify fluctuations in power generation and makes comparison with day-to-day demand variability. Finally, a preliminary capacity credit calculation is conducted to quantify the contribution of the envisaged future tidal energy generation development scenario towards ensuring demand security.

II. Tidal Resource Development Scenarios

A number of studies have been conducted to assess the total exploitable tidal energy resource in the UK. It is of value to accurately define the exploitable resource as this quantifies the potential scale of industry development that can be supported. The next section discusses the latest estimates for tidal current energy in the UK and highlights the need for additional analysis of the variability of the resource in an energy context.

A. Resource Assessment

Under the Marine Energy Challenge, Black & Veatch (B&V) [3] estimate the extractable resource to be 18 TWh/yr (±30% uncertainty). This is the most widely referenced assessment at a national scale. The analysis in [3] utilises input data from a combination of sources, the UK Marine Renewable Energy Resource Atlas [8] by the (then) Department of Trade and Industry (DTI), Admiralty chart data from the UK Hydrographic Office [9], and local port data where available.

A 'Significant Impact Factor' (SIF) is proposed to limit the energy that can be exploited without adversely affecting the environment and the overall resource itself. A constant value of 20% of the total available kinetic energy flux is applied in [3].

Sinden [10] has furthered the work conducted in [3] by extracting power output time series for wave and tidal current energy. The analysis in [10] assumes a scenario where all the available tidal energy resource identified in [3] is developed, after accounting for SIF restrictions. The analysis does not differentiate between shallow and deeper sites where a different generation of technology will need to be deployed. First generation devices are considered to be the driver for tidal current energy development until at least 2025. Installation and operation in deeper water requires more radical 'second' and 'third' generation approaches that are as yet only in the very early stages of research and development. Therefore an analysis based on just first generation device specification is required. The application of the SIF has since been superseded, therefore a revision of the 'Extractable Power' considered in [3] and [10] is also necessary.

An interesting aspect that is yet to be fully understood is whether the aggregate output from different tidal sites can represent a form of 'firm' generation by diversifying the phasing of the incoming tidal waves. [11] demonstrates the potential for baseload provision using tidal currents based on analysis of three locations. Nautical Almanacs are used as the input data in [11]. This data is primarily used by yachtsmen for navigation purposes and it has not previously or since been used for tidal current evaluation purposes. Interrogating the BERR Marine Atlas [12], an updated version of the DTI Atlas [8] at the locations used by [11] indicates significant discrepancies. The data in the almanac is likely to refer to high resolution flow features as is necessary for safe navigation. The nearest TotalTide tidal diamond [13] (digitised Admiralty chart data [9]) and the BERR Marine Atlas [12] indicate that these locations would not be suitable for large scale tidal current energy development. Similarly the depths in the regions identified in [11] are not appropriate for even relatively small scale tidal current energy development.

Another attempt to assess potential for firm aggregate generation is presented by [14] where it is proposed that a careful selection of sites can generate a steady output. Back-testing this analysis, the authors have found significant discrepancies. For instance, [14] purports to use data relating to tidal diamond SN040A and suggests that it has a spring peak velocity of 2.1 m/s. Interrogating the same tidal diamond using UKHO TotalTide software [13] indicates that SN040A only reaches a spring peak of 0.57 m/s – this would be inappropriate for tidal current energy development. Other discrepancies with reported tidal diamond data were also observed. Hence the outcomes of the analysis presented in [14] are considered to be flawed.

For the analysis presented herein, only first generation devices are considered, where first generation technology is defined as prototype devices already undergoing pre-commercial demonstration. These devices are typically deployable in water depths of 25 to 50 meters. An additional concern with operating in deeper water is the implication of being further from shore – this would suggest a substantial increase in project cost due to the need for extended undersea cabling. Other limitation imposed within this analysis is site selection based on regions where tidal current velocity is above 2.5 m/s at the time of spring peak. Such a stipulation is a simple means of ensuring that there is potential for economic development of the site due to the energy density that will be available for capture by tidal current devices.

B. Tidal Resource Phasing

The timing of local tidal conditions stems from the fundamental concept of tidal wave propagation. In the deep ocean, tides predominantly propagate as progressive waves. However, as they approach nearshore regions on the northern European continental shelf, their behaviour tend towards a standing wave characteristic where high and low water coincides with slack tide. Hence nearshore tidal velocities tend to peak when the gradient of the surface elevation is at a maximum. Figure 1 illustrates the current velocity and tidal heights for a random location

around the UK (Amlwch, near Holyhead - tidal diamond SN048J). Slack tide occurs when the tidal current (solid line) changes direction. The change in flood to ebb direction is at the time of high water indicating standing wave characteristics. Holyhead data is used here as being generically representative of large swathes of UK coastal waters. What Figure 1 represents is the tidal wave characteristics throughout UK waters. Slight time lead/lag may be experienced at specific sites but the current will typically change direction at the time of highest gradient of local surface elevation. Figure 2 presents co-tidal lines around the UK that represent the time of high water – the propagation of the tidal wave is easily observed. Assuming that the relationship between tidal height and current is similar as indicated in Figure 1, then Figure 2 also broadly illustrates the relative timing of tidal current propagation.

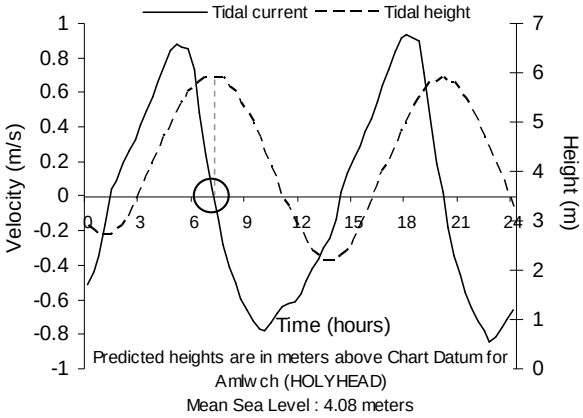

FIG. 1 Tidal currents (solid line) and height data (dotted line) at Holyhead indicating relative phasing of current and surface elevation (source data [12]).

The locations circled in Figure 2 have been identified by Black & Veatch [3] as being sites of major interest for tidal current energy extraction. Ideally a phase difference of 90° or 270°, relating to a time variation of three or nine hours would be optimal for tidal sites to formulate a combined output for firm power generation. However, the sites highlighted in Figure 2 experience high water at approximately the same time (some sites show a variation of up to an hour). If these identified sites are characterised by similar tidal height and current relationships as in Figure 1, then all these sites can be expected to experience ebb and flood in phase with each other.

Coincidence between two of the biggest sites can have a significant negative impact in terms of tidal current energy's contribution towards firm power. The Pentland Firth and Channel Islands have been identified as locations that embody about 70% of the technically extractable resource [15]. As these two sites are potentially in phase, the aggregated power output will also be in phase. From an electricity network perspective this is the worst case scenario, as the system will have to absorb surges of power over relatively short periods assuming large-scale tidal current energy development. This potentially in-phase characteristic of the most important sites is entirely coincidental and specific to the UK context due to its unique shape and size. The above theory relating potential 'locking' of tidal phase around the UK at major tidal current energy development sites will now be examined further.

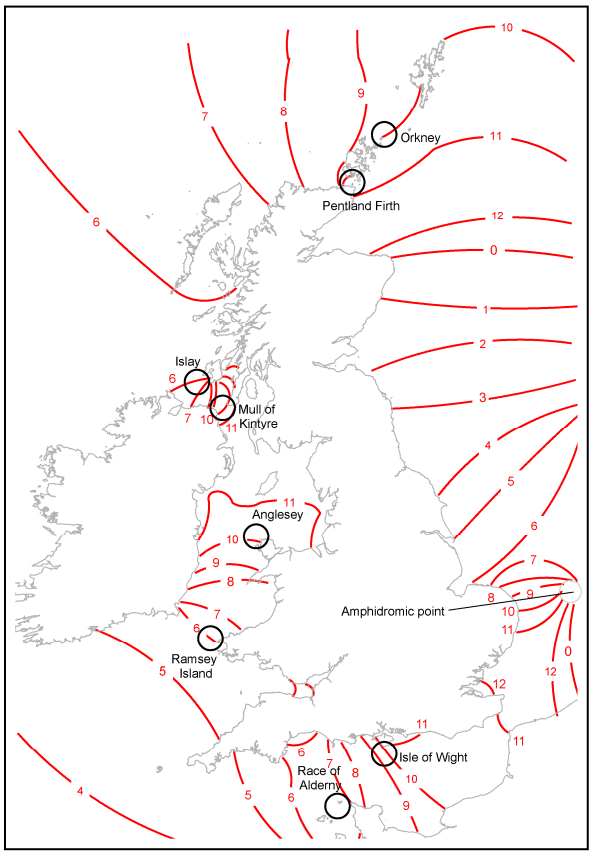

FIG. 2 Co-tidal lines for the coast of the UK. Areas marked in the circle show regions of interest for tidal current energy development.

III. METHODOLOGY FOR RESOURCE ASSESSMENT

Resource assessment analysis in this section follows the methodologies demonstrated in [6]. Only first generation sites are considered, as mentioned earlier. A Geographical Information System (GIS) setup was used to interrogate the BERR Marine Atlas [12].

A. Site Selection

Resource assessment analysis in this section follows the methodologies demonstrated in [6]. The Marine Atlas dataset provides mean spring and neap tide velocity values and water depths for the UK continental shelf (UKCS) at a spatial resolution of approximately 1.8 km^2.The Marine Atlas provides wide spatial coverage but lacks temporal resolution. Therefore the Atlas was used to identify cells meeting certain criteria: cells were only considered appropriate for economic development where the spring peak velocity exceeded 2.5 m/s. This criterion is based on the findings of [3] which suggest that sites that do not experience peak velocity of this magnitude are considered uneconomic.

A number of sites included in [3] are not identified in this study as they do not meet the criteria outlined for site selection for first generation development. Narrow channels such as Strangford Narrows are not included in this study as the Marine Atlas is unable to resolve these regions, although the location has been

identified as an energetic site for economic development [16]. Hence, insufficient data exists in the public domain to effectively generate reliable time series. All the sites identified using the above criteria are listed in Table 1 with data synthesised from [12].

The UK Hydrographic Office software (TotalTide) [13] is used to determine time series spanning the calendar year 2009 by accessing tidal diamond current velocity data. A limitation is that the tidal diamonds do not necessarily coincide with the location of the specific cells. Therefore 'pseudo diamonds' have been created using interpolation techniques outlined in [18]. The authors have already utilised this approach for application to tidal diamond data as identified in [6] where more detail is provided. The combination of applying the velocity magnitude from one source, Marine Atlas [8] and temporal variation from another, TotalTide [13] is sub-optimal. However given the lack of more effective and robust data coverage across the UK, this is deemed an appropriate method as discussed in detail in [6]; combining two source datasets to provide appropriate spatial and temporal resolution.

TABLE I
LIST OF SITES IDENTIFIED FOR THIS STUDY

Site name	No. of Cells	Region	Avg. Depth (m)	Avg. Spring Peak (m/s)
Pentland Skerries	2	Scotland	35.50	3.60
S. Ronaldsay P. Firth	1	Scotland	39.00	3.19
S. Ronaldsay/ P. Skerries	5	Scotland	43.20	2.93
Duncansby Head	1	Scotland	36.00	3.25
Inner Sound	3	Scotland	28.67	3.27
Stroma P. Firth	7	Scotland	39.29	3.44
Westray Firth	2	Scotland	29.00	3.81
N. Ronaldsay Firth	1	Scotland	34.00	2.57
Islay North	7	Scotland	29.00	2.75
Islay Centre	12	Scotland	27.75	2.76
Islay South	8	Scotland	38.88	2.63
Sound of Islay	2	Scotland	50.00	2.95
Anglesey North	4	Wales	30.00	2.59
Anglesey South	1	Wales	31.00	2.60
Ramsey Island	3	Wales	35.00	2.66
Race of Alderney	19	England	31.68	3.38
Isle of Wight	2	England	27.50	2.76

More robust in-situ Acoustic Doppler Current Profiler (ADCP) data was obtained for sites where possible. For example in the Orkney region, data was purchased from EMEC for Westray Firth. The ADCP measurements were taken over a month long period in 2005 and did not coincide with the selected tidal diamond time series for the other locations. Therefore harmonic constituents were derived from the ADCP data using the NOAA least–squared analysis approach [16]. 23 principal constituents were obtained using this methodology and were then used to recreate the time series coincident in spatial and temporal resolution to the rest of the datasets (i.e. spanning 2009). Additional ADCP data for Sound of Islay was kindly provided by ScottishPower Renewables [19]. The final additional dataset covers the area around Anglesey. This data was accessed via the British Oceanographic Data Centre (BODC) [20]. Datasets spanning periods above 29 days were once again used in conjunction with harmonic analysis and reconstruction for the common time series via harmonic prediction. A detailed discussion of this analysis and the methodology can be found in [21].

IV. Scenario Development and Analysis

The device characteristics in this study are based on the assumption of a generic horizontal axis device. Previous analysis [6] has utilised a rated velocity determined for each device by taking 70% of the spring peak velocity as suggested by [3]. However, during the analysis in [6] it was thought that the capacity factors of some of the sites that are otherwise known to be high-energy sites were lower than expected. In this context, capacity factor is defined as a ratio of actual power output over the nameplate capacity of the plant over a period of time.

Discussion with the authors of [3] highlighted that this method does not fully consider the site economics and they have since moved on to an in house cost optimisation model that chooses a device rated velocity accordingly. Unfortunately this cost model is not available in the public domain. Therefore, in order to strike the right balance between maximum power generation and economic capacity factor an alternative simplified method of assigning the rated velocity has been identified.

Figure 3 is a velocity exceedance curve for all the cells of interest identified in Table 1. All the sites experience spring peak velocity above 2.5 m/s, but examining the exceedance curves it becomes clear that for some sites this occurrence is very low. Therefore to choose a rated velocity based on the spring peak characteristics for a site could mean that the device would spend only a small proportion of its time operating at rated power and hence have a low capacity factor.

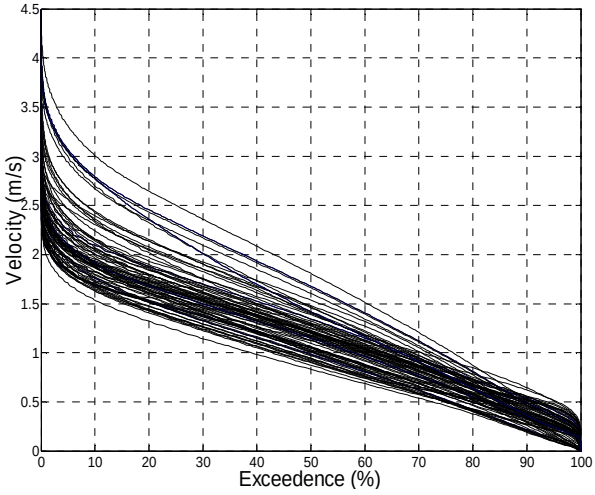

FIG. 3 Velocity exceedance curve from all the selected cells.

The interpretation of capacity factor statistics is complicated by the fact that increasing the rated power

of a turbine increases the energy harvested but decreases the overall capacity factor. A compromise needs to be made between maximising generation at the expense of engineering the device to withstand the forces at higher rated velocity. It is considered uneconomic to engineer a device that will only be operating at its rated value for a small percentage of the time. Therefore, in order to reach an effective balance, the approach adopted herein specified the rated velocity as the velocity value associated with 10% velocity exceedance. The idea behind choosing the rated velocity this way is that using the 10th percentile value forces the device specified in each cell to operate at rated power for 10% of the operational time (assuming no downtime). Examining the exceedance curve in Figure 3 indicates that for roughly 20% of the time, the majority of sites experience velocity below 0.7 m/s. This equates to the cut in velocity expected of first-generation tidal current technologies; below 0.7 m/s the device will not generate. For the remaining 70% of the time the device will be generating but will be operating somewhere between cut-in and rated velocity.

Capacity factor is used here as a simplified indicator of how 'economic' a site is (assuming common turbine design). A low capacity factor indicates low economic performance. This method of using the exceedance plot therefore provides a sensible way of understanding the power generation distribution over tidal cycles and assists in identifying a rated velocity appropriate for each cell location that will lead to a capacity factor of around 30% which is deemed a likely economic balance for first generation tidal devices in light of wind energy developmental experience.

Having established the rated velocity, the power generated from a device can be characterised using the equation:

$$P = \frac{1}{2} C_p \rho A v^3 \qquad (1)$$

where C_p is the device efficiency, assumed to be a constant value of 40% based on [22], the water density, ρ = 1025 kg/m^3, A (m^2) is the rotor swept area and v (m/s) is the depth-averaged current velocity. Two energy capture device models are utilised in the analysis to reflect the difference required for operating across a range of water depths: in cells of depth between 25 to 30 meters, a device diameter of 15 meters is used to provide appropriate surface and seabed clearance and avoid conflict with vessel navigation. In water depths of 30 meters or more (up to 50 meters) a device diameter of 20 meters is specified. Cut-in velocity in all cases is assumed to be 0.7 m/s. The device maintains rated power for velocities higher than rated velocity.

Figure 4 shows the capacity factor for each of the cells already identified in the analysis using the two different approaches for selecting the rated power. From the graph, it can be seen that the updated method of assessing the rated velocity maintains better consistency of capacity factor (around 30% as desired). Hence this new method is carried forward throughout the analysis. This standardised approach is being used to inform a national scale resource assessment. For project scale and site-specific design, much more detailed analysis would be necessary.

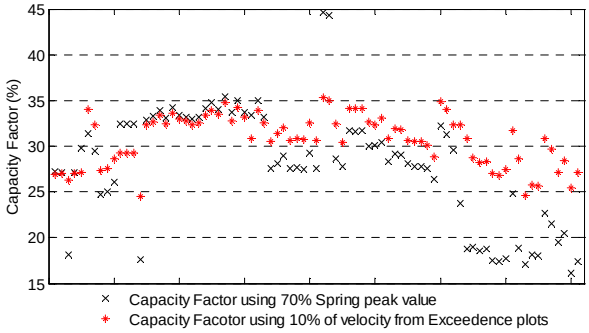

FIG. 4 Summary of Capacity Factor evaluation for all the cells of interest appropriate for first-generation device deployment

V. ACCEPTABLE POWER

The installed capacity for each cell is based on the rated velocity and device spacing as in [6]. Two scenarios are considered, the unconstrained scenario considers all the energy that can be extracted from the site without considering consequences of extraction on the local environment (also known as the farm approach).The second scenario considers constrained power generation, Technically Acceptable Power, (TAP) that can be extracted from the site without significantly impacting the environment based upon current understanding of the engineering potential of the technology. While the analysis presented here lacks the very high temporal and spatial resolution data necessary to inform individual project development and detailed device design characteristics, it offers a credible and broad resource analysis suitable for understanding the nature of the UK tidal resource and its phasing. A true understanding with a high level of accuracy of the resource will only be gained by extensive site measurements combined with tidal hydrodynamic models incorporating the complex interaction of device operation alongside the evolving hydrodynamics.

A. Total Power

Aggregating the output from each of the sites, in the unconstrained scenario, there is potential for energy harvesting of 31.22 TWh/yr utilising a total installed capacity of 11.44 GW. Within this scenario there are a range of installed capacities across various locations, the smallest being Isle of Wight at 0.23 GW. The largest installed capacity of 3.4 GW is at Race of Alderney. The productivity of each site broadly reflects the installed capacity as the scenario developed achieved a consistent capacity factor of 30.2% nationally.

B. Technically Acceptable Power

The national resource assessment presented in the preceding section has been conducted without considering the effect energy extraction may have on the underlying tidal system. The SIF approach utilised by [3] and [10] is now outdated and needs to be revised to update and reflect enhanced understanding

of the resource. Numerical modelling in [7] suggests that tidal hydrodynamic mechanisms can be grouped into hydrodynamic mechanisms – tidal streaming, resonance and hydraulic current. These flow phenomena are necessary to generate tidal current flow conditions extreme enough to warrant considering the location appropriate for economic development. [7] also identifies that there is a limit to the amount of energy that can be extracted before the energy extraction process starts affecting the local hydrodynamic mechanism. [23] has already identified that beyond a theoretical harvesting limit, any more energy extraction would in fact reduce the cumulative energy harvested as a result of reduction in kinetic energy flux.

To evaluate the level of power that can be harvested from each of the sites, their respective hydrodynamic mechanism is identified and a TAP value defined in [6]. Regions with multiple sites are treated in one of two ways: the sites at Orkney, Islay and Anglesey are considered to be sufficiently geographically and hydraulically dispersed to be evaluated separately while for the Pentland Firth, sites are considered interdependent and are handled jointly by a single set of limits. For many sites the high flow velocities experienced are as a result of a combination of mechanisms.

Where a site needs to be constrained, the capacity factor of each cell is considered. Cells with the lowest capacity factor are sequentially removed until the restricted TAP generation conditions are met. This was achieved either by removing the cell entirely or by reducing the number of devices deployed in the identified cell to meet TAP constraints. Details of the limitations for the sites considered in this scenario can be found in [6]. For the UK wide constrained scenario using the locations identified in this analysis, a TAP of 14.25 TWh/yr is extractable utilising an optimised total installed capacity of 5.4 GW. The limit imposed by the constraint reduces the total power output by more than half from the unconstrained to the constrained scenario. A breakdown of unconstrained and constrained generation for all the sites is listed in Table II, using data provided in [6].

Figure 5 shows the combined power output from all the sites for the constrained and the unconstrained scenario. Only the peak value far each 12 hour period is plotted so an envelope of the generation can be seen representative of the variation of the spring-neap cycle. What is not shown in the graph is the daily cycle with two peaks and two troughs generated in every 12.4 hour period. Hence, the power output varies every three hours, ranging from 12 GW to 0 GW and 6 GW to 0 GW in the unconstrained and constrained scenario respectively.

TABLE II
POWER GENERATION POTENTIAL FOR ALL THE SITES CONSTRAINED AND UNCONSTRAINED. DATA DERIVED FROM [6].

Site name	Generation Unconstrained (TWh/yr)	Generation Constrained (TWh/yr)
Pentland Skerries	1.173	1.173
S. Ronaldsay P. Firth	0.287	0.287
S. Ronaldsay/ P. Skerries	1.085	1.085
Duncansby Head	0.410	0.410
Inner Sound	0.886	0.886
Stroma P. Firth	2.658	2.658
Westray Firth	2.877	0.746
N. Ronaldsay Firth	0.144	0.144
Islay North	2.580	0.493
Islay Centre	4.614	0.580
Islay South	2.099	1.173
Sound of Islay	0.104	0.104
Anglesey North	0.871	0.832
Anglesey South	0.288	0.288
Ramsey Island	0.726	0.625
Race of Alderney	9.766	2.115
Isle of Wight	0.664	0.664
Total (TWh/yr)	**31.23**	**14.26**

Since the output from all the sites are predominantly in-phase, the potential for tidal current toprovide significant firm generation is limited. Continuous output can be achieved for a number of days around Spring peak, however the continuous output is sustained as a small fraction of the peak generation potential. An informative way of summarising the data is using an exceedance curve as shown in Figure 6. It can be seen that for the constrained and unconstrained case, the power output drops to zero near 100% exceedance indicating that tidal current energy cannot generate firm power, at least not within this scenario considering the major tidal current energy locations around the UK coastline.

As the unconstrained scenario is likely to be deemed unacceptable due to the associated environmental impact. For example extracting 9.76 TWh/yr from Race of Alderney as developed for the unconstrained case would reduce the free stream velocity by 25% and alter tidal height variation by more than 35%, only the

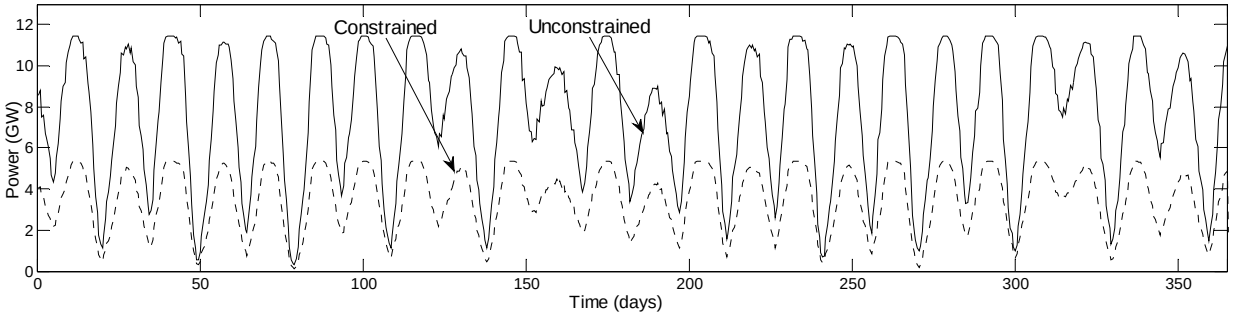

FIG. 5 Power output for 2009 in the constrained and unconstrained scenario.

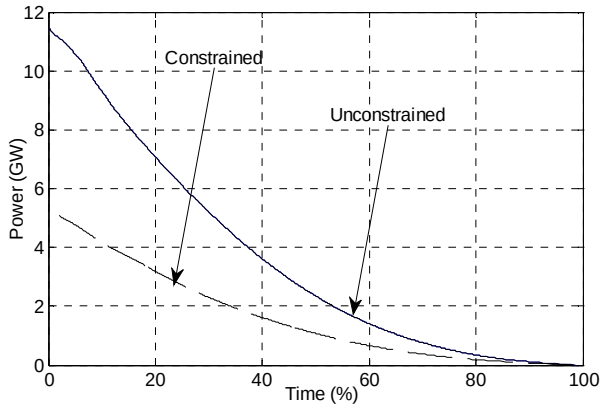

FIG. 6 Power exceedance for the constrained and unconstrained scenario.

constrained scenario will be considered hereafter. The analysis indicates that for most of the identified key sites, the limit to how much energy can be extracted is determined by the TAP constraint limiting energy harvesting due to excessive environmental impact. In the constrained scenario presented here, most of the sites meet or exceed the TAP limitations imposed. The only exceptions are Pentland Firth (consisting of Pentland Skerries, S. Ronaldsay P. Firth, S.Ronaldsay/P.Skerries, Duncansby Head, Inner Sound and Stroma P. Firth), N. Ronaldsay Firth, Sound of Islay, Anglesey South and Isle of Wight. At these locations if suitable depth conditions are available, further development potential would be possible when second/ third generation tidal energy devices become available. However at locations where the TAP constraint has already been reached, further development with newer generations of technology will be constrained by the existing first generation deployments.

VI. Matching Tidal Generation and Demand

For this study, half hourly demand data is obtained from National Grid, the Transmission System Operator in Great Britain. IO14_DEM demand values are used for this analysis, which takes into account station load but no pump storage activity [24].

A. Tidal Variability

The addition of renewable generation to the existing electricity network will further complicate the operation of the system, particularly during periods of high demand expectation. Although the inherent predictability of tidal generation is beneficial, there is no obvious casual relationship to expect that strong periods of generation will coincide with high demand. Figure 7 shows tidal generation fluctuation potential simulated every half hour using the constrained development scenario data for 2009 already detailed. This graph presents the aggregated output of the complete tidal generation scenario. Extreme fluctuations of -2 to +2 GW are observed. Considering the total installed tidal capacity under the constrained scenario is 5.4 GW, the maximum indicated half-hourly swing is a significant proportion of installed capacity. However smaller swings are generally the norm. The modular approach to tidal current generation installation ensures that intermittency is avoided. Key distinction to be made here is that near–zero output from an entire fleet of conventional generation units does not occur, while for tidal generation the output is constantly variable dependent upon the forcing of the resource. However an unexpected shutdown is highly unlikely.

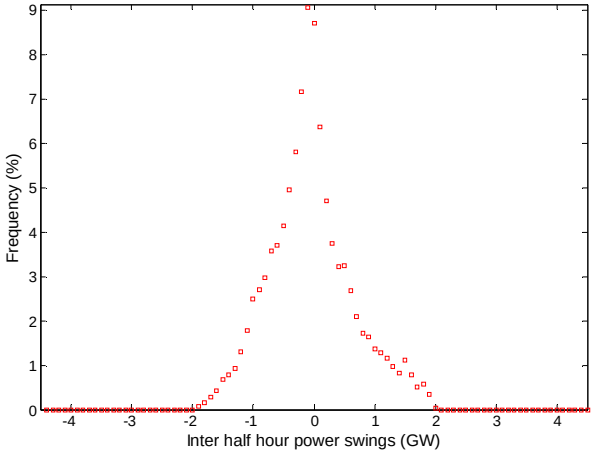

FIG. 7 Inter half hourly power output fluctuations from constrained scenario.

An advantage tidal generation has over wind and wave power is the absence of extremities of operation. For example, a standard wind turbine may be rated at 12 m/s and cut out at 25 m/s. This is necessary as gust speeds of 50 m/s are not uncommon across the UK [25]. A cut-out velocity or survival strategy is therefore necessary for these technologies as sites can experience extreme gust speeds (wind) or wave heights (wave) that are far beyond the operating region of the energy extraction device. For tidal current this is not a major issue as the operating conditions are not that far removed from the extreme conditions as shown in Figure 3; most tidal devices are therefore not designed to cut out and can operate at rated power during extremes by pitching the blades to alter the angle of attack and hence shed load.

B. Demand Variability

Demand for electricity is characterised by variation at different time scales. Northern European countries, including the UK experience winter periods that are dominated by cold weather and short daylight periods. Peak electricity demand is therefore concentrated in the winter period with the increase in consumption of electricity associated with the need for domestic heat and lighting along with the usual underlying load. Electricity consumption patterns are well understood and the extent of the variability can be estimated with a high degree of certainty. Detailed weather forecasting systems can help prepare for cold spells and provide early warning for the system to secure more reserve.

The UK electricity system has an average demand of 36.4 GW, with a standard deviation of 7.7 GW. In 2009 electricity demand peaked at 59.1 GW (6th January, 17:30) and is expected to grow at a 1.2% growth rate per year [26]. Figure 8 shows the mean demand for each half hour period in a standard day

determined from the complete 2009 data record. Although the average demand for the entire year is 36.4 GW, it can fall as low as 20.15 GW (2nd August), 34% of the peak value.

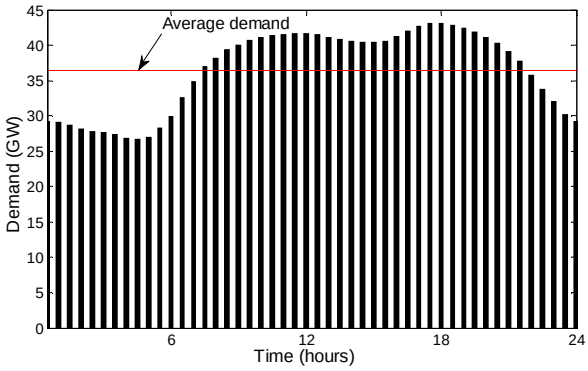

FIG. 8 Mean demand for each half hour period in the day (2009).

The system is most vulnerable at times of peak demand, so any generation that contributes towards meeting peak demand has a positive influence and reduces the burden on the network. Figure 9 shows two curves, the UK demand profile spanning over the week when peak demand occurred, from the 5th to 11th of January with peak demand occurring on the 6th. The second curve shows net demand with tidal generation imposed as a negative load (demand – tidal generation) utilising 5.4 GW installed capacity (the constrained scenario). The contribution of tidal current energy to the system would only reduce the system peak on the 6th by 0.5 GW. Two days later, on the 8th, maximum demand for the day was 57.3 GW, 12th highest for the year. Under the envisaged constrained scenario, this demand would be reduced by 3 GW with the inclusion of tidal in the system. The biggest reduction that can be obtained with the inclusion of tidal in the system will be in the order of 5 GW, which occurs around midnight on the 11th; in this instance, peak generation does not coincide with a significant demand peak. Examining Figure 9 indicates the importance of timing of demand and tidal generation cycles.

A key question to be addressed is what consequences will the addition of variable generation from tidal current have on the network and the system operator with increasing levels of penetration? In the constrained case, tidal current plays a small role meeting 3.8% of existing UK demand. A method of assessing the variability for the whole year is presented in Figure 10.

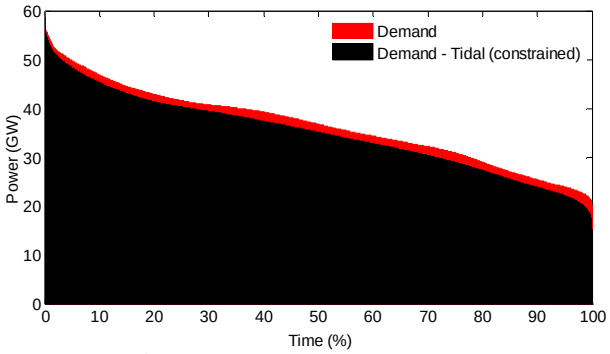

FIG. 10 The half hourly demands and tidal generation presented as Load Duration curve.

The two curves show demand with the inclusion of tidal in the system. The reduction in the load duration curve with tidal in the system is an even spread indicating a potential correlation, however the tidal resource is independent of demand due to the lack of any causal relationship.

Despite its usefulness the load duration curve does not show how demand and generation are responding with respect to time. Therefore, matching of demand and supply is shown in Figure 11, each column in the bivariate histogram presents the amount of time (in %) for which a particular combination of generation is presented as a percentage of the total installed capacity and demand is presented as a percentage of peak demand. The worst-case as defined by [27] is identified as the period when demand is ≥90% and tidal generation is ≤10%, the right-most column in the histogram. This corner is significant as it defines the time when generation is low and demand is high. The histogram highlights that the largest match occurs when generation is ≤10% and demand is between 50-60%.

The effect of this variability on the system can be examined by considering the net demand that generation sources other than tidal must provide. Figure 12 shows the frequency of inter-half hourly demand changes before and after tidal is introduced. The impact of inclusion of tidal to the overall system is rather small although there are few occasions with near zero (0 GW) residual demand change. The Y-axis uses a log scale to highlight excursions occurring at the tails of the distribution; an important characteristic of this graph from the perspective of network management. Table III summarises the key changes and highlights that the largest swings are increased and become more frequent with the addition of tidal to the

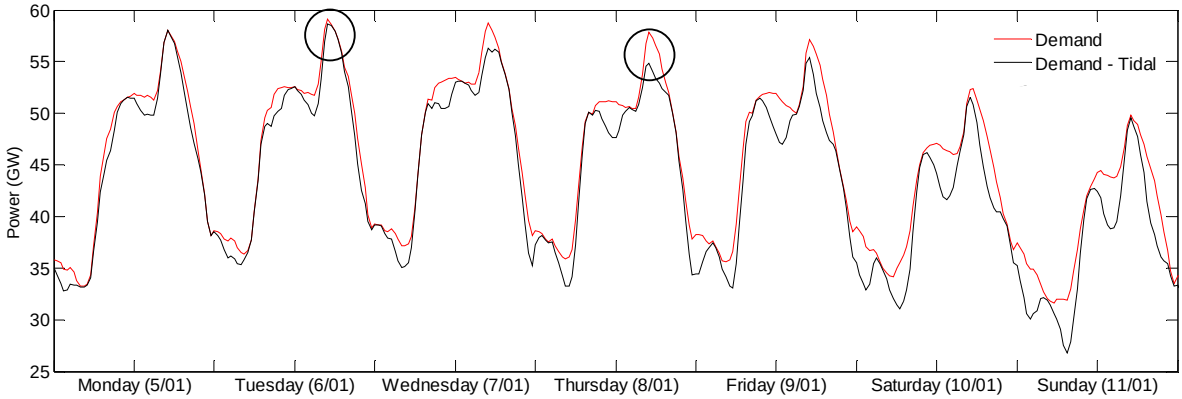

FIG. 9 Demand change with tidal generation in the system.

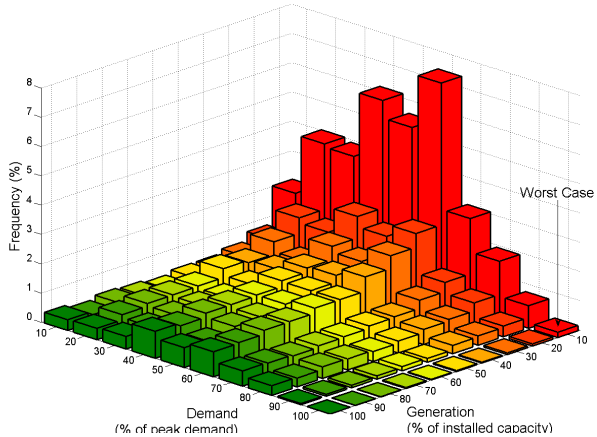

2.08	4.08	3.97	6.19	5.59	7.42	3.11	1.97	0.77	0.18	10
0.8	1.84	1.67	2.52	2.16	2.57	1.22	0.84	0.37	0.07	20
0.5	1.31	0.98	1.79	1.59	2.11	0.91	0.57	0.32	0.06	30
0.36	0.89	0.98	1.34	1.41	1.67	0.63	0.51	0.29	0.03	40
0.36	0.98	0.75	1.2	1.18	1.19	0.61	0.41	0.13	0.03	50
0.25	0.67	0.59	1	1	1.19	0.53	0.34	0.14	0.02	60
0.33	0.66	0.62	0.96	0.86	1.02	0.51	0.38	0.11	0.03	70
0.37	0.66	0.58	0.96	0.82	1.01	0.45	0.39	0.09	0.01	80
0.25	0.57	0.47	0.82	0.59	0.88	0.5	0.3	0.06	0.01	90
0.37	0.39	0.43	0.92	0.68	0.86	0.52	0.33	0.04	0	100
10	20	30	40	50	60	70	80	90	100	

Generation (% of installed capacity)

Demand (% of peak demand)

FIG. 11 Coincident half hourly histogram and table.

system. his outcome obviously relates back to the initial findings of the relative phasing of UK tidal current energy resources – if the resource was more out of phase, the variability felt by the system would be reduced as power generation would vary more smoothly with potential for continuous generation.

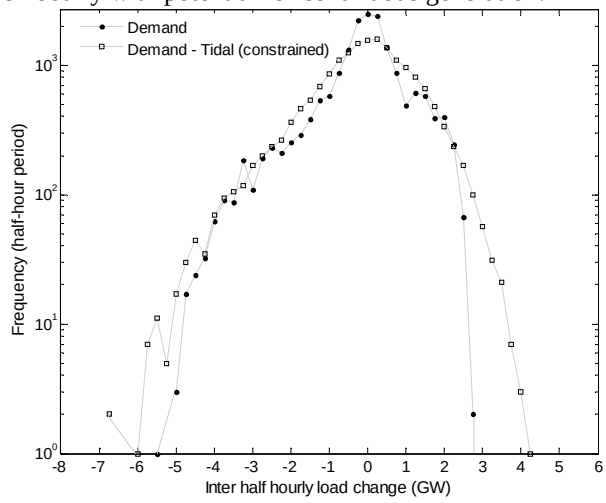

FIG. 12 Inter half hourly demand change with and without tidal current in the system.

Capacity value is another important concept that can help understand the potential contribution made by tidal current energy in supporting demand. The commonly used Effective Load Carrying Capability (ELCC) can be defined as the additional demand which the generation can support without increasing the system risk. The empirical distribution across all days of available tidal capacities at 1700 hours (the time of day at which extreme high demands typically occur in GB) may be used as the distribution of available capacity at time of annual peak. This may be used in an annual peak loss-of- load-probability (LOLP) based generation adequacy risk calculation [28]. LOLP is the probability that generation will be insufficient to meet demand at a particular time. A preliminary calculation has been performed using a Gaussian distribution of available conventional capacity with mean 65 GW and standard deviation 2 GW; this is representative of a sustainable long-term level of adequacy risk. The ELCC is then 1.15 GW (10.05% of the unconstrained scenario installed capacity) and 0.82 GW (15.19% of the constrained scenario installed capacity). The small difference between the two cases arises because in the unconstrained case the possibility of very low percentage output is more significant than the substantial mean of 3.39 GW (the mean in the constrained case is 1.55 GW). A more detailed study of adequacy risk will be presented in future.

TABLE III

KEY DATA FOR HALF HOURLY POWER EXCURSIONS WITH THE INCLUSION OF TIDAL IN THE SYSTEM.

Tidal Penetration		
	None	**Constrained**
Maximum decrease: GW	5.47	6.65
Number of decreases of 5.25 GW and above	1	21
Maximum increase: GW	2.77	4.36
Number of increases of 2.5 GW and above	2	220

VII. CONCLUSION

This work presents an improved method of assessing the total UK tidal current resource by combining multiple datasets including Marine Atlas, TotalTide tidal diamonds and measured tidal current information where available. First generation device installation is considered in regions where spring peak velocity exceeds 2.5 m/s in water depths of 25 to 50 meters. Based on an economic assessment of the capacity factors for each of the sites considered it is concluded that 14.25 TWh/yr can be extracted without significantly impacting the underlying resource at the identified sites, as further detailed in [6]. A new approach to identifying the device rated velocity is introduced to help achieve an overall economic capacity factor and aid development of realistic scenarios.

The nature of tidal wave propagation around the UK coast indicates that the high energy sites considered are largely in-phase and that tidal current *cannot* be seen as offering significant 'base load' generation potential in the UK. Numerous small sites exist that may provide a small percentage of generation out of phase but this will amount to a small proportion of the total installed capacity. Generation from the constrained scenario presented here can meet 3.8% of present UK demand. Two of the largest sites, Pentland Firth and Race of Alderney together contribute 60.4% of the total generation.

The impact of aggregated tidal current generation on the electricity network is considered. Inclusion of

tidal in the system increases the number of extreme short-term changes in net demand but they do not appear to be severe and seem manageable as suggested by National Grid [26]. The capacity value of the preferred scenario is 15.19% with an ELCC of 0.82 GW.

The analysis presented here makes specific assumptions about how much resource can be extracted and what type of devices will be used, their efficiency, operating conditions etc. Varying any of these parameters can significantly vary the final output. The intention has been to develop scenarios representative of realistic large-scale uptake of tidal current energy in the UK using conservative assumptions of device characteristics based upon existing prototype devices. On this basis, the relative phasing of the key tidal energy sites around the UK have been demonstrated to be largely in phase.

ACKNOWLEDGMENT

This research was supported by funding from the EPSRC Supergen FlexNet (Grant no. [EP/E04011X/1]) and Supergen Marine (Grant no. [EP/E040136/1]) Consortia. The buoy records were supplied by the British Oceanographic Data Centre as part of the Inter-Agency Committee on Marine Science and Technology funded, 'UK Moored Current Meter Data Set' DVD electronic publication. The data were collected by the Proudman Oceanographic Laboratory during the Mixing and sediment resuspension in shelf seas which was funded by the Natural Environment Research Council (NERC). The authors wish to acknowledge EMEC and ScottishPower Renewables for the provision of ADCP data as well as Chris Zervas at NOAA for providing tidal analysis software. The authors would also like to thank Chris Dent from Durham University for supplying the capacity credit assessment. The map shown is based on UK Crown copyright material supplied through EDINA, www.edina.ac.uk.

REFERENCES

[1] House of Lords, The EU's Target for Renewable Energy: 20% by 2020. Volume I: Report. London, 2008.

[2] HM Government, The UK Renewable Energy Strategy. Surrey, July 2009.

[3] BLACK & VEATCH, Phase II.UK Tidal Stream Energy Resource Assessment, The Carbon Trust. London, 2005.

[4] R. Burrows, I.A. Walkington, N.C. Yates, T.S. Hedges, J. Wolf and J. Holt, The Tidal Range Energy Potential of the West Coast of the United Kingdom. Applied Ocean Research, 31, 229-238, 2009.

[5] Crown Estate, Press Release: World's First Wave and Tidal Energy Leasing Round to Power up to Three Quarters of a Million Homes, 16 May 2010 (http://www.thecrownestate.co.uk/newscontent/92-pentland-firth-developers.htmCrown Estate)

[6] A.S. Iyer, S. Couch, G.P. Harrison, A.R. Wallace. Variability and phasing of tidal current energy around United Kingdom. Renewable Energy 2011 [In review.]

[7] BLACK & VEATCH, UK Tidal Current Resource and Economics, The Carbon Trust, London, 2011.

[8] Department for Trade and Industry, Atlas of UK Marine Renewable Energy Resource. A Strategic Environmental Assessment Report, DTI, London, 2004.

[9] UK Hydrographic Office, Admiralty Charts, UKHO, Taunton, UK, (http://catalogue.ukho.gov.uk/home.asp.)

[10] G. Sinden, Variability of UK Marine Resource, The Carbon Trust, London, 2005.

[11] J.A. Clarke, G. Connor, A.D. Grant, C.M. Johnstone, Regulating the output characteristics of tidal current power stations to facilitate better base load matching over the lunar cycle, Renewable Energy, 31 (2006) 173-180.

[12] Department of Business, Enterprise and Regulatory Reform, Atlas of UK Marine Renewable Energy Resource, BERR, London, (http://www.renewables-atlas.info/)

[13] UK Hydrographic Office, Admirality TotalTide (version 2007), UKHO, Taunton, UK.

[14] J. Hardisty, Power intermittency, redundancy and tidal phasing around the United Kingdom, Geographical Journal, 174 , 76-84. 2008

[15] BLACK & VEATCH, Phase I.UK Tidal Stream Energy Resource Assessment, The Carbon Trust, London, 2004.

[16] MCT at Strangford: SeaGen the world's first commercial scale tidal energy turbine deployed in Northern Ireland. http://www.marineturbines.com/3/news/article/7/seagen__the_world_s_first_commercial_scale_tidal_energy_turbine_deployed_in_northern_ireland/

[17] Donald Shepard. A two-dimensional interpolation function for irregularly-spaced data. *In Proc. 1968 ACMNational Conference.*

[18] C. Zervas, Tidal Current Analysis Procedures and Associated Computer Programs NOAA Technical Memorandum NOS CO-OPS 0021, National Oceanic and Atmospheric Administration, Washington DC, 1999.

[19] Scottish Power Renewables in Sound of Islay: http://www.scottishpowerrenewables.com/pages/sound_of_islay.asp

[20] British Oceanographic Data Centre, Moored current data, (http://www.bodc.ac.uk/.)

[21] A.S. Iyer, S.J. Couch, G.P. Harrison, A.R. Wallace, Analysis and comparison of Tidal Datasets. Proc. 8th European Wave and Tidal Energy Conference.(EWTEC), Uppsala, Sweden, Sept. 2009.

[22] J. Thake, Development Installation and Testing of a Large Scale Tidal Current Turbine, Department for Trade and Industry, London 2005.

[23] G. Sutherland, M. Foreman, C. Garrett. Tidal current energy assessment for Johnstone Strait, Vancouver Island. Proc. IMechE Part A: Journal of Power and Energy, 221, 2007, pp. 147-157.

[24] National Grid (2009): Demand Data (http://www.nationalgrid.com/uk/Electricity/Data/Demand+Data/)

[25] Met Office: Gust speed records by district. http://www.metoffice.gov.uk/climate/uk/extremes/gust_district.html (Accessed on 28/04/11)

[26] 2010 National Electricity Transmission System Seven Year Statement.

[27] T. Boehme, Matching Renewable Electricity Generation with Demand in Scotland (PhD Theise). Institute for Energy Systems. Edinburgh, University of Edinburgh, 2006.

[28] C.J. Dent, A. Keane and J.W. Bialek, Simplified Methods for Renewable Generation Capacity Credit Calculation: A Critical Review, IEEE PES GM, 2010.

Elsevier Editorial System(tm) for Renewable Energy

Manuscript Draft

Manuscript Number: RENE-D-11-00146

Title: Variability and phasing of tidal current energy around United Kingdom

Article Type: Research Paper

Keywords: Renewable Energy; Tidal Current Energy; Intermittency; Tidal phasing

Corresponding Author: Miss Abhinaya Sankaran Iyer, BEng

Corresponding Author's Institution: Institute for Energy systems

First Author: Abhinaya Sankaran Iyer, BEng

Order of Authors: Abhinaya Sankaran Iyer, BEng; Scott Couch, PhD; Gareth Harrison, PhD; Robin Wallace, PhD

Abstract: Tidal energy has the potential to play a key role in meeting renewable energy targets set out by the United Kingdom (UK) government and devolved administrations. Attention has been drawn to this resource as a number of locations with high tidal current velocity have recently been leased by the Crown Estate for commercial development. Although tides are periodic and predictable, there are times when the current velocity is too low for any power generation. However, it has been proposed that a portfolio of diverse sites located around the UK will deliver a firm aggregate output due to the relative phasing of the tidal signal around the coast. This paper analyses whether firm tidal power is feasible with 'first generation' tidal current generators suitable for relatively shallow water, high velocity sites. This is achieved through development of realistic scenarios of tidal current energy industry development. These scenarios incorporate constraints relating to assessment of the economically harvestable resource, tidal technology potential and the practical limits to energy extraction dictated by environmental response and spatial availability of resource. The final scenario is capable of generating 17 TWh/year with an effective installed capacity of 7.8 GW, at an average capacity factor of 29.9% from 7 major key locations. However, it is concluded that there is insufficient diversity between sites suitable for first generation tidal current energy schemes for a portfolio approach to deliver firm power generation.

Variability and phasing of tidal current energy around United Kingdom

A.S. Iyer*, S.J. Couch, G.P. Harrison and A.R. Wallace

*** Corresponding author**

Address:

Institute for Energy Systems

School of Engineering

University of Edinburgh

Mayfield Road

Edinburgh EH9 3JL

E-mail address:

A.Sankaran-Iyer@ed.ac.uk

Scott.Couch@ed.ac.uk

Gareth.Harrison@ed.ac.uk

Robin.Wallace@ed.ac.uk

Phone:	**Fax:**
+44 (0) 131 650 5612	+44 (0)131 650 6554

Abstract

Tidal energy has the potential to play a key role in meeting renewable energy targets set out by the United Kingdom (UK) government and devolved administrations. Attention has been drawn to this resource as a number of locations with high tidal current velocity have recently been leased by the Crown Estate for commercial development. Although tides are periodic and predictable, there are times when the current velocity is too low for any power generation. However, it has been proposed that a portfolio of diverse sites located around the UK will deliver a firm aggregate output due to the relative phasing of the tidal signal around the coast. This paper analyses whether firm tidal power is feasible with 'first generation' tidal current generators suitable for relatively shallow water, high velocity sites. This is achieved through development of realistic scenarios of tidal current energy industry development. These scenarios incorporate constraints relating to assessment of the economically harvestable resource, tidal technology potential and the practical limits to energy extraction dictated by environmental response and spatial availability of resource. The final scenario is capable of generating 17 TWh/year with an effective installed capacity of 7.8 GW, at an average capacity factor of 29.9% from 7 major key locations. However, it is concluded that there is insufficient diversity between sites suitable for first generation tidal current energy schemes for a portfolio approach to deliver firm power generation.

Keywords

Renewable Energy, Tidal Current Energy, Intermittency, Tidal phasing

Abbreviations

ADCP	Acoustic Current Doppler Profiles
BODC	British Oceanographic Data Centre
EMEC	European Marine Energy Centre
GIS	Geographical Information System
IDW	Inverse Distance Weighting
NOAA	National Oceanic Atmospheric Administration
SIF	Significant Impact Factor
TAP	Technically Acceptable Power

Nomenclature and units

A	= area (m^2)
a_o	= amplitude
c	= wave celerity (m/s)
C_p	= Device efficiency
d	= distance (m)
g	= gravitational acceleration (m/s^2)
h	= water depth (m)
P	= Power (W)
T	= time period (s)
v	= velocity (m/s)
ρ	= density (kg/m^3)
λ	= wavelength (km)

1. Introduction

The European Union's ambitious target of meeting 20% of energy demand from renewable energy by 2020 [1] is driving interest and investment in the renewable sector. The UK 2020 target of 15% renewable energy implies a need for around 34% reduction in emissions [2]. Meeting these targets will require substantial investment in new on- and offshore wind, wave and tidal energy developments, drawing on the UK's abundant resource potential. There is however concern regarding the integration requirements of the large capacities of new renewable generation implied by UK targets given the inherent variability of the major renewables, and the relative timing of their output with electricity demand. In reality, no energy source is 100% reliable and outages (scheduled or unscheduled) do occur. Demand patterns are also variable, hence the power system and network have historically, and will continue to be required to be designed and managed to handle variability [3]. As tidal current energy generation is driven by the gravitational interaction of the Earth–Sun-Moon system, tidal energy production patterns can be reliably predicted on both short and long timescales. Accurate predictions of the output and variability of individual tidal current sites and the impact of aggregation of output from various sites will be highly desirable to facilitate network planning and operation.

The Carbon Trust has commissioned a number of studies that have been used to assess the tidal current resource, its variability and its implications for development [4-6]. As part of the Marine Energy Challenge Black and Veatch (B&V) [4] estimated the extractable tidal current resource to be 18 TWh/yr (±30% uncertainty) [4], that this 'Technically Extractable Resource' can meet about 5% of current UK demand and that the UK has around 50% of the EU tidal current resources. The study used output from the DTI Atlas of UK Marine Renewable Energy Resources [7], Admiralty Chart data from the UK Hydrographic Office [8], and local current meter data to select and characterise specific locations of tidal energy generation. It also applied a 'Significant Impact Factor' (SIF) to assess the 'Technically Acceptable Resource' tat places a limit on the amount of available kinetic energy that can be harvested without undue impacts on the environment and the tidal current resource itself. This SIF value was estimated as being 20% of available kinetic energy flux [4] although understanding of the extraction limits has since advanced considerably [e.g. 9, 32].

Analysis of tidal current energy generation potential has been further progressed by Sinden [5] by extracting power output time series for wave and tidal energy. Comparing the variability of the identified tidal sites was conducted using data extracted from the Proudman Oceanographic Laboratory POL CS20 tidal model [11] (also the basis for the DTI Atlas tidal component [7]). Although the variations were examined at specific locations, and SIF constraints (as in [4]) were taken into account, the analysis assumed a scenario where all the sites are fully developed without any further constraints. While this may be possible in a few decades time, 'first generation' tidal current devices are unlikely to be able to be deployed in water depth over 50 meters deep. Also as the analysis in [5] focuses on a portfolio of tidal and wave energy generation, the effect of tidal current energy alone cannot be easily discerned.

Boehme *et al*. [12] examined tidal current resource variability in Scotland as part of the 'Matching Study' for the (then) Scottish Executive. It used the DTI Atlas and Admiralty charts to define current

flows within Scottish waters. It applied a generic twin-rotor tidal turbine to estimate production levels and variability. The study estimated the Scottish tidal resource as 2.2 TWh/yr when a 750 MW installed capacity development scenario is considered.

1.1 Firm Tidal Power Generation

An important area that these studies have not tackled directly is whether the aggregate outputs from tidal sites can represent a form of 'firm' energy generation through diversity in the phasing of energetic sites. Two other studies have offered some analysis of this issue. Clarke *et al*. [13] suggest that aggregate output from a number of sites can provide base load. Unfortunately, the sites selected are less energetic and/or generally too deep for first generation deployment. For example, Sanda (Mull of Kintyre) has tidal current velocity above 2.5 m/s but the water depth at this site ranges from 100-120 m. While this site may eventually be developed for tidal current energy harvesting, it is not credible for first generation tidal projects. Hardisty [14] also reports that by careful selection of tidal current site locations a continuous – or firm – level of generation could be achieved. However, when interrogating the same data source as referenced in [14] (Admiralty Total Tide software [15]), the authors were unable to reproduce this outcome as the sites selected generally had current velocities below 1 m/s. Additionally, considering the local bathymetric depth data [7], indicates that some of the sites identified in [14] are too shallow for full scale device deployment. Hence, the authors contend that the locations identified in [14] are not likely to be considered for large scale development of tidal current energy even if they are out-of-phase, as they are wholly inappropriate for economic energy generation.

Given the identified deficiencies of existing efforts to assess the potential for 'firm' tidal current energy generation, this paper is concerned with understanding the scope for portfolios of credible first generation tidal current development scenarios to provide firm power. This involves a reassessment of the UK tidal current resource by identifying appropriate development locations incorporating the latest thinking on power extraction limits and examines aspects of generation yield, variability and temporal phasing.

For the purposes of the analysis to be presented herein, first generation technology is defined as iterations of existing prototype devices that are already undergoing pre-commercial demonstration. A second generation of technology is defined as being able to be deployed in deeper waters. Examples of second generation technology solutions are under development, but are currently at the early stages of technology readiness, and hence unlikely to make a significant contribution to meeting 2020 energy generation targets.

1.2 Data sources

The majority of the data used in this study are publically available. Two different datasets are used to provide spatial and temporal accuracy. With additional processing, the datasets are combined to achieve considerable improvement in analysing the resource. The data obtained from the DTI Atlas of UK Marine Renewable Energy Resource [7] has been taken forward by The Department for Business, Enterprise and Regulatory Reform (BERR) and the underlying Marine Atlas data is now available through a web interface [10]. The Geographic Information System (GIS) data layers downloadable

from the web interface are interrogated in the analysis presented using ArcGIS and integrated with manipulated Admiralty chart data [8] accessed utilising Admiralty Total Tide software [15] to provide time series at identified locations.

Acoustic Doppler Current Profiler (ADCP) data can also be used to measure current velocity, using the principles of Doppler Effect and reflecting sound off small particles in the water column [16]. ADCP data was made available to the author on request for Orkney by the European Marine Energy Centre (EMEC) [17] and measured buoy data was obtained from British Oceanographic Data Centre (BODC) for Anglesey [18]. Time series for all the sites need to be coincident in time, therefore this additional buoy and ADCP data had to be recreated using harmonic decomposition and prediction, in this case using the methodology advocated by the US National Oceanic Atmospheric Administration (NOAA) [19].

The paper is laid out as follows: section 2 examines the theory behind tidal currents and their phasing around the UK. Section 3 sets out the methodology for assessing the resource available at first generation tidal sites and section 4 reports on the outcomes of the analysis. Sections 5 and 6 discuss the implications and conclusion of the study.

2. Tidal Resource Phasing

The timing of the tidal phasing stems from the fundamental concept of tidal wave propagation. The velocity of tidal wave propagation (wave celerity '*c*') in shallow water is given by:

$$c = \sqrt{gh} \tag{1}$$

where *c* is the wave celerity (m/s), *g* is the gravitational acceleration (m/s^2), and *h* is the water depth. For the purpose of elucidating the discussion, a depth of 50 m is selected as being representative of UK coastal waters. From this, the wavelength λ of the tidal wave can be calculated as:

$$\lambda = cT \tag{2}$$

where *T* in this case is taken as the time period 12.4 hours of the dominant tidal constituent (M2 - the diurnal pattern of the Moon). The wavelength of the M2 tidal component in 50 metres water depth is 988 km, which is around the length of the UK landmass. This would suggest that that there are substantial differences in phase around the UK coastline, however the topology of the British Isles serves to complicate matters: Figure 1 shows the co-tidal lines around the UK that represent the time of high water at each location. This broadly illustrates the phasing of tidal currents although coincidence in the time of high water does not necessarily mean that the tidal currents in each location are also in phase as this is highly dependent upon the local variation of surface elevation. Tidal interaction with local bathymetry and the coastal topography also play an important role in the local phasing of tidal currents. In addition the characteristics of tidal current generators, particularly the shape of the power extraction curve will also play a significant role in the phasing of production.

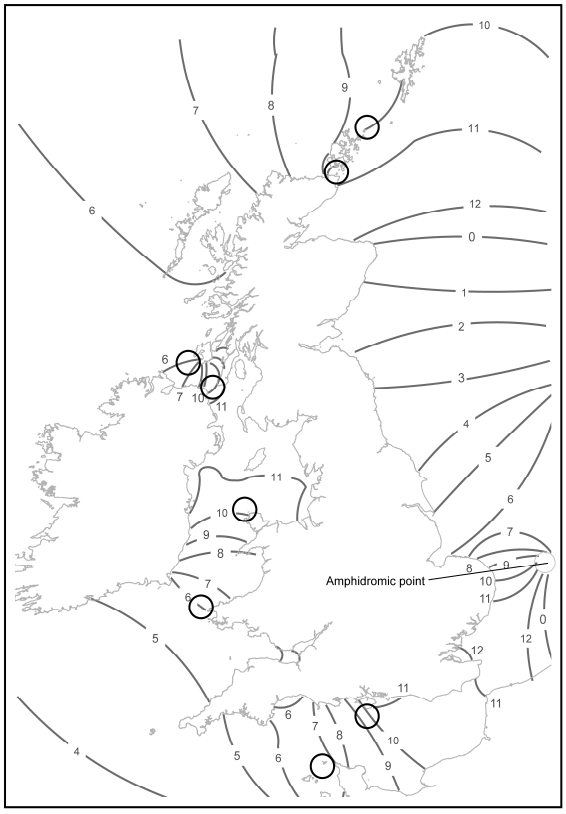

Figure 1. Co-tidal lines for the coast of UK. Areas indicated by the circles are regions identified to be of interest for tidal current energy development.

The locations circled in Figure 1 have been identified by Black and Veatch [4] as being sites of interest for tidal current energy extraction. Ideally a phase difference of 90 or 270 degrees (around three or nine hours) between two locations is optimal for tidal sites to provide best potential for generating firm power. However, the locations highlighted in Figure 1 experience high water at broadly similar times. This suggests that there is also a good likelihood that these locations will also exhibit tidal current patterns that are also likely to be in phase. If this coincidence of tidal velocity phasing can be verified for instance in the case of the Pentland Firth and Channel Islands this will have significant negative impact on the potential for tidal current energy to generate a large proportion of its output as firm power, as these two locations alone have been identified as embodying about 70% of the technically extractable UK tidal current energy resource [6]. Sites in the Pentland Firth have already been identified as likely to witness the first significant tidal current energy developments, as established by the recent round of site leasing by the Crown Estate with 1.2 GW installed capacity of wave and tidal energy originally proposed for this region [20]. An additional 400 MW of tidal energy developments have since been leased in the Inner Sound region of the Pentland Firth [21]. As a result of these geographically clustered developments, there will likely be very small phase difference between the tidal sites. This will become relevant in section 4 where specifics of site selection and their outputs are discussed. The ‘in phase’ character of the tidal sites is entirely coincidental and specific to the UK context under investigation; such coincidence of phasing of so many key locations in one country is unlikely to be replicated in other territories when the tidal current energy resource is accurately assessed.

3. Methodology

The methodology aims to make best use of publicly available data to identify locations suitable for deployment of first generation tidal current devices and to generate credible time series of energy production from generic tidal current technologies at these locations. It also allows the latest methods on power extraction limits to be incorporated. The three main stages of the method outlined in Figure 2 are:

1. Identification of locations suitable for large scale first generation tidal current device developments;
2. Estimation and validation of the tidal current time series at these locations;
3. Estimation of generic tidal generator size, rating and hence time series of energy generation at each identified location.

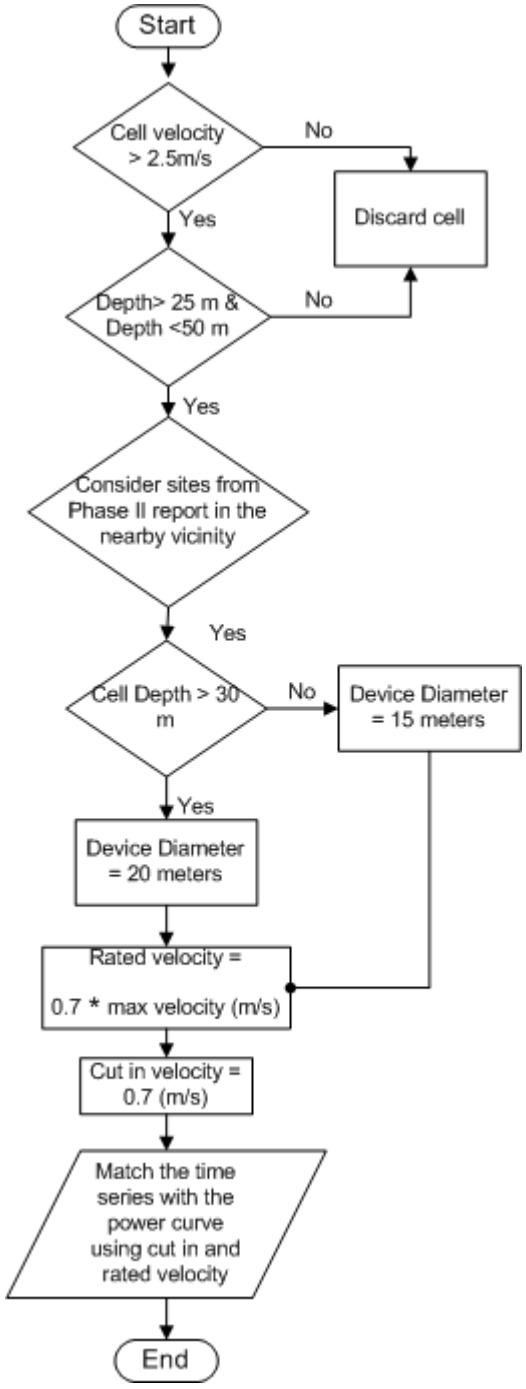

Figure 2. Flowchart showing the steps embodying the methodology

The final time series generated provide a suitable format to enable comparison between and aggregate assessment of the energy generation potential of specific regions or for the UK as a whole.

3.1 Identification of locations suitable for first generation tidal devices

The first stage of the process outlined in Figure 2 aims to identify sites that are viable for the deployment of first generation tidal current devices. Data accessed from downloadable GIS layers of the Atlas of UK Marine Renewable Energy Resources [10] are utilised for this purpose. This is a similar approach to that adopted by B&V [4]. The GIS data itself is derived from the POL CS20 Model [11], data also utilised in the analysis conducted by Sinden [5]. The Atlas provides mean spring and neap tide velocity magnitude and water depth data within the UK territorial waters at a spatial resolution of approximately 1.8km^2. Figure 3 shows the mean spring peak current for the UK and several regions of particular interest for first generation tidal deployment.

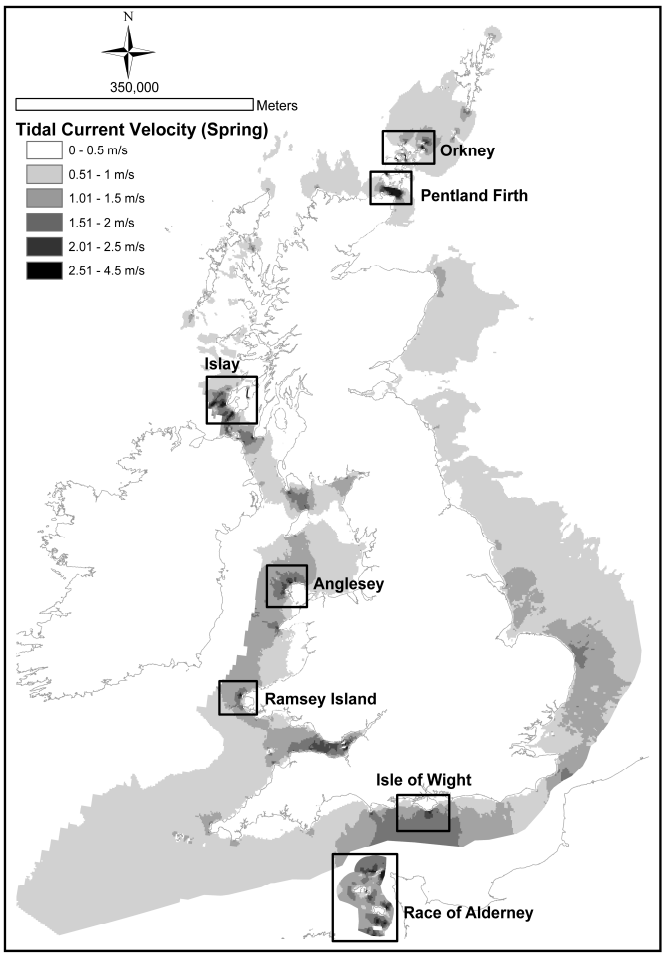

Figure 3. Figure showing mean spring peak current and specific regions of interest.

BERR Marine Atlas. © Crown Copyright. All rights reserved 2008.

Using ArcGIS, the Marine Atlas data [10] was interrogated to select specific cells meeting certain criteria. For a site to be considered economically viable for first generation tidal farms the mean spring peak current velocity must exceed 2.5 m/s [4]. The second criterion is the need for the water depth to be within the range 25 to 50 meters which is the expected operational parameter for first generation devices. A list of all the sites selected using these criteria are indicated in Table 1 and Figure 3. The

number of (approximately 1.8 km^2) cells identified as meeting these criteria at each of the listed sites are included to give an estimate of the extent of each of the sites.

To simplify relaying the findings, where appropriate, the sites in a particular region have been grouped together. It is interesting to note that Table 1 does not include all the sites identified by B&V [4] as many of the sites identified by their analysis are in water depths greater than 50 meters or do not meet the velocity criteria applied here. In some cases, smaller sites like Strangford Narrows – the test site for one of the few existing full scale tidal current energy technologies – have not been included in the Marine Atlas [10]. The Marine Atlas does not resolve the Narrows regions or similar narrow channels, and insufficient data to generate a time-series of resource variability was available in the public domain for the Narrows. An additional variation is that although depth data from [10] suggests that the Sound of Islay is not deep enough to be considered for device deployment, Scottish Power Renewables [22] indicate that the Sound of Islay reaches 48 meters deep and therefore is appropriate for first generation development. This example is indicative of some of the limitations of the Marine Atlas as a data source – it has wide area coverage, but this is only achievable because the resolution is still relatively coarse (from an end-users context). It should also be noted that the majority of the identified sites are located in Scotland in relatively close proximity to each other: the Pentland Firth alone houses six major sites.

	Site name	Grid reference		No. of cells	Region	Average Depth (m)	Average Velocity Spring Peak (m/s)
Pentland Firth	Pentland Skerries	58.72 N	-2.95 W	2	Scotland	35.50	3.60
	S. Ronaldsay P.Firth	58.74 N	-3.06 W	1	Scotland	39.00	3.19
	S. Ronaldsay/ P.Skerries	58.69 N	-2.92 W	5	Scotland	43.20	2.93
	Duncansby Head	58.64 N	-3.01 W	1	Scotland	36.00	3.25
	Inner Sound	58.66 N	-3.06 W	3	Scotland	28.67	3.27
	Stroma P.Firth	58.68 N	-3.12 W	7	Scotland	39.29	3.44
Orkney	Westray Firth	59.17 N	-2.86 W	2	Scotland	29.00	3.81
	N. Ronaldsay Firth	59.39 N	-2.34 W	1	Scotland	34.00	2.57
Islay	Islay North	55.67 N	-6.84 W	7	Scotland	29.00	2.75
	Islay Centre	55.67 N	-6.63 W	12	Scotland	27.75	2.76
	Islay South	55.54 N	-6.39 W	8	Scotland	38.88	2.63
	Sound of Islay	55.86 N	-6.09 W	2	Scotland	50.00	2.95
Anglesey	Anglesey North	53.42 N	-4.61 W	4	Wales	30.00	2.59
	Anglesey South	53.29 N	-4.71 W	1	Wales	31.00	2.60
	Ramsey Island	51.41 N	-5.41 W	3	Wales	35.00	2.66
	Race of Alderney	49.69 N	-2.11 W	19	England	31.68	3.38
	Isle of Wight	50.56 N	-1.23 W	2	England	27.50	2.76

Table 1. List of all the sites considered in this study as identified using the methodology in Figure 2.

3.2 Estimation and validation of tidal current time series

The next stage of the analysis is to generate credible tidal current time series data for each of the sites identified in Table 1. The first step is to use information from the UK Hydrographic Office (UKHO) Admiralty chart data [8], often referred to as 'tidal diamonds', as their respective positions are indicated on Admiralty charts by diamond symbols. The TotalTide software package [15] contains fundamentally the same information as the Admiralty charts but provides a convenient means of interrogating the tidal current data through time at the tidal diamond locations. The limitation of the TotalTide data is that it only encapsulates the variability of the currents as described by the two

dominant tidal harmonic constituents, M2 and S2 [23]. A limitation is that the tidal diamonds do not always coincide spatially with the locations of specific cells of interest within each site. Therefore, to allow generation of time series of current flows, 'pseudo diamonds' were created at these points based on interpolation from surrounding tidal diamonds. This approach is similar to that applied by Boehme *et al* [12]. The inverse distance weighting (IDW) interpolation methodology [24] was applied to create a site specific flow velocity v by weighting the velocities v_k at nearby tidal diamond locations k according to their relative distance d_k from the specific site of interest:

$$v = \frac{\sum_k v_k \cdot d_k^p}{\sum_k d_k^p} \quad (3)$$

where the value of p describes the relative influence of nearby over more distant points. A value of 2 is adopted here as recommended by [24]. Multiple calibrations between different tidal diamonds were employed to find IDW's that best represented the sites. To improve the accuracy of the data set, the time series was scaled up to the spring peak current value obtained from the nearest grid cell reported in the Marine Atlas. This maintains the local phasing and spring-neap variability as prescribed by the tidal diamond data obtained from the TotalTide software, while also utilising the improved resolution of the numerical model output to identify local peak current velocities. Outputs from the numerical model as time-series are unfortunately not available in the public domain, hence the need to combine various data sources. Using this approach helps maintain the correct phase of tidal propagation and provides credible current velocity estimates at each of the sites of interest. All the tidal diamond datasets generated are for the year 2009 when the analysis was initiated using appropriate available datasets.

Although tides are highly spatially variable as highlighted in [25], the methodology presented represents a consistent means of combining datasets without the need to perform full-scale site assessment modelling, necessitating an extensive and expensive in-situ survey data and numerical modelling campaign beyond the scope of this analysis (and although highly desirable is, as yet, unavailable on a UK wide scale).

The authors consider in-situ data measurements to be the preferred 'gold-standard' data source, and were obtained where possible. Acoustic Doppler Current Profiler (ADCP) data for various sites were obtained through purchasing data sets and via personal communication. For example, data for the Orkney region obtained from the European Marine Energy Centre (EMEC) [17]. ADCP measurements are very accurate when set up correctly and hence are highly desirable for conducting detailed site analysis and characterisation. The ADCP data used for analysis at the Orkney location is a 1 month long measurement taken in 2005 and hence does not coincide in time with the tidal diamond time series obtained for all the other locations. Therefore harmonic constituents for theses locations were determined from the ADCP data records using least-squared analysis. 23 principal constituents were obtained following the recommended practice of the NOAA in their Tidal Current Analysis Procedures and Associated Computer Programs documentation [19]. The principal constituents were then used to recreate the time series coincident in time and in temporal resolution to all the other time series created from tidal diamonds.

Similarly, recording current meter data measurements for Anglesey were obtained from the British Oceanographic Data Centre (BODC) [18]. The minimum data length used in the analysis was 29 days which enabled a detailed harmonic analysis to be conducted: the specifics of this analysis can be found in [25].

Where ADCP data is obtained, velocity from the 'mid bin' of the water column is used, usually where the hub is placed. This is done so that the resource is not under estimated. Tidal diamond data is measure near surface (at about 5 meters from surface). This data has not been processed further. Therefore although mentioned velocity as *v,* for tidal diamond data its near surface and for ADCP data it is mid depth velocity.

3.3 Estimation of generic tidal generator size, rating and production time series

The third stage of the method uses a simple generic model of a 3-bladed horizontal axis tidal current device to estimate time series of power generation at each site from local current velocity time-series. For the purpose of assessing energy extraction, it is assumed that each device is sited such that the flow direction is aligned perpendicular to the device axis of rotation. Two device models are used to reflect the differences required for operating in different water depths: in cells with minimum water depths of 25 to 30 meters a device rotor diameter of 15 meters provides appropriate surface and seabed clearance, avoiding conflict with vessel navigation in the region. In depths greater than 30 meters, a device diameter of 20 meters is specified.

An appropriate rated current velocity for each cell is determined by taking 70% of the Spring peak velocity of the specific cell. This follows similar practice to [4], utilising understanding of the optimal economic balance between capturing maximum available energy and the cost of the energy capture device. If, for instance, the device was rated to coincide with maximum Spring peak velocity, then the drivetrain would have to be rated to operate for a condition that occurs only for a short instant each month, and the structural support element of the device would similarly have to be designed to withstand the thrust acting on the turbine for only a minute fraction of the operational period. Having established the rated velocity, the power can be assessed across the operational cycle as:

$$P = \frac{1}{2} C_p \rho A v^3 \tag{4}$$

where C_p is the device efficiency and assumed to be 40% on the basis of [26], the water density, ρ = 1025 kg/m^3, A (m^2) is the rotor swept area and v (m/s) is the depth-averaged current velocity. Figure 4 illustrates the hypothetical power curve for a generic 0.5 MW rated turbine, and demonstrates the difference in rated velocity necessary to generate 0.5 MW with a 15 and a 20 meter rotor diameter. A cut in velocity of 0.7 m/s is assumed for all the hypothesised generic tidal turbines [26].

Multiple tidal devices populate each of the 1.8km^2 cells. EMEC standards [27] suggest devices are spaced two and a half diameters between the rotor axis perpendicular to the current and ten diameters apart parallel to the current. Here the assumed device array spacing is more conservative with three diameters apart laterally and ten diameters spacing upstream/downstream of each device. This means that 480, 15 m diameter devices or 270, 20 m diameter devices can populate each 1.8km^2 cell. It is

acknowledged that actual array layout is unlikely to be as regimented, employing staggering of devices, and would have to adapt to the real world variability of appropriate bathymetric conditions (e.g. bed slope). The device rating varied for each cell based on the local bathymetry (impacting diameter) and maximum Spring peak velocity (impacting rated velocity) reported for that cell as previously outlined.

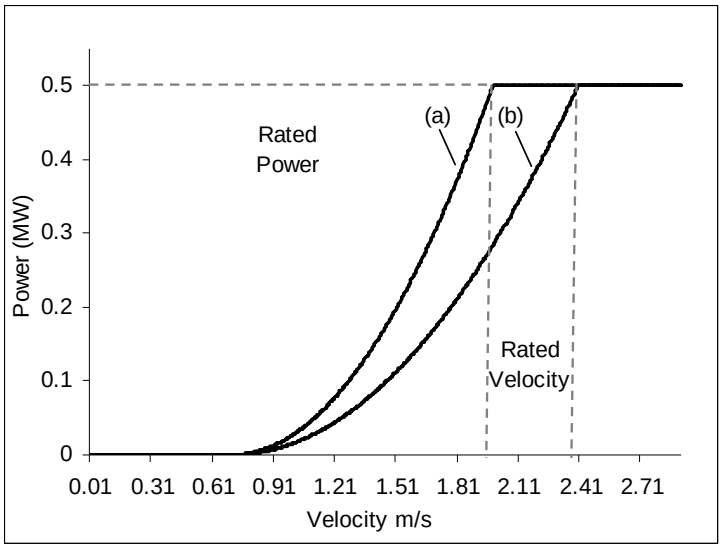

Figure 4. Hypothetical power curve for a generic 0.5 MW tidal current device: (a) rated velocity of 1.98 m/s with 20 m diameter rotor; (b) rated velocity of 2.39 m/s for a 15 m rotor.

4. Analysis

This section reports the results obtained from application of the methodology described in section 3 when applied to the sites identified in table 1 as being suitable for first generation tidal current sites (also see figure 3). The power potential of each site, the phasing of the sites and the impact of the environmental extraction limits at each location are presented.

4.1 First Generation Tidal Current Resource

The installed capacity of each cell was calculated from the relevant cell rated velocity and peak power output. These are aggregated for each site as shown in Table 2 along with a breakdown of the number of each turbine size. This shows that, overall, first generation sites would support an installed capacity of 13.4 GW of tidal current devices. The installed capacity is a simple assessment of the number of devices that can be placed in each of the identified cells without considering any impact this may have on the current flow velocity or the environment. There is a substantial range of installed capacity, with the largest single site capacity identified as 3855 MW in the Race of Alderney and the smallest being the 105 MW Anglesey South site. The largest regional group is the Pentland Firth at 4352 MW. For the purposes of the analysis presented here, the interaction of devices with wakes generated by upstream devices and device downtime due to planned or unplanned maintenance have been ignored, as these aspects are likely to be highly site- and project-specific. These aspects are more appropriate for consideration at a project assessment scale as opposed to a higher level national assessment.

	Site name	No. of cells	No. of device (20 m)	No. of device (15 m)	Installed Capacity MW	Yield TWh/yr	Capacity Factor %
Pentland Firth	Pentland Skerries	2	540		708	1.8	28.8
	S. Ronaldsay P.Firth	1	270		194	0.4	26.2
	S. Ronaldsay/ P.Skerries	5	1350		759	1.7	25.2
	Duncansby Head	1	270		205	0.6	32.6
	Inner Sound	3	270	960	813	1.4	23.3
	Stroma P.Firth	7	1890		1673	3.9	24.7
	Regional Total				**4352**	**9.7**	
Orkney	Westray Firth	2	540		620	2.6	32.4
	N. Ronaldsay Firth	1		480	180	0.2	23.8
	Regional Total				**800**	**2.9**	
Islay	Islay North	7	810	1920	875	2.5	32.5
	Islay Centre	12	2160	1920	1526	4.5	33.2
	Islay South	8	1620	960	879	2.6	33.3
	Sound of Islay	2	40		23	0.1	43.6
	Regional Total				**3302**	**9.6**	
Anglesey	Anglesey North	4	270	1440	418	1.0	26.2
	Anglesey South	1	270		105	0.3	32.4
	Regional Total				**523**	**1.3**	
	Ramsey Island	3	540	480	**340**	**0.7**	24.8
	Race of Alderney	19	3658	1178	**3855**	**10.4**	30.0
	Isle of Wight	2		960	**255**	**0.7**	29.6
	TOTAL				**13427**	**35.2**	

Table 2. All the sites with installed capacity, annual energy yield and capacity factor

The gross annual energy yield from each of the cells is calculated from the tidal current time series at each cell matched with the device power curve identified as appropriate for that cell. As reported in table 2, the results from each cell within a site are summated and suggest that over 35 TWh per year could be produced across each of the sites, which equates to approximately 10% of UK electricity demand [28]. The productivity of each site broadly reflects the installed capacity, although the match between current flow conditions and generator characteristics means that the production from each site varies. For example, the Race of Alderney has the highest energy yield despite not possessing the largest installed capacity. This is reflected in the site capacity factors (Table 2; the ratio of production from a given generator to the production if the same generator operated at rated output with 100% availability). The overall average capacity factor across all the sites is 29.9% but the values for individual sites vary between 23.3 and 43.6%. For comparison, the average load factor for onshore wind across the UK in 2009 was 27.4% [29]. The load factor differs from the capacity factor by accounting for planned and unplanned outages – the load factor is a measurement of performance, the capacity factor an assessment of performance potential.

Capacity factor can be used as a simplified indicator of how 'economic' a site is by indicating how well the capital investment in generation capacity is being utilised. A low capacity factor is indicative of a lower economic performance on a per kW basis but the overall investment may still perform very well. The variation in capacity factor may partially also be a consequence of the simple generic turbine sizing utilised under-rating device characteristics at some of the higher capacity factor sites, and being too large for low capacity factor sites. The important point in decision-making however, is the balance between revenue from energy sales and the cost of the installation. With the cost of the devices and

importantly the grid connections not part of the selection criteria, it would be anticipated that sites further from land represent a more challenging investment, particularly at prices of £52,000/MW/km for underwater provision of 132-275 kV HVAC cable [30]. It is important to highlight that such additional externalities will impact on potential site selection, as distance to shore as an example is an important criterion differentiating projects.

4.2 Site Phasing

The generation time series are now used to examine the relative phasing of production from each site. Figure 5 is a plot for a typical spring peak day, highlighting that the majority of generation contributions are from the Pentland Firth, Islay region and the Race of Alderney. The periods of generation at rated output can be clearly seen in many of the traces particularly for the Pentland Firth, as can the asymmetric nature of the production cycle with aggregated output increasing more slowly than it reduces. The location of the individual sites determines their phasing and in terms of tidal wave propagation, Islay and Pentland Firth are in phase due to the coincidence of the local tidal phasing at these locations. The Race of Alderney is out of phase (behind) by approximately one hour. The aggregate effect of this can be seen in the total power output generated which highlights the inter daily variability. What is notable is that the base of aggregate generation is much wider than any of the individual outputs: this shows that there is a portfolio aggregating effect exploiting the phase variations between sites. However, this effect is not sufficient to generate significant firm output as none of the large sites are appropriately out of phase. Even the smaller contributions from the Orkney, Anglesey, Isle of Wight and Ramsey Island sites are more or less in phase with each other, and with the Pentland Firth and Islay.

4.3 Technically Acceptable Power Extraction

So far the analysis has not taken any account of the fact that there is a limit to the amount of energy that can be extracted from the tidal system. The original Significant Impact Factor of 20% extractable kinetic energy used in many tidal assessments has been substantially revised in [9] to reflect improved understanding of the hydrodynamic mechanisms that underly the tidal current resource.

The numerical modelling carried out by the authors in support of [9] assesses representations of various relevant hydrodynamic mechanisms – tidal streaming, resonance and hydraulic currents – the flow phenomena that create tidal current conditions necessary for economic project development. The same analysis also demonstrated that when too much energy is extracted from the system, this impacts on the underlying dynamics of the tidal system. The evidence suggest that beyond what is referred to as the theoretical harvesting limit, attempts to extract more energy by installing additional devices would in fact result in a reduction of the overall energy harvested as each device in the farm would experience a reduction in kinetic energy flux. This has previously been demonstrated analytically for hydraulic current tidal flow regimes by [31] and [32]. A further ‘Technically Acceptable Power’ (TAP) limit has also been defined in [9] by imposing constraints to limit far field environmental impacts beyond which energy harvesting is likely to be restricted by environmental regulation.

Tidal Mechanisms	Theoretical limit of tidal current energy harvesting.	'Technically acceptable' limit of tidal current energy harvesting.	Hydrodynamic response limiting energy harvesting.
Hydraulic current	$P_{Theoretical} = 0.2\rho g Q_{\max} a_o$	$P_{acceptable} = 0.086\rho g Q_{\max} a_o$	Velocity reduction
Resonant basin	$P_{Theoretical} = 0.2\rho g Q_{\max} a_o$	$P_{acceptable} = 0.033\rho g Q_{\max} a_o$	Downstream tidal range
Tidal streaming	$P_{Theoretical} = 0.16\rho g Q_{\max} a_o$	$P_{acceptable} = 0.020\rho g Q_{\max} a_o$	Downstream tidal range

Table 3. Summary of technically acceptable power (TAP) extraction limits for the three identified tidal flow driving mechanisms.

The parameters needed for this calculation are shown in Table 3 where Q_{max} is the maximum flow rate and a_o the amplitude of the sea level difference between the two ends of the channel in the case of a hydraulic current. For tidal streaming and resonance a_o is the local tidal elevation amplitude. To evaluate the level of power that can be harvested from each of the sites, their respective hydrodynamic mechanism is identified and a TAP value defined. Regions with multiple sites are treated in one of two ways: the sites at Orkney, Islay and Anglesey are considered to be sufficiently geographically and hydraulically dispersed to be evaluated separately while for the Pentland Firth, sites are considered interdependent and are handled jointly by a single set of limits. For many sites the high flow velocities experienced areas are a result of a combination of mechanisms; Table 4 lists all the sites and attempts to identify the dominant hydrodynamic mechanism experienced. Using the dominant system, the annual 'Environmentally acceptable' power that can be extracted from each of the sites is assessed as reported in Table 4 using the extraction limits identified (Table 3).

The TAP yield values listed in Table 4 are used to place limits on the development at each site – defined as the TAP yield. In order to incorporate this, the capacity factor for each cell was used to define the 'least economic', and these cells are prioritised for removal from the analysis when limitation of the site output is necessary to meet TAP constraints. This was achieved either by removing the cell entirely or by reducing the number of devices deployed in the identified cell to meet TAP constraints. The energy yield reductions imposed by TAP constraints range from 5% for the Pentland Firth to 80% for the Race of Alderney, with an overall reduction of 52% (from 35.2 TWh/yr to 17 TWh/yr). In some cases, there is no reduction in capacity and yield (N. Ronaldsay Firth, Sound of Islay, Anglesey North and Isle of Wight) as the original unconstrained energy yield is less than those implied by the TAP limits. This is because the power that can be extracted using first generation devices is less than the identified TAP and hence these locations do not require further constraint beyond the initial spatial availability for device deployment.

Figure 5 presents the time series of aggregate unconstrained production from the sites from a day coincident with a Spring tide. In contrast Figure 6 shows the same time series with the TAP limits applied and indicates the significant overall reduction in aggregate energy generation. Most significant is the impact on the Race of Alderney power output, and its impact on the aggregate generation potential is obvious. This is of particular significance from a phasing perspective, as the Race of Alderney is the only site that made any significant (partial) out of phase contribution.

	Site name	Tidal Site System	ANNUAL YIELD TWh/yr Unconstrained	TAP (Constrained)	Actual	% Reduced	CAPACITY MW Unconstrained	Constrained	% Reduced
Pentland Firth	Pentland Skerries	HC	1.8	Calculated as one system	1.8		708	708	
	S. Ronaldsay P.Firth	HC	0.4		0.4		194	194	
	S. Ronaldsay/ P.Skerries	HC	1.7		1.7		759	759	
	Duncansby Head	HC	0.6		0.6		205	205	
	Inner Sound	HC	1.4		1.4		813	813	
	Stroma P.Firth	HC	3.9		3.4		1673	*1526*	
	Regional Total		**9.7**	**9.2**	**9.2**	-5%	**4352**	**4205**	-3%
Orkney	Westray Firth	HC	2.6	0.7	0.7		620	*259*	
	N. Ronaldsay Firth	TS	0.2	0.2	0.2		180	180	
	Regional Total		**2.9**	**1.0**	**1.0**	-67%	**800**	**439**	-45 %
Islay	Islay North	TS	2.5	0.5	0.5		875	*167*	
	Islay Centre	TS	4.5	0.6	0.6		1526	*192*	
	Islay South	TS	2.6	1.2	1.2		879	*393*	
	Sound of Islay	HC	0.1	0.7	0.1		23	23	
	Regional Total		**9.6**	**2.9**	**2.3**	-76%	**3303**	**775**	-77 %
Anglesey	Anglesey North	TS	1.0	0.8	0.8		418	*363*	
	Anglesey South	TS	0.3	0.4	0.3		105	105	
	Regional Total		**1.3**	**1.2**	**1.1**	-10%	**523**	**468**	-11 %
	Ramsey Island	TS	**0.7**	**0.6**	**0.6**	-16%	**340**	**285**	-16 %
	Race of Alderney	TS	**10.4**	**2.1**	**2.1**	-80%	**3855**	**747**	-81 %
	Isle of Wight	HC	**0.7**	**1.2**	**0.7**	-	**255**	**255**	-
	TOTAL		**35.2**	**18.2**	**17.0**	-52%	**13428**	**7174**	-42 %

HC = Hydraulic current TS = Tidal streaming

Table 4. Technically Acceptable Power that can be extracted from each of the sites and the final annual energy yield including TAP constraints

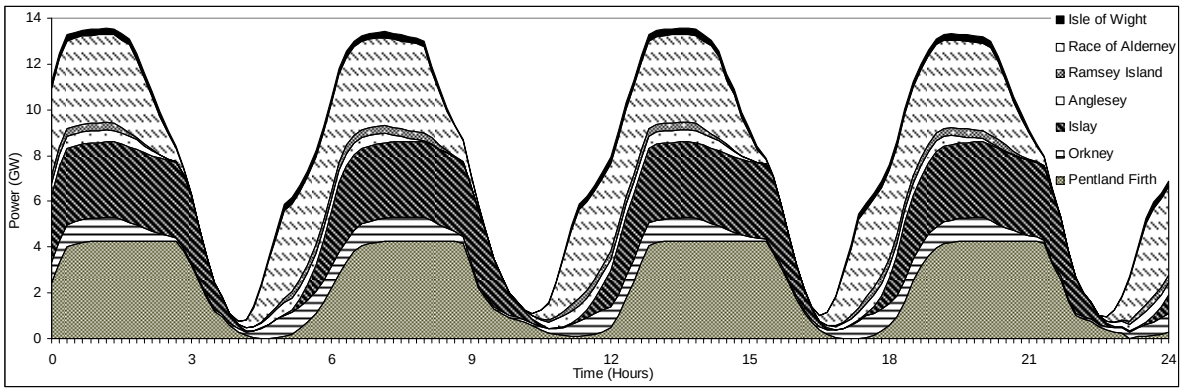

Figure 5. Stacked time series of all sites showing aggregate production at spring peak with environmental constraints ignored.

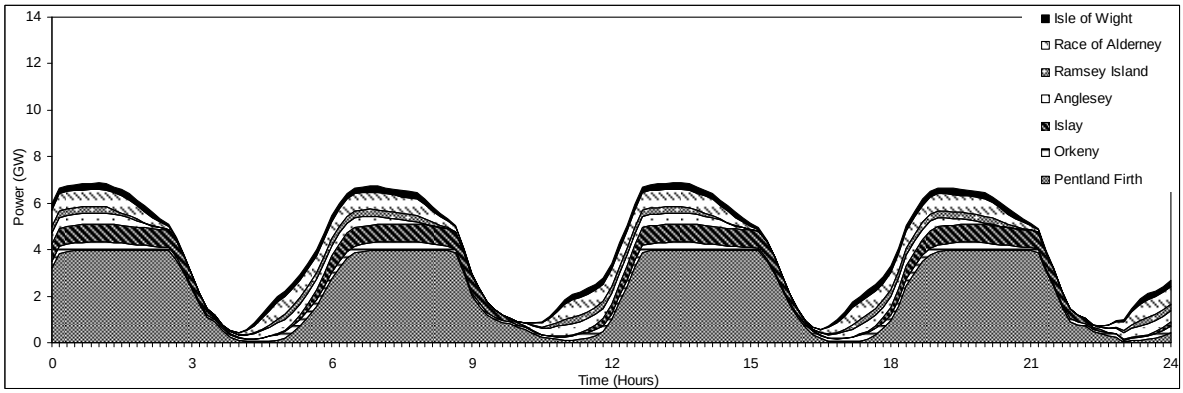

Figure 6. Stacked time series of all sites showing aggregate production at spring peak with environmental constraints included

Figure 6 represents the final scenario that is used for further assessment, representing a realistic scenario of tidal current energy development that can be undertaken with first-generation depth limited

devices. Over a three hour period during a typical spring tide, the power output varies from 7 GW to 1 GW or less and this variation occurs four times daily. During the neap cycle (not shown) the peak power generation will be of the order of 4 GW and falls to near zero four times a day.

5. Discussion

The analysis presented here suggests that with an installed capacity of 13.4 GW around 35 TWh/year of tidal current energy could be extracted using only first generation tidal current devices installed at suitable UK sites. However, when accounting for environmental acceptability limitations and the consequent reduction of the in-situ resource, a lower overall Technically Acceptable Power output of 17 TWh/yr is suggested based on the restricted site selection and assumptions detailed. Approximately 7.8 GW of installed capacity is necessary to meet this scenario of generation. While the analysis presented here lacks the very high temporal and spatial resolution data necessary to inform individual project development detailed design, it offers a credible and broad resource analysis suitable for understanding the nature of the UK tidal resource and its phasing. A true understanding with a high level of accuracy of the resource will only be gained by extensive site measurements combined with new generations of hydrodynamic tidal models incorporating the complex interaction of device operation alongside the evolving hydrodynamics.

In terms of answering the original question as to whether first generation tidal current devices can offer a significant degree of firm power supply in the UK, the results suggest that it is not possible. Continuous output can be achieved for a number of days around Spring peak. However the level of continuous generation is only a small fraction of peak generation. This can be confirmed by aggregating the time series output of all the sites and presenting them as a power exceedance curve over a period of a year (showing the percentage of time the aggregate power output is exceeded). Figure 7 shows curves for aggregate tidal current generation with and without the TAP limit enforced.

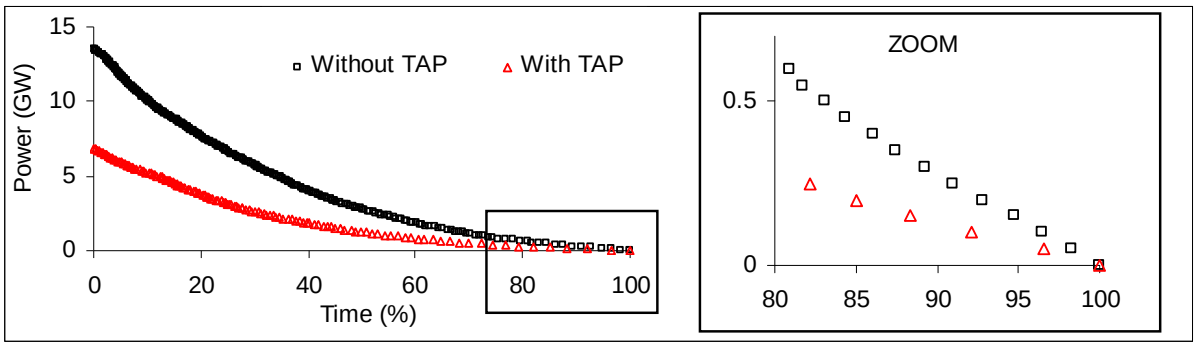

Figure 7. Power Exceedance curve from instantaneous tidal generation with and without TAP over a year

In both cases aggregate output at or near 100% exceedance is zero, meaning that there is no true capability for firm power generation with first generation tidal current devices. Other definitions of ‘firm’ output exist with, for example, the hydropower sector often adopting the 95% exceedance figure as firm output. Adopting this definition for the tidal current case, represents a firm capacity of around 75 to 150 MW with and without TAP constraints respectively – still negligible in comparison with the peak generation potential, or as a percentage of the installed capacity.

To further investigate this phasing aspect, the correlation between production at individual sites is presented in Table 5 to indicate the relationship between their various timings; all combinations showing a correlation in excess of 0.5 are shown in bold. This analysis obviously does not take any consideration of the relative magnitudes of each site, only the relative phasing. The majority of the locations in the study show either some or strong positive correlation. Maximum correlation is observed between Pentland Firth, Orkney and Islay and between Anglesey, Race of Alderney, Ramsey Island and Isle of Wight. It is also interesting to observe the high correlation between Orkney and Race of Alderney, Ramsey Island and Isle of Wight, particularly as they are geographically distant. It would be preferable from the point of view of generating continuous base load profile if the sites indicated a wide spread of both positive and negative correlations. It is anticipated that the use of second generation tidal current devices will open up more areas to exploitation, potentially improve the spread of phasing and raise the opportunity for firm aggregate production from tidal current sources.

Site name	Pentland Firth	Orkney	Islay	Anglesey	Race of Alderney	Ramsey Island	Isle of Wight
Pentland Firth	1	**0.69**	**0.96**	0.21	0.37	0.35	0.49
Orkney	**0.69**	1	**0.70**	0.48	**0.75**	**0.73**	**0.79**
Islay	**0.96**	**0.70**	1	0.26	0.38	0.35	0.49
Anglesey	0.21	0.48	0.26	1	**0.82**	**0.72**	**0.76**
Race of Alderney	0.37	**0.75**	0.38	**0.82**	1	**0.95**	**0.97**
Ramsey Island	0.35	**0.73**	0.35	**0.72**	**0.95**	1	**0.93**
Isle of Wight	0.49	**0.79**	0.49	**0.76**	**0.97**	**0.93**	1

Table 5. Correlation coefficient for production between each site

Despite the apparent lack of a firm production capability, tidal current energy can be predicted accurately over long periods. As such, it provides an opportunity for network operators to accurately schedule generation and reserve to meet demand and accommodate tidal generation, although swings of 7 GW over several hours will represent a challenge. In addition like all variable renewable sources, tidal current devices possess a ‘capacity credit’ or capacity value that describes the degree of conventional generation mix can be substituted by tidal current energy generation. Assessment of the capacity credit of tidal current energy generation building upon the scenarios presented in this work is an area for future work.

Overall this study highlights that tidal current energy production is highly variable and site specific, but this variability can be accurately predicted. A credible high level analysis of the aggregate potential of tidal current production from first generation tidal current devices sited in location with high current velocities and relatively shallow water has been presented. The analysis presented lacks the high (temporal and spatial) resolution data necessary to conduct a rigorous detailed resource analysis on a site-by-site basis as would be appropriate for detailed project design and financing. However, the approach utilised is tractable within the framework of the research and, on a site-by-site basis is analogous to preliminary site assessment in a project development context. To provide a more detailed understanding with a high degree of accuracy, extensive in-situ measurements would be necessary. Such detailed data would enable reliable assessment of additional aspects such as short–term variability for system balancing.

6. Conclusions

This study presents a high level analysis of the aggregate behaviour of the tidal current energy resource in the UK and credible scenarios for exploiting the resource using first generation tidal current technology. With due consideration to the environmentally acceptable limits to energy extraction identified, the resource available at first generation sites was estimated to be 17 TWh/year for an installed capacity of 7.8 GW. Unfortunately, the nature of tidal wave propagation around the west coast of the UK means that most tidal energy hot spots suitable for first generation technologies are largely in phase, with only the Race of Alderney in the Channel Isles differing significantly. It is concluded that there is insufficient diversity between the sites identified for first generation tidal current schemes to be considered as a firm power source.

Acknowledgements

This research was supported by funding from the EPSRC Supergen FlexNet and Supergen Marine Consortia. The buoy records were supplied by the British Oceanographic Data Centre as part of the, Inter-Agency Committee on Marine Science and Technology funded, 'UK Moored Current Meter Data Set' DVD electronic publication. The data were collected by the Proudman Oceanographic Laboratory during the Mixing and sediment resuspension in shelf seas which was funded by the Natural Environment Research Council (NERC). The authors wish to acknowledge EMEC and ScottishPower Renewables for the provision of ADCP data as well as Chris Zervas at NOAA for providing tidal analysis software. The map shown is based on UK Crown copyright material supplied through EDINA, www.edina.ac.uk.

Reference

[1] House of Lords, The EU's Target for Renewable Energy :20% by 2020. Volume 1: Report. 2008.

[2] Department for Energy and Climate Change, The UK Renewable Energy Strategy. DECC, London, 2009.

[3] R. Gross, P. Heptonstall, D. Anderson, T. Green, M. Leach, J. Skea, The Cost and Impact of Intermittency: An assessment of the evidence on the cost and impacts of intermittent generation on the British electricity network. UK Energy Research Centre, London, 2006.

[4] BLACK & VEATCH, Phase II.UK Tidal Stream Energy Resource Assessment, The Carbon Trust, London, 2005.

[5] G. Sinden, Variability of UK Marine Resource, The Carbon Trust, London, 2005.

[6] BLACK & VEATCH, Phase I.UK Tidal Stream Energy Resource Assessment, The Carbon Trust, London, 2004.

[7] Department for Trade and Industry, Atlas of UK Marine Renewable Energy Resource. A Strategic Environmental Assessment Report, DTI, London, 2004.

[8] UK Hydrographic Office, Admiralty Charts, UKHO, Taunton, UK, http://catalogue.ukho.gov.uk/home.asp.

[9] BLACK & VEATCH, UK Tidal Current Resource and Economics, The Carbon Trust, London, 2011.

[10] Department of Business, Enterprise and Regulatory Reform, Atlas of UK Marine Renewable Energy Resource, BERR, London, http://www.renewables-atlas.info/

[11] Proudman Oceanographic Laboratories, POL High Resolution 3D Continental Shelf Model (CS20), POL, Liverpool, UK, http://www.pol.ac.uk/.

[12] T. Boehme, J. Taylor, A.R. Wallace, J. Bialek, Matching Renewable Electricity Generation with Demand. The Scottish Exectutive, Edinburgh, 2006.

[13] J.A. Clarke, G. Connor, A.D. Grant, C.M. Johnstone, Regulating the output characteristics of tidal current power stations to facilitate better base load matching over the lunar cycle, Renewable Energy, 31 (2006) 173-180.

[14] J. Hardisty, Power intermittency, redundancy and tidal phasing around the United Kingdom, Geographical Journal, 174 (2008) 76-84.

[15] UK Hydrographic Office, Admirality TotalTide (version 2007), UKHO, Taunton, UK.

[16] RD Instruments, Acoustic Doppler Current Profiler. Principles of Operation. A Practical Primer.
1996.

[17] European Marine Energy Centre Ltd, ADCP data, EMEC, Orkney, Scotland,. http://www.emec.org.uk/index.asp.

[18] British Oceanographic Data Centre, Moored current data, http://www.bodc.ac.uk/.

[19] C. Zervas, Tidal Current Analysis Procedures and Associated Computer Programs NOAA Technical Memorandum NOS CO-OPS 0021, National Oceanic and Atmospheric Administration, Washington DC, 1999.

[20] Crown Estate, Press Release: World's First Wave and Tidal Energy Leasing Round to Power up to Three Quarters of a Million Homes, 16 May 2010
http://www.thecrownestate.co.uk/newscontent/92-pentland-firth-developers.htm

[21] Crown Estate, Press release: Inner Sound Tidal Project Awarded, Crown Estate, London, 27 Oct 2010, http://www.thecrownestate.co.uk/newscontent/92-inner-sound-tidal-project-awarded.htm

[22] Scottish Power Renewables, Sound of Islay Demonstration Tidal Array Environmental Statement. Non Technical Summary. Scottish Power Renewables , Glasgow, 2010

[23] C. Bell, L. Carlin, Generation of UK Tidal Stream Atlases from Regularly Gridded Hydrodynamic Modelled Data, The Journal of Navigation, 51 (1998) 73-78.

[24] D. Shepard, A two-dimensional interpolation function for irregularly-spaced data, Proc. 23rd ACM national conference, New York, 1968.

[25] A.S. Iyer, S.J. Couch, G.P. Harrison, A.R. Wallace, Analysis and comparison of Tidal Datasets. Proc. 8th European Wave and Tidal Energy Conference.(EWTEC), Uppsala, Sweden, Sept. 2009.

[26] J. Thake, Development Installation and Testing of a Large Scale Tidal Current Turbine, Department for Trade and Industry, London 2005.

[27] C. Legrand, Assessment of Tidal Energy Resource. European Marine Energy Centre

Ltd, Orkney, 2009.

[28] National Grid Electricity Transmission plc, 2010 National Electricity Transmission System (NETS) Seven Year Statement, London, 2010; http://www.nationalgrid.com/uk/Electricity/SYS/

[29] Department of Energy & Climate Change, Digest of United Kingdom Energy Statistics (DUKES), London, 2010

[30] T. Boehme, Matching Renewable Electricity Generation with Demand in Scotland, PhD Thesis, Institute for Energy Systems, University of Edinburgh, Edinburgh, 2006.

[31] G. Southerland, M. Foreman, C. Garrett, Tidal current energy assessment for Johnstone Strait, Vancouver Island. Proc. IMechE Part A: Journal of Power and Energy, 221, 2007, pp. 147-157.

[32] B. Polagye, M. Kawase, P. Malte, In-stream tidal energy potential of Puget Sound, Washington. Proc IMechE Part A: Journal of Power and Energy, 223, 2009, pp. 571- 587